# Diels–Alder Reactions in I. the Biosynthesis of Paracaseolide A and II. the De Novo Construction of Benzenoid Structures

A DISSERTATION
SUBMITTED TO THE FACULTY OF THE GRADUATE SCHOOL
OF THE UNIVERSITY OF MINNESOTA
BY

Tao Wang

IN PARTIAL FULFILLMENT OF THE REQUIREMENTS
FOR THE DEGREE OF
DOCTOR OF PHILOSOPHY

Thomas R. Hoye, Advisor

December 2016

# Acknowledgements

As I reach this important milestone of my career, I want to express my sincere gratitude to all people who have been tremendously helpful in my doctoral studies. First and foremost, I would like to thank Juanjuan Bu for her unconditional love and support. She helped me on countless things, many of which I may not even be aware of. She is my best friend, my soul mate and will soon become my life-long companion. I want to thank her for making me who I am today.

I want to thank my parents, who have been working tirelessly in the past 27 years to give me the best education. I want to thank them for answering probably millions of questions I had about Nature when I was still a kid. Their patience in taking care of my curiosity encouraged me to become a researcher myself and to probe more of those interesting phenomena. I am also very grateful for all the great foods made by them.

I would like to thank my advisor, Professor Thomas R. Hoye. I met Tom in the winter (mid-December) of 2010 during his lecture at Peking University. At that time, I was not yet able to fully capture every detail in his presentation. However, I knew immediately that he is a great advisor and is someone who will guide students with extreme patience and care. Now, six years later, I feel exceedingly fortunate to have become a member of his lab. Tom is not only a research advisor with great knowledge, but also a friend with good sense of humor, a counselor with extreme patience, a chemist with cutting-edge skills of communication, a role model with high self-discipline, and a senior who we can trust, rely on, and admire. I cannot say enough good things about Tom, but I would like to end my acknowledgement to him by telling a story. I was once asked by an incoming new student “can you describe what it’s like working in the Hoye lab?” I concluded my answer in two words: “freedom & independent”. Tom has always been open-minded and allow us to freely explore chemistry driven by our own curiosity. He also treats students with great respect and trust, which is not easy. He is willing to adapt to our styles of working and give us a hand whenever we are in trouble.

I also want to thank Dawen Niu, a former member of the Hoye lab and one of the best colleague I have ever had. Without doubt, he is one of the smartest person I know of. He is knowledgeable, easy to work with, and willing to offer help to young members in the lab. I am also impressed by his love of chemistry and familiarity of literature. When chatting with other chemists, he will never waste more than five sentences before rushing to the main topic of chemistry. He taught me a lot in reaction setup, problem solving, and spectroscopic analysis. My doctoral study would be a lot harder without his generous help. He has also been a great role model in career planning.

I am very grateful for all the suggestions and guidance on computational chemistry from Professor Christopher J. Cramer during his class and throughout my graduate research. I found myself learned much more than I could imagined during his lecture, in which he has completely changed my view of this unique science. I gained a lot of confidence in his class to use calculation as a powerful tool in research. I also want to thank Kaining Duanmu in Truhlar lab for sharing his expertise in theoretical chemistry and being a great friend of mine.

I appreciate all the healthy discussion I had with Sean Ross and Junhua Chen in the lab. I also want to thank Dr. Beeraiah Baire, Dr. Vedamayee Pogula, Dr. Patrick Willoughby, and Dr. Brian Woods for being great coworkers. I want to thank all other members in the Hoye group for creating a happy atmosphere in the lab.

I want to thank Wayland Noland Fellowship, Doctoral Dissertation Fellowship, and Chinese Government Award for Outstanding Self-Financed Students Abroad for their financial support.

Lastly, I would like to thank my cat Wu, who has been able to maintain cute and stupid at the same time in the past three years. I want to thank him for petting away my stress and worries and being a wonderful companion.

*To Juanjuan Bu,*

*My source of happiness and spiritual support*

# Abstract

**Part I:** Paracaseolide A, a natural product characterized by a tetracyclic dilactone core structure containing six adjacent stereocenters, has an unprecedented skeleton and occupies unique structural space among the >200,000 characterized secondary metabolites. Researchers from six different groups have published a chemical synthesis of this compound; five used a thermal, net Diels–Alder cycloaddition and dehydration at high temperature under neat and $O_2$-free condition to access this target by dimerization of a simple butenolide precursor. In my study, I found (i) that this dimerization proceeds under much milder (ambient temperature) conditions and with a different stereochemical outcome (*exo* instead of *endo*), rationalizable by a bis-pericyclic transition state, than previously recognized; (ii) that spontaneous epimerization, necessary to correct the configuration at one key stereocenter, is viable; and (iii) that natural paracaseolide A is racemic—a fact that directly points to the absence of enzymatic catalysis (namely, Diels–Alderase activity) in the cycloaddition. Together these results strongly suggest that a non-enzyme-mediated dimerization of butenolide monomer is the actual event by which paracaseolide A is produced in Nature.

**Part II:** The hexadehydro-Diels–Alder (HDDA) reaction has recently grown as a powerful alternative in the generation of benzyne intermediates as well as a de novo approach in accessing highly substituted aromatic systems. Like other members of the venerable Diels–Alder cycloaddition, HDDA reaction starts from linear precursors and is also highly atom economical. I have contributed to several projects in this area of study. These includes (i) mechanism of cycloisomerization step (concertedness of reaction), (ii) origin of distortion in the geometry of benzyne, (iii) mechanism in the trapping reactions of tethered silyl ether, tethered arene and intermolecular trapping of alcohols, and (iv) synthesis of dichloroarene and carbazole derivatives via a HDDA-based strategy.

# Table of Contents

# List of Figures

# List of Schemes

# List of Tables

# List of Abbreviations

| | |
|---|---|
| **ACN** | Acetonitrile |
| **$Ac_2O$** | Acetic anhydride |
| **au** | Atomic unit |
| **Bcat** | Catecholboranyl |
| **Bn** | Benzyl |
| **BRSM** | Based on recovered starting material |
| **Bz** | Benzoyl |
| **CAN** | Cerric ammonium nitrate |
| **CSA** | Camphor sulfonic acid |
| **DA** | Diels–Alder |
| **DBU** | Diaza(1,3)bicyclo[5.4.0]undecane |
| **DIBAL** | Diisobutylaluminum hydride |
| **DCC** | Dicyclohexylcarbodiimide |
| **DCM** | Dichloromethane |
| **DCE** | 1,2-Dichloroethane |
| **DFT** | Density functional theory |
| **DMAD** | Dimethyl acetylenedicarboxylate |
| **DMAP** | *N*,*N*-4-Dimethylaminopyridine |
| **DME** | Dimethoxyethane |
| **DMF** | *N*,*N*-Dimethylformamide |
| **DMS** | Dimethyl sulfide |
| **dr** | Diastereomeric ratio |
| **E** | Methoxycarbonyl |
| **ee** | Enantiomeric excess |
| ***epi*** | Epimer |
| **EtOAc** | Ethyl acetate |
| **$Et_3N$** | Triethylamine |
| **$Et_2O$** | Diethyl ether |

| | |
|---|---|
| **GC/MS** | Gas chromatography-mass spectrometry |
| **HDDA** | Hexadehydro-Diels–Alder |
| **HF** | Hartree-Fock |
| **HMPA** | Hexamethylphosphoramide |
| **HR ESI-MS** | High resolution electrospray ionization-mass spectrometry |
| **$IC_{50}$** | Half maximal inhibitory concentration |
| **IEFPCM** | Integrated equation formalism polarized continuum model |
| **INT** | Intermediate |
| **IR** | Infrared |
| **IRC** | Intrinsic reaction coordinate |
| **LC/MS** | Liquid chromatography-mass spectrometry |
| **LDA** | Lithium diisopropylamide |
| **LiHMDS** | Lithium *bis*(trimethylsilyl)amide |
| **LUMO** | Lowest unoccupied molecular orbital |
| **MB** | Methylene blue |
| **MeCN** | Acetonitrile |
| **MS** | Molecular sieve |
| **mp** | Melting point |
| **NaAsc** | Sodium ascorbate |
| **NBS** | *N*-Bromosuccinimide |
| **NMP** | *N*-Methyl-2-pyrrolidone |
| **NMR** | Nuclear magnetic resonance |
| **nOe** | Nuclear Overhauser enhancement |
| **PES** | Potential energy surface |
| **$PhCH_3$** | Toluene |
| **phen** | 1,10-phenanthroline |
| **PhH** | Benzene |
| **PMB** | 4-Methoxybenzyl |
| **PPTS** | Pyridinium *para*-toluenesulfonate |
| **psi** | Pounds per square inch |

| | |
|---|---|
| **Py** | Pyridine |
| **SM** | Starting material |
| **SMD** | Solvation model density |
| **TBAF** | Tetra-*n*-butylammonium fluoride |
| **TBAI** | Tetra-*n*-butylammonium iodide |
| **TBS** | *t*-Butyldimethylsilyl |
| **TBDPS** | *t*-Butyldiphenylsilyl |
| **TC-PTP** | T-cell protein tyrosine phosphatase |
| **TDDA** | Tetradehydro-Diels–Alder |
| **TEA** | Triethylamine |
| **TES** | Triethylsilyl |
| **Tf** | Trifluoromethanesulfonyl |
| **TFA** | Trifluoroacetic acid |
| **THF** | Tetrahydrofuran |
| **TIPS** | Triisopropylsilyl |
| **TLC** | Thin layer chromatography |
| **TMEDA** | Tetramethylethylenediamine |
| **TMS** | Trimethylsilyl |
| **Tol** | 4-Methylphenyl |
| **TPCP** | Tetraphenylcyclopentadienone |
| **Ts** | *p*-Toluenesulfonyl |
| **TS** | Transition state |

# ◊ Part I ◊

## Diels–Alderase-free, bis-pericyclic, [4+2] dimerization in the biosynthesis of (±)-paracaseolide A

# Chapter 1. Hypotheses in the biosynthesis of paracaseolide A

## 1.1 Isolation, bioactivity and structure paracaseolide A

Paracaseolide A (**101**, Figure 1) is a secondary metabolite first reported by Guo and coworkers in 2011.[1] It was isolated from the stem bark of *Sonneratia paracaseolaris*, which is a mangrove plant that was collected in Zhanjiang, Guangdong Province of China. In this initial report, 12 mg of paracaseolide A (**101**) was obtained from 1.5 kg of dried stem bark via repeated chromatographic purification of the methanol extract.

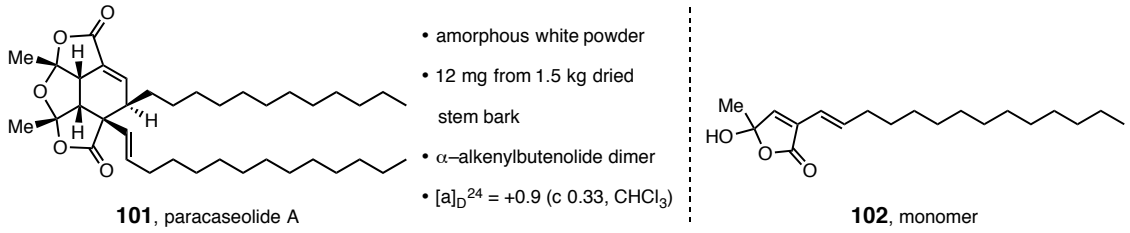


**Figure 1.** Structure of paracaseolide A **101** and monomer **102**

Paracaseolide A (**101**) exhibited significant inhibitory activity against dual specificity phosphatase CDC25B, which is a key enzyme for cell cycle progression, with an $IC_{50}$ value of 6.44 $\mu$M.[1,2] Recent studies also showed its inhibitory activity against PTP1B and T-cell protein tyrosine phosphatase (TC-PTP) with $IC_{50}$ values of 1.50 $\mu$M and 6.01 $\mu$M respectively.[3]

The ubiquitous structure of paracaseolide A (**101**) was elucidated through extensive spectroscopic studies by Guo and coworkers.[1] It is characterized by a tetraquinane oxa-cage bislactone skeleton bearing two linear alkyl chains. One most prominent skeletal

---

[1] Chen, X.-L.; Liu, H.-L.; Li, J.; Xin, G.-R.; Guo, Y.-W. Paracaseolide A, first α-alkylbutenolide dimer with an unusual tetraquinane oxa-cage bislactone skeleton from Chinese mangrove *Sonneratia paracaseolaris*. *Org. Lett.* **2011**, *13*, 5032–5035.

[2] Lammer, C.; Wagerer, S.; Saffrich, R.; Mertens, D.; Ansorge, W.; Hoffmann, I. The cdc25B phosphatase is essential for the G2/M phase transition in human cells. *J. Cell Sci.* **1998**, *111*, 2445–2453.

[3] Yin, J.-P.; Tang, C.-L.; Gao, L.-X.; Ma, W.-P.; Li, J.-Y.; Li, Y.; Li, J.; Nan, F.-J. Design and synthesis of paracaseolide A analogues as selective inhibitors of protein tyrosine phosphatase 1B inhibitors. *Org. Biomol. Chem.* **2014**, *12*, 3441–3445.

feature of **101** is its dimeric nature—it is a dimer of the simple α–alkenylbutenolide **102** (Figure 1). While the α–alkylbutenolide substructure is common among a variety of isolated pharmacologically active natural products,[4] the dimeric α–alkylbutenolide, to the best of our knowledge, has not been reported previously.

## 1.2 Our hypothesis

The structure of **101** is intriguing both as a target for synthesis as well as from the perspective of its biosynthetic origin. We have focused particular attention on the question of whether the dimerization of butenolide **102** could be the actual event involved in the biosynthesis of **101**. More specifically, we wondered if that reaction is sufficiently fast to be operative in the absence of any enzymatic catalysis (here, Diels–Alderase-free?). This type of question, i.e., is a spontaneous event occurring in the organism, is one that we frequently find ourselves asking when faced with the structure of a secondary metabolite that is unique—Nature's equivalent of a one hit wonder. Why shouldn't it be that some biosynthetic intermediates are inherently endowed with sufficiently high, inherent reactivity such that they will spontaneously react—either uni- or bi-molecularly, the latter often in a dimerization mode—to produce a new product that proves to be of benefit to the organism? [5]

First, we asked if it is reasonable that the requisite alkenyl butenolide **102** could be generated by common, biosynthetic pathways and their associated enzymatic machinery. On the basis of a search of relevant known natural product structures, we conclude that it is. Namely and as we have summarized in Figure 2, there are many known secondary

---

[4] For example: (a) Shults, E. E.; Velder, J.; Schmalz, H.-G.; Chernov, S. V.; Rubalava, T. V.; Gatilov, Y. V.; Henze, G.; Tolstikov, G. A.; Prokop, A. Gram-scale synthesis of pinusolide and evaluation of its antileukemic potential. *Bioorg. Med. Chem. Lett.* **2006**, *16*, 4228–4232 and references cited therein. (b) Koo, K. A.; Lee, M. K.; Kim, S. H.; Jeong, E. J.; Oh, T. H.; Kim, Y. C. Pinusolide and 15-methoxypinusolidic acid attenuate the neurotoxic effect of staurosporine in primary cultures of rat cortical cells. *Br. J. Pharmacol.* **2007**, *150*, 65–71. (c) Kikuchi, H.; Tsukitani, Y.; Nakanishi, H.; Shimizu, I.; Saitoh, S.; Iguchi, K.; Yamada, Y. Studies on marine natural products. VIII. New Butenolides from the Gorgonian Euplexaura flava (Nutting). *Chem. Pharm. Bull.* **1983**, *31*, 1172–1176. (d) Boukouvalas, J.; Loach, R. P. General, regiodefined access to α-substituted butenolides through metal−halogen exchange of 3-bromo-2-silyloxyfurans. Efficient synthesis of an anti-inflammatory gorgonian lipid. *J. Org. Chem.* **2008**, *73*, 8109–8112.

[5] Gravel, E.; Poupon, E. Biogenesis and biomimetic chemistry: Can complex natural products be assembled spontaneously? *Eur. J. Org. Chem*. **2008**, 27–42

metabolites that contain the 2-alkenylbutenolide subunit shown as **103**. In Figure 2A these are grouped as families of compounds that bear various kinds of substituents at C4 of the butenolide and Cβ of the alkenyl side chain. Five of these compounds contain a free C4-hydroxyl group (Figure 1B).[6a–e] In particular, **104** and **105** each contains a bulky substituent at Cβ of the alkenyl side chain while **106** has a *cis*-alkenyl side chain. Their self-dimerization via Diels–Alder cycloaddition are expected to be slow due to steric hindrance (**104** and **105**) or low concentration of the active *s-cis* conformer (**106**). Finally, over one-thousand 2-*alkyl*butenolides have been isolated from nature, over 200 of which contain a C4-OH group. The most relevant one to this discussion is compound **107** (Figure 2B),[6f] which is a dihydro-analogue of **102** containing two addition carbon atoms (i.e., one acetate unit) in its lipophilic side chain. All told, the existence of this collection of natural products implies that the requisite polyketide enzymatic machinery to produce the butenolide **102** is well in place in the natural world.

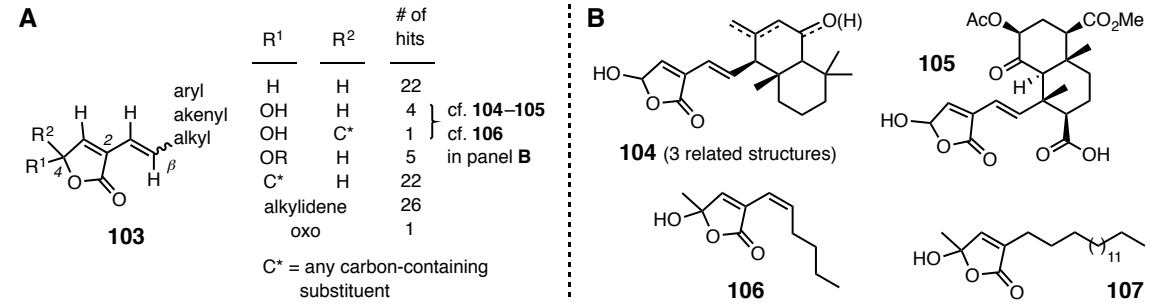


**Figure 2.** Structually related 2-alkenylbutenolides isolated in Nature

Another relevant question can be put as "what's known about the innate propensity of a

[6] (a) Zhao, Q.; Qing, C.; Hao, X. J.; Han, J.; Zuo, G. Y.; Zou, C.; Xu, G. L. Cytotoxicity of labdane-type diterpenoids from Hedychium forrestii. *Chem. Pharm. Bull.* **2008**, *56*, 210–212. (b) Nakamura, S.; Okazaki, Y.; Ninomiya, K.; Morikawa, T.; Matsuda, H.; Yoshikawa, M. Medicinal flowers. XXIV. Chemical structures and hepatoprotective effects of constituents from flowers of Hedychium coronarium. *Chem. Pharm. Bull.* **2008**, *56*, 1704–1709. (c) Suresh, G.; Reddy, P. P.; Babu, K. S.; Shaik, T. B.; Kalivendi, S. V. Two new cytotoxic labdane diterpenes from the rhizomes of Hedychium coronarium. *Bioorg. Med. Chem. Lett.* **2010**, *20*, 7544–7548. (d) Shirota, O.; Nagamatsu, K.; Sekita, S.; Neo-clerodane diterpenes from the hallucinogenic sage Salvia divinorum. *J. Nat. Prod.* **2006**, *69*, 1782–1786. (e) Gamard, P.; Sauriol, F.; Benhamou, N.; Belanger, R. R.; Paulitz, T. C. Novel butyrolactones with antifungal activity produced by Pseudomonas aureofaciens strain 63-28. *J. Antibiot.* **1997**, *50*, 742–749. (f) Kikuchi, H.; Tsukitani, Y.; Nakanishi, H.; Shimizu, I. New butenolides from the gorgonian euplexaura flava(nutting). *Chem. Lett.* **1982**, *11*, 233–236.

1,3-butadiene bearing and electron-withdrawing substituent at C2 to undergo a Diels-Alder dimerization reaction?" This represents the minimalist substructure in **102** essential to the main thesis here. 1,3-Butadiene-2-carboxylic acid esters (e.g., **108**) have many times been observed to self-dimerize in a [4+2] sense under very mild conditions (Scheme 1A) to give the corresponding esters of mikanecic acid (e.g., **109**), which has a similar carbon skeleton compared to paracaseolide A **101**. The activation Gibbs free energy of this transformation was determined to be as low as 21 kcal $mol^{-1}$.[7] Interestingly, we can find no evidence in the literature of characterization of the parent 3-butadiene-2-carboxylic acid. Also, previous studies in our lab revealed that simple α–vinylbutenolide **110** can undergo spontaneous dimerization reaction at room temperature via Diels–Alder reaction to give differolide, which arises from a reaction where the vinyl group has functioned as the dienophile (**111**, Scheme 1B).[8] When a neat sample of **110** was kept at room temperature for 14 days, dimeric species **111** and **112** can be isolated in 31% and 4% yield respectively, along with 18% yield of the recovered starting material. It is worth pointing out that differolide was isolated as a racemic mixture in Nature,[9] which is more consistent with a non-enzyme catalyzed Diels–Alder dimerization.

**Scheme 1.** Facile dimerization reaction of diene ester **108** and vinylbutenolide **110** at room temperature via Diels–Alder reaction

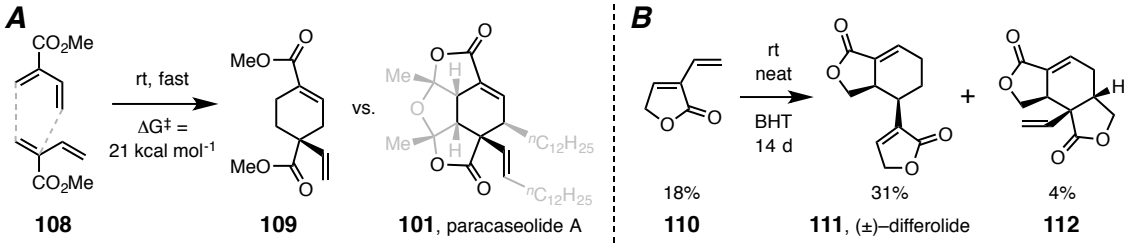


[7] Jung, M. E.; Zimmerman, C. N. New synthesis of methyl 1,3-butadiene-2-carboxylate by the cheletropic extrusion of carbon monoxide from 3-carbomethoxy-3,4-pentadienal and a study of its dimerization to give dimethyl mikanecate (dimethyl 4-ethenyl-1-cyclohexene-1,4-dicarboxylate). *J. Am. Chem. Soc.* **1991**, *113*, 7813–7814.

[8] Hoye, T. R.; Donaldson, S. M.; Vos, T. J. An enyne metathesis/(4 + 2)-dimerization route to (±)-differolide. *Org. Lett.* **1999**, *1*, 277–279.

[9] Keller-Schierlein, W.; Bahnmüller, U.; Dobler, M.; Bielecki, J.; Stümpfel, J.; Zähner, H. Isolation and structure elucidation of differolide. *Helv. Chim. Acta* **1986**, *69*, 1833–1836.

There are additional specific issues germane to the question of whether the spontaneous dimerization of diene **102** is the actual event involved in the biosynthesis of paracaseolide A (**101**). First, if the reaction is not catalyzed by an enzyme, one would expect the isolated natural sample of **101** to be racemic. That material was reported to show a specific rotation of +0.9°. In our view, particularly in light of minor resonances in the $^{1}$H NMR spectrum for **101** that indicate the presence of some contaminants, this small value is within experimental error of zero and is not sufficient to rule out the possibility that natural paracaseolide A is, indeed, a racemate. We revisit this point later. Second, a concerted Diels–Alder reaction between two molecules of **102** would produce an initial cyclohexene adduct in which the substituents on the two allylic carbons, C5 and C7c, have a *cis*-orientation to one another. These are structures **113-endo** or **113-exo** (Scheme 2), the diastereomers formed through *endo* addition of the diene with respect to the lactone carbonyl vs. the alkene side chain in **102**, respectively. Importantly however, in either instance this results in an unnatural relative configuration among the four newly created stereocenters embedded in the cyclohexene ring. In order for either of **113-endo** or **113-exo** to proceed to paracaseolide A (**101**) would be necessary to epimerize the configuration at either C5 or C7c, respectively, as well as, of course, to lose a molecule of water.

**Scheme 2.** Two possible modes of Diels–Alder reaction in the dimerization event

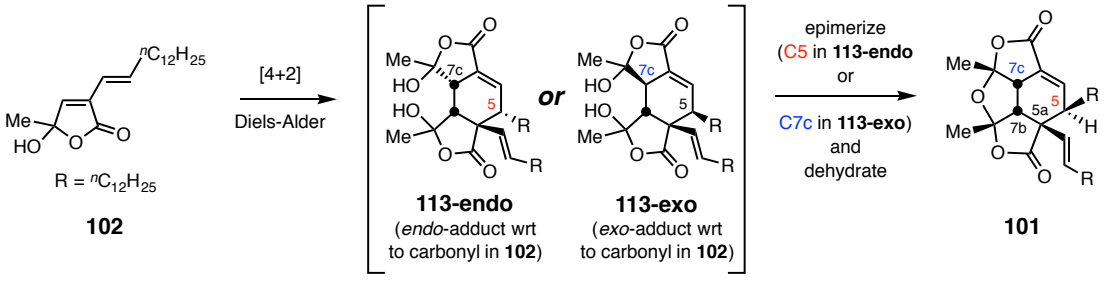


With these considerations in mind, we felt that mechanistic studies of the dimerization pathway of **102** (to give paracaseolide A **101**) would be particularly interesting and valuable due to its strong relevance to Diels–Alderase enzymatic action (or lack thereof)

in biosynthesis.[10,11] Other biosynthetically relevant, spontaneous Diels–Alder (DA) dimerizations have been proposed and demonstrated; notable examples include those leading to carpanone[12] and the endiandric acids.[13]

## 1.3 Previous studies of the dimerization reaction in the synthesis of paracaseolide A

The fascinating, skeletally unique structure of paracaseolide A (**101**) quickly captured the attention of synthetic chemists. In a short period of time, researchers in five different laboratories have reported a total synthesis of **101** involving the same final key step.[3,14] Namely, dimerization of the butenolide **102** (Scheme 3) accompanied by dehydration has been repeatedly used to produce **101**. In every instance **102** was heated to 110 °C to effect this overall transformation. In every instance the researchers initially rationalized the reaction to occur via an *endo* orientation of the two reacting monomers (see Scheme 3) and via the intermediacy of the *endo* Diels–Alder dimer **113-endo** and its dehydrated product **5-epi-101**. (In this document, *endo* and *exo* refer to the relative orientation between the carbonyl group on the dienophilic component and the internal carbons of the

---

[10] (a) Stocking, E. M.; Williams, R. M. Chemistry and biology of biosynthetic Diels–Alder reactions. *Angew. Chem. Int. Ed.* **2003**, *42*, 3078–3115. (b) Hideaki Oikawa, H.; Tokiwano, T. Enzymatic catalysis of the Diels–Alder reaction in the biosynthesis of natural products. *Nat. Prod. Rep.* **2004**, *21*, 321–352.

[11] (a) Kim, A. H. J.; Ruszczycky, M. W.; Choi, S.-H.; Liu, Y.-N.; Liu, H.-W. Enzyme-catalyzed [4+2] cycloaddition is a key step in the biosynthesis of spinosyn. *Nature* **2011**, *473*, 109–112. (b) Hashimoto, T.; Hashimoto, J.; Teruya, K.; Hirano, T.; Shin-Ya, K.; Ikeda, H.; Liu, H-w.; Nishiyama, M.; Kuzuyama, T. Biosynthesis of versipelostatin: Identification of an enzyme-catalyzed [4+2]-cycloaddition required for macrocyclization of spirotetronate-containing polyketides. *J. Am. Chem. Soc.* **2015**, *137*, 572–575.

[12] (a) Brophy, G. C.; Mohandas, J.; Slaytor, M.; Sternhell, S.; Watson, T. R.; Wilson, L. A. Novel lignans from a *Cinnamomum* sp. from Bougainville. *Tetrahedron Lett.* **1969**, *10*, 5159–5162. (b) Chapman, O. L.; Engel, M. R.; Springer, J. P.; Clardy, J. C. The total synthesis of carpanone. *J. Am. Chem. Soc.* **1971**, *93*, 6696–6698.

[13] (a) Bandaranayake, W. M.; Banfield, J. E.; Black, D. St. C. Postulated electrocyclic reactions leading to endiandric acid and related natural products. *J. Chem. Soc. Chem. Comm.* **1980**, 902–903. (b) Nicolaou, K. C.; Petasis, N. A.; Zipkin, R. E.; Uenishi, J. The endiandric acid cascade. Electrocyclizations in organic synthesis. 1. Stepwise, stereocontrolled total synthesis of endiandric acids A and B. *J. Am. Chem. Soc.* **1982**, *104,* 5555–5557.

[14] (a) Noutsias, D.; Vassilikogiannakis, G. First total synthesis of paracaseolide A. *Org. Lett*. **2012**, *14*, 3565–3567. (b) Vasamsetty, L.; Khan, F. A.; Mehta G. Total synthesis of a novel oxa-bowl natural product paracaseolide A via a 'putative' biomimetic pathway. *Tetrahedron Lett*. **2013**, *54*, 3522–3525. (c) Giera, D. S.; Stark, C. B. W. Total synthesis of (±)-paracaseolide A and initial attempts at a Lewis acid mediated dimerization of its putative biosynthetic precursor. *RSC Adv.* **2013**, *3*, 21280–21284. (d) Boukouvalas, J.; Jean, M.–A. Streamlined biomimetic synthesis of paracaseolide A via aerobic oxidation of a 2-silyloxyfuran. *Tetrahedron Lett*. **2014**, *55*, 4248–4250.

1,3-butadiene derivative in the cycloaddition transition state geometry and products derived therefrom.) This necessitated the supposition of a subsequent epimerization at C5 in the cyclohexenyl ring of **5-epi-101** in order to account for the final formation of **101**.

**Scheme 3.** Previous syntheses of paracaseolide A (**101**) via dimerization of **102** and the proposed reaction pathway

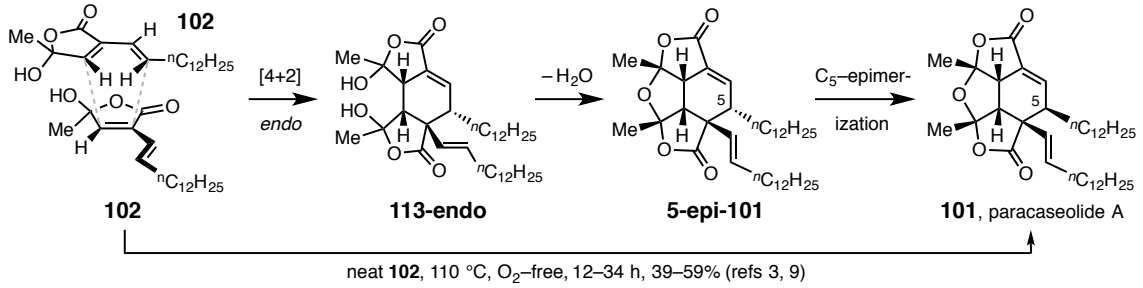


It is noteworthy that attempts to interconvert **5-epi-101** with **101** (and vice-versa) by two groups of workers have been unsuccessful.[14b,c] These mechanistic and stereochemical dilemmas have recently been explored computationally by the research groups of Ganguly, Khan, and Mehta, leading those workers to conclude that a "stepwise mechanism (leading to **5-epi-101**) is the likely pathway" and that "a concerted [4+2] cycloaddition and post-DA epimerization" is less likely.[15]

[15] Vasamsetty, L.; Sahu, D.; Ganguly, B.; Khan, F. A.; Mehta, G. Total synthesis of novel bioactive natural product paracaseolide A and analogues: Computational evaluation of a 'proposed' biomimetic Diels–Alder reaction. *Tetrahedron* **2014**, *70*, 8488–8497.

# Chapter 2. Total synthesis of paracaseolide A

## 2.1 Preparation of paracaseolide A

Our study began with the preparation of α–vinylbutenolide monomer **202a** (= **102**, the natural monomer with long alkenyl side chain). As shown in Scheme 4, the synthesis of **202a** commenced with propargyl alcohol (**203**). Tetrahydropyranyl ether formation followed by acylation of the terminal alkyne gave ynone **204**, which was treated with concentrated aqueous hydrobromic acid to give 4-bromo-2-methylfuran (**205**) as the key building block. To install the alkenyl side chain in **202a**, this bromofuran derivative was coupled with tetradecenylboronic ester under Suzuki condition. The product furan **206** was then silylated at the C2 position before subjecting to singlet oxygen oxidation using methylene blue as sensitizer and incandescent lamp as the mild light source to produce the natural monomer **202a** as a waxy white solid.

**Scheme 4.** Our total synthesis of paracaseolide A

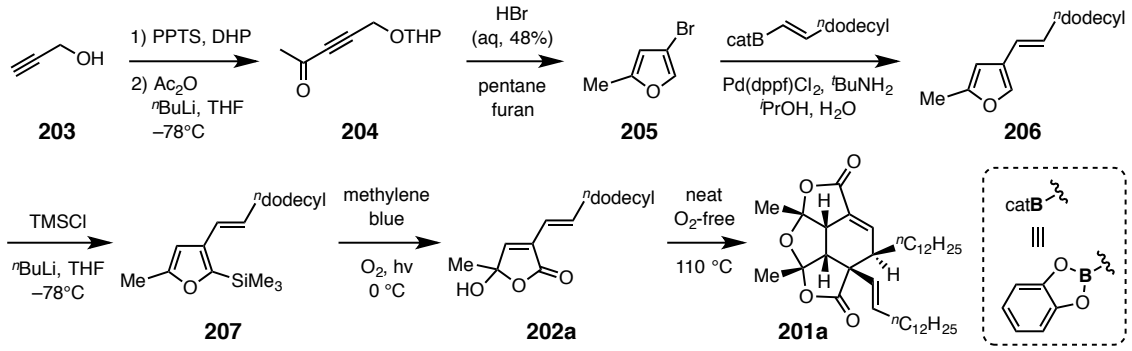


203 204 205 206 207 202a 201a

With this monomer in hand, we explored various dimerization condition. Similar to later reports,[3,10] we found when a neat sample of **202a** was kept under 110 °C and $O_2$-free condition, paracaseolide A (**201a** = **101**, Scheme 4) can be isolated in 42% yield along with its C5-epimer **5-epi-201a** (7% yield, not shown here, see Figure 3 for structure). However, efforts to obtain single crystals of either of these two epimers remained unsuccessful. We rationalized that this is due to the surfactant like molecular structure, in

which the tetracyclic bislactone moiety is highly polarized and hydrophilic while the two long alkenyl side chain is hydrophobic and hard to form regulated packing in the crystal lattice.

## 2.2 Total synthesis of the truncated paracaseolide A

To solve this difficulty in crystal formation and unambiguously confirm the relative configurations in paracaseolide A. We have also designed and prepared the truncated monomer **202b** where the $^{n}$dodecyl substituent in the alkenyl side chain was replaced by a simple methyl group. (Scheme 5) Following a similar strategy, lithium halogen exchange of furan **205** using *tert*-butyllithium followed by trapping with propanal gave secondary alcohol **208**. This was then protected as the TBS ether **209** before subjecting to subsequent retro-Brook rearrangement. When **209** was treated with $^{n}$BuLi and HMPA in THF, 1,4-silyl migration from alcohol oxygen to the C2-carbon of furan proceeded smoothly to deliver 2-silylated furan compound **210**. The hydroxyl moiety was eliminated under dehydration condition ($^{p}$TsOH, reflux toluene) to give a E/Z mixture (5:1) of **211**. Subsequent singlet oxygen oxidation produced O-silylated ketoester **212** as a labile intermediate, [16] which was conveniently hydrolyzed upon treatment of silica gel in wet solvent such as $CH_2Cl_2$. Monomer **202b** was obtained as 7 to 1 mixture of side chain E/Z isomers (pale yellow oil).

**Scheme 5.** Synthesis of truncated monomer **202b**

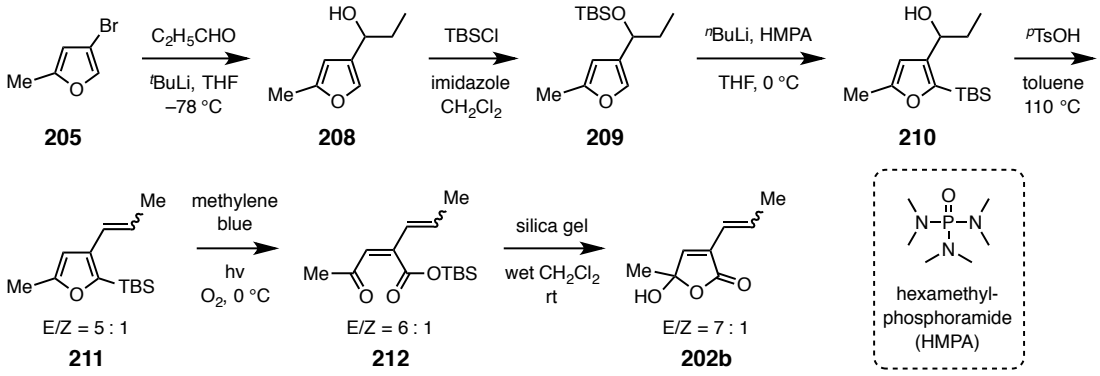


[16] Adam, W.; Rodriguez, A. Intramolecular silyl migration in the singlet oxygenation of 2-methyl-5-trimethylsilylfuran. *Tetrahedron Lett.* **1981**, *22*, 3505–3508.

Like the natural monomer, when truncated monomer **202b** was subjected to neat, 110 °C, and $O_2$-free condition, a dimeric product **201b**, namely the truncated analogue of paracaseolide A, can be isolated as the major product in 42% yield (Figure 3A). $^1$H NMR analysis showed close correlation between the peaks that were attributed to the each of the two tetracyclic core of **201a** and **201b** (Figure 3B).

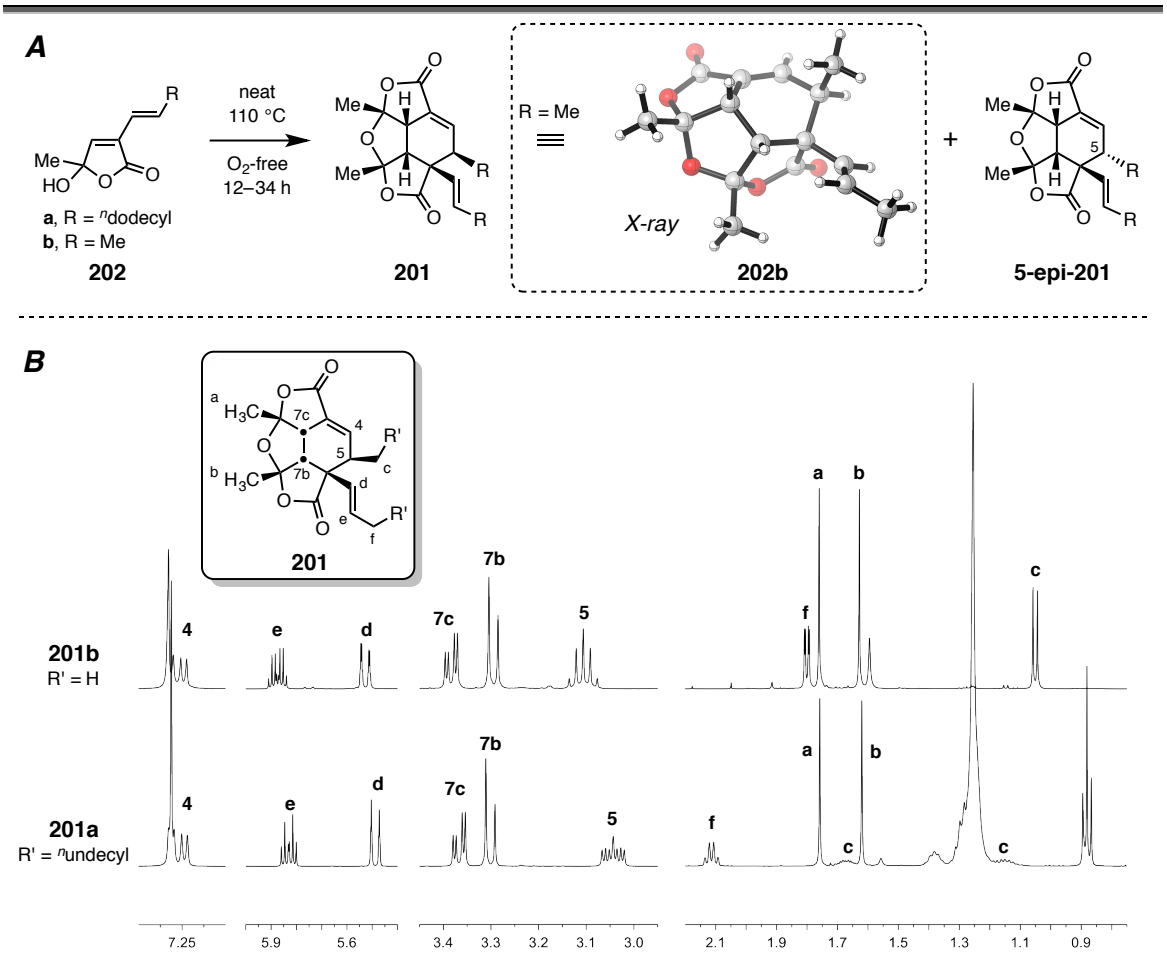


**Figure 3.** Dimerization of monomers and structural validation of paracaseolide A from a combination of X-ray and $^1$H NMR analysis

To our great delight, truncated paracaseolide A **201b**, unlike its long chain analogue **201a**, is a crystalline white solid. This allowed us to perform X-ray analysis of the obtained **201b** single crystal and, for the first time, definitively establish the relative configuration in the structure of paracaseolide A.

Throughout part I of this document, compound structure numbers ending in "**a**" all contain $^{n}$dodecyl groups that correspond to the substituents present in the natural product; the structure numbers ending in "**b**" all contain a methyl in place of the $^{n}$dodecyl group and comprise a series of unnatural, truncated analogues.

## 2.3 Previous synthetic efforts towards paracaseolide A

### *2.3.1. Reported total synthesis via dimerization of monomer*

Vassilikogiannakis lab were the first to publish a total synthesis of paracaseolide A via the dimerization reaction of **202a** (June 2012). In their synthesis of the monomer **202a** (Scheme 6), tridecan-1-ol (**213**) was first converted to 1-iodotridecane (**214**) under Appel reaction condition. Lithium halogen exchange using *tert*-butyllithium followed by trapping with furan-3-carbaldehyde yielded alcohol **215**, which was then protected as TBS ether **216**. Subsequent retro-Brook rearrangement (**216** to **217**), acid catalyzed dehydration (**217** to **218**), and methylation of the furan ring gave furan **219** as the key intermediate. This C2-silylated furan derivative was then converted to monomer **202a** via singlet oxygen oxidation.

**Scheme 6.** Vassilikogiannakis's synthesis of monomer (June 2012)

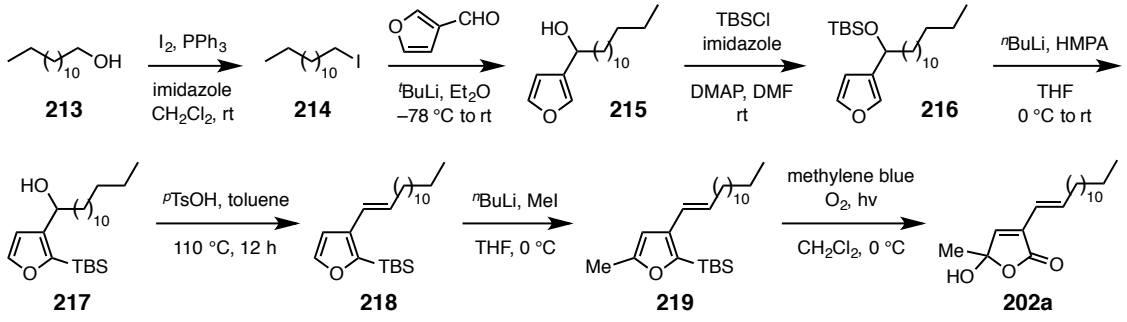


July 2013, Mehta and coworkers reported their synthesis starting from 5-methylfuran-2-carbaldehyde (**220**, Scheme 7A). Singlet oxygen oxidation led to butenolide **221**, which was subjected to α–iodination (to give **222**) and Suzuki coupling to furnish the monomer **202a**. Finally, **202a** was converted to **201a** under the same neat dimerization condition.

September 2013, Stark group reported their total synthesis using the same dimerization strategy starting from furanone **223** (Scheme 7B). Palladium-catalyzed acyloxylation employing sodium perborate as oxidant furnished butenolide **224**, which was converted to monomer **202a** via an α–iodination, Suzuki coupling, and hydrolysis sequence.

**Scheme 7.** Mehta (July 2013, panel A), Stark (September 2013, panel B), Li (March 2014, panel C), and Boukouvalas (July 2014, panel D) synthesis of monomer

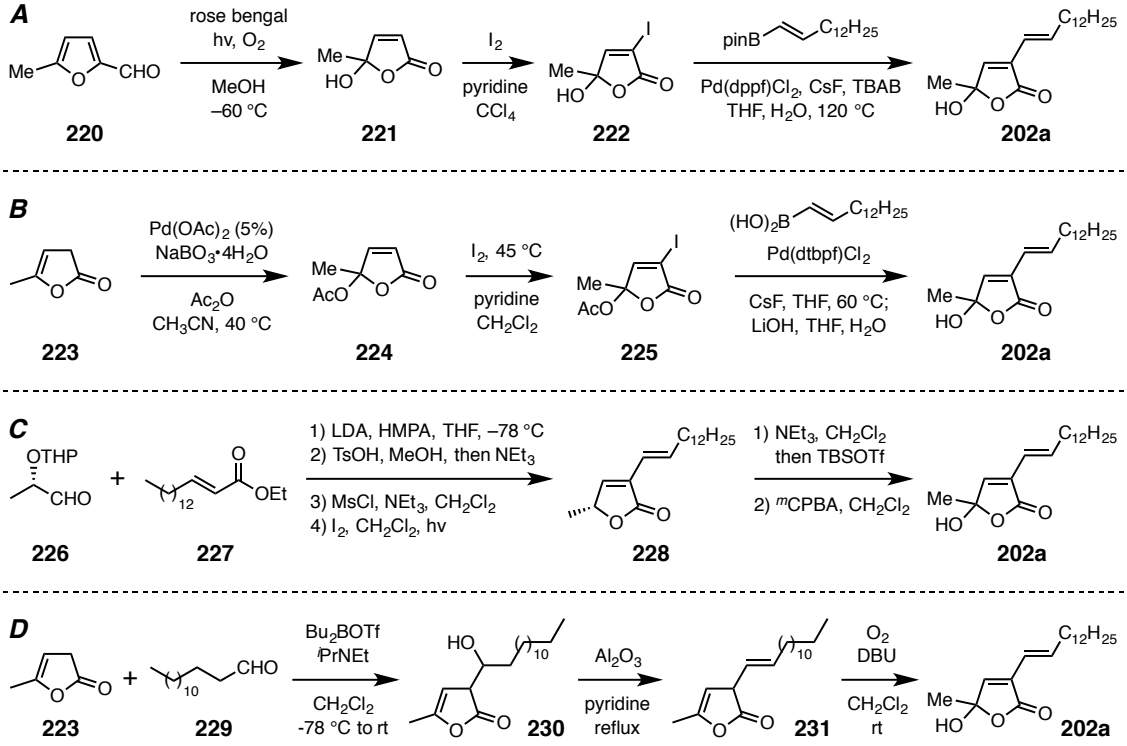


March 2014, Li and coworkers reported an alternative approach starting from aldehyde **226** and *α,β*–unsaturated ester **227** (Scheme 7C). The synthesis commenced with deprotonation of **227** using LDA and HMPA in THF. The resulting lithium enolate was trapped with aldehyde **226**, followed by THP deprotection, and lactonization. Product *β*–hydroxyllactone was eliminated to give an E/Z mixture of butenolide **228**. The *Z*-isomer of **228** can be converted to the *E*-isomer under sunlight irradiation in presence of $I_2$. Compound *E*-**228** was then convert to monomer **202a** via *tert*-butyldimethylsiloxy furan formation and $^{m}$CPBA oxidation.

July 2014, Boukouvalas reported yet another total synthesis via the dimerization strategy starting from 5-methylfuran-2(*3H*)-one (**223**, Scheme 7D). Aldol reaction of **229** with the *in situ* generated boron 2-furanolate of **223** proceeded with complete regiocontrol to afford butenolide **230** as a mixture of diastereoisomers. This mixture was directly dehydrated with alumina in refluxing pyridine (to yield **231**) and oxidized under basic condition via bubbling of oxygen gas into the acetonitrile solution to give monomer **202a**.

*2.3.2. Kraus's total synthesis of paracaseolide A*

January 2013, Kraus and coworkers reported the first and the only non-dimerization based synthesis of paracaseolide A (**201a**, Scheme 8).[17] Their approach began with the Diels–Alder reaction of enedione **232** and 1,3-cyclohexadiene to give bicyclic diketone **233**. The endocyclic double bond was cleaved via ozonolysis followed by oxidation of the resulting bis-hemiacetal with PCC to give the symmetric bis-lactone **234**. Subsequent α–functionalization through enolate formation and trapping with excess diphenyl disulfide furnished **235**, which was desymmetrized through an oxidation/elimination protocol to give **236**. The two vicinal side chains were then installed via a tandem Cu-assisted 1,4-addition/aldol reaction to generate **237**. The final steps in this total synthesis included elimination of the secondary alcohol (**237** to **238**) and oxidation/elimination to furnish the two double bonds to ultimate arrive the structure of paracaseolide A (**201a**).

**Scheme 8.** Kraus's total synthesis of paracaseolide A

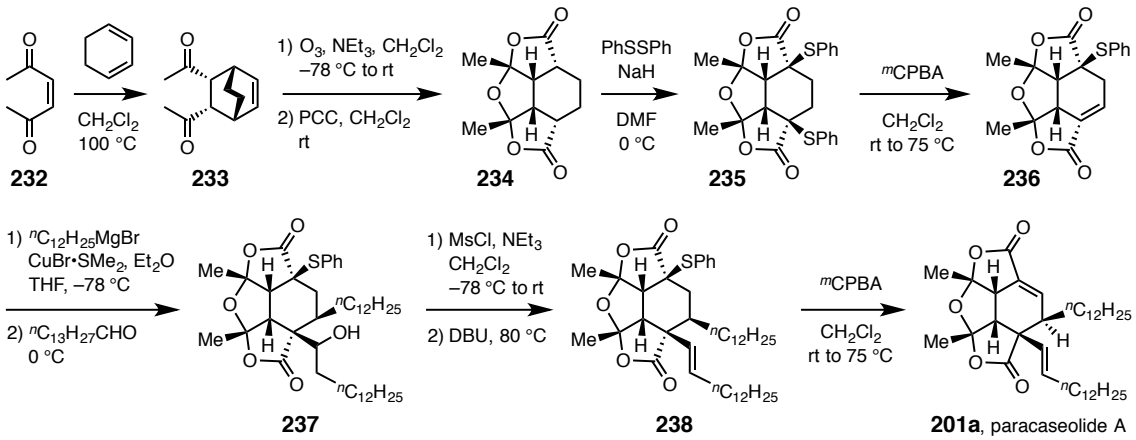


[17] Guney, T.; Kraus, G. A. Total synthesis of paracaseolide A. *Org. Lett.* **2013**, *15*, 613–615.

# Chapter 3. Mechanistic studies of the dimerization event[18]

## 3.1 Model study with truncated series

### *3.1.1 Unexpected Diels–Alder reaction at ambient temperature*

Our mechanistic studies were initiated by a serendipitous observation: when store in neat form, significant instability of the truncated monomer **302b** was observed even at –20 °C while the natural monomer **302a** appeared to be stable at room temperature. It should be pointed out that one key difference between **302a** and **302b** is their physical state at ambient temperature: unlike **302a**, which is a waxy solid that melts around 40 °C, the shorter side chain analogue **302b** exists as a liquid (Scheme 9). This thought-provoking instability of **302b** indicated the high intrinsic reactivity of α-alkenylbutenolide, presumably towards another copy of itself, when free movements and collisions of molecules are permitted (cf. **302b** and **302a**, liquid vs. solid).

**Scheme 9.** Unexpected *exo* adduct **303b** from dimerization of **302b** at ambient temperature

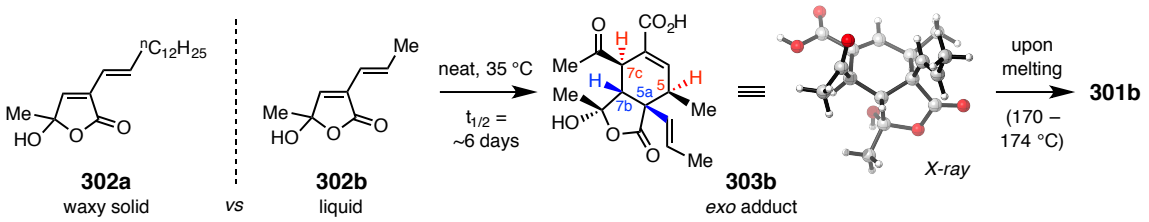


More excitingly, we can observe appearance of a new dimeric product under more controlled condition (neat **302b**, 35 °C, $O_2$-free), which is much milder than that had been reported for **302a** (110 °C). The resulting dimer had not yet dehydrated. A crystalline sample of that new material was subjected to single crystal X-ray analysis, which revealed it to be the Diels–Alder adduct **303b** (Scheme 9). This dimerization occurs with

[18] This chapter is largely adapted from: Wang, T.; Hoye, T. R. Diels–Alderase-free, bis-pericyclic, [4+2] dimerization in the biosynthesis of (±)-paracaseolide A. *Nature Chem.* **2015**, *7*, 641–645.

a very high level of regio- and stereoselectivity. Most notably, the relative configuration among carbons 5/5a/7b/7c indicated that the [4+2] cycloaddition had proceeded by a pathway in which the diene had approached the dienophile with an *exo* orientation with respect to the carbonyl group on the dienophile (Scheme 9)! We also established that dimer **303b** was a competent precursor to the paracaseolide A analogue **301b**. When the solid sample of **303b** was melted (melting point of 170–174 °C), the resulting cooled substance had been transformed cleanly to **301b** (Scheme 9). Moreover, holding crystalline **303b** well below its melting point (110 °C) resulted in its virtually quantitative conversion to crystalline **301b**. It should be noted that the stereochemical outcome of this transformation requires a change in the configuration at C7c, a point that is discussed further below.

*3.1.2 DFT Study: Locating the exo and endo Diels–Alder transition states*

In an attempt to understand this stereochemical outcome, we performed density functional theory [DFT; SMD/M06-2X/6-311+G(d,p) in 2-butanol] calculations to evaluate the relative energies of transition state structures corresponding to the *exo* vs. the *endo* modes of dimerization of **302b** (Figure 4).

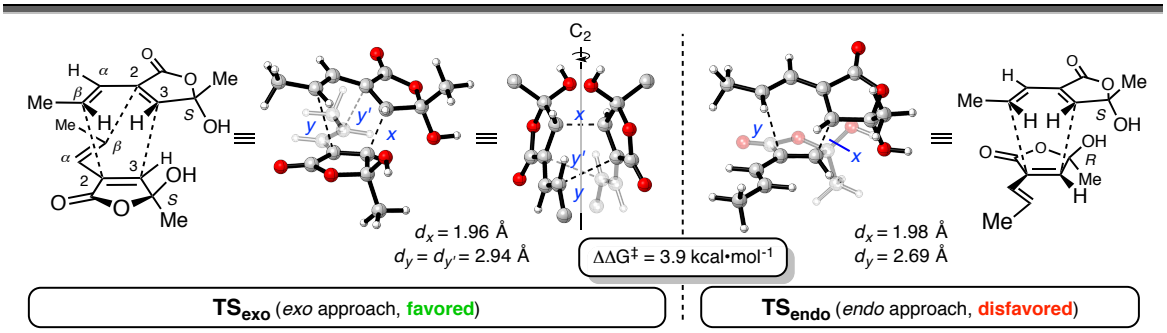


**Figure 4.** DFT calculated transition states of *exo* and *endo* Diels–Alder cycloaddition

Consistent with the experimental observation, the lowest energy transition state (TS) structure for all possible *exo* modes of dimerization is favored by 3.9 kcal•mol$^{-1}$ relative to the overall lowest energy for an *endo* approach of the two reactants. Moreover, the computed free energy of activation for the *exo* dimerization of **302b** to **303b** was 25.2 kcal•mol$^{-1}$ (cf. Scheme 9). That this value is in reasonably good agreement with the

observed dimerization rate provides validity to the computational methodology. The overall reaction of two molecules of **302b** to the initial bis-acylal-containing dimer, which subsequently ring-opens to the more stable keto acid **303b**, is computed to be exergonic by 14.0 kcal•mol$^{-1}$, suggesting that the dimerization should not be significantly reversible under the experimental conditions. We also admixed dimer **303b** with the "real" dimeric diacid **303a** (formed in analogous fashion) and incubated that neat sample at 35 °C for 7 days. Analysis by ESI-MS gave no evidence of any mixed dimer, which presumably would have formed had there been any appreciable reversibility back to **302b** and **302a**.

*3.1.3 Bis-pericyclic dimerization in the synthesis of paracaseolide A*

How can one rationalize this atypical preference for an *exo* over an *endo* approach for a Diels–Alder reaction (i.e., $\mathbf{TS_{exo}}$ rather than $\mathbf{TS_{endo}}$)? It is enlightening to recognize that the geometry of the lowest energy TS ($\mathbf{TS_{exo}}$, Figure 4) is $C_2$-symmetric, as reflected, for example, by the identical distance between carbons C2–Cβ in both pairs of reactants, (cf. *y* and *y′* in Figure 4). This is an example of a bis-pericyclic process,[19] passing through a TS in which the two possible modes of cycloaddition, [4+2] vs. [2+4], have fully merged. Subsequent (and degenerate) bifurcation,[20] in which the partial bonding in $\mathbf{TS_{exo}}$ between one or the other of the two C2–Cβ pairs is forfeited, forms the product **303b**.

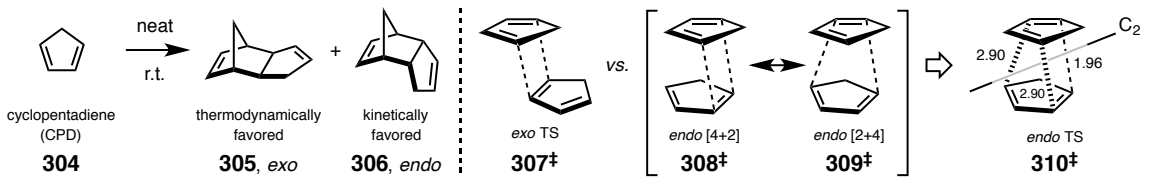


**Figure 5.** Bis-pericyclic transition state in the dimerization of cyclopentadiene

This type of symmetrical TS structure was first invoked to account for Diels–Alder

[19] Caramella, P.; Quadrelli, P.; Toma, L. Unexpected bispericyclic transition structure leading to 4+2 and 2+4 cycloadducts in the endo dimerization of cyclopentadiene. *J. Am. Chem. Soc.* **2002**, *124*, 1130–1131.

[20] Ess, D. H.; Wheeler, S. E.; Iafe, R. G.; Xu, L.; Çelebi-Ölçüm, N.; Houk, K. N. Bifurcations on potential energy surfaces of organic reactions. *Angew. Chem. Int. Ed.* **2008**, *47*, 7592–7601.

dimerizations of simple 4π-systems.[19,21] For example, cyclopentadiene (**304**) is well known to undergo self-dimerization at ambient temperature to give both *exo* and *endo* dicyclopentadiene (**305** and **306**, respectively, Figure 5). In this spontaneous event, *endo* isomer **306** is initially formed as the kinetically favored product, which will slowly isomerize to the thermodynamically more stable *exo* isomer **305**. Traditionally, this preference was rationalized by the secondary orbital interaction[22] in the *endo* [4+2] transition state **308**‡. However, as pointed out by Caramella and coworkers,[19] the geometry of **308**‡ was also well suited for the alternative [2+4] cycloaddition (**309**‡), which also gives the *endo* educt **306**. In fact, in their DFT studies, these two transition states merged to give a single $C_2$-symmetric TS structure **310**‡. This TS was found to be highly asynchronous in which there was almost a 1 Å difference between the longer and shorter forming bonds (2.90 Å vs. 1.96 Å).

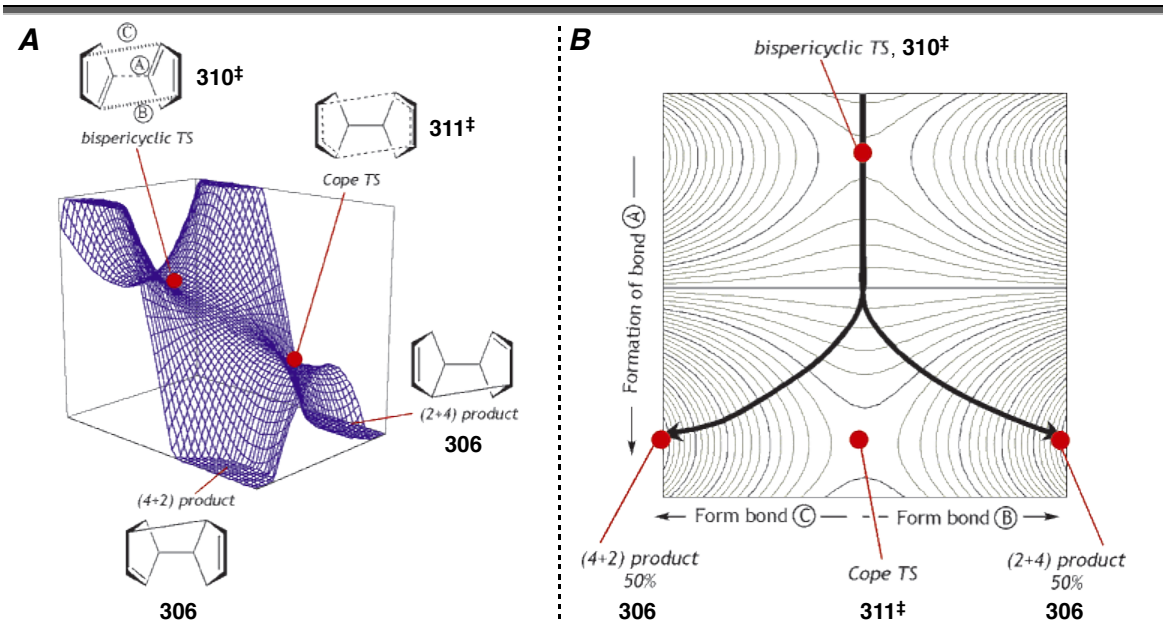


**Figure 6.** Potential energy surface in the bis-pericyclic dimerization of cyclopentadiene (adapted from reference 23)

[21] Toma, L.; Romano, S.; Quadrelli, P.; Caramella, P. Merging of 4+2 and 2+4 cycloaddition paths in the regiospecific dimerization of methacrolein. A case of concerted crypto-diradical cycloaddition. *Tetrahedron Lett.* **2001**, *42*, 5077–5080.

[22] Alston, P. V.; Ottenbrite, R. M.; Shillady, D. D. Secondary orbital interactions determining regioselectivity in the Diels-Alder reaction. *J. Org. Chem.* **1973**, *38*, 4075–4077.

The landscape of the potential energy surface (PES) is also worth commenting. As shown in Figure 6, after reaching the highest energy point, namely the bis-pericyclic TS **310**‡, intrinsic reaction coordinate (IRC) bifurcates into two directions (bold curved arrows in Figure 6B): one leading to the [4+2] product while the other leading to the [2+4] adduct.[23] Both routes are degenerate and give *endo* dimer **306** as the only product. There also exists a Cope TS **311**‡ connecting the products of two pathways. The shape of this PES is unique in that, a single rate-determining TS led to two downhill pathways and a second saddle point connecting the two products.

More recently, a $C_2$-symmetric, bis-pericyclic TS assembly has also been used to rationalize the stereochemical outcome of the self-dimerization of a complex orthoquinol in a synthesis of the secondary metabolite aquaticol.[24] The extra stabilization that attends a bis-pericyclic TS has been nicely explained as its being "admirably suited to take advantage of the maximum accumulation of unsaturated centers".[19]

*3.1.4 Close vs. open-chain ketoester*

**Scheme 10.** Open-chain (**312b**) vs. close-chain (**302b**) tautomer

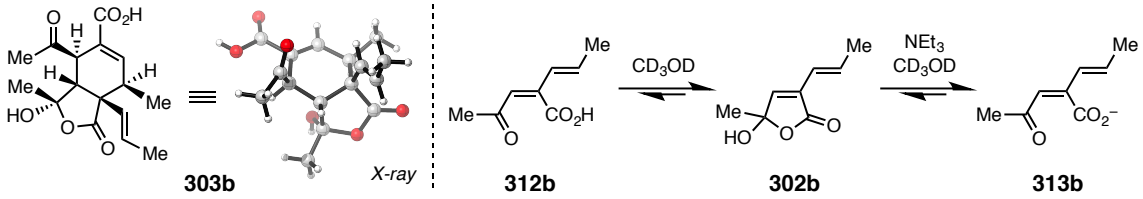


The dimeric intermediate **303b** isolated from room temperature dimerization of **302b** contains a ring-opened keto acid in its "northern" region in both the solid state (X-ray, Scheme 10) as well as in solution ($^1$H NMR). This observation led us to wonder about the role of the analogous ring-opened "tautomer" of the precursor hemiacylal **302b** as a participant in the Diels–Alder reaction itself. The $^1$H NMR spectrum of **302b** in $CD_3OD$

[23] Limanto, J.; Khuong, K. S.; Houk, K. N.; Snapper, M. L. Intramolecular cycloadditions of cyclobutadiene with dienes: Experimental and computational studies of the competing (2 + 2) and (4 + 2) modes of reaction. *J. Am. Chem. Soc.* **2003**, *125*, 16310–16321.

[24] Gagnepain, J.; Castet, F.; Quideau, S. Total synthesis of (+)-aquaticol by biomimetic phenol dearomatization: Double diastereofacial differentiation in the Diels–Alder dimerization of orthoquinols with a *C*2-symmetric transition state. *Angew. Chem.* **2007**, *119*, 1555–1557.

showed no clear evidence for any of the isomeric keto acid **312b** (Scheme 10). However, when this solution was treated with slightly over one equivalent of the weak base $Et_3N$, the NMR spectral data indicated that the $Et_3NH^+$ salt of the ring-opened carboxylate **313b** was now the dominant species (Scheme 10).[25]

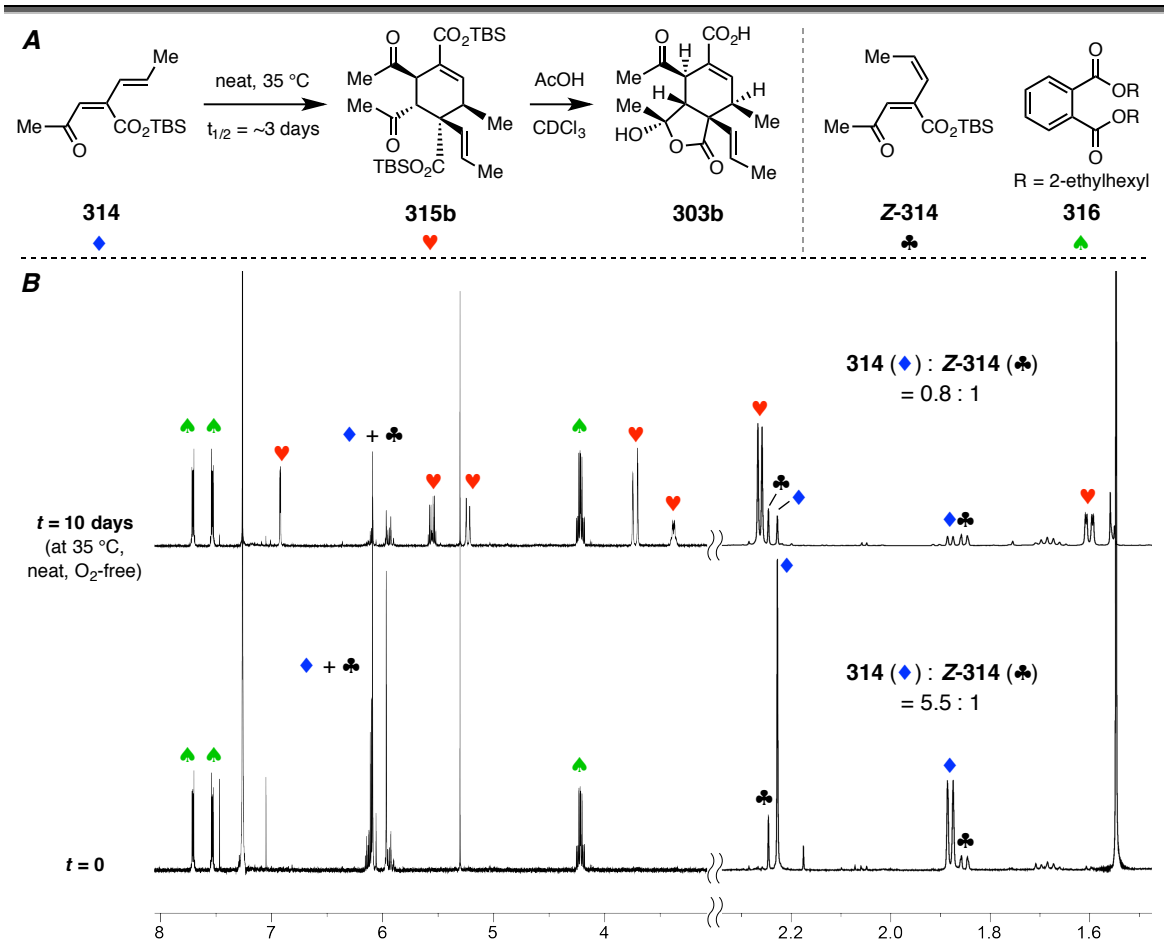


**Figure 7.** Dimerization of open-chain *tert*-butyldimethylsilyl ester **314**

These observations raised the question of the relevance of a ring-opened keto acid like **312b** or carboxylate like **313b** as a potential reactant in the dimerization involved in the biosynthesis of paracaseolide A (**301a**) itself. In particular, it might be expected that either of **312b** or **313b**, each having an alkene bearing two electron-withdrawing groups,

[25] Miles, W. H.; Duca, D. G.; Selfridge, B. R.; Palha De Sousa, C. A.; Hamman, K. B.; Goodzeit, E. O.; Freedman, J. T. Amine-catalyzed epimerization of γ-hydroxybutenolides. *Tetrahedron Lett.* **2007**, *48*, 7809–7812.

would be a more reactive dienophile than the butenolide **302b**. Previous workers have not considered the Diels–Alder reactivity of an open-chain tautomer like **312b** or **313b**. We used the TBS ester **314**, the direct product of singlet oxygen oxidation of furan **211** (Figure 7, also see Scheme 5 for synthesis of **314**), to probe this possibility. Interestingly, a neat sample of this acyclic analog of **302b** dimerized ($t_{1/2}$ = ca. 3 days, Figure 7A) to give, highly selectively, **315b** with a rate about two times faster than that of **302b** ($t_{1/2}$ = ca. 6 days). The relative configuration of **315b** was securely established by its conversion to **303b** upon removal of both TBS esters. The structure of **315b** indicated that the dimerization of **314** had also occurred through an approach involving an *exo* orientation of the two reacting molecules.

To showcase the cleanness of this dimerization reaction, the crude NMR is provided in Figure 7B. In this experiment, a neat sample containing monomer **314** and its *Z*-isomer **Z-314** (E/Z = 5.5:1, Figure 7B, *t* = 0, bottom spectrum) as well as bis(2-ethylhexyl) phthalate (**316**, inert internal standard) was hold at 35 °C under $O_2$-free condition. After 10 days, the crude mixture was directly analyzed by $^1$H NMR (Figure 7B, *t* = 10 days, top spectrum). Dimeric product **315b** was formed in 98% yield based on reacted portion of **314**. Interesting, the *Z*-isomer **Z-314** remain largely unreacted. This is likely due to its inability to form the *s-cis* conformer, which is a prerequisite in the homo- (with **Z-314**) or hetero- (with **314**) dimerization via bis-pericyclic Diels–Alder cycloaddition.

## 3.2 Studies on the dimerization of natural monomer

We then examined the ambient temperature behavior of the 'parent' hydroxybutenolide **302a**. By extrapolation, the fact that **302b** dimerized exclusively to the *exo* adduct **303b** implied that **303a** should be formed in the dimerization of **302a** that ultimately gives rise to (±)-paracaseolide A (**301a**). Recall that, in contrast, it is the *endo* adduct **317** (Scheme 11A) that has been previously invoked by those who have delineated a structure for the initial Diels–Alder dimer.[14a–c] Indeed, when held as a highly concentrated sample (in ethyl acetate) at ambient temperature, **302a** was observed to slowly but cleanly dimerize to the *exo* adduct **303a** (Scheme 11B). This transformation is *much* faster (ca. 2% conversion per day at 21 °C) than what is implied by every previous experiment, all of

which were carried out at 110 °C for 12-34 hours. Presumably these more forcing conditions were used because only the formation of the final dehydrated product **301a** was being monitored. The relative configuration of **303a** was confidently assigned in view of its many analogous $^{1}$H NMR spectroscopic features vis-à-vis those of its lower homolog **303b**. In turn, this revised stereochemical outcome now requires adjustment of the configuration at C7c in **303b** in order to ultimately arrive at the proper relative configuration present in **301a**. This contrasts with previous presumptions that epimerization at C5 was necessary, a consequence of the incorrect assumption that the structure of the initial DA adduct was the *endo* intermediate **317** (Scheme 11A).

**Scheme 11.** (A) Conversion of dimeric intermediate **303** to **301** vs previously proposed mechanism of dimerization. (B-C) Dimerization of monomer **302a** and its open-chain methyl ester **318**

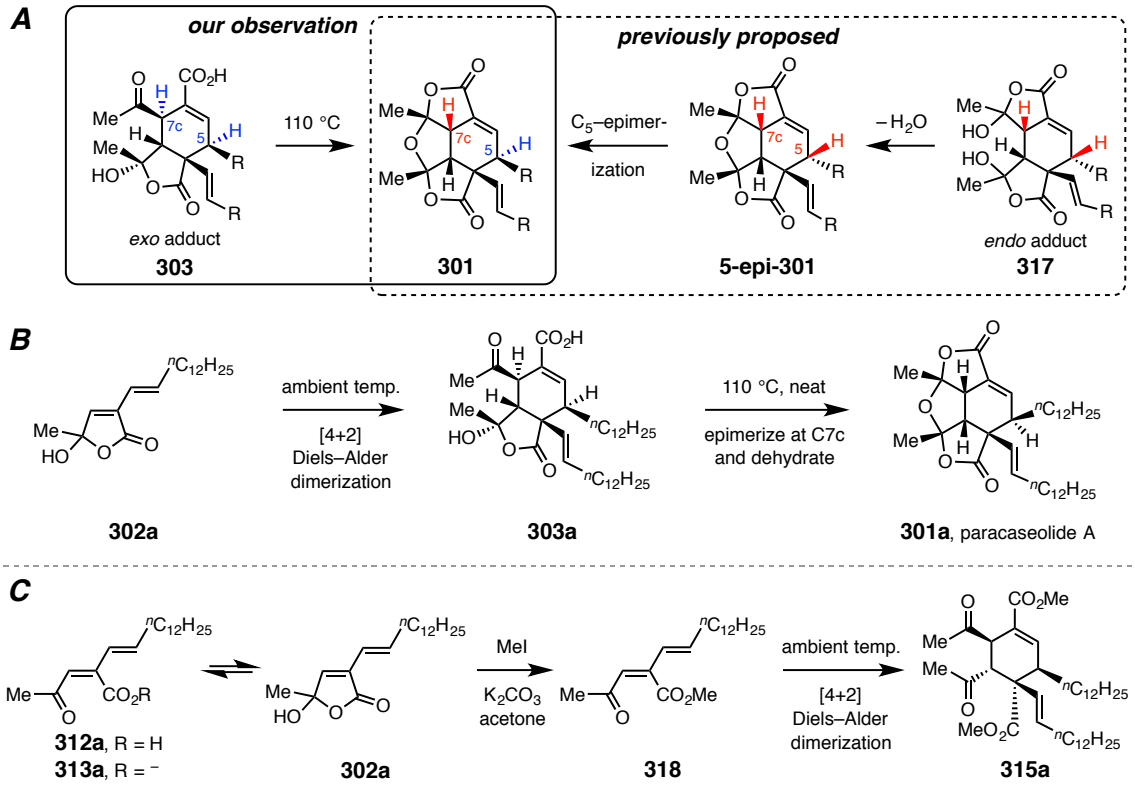


We have also examined the potential of an open-chain analog of the hemiacylal **302a** to undergo spontaneous [4+2] cycloaddition (Scheme 11C). A neat sample of the methyl

ester **318** (obtained by treatment of **302a** with MeI/$K_2CO_3$/acetone) also slowly dimerized at room temperature to give the *exo* adduct **315a** in a highly diastereoselective process (≤3% of any other single compound was observed). The rate of this reaction was slightly faster than that of the dimerization of **302a** itself. The structure of **315a** was assigned on the basis of analogy, nOe (nuclear Overhauser enhancement) analysis, and $^1$H NMR spectroscopic comparisons with **315b**. Because the methyl ester in **318** (as well as the TBS ester in the analogous open-chain analog **314**, Figure 7A) represents a significant perturbation of the structure of the ring-open keto acid **312a** (or its carboxylate **313a**), we believe that drawing a definitive conclusion about the relative reactivities of the open vs. closed isomers of the acid **312a** (or its carboxylate **313a**, which might well be the species most relevant to the natural event enroute to **301a** in the mangrove) vs. the hemiacylal **302a** is unwarranted.

## 3.3 Mechanistic insights in the epimerization step

But how might epimerization at C7c in **303a** (or **303b**) occur? Quite serendipitously, we made a remarkable observation, first using the truncated analog **303b-H**. When this compound was held in methanol-$d_4$ at room temperature, the C7c-proton *spontaneously exchanged*, quite cleanly, with a deuterium atom from the solvent to give **303b-D** ($t_{1/2}$ = 3.2 days at room temperature, Figure 8B)! One rationale for this exchange is by way of intramolecular formation of the zwitterion **319b** (Figure 8A, R = Me) followed by internal removal of the allylic C7c-proton by the proximal carboxylate to produce the enol **320b**. Intervention of a hydroxyl group, specifically the MeO–D bond here, as a proton shuttle to aid this process can also be envisioned. This interconversion of **303** with **320** constitutes an intramolecular, self-organocatalyzed, keto-enol tautomerization. Rapid solvent exchange of RCOOH to RCOOD in **320b** followed by the microscopic reverse would return the observed mono-deuterated analog **303b-D**. Importantly, this facile process provides access to an intermediate having a planar, $sp^2$-hydribized C7c carbon atom, protonation of which from the β-face would effect the requisite C7c-epimerization leading to the relative configuration mandatory for final dehydration to **301**.

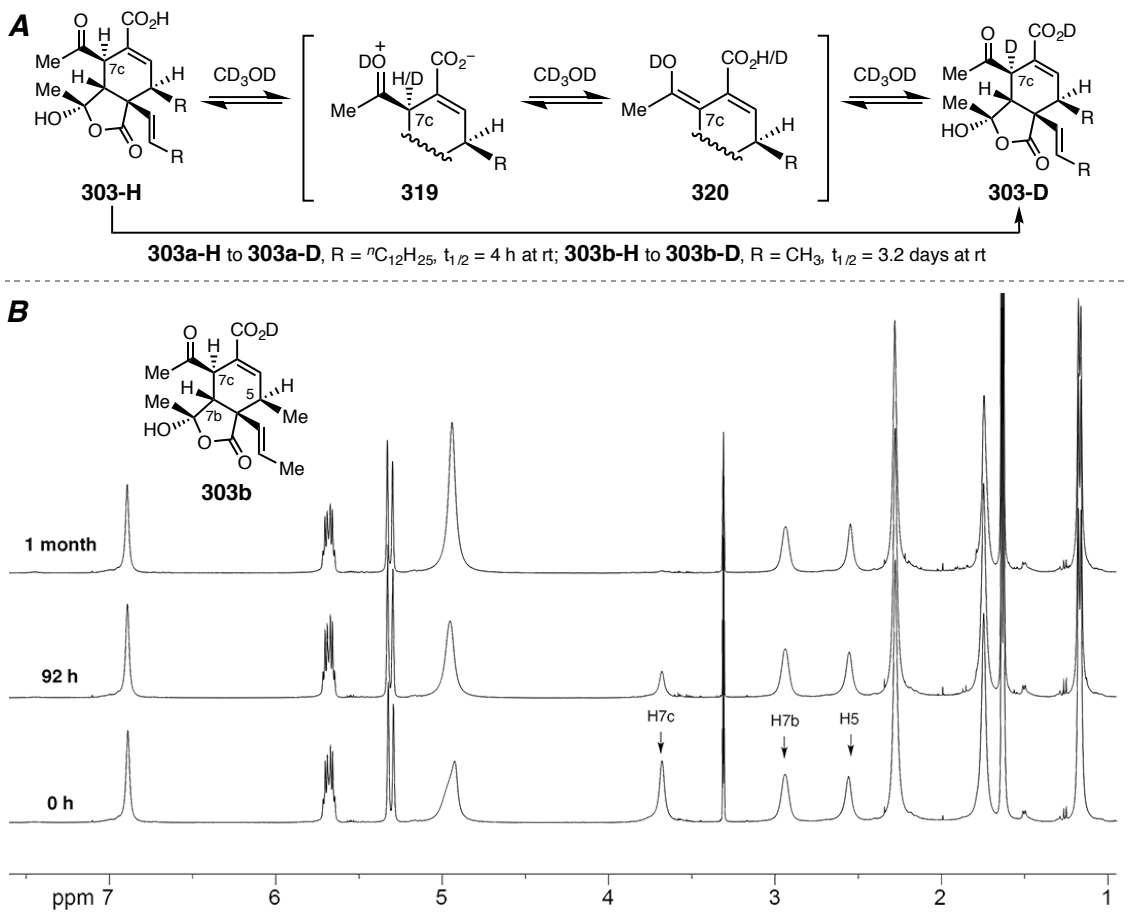


**Figure 8.** Mild H/D exchange of **303** at C7c proton in neutral methanol-$d_4$ solvent

The analogous adduct **303a-H** (Figure 8A) underwent even more facile H-D exchange at C7c to give **303a-D** when dissolved in $CD_3OD$ ($t_{1/2}$ ca. 4 h at room temperature). The same experiment using the dimethyl ester **315a-H** (Scheme 12A) showed that this substrate had a much slower rate of deuteration at C7c ($t_{1/2}$ ca. 400 h at room temperature, two orders of magnitude slower), clearly suggesting a catalytic role for the carboxylic acid in **303a-H** (cf. **319** and **320** in Figure 8A). To judge if that process was unimolecular or bimolecular in nature, we prepared a $CD_3OD$ solution containing both **303a-H** and **315a-H**. (Scheme 12B) After 12 hours, ESI-MS analysis indicated that the former had undergone exchange to the extent of ca. 75% whereas exchange in **315a-H** was not detected. This argues against a bimolecular process in which a carboxylic acid in one molecule promotes the enolization and exchange of H7c alpha to the acetyl group in a second molecule of **303a-H** or **315a-H**.

**Scheme 12.** Deuteration experiments of **303a-H** vs its dimethyl ester **315a-H**

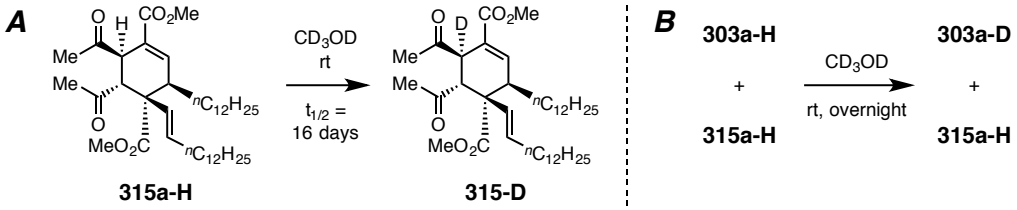


## 3.4 Specific rotation of paracaseolide A

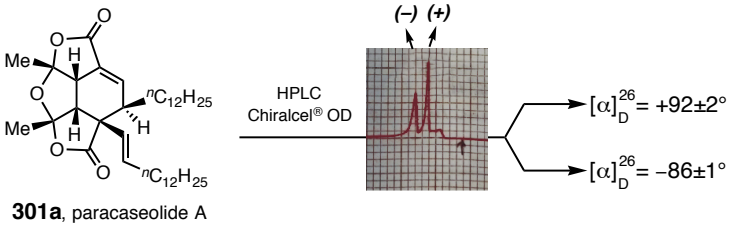


**Figure 9.** Resolution of the synthetic racemic sample of paracaseolide A

Finally, we return to a key issue that is highly germane to the question of whether the spontaneous dimerization of diene **302a** is the true biosynthetic event involved in the biosynthesis of paracaseolide A (**301a**). If this reaction is not catalyzed by an enzyme, one would expect the isolated natural sample of **301a** to be racemic. The natural substance was reported to have a specific rotation of $[\alpha]^{24}_{d} = +0.9$.[1] As I mentioned in chapter 1.2, we believe the small value of this rotation is within experimental error of zero in light of minor resonances in the $^{1}$H NMR spectrum that indicate the presence of contaminants in that sample. To interrogate this point further, we resolved a sample of our synthetic (±)-**301a** on a Chiralcel® OD HPLC column (Figure 9). (Our attempts to obtain a small amount of the natural sample of paracaseolide A to analyze by this method were unsuccessful.) Essentially equal amounts (4.5 and 4.4 mg) of each enantiomer were recovered following semi-preparative-scale separation. The rotation values measured for the faster and the slower eluting enantiomers were +92° and -86°, respectively. This evidence strongly suggests that the natural material, like the synthetic, is racemic. This, in turn, is further support of our hypothesis that a Diels–Alderase is neither required nor

responsible for the biosynthesis of paracaseolide A (**301a**).

## 3.5 Summary

Immediately upon contemplating the structure of paracaseolide A and in parallel with our interpretation of the fact that the natural material showed a near-zero value for its specific rotation,[1] we hypothesized that its biosynthesis proceeded by *spontaneous* dimerization of the hydroxybutenolide **302a**. To test this required that we examine the chemical reactivity of **302a** to learn if it is sufficiently innately active to produce an adduct like **317** or **303a**. Our conviction in that hypothesis led us to undertake the experiments reported here, through which we have established: (i) that the DA dimerization of **302a** (or the isomeric ring-opened keto acid **312a**) is sufficiently energetically accessible to be biosynthetically relevant, (ii) that this DA dimerization is *exo* selective, unlike what previous workers have presumed, (iii) using DFT computational studies, that this stereoselectivity can be explained by a bis-pericyclic pathway involving a $C_2$-symmetric TS geometry, (iv) that facile H/D exchange of the C7c-hydrogen atom in **303a-H** shows that the obligate planarization of C7c is a feasible process and enables a pathway for the required epimerization at C7c in **303a-H**, and (v) that the natural sample of paracaseolide A is, in all likelihood, racemic—a fact incompatible with its formation under the action of a Diels–Alderase in *Sonneratia paracaseolaris*. Collectively, these observations lend substantial support to the idea that a spontaneous DA dimerization of the butenolide **302a** is the key biosynthetic event leading to paracaseolide A—conceptualization that, until now, has been obscured by biased, but incorrect, assumptions that the dimerization required high temperature and occurred with either *endo* selectivity or by a stepwise mechanism.

# ◊ Part II ◊

## The Hexadehydro-Diels–Alder (HDDA) Cascade: Mechanistic Insights and New Reactions Development

# Chapter 4. The Hexadehydro-Diels–Alder Reaction

The famous Diels–Alder cycloaddition reaction[26] has been regarded as one of the most fundamental transformation in organic chemistry.[27] The prototypical Diels–Alder (DA) event shown in Scheme 13A can be found in every introductory organic chemistry textbook: a cycloaddition reaction occurred between a 2π-component like ethylene (**401**, the dienophile) and 4π-component like 1,3-butadiene (**402**, the diene) to give cyclohexene (**403**) – a product at the tetrahydrobenzene oxidation state. In comparison, the most highly oxidized version of this chemistry between acetylene (**404**, diynophile) and 1,3-butadiyne (**405**, diyne) is shown in Scheme 13B. Although closely related, it is surprising to point out that this particular transformation remain unexploited for more than 100 years since the very first report of Diels–Alder cycloaddition![28] The immediate product—cyclic cumulene (**406**) is just another resonance form of benzyne (**407**, or didehydrobenzene), which will then undergo trapping reactions to generate benzene derivatives like **408**. Compared to traditional DA cycloaddition, six protons were removed in the prototype reaction (cf. **403** and **408**, Scheme 13). Therefore, it is termed as the hexadehydro-Diels–Alder (HDDA) reaction to reflect this change of oxidation state. In this chapter, I will cover some of the key contributions in the discovery and early development of HDDA chemistry, *more specifically*, from *other* researchers.

**Scheme 13.** Diels–Alder vs. hexadehydro-Diels–Alder reaction

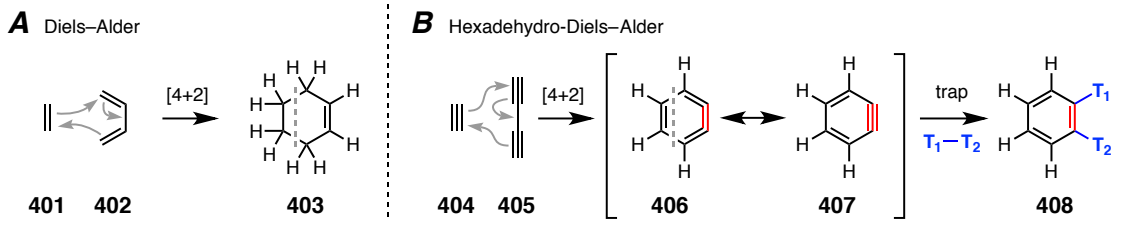


[26] Diels, O. & Alder, K. Syntheses in the hydroaromatic series [in German]. *Justus Liebigs Ann. Chem.* **1928**, *460*, 98–122.

[27] (a) Onishchenko, A. S. Diene Synthesis (Israel Program for Scientific Translations,1964). (b) Nicolaou, K. C., Snyder, S. A., Montagnon, T.; Vassilikogiannakis, G. The Diels–Alder reaction in total synthesis. *Angew. Chem. Int. Ed.* **2002**, *41*, 1668–1698.

[28] Michael, A.; Bucher, J. E. Über die einwirkung von eissigsäureanhydrid auf phenylpropiolsäure. *Chem. Zentrblt.* **1898**, 731–733.

## 4.1 Discovery of the hexadehydro-Diels–Alder (HDDA) reaction

In 2012, our lab reported the first systematic study of the hexadehydro-Diels–Alder reaction.[29] In the course of an otherwise unrelated study, Dr. Baire in our lab attempted to prepare ketotetrayne **410** through manganese dioxide oxidation of alcohol **409**. To his surprise, a hexasubstituted benzene derivative **411** was isolated after purification of reaction. This intriguing result was rationalized by proposing an intramolecular [4+2] cycloaddition between the ynone alkyne moiety and 1,3-diyne moiety in **410** to give the cyclocumulene structure **412**, or benzyne **413**. The tethered silyl ether group then engages to form zwitterion **414**, which would then undergo a retro-Brook rearrangement to yield **411** as the ultimate stable product.

**Scheme 14.** Serendipitous discovery of the HDDA reaction in our lab

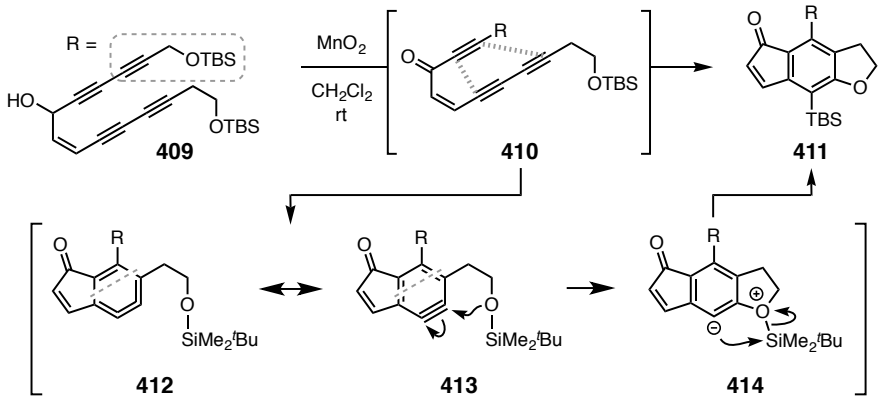


## 4.2 HDDA vs. traditional methods of benzyne formation

*ortho*-Benzyne is one of the oldest,[30] most interesting, and most well-studied intermediate in organic chemistry. The versatile trapping reactions has gained significant attention among generations of synthetic chemists and provided access to a wide range of benzenoid structures. Many of these fundamental modes of trapping events were known

[29] Hoye, T. R.; Baire, B.; Niu, D.; Willoughby, P. H.; Woods, B. P. The hexadehydro-Diels–Alder reaction. *Nature*, **2012**, *490*, 208–212.

[30] Wenk, H. H.; Winkler, M.; Sander, W. One century of aryne chemistry. *Angew. Chem. Int. Ed.* **2003**, 42, 502–528.

even by 1967.[31] Nevertheless, new modes of benzyne reactions continue to emerge, especially so within the last decade.[32]

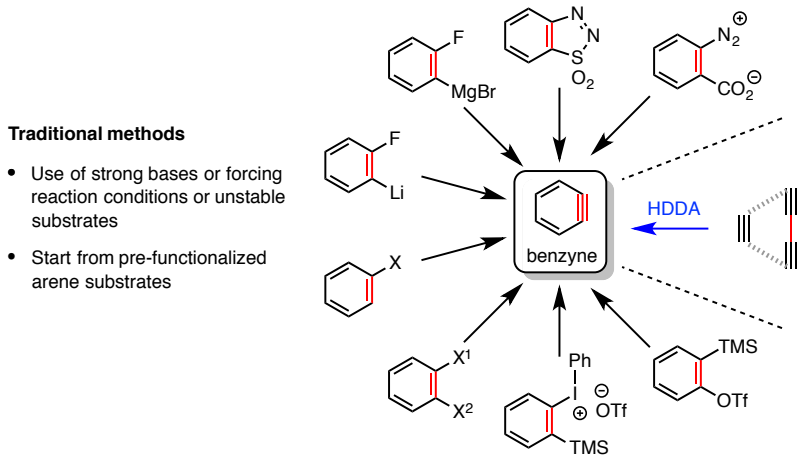


**Figure 10.** HDDA vs. other benzyne generation methods

In sharp contrast with the multifaceted benzyne trapping reactions, strategies to generate this key intermediate remain largely the same: namely, through elimination of arene derivatives (Figure 10). This method usually requires use of a strong base or unstable substrates, which significantly limited their scope of application and overall reaction efficiency. Alternatively, the HDDA reaction provided an entirely orthogonal approach to synthesize benzyne via thermal cycloaddition reactions (Figure 10). Like other Diels–Alder reactions, one most prominent feature of the HDDA chemistry is its high atom economy, in which all structural components in the substrate were retained in the final product. Benzyne was produced under pristine environment (i.e. free of added reagents

[31] Hoffmann, R. W. Dehydrobenzene and cycloalkynes (Organic chemistry, a series of monographs, vol. 11, academic, 1967).

[32] (a) Pellissier, H.; Santelli, M. The use of arynes in organic synthesis. *Tetrahedron* **2003**, *59*, 701–730. (b) Dyke, A. M.; Hester, A. J.; Lloyd-Jones, G. C. Organometallic generation and capture of ortho-arynes. *Synthesis* **2006**, 4093–4112. (c) Sanz, R. Recent applications of aryne chemistry to organic synthesis. A review. *Org. Prep. Proced. Int.* **2008**, *40*, 215–291. (d) Gilchrist, T. L. in Science of Synthesis Vol.43 (ed. Hopf, H.) 151–215 (Georg Thieme, 2008). (e) Chen, Y.; Larock, R. C. in Modern arylation methods (ed. Ackermann, L.) 401–473 (Wiley-VCH, 2009). (f) Kitamura, T. Synthetic methods for the generation and preparative application of benzyne. *Aust. J. Chem.* **2010**, *63*, 987–1001. (g) Tadross, P. M.; Stoltz, B. M. A comprehensive history of arynes in natural product total synthesis. *Chem. Rev.* **2012**, 112, 3550–3577. (h) Gampe, C. M.; Carreira, E. M. Arynes and cyclohexyne in natural product synthesis. *Angew. Chem. Int. Ed.* **2012**, *51*, 3766–3778.

and byproducts) which allows us to fully probe its original reactivity and unleash new and interesting modes of reactions.

## 4.3 Scope of HDDA reaction: initial report

**Table 1.** Reaction scope of the HDDA cascade reaction

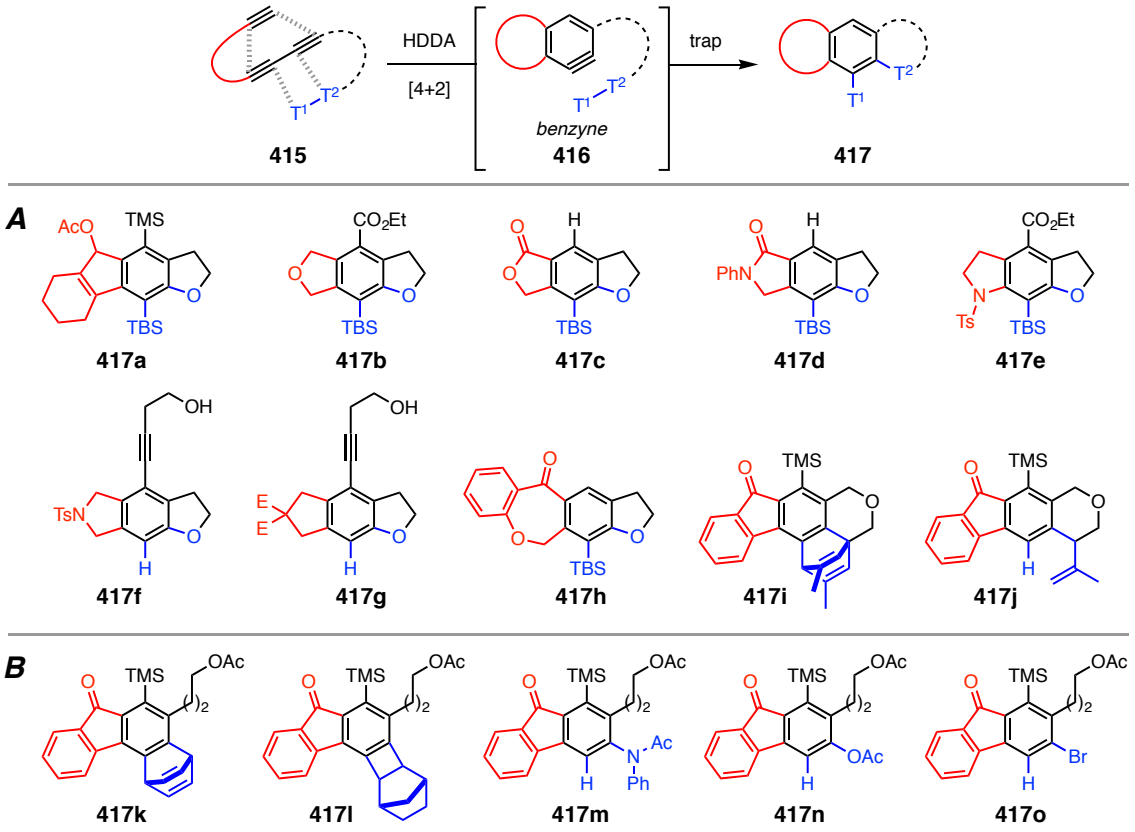


As shown in Table 1, various triynes (**415a–e**, **h–o**) and tetraynes (**415f–g**) proved to be effective precursors to produce benzyne **416** under purely thermal condition.[29] To date, all reported examples of HDDA reactions are intramolecular. Namely, the 2π-component (monoyne, or diynophile) and 4π-component (diyne) are always connected with a linker (Table 1, colored as red). A wide range of these linker structures, including all carbon (entry a, g, i–o), ether (entry b), ester (entry c), amide (entry d), and other heteroatom containing linkers (entry e, f, h), can be used. Trapping agents (colored in blue) of the resulting benzyne **416** can be either intramolecular (tethered to the terminal of diyne, see

examples in panel A) or intermolecular (panel B), and give a stable arene product **417**. Like benzyne generated by other methods, HDDA generated benzyne **416** is also highly electrophilic, and will engage nucleophilic reagents like alcohol (entry f, g) amine (entry m), carboxylic acid (entry n), or bromide anion (entry o). Benzyne **416** can also undergo cycloaddition reactions with other 4π-systems ([4+2], entry k) or strained 2π-component ([2+2], entry l) to quickly construct benzo-fused polycyclic skeletons in one step.

## 4.4 Discovery of new benzyne reactivities enabled by HDDA chemistry

In addition to the strategic power offered by the HDDA cycloisomerization, this reaction also provides the opportunity to uncover previously unprecedented modes of benzyne reaction. This is because HDDA cyclizations produce reactive benzyne intermediates in the absence of added reagents, by-products or catalysts.

*4.4.1 Alkane desaturation by concerted double hydrogen atom transfer to benzyne*

**Scheme 15.** Alkane desaturation by concerted double hydrogen atom transfer to benzyne

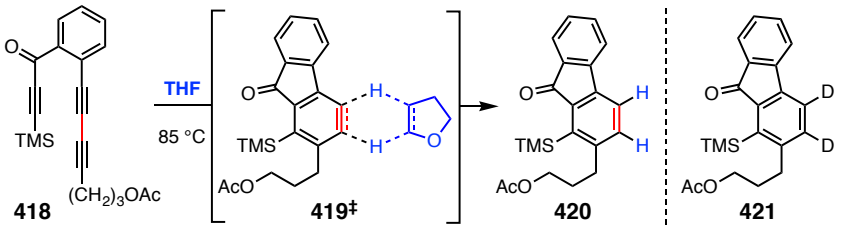


| Solvent | **420** : **421** |
|---|---|
| THF-$h_8$ | 100 : 0 |
| THF-$d_8$ | 0 : 100 |
| THF-$h_8$: THF-$d_8$ = 1 : 1 | 6 : 1 |
| THF-$h_8$: THF-$d_8$ = 1 : 6 | 1 : 1 |

In 2013, Dawen Niu in our lab discovered an interesting dihydrogen transfer reaction between HDDA-generated benzyne and various cyclic compounds.[33] For example, when a THF solution of triyne **418** was heated to 85 °C, arene **420** can be isolated (Scheme 15). Accordingly, THF-$d_8$ led to dideuterated product **421**. To throw light upon the reaction mechanism, a 1:1 THF-$h_8$ and THF-$d_8$ mixed solution was used and led to a 6:1 mixture of **420** and **421**. The 6:1 kinetic isotope effect (KIE) ratio was confirmed by using a 1:6 mixture of THF-$h_8$ and THF-$d_8$, which led to formation of equal amounts of **420** and **421**.

[33] Niu, D.; Willoughby, P. H.; Woods, B. P.; Baire, B.; Hoye, T. R. Alkane desaturation by concerted double hydrogen atom transfer to benzyne. *Nature* **501**, 531–534.

In this set of experiments, mono-deuterated **421** was never observed, together with the large KIE value, suggesting a concerted dihydrogen transfer transition state like **419**‡. It is worth pointing out that, THF has commonly been employed as the solvent in previous studies of benzyne trapping reactions.[34] It is reasonable to speculate that these reactions of benzynes generated in THF are compromised in their efficiency as a result of competitive reduction by that solvent.

*4.4.2 Divergent modes of reaction in phenol trapping*

**Scheme 16.** Two modes of phenol trapping reactions

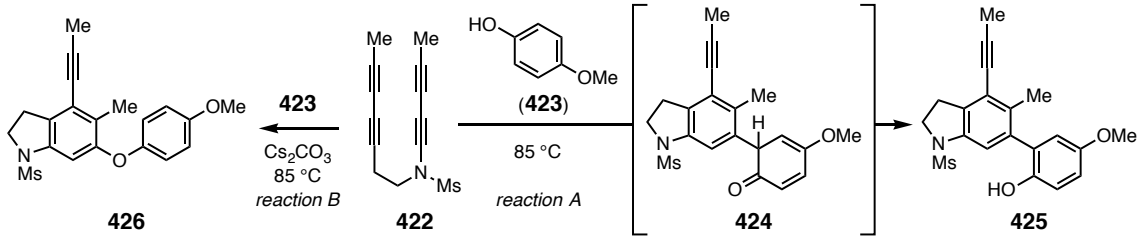


More recently, Juntian Zhang and co-workers from our lab reported the interesting divergent reactivity of phenol in its trapping reaction with HDDA-generated benzyne.[35] For instance, when tetrayne **422** was heated in presence of *p*-methoxyphenol (**423**), biaryl compound **425** was isolated (reaction A, Scheme 16). This is in sharp contrast with previously reported mode of phenol trapping reactions, in which the nucleophilic phenol oxygen engaged and form biaryl ethers like **426**. This dramatic discrepancy is likely due to the difference in the reaction environment. In case of HDDA cycloisomerization, benzynes are generated under neutral condition. A phenol-ene reaction occurred between **423** and **422** derived benzyne to form cyclohexadienone **424**, which will then isomerize to the ultimate product **425** (reaction A, Scheme 16). On the other hand, benzynes formed by traditional elimination method usually contains base in the reaction mixture, which will deprotonate phenol and considerably increase its O-nucleophilicity. To mimic and

[34] Himeshima, Y.; Sonoda, T.; Kobayashi, H. Fluoride-induced 1,2-elimination of *o*-trimethylsilylphenyl triflate to benzyne under mild conditions. *Chem. Lett.* **1983**, *12*, 1211–1214.

[35] Zhang, J.; Niu, D.; Brinker, V. A.; Hoye, T. R. The phenol–ene reaction: biaryl synthesis via trapping reactions between HDDA-generated benzynes and phenolics. *Org. Lett.* **2016**, *18*, 5596–5599.

closely compare these two events, 1.5 equivalents of $Cs_2CO_3$ was added to the otherwise identical HDDA condition (reaction B vs. reaction A, Scheme 16). Indeed, diaryl ether product **426** was observed as the major product under this basic condition.

## 4.5 Further expansion of HDDA chemistry

### *4.5.1 Cascade reactions*

Recognized as one of the most reactive intermediate in organic chemistry, benzyne is endowed with sufficient potential energy to enable numerous otherwise unattainable modes of reactivity. This large thermodynamic driving force allowed chemists to design and execute various tandem reactions and introduce molecular complexity in short and atom economical fashion. When coupled with an HDDA cycloisomerization, which construct benzyne moiety from strategic disconnection via a Diels–Alder cycloaddition process, such multi-stage cascade events are particularly efficient and powerful. One such example developed in our lab is shown in Scheme 17.

**Scheme 17.** The HDDA // aromatic ene // Alder ene cascade

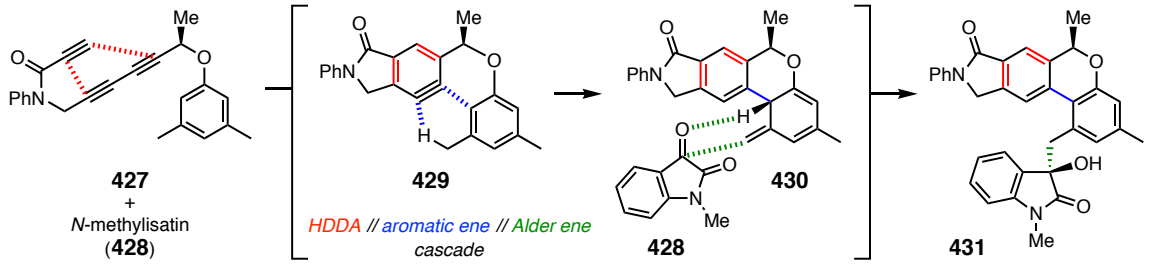


In 2013, Dawen Niu and co-workers reported a remarkable HDDA // aromatic ene // Alder ene cascade reaction.[36] When the triyne **427**, a precursor bearing a tethered 3,5-dimethylphenyl group, was heated in presence of 1.2 equivalents of *N*-methylisatin (**428**) in 1,2-dichloroethane (120 °C, 18 h), tetracyclic compound **431** can be isolated in 76% yield (4:1 dr). A total of three new rings, four new C–C bonds were formed in this single step transformation. The overall transformation consists of 1) HDDA cycloisomerization

[36] Niu, D.; Hoye, T. R. The aromatic ene reaction. *Nat. Chem.* **2014**, *6*, 34–40.

of triyne **427** to form benzyne **429**, 2) aromatic-ene reaction of benzyne **429** with tethered 3,5-dimethylphenyl moiety to give isotoluene intermediate **430**, and 3) Alder ene reaction of **430** with *N*-methylisatin **428** to yield the final product **431**. It is worth commenting that ene reactions with aromatic ring systems are rare[37] due to the energy penalty from dearomatization. The two atom linker in **429** is critical to reveal this unusual reactivity—the alternative intramolecular Diels–Alder (IMDA) mode of trapping is suppressed by the ring strain induced by the tether.[36] It's also interesting to point out that the stereocenter in the tether is able to induce a 4:1 dr at C3 position of the isatin moiety in **431**, which is 6 atoms away! Presumably this remote stereo-induction is relayed by the stereocenter at the benzylic position of isotoluene intermediate **430**.

*4.5.2 Multi-component reactions*

**Scheme 18.** Multi-component reaction with HDDA-generated benzyne

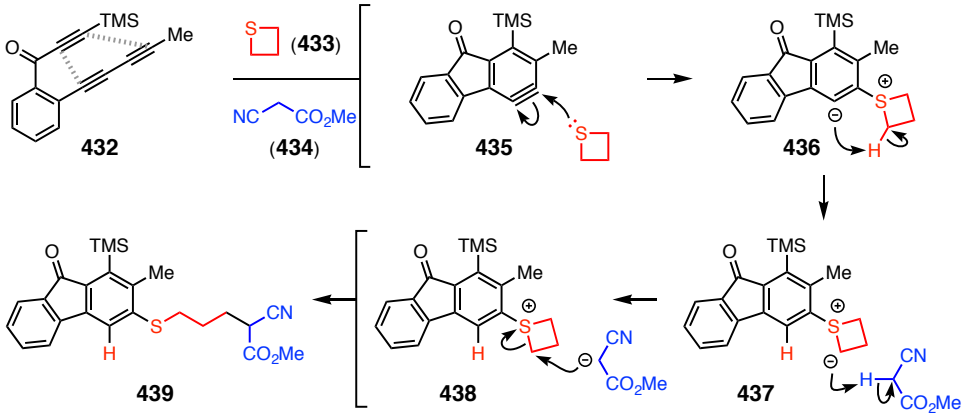


Another characteristic aspect of benzyne chemistry is its potential to initiate a variety of highly efficient multi-component reactions (MCRs). For instance, Junhua Chen and co-workers in our lab reported a three component reaction between an HDDA-generated benzyne, a cyclic thioether, and a nucleophile.[38] As shown in Scheme 18, after formation of benzyne **435** (from **432**), the thietane (**435**) sulfur quickly traps to give zwitterion **436**.

[37] (a) Brinkley, Y. J.; Friedman, L. Novel ene and insertion reactions of benzyne and alkylbenzenes. *Tetrahedron Lett.* **1972**, *13*, 4141–4142. (b) Tabushi, I.; Yamada, H.; Yoshida, Z.; Oda, R. Reactions of benzyne with substituted benzenes. *Bull. Chem. Soc. Jpn.* **1977**, *50*, 285–290.

[38] Chen, J.; Palani, V.; Hoye, T. R. Reactions of HDDA-derived benzynes with sulfides: mechanism, modes, and three-component reactions. *J. Am. Chem. Soc.* **2016**, *138*, 4318–4321.

After proton transfer, the ester enolate of methyl 2-cyanoacetate (**434**) then engages as the third component by nucleophilic attack and ring-opening of the cationic intermediate **438** to give **439** as the final coupled product. Deuterium labelling study revealed that a sulfur ylide (**437**) is presented in this transformation, formation of which required an intramolecular proton transfer as indicated in Scheme 18.

*4.5.3 Material science applications*

Recently, Dr. Feng Xu reported an expedient synthesis of compound **443**, which is a promising lead compound for the identification of emissive component of organic LEDs (OLED).[39] As portrayed in Scheme 19, this short synthesis commenced with a Cadiot-Chodkiewicz coupling between diyne bromide **440** and arylacetylene **441** to make the linear tetrayne precursor **442**. A solution (1:1 chloroform/ethyl acetate) of this compound was then heated to 80 °C in presence of tetraphenylcyclopentadienone (TPCP) in order to forge the tricyclic core skeleton in **443**. This example clearly demonstrated the strategic advantage of HDDA chemistry in terms of quickly assemble large aromatic systems.

**Scheme 19.** Expedient synthesis of a lead compound for the identification of emissive component of organic LEDs using HDDA based strategy

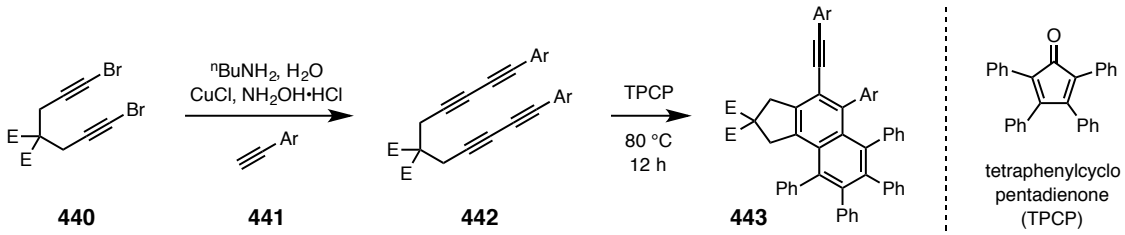


## 4.6 Summary

Since our first report of the systematic study of the hexadehydro-Diels–Alder reaction, we have witnessed a renaissance of the benzyne chemistry. The synthetic advantage provided by HDDA chemistry, specifically to be able to generate benzyne under purely

[39] Xu, F.; Hershey, K. W.; Holmes, R. J.; Hoye, T. R. Blue-Emitting Arylalkynyl Naphthalene Derivatives via a Hexadehydro-Diels–Alder Cascade Reaction. *J. Am. Chem. Soc.* **2016**, *138*, 12739–12742.

thermal condition empowered the investigation of 1) new reactivities of benzyne 2) new structural scaffold of aryne 3) de novo construction of benzenoids 4) mechanistic insights that were previously masked/restrained by byproducts, catalysts, or reagents presented in the reaction media.

**Scheme 20.** The prototypical hexadehydro-Diels–Alder event

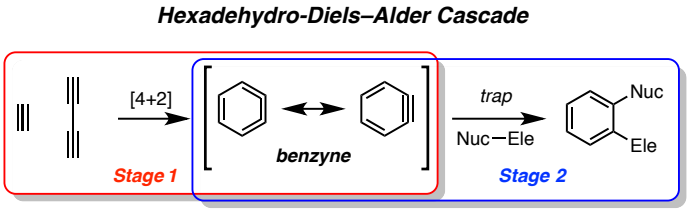


In contrast with other members of Diels–Alder reactions, the HDDA cyclization consists of two stages: cycloisomerization to form benzyne and subsequent trapping (Scheme 20). We have termed this overall process the HDDA cascade. In this chapter, I have briefly covered the historical background in the early discovery of the HDDA chemistry as well as several more recent contributions from other chemists in the Hoye research group. In the next two chapters, I will be more focus on the part of chemistry I was able to directly contribute to. These projects are grouped into two main parts: chapter 5 will describe my efforts to understand the mechanistic details in HDDA cascade reactions while chapter 6 will be devoted to my experimental work in order to expand the synthetic utility of the HDDA cycloisomerization.

# Chapter 5. Mechanistic insights in the HDDA cascade

## 5.1 Previous studies on the mechanism of HDDA cycloisomerization

Since the first report of the HDDA cycloisomerization by Ueda and co-workers,[40] the mechanism for this transformation has been under debate. Namely, whether the reaction proceeds via a concerted pericyclic pathway or stepwise diradical route? Computational [density functional theory (DFT)] studies have been used to explore this intriguing and important mechanistic question.[41] These encompass both (hypothetical) intermolecular as well as prototypical intramolecular examples.

### *5.1.1 Comparison of concerted vs stepwise mechanisms in various dehydro-Diels−Alder reactions by Johnson and co-workers[41a]*

In 2011, Johnson and co-workers reported a detailed computational study to compare the concerted vs stepwise mechanism in various dehydro-Diels–Alder (DDA) reactions. In their model study of the hexadehydro-Diels–Alder reaction, the potential energy surface (PES) for the cycloaddition between acetylene (**501**) and 1,3-butadiyne (**502**) is carefully mapped (Figure 11). The calculated barriers of the rate determining step (RDS) of the concerted (**503**$^{‡}$, 36.5 kcal mol$^{-1}$) vs stepwise (**505**$^{‡}$, 37.0 kcal mol$^{-1}$) pathway are similar with a small preference for the concerted pathway. As pointed out in our first HDDA publication,[29] it is remarkable that such cycloaddition produces benzyne (**504**, -51.4 kcal

---

[40] Miyawaki, K.; Suzuki, R., Kawano, T.; Ueda, I. Cycloaromatization of a nonconjugated polyenyne system: synthesis of 5H-benzo[d]fluoreno[3,2-b]pyrans via diradicals generated from 1-[2-{4-(2-alkoxymethylphenyl)butan-1,3-diynyl}]phenylpentan-2,4-diyn-l-ols and trapping evidence for the 1,2-didehydrobenzene diradical. *Tetrahedron Lett.* **1997**, *38*, 3943–3946.

[41] (a) Ajaz, A.; Bradley, A. Z.; Burrell, R. C.; Li, W. H. H.; Daoust, K. J.; Bovee, L. B.; DiRico, K. J.; Johnson, R. P. Concerted vs stepwise mechanisms in dehydro-Diels–Alder reactions. *J. Org. Chem.* **2011**, *76*, 9320–9328. (b) Liang, Y.; Hong, X.; Yu, P.; Houk, K. N. Why alkynyl substituents dramatically accelerate hexadehydro-Diels–Alder (HDDA) reactions: stepwise mechanisms of HDDA cycloadditions. *Org. Lett.* **2014**, *16*, 5702–5705. (c) Kerisit, N.; Toupet, L.; Larini, P.; Perrin, L.; Guillemin, J.-C.; Trolez, Y. Straightforward synthesis of 5-bromopenta-2,4-diynenitrile and its reactivity towards terminal alkynes: a direct access to diene and benzofulvene scaffolds. *Chem.-Eur. J.* **2015**, *21*, 6042−6047. (d) Skraba-Joiner, S. L.; Johnson, R. P.; Agarwal, J. Dehydropericyclic reactions: symmetry-controlled routes to strained reactive intermediates. *J. Org. Chem.* **2015**, *80*, 11779–11787. (e) Marell, D. J.; Furan, L. R.; Woods, B. P.; Lei, X.; Bendelsmith, A. J.; Cramer, C. J.; Hoye, T. R.; Kuwata, K. T. Mechanism of the intramolecular hexadehydro-Diels–Alder reaction. *J. Org. Chem.* **2015**, *80*, 11744–11754. (f) [SMD(*o*-dichlorobenzene)/B3LYP-D3BJ/6-311+G(d,p)//M06-2X/6-311+G(d,p)]

mol$^{-1}$), one of the most reactive organic intermediate, in an *exo*thermic fashion!

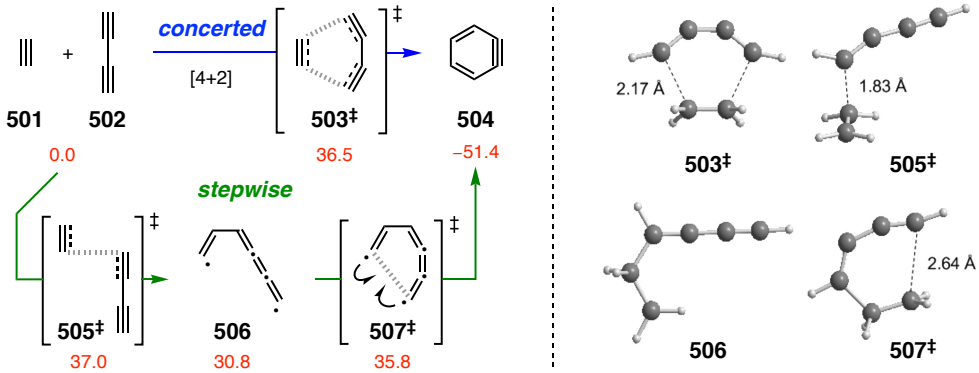


**Figure 11.** CCSD(T)//M05-2X energetics of diyne−yne cycloadditions (in kcal/mol)

*5.1.2 Distortion/interaction analysis of the HDDA reaction by Houk and coworkers*[41b]

In 2014, Houk and co-workers reported their approach towards revealing the mechanism of the HDDA reaction via distortion/interaction analysis.[42] The stepwise (with suffix "-s" in numbering) and concerted (with suffix "-c" in numbering) transition states (TSs) are located for model reactions between 1,3-butadiyne and three differently substituted monoynes (**508**–**510**, Table 2).

**Table 2.** (U)M06-2X/6-311+G(d,p)-Computed activation, distortion, and interaction energies in kcal mol$^{-1}$ (adapted from reference 41b)

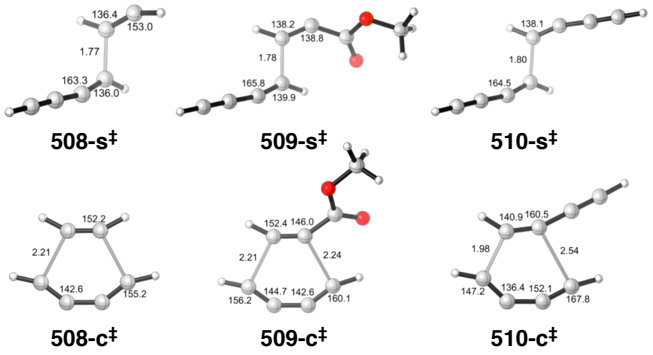


| TS | $E_{act}$ | $E_{dist\text{-}2\pi}$ | $E_{dist\text{-}4\pi}$ | $E_{dist}$ | $E_{int}$ |
|---|---|---|---|---|---|
| **508-s‡** | 35.2 | 14.6 | 12.9 | 27.5 | 7.7 |
| **508-c‡** | 36.0 | 14.0 | 29.3 | 43.3 | −7.3 |
| **509-s‡** | 28.8 | 18.8 | 10.7 | 29.5 | −0.7 |
| **509-c‡** | 32.4 | 17.2 | 26.7 | 43.9 | −11.5 |
| **510-s‡** | 28.4 | 11.6 | 11.6 | 23.2 | 5.2 |
| **510-c‡** | 35.4 | 16.1 | 27.9 | 44.0 | −8.6 |

[42] Paton, R. S.; Kim, S.; Ross, A. G.; Danishefsky, S. J.; Houk, K. N. Experimental Diels–Alder reactivities of cycloalkenones and cyclic dienes explained through transition-state distortion energies. *Angew. Chem. Int. Ed.* **2011**, *50*, 10366–10368.

In all three cases, the activation energies ($E_{act}$) are lower for the stepwise TSs. This is likely due to the large distortion energy ($E_{dist}$) required in the concerted mechanism, specifically, the distortion energy of the 4π-component 1,3-butadiyne ($E_{dist\text{-}4\pi}$). On the other hand, although concerted pathway enjoyed a bigger interaction energy, such stabilizing effect was not as dramatic as the increase in distortion energy and therefore led to a higher reaction barrier. It's also worth noting that, compared to the reaction of non-substituted monoyne as in TS **508-s**‡, HDDA of monoyne bearing an electron-withdrawing group (cf. **509-s**‡) has a larger interaction energy and thus lower overall activation energy. When alkynyl substituent is placed on the terminal of monoyne (cf. **510-s**‡), the overall activation energy ($E_{act}$) is also lower, which was attributed to the smaller distortion energy of the 2π-unit (cf. $E_{dist\text{-}2\pi}$). The authors also pointed out that the radical stabilizing effect of the alkynyl group is likely responsible for this phenomena. In this report, all the conclusions are based on model studies of hypothetical intermolecular HDDA cycloaddition reactions.

*5.1.3 Calculated PES of HDDA processes from Trolez lab and Johnson lab in 2015*[41c,d]

In 2015, Johnson and coworkers computed the potential energy surfaces for a series of intramolecular HDDA cycloisomerization reactions (Table 3, entries a–e). These data suggested that both concerted and stepwise pathway are possible and the preference between the two is substrate dependent. For instance, the reaction of *tri*yne **511a** and **511c** favors the concerted pathway while *tetra*yne **511b** showed high preference for a stepwise mechanism. For substrates like **511d** and **511e**, both pathways are similar in energy (< 1 kcal $mol^{-1}$). However, when compared to experimentally observed rate of reaction, these computed reaction barriers appeared to be slightly higher. For example, **511d** is expected to react at room temperature,[29] but the calculated activation free energy is as high as 30 kcal $mol^{-1}$.

Trolez and coworkers calculated the reaction energetics for the low temperature HDDA reaction observed in their experiment (entry f, Table 3). In the published manuscript, only the stepwise pathway is considered.

**Table 3.** Calculated PESs for HDDA reactions*

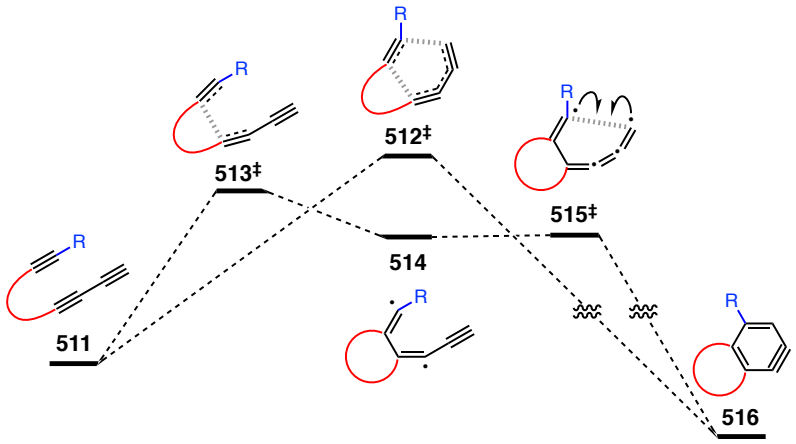


| entry (# suffix) | **511** reactant $G_{rel}$ = 0.0 | **512‡** concerted TS | **513‡** stepwise TS1 | **514** diradical intermediate | **515‡** stepwise TS2 | **516** benzyne product |
|---|---|---|---|---|---|---|
| **a** | 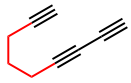 | 41.1 | 43.9 | 37.8 | 49.3 | –29.9 |
| **b** | 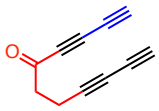 | 39.0 | 34.7 | 22.6 | 32.7 | –38.3 |
| **c** | 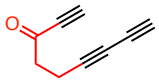 | 36.9 | 37.8 | 29.0 | 34.2 | –50.3 |
| **d** | 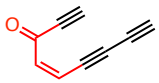 | 30.8 | 30.1 | 21.8 | 28.2 | –46.2 |
| **e** | 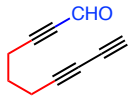 | 33.1 | 33.8 | 25.4 | 32.3 | –45.5 |
| **f** | 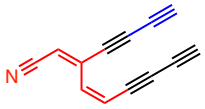 | – | 26.1 | 16.4 | 26.7 | –30.9 |
| **g** | 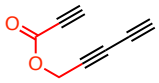 | 31.5 | 25.5 | 18.8 | 18.1 | –56.9 |

* Entries a–e are from reference 41d [Gibbs free energies at (U)M05-2X/6-311+G(d,p) level, entry a is calculated at 500 °C, entries b–e are at 25 °C]; Entry f is from reference 41c [Gibbs free energies at SMD/M06/6–311G(d,p) level]; Entry g is from reference 41e [enthalpy at SMD(o-dichlorobenzene)/B3LYP-D3BJ/6-311+G- (d,p)//M06-2X/6-311+G(d,p) level].

*5.1.4 Calculation method benchmarking*[41e]

Our group also reported a mechanistic study of the HDDA reaction in collaboration with Cramer group and Kuwata group in 2015. In this work, Brian Woods in our lab carefully measured the experimental kinetic data of a set of closely related HDDA substrates. Accordingly, various levels of computational methods were tested and the "best" DFT electronic energies were computed using the B3LYP functional[43] along with the 6-311+G(d,p) basis set and a D3 dispersion correction[44] damped according to the scheme of Becke and Johnson.[45] Additionally, SMD solvation model[46] were used in these single-point calculations to account for the solvation effects. This level of theory, which can be denoted in full as SMD(o-dichlorobenzene)/B3LYP-D3BJ/6-311+G-(d,p)//M06-2X/6-311+G(d,p), was further tested by comparing its calculated reaction energetics with several additional examples where experimental kinetic data were available. The results showed remarkable correlation between theory and experimental observation.

With this optimal level of theory in hand, a more reliable picture of the HDDA potential energy surface was revealed. As shown in entry g of table 3, the RDS transition state in the stepwise pathway (**513g**$^{‡}$) is 6 kcal mol$^{-1}$ lower in energy than the alternative TS in the concerted route (**512g**$^{‡}$). This is a large preference favoring the stepwise mechanism. However, this energy diagram also revealed that the second step in the stepwise pathway (from **514g** to **516g** via **515g**$^{‡}$) is essentially barrierless. This is consistent with the fact that we have seen no consequences of radical character in any of the many modes of HDDA trapping reactions we have studied. We have therefore termed this pathway a

---

[43] (a) Becke, A. D. Density-functional exchange-energy approximation with correct asymptotic behavior. *Phys. Rev. A: At., Mol., Opt. Phys.* **1988**, *38*, 3098−3100. (b) Lee, C.; Yang, W.; Parr, R. G. Development of the Colle-Salvetti correlation-energy formula into a functional of the electron density. *Phys. Rev. B: Condens. Matter Mater. Phys.* **1988**, *37*, 785−789. (c) Becke, A. D. Density‐functional thermochemistry. III. The role of exact exchange. *J. Chem. Phys.* **1993**, *98*, 5648−5652. (d) Stephens, P. J.; Devlin, F. J.; Chabalowski, C. F.; Frisch, M. J. Ab initio calculation of vibrational absorption and circular dichroism spectra using density functional force fields. *J. Phys. Chem.* **1994**, *98*, 11623−11627.

[44] Grimme, S.; Antony, J.; Ehrlich, S.; Krieg, H. A consistent and accurate ab initio parametrization of density functional dispersion correction (DFT-D) for the 94 elements H-Pu. *J. Chem. Phys.* 2010, 132, 154104.

[45] Johnson, E. R.; Becke, A. D. A post-Hartree-Fock model of intermolecular interactions: Inclusion of higher-order corrections. *J. Chem. Phys.* **2006**, *124*, 174104.

[46] Marenich, A. V.; Cramer, C. J.; Truhlar, D. G. Universal solvation model based on solute electron density and on a continuum model of the solvent defined by the bulk dielectric constant and atomic surface tensions. *J. Phys. Chem.* B **2009**, *113*, 6378−6396.

"stepwise-like" mechanism.

In conclusion, the calculations indicate that the activation energies for stepwise and concerted processes are similar, although a preference for a stepwise mechanism through a diradical intermediate[47] was often seen.

5.1.5 Impact of linker structure.

In a related work published in 2014, Brian Woods and coworkers in our lab studied the impact of linker structure to the relative rates of HDDA cyclization.[48] One particular attractive result is shown in Table 4: A series of triyne substrates (**517**) containing various sizes of carbocycles (5–8 membered) in the linker structure and a tethered silyl ether trap were prepared and their reaction half-lives were carefully measured. Consistent with our earlier observation,[29] when a six-membered ring is embedded (i.e. n = 2), the HDDA reaction occurred at room temperature to give **518** with a half-life of 7 hours. When the size of the ring increases (n = 3, 4), the reactivity of **517** increased accordingly. This is likely due to the geometry of substrate, in which larger rings led to decreased distance between the two reacting partner (namely, diynophile and diyne) in **517**. In contrast, the substrate containing a five membered carbocycle (n = 1) in the linker reacts drastically (ca. 1,000,000 times!) slower, which clearly demonstrated the impact of linker structure. Another important conclusion from this work is that electron-withdrawing substituent like carbonyl in the linker also accelerates the reaction.

**Table 4.** HDDA cycloisomerization rates of substrates containing various sizes of carbocycles embedded in the linker

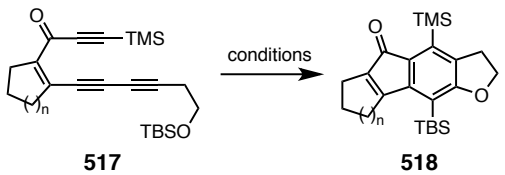


**517** **518**

| n | temperature | $t_{1/2}$ | ca. $k_{rel}$ |
|---|---|---|---|
| 1 | 150 °C | 4 h | 1 x $10^{-6}$ |
| 2 | 23 °C | 7 h | 1 |
| 3 | 24 °C | 1 h | 6 |
| 4 | 3 °C | 3 h | 20 |

[47] For a review describing cycloaromatization reactions via diradicals, see: Mohamed, R. K.; Peterson, P. W.; Alabugin, I. V. *Chem. Rev.* **2013**, *113*, 7089–7129.

[48] Woods, B. P.; Baire, B.; Hoye, T. R. Rates of hexadehydro-Diels−Alder (HDDA) cyclizations: impact of the linker structure. *Org. Lett.* **2014**, *16*, 4578−4581.

## 5.2 Our experimental design to distinguish between the two pathways[49]

We decided to systematically examine diynophile substituent effects on the rate of the HDDA cycloisomerization to see whether experimentation could distinguish between a stepwise vs. concerted reaction pathway. Accordingly, we identified the series of triynes **519a–g** (Figure 12) as an appropriate group of compounds for measuring their relative rates of HDDA cyclization. The choice of this set of substituents was guided by the prevalent use of many as activators of classical Diels-Alder reactions. The inclusion of the alkynyl substituent in tetrayne **519f** was based on the observation of Houk and coworkers that an alkynyl substituent on the terminus of the diynophile significantly lowered the activation barrier computed for the HDDA reaction for the intermolecular HDDA net cycloaddition reaction of 1,3-butadiyne with itself vs. with ethyne.[41b]

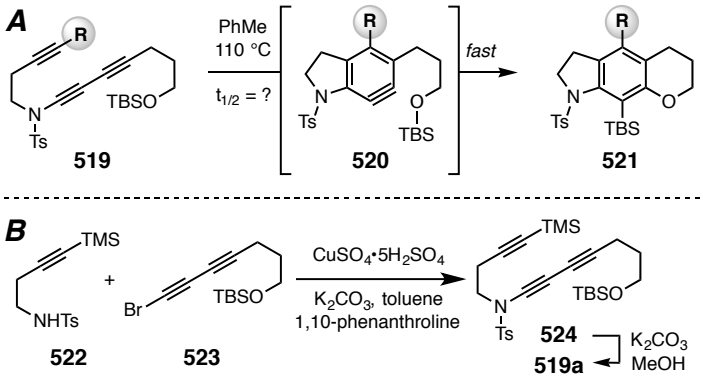


| triyne | R | conditions (from 525a) |
|---|---|---|
| ***519a*** | H | — |
| ***519b*** | $CONEt_2$ | 1) *n*-BuLi, THF, $CO_2$<br>2) EDCI, $Et_2NH$, DMAP, DMF |
| ***519c*** | $CO_2Me$ | *n*-BuLi, THF, $ClCO_2Me$ |
| ***519d*** | COMe | *n*-BuLi, THF, $Ac_2O$ |
| ***519e*** | CHO | 1) *n*-BuLi, THF, $(CH_2O)_n$<br>2) DMP, $NaHCO_3$, $CH_2Cl_2$ |
| ***519f*** | C≡C−Me | 1-bromoprop-1-yne, CuCl,<br>$NH_2OH$•HCl, *n*-$BuNH_2$, $CH_2Cl_2$ |
| ***519g*** | $CF_3$ | $TMSCF_3$, CuI, $K_2CO_3$,TMEDA, DMF, air |

**Figure 12.** Preparation and HDDA reaction of **519**

[49] This part is largely adapted from: Wang, T.; Niu, D.; Hoye, T. R. The hexadehydro-Diels−Alder cycloisomerization reaction proceeds by a stepwise mechanism. *J. Am. Chem. Soc.* **2016**, *138*, 7832−7835.

Diynamide substrates like **519** are known to be well behaved, cyclizing at convenient rates and giving rise to indoline products in good yields.[50,51] The products **521a–g** are formed via the HDDA cascade comprising initial, rate-limiting cycloisomerization of **519** to benzynes **520** followed by rapid trapping by the pendant silyl ether. In every instance, product **521** was, by far, the major product formed and, most often, the only product observed. The yields of **521a-g** following isolation ranged from 42–82%.[52]

The relative rates of the HDDA cyclization were measured by $^1$H NMR spectroscopic analysis of reactions performed in toluene-$d_8$ at 110 °C.[48] Integration of the growth of resonances from products **521** vs. those of an inert internal standard (*p*-nitrotoluene) as a function of time allowed identification of the reaction half-lives. These results are listed in Table 5.

First, consider the reactivities within the set **519a–e**. These correlate reasonably well with the expected substituent effects (see below) in classical Diels-Alder dienophile activation (i.e., approximately, CHO > COR > $CO_2R$ > $CONR_2$ > H). This trend is also suggested by comparison to the Hammett $\sigma_p$ values,[53] which reflect the electron withdrawing character of the groups present in **519a–e**. It is tempting to be satisfied that this trend mirrors that of dienophile reactivity in classical Diels-Alder reactions.[54] However, a less often used parameter, the radical stabilizing energy (RSE),[55] is also given in Table 5. These also are, qualitatively, in line with the reactivity trend observed for **519a–e**. We

---

[50] Baire, B.; Niu, D.; Willoughby, P. H.; Woods, B. P.; Hoye, T. R. Synthesis of complex benzenoids via the intermediate generation of o-benzynes through the hexadehydro-Diels–Alder reaction. *Nat. Protoc.* **2013**, *8*, 501−508.

[51] Yun, S. Y.; Wang, K.-P.; Lee, N.-K.; Mamidipalli, P.; Lee, D. Alkane C–H insertion by aryne intermediates with a silver catalyst. *J. Am. Chem. Soc.*, **2013**, *135*, 4668–4671.

[52] In the case of the slowest reacting members, formation of 3-butynyl *p*-toluenesulfonamide-containing byproducts were observed, presumably arising from a slow hydrolysis of the ynamide bond in **519a** or **519g** under the HDDA cyclization conditions. Other than **521**, no product arising from an initial HDDA cyclization event was ever observed for any of the examples.

[53] Hansch, C.; Leo, A.; Taft, R. W. A survey of Hammett substituent constants and resonance and field parameters. *Chem. Rev.* **1991**, *91*, 165–195.

[54] (a) Onishchenko, A. S. *Diene Synthesis* (Israel Program for Scientific Translations, 1964). (b) Diels-Alder reactions with ethylenic and acetylenic dienophiles: Holmes, H. L. *Org. React*. **1948**, 4, 60.

[55] (a) Pasto, D. J.; Krasnansky, R.; Zercher, C. Stabilization energies and structures of substituted methyl radicals. *J. Org. Chem.* **1987**, *52*, 3062–3072. (b) Henry, D. J.; Parkinson, C. J.; Mayer, P. M.; Radom, L. Bond dissociation energies and radical stabilization energies associated with substituted methyl radicals. *J. Phys. Chem. A* **2001**, *105*, 6750–6756. (c) Zipse, H. Radical stability—a theoretical perspective. *Top. Curr. Chem.* **2006**, *263*, 163–189.

return below to consider the rates of the alkynyl- and trifluoromethyl-bearing triynes **519f** and **519g**.

**Table 5.** Relative HDDA reaction rates of triynes **519a–g** and their comparisons with $\sigma_p$ (Hammett constant) and radical stabilizing energies (RSEs)

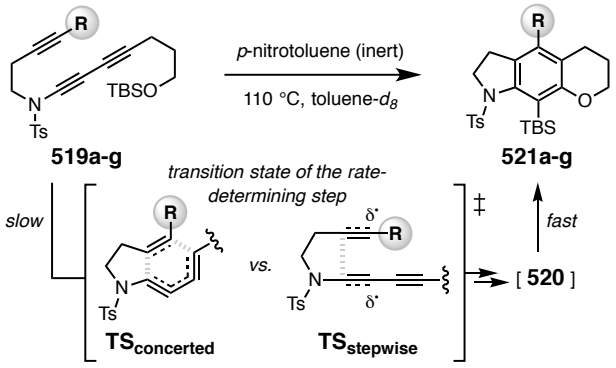


| triyne | R | $t_{1/2}$[a] | $k_{rel}$ | $\sigma_p$ | RSE[b] |
|---|---|---|---|---|---|
| **519f** | −C≡CMe | 0.26 | 320 | 0.03 | −12.1 |
| **519e** | −CHO | 0.82 | 100 | 0.42 | −7.7 |
| **519d** | −COMe | 5.1 | 16 | 0.34 | −6.7 |
| **519c** | $-CO_2Me$ | 9.2 | 9.1 | 0.34 | −4.9 |
| **519b** | $-CONEt_2$ | 84 | 1 | 0.26 | −4.9 |
| **519a** | −H | > 400 | – [c] | 0 | 0 |
| **519g** | $-CF_3$ | > 600 | – [c] | 0.54 | +1.9 |

[a] Experimentally measured half-lives in hours. [b] Radical stabi-lizing energy (kcal $mol^{-1}$) of the substituent on a ($C_{sp3}$-centered) radical. [c] Reaction rates were sufficiently slow at 110 °C for triynes **519a** and **519g** that 50% conversions were not achieved. At 145 °C **519a** converted ca. 1.5 times faster than **519g**.

How well do the relative HDDA reactivities for the specific set of **519a-g** compare with dienophile substituent effects in classical Diels-Alder cycloadditions? We were surprised to find a relative paucity of data addressing, in a quantitative way, dienophilic reactivity in a set of analogs in which only a single substituent has been varied. In fact, we can find only two reports of such studies[56] and neither encompassed the array of substituents we

[56] (a) Sauer, J.; Wiest, H.; Mielert, A. *Chem. Ber.* **1964**, *97*, 3183–3207. (b) Konovalov, A. I.; Kamasheva, G. I.; Loskutov, M. P. *J. Org. Chem. USSR* **1973**, *9*, 2064–2071.

desired for comparison with the full set of analogs **519a-g**. Therefore, we prepared the series of electron deficient alkynes **525a-g**. These again differ only in the substituents R, the nature of which corresponds directly to those in triynes **519a-g**. Competition studies were used to determine, in pairwise fashion, the relative reactivities of these dienophiles. We used the classic approach of exposing a substantial excess of each of the two competing reactants, in this case 10 equivalent each of two different dienophiles **525**, with the limiting reactant, here cyclopentadiene. Under the assumption that the reaction is essentially irreversible, the product ratio is a direct reflection of the relative rate constants for the two competing DA reactions, because the initial relative concentration of both dienophiles remains nearly constant throughout the course of the reaction.

**Table 6.** Relative rates of Diels–Alder reaction of alkynes **525a-g** with cyclopentadiene

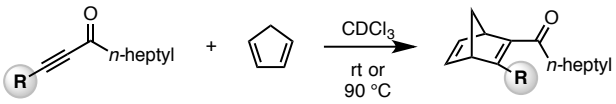


**525a-g** **526a-g**

| dienophile | R | $k_{rel}$[a] | $\sigma_p$ | RSE |
|---|---|---|---|---|
| **525e** | −CHO | 47,000 | 0.42 | −7.7 |
| **525g** | **−$CF_3$** | 16,800 | **0.54** | +1.9 |
| **525d** | −COEt | 2,100 | 0.34 | −6.7 |
| **525c** | −$CO_2$Me | 840 | 0.34 | −4.9 |
| **525b** | −$CONMe_2$ | 50 | 0.26 | −4.9 |
| **525a** | −H | 10 | 0 | 0 |
| **525f** | **−C≡CMe** | 1 | **0.03** | −12.1 |

[a] Determined by $^1$H NMR analysis of pairwise competition reactions using two dienophiles (10 equiv each) and cyclopentadiene in $CDCl_3$ in a sealed vessel.

The dienophiles are listed in Table 6 in order of decreasing reaction rate (red to blue). Note that the propynyl substituted compound **525f** is the slowest of all[41b] and that the trifluoromethylated alkyne **525g** is one of the fastest. The Hammett $\sigma_p$ and RSE parameters are also listed. The results are much better aligned with the electron withdrawing nature of the substituent, as expressed by $\sigma_p$, rather than with their radical stabilizing character, as reflected in the RSE values.

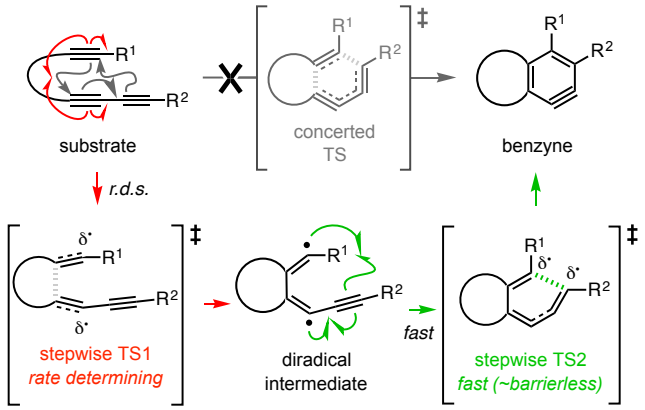


**Figure 13.** The HDDA cycloisomerization proceeds via diradical intemediate rather than through a "concerted TS" geometry; the relative rate data indicate that the "stepwise TS1" defines the rate of reaction.

What have we learned from the HDDA reactivity of compounds **519f** and **519g** vis-à-vis the rates of Diels–Alder cycloaddition of the ynones **525f** and **525g**? Indeed, it was the dichotomous nature of the electron withdrawing ($\sigma_p$) vs. the radical stabilizing effects (RSEs) of alkynyl vs. $CF_3$ substituents (see Table 5) that led us to include tetraynes **519f** and **519g** among the HDDA substrates we studied. The results are quite definitive. The tetrayne **519f**, whose alkynyl substituent has the largest RSE but only negligible electron withdrawing power, reacts the fastest, and the trifluoromethylated alkyne **519g**, with its non-radical-stabilizing and strongly electron withdrawing $CF_3$ substituent, the slowest (Table 5, red vs. blue, respectively) of all the HDDA substrates we studied. This is clearly supportive of a stepwise mechanism for the HDDA cycloisomerization reaction, in which the substrate proceeds via an initial (and rate-determining) closure to the diradical intermediate via "stepwise TS1" (red) rather than proceeding directly to benzyne via the "concerted TS" (Figure 13). This conclusion is in accordance with earlier computational analyses.[41b,c,e] Finally, recall that those studies also indicated that recombination within the diradical to complete the formation of the carbocyclic benzyne occurs with an extremely low activation barrier (green, stepwise TS2). Circumstantial evidence supports this view; we have never observed a product from any HDDA cascade experiment that suggests that the diradical intermediate is of any practical consequence. All told, our experimental data validate the mechanistic pathway laid out in Figure 13 for

the HDDA cycloisomerization.

## 5.3 The regioselectivity in benzyne trapping reactions

*5.3.1 Previous study: regioselectivity in trapping reaction of pre-distorted benzyne*

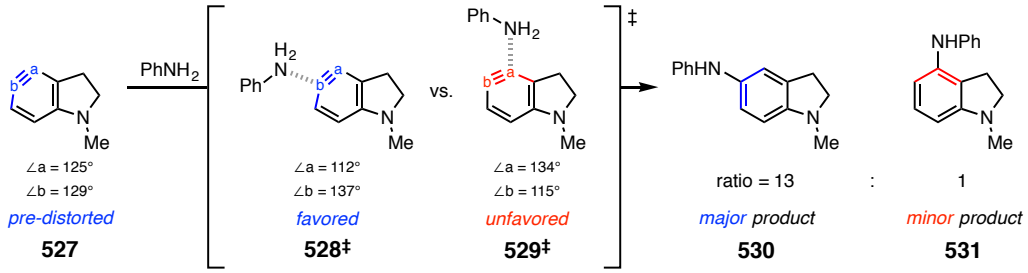


**Figure 14.** Regioselectivity in the trapping reaction of 4,5-indolyne (**527**)

One characteristic feature of benzyne as a reactive intermediate is that it has two possible sites of reaction. The regioselectivity of an asymmetric benzyne in its trapping event has been previously probed by computational approaches.[57] For instance, density functional theory (DFT) modeling showed that the benzyne moiety present in 4,5-indolyne (**527**) is pre-distorted with the internal angle of $C_a$ smaller than the alternative reaction center $C_b$ (125° vs 129°, Figure 14).[57b] As the nucleophile (aniline) approaches, benzyne become more obtuse at the electrophilic carbon (cf. $C_b$ in **528**$^‡$ and $C_a$ in **529**$^‡$) in the transition state geometry. As a result, because the TS geometry of **528**$^‡$ is distorted in a "matched" fashion (namely, $\angle C_a$ *smaller* than $\angle C_b$) with respect to **527**, reaction via **528**$^‡$ is faster. Accordingly, the alternative TS **529**$^‡$ is penalized by distorting benzyne in the opposite direction ($\angle C_a$ *larger* than $\angle C_b$, i.e. the "mismatched" case). This is fully consistent with the experimentally observed preferences: the major (**530**) and minor products (**531**) were isolated in 13 to 1 ratio. Further analysis showed that this conclusion is broadly

[57] (a) Hamura, T.; Ibusuki, Y.; Sato, K.; Matsumoto, T.; Osamura, Y.; Suzuki, K. Strain-induced regioselectivities in reactions of benzyne possessing a fused four-membered ring. *Org. Lett.* **2003**, *5*, 3551−3554. (b) Cheong, P. H. Y.; Paton, R. S.; Bronner, S. M.; Im, G.-Y. J.; Garg, N. K.; Houk, K. N. Indolyne experimental and computational studies: synthetic applications and origins of selectivities of nucleophilic additions. *J. Am. Chem. Soc.* **2010**, *132*, 1267−1269. (c) Garr, A. N.; Luo, D.; Brown, N.; Cramer, C. J.; Buszek, K. R.; VanderVelde, D. Experimental and theoretical investigations into the unusual regioselectivity of 4,5-, 5,6-, and 6,7-indole aryne cycloadditions. *Org. Lett.* **2010**, *12*, 96−99.

applicable to regioselectivity prediction in other benzyne trapping reactions. For pre-distorted arynes, nucleophilic additions are favored at the more obtuse carbon. Similar conclusions were reached in other studies as well.[57a,c]

*5.3.2 Potential energy and partial charge in a distorted benzyne*

To better understand the nature of benzyne, especially in light of the above mentioned study in which a clear connection between regioselectivity and distortion was established, the energy required to distort such an intermediate is important.

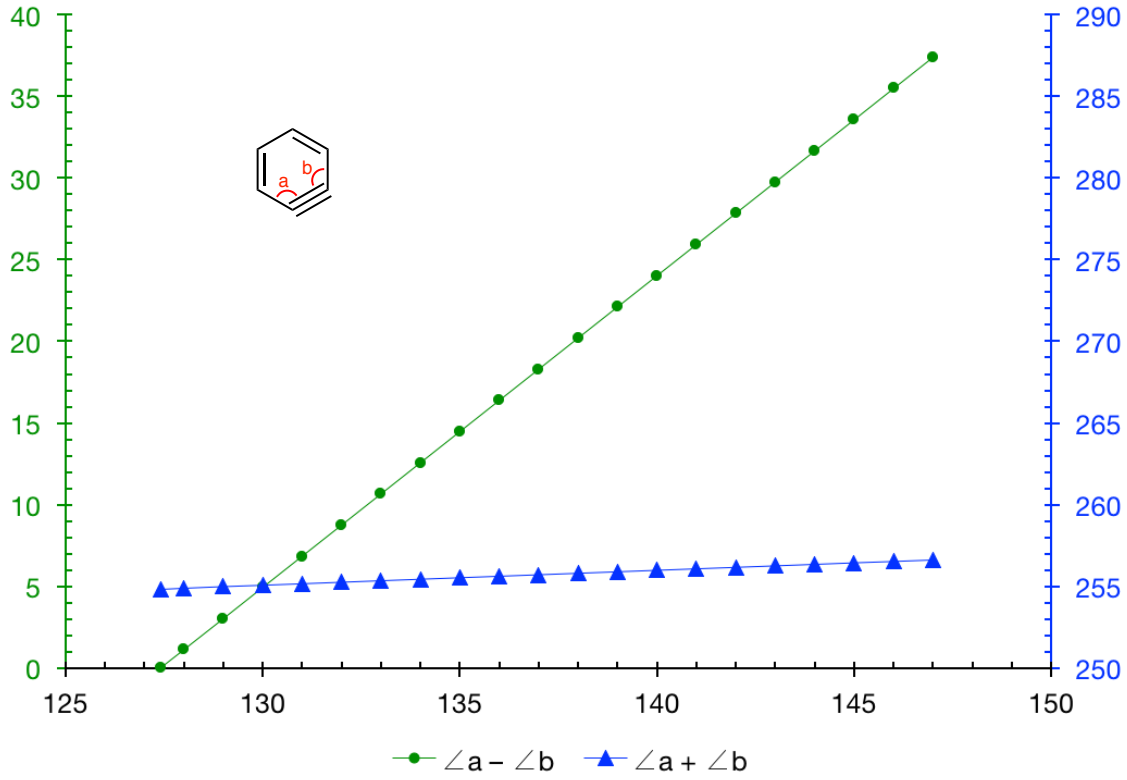


**Figure 15.** Change of ∠a – ∠b and ∠a + ∠b as ∠a changes (x axis: ∠a; green y axis: ∠a – ∠b; blue y axis: ∠a + ∠b; Optimized at SMD(chloroform)/M06-2X/6-311+G(d,p) //SMD(chloroform)/M06-2X/6-31G(d) level of theory)

My preliminary study to probe this problem started by DFT modeling of the parent benzyne. As shown in Figure 15, a series of distorted benzyne geometries were located

by fixing the internal angle ∠a while allowing all other structural parameters to relax in the optimization. By switching to different ∠a values, an array of benzyne geometries of varying degrees of distortion were obtained. We first examined how the geometry of benzyne react to different ∠a values. As shown in Figure 15, the overall magnitude of distortion (as represented by ∠a – ∠b) was plotted against ∠a and showed great linear correlation (green). On the other hand, the values of ∠a + ∠b remain largely the same across the series as indicated by the negligible slope in the plot of ∠a + ∠b against ∠a (blue). These facts pointed out that 1) the distortion is largely localized in the strained benzyne triple bond and 2) either the internal angle (e.g. ∠a) or the difference between the two internal angles (∠a – ∠b) can reflect the overall degree of benzyne distortion.

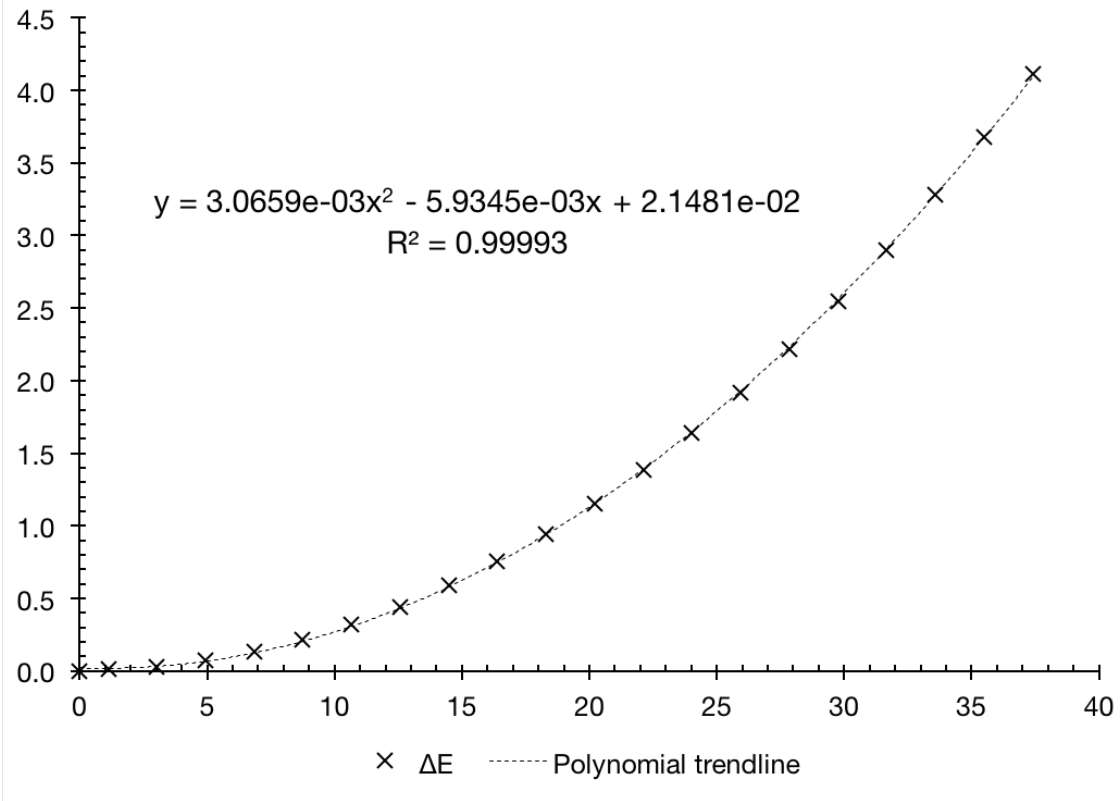


**Figure 16.** Distortion energy (in kcal $mol^{-1}$) vs. degree of distortion (∠a – ∠b)

I then turned focus to the key question of distortion energy versus the extent of distortion. As shown in Figure 16, the electronic energy of these distorted benzynes were plotted

against ∠a – ∠b (namely, x axis = ∠a – ∠b; y axis = electronic energy of these distorted benzyne structures). Remarkably, these data points can be fitted with a parabola trendline with a $r^2$ of 0.99993. This second-order relation between the magnitude of deformation and potential energy is reminiscent of the famous Hooke's law, in which the potential energy increases parabolically as the spring stretches/compresses. Guided by this thinking, one can conclude that benzyne is relatively easy to distort from the equilibrium position. However, as the amount of deformation increases, each degree of change would be more and more disfavored energetically.

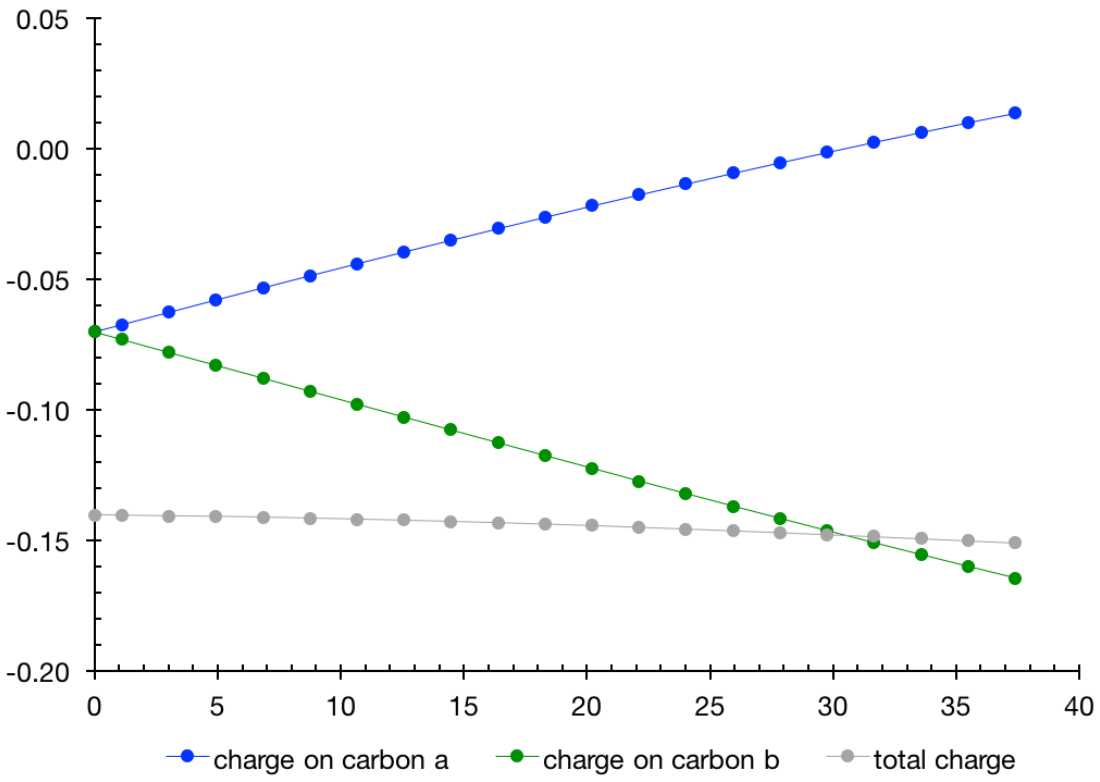


**Figure 17.** CM5 partial atomic charge vs. degree of distortion (∠a – ∠b)

Furthermore, I have calculated the CM5 partial atomic charges[58] on both carbon a and

[58] (a) Duanmu, K.; Wang, B.; Marenich, A. V.; Cramer, C. J.; Truhlar, D. G. CM5PAC version 2015, University of Minnesota, Minneapolis, 2015. http://comp.chem.umn.edu/cm5pac/ (b) Marenich, A. V.; Jerome, S. V.; Cramer, C. J.; Truhlar, D. G. Charge Model 5: an extension of Hirshfeld population analysis for the accurate description of molecular interactions in gaseous and condensed phases. *J. Chem. Theor.*

carbon b of these distorted benzyne geometries. As shown in Figure 17, as ∠a increases, carbon a becomes more and more positively charged (line in blue). At the same time, as ∠b decreases, more negative charge on carbon b starts to build up (line in green). This observation is, again, consistent with previous studies. Interestingly, we have observed a linear (first-order) relation between partial charge on carbon atom versus degree of distortion (∠a – ∠b). I also wanted to point out that, the total charge on carbon a and b remain mostly the same (grey line) and is insensitive to the amount of distortion. Here, deformation induces electron density to relocate between carbon a and b.

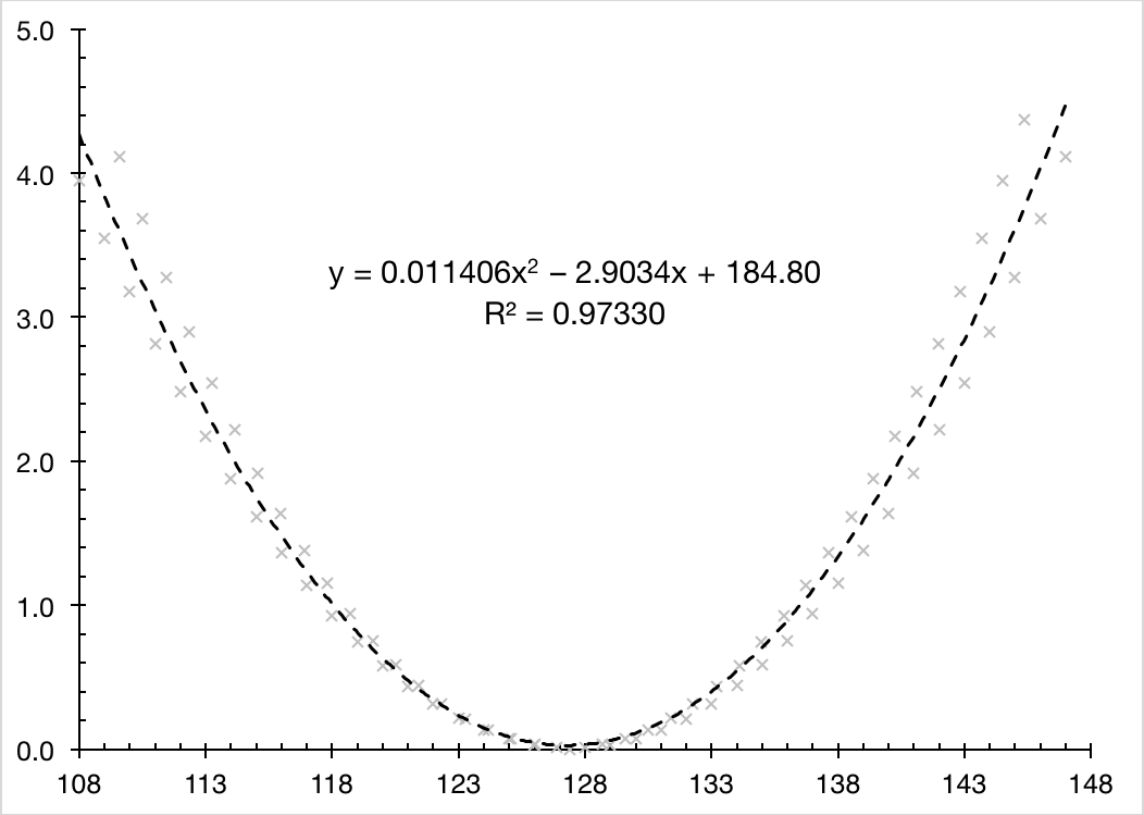


**Figure 18.** Distortion energy vs. internal angle of benzyne carbon

However, there exists a certain extent of systematic error in this approach, especially in geometry optimization. To be more specific, when benzyne is optimized with ∠a fixed

*Comput.* **2012**, *8*, 527–541. (c) Duanmu, K.; Truhlar, D. G. Partial ionic character beyond the pauling paradigm: metal nanoparticles. *J. Phys. Chem. C* **2014**, *118*, 28069–28074.

to 120°, ∠b is roughly 134° in the obtained geometry. However, when ∠a was fixed to 134°, ∠b is 121.4° in the obtained optimized structure, instead of 120°!

As an attempt to average out this systematic error and provide reasonable estimation of distortion energy and partial atomic charge based solely on the internal angle of benzyne carbon, each distorted benzyne structure was plotted twice and average in the trendline. For example, in Figure 18, x axis is the internal angle while y axis represents the relative electronic energy. For each structure, two data points with coordinates (∠a, E) and (∠b, E) can be drawn in the diagram. The final parabola trendline was calculated based on all data points. The relation between partial atomic charge on carbon and benzyne internal angle was established in similar way as shown in Figure 19.

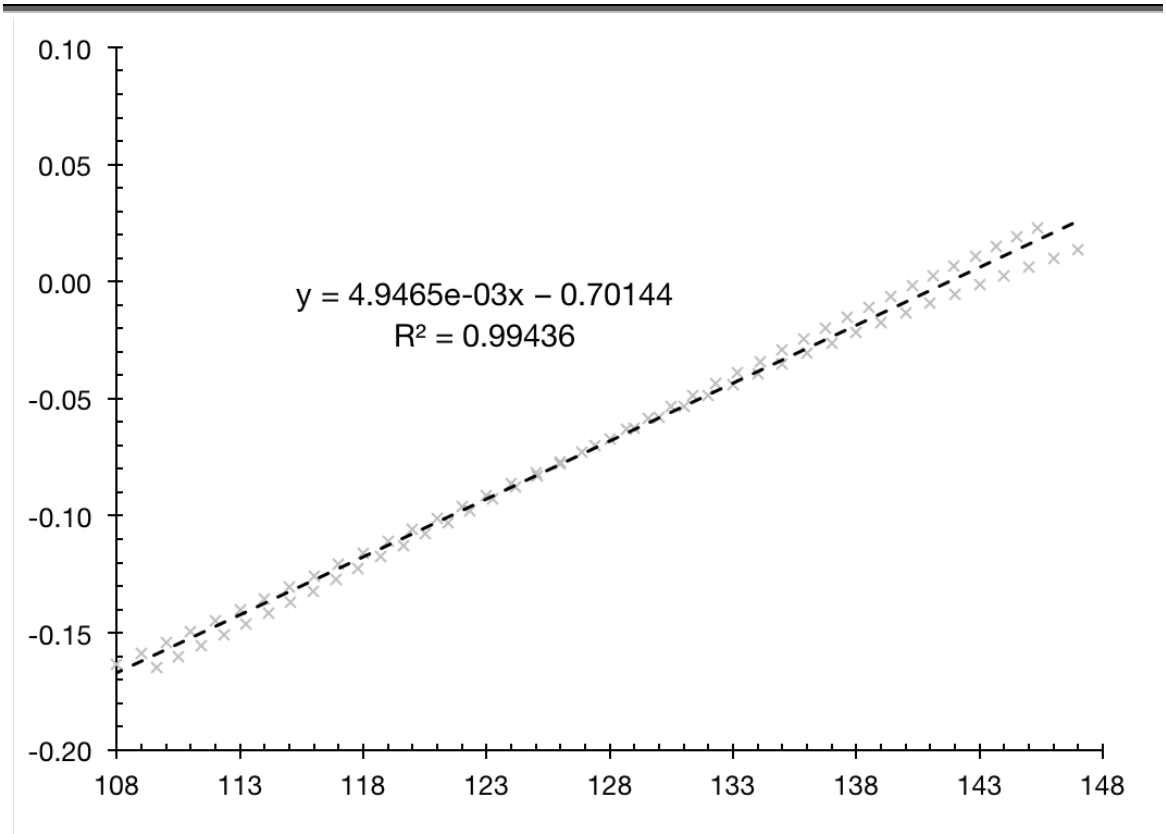


**Figure 19.** CM5 partial atomic charge on carbon vs. internal angle of benzyne carbon

*5.3.3 Substituent effect in benzyne geometry*

Substitution adjacent to the aryne triple bond can dramatically affect its structure and reactivity. For example, Garg and coworkers reported a significant change in geometry for C5 or C2 substituted 3,4-pyridyne.[59] As shown in Table 7A, when σ-inductive groups like halogen atom or oxygen based substituents like dimethylsulfamoyloxy or methoxy were attached to C5 of 3,4-pyridyne, C3 became flattened, as indicated by the larger C3 internal angle. Nucleophilic attack favors C3 position over C4 to give 3,5-disubstituted pyridine product. Remarkably, when the same set of groups were attached to the C2 position, as shown in Table 7B, C4 now became the more obtuse carbon and therefore more electrophilic. The high synthetic value in this regiochemistry inversion urged us to understand the effect of other common functional groups.

**Table 7.** Effect of substituents at either C2 or C5 on the distortion of 3,4-pyridyne

**A**

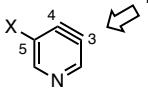


5-substituted 3,4-pyridynes

| X | C3 | C4 | difference |
|---|---|---|---|
| Cl | 129.8° | 119.8° | 10.0° |
| Br | 129.1° | 120.6° | 8.5° |
| I | 127.1° | 122.8° | 4.3° |
| $OSO_2NMe_2$ | 130.5° | 118.8° | 11.7° |
| OMe | 131.9° | 118.3° | 13.6° |

**B**

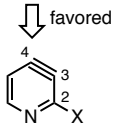


2-substituted 3,4-pyridynes

| X | C3 | C4 | difference |
|---|---|---|---|
| Cl | 121.8° | 127.6° | 5.8° |
| Br | 122.1° | 127.2° | 5.1° |
| I | 123.3° | 128.9° | 3.0° |
| $OSO_2NMe_2$ | 120.3° | 128.9° | 8.6° |
| OMe | 121.6° | 128.1° | 6.5° |

I have performed DFT calculations [SMD(chloroform)/M06-2X/6-31G(d)] to model the geometry of a number of benzynes with various common substituents attached *ortho* to the strained alkyne. As shown in Table 8, the internal angle values of these benzyne structures were recorded and sorted based on ∠a. Consistent with Garg's report,[59] σ-inductive groups like fluoride, nitro and methoxy are among the strongest "*meta*" directing groups (i.e. distort the benzyne and lead to nucleophilic attack meta to R group). On the other hand, substituents with lower electronegativity like $sp^3$-hybridized carbon or

[59] Goetz, A. E.; Garg, N. K. Regioselective reactions of 3,4-pyridynes enabled by the aryne distortion model. *Nat. Chem.* **2013**, *5*, 54–60.

silyl groups are σ-donating and therefore favors addition "*ortho*" to the R group.

**Table 8.** Substituent effect in benzyne geometry

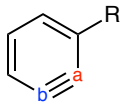


| Selectivity | R | ∠a | ∠b | ∠a –∠b |
|---|---|---|---|---|
| ***meta*** | F | 115.7 | 137.4 | -21.8 |
| | $NO_2$ | 116.2 | 136.0 | -19.8 |
| | OMs | 117.3 | 136.2 | -18.9 |
| | OMe | 118.6 | 135.9 | -17.3 |
| | $SO_2Me$ | 118.9 | 134.1 | -15.3 |
| | Cl | 119.1 | 134.7 | -15.6 |
| | NHMs | 120.0 | 134.8 | -14.8 |
| | Br | 120.1 | 133.8 | -13.7 |
| | $CF_3$ | 121.7 | 132.1 | -10.4 |
| | CN | 121.8 | 132.2 | -10.4 |
| | CHO | 123.8 | 130.3 | -6.6 |
| | $CO_2Me$ | 124.2 | 130.0 | -5.9 |
| | ethynyl | 124.9 | 130.1 | -5.2 |
| | COMe | 125.3 | 129.2 | -3.9 |
| | $CONH_2$ | 125.7 | 129.0 | -3.3 |
| | **H** | **127.4** | **127.4** | **0.0** |
| | $CH_3$ | 128.7 | 127.2 | 1.5 |
| | $^t$Bu | 129.0 | 126.8 | 2.2 |
| ***ortho*** | TMS | 135.6 | 120.7 | 14.9 |

## 5.4 Mechanistic details in the trapping event

### *5.4.1 Retro-Brook rearrangement in intramolecular silyl ether trapping event*[60]

In our first example of HDDA reaction reported in 2012, we found that tethered silyl ether could serve as an efficient intramolecular trapping agent (Scheme 21). For example,

[60] This section is largely adapted from: Hoye, T. R.; Baire, B.; Wang, T. Tactics for probing aryne reactivity: mechanistic studies of silicon-oxygen bond cleavage during the trapping of (HDDA-generated) benzynes by silyl ethers. *Chem. Sci.* **2014**, *5*, 545–550.

triyne **532** could cyclize at 26 °C to give **533** with a half-life of 7 hours. After formation of the key benzyne intermediate with HDDA cycloisomerization, two reaction pathways are possible. As shown in Scheme 21, the tethered silyl ether could either engage the benzyne and form zwitterionic intermediate like **535**, which could undergo subsequent retro-Brook rearrangement to give the ultimate stable compound **533** (red pathway), or directly generate **533** in a concerted fashion (green pathway). Although retro-Brook rearrangements are known, example of concerted O–Si bond insertion, as in the later proposed route, is not reported.

**Scheme 21.** The HDDA reaction of **532** to give **533** via benzyne **534**

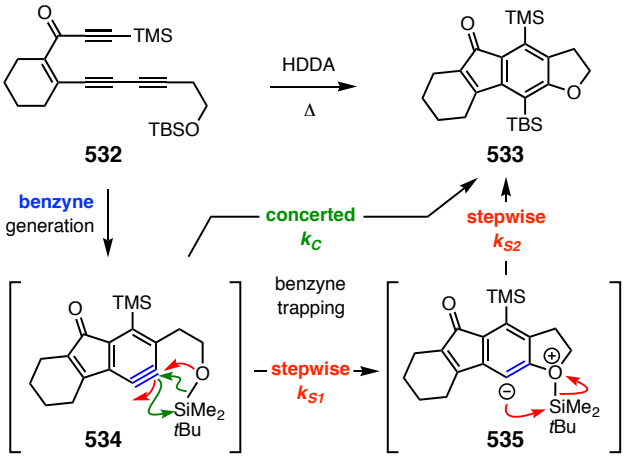


To study the mechanism of this interesting trapping event, Dr. Baire in our lab cleverly designed and performed cross-over experiments using symmetrical, doubly labeled bis-silyl ether substrates to establish that the reaction is unimolecular in nature. A series of competition experiments involving either intramolecular or intermolecular dihydrogen transfer clock reactions (from within a TIPS isopropyl group or cyclooctane, respectively) vs. the silyl ether cyclization were used to gain additional insights. The effects of the steric bulk of the silyl ether trapping group and the ring-size of the cyclic ether being formed (furan vs. pyran) were also evaluated. These types of competition experiments allow the relative rates of various product-determining steps to be measured. This previously has only rarely been possible because aryne formation is typically rate-limiting, making it challenging to probe the kinetics of subsequent trapping reactions.

The solvent effect was also evaluated and showed a modest rate enhancement in solvents of higher polarity. This can be interpreted as evidence for only a moderate degree of polarization in the transition structure for the rate-limiting step. It was also found that larger alkyl groups on the silyl ether would slow the rate of trapping (ca. 20-fold between TES and TIPS). Precursors to form benzofuran vs. benzopyran products were also tested and showed essentially same cyclization rate, suggesting that enthalpic and entropic factors in these two types of tethers are self-compensating.

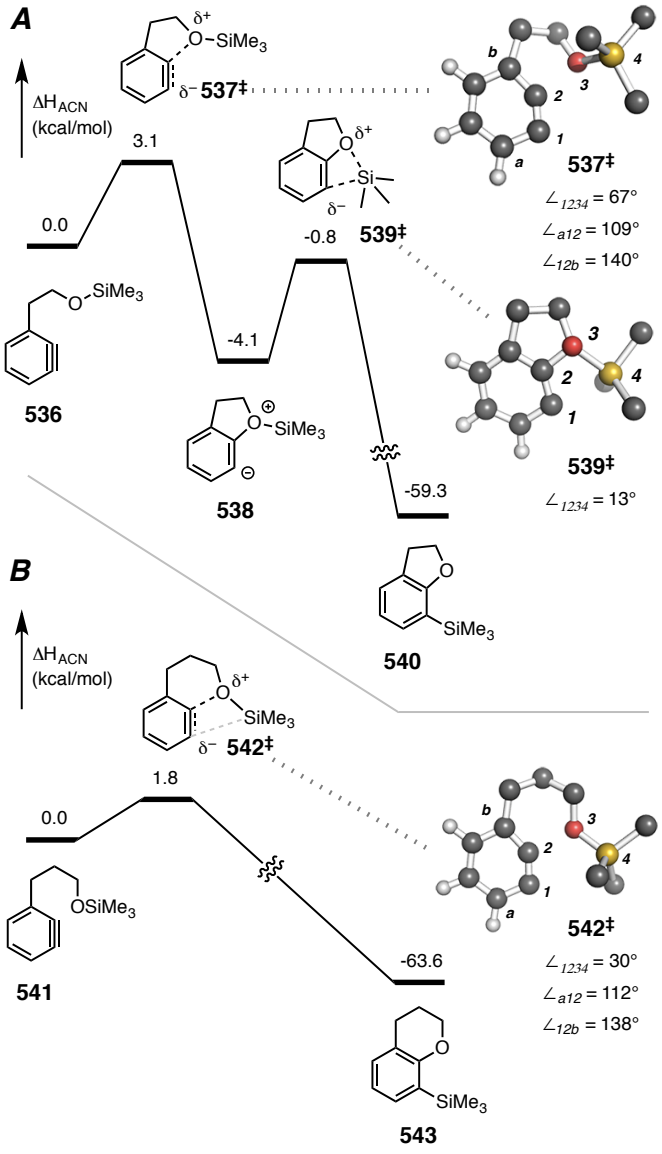


**Figure 20.** PES of benzyne trapping with tethered silyl ether

To gain more information relevant to the possibility of single-step insertion into the Si–O σ bond, I have examined this benzyne trapping process computationally. I have studied each of the model benzyne-containing substrates **536** and **541** (Figure 20, panels A and B, respectively). Each comprises a simple trimethylsilyl ether and a mono-substituted benzyne, and the two differ only in the length of the methylene chain (two vs. three $CH_2$s) linking the aryne and silyl ether moieties. Benzyne **536** leads to the benzofuran product **540**, the homolog **541** to the benzopyran **543**. The reaction potential energy surface (PES) for each substrate/product pair was modeled at SMD(acetonitrile)/M06-2X/6-31G(d)] level of theory. We were able to locate a zwitterionic species as an intermediate only when an implicit (or continuum) solvation model (SMD[46]) were applied during geometry optimization and, then, only in the five-membered series (cf. the pathway involving **536**–**540**). The barrier heights leading away from the zwitterion (**538**) are quite low, especially so in the forward direction, suggesting that it is a fleeting intermediate. Computational results (energies for **536**–**543** and geometries for TSs **537**$^{‡}$, **539**$^{‡}$, and **542**$^{‡}$) are given in Figure 20. The trends and conclusions are qualitatively the same regardless of the nature of the basis set that was used.

The overall transformation for either trapping reaction (**536** to **540** or **541** to **543**) is highly exothermic (>50 kcal•mol$^{-1}$). The geometry of each of the initial (and early) TSs **537**$^{‡}$ or **542**$^{‡}$ shows only a slight lengthening of the O–Si bond. The major difference in the two (cf. TS geometries in Figure 20) is seen in the dihedral bond angle across the pair of benzyne carbon atoms and the silyl ether oxygen and silicon atoms ($\angle_{1234}$ = 67° in **537**$^{‡}$ vs. 30° in **542**$^{‡}$). TS **537**$^{‡}$ was able to settle into the zwitterionic intermediate **538**, in which this dihedral angle has been significantly reduced to 18°. This then proceeds via the second TS **539**$^{‡}$ (dihedral = 13°) to product **540** (dihedral = 0°) via a second, low barrier and very exothermic elementary step. The TS **542**$^{‡}$ for the six-membered substrate is very similar to **538** in both geometry and energy. However, it directly evolves into benzopyran **543** (dihedral = 0°) without indication of encountering an intervening energy minimum species (i.e., an analogous zwitterionic intermediate). It is also of interest that the benzyne moiety in each of TSs **537**$^{‡}$ and **542**$^{‡}$ has undergone an appreciably large, induced distortion of geometry in response to the approach of the oxygen nucleophile.

Specifically, the two bond angles within the benzyne ring at atoms C1 ($\angle_{a12}$) vs. C2 ($\angle_{12b}$) reveal a large distortion of the benzyne in each ($\angle_{12b}$ - $\angle_{a12}$ = 31° for **537**‡ and 26° for **542**‡). This induced distortion of the transition structure represents an extrapolation of previous explanations of ground-state benzyne distortions that effectively explain the site of greater electrophilic character in unsymmetrical benzynes.[57]

*5.4.2 Alcohol trapping reaction*[61]

In 2014, Patrick Willoughby, Dawen Niu and coworkers in our lab studied the reaction between primary and secondary alcohols with HDDA-generated benzyne. Although such trapping event of benzynes generated by traditional methods has been previously probed, study of alcohol trapping of HDDA-generated benzyne revealed new knowledge. For instance, as shown in Figure 21A, starting from triyne precursor **544** and alcohol **545**, a competition has been observed between addition vs. dihydrogen transfer to produce arylethers (eg. **546**) vs. reduced benzenoid products (eg. **547**), respectively. During the latter process, an equivalent amount of oxidized ketone (or aldehyde) is formed. Using deuterium labeling studies, we determined that (i) it is the carbinol C–H and adjacent O–H hydrogen atoms that are transferred during this process and (ii) the mechanism is consistent with a hydride-like transfer of the C–H. Substrates bearing an internal trap attached to the reactive, HDDA-derived benzyne intermediate were used to probe the kinetic order of the alcohol trapping agent in the $H_2$-transfer as well as in the alcohol addition process. The $H_2$-transfer reaction is first order in alcohol. These results are suggestive of a concerted $H_2$-transfer process, which is further supported by DFT computational studies and results of a kinetic isotope effect experiment. In contrast, the alcohol addition to the benzyne is second order in alcohol—a previously unrecognized phenomenon. My major contribution in this project was to understand this intriguing second-order rate dependence as well as to reveal the relative energetics in each competing pathway via DFT calculations.

---

[61] This section is largely adapted from: Willoughby, P. H.; Niu, D.; Wang, T.; Haj, M. K.; Cramer, C. J.; Hoye, T. R. Mechanism of the reactions of alcohols with o-benzynes. *J. Am. Chem. Soc.* **2014**, *136*, 13657–13665.

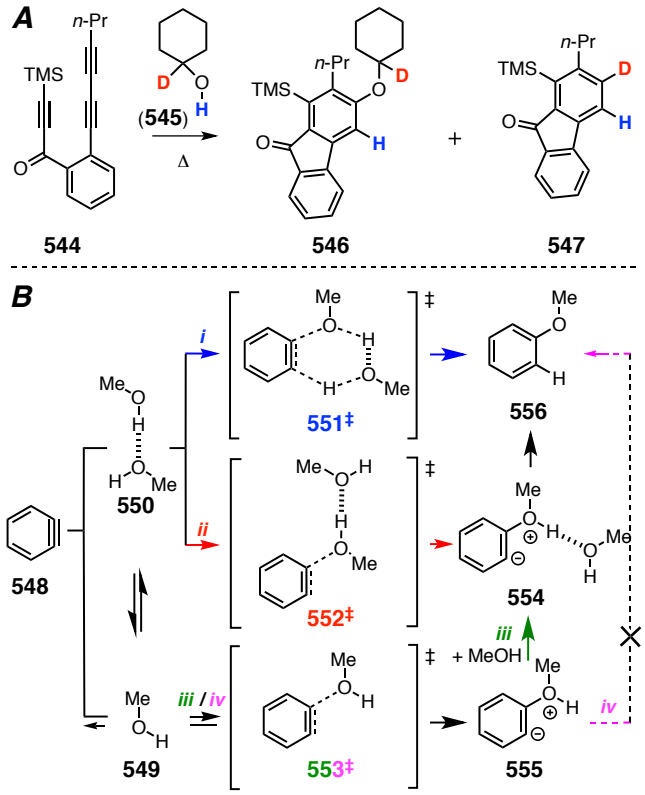


**Figure 21.** Reaction between alcohol and benzyne

Three mechanistic interpretations for the addition of an alcohol [eg. Methanol (**549**)] to a benzyne, consistent with the second-order dependency on alcohol, are shown in Figure 21B. For simplicity, they are represented with *o*-benzyne (**548**) to give the alkyl phenyl ether **556**. In pathway ***i*** alcohol addition occurs by a single encounter between a preformed alcohol dimer **550** and **548** via TS structure **551**‡. In pathway ***ii*** dimer **550** adds to **548** to produce a discrete intermediate **554**, having one new C–O bond by way of a TS structure like **552**‡. Adduct **554** would then proceed to **556** by an intramolecular proton shuttling event. Assistance of intramolecular 1,3-proton migration by an external hydroxyl-containing molecule has been invoked in classical (keto–enol and 2-pyridone–2-hydroxypyridine) tautomerization reactions. In pathway ***iii*** initial rapid and reversible addition of the first molecule of monomeric alcohol gives zwitterion **555** by way of TS structure **553**‡. This is followed by a coordination with a second molecule of alcohol to intersect with intermediate **554** invoked in pathway ***ii***. It is noteworthy that the results from our kinetic studies are inconsistent with an intramolecular proton transfer that would

convert **555** directly to **556** (pathway ***iv***) because this would show a simple first-order dependency on the alcohol concentration.

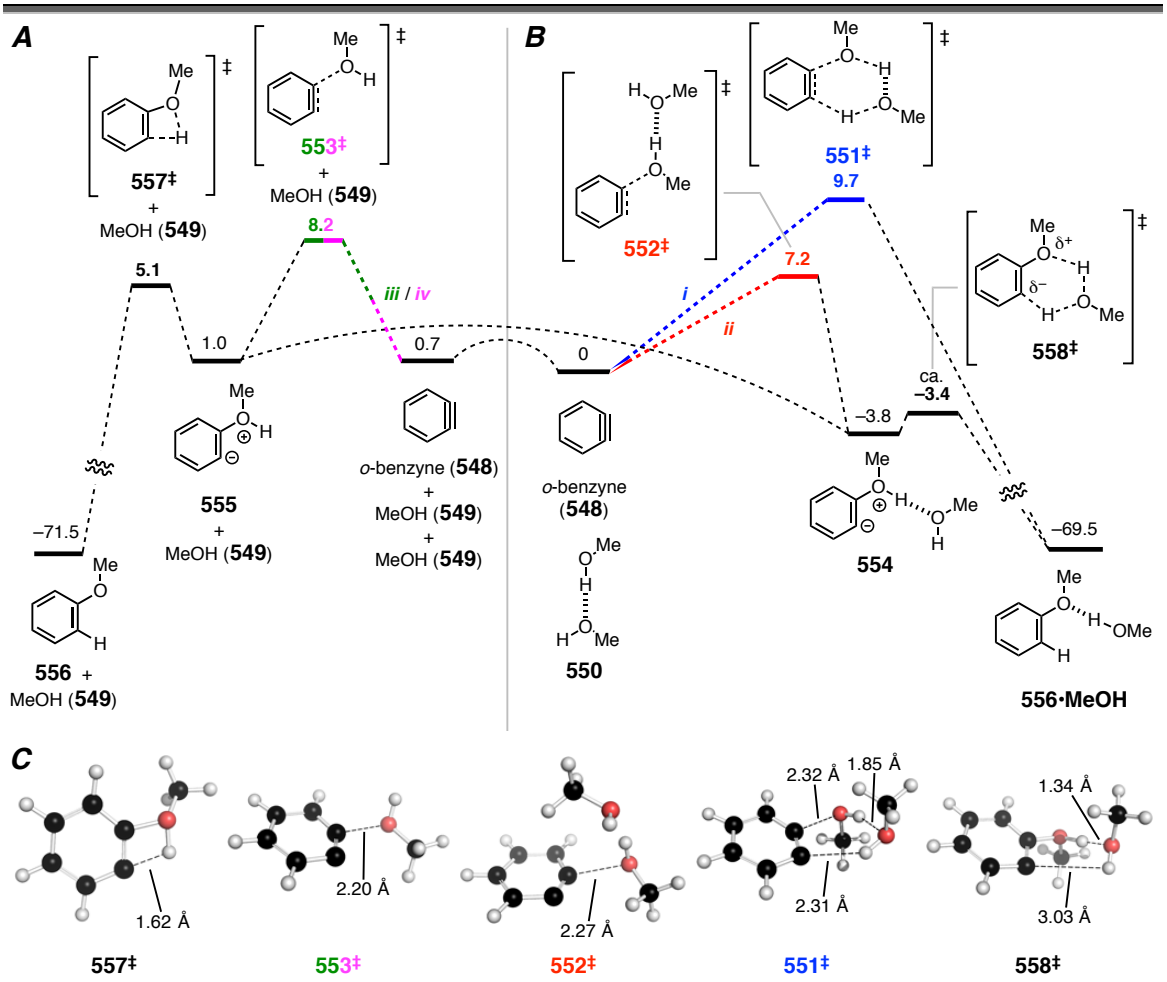


**Figure 22.** The calculated PES of all four pathways in methanol trapping of benzyne

As shown in Figure 22, DFT calculations were performed using M06-2X/6-311+G(d,p) and the SMD solvation model (MeOH). Standard state corrections (gas phase to 1 M solution) were applied to all structures and the concentration of methanol was adjusted to 24.7 M (neat methanol). All values are of the free energies in kcal $mol^{-1}$. Minima and TS structures of species in which *one* vs. *two* methanol molecules have engaged *o*-benzyne (**548**) are shown in panel A vs. B, respectively. The curved dashed lines represent low barrier processes in which a new hydrogen bond to methanol is being formed to convert a species in panel A to one in panel B. In panel C, a 3D view of the geometry of each of the

five TS structures was provided. The dashed lines in each represent atom pairs between which bond order is increasing in the forward reaction direction. For each of the four pathways, the level of the highest energy TS structure and rate determining step is shown in color. The relative zero of free energy corresponds to an isolated *o*-benzyne and a methanol dimer (all species in Figure 22 include continuum methanol solvation). The stoichiometrically equivalent combination of *o*-benzyne and two isolated methanol monomers is 0.7 kcal $mol^{-1}$ higher in free energy.

The addition of methanol monomer (**549**) to **548** to produce the zwitterion **555** is a step common to both pathways ***iii*** and ***iv*** (green/magenta). The associated TS structure **553**‡ was found to have a relative free energy of 8.2 kcal $mol^{-1}$. The subsequent, low barrier, for unimolecular proton transfer within **555** via **557**‡ was suggestive of rapid conversion to product **556** to complete pathway ***iv***—the reaction that would be first order in alcohol concentration.[62] Alternatively, we envision that **555** could coordinate a second molecule of methanol[63] to produce **554** by another presumably very low barrier process merely involving hydrogen bond formation (a librational motion in neat alcohol or a solvent-shell exchange reaction in a mixed solvent). Knowing the relative ease of that event vis-à-vis that passing through **557**‡ is somewhat moot, however, since (i) irrespective of the barrier, a path to product having first-order dependence on methanol would be available and, more importantly, (ii) TS structure **553**‡ (green/magenta) is *not* associated with the overall lowest energy pathway in Figure 22.

The most favored computed pathway is ***ii*** (red), the stepwise addition of the methanol dimer (**550**) to **548**, which passes through the TS structure **552**‡ having a relative free

---

[62] (a) The possibility of a direct, single-step, O-H insertion mechanism[62b] to produce anisole directly from methanol and *o*-benzyne (not shown) was considered. Numerous attempts to locate a TS structure were unsuccessful. (b) Im, G.-Y. J.; Bronner, S. M.; Goetz, A. E.; Paton, R. S.; Cheong, P. H.-Y.; Houk, K. N.; Garg, N. K. Indolyne experimental and computational studies: synthetic applications and origins of selectivities of nucleophilic additions. *J. Am. Chem. Soc.* **2010**, *132*, 17933–17944.

[63] (a) Xia, Y.; Liang, Y.; Chen, Y.; Wang, M.; Jiao, L.; Huang, F.; Liu, S.; Li, Y.; Yu, Z.-X. An unexpected role of a trace amount of water in catalyzing proton transfer in phosphine-catalyzed (3 + 2) cycloaddition of allenoates and alkenes. *J. Am. Chem. Soc.* **2007**, *129*, 3470–3471. (b) Patil, M. P.; Sunoj, R. B. Insights on Co-catalyst-promoted enamine formation between dimethylamine and propanal through ab initio and density functional theory study. *J. Org. Chem.* **2007**, *72*, 8202-8215. (c) Cheong, P. H.-Y.; Legault, C. Y.; Um, J. M.; Çelebi-Ölcüm, N.; Houk, K. N. Quantum mechanical investigations of organocatalysis: mechanisms, reactivities, and selectivities. *Chem. Rev.* **2011**, *111*, 5042–5137.

energy of 7.2 kcal•mol$^{-1}$. The resulting adduct **554** was located as a minimum and would be expected to proceed rapidly to product **556•MeOH** through some TS structure **558**$^{‡}$. However, we were unsuccessful in finding a fully converged TS structure (i.e., a species having only one imaginary frequency) for this final step, presumably owing to a very flat potential-energy surface along the reaction coordinate and some numerical noise associated with non-analytic density functional integrals determined on necessarily finite integration grids; such situations can defeat optimization algorithms in their search for a stationary TS structure. Instead, we approximately identified **558**$^{‡}$ (Figure 22) by manually distorting the geometry of **554** in very small increments toward that of the requisite product and computing the energy with restrained internal coordinates. The energy increased by only 0.4 kcal mol$^{-1}$ with respect to **554** until a final small change (0.1° in one internal angle) resulted in exergonic collapse to product upon geometry optimization. This approach can be used to identify approximate TS structures for processes for which optimization algorithms fail to converge to stationary points.[64]

An alternative reaction pathway involving dimer **550** (i.e., ***i***; blue) invokes its concerted addition to **548**. The requisite TS structure **551**$^{‡}$ shows the highest free energy (9.7 kcal mol$^{-1}$) for the rate limiting step of any of the four pathways. In summary, although it is prudent not to place excessive weight on the merit of computed energetics for reactions having activation barriers that vary by only a few kcal mol$^{-1}$, it is encouraging that the results of this study are in concert with a lowest-energy process that involves two molecules of methanol prior to its rate-limiting event.

### *5.4.3 Competition in IMDA trapping*[65]

In 2015, Vedamayee Pogula observed the efficient, intramolecular trapping in a Diels–Alder sense of thermally generated benzynes by one of two pendant arene rings. A more electron rich ring (*p*-methoxyphenyl) reacted substantially faster than a simple phenyl

---

[64] (a) Hull, J. F.; Balcells, D.; Sauer, E. L. O.; Raynaud, C.; Brudvig, G. W.; Crabtree, R. H.; Eisenstein, O. Manganese catalysts for C−H activation: an experimental/theoretical study identifies the stereoelectronic factor that controls the switch between hydroxylation and desaturation pathways. *J. Am. Chem. Soc.* **2010**, *132*, 7605-7616. (b) Lonsdale, R.; Harvey, J. N.; Mulholland, A. J. A practical guide to modelling enzyme-catalyzed reactions. *Chem. Soc. Rev.* **2012**, *41*, 3025-3038.

[65] This part is largely adapted from: Pogula, V. D.; Wang, T.; Hoye, T. R. Intramolecular [4 + 2] trapping of a hexadehydro-Diels–Alder (HDDA) benzyne by tethered arenes. *Org. Lett.* **2015**, *17*, 856–859.

ring, which was in turn, slightly more reactive vs. a 4-carbomethoxyphenyl ring.

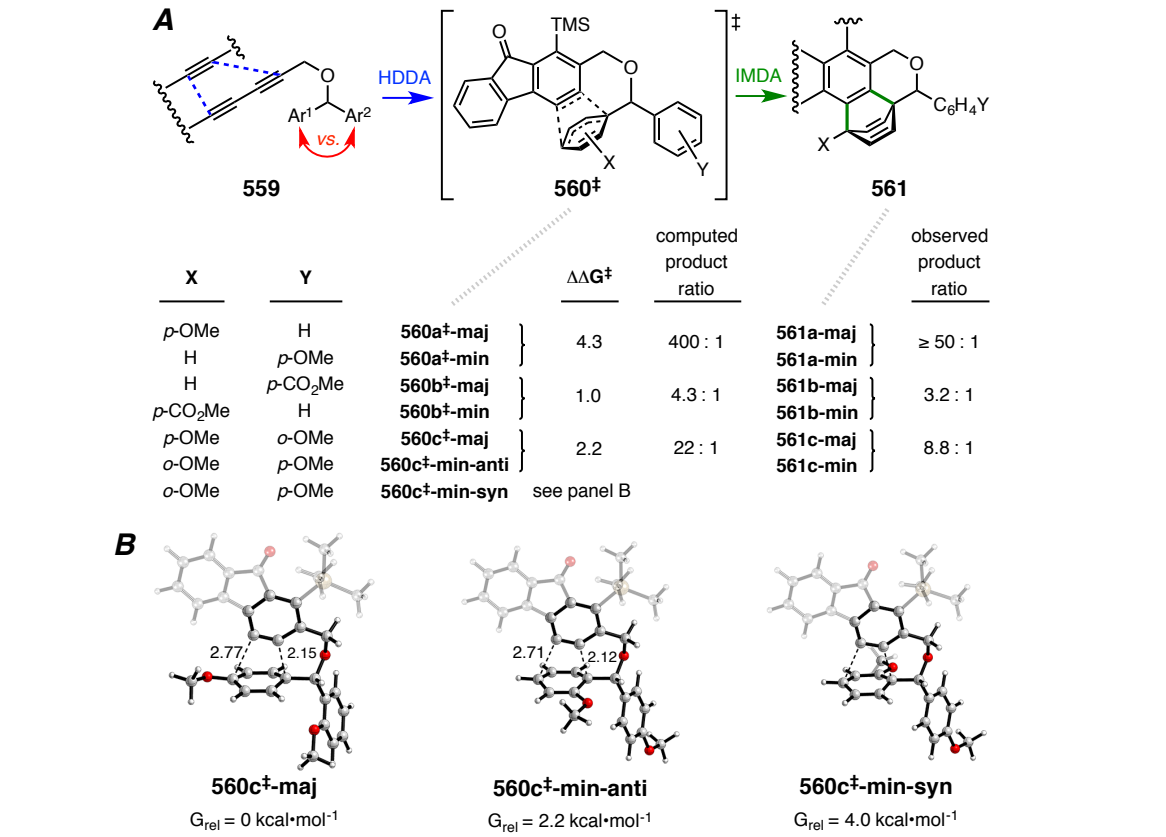


**Figure 23.** Selectivity in the competitive IMDA trapping of HDDA-generated benzynes

I have examined whether DFT calculations are effective at rationalizing these observed selectivities. Specifically, I have computed [SMD(chloroform)/M06-2X/6-31G(d)] the transition state structures for the competing IMDA trapping reactions of the benzynes derived from **559a**, **559b**, and **559c**. These lead via **560**‡ (Figure 23A) to the major and minor products of **561a**, **561b**, and **561c**. Also given in Figure 23A are the differences in computed free energy of activation ($\Delta\Delta G^{\ddagger}$) along with the associated computed and experimentally observed product ratios. DFT does a good job of accounting for the relative energies of the competing TS structures for the trapping of the benzyne. The geometries of those TSs all indicated a high degree of asynchroneity to these concerted IMDA reactions (Figure 23B). I was also successful in using DFT to account for the sense of diastereoselectivity (i.e., *anti*) observed in the formation of **561c-min**. The

**560c$^{‡}$-min-anti** was favored by 1.8 kcal•mol$^{-1}$ over the alternative **560c$^{‡}$-min-anti** (Figure 22B), presumably reflecting the greater steric congestion in the latter, which possesses *cis*-(and *endo*-)oriented methoxy and aryl groups.

# Chapter 6. De novo synthesis of benzenoids via HDDA

The hexadehydro-Diels–Alder cascade involves a sequential net 4+2 cycloisomerization reaction between a 1,3-diyne and a diynophile to produce a benzyne intermediate,[40] followed by one of several different modes of trapping reactions.[29,66,67,68] This cascade constitutes a powerful and versatile strategy for synthesis of benzenoid derivatives in

---

[66] (a) Yun, S. Y.; Wang, K.; Lee, N.; Mamidipalli, P.; Lee, D. Alkane C–H insertion by aryne intermediates with a silver catalyst. *J. Am. Chem. Soc.* **2013**, *135*, 4668−4671. (b) Karmakar, R.; Mamidipalli, P.; Yun, S. Y.; Lee, D. Alder-ene reactions of arynes. *Org. Lett.* **2013**, *15*, 1938−1941. (c) Wang, K.; Yun, S. Y.; Mamidipalli, P.; Lee, D. Silver-mediated fluorination, trifluoromethylation, and trifluoromethylthiolation of arynes. *Chem. Sci.* **2013**, 4, 3205−3211. (d) Mamidipalli, P.; Yun, S. Y.; Wang, K.; Zhou, T.; Xia, Y.; Lee, D. Formal hydrogenation of arynes with silyl $C_{\beta}$–H bonds as an active hydride source. *Chem. Sci.* **2014**, *5*, 2362−2367. (e) Lee, N.; Yun, S. Y.; Mamidipalli, P.; Salzman, R. M.; Lee, D.; Zhou, T.; Xia, Y. Hydroarylation of arynes catalyzed by silver for biaryl synthesis. *J. Am. Chem. Soc.* **2014**, 136, 4363−4368. (f) Karmakar, R.; Yun, S. Y.; Wang, K.; Lee, D. Regioselectivity in the nucleophile trapping of arynes: the electronic and steric effects of nucleophiles and substituents. *Org. Lett.* **2014**, *16*, 6−9. (g) Karmakar, R.; Yun, S. Y.; Chen, J.; Xia, Y.; Lee, D. Benzannulation of triynes to generate functionalized arenes by spontaneous incorporation of nucleophiles. *Angew. Chem. Int. Ed.* **2015**, *54*, 6582−6586. (h) Karmakar, K.; Ghorai, S.; Xia, Y.; Lee, D. Synthesis of phenolic compounds by trapping arynes with a hydroxy surrogate. *Molecules* **2015**, *20*, 15862−15880. (i) Karmakar, R.; Wang, K.-P.; Yun, S. Y.; Mamidipalli, P.; Lee, D. Hydrohalogenative aromatization of multiynes promoted by ruthenium alkylidene complexes. *Org. Biomol. Chem.* **2016**, *14*, 4782–4788.

[67] (a) Vandavasi, J. K.; Hu, W.; Hsiao, C.; Senadia, G. C.; Wang, J. J. A new approach for fused isoindolines via hexadehydro-Diels–Alder reaction (HDDA) by Fe(0) catalysis. *RSC Adv.* **2014**, *4*, 57547−57552. (b) Liang, Y.; Hong, X.; Yu, P.; Houk, K. N. Why alkynyl substituents dramatically accelerate hexadehydro-Diels–Alder (HDDA) reactions: stepwise mechanisms of HDDA cycloadditions. *Org. Lett.* **2014**, *16*, 5702−5705. (c) Nobusue, S.; Yamane, H.; Miyoshi, H.; Tobe, Y. [4.2](2,2')(2,2')Biphenylophanetriyne: a twisted biphenylophane with a highly distorted diacetylene bridge. *Org. Lett.* **2014**, *16*, 1940−1943. (d) Kerisit, N.; Toupet, L.; Larini, P.; Perrin, L.; Guillemin, J.; Trolez, Y. Straightforward synthesis of 5-bromopenta-2,4-diynenitrile and its reactivity towards terminal alkynes: a direct access to diene and benzofulvene scaffolds. *Chem. - Eur. J.* **2015**, *21*, 6042−6047. (e) Watanabe, T.; Curran, D. P.; Taniguchi, T. Hydroboration of arynes formed by hexadehydro-Diels–Alder cyclizations with N-heterocyclic carbene boranes. *Org. Lett.* **2015**, *17*, 3450−3453. (f) Chen, Z.; Shan, W.; Yin, J.; Yu, G.; Liu, S. Efficient construction of carbazole derivatives via new benzyne precursors of four acetylene modules. *Acta Chimica Sinica* **2015**, *73*, 1007–1012. (g) Zhang, M.-X.; Shan, W.; Chen, Z.; Yin, J.; Yu, G.-A.; Liu, S. H. Diels–Alder reactions of arynes in situ generated from DA reaction between bis-1,3-diynes and alkynes. *Tetrahedron Lett.* **2015**, *56*, 6833–6838.

[68] (a) Niu, D.; Hoye, T. R. The aromatic ene reaction. *Nat. Chem.* **2014**, 6, 34−40. (b) Chen, J.; Baire, B.; Hoye, T. R. Cycloaddition reactions of azide, furan, and pyrrole units with benzynes generated by the hexadehydro-Diels–Alder (HDDA) reaction. *Heterocycles* **2014**, *88*, 1191−1200. (c) Woods, B. P.; Baire, B.; Hoye, T. R. Rates of hexadehydro-Diels–Alder (HDDA) cyclizations: impact of the linker structure. *Org. Lett.* **2014**, *16*, 4578−4581. (d) Woods, B. P.; Hoye, T. R. Differential scanning calorimetry (DSC) as a tool for probing the reactivity of polyynes relevant to hexadehydro-Diels–Alder (HDDA) cascades. *Org. Lett.* **2014**, *16*, 6370−6373. (e) Pogula, V. D.; Wang, T.; Hoye, T. R. Intramolecular [4 + 2] trapping of a hexadehydro-Diels–Alder (HDDA) benzyne by tethered arenes. *Org. Lett.* **2015**, *17*, 856−859. (f) Luu Nguyen, Q.; Baire, B.; Hoye, T. R. Competition between classical and hexadehydro-Diels–Alder (HDDA) reactions of HDDA triynes with furan. *Tetrahedron Lett.* **2015**, *56*, 3265−3267. (g) Chen, J.; Palani, V.; Hoye, T. R. Reactions of HDDA-derived benzynes with sulfides: mechanism, modes, and three-component reactions. *J. Am. Chem. Soc.* **2016**, *138*, 4318–4321.

which the benzene ring itself has been assembled in de novo fashion from the six reacting alkyne carbon atoms. The purely thermal nature of the reaction conditions lends itself to the discovery of new types of aryne trapping reactions that can be complementary to those possible with arynes generated by conventional[69] means.

## 6.1 Synthesis of carbazoles via HDDA reaction[70]

### *6.1.1 Introduction*

Carbazoles have a long[71] and rich history in the fields of heterocyclic and medicinal chemistries and recently have garnered considerable attention as a chromophoric platform for the development of organic electroluminescent[72] materials. Hundreds of carbazole-containing alkaloid secondary metabolites are known.[73] Collectively these exhibit manifold categories of bioactivity.[74]

Numerous approaches for carbazole synthesis use construction of one of the benzenoid rings as a strategic tactic.73,[75] Methods using condensation, elimination, or oxidative aromatization reactions are common. Cyclizations or cycloadditions involving alkynes or allenes have also been used. These often give rise to the new six-membered carbocycle at precisely the oxidation state of benzene. The examples shown in Figures 24A–C include

---

[69] For a summary of these methods see, e.g.: Tadross, P. M.; Stoltz, B. M. A comprehensive history of arynes in natural product total synthesis. *Chem. Rev*. **2012**, *112*, 3550–3577 and references therein.

[70] This section is largely adapted from: Wang, T.; Hoye, T. R. Hexadehydro-Diels–Alder (HDDA)-enabled carbazolyne chemistry: single step, de novo construction of the pyranocarbazole core of alkaloids of the murraya koenigii (curry tree) family. *J. Am. Chem. Soc.* **2016**, *138*, 13870–13873.

[71] Campbell, N.; Barclay, B. M. Recent advances in the chemistry of carbazole.*Chem. Rev.* **1947**, 359-380.

[72] Jiang, H.; Sun, J.; Zhang, J. A review on synthesis of carbazole-based chromophores as organic light-emitting materials. *Curr. Org. Chem.* **2012**, *16*, 2014–2025.

[73] (a) Knölker, H.-J.; Reddy, K. R. Isolation and synthesis of biologically active carbazole alkaloids. *Chem. Rev*. **2002**, *102*, 4303–4427. (b) Knölker, H.-J.; Reddy, K. R. In *The Alkaloids: Chemistry and biology of carbazole alkaloids*; Cordell, G. A., Ed.; Academic Press: New York, 2008; Vol. 65, pp 1–430. (c) Occurrence, biogenesis, and synthesis of biologically active carbazole alkaloids.Schmidt, A. W.; Reddy, K. R.; Knölker, H.-J. *Chem. Rev*. **2011**, *112*, 3193–3328.

[74] Głuszyńska, A. Biological potential of carbazole derivatives. *Eur. J. Med. Chem*. **2015**, *94*, 405–426.

[75] For recent reviews of carbazole synthesis see: (a) Roy, J.; Jana, A. K.; Mal, D. Recent trends in the synthesis of carbazoles: an update. *Tetrahedron*, **2012**, *68*, 6099–6121. (b) Bauer, I.; Knölker, H.-J. Synthesis of pyrrole and carbazole alkaloids. *Top. Curr. Chem.* **2012**, *309*, 203–253.

electrocyclic ring closure,[76] [2+2+2] cyclization of three isolated alkyne units,[77] and the tetradehydro-Diels–Alder[78,50] reaction.

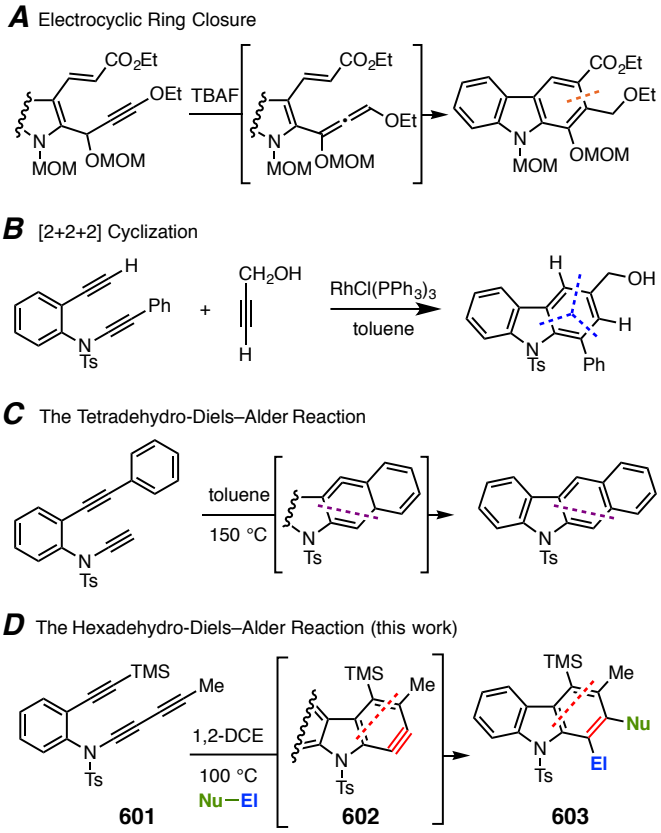


**Figure 24.** (A–C) Previous synthesis of carbazoles from alkyne-containing substrates and (D) HDDA-enabled carbazole synthesis

Here we describe a new strategy for carbazole assembly that capitalizes on the HDDA cascade. The relevant and enabling intermediate is a carbazolyne (**602**, Figure 24D), a rare member[79] of the family of arynes. We have used a number of different trapping

[76] Tohyama, S.; Choshi, T.; Azuma, S.; Fujioka, H.; Hibino, S. A new synthetic route to the 1-oxygenated carbazole alkaloids, mukonine and clausine E (clauzoline I). *Heterocycles*, **2009**, *79*, 955–965.

[77] Witulski, B.; Alayrac, C. A highly efficient and flexible synthesis of substituted carbazoles by rhodium-catalyzed inter- and intramolecular alkyne cyclotrimerizations. *Angew. Chem. Int. Ed.* **2002**, *41*, 3281–3284.

[78] Martínez-Esperón, M. F.; Rodríguez, D.; Castedo, L.; Saá, C. Synthesis of carbazoles from ynamides by intramolecular dehydro Diels−Alder reactions. *Org. Lett.* **2005**, *7*, 2213–2216.

[79] (a) Brown, R. F. C.; Choi, N.; Coulston, K. J.; Eastwood, F. W.; Ercole, F.; Horvath, J. M.; Mattinson, M.; Mulder, R. J.; Ooi, H. C. Pyrolytic generation and rearrangement of n-substituted 1,2-

agents Nu–El to capture the intermediate carbazolynes. Collectively, these demonstrate the versatility of this approach for preparing carbazoles bearing a wide variety of substituents and other structural variations. Finally, we further demonstrate the strategic power of this approach through efficient chemical syntheses of the mahanine alkaloids mahanimbine (**612**)[80] and koenidine (**619**)[81] in which three of the four rings in these pyranocarbazoles are constructed in a single operation.

**Table 9.** HDDA construction[a] of carbazoles **606** from triyne substrates **604** via **605**

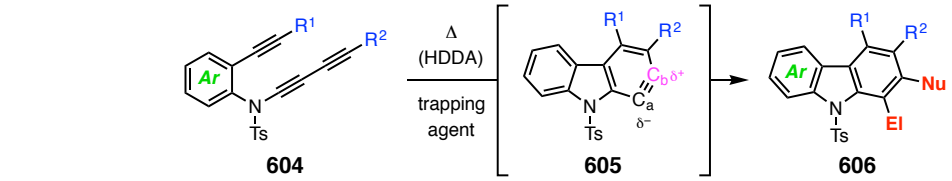


| Product (trapping agent, isolated yield) | | | | |
|---|---|---|---|---|
| 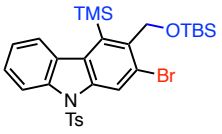 | 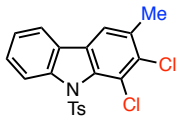 | 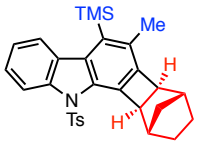 | 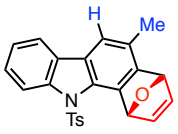 | 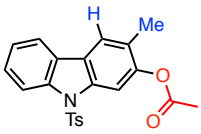 |
| **606a** (NEt$_3$•HBr,[b] 87%) | **606b** (Li$_2$CuCl$_4$,[c] 94%) | **606c** (norbornene,[d] 37%) | **606d** (furan,[c] 72%) | **606e** (acetic acid,[b] 71%) |
| 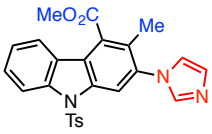 | 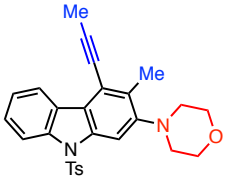 | 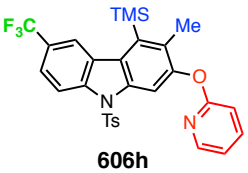 | 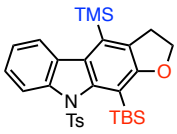 | 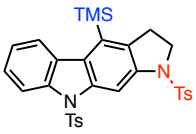 |
| **606f** (imidazole,[c] 79%) | **606g** (morpholine,[c] 80%) | **606h** (2-pyridone,[d] 97%) | **606i** (internal OTBS, 72%) | **606j** (internal NHTs, 72%) |

didehydrocarbazoles. *Liebigs Ann./Recueil* **1997**, 1931−1940. (b) Goetz, A. E.; Silberstein, A. L.; Corsello, M. A.; Garg, N. K. Concise enantiospecific total synthesis of tubingensin A. *J. Am. Chem. Soc.* **2014**, *136*, 3036−3039.

[80] Isolation: (a) Joshi, B. S.; Kamat, V. N.; Gawd, D. H. On the structures of girinimbine, mahanimbine, isomahanimbine, koenimbidine and murrayacine. *Tetrahedron* **1970**, *26*, 1475−1482. Recent syntheses: (b) Hesse, R.; Gruner, K. K.; Kataeva, O.; Schmidt, A. W.; Knölker, H.-J. Efficient construction of pyrano[3,2-a]carbazoles: application to a biomimetic total synthesis of cyclized monoterpenoid pyrano[3,2-a]carbazole alkaloids. *Chem. Eur. J.* **2013**, *19*, 14098–14111. (c) Li, X.; Song, W.; Tang, W. Rhodium-catalyzed tandem annulation and (5 + 1) cycloaddition: 3-hydroxy-1,4-enyne as the 5-carbon component. *J. Am. Chem. Soc.* **2013**, *135*, 16797–16800.

[81] Isolation: (a) Narasimhan, N. S.; Paradkar, M. V.; Chitguppi, V. P.; Kelkar, S. L. *Indian J. Chem.* **1975**, *13*, 993−999. Recent synthesis: (b) Schuster, C.; Rönnefahrt, M.; Julich-Gruner, K. K.; Jäger, A.; Schmidt, A. W.; Knölker, H.–J. Synthesis of the pyrano[3,2-a]carbazole alkaloids koenine, koenimbine, koenigine, koenigicine, and structural reassignment of mukonicine. *Synthesis* **2016**, *48*, 150–160.

[a]Reactions were carried out in 1,2-dichloroethane (DCE), chloroform, or THF at temperatures of 90–100 °C with an initial concentration of **604** = 0.02 M; the following amounts of external trapping agents were used: [b]2 equiv, [c]5 equiv, [d]10 equiv.

In Table 9 we have shown examples of the types of carbazoles that can be prepared using this HDDA approach. Many different types of trapping agents, both internal (tethered) and external, are effective, and often highly so. Various substituents $R^1$ and $R^2$ are accommodated on the alkyne termini [e.g., TMS, H, $CO_2Me$, and alkynyl (on the diynophile) and alkyls (on the diyne)] and the benzene ring in the triyne **604** can carry an additional substituent (e.g., **606h**). Taken together, these types of modifications can be envisioned to allow for considerable flexibility in the substitution pattern that can be accessed in the carbazole products **606**.

**Table 10.** Computed (DFT) geometric distortion of **602** vs. analogous benzynes lacking the TMS and/or having the electronegative NTs moiety replaced by a methylene group

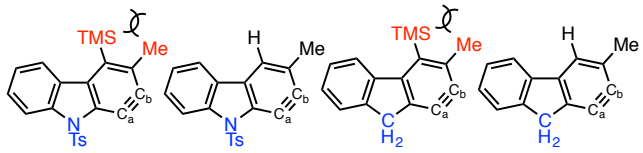


| Angle (°) | 602 | 602(–TMS) | 602(CH2) | 602(CH2–TMS) |
|---|---|---|---|---|
| ∠a | 114.8° | 117.7° | 120.8° | 125.3° |
| ∠b | 138.8° | 136.0° | 134.1° | 129.9° |
| ∠b–∠a | 24.0° | 18.3° | 13.3° | 4.6° |

For trapping reactions that involve inequivalent trapping atoms or groups, the nucleophilic component could add to either $C_a$ or $C_b$ in the electrophilic carbazolynes **605**. However, we never observed an isomeric product arising from attack of the nucleophile at $C_a$ (cf. **606a**, **606e**, **606f**, **606g**, and **606h**).[82] This essentially perfect level of regioselectivity is deserving of comment. Aryne **605** ($R^1$ = TMS and $R^2$ = Me; i.e., **602** in Figure 24) is computed [DFT: SMD($ClCH_2CH_2Cl$)/M06-2X/6-31G(d)] to be significantly distorted, having a very large difference of 24° (see Table 10) between the

[82] Our analytical methods should have allowed detection of as little as 1% of such a byproduct.

intra-annular angles at its nominally sp-hybridized atoms $C_a$ vs. $C_b$. It is now well established[57] that this ring-distortion allows one to account for (or predict in advance) the sense of the regioselectivity shown by unsymmetrical trapping agents of the Nu–El class. Consistent with this, the nucleophilic portion of the trapping agent (Nu) shows a high preference for adding to $C_b$, the atom having higher in-plane p-character and, accordingly, greater electrophilicity ($\delta^+$) in the reactive, strained alkyne. This is portrayed in **605** at the top of Table 9.

To gain a better sense of the factors that contribute to the highly biased geometry of these carbazolynes, we also calculated the extent of distortion in several analogs of **602**. These are shown in Table 10. The remote TMS substituent is more than an innocent bystander. Its removal results in a reduction of the ring distortion (see **602$_{(-TMS)}$**, where $\angle b - \angle a$ = 18.3°), presumably a response to the change in the buttressing force the TMS imposes on its adjacent substituents. Nonetheless, the trapping of **605** ($R^1$ = H and $R^2$ = Me) with, for example, acetic acid also proceeded with high regioselectivity, giving **606e** as the only observed product. To understand the impact of the electronegative NTs substituent adjacent to carbon a, the geometries of the methylene replacement analogs **602$_{(CH2)}$** and **602$_{(CH2\text{-}TMS)}$** were also computed. These show, in turn, a substantial reduction in the extent of the internal distortion ($\angle b - \angle a$ = 13.3° and 4.6°, respectively), which shows that the inductive effect of the NTs is a major contributor to the polarization of the alkyne in carbazolyne **602**. A similar effect has been observed for the computed geometric distortions of 6,7-indolyne vs. 4,5-indanyne.[57b]

We then explored whether this type of reaction could serve as an enabling strategy for the synthesis of mahanine alkaloids like mahanimbine (**612**, Scheme 22) and koenidine (**619**, Scheme 23). These natural substances are found in *Murraya koenigii* (the curry tree) and have been ingested by humans, including for medicinal purposes, for eons. Koenidine was recently reported to show insulin sensitizing and blood glucose lowering properties in mice.[83] Each of the carbazoles **612** and **619** bears a fused pyran ring, a hallmark of

[83] Patel, O. P. S.; Mishra, A.; Maurya, R.; Saini, D.; Pandey, J.; Taneja, I.; Raju, K. S. R.; Kanojiya, S.; Shukla, S. K.; Srivastava, M. N.; Wahajuddin, M.; Tamrakar, A. K.; Srivastava, A. K.; Yadav, P. P.

many of the carbazoles found in *Murraya koenigii*, indigenous to Asia.

Enals were recently reported to produce benzopyrans (or chromenes) by trapping *o*-benzyne.[84] If the engagement of the benzyne by the nucleophilic carbonyl oxygen atom in the enal initiates the capture event, then the distortion present in a benzyne like **602** should dictate the proper outcome required for assembly of the requisite skeleton for mahanimbine (**612**) and koenidine (**619**). In the event (Scheme 22), when triyne **601** was heated in the presence of citral (**609**, 2.0 equiv), a very clean transformation to **611** allowed its isolation in 89% yield after chromatographic purification. This reaction proceeds, presumably, through the intermediate 1,3-zwitterion **610a**, benzoxetene **610b**, and alkenyl quinonemethide **610c**, prior to the ultimate electrocyclic ring-closure to the pyran. This transformation proceeds with 100% atom efficiency and is mediated solely by thermal energy—no reagents or catalysts are used. Removal of the TMS and Ts groups in **611** proved to be trivial under the action of tetrabutylammonium fluoride (TBAF) in THF at 80 °C, which smoothly provided **612**.

**Scheme 22.** Key step in the enal trapping of benzyne **602**, establish-ing the tetracyclic pyranocarbazole core structure of mahanimbine (**612**)

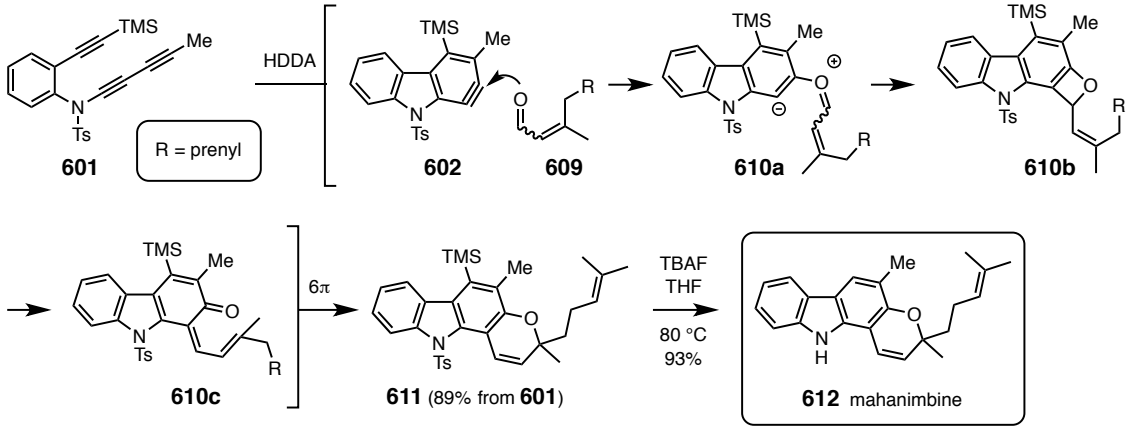


To prepare koenidine (**619**), the triyne **617**, the dimethoxy analog of **601**, was required.

---

Naturally occurring carbazole alkaloids from murraya koenigii as potential antidiabetic agents. *J. Nat. Prod*. **2016**, *79*, 1276–1284.

[84] Zhang, T.; Huang, C.; Wu, L. A facile synthesis of 2H-chromenes and 9-functionalized phenanthrenes through reactions between α,β-unsaturated compounds and arynes. *Eur. J. Org. Chem*. **2012**, 3507–3519.

The preparation of this substrate, starting from the commercially available bromide **613**, is shown in Scheme 23. This is representative of the strategy used to prepare each of the HDDA substrates used in this study. Particularly noteworthy is the construction of the ynamide bond[85] in **616** via the 1,2-dichlorovinylsulfonamide **615**.[86] In our hands this strategy proved to be more reproducible and serviceable for the sulfonamide **614** than one using the ethynyl iodonium salt HC≡C(Ph)I$^+$TfO$^-$.[87] Heating **617** with β,β-dimethylacrolein followed by TBAF treatment to strip away the TMS and Ts groups completed this efficient synthesis of koenidine.

**Scheme 23.** Synthesis of koenidine (**619**)

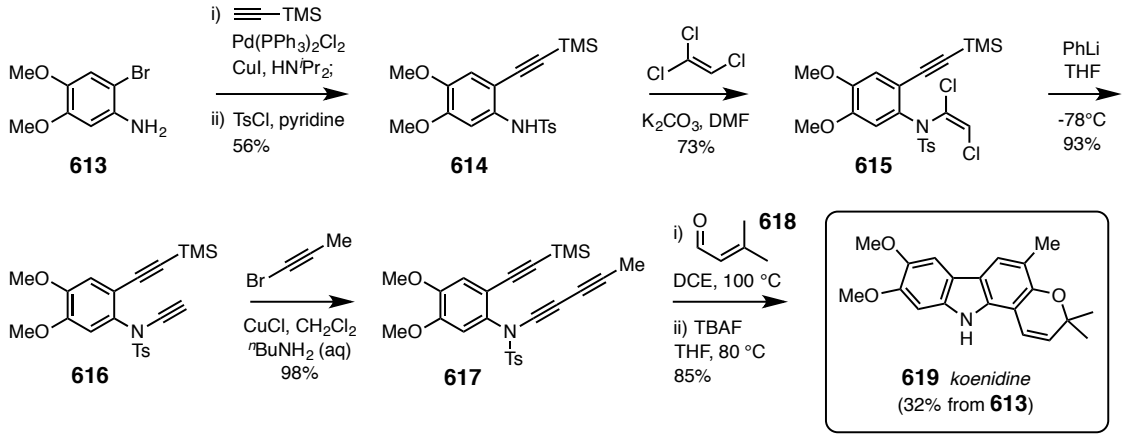


Finally and as evidence of the potential that this benzyne plus enal trapping reaction has for the construction of additional types of polycyclic skeletons, we show the reaction between the triyne **620a** (which happens to bear a trifluoromethyl substituent[88] on the

[85] DeKorver, K. A.; Li, H.; Lohse, A. G.; Hayashi, R.; Lu, Z.; Zhang, Y.; Hsung, R. P. Ynamides: a modern functional group for the new millennium. *Chem. Rev*. **2010**, *110*, 5064–5106.

[86] Mansfield, S. J.; Campbell, C. D.; Jones, M. W.; Anderson, E. A. A robust and modular synthesis of ynamides. *Chem. Commun*. **2015**, *51*, 3316–3319.

[87] (a) Witulski, B.; Stengel, B. Rhodium(I)-catalyzed [2+2+2] cycloadditions with N-functionalized 1-alkynylamides: a conceptually new strategy for the regiospecific synthesis of substituted indolines. *Angew. Chem., Int. Ed.* **1999**, *38*, 2426–2430. (b) Alayrac, C.; Schollmeyer, D.; Witulski, B. First total synthesis of antiostatin $A_1$, a potent carbazole-based naturally occurring antioxidant. *Chem. Commun.* **2009**, 1464–1466.

[88] Tresse, C.; Guissart, C.; Schweizer, S.; Bouhoute, Y.; Chany, A.-C.; Goddard, M.-L.; Blanchard, N.; Evano, G. Practical methods for the synthesis of trifluoromethylated alkynes: oxidative trifluoromethylation of copper acetylides and alkynes. *Adv. Synth. Catal.* **2014**, *356*, 2051–2060.

diynophile) and the designer exocyclic enal **621a** (Scheme 24).[89] When heated at 120 °C for 15 h,[90] the spirocyclic pyran **622a** was smoothly produced. Other exocyclic enals containing different ring systems (eg., six-membered, saturated ring in **621b** and five-membered, aromatic ring in **621c**) can also be used as efficient trapping agents to give the desired spiropyran products in moderate to excellent yields (94% for **622b**, 72% for **622c**).

**Scheme 24.** Trapping reaction of exocyclic enal **621** to introduce the spirocyclic pyran subunit in product **622**

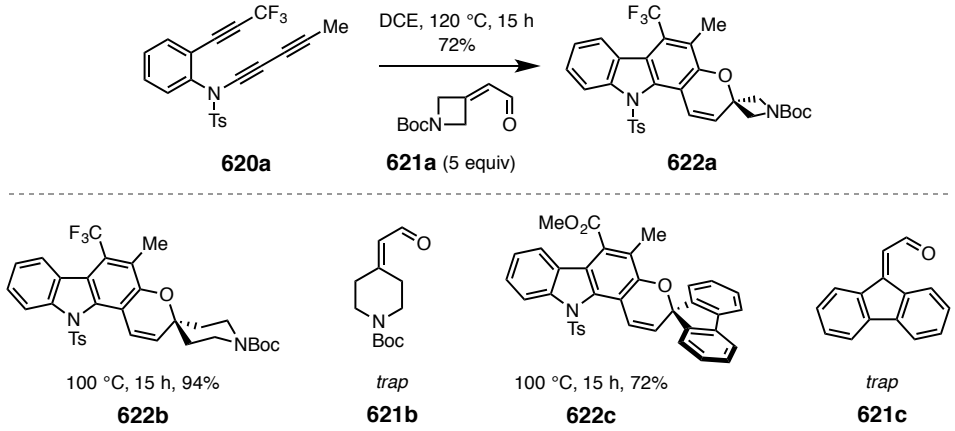


In summary, we have shown that an HDDA cascade is a general strategy for the preparation of substituted carbazoles. The intermediate, unsymmetrical carbazolynes can be captured by a variety of nucleophilic trapping agents with perfect regioselectivity. Factors that contribute to the distortion of these intermediate arynes have been probed through a simple DFT study. Efficient reactions of carbazolynes with 3,3-disustituted enals comprise a key strategy for construction of the tetracyclic pyranocarbozole rings of the alkaloids mahanimbine (**612**) and koenidine (**619**). The de novo construction of a

[89] Burkhard, J. A.; Guérot, C.; Knust, H.; Rogers-Evans, M.; Carreira, E. M. Synthesis and structural analysis of a new class of azaspiro[3.3]heptanes as building blocks for medicinal chemistry. *Org. Lett.* **2010**, *12*, 1944–1947.

[90] (a) This HDDA cycloisomerization proceeds more slowly than the other examples reported here, consistent with the presence of the $CF_3$-group, one of the rare substituents that destabilizes adjacent radical character relative to a hydrogen atom. In turn, this outcome is entirely in line with previous mechanistic studies supporting the stepwise (diradical) nature of the HDDA cyclization reaction.[49]

highly substituted, central benzenoid ring constitutes a significant strategic advance.[66i,91]

## 6.2 Dichlorination of HDDA-generated benzyne[92]

Aryl chlorides are commonly encountered in, for example, agrochemicals, pharmaceuticals, natural products, and photonic materials. Aryl chlorides have also grown in importance as synthetic intermediates in light of improved methodologies capable of activating the relatively inert $C_{sp2}$-Cl bonds.[93] Classically, aryl chlorides are made from the Sandmeyer reaction or electrophilic aromatic halogenation. One of the benzyne trapping reactions we have reported[29] is that with an ammonium bromide salt to produce the monobromoarenes **625** (Figure 25A, Hal = Br). Since then, we also found that treatment with various ammonium chlorides can form monochloroarenes as well.

1,2-Dichlorobenzene derivatives are seen in target compounds of interest, as represented by the structures **626a-d** (Figure 25B). The preparation of *ortho*-dichlorinated arenes is more challenging than that of monochloroarenes. There are only a few reports of direct 1,2-dihalogenation of arynes. These are limited to (i) diiodination[94,95] (with $I_2$) or dibromination[94a] (with $Br_2$), in which the reactions tend to proceed less effectively for arynes more elaborate than those of benzyne itself (from anthranilic acid or *ortho*-TMSPhOTf)[94c] and (ii) vicinal, mixed fluorohalogenation via silver(I)-promoted, net addition of FCl, FBr, or FI to HDDA-generated benzynes.[66b] A strategy to make 1,2-dichlorinated arenes from triynes via the intermediate benzynes would be valuable to provide an orthogonal approach to such an important class of compounds.

---

[91] It was once deemed that "bonds within aromatic rings are not considered to have potential strategic character."Corey, E. J.; Howe, W. J.; Orf, H. W.; Pensak, D. A.; Petersson, G. General methods of synthetic analysis. Strategic bond disconnections for bridged polycyclic structures. *J. Am. Chem. Soc.* **1975**, *97*, 6116–6124.

[92] This part is largely adapted from: Niu, D.; Wang, T.; Woods, B. P.; Hoye, T. R. Dichlorination of (hexadehydro-Diels–Alder generated) benzynes and a protocol for interrogating the kinetic order of bimolecular aryne trapping reactions. *Org. Lett.* **2014**, 16, 254–257.

[93] Noyori, S.; Nishihara, Y. "Recent advances in cross-coupling reactions with aryl chlorides, tosylates, and mesylates." In *Applied Cross-Coupling Reactions*, pp. 177-202. Springer Berlin Heidelberg, 2013.

[94] a) Friedman, L.; Logullo, F. M. *Angew. Chem., Int. Ed.* **1965**, *4*, 239–240. b) Birkett, M. A.; Knight, D. W.; Little, P. B.; Mitchell, M. B. *Tetrahedron* **2000**, *56*, 1013. c) Perry, R. J.; Turner, S. R. *J. Org. Chem.* **1991**, *56*, 6573. d) Rodríguez-Lojo, D.; Cobas, A.; Peña, D.; Pérez, D.; Guitián, E. *Org. Lett.* **2012**, *14*, 1363–1365.

[95] Buchwald, S. L.; Lucas, E. A.; Davis, W. M. *J. Am. Chem. Soc.* **1989**, *111*, 397.

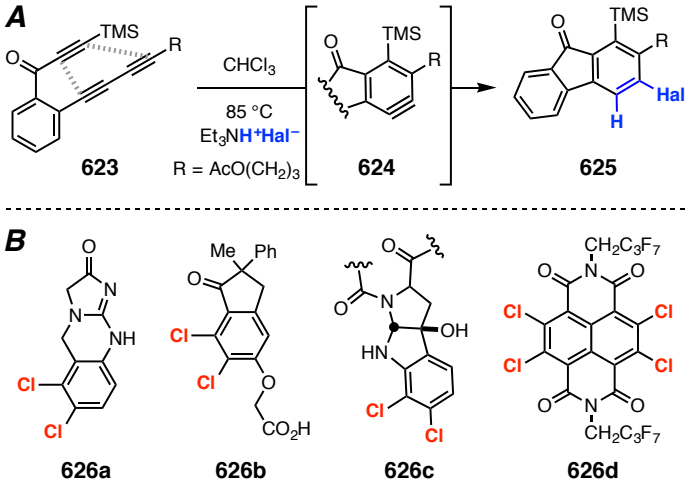


**Figure 25.** (A) Monohalogenation by benzyne trapping with ammonium halide salts (B) Examples of 1,2-dichlorinated target compounds: **626a**, Agrylin®, platelet reducing agent for treatment of thrombocytosis; **626b**, indacrinone, diuretic developed for treatment of gout and hypertension; **626c**, kutznerides, antimicrobial cyclic peptides; and **626d**, for organoelectronic applications

We initially explored the possibility of trapping the HDDA-generated benzyne **624** with either $I_2$ or $Br_2$. We were not surprised that this experiment did not produce observable amounts of the desired dihalobenzenes. In general, one practical feature of HDDA chemistry is that the alkynes in the triyne reactant need to be compatible with the agents intended to trap the intermediate benzynes under the conditions required to generate the benzyne. For example, addition of $Cl_2$ (and $Br_2$) to alkynes is relatively fast and is not expected to be compatible with most HDDA substrates. However, various metal halides are known to act as milder dihalogen surrogates for some dihalogen addition reactions.[96] We have learned that dilithium tetrachlorocuprate ($Li_2CuCl_4$) functions as an effective dichlorinating agent of HDDA-generated benzynes and report those observations here.

*My major contribution* to this project is optimization of reaction condition. I found the symmetrical tetrayne **627** a particularly well behaved substrate, and is later used for our

[96] a) Rodebaugh, R.; Debenham, J. S.; Fraser-Reid, B.; Snyder, J. P. *J. Org. Chem.* **1999**, *64*, 1758–1761. b) Uemura, S.; Sasaki, O.; Okano, M. *J. Chem. Soc. D*, **1971**, 1064–1065. c) Uemura, S.; Onoe, A.; Okano, M. *Bull. Chem. Soc. Jap.* **1974**, *47*, 692–697. See also, d) Kovacic, P.; Brace, N. O. *J. Am. Chem. Soc.* **1954**, *76*, 5491–5494. e) Yang, L.; Lu, Z.; Stahl, S. S. *Chem. Commun.* **2009**, 6460–6462.

initial explorations; it is both quite easy to prepare and has relatively high reactivity as a HDDA substrate. When a solution of **627** in $CH_3CN$ was heated in the presence of $FeCl_3$, no desired dichlorination product **628** was formed, as judged by GC or TLC analysis (entry 1, Figure 26A). The first indication of a successful outcome was seen with the use of $CuCl_2$ in acetonitrile. Addition of **627** and warming the resulting solution to 68 °C led to the formation of **628** in 67% yield following purification. Use of $Li_2CuCl_4$, formed in situ by mixing $CuCl_2$ with solid LiCl, in acetonitrile gave the desired dichlorination product in a similar yield. The efficiency of the reaction was increased when the solvent was changed to THF; **628** was isolated in 85% yield. Under these conditions, no noticeable amount of dihydrogenation (by THF)[33] or HCl addition products derived from competitive trapping of the intermediate benzyne was observed. Notably, dioxane was an ineffective solvent for this transformation, presumably due to the low solubility of $Li_2CuCl_4$, a feature that stands in contrast to its high solubility in THF.

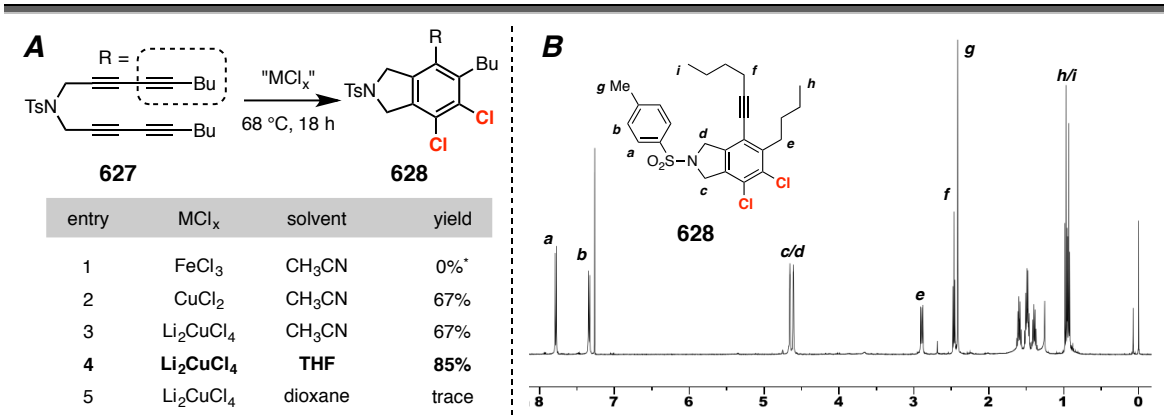


| entry | $MCl_x$ | solvent | yield |
|---|---|---|---|
| 1 | $FeCl_3$ | $CH_3CN$ | 0%* |
| 2 | $CuCl_2$ | $CH_3CN$ | 67% |
| 3 | $Li_2CuCl_4$ | $CH_3CN$ | 67% |
| **4** | **$Li_2CuCl_4$** | **THF** | **85%** |
| 5 | $Li_2CuCl_4$ | dioxane | trace |

**Figure 26.** (A) Identification of $Li_2CuCl_4$ as an effective reagent for dichlorination of the benzyne derived from tetrayne **627**. (B) $^1$H NMR spectrum of the *crude product mixture* following simple extractive workup of the entry 4 experiment.

Dawen Niu and Brian Woods further expanded the scope of substrate and demonstrated that various types of 1,2-dichlorinated products can be accessed.[92] The conditions are compatible with a considerable variety of functional groups in the benzyne precursor and resultant benzenoid product. In the course of the studies, Dr. Niu have also developed a strategy for probing some important kinetic aspects of benzyne trapping reactions. In

particular, competitive intramolecular Diels–Alder (IMDA) reaction of benzyne was used as an internal clock reaction and the observed change in ratio of the dichlorination to IMDA products as a function of the concentration of the dichlorinating agent was carefully measured. A first order dependence on the concentration of $Li_2CuCl_4$ can be concluded from this experiment.

## 6.3 Copper assisted terminal alkyne addition to HDDA-generated benzyne

The hexadehydro-Diels–Alder reaction has enabled numerous new methodologies to access highly substituted aromatic systems via de novo construction of benzene ring.[29,66,67,68] By capitalizing the broad scope of aryne chemistry, a wide variety of functionalities can be introduced in short fashion via trapping of nucleophilic reagents (Scheme 24A). Common instances include trapping with nitrogen, oxygen, sulfur, phosphine or halogen based nucleophiles to produce mono-substituted arene derivatives.

**Scheme 25.** (A) Previously developed modes of benzyne trapping reactions (B) Reported example of carbon-based nucleophiles used in benzyne trapping reactions (C) Previous strategy to achieve mono-functionalization with carbon-based groups on benzyne via a 2-step halogen trapping/coupling sequence

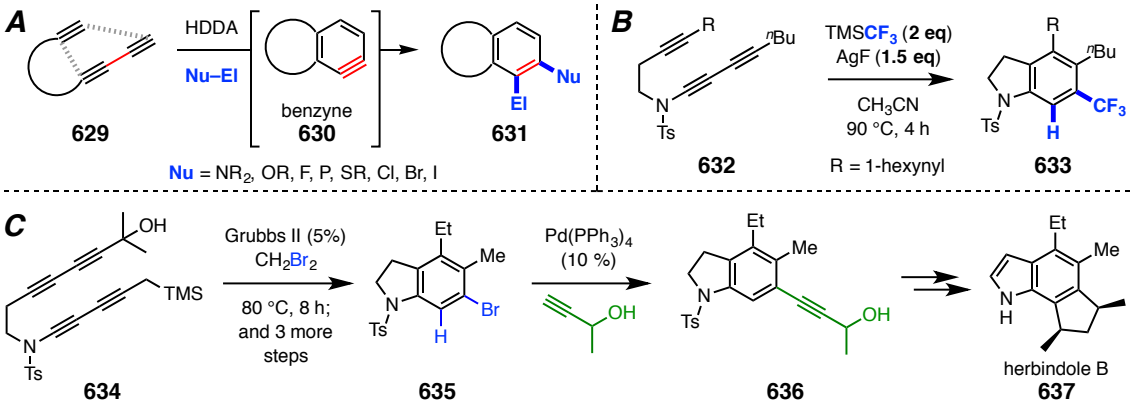


However, C–C bond formation in the trapping event was largely limited to cycloaddition reactions. Attempts to exploit carbon based nucleophiles and form mono-functionalized

product proved to be much more challenging due to their high basicity. One recently reported example introduces trifluoromethyl group via a silver catalyzed reaction.[66c] As shown in Scheme 25B, $TMSCF_3$ was used as the source of carbon, which was desilylated in presence of AgF. The in situ formed $AgCF_3$ then engages HDDA-generated benzyne (from **632**) to give compound **633** as the product. In this transformation, stoichiometric amount (1.5 eq) of silver was required to allow for an efficient trapping reaction.

Alternatively, a two-step halogen trapping/coupling reaction sequence was recently used to establish the C–C bond in benzyne trapping event.[66i] As shown in Scheme 25C, in the formal total synthesis of herbindole B (**637**), tetrayne **634** was converted to alkynyl-substituted arene **636** by first mono-bromination of the HDDA-generated benzyne. After functional group manipulation, a second palladium catalyzed coupling reaction was subsequently used to install the required alkynyl moiety. Therefore, methods to directly effect C–C bond formation and introduce carbon based substituents (eg., alkynyl) in the benzyne trapping event would be of great synthetic value.

**Scheme 26.** Reported alkyne–aryne coupling reaction catalyzed by copper

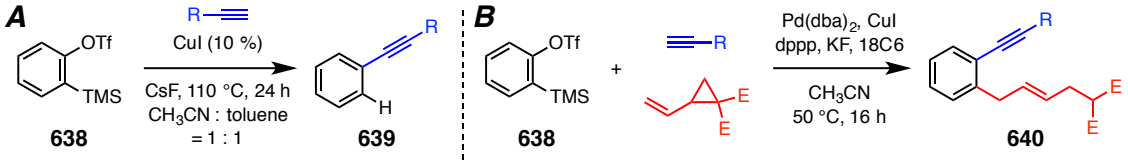


In 2008, Zhang group reported a copper catalyzed alkyne–aryne coupling reaction.[97] As shown in Scheme 26A, benzyne generated by Kobayshi method[34] (from **638**) was coupled with terminal alkyne (blue) in presence of 10 mol% of CuI to form phenyl-acetylene derivative **639**. An aryl copper species was proposed to be the key intermediate, which can further engage in other coupling events via transmetallation as demonstrated in the multicomponent reaction shown in Scheme 26B.[98]

[97] Xie, C.; Liu, L.; Zhang, Y.; Xu, P. Copper-catalyzed alkyne-aryne and alkyne-alkene-aryne coupling reactions. *Org. Lett.* **2008**, *10*, 2393–2396.

[98] Garve, L. K. B.; Werz, D. B. Pd-catalyzed three-component coupling of terminal alkynes, arynes, and vinyl cyclopropane dicarboxylate. *Org. Lett.* **2015**, *17*, 596−599.

Guided by these reports, we were wondering if a direct coupling between HDDA-generated benzyne and terminal alkyne is possible under copper catalysis. Such proposed event is challenging because (1) copper acetylide formation is suppressed under neutral HDDA condition, (2) commonly used bases for copper acetylide formation, such as tertiary amines, are also great trapping agents for benzyne. In 2015, Trolez and coworkers isolated an unexpected bicyclic product **644** in the reaction between terminal diyne **641** and bromodiyne **642** under Sonogashira coupling condition [$Pd(PPh_3)_2Cl_2$, CuI, $^iPr_2NH$, Scheme 27A].[41c] Tetrayne **643** was proposed to be the key intermediate, which would undergo HDDA cycloisomerization and Cu assisted terminal diyne (**641**) addition to give the ultimate product. Feng Xu, a postdoc researcher in our lab, further discovered that, in presence of substoichiometric amount of CuCl, phenylacetylene (**646**) could efficiently trap benzyne generated from tetrayne **645**, and form a mixture of two regioisomeric products **647** and **648** under oxygen-free condition.

**Scheme 27.** (A) Preiously proposed Cu assisted diyne addition to HDDA-generated benzyne. (B) Initial discovery by Feng Xu in our lab

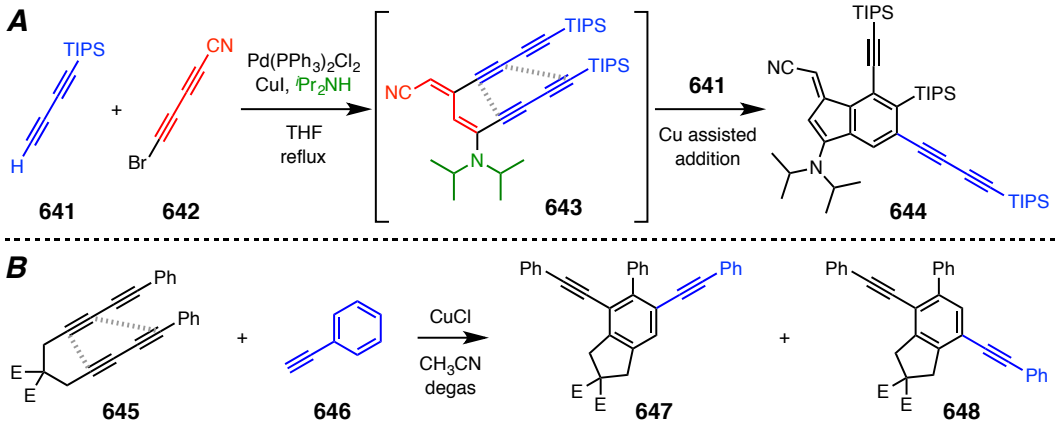


With this initial hit in hand, I have performed a series of systematic studies to optimize the reaction condition. Some selected results are shown in Table 11. The "best" set of reagents are 5% CuCl (catalyst), 1.1 equivalents of terminal alkyne and 0.5 equivalents of sodium ascorbate (NaAsc) in acetonitrile as the solvent (0.02 M). Starting with tetrayne **649** as the benzyne-precursor and phenylacetylene as the coupling alkyne, product **650** can be isolated in 91% yield as a ca. 2:1 mixture of regioisomers under standard

condition (entry 1, Table 11). Copper(I) catalyst is required for this coupling reaction to occur, as indicated by 0% yield when either CuCl or NaAsc [as the Cu(II) reducing agent] was absent in the reaction condition (entries 2–3). Sodium ascorbate merely served as a Cu(II) reducing agent, as evidenced by similar isolated yield after degassing the reaction solution (entry 4). Other frequently used Cu(I) sources like CuBr, CuI also works for this particular transformation (entries 5–6). Readily available copper (II) reagents like $CuSO_4$ can also be used (entry 7). However, CuCl gave the best isolated yield among all copper sources we have screened in the optimization.

**Table 11.** Reaction conditions optimization for Cu-assisted terminal alkyne addition to HDDA-generated benzyne

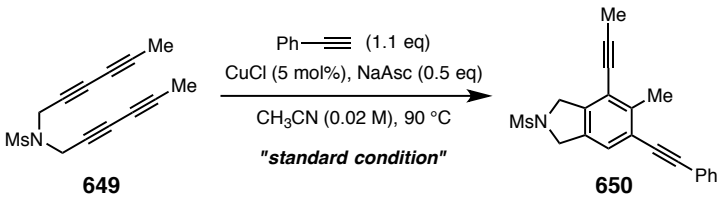


649 650

| entry | change to standard condition | yield |
|---|---|---|
| 1 | none | 91% |
| 2 | no CuCl | 0% |
| 3 | no NaAsc | 0% |
| 4 | no NaAsc, remove $O_2$ by bubbling $N_2$ | 89% |
| 5 | use 5 mol% CuBr instead of CuCl | 72% |
| 6 | use 5 mol% CuI instead of CuCl | 68% |
| 7 | use 5 mol% $CuSO_4$ instead of CuCl | 68% |
| 8 | use 1 mol% CuCl instead of 5 mol% | 76% |
| 9 | use 10 mol% CuCl instead of 5 mol% | 91% |
| 10 | use 3 eq phenylacetylene instead of 1.1 eq | 91% |
| 11 | 0.2 eq DIPEA added | 86% |
| 12 | 0.2 eq 2,6-lutidine added | 89% |
| 13 | 0.2 eq 1,10-phenanthroline added | 84% |
| 14 | 0.2 eq TMEDA added | 61% |
| 15 | use $CH_3CN$ : $H_2O$ = 1:1 as the solvent | 41% |

The effect of catalyst loading was also examined. Although 1 mol% of CuCl led to decreased yield (76%, entry 8), 5 mol% loading performed equally well compared to higher load of copper (entry 9). This result is especially remarkable because the active trapping agent in the reaction mixture is the copper-alkyne complex, which is less or

equal than only 5 mol% or 0.05 equivalent! This is in sharp contrast with almost all previous examples of benzyne trapping reactions, in which the trapping agent was always used in large excess to guarantee efficient trapping. Indeed, use of 3 equivalents of terminal alkyne gave essentially identical result compared to standard condition (1.1 equivalents, entry 10 vs entry 1). Alkyne only served to maintain a low concentration (≤ 5 mol%) of the active copper-containing trapping agent.

Despite the fact that no ligand or base is required for this Cu-assisted terminal alkyne addition to HDDA-generated benzyne, addition of several commonly used bases (eg., DIPEA, 2,6-lutidine, entries 11 and 12) or bidentate ligands (eg., 1,10-phenanthroline, TMEDA, entries 13 and 14) did not change the result of reaction significantly. It was also worth mentioning that, this alkyne addition reaction out-competed amine trapping event, which was believed to be one of the fastest benzyne trapping reaction. Finally, I found this reaction to be fairly tolerant of water. In fact, the reaction can be performed even in a 1:1 mixture of acetonitrile and water (entry 15)!

With the optimized condition in hand, I then tested to see if this methodology can be applied to other HDDA precursors. As shown in Figure 27, both triynes (**653**) and tetraynes (**651**, **652**, **654**) are good substrates for the reaction.

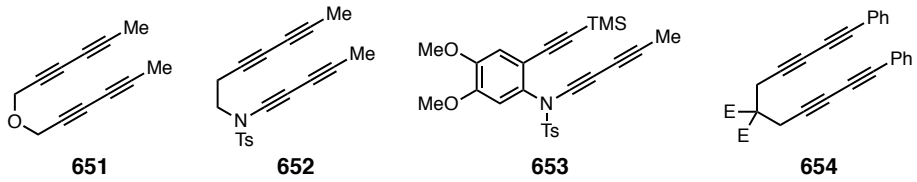


**651** **652** **653** **654**

**Figure 27.** Scope of HDDA substrates

More importantly, I have explored the scope of alkyne trapping agents and found this reaction to be tolerant of a great array of functionalities. As shown in Figure 28, both aromatic (**655a–f**) and aliphatic (**655g–l**) alkynes can be used as the coupling partner. For aromatic alkynes, the impact of electronic effects from substituents was minimal: Phenyl acetylene derivatives containing electron-withdrawing groups like fluorine atom (**655b**) or methoxycarbonyl (**655d**), or electron-donating substituents like *N*,*N*-diphenylamino

(**655c**) or methoxy (**655e, f**) on the phenyl ring are all great substrates for the reaction. ortho-Substitution on the phenyl ring (eg., **655e**) was also tolerated.

The chemo-selectivity in this chemistry is well-worth commenting. For example, we have previous showcased that alcohols, especially primary alcohols like **655i**, to be great trapping agents. The nucleophilic oxygen quickly attacks the highly electrophilic benzyne alkyne to form aryl ether products. However, under the standard condition reported here, alkynyl addition product (**656i**, not shown) was observed instead. This fascinating switch of reactivity suggested the possibility of a site-selective alkyne arylation reaction, in which copper is used to direct exclusive C–C bond coupling between benzyne and terminal alkyne in presence of numerous other functionalities. The potential of this chemistry is still under investigation.

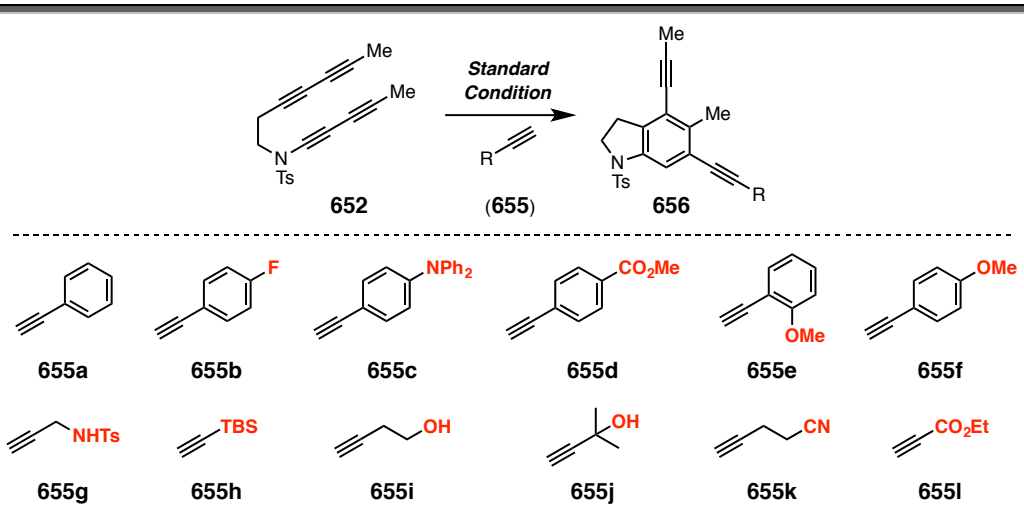


**Figure 28.** Scope of terminal alkyne

# ◊ Part III ◊

## Supplementary information

# Supplementary information for Chapters 2 – 3

## General Experimental Protocols

NMR ($^{1}$H and $^{13}$C) spectra were recorded on Bruker Avance 500 (500 MHz) or Varian Inova 500 (500 MHz) spectrometers. $^{1}$H NMR chemical shifts ($CDCl_3$, $CD_3OD$) are referenced to TMS (0.00 ppm) and $CHD_2OD$ (3.31 ppm), respectively. The designation "nfom" is used to denote non-first order multiplets. $^{13}$C NMR chemical shifts are referenced to chloroform (77.23 ppm) and methanol (49.15 ppm). The following format is used to report each resonance: chemical shift in ppm (multiplicity, *J* values (coupling constant(s)) in Hz, integral value, and assignment). Coupling constant analysis was aided by protocols we have reported elsewhere.[1] The skeleton of some of the more complex structures are numbered to simplify identification of the proton assignment. Infrared (IR) spectra were recorded of thin film samples on a ZnSe plate (ATR) on a Prospect MIDAC FT-IR spectrometer. Bands are reported in $cm^{-1}$. Mass spectrometric measurements were made: i) at low resolution on an Agilent 5975 GC-MS instrument using an electron impact ionization method at 70 eV and ii) at high resolution on a Bruker BioTOF II instrument using electrospray ionization and PEG as an internal calibrant. Optical rotation values were measured on a Rudolph Research Analytical (Autopol III) instrument.

MPLC refers to medium pressure liquid chromatography (50-200 psi) using hand-packed silica gel columns (25-35 μm, 60 Å pores) and a Waters HPLC pump outfitted with a Waters R401 differential refractive index detector. Flash chromatography was carried out on columns packed with E. Merck silica gel (40-63 μm). Reactions needing anhydrous conditions were carried out under an atmosphere of argon or nitrogen in flame- or oven-dried glassware. Anhydrous diethyl ether, THF, toluene, and methylene chloride were collected after being passed through a column of activated alumina immediately prior to use.

## Preparation procedures and characterization data for all key compounds

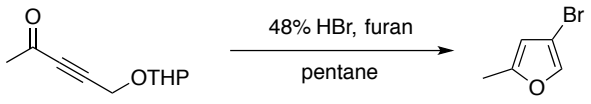


**205**

**Preparation of 4-bromo-2-methylfuran (205)**

Furan (2 mL) was added to a solution of 5-(tetrahydro-2*H*-pyran-2-yloxy)pent-3-yn-2-one[99] (495 mg, 2.72 mmol) in pentane (8 mL). The solution was cooled to 0 °C in an ice bath and concentrated aqueous hydrobromic acid (48%, 0.4 mL) was added. The reaction mixture was stirred at room temperature for 18 h and a solution of saturated aqueous $NaHCO_3$ was added. The resulting mixture was extracted with pentane (5 mL x 2). The combined organic layers were directly applied to a silica gel column and eluted with pentane. The eluent was concentrated on a rotary evaporator in an ambient temperature bath to a volume of ca. 0.3 mL. NMR analysis of this colorless solution allowed estimation of the percent content of 4-bromo-2-methylfuran **205** (est. 286 mg, 1.78 mmol, 65%). The $^1$H NMR and MS data were consistent with the structure of this known compound.[99] This material was carried forward into the next reaction.

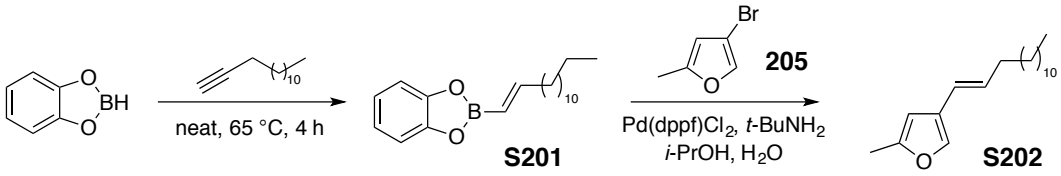


**Preparation of (*E*)-2-methyl-4-(tetradec-1-enyl)furan (S202) via (*E*)-2-(tetradec-1-enyl)benzo[d][1,3,2]dioxaborole (S201)**

[99] Abson, A.; Broom, N. J. P.; Coates, P. A.; Elder, J. S.; Forrest, A. K.; Hannan, P. C. T.; Hicks, A. J.; O'Hanlon, P. J.; Masson, N. D.; Pearson, N. D.; Pons, J. E.; Wilson, J. M. Chemistry of Pseudomonic Acid. Part 16 Aryl and Heteroaryl Ketone Derivatives of Monic Acid. *J. Antibiot.* **49**, 390–394 (1996).

Under an Ar atmosphere, a 20 mL vial was charged with catecholborane (2.3 mL, 19.2 mmol) and tetradecyne (4.7 mL, 19.1 mmol) and then sealed with a Teflon cap. The mixture was heated to 55 °C for 15 h. The resulting colorless liquid sample of **S201** was used directly without further purification.

To a solution of 4-bromo-2-methylfuran (**205**, 0.58 g, 3.6 mmol) in *i*-PrOH/$H_2O$ (11.5 mL/5.6 mL) was added Pd(dppf)$Cl_2$ (53.5 mg, 0.07 mmol, 2 mol%) and *t*-Bu$NH_2$ (1.15 mL, 10.9 mmol). (*E*)-2-(Tetradec-1-enyl)benzo[d][1,3,2]dioxaborole (**S201**, 3.8 mL) was added dropwise. The headspace was flushed with $N_2$ and the vessel was sealed with a Teflon cap. The mixture was heated to 80 °C for 26 h. The resulting mixture was directly filtered through a short plug of Celite® (EtOAc elution), the filtrate concentrated, and the residue chromatographed on silica (pure hexanes) to afford (*E*)-2-methyl-4-(tetradec-1-enyl)furan (**S202**, 0.95 g, 3.44 mmol, 96%) as a colorless oil.

**$^1$H NMR** ($CDCl_3$, 500 MHz) δ 7.19 (d, *J* = 0.4 Hz, 1H, *H5*), 6.16 (dt, *J* = 15.7, 1.6 Hz, 1H, ArC*H*=CHC$H_2$), 6.10 (dq, *J* = 0.4 and 1.0 Hz, 1H, *H3*), 5.86 (dt, *J* = 15.7, 6.9 Hz, 1H, ArCH=C*H*C$H_2$), 2.25 (d, *J* = 1.0 Hz, 3H, Ar-C$H_3$), 2.12 (ddt, *J* = 7.0, 1.5, 7.0 Hz, 2H, ArCH=CHC$H_2$), 1.41 (br quintet, 2H, CH=CHC$H_2$C$H_2$), 1.34–1.19 (m, 18H), and 0.88 (t, *J* = 7.0 Hz, 3H, C$H_2$C$H_3$).

**$^{13}$C NMR** (125 MHz, $CDCl_3$) δ 153.1, 137.9, 130.5, 125.7, 119.8, 103.7, 33.1, 32.2, 29.9 (4C), 29.8, 29.7, 29.6, 29.5, 22.9, 14.3, and 13.8.

**IR** (neat): 2924, 2853, 1687, 1606, 1544, 1464, 1381, 1126, 959, 917, 797, and 735 $cm^{-1}$.

**GC-LRMS** (ES, 70 eV): $t_R$ = 10.08 min. *m/z*: 276 ($M^+$), 135 ($M^+$-$C_{10}H_{21}$) and 121 ($M^+$-$C_{11}H_{23}$).

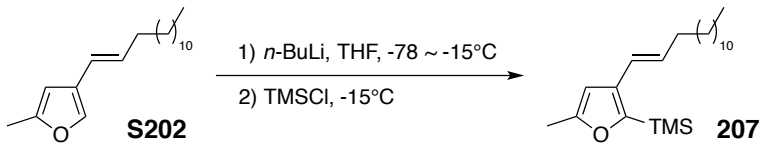


**S202** **207**

**Preparation of (*E*)-trimethyl(5-methyl-3-(tetradec-1-enyl)furan-2-yl)silane (207)**

To a dry 100 mL flask was added (*E*)-2-methyl-4-(tetradec-1-enyl)furan (**S202**, 0.95 g, 3.44 mmol) and THF (20 mL). The headspace was flushed with $N_2$ and the mixture was cooled to -78 °C in a dry ice-acetone acetone bath. *n*-BuLi (2.7 mL, 6.75 mmol, 2.5 M solution in hexanes) was added dropwise. The mixture was allowed to warm to -10 °C over 40 min, and freshly distilled TMSCl (0.74 g, 6.8 mmol) was added. The mixture was allowed to stir at room temperature for 1 h and saturated aqueous $NH_4Cl$ was added. The water layer was extracted with diethyl ether. The combined organic phase was dried over $Na_2SO_4$, filtered, and concentrated to give (*E*)-trimethyl(5-methyl-3-(tetradec-1-enyl)furan-2-yl)silane (**207**, 1.0 g, 3.0 mmol, 86%) as a colorless oil that was used without further purification.

**$^1$H NMR** ($CDCl_3$, 500 MHz) δ 6.31 (ddt, *J* = 15.6, 0.3, 1.5 Hz, 1H, ArC*H*=CH), 6.12 (br s, 1H, Ar*H*), 5.86 (dt, *J* = 15.5, 7.0 Hz, 1H, ArCH=C*H*), 2.27 (d, *J* = 0.9 Hz, 3H, Ar-C$H_3$), 2.13 (ddt, *J* = 7.0, 1.6, 7.0 Hz, 2H, CH=CHC$H_2$), 1.45–1.35 (m, 2H, CH=CHCH$_2$C$H_2$), 1.34–1.20 (m, 18H), 0.88 (t, *J* = 6.9 Hz, 3H, CH$_2$C$H_3$), and 0.29 (s, 9H, Si(C$H_3$)$_3$).

**$^{13}$C NMR** (125 MHz, $CDCl_3$) *δ* 156.4, 154.3, 135.5, 130.7, 121.1, 104.0, 33.3, 32.2, 29.9 (2C), 29.8, 29.7 (2C), 29.6, 29.4 (2C), 22.9, 14.4, 13.9, and 0.6.

**IR** (neat): 2954, 2923, 2853, 1248, 957, 841, 794, and 758 cm$^{-1}$.

**GC-LRMS** (ES, 70 eV): $t_R$ = 10.90 min. *m/z*: 348 ($M^+$), 333 ($M^+$-$CH_3$), 275 ($M^+$-TMS), and 73 ($TMS^+$).

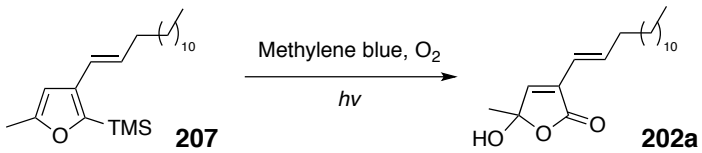


**Preparation of (±)-(*E*)-5-hydroxy-5-methyl-3-(tetradec-1-enyl)furan-2(5*H*)-one**

**(202a)**

Methylene blue (1 mg) was added to a solution of (*E*)-trimethyl(5-methyl-3-(tetradec-1-enyl)furan-2-yl)silane (**207**, 0.90 g, 2.59 mmol) in $CH_2Cl_2$ (50 mL) in a round bottomed flask. The mixture was cooled to -40 °C in a dry ice-acetone bath. $O_2$ was introduced into the solution via a fritted glass tube. A 175 W mercury lamp was placed directly above the reaction flask (distance < 5 cm). After 1.5 h full consumption of furan **207** was confirmed by TLC analysis. The mixture was concentrated and purified by flash column chromatography to give (*E*)-5-hydroxy-5-methyl-3- (tetradec-1-enyl)furan-2(5H)-one (**202a**) as a colorless waxy solid (602 mg, 1.95 mmol, 76%), whose spectral data closely matched those reported for this butenolide.[14]

**$^1$H NMR** (500 MHz, $CDCl_3$) δ 6.84 (br dt, *J* = 15.8, 7.1 Hz, 1H, CH=C*H*$CH_2$), 6.83 (br s, 1H, C(OH)($CH_3$)C*H*=C), 6.07 (dt, *J* = 15.8, 1.7 Hz, 1H, C*H*=C$HCH_2$), 2.87 (br s, 1H, -O*H*), 2.17 (ddt, *J* = 1.6, 7.1, 7.4 Hz, 2H, CH=CHC$H_2$), 1.71 (s, 3H, C(OH)-C$H_3$), 1.47–1.40 (m, 2H, CH=CHC$H_2$C$H_2$), 1.35–1.21 (m, 18H), and 0.88 (t, *J* = 7.0 Hz, 1H, $CH_2$C$H_3$).

**$^{13}$C NMR** (125 MHz, $CDCl_3$) δ 170.1, 144.0, 141.4, 131.1, 118.0, 104.1, 33.7, 32.1, 29.9 (3C), 29.8, 29.7, 29.6, 29.5, 28.9, 25.1, 22.9, and 14.3.

**IR** (neat): 3356, 2924, 2853, 1746, 1662, 1463, 1414, 1372, 1260, 1170, 1106, 1056, 971, and 931 $cm^{-1}$.

**HRMS** (ESI-TOF): Calcd for $(C_{19}H_{33}O_3)^+$ 309.2424. Found: 309.2412

**mp** 36–42 °C.

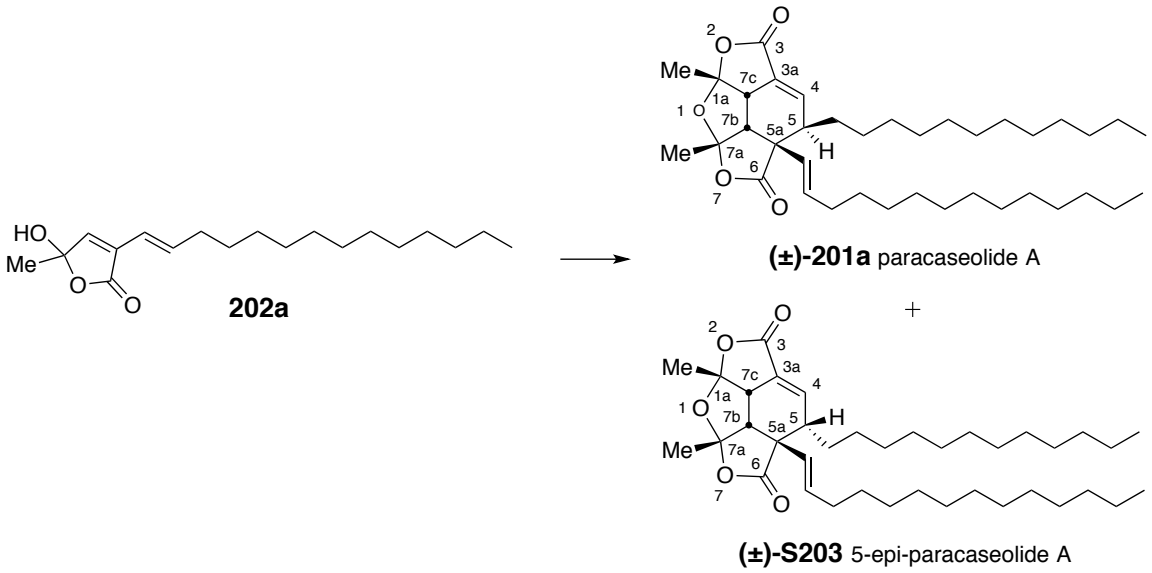


**Preparation of (±)-paracaseolide A (1a*R*,5*R*,5a*S*,7a*S*,7b*R*,7c*S*)-rel-(±)-5-dodecyl-1a,5,5a,7a,7b,7c-hexahydro-1a,7a-dimethyl-5a-(1*E*)-1-tetradecen-1-yldifuro[2,3,4-cd:4',3',2'-hi]isobenzofuran-3,6-dione [(±)-201a] and its C5-epimer (1a*R*,5*S*,5a*S*,7a*S*,7b*R*,7c*S*)-rel-(±)-5-dodecyl-1a,5,5a,7a,7b,7c-hexahydro-1a,7a-dimethyl-5a-(1*E*)-1-tetradecen-1-yldifuro[2,3,4-cd:4',3',2'-hi]isobenzofuran-3,6-dione [(±)-S203]**

(±)-(*E*)-5-Hydroxy-5-methyl-3-(tetradec-1-enyl)furan-2(5H)-one (**202a**, 33.2 mg, 0.11 mmol) was placed in a 1 mL vial with a Teflon cap. The headspace was flushed with Ar. The reaction vial was heated to 110 °C for 43 h. The crude mixture was directly subjected to flash column chromatography on silica gel (hexanes:ethyl acetate = 12:1, then 5:1, then 3:1) to give (±)–paracaseolide A (**201a**, 13.4 mg, 42%) and (±)–5-*epi*-paracaseolide A (**S203,** 2.0 mg, 7%), each as a white powder.

**(±)–paracaseolide A (201a):**

**$^1$H NMR** ($CDCl_3$, 500 MHz): $\delta$ 7.25 (dd, $J$ = 7.6, 3.2 Hz, 1H, *H*4), 5.83 (dt, $J$ = 15.7, 6.9 Hz, 1H, HC=C*H*$CH_2$), 5.49 (dt, $J$ = 15.8, 1.5 Hz, 1H, *H*C=$CHCH_2$), 3.37 (dd, $J$ = 9.5, 3.3 Hz, 1H, *H*7c), 3.30 (d, $J$ = 9.6 Hz, 1H, *H*7b), 3.04 (ddd, $J$ = 11.6, 7.6, 3.7 Hz, 1H, *H*5), 2.11 (ddt, $J$ = 1.3, 7, 7 Hz, 2H, HC=CHC$H_2$), 1.76 [s, 3H, C(1a)C$H_3$], 1.71–1.64 [m, 1H,

C(5)C$H_a$H$_b$], 1.62 [s, 3H, C(7a)C$H_3$], 1.45–1.34 (m, 2H, HC=CHCH$_2$C$H_2$), 1.34–1.16 (m, many H), 1.20–1.05 [m, 1H, C(5)CH$_a$$H_b$], and 0.88 [t, $J$ = 7.0 Hz, 6H, (C$H_3$CH$_2$)$_2$].

**$^{13}$C NMR** (125 MHz, $CDCl_3$) $\delta$ 175.3, 166.4, 144.9, 135.3, 129.5, 126.5, 115.6, 114.0, 58.5, 50.5, 46.9, 45.3, 32.9, 32.1 (2x), 29.91, 29.88 (2x), 29.87 (2x), 29.86 (2x), 29.84 (2x), 29.77, 29.64 (2x), 29.58 (2x), 29.3, 29.2, 28.4, 28.2, 26.8, 25.9, 22.9 (2x), and 14.3 (2x).

**IR** (neat): 2923, 2853, 1774, 1465, 1390, 1312, 1272, 1129, 1056, and 913 cm$^{-1}$.

**HRMS** (ESI-TOF): Calcd for $(C_{38}H_{62}NaO_5)^+$ 621.4489, Found: 621.4499.

**mp** 59–64 °C.

**(±)–5-*epi*-paracaseolide A (S203):**

**$^1$H NMR** ($CDCl_3$, 500 MHz): δ 6.98 (dd, $J$ = 4.2, 3.5 Hz, 1H, $H$4), 5.69 (dt, $J$ = 15.7, 6.9 Hz, 1H, HC=C$H$CH$_2$), 5.43 (dt, $J$ = 15.7, 1.4 Hz, 1H, $H$C=CHCH$_2$), 3.27 (ddd, $J$ = 9.9, 3.3, 2.0, $H$7c), 3.20 (d, $J$ = 9.9 Hz, 1H, $H$7b), 2.20–2.07 (m, 3H, $H$5, CH=CHC$H_2$), 2.01 [dddd, $J$ = 13.8, 12.1, 10.2, 4.6 Hz, 1H, C(5)HC$H_a$H$_b$], 1.75 (dddd, $J$ = 13.6, 10.6, 6.0, 3.0 Hz, 1H, C(5)HCH$_a$$H_b$) 1.74 [s, 3H, C(1a)C$H_3$], 1.59 [s, 3H, C(7a)C$H_3$], 1.53–1.45 (m, 1H), 1.41–1.35 (m, 2H), 1.35–1.17 (m, many H), and 0.88 [t, $J$ = 7.0 Hz, 6H, (C$H_3$CH$_2$)$_2$].

---

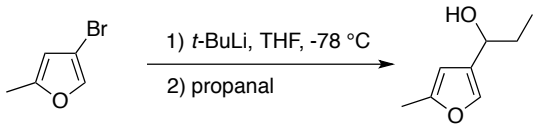


**205** **208**

**Preparation of 1-(5-methylfuran-3-yl)propan-1-ol (208)**

An oven-dried 250 mL round bottom flask was charged with dry THF (75 mL). The flask was cooled to -78 °C before dropwise addition of a solution of *t*-BuLi (38 mL, 1.7 M, in hexanes; 65 mmol). 4-Bromo-2-methylfuran (**205**) containing ca. 5 wt% of pentane (4.98 g, 29 mmol) was added dropwise at -78 °C to form an orange solution. This mixture was

stirred at -78 °C for 10 min before dropwise addition of dry propionaldehyde (6 mL, 84 mmol). The reaction mixture was allowed to warm to room temperature, quenched with aqueous $NH_4Cl$ solution, and extracted with ethyl acetate The organic layer was washed with brine, dried with $Na_2SO_4$, filtered, concentrated, and subjected to flash column chromatography on silica gel (hexanes:ethyl acetate = 5:1) to give 1-(5-methylfuran-3-yl)propan-1-ol (**208**, 3.8 g, 95% yield) as a colorless liquid.

**$^1$H NMR** (500 MHz, $CDCl_3$) δ 7.22 (br s, 1H, *H2*), 5.98 (br s, 1H, *H4*), 4.49 (br t, $J$ = 6.5 Hz, 1H, C*H*(OH)$CH_2$), 2.27 (s, 3H, ArC*H*$_3$), 1.75 (ddq, $J$ = 14, 7.4, 7.4 Hz, 1H, C$H_a$H$_b$$CH_3$), 1.71 (ddq, $J$ = 14, 7.2, 7.2 Hz, 1H, $CH_a$*H*$_b$$CH_3$), 1.71 (br s, 1H, OH), and 0.93 (t, $J$ = 7.5 Hz, 3H, $CH_2$C*H*$_3$).

**$^{13}$C NMR** (125 MHz, $CDCl_3$) δ 153.1, 137.4, 129.9, 104.6, 68.8, 30.8, 13.8, and 10.2.

**IR** (neat): 3384, 2964, 2933, 2877, 1555, 1452, 1381, 1266, and 1208 $cm^{-1}$.

**HRMS** (ESI-TOF): Calcd for $(C_{19}H_{33}O_3)^+$ 309.2424. Found: 309.2412.

**GC-LRMS** (ES, 70 eV): $t_R$ = 4.08 min. *m/z*: 140 ($M^+$), 111 ($M^+$-$CH_2CH_3$), and 83 ($M^+$-$COCH_2CH_3$).

---

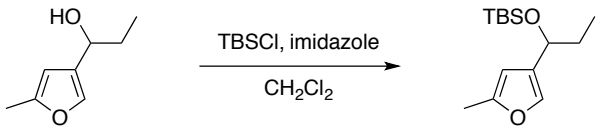


**208** **209**

**Preparation of *tert*-butyldimethyl(1-(5-methylfuran-3-yl)propoxy)silane (209)**

To a $CH_2Cl_2$ (150 mL) solution of 1-(5-methylfuran-3-yl)propan-1-ol (**208**, 3.6 g, 26 mmol) was added TBSCl (8.8 g, 58 mmol) and imidazole (3.9 g, 58 mmol) at room temperature. The reaction mixture was stirred for 20 h, and the resulting slurry was filtered through a cotton plug, using DCM to wash the solid filter cake. The filtrate was concentrated and the residue redissolved in ethyl acetate. This solution was washed with

deionized water, dried over $Na_2SO_4$, filtered, and concentrated. The residue was purified using flash column chromatography on silica gel (hexanes:ethyl acetate = 12:1) to give *tert*-butyldimethyl(1-(5-methylfuran-3-yl)propoxy)silane (**209**, 5.9 g, 90% yield) as a colorless liquid.

**$^1$H NMR** (500 MHz, $CDCl_3$) δ 7.11 (br s, 1H, *H2*), 5.90 (br s, 1H, *H4*), 4.51 (t, $J$ = 6.0 Hz, 1H, C*H*(OTBS)$CH_2CH_3$), 2.25 (s, 3H, Ar$CH_3$), 1.67 (ddq, $J$ = 6.7, 13.9, 7.4 Hz, 1H, $CH_aH_bCH_3$), 1.61 (ddq, $J$ = 5.8, 13.9, 7.6 Hz, 1H, $CH_aH_bCH_3$), 0.88 (s, 9H, $SiC(CH_3)_3$), 0.86 (t, $J$ = 7.4 Hz, 3H, $CH_2CH_3$), 0.04 (s, 3H, $SiMe_aMe_b$), and –0.04 (s, 3H, $SiMe_aMe_b$).

**$^{13}$C NMR** (125 MHz, $CDCl_3$) δ 152.4, 137.1, 130.8, 105.0, 69.3, 32.4, 26.1, 18.5, 13.9, 9.9, –4.4, and –4.7.

**IR** (neat): 2958, 2930, 2858, 1473, 1255, 1059, 1017, 836, and 776 $cm^{-1}$.

**GC-LRMS** (ES, 70 eV): $t_R$ = 6.09 min. *m/z*: 239 ($M^+$-$CH_3$), 225 ($M^+$-$CH_2CH_3$), and 197 ($M^+$-$C(CH_3)_3$).

---

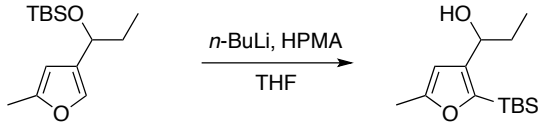


**209** **210**

**Preparation of 1-(2-(*tert*-butyldimethylsilyl)-5-methylfuran-3-yl)propan-1-ol (210)**

To a solution of *tert*-butyldimethyl(1-(5-methylfuran-3-yl)propoxy)silane (**209**, 5.4 g, 21 mmol) in dry THF (330 mL) was added HPMA (4.2 mL, 24 mmol) at room temperature. The reaction flask was then cooled to 0 °C followed by dropwise addition of *n*-BuLi solution (15 mL, 2.5 M in hexanes). The reaction solution was allowed to warm to room temperature and stirred for 45 min before being quenched by the addition of $Et_2O$ and aqueous $NH_4Cl$ solution. The organic layer was washed with brine, dried with $Na_2SO_4$, and concentrated. The residue was purified using flash column chromatography on silica gel (hexanes:ethyl acetate = 5:1) to give 1-(2-(*tert*-butyldimethylsilyl)-5-methylfuran-3-

yl)propan-1-ol (**210**, 4.67 g, 86% yield) as an off-white solid.

**$^1$H NMR** (500 MHz, $CDCl_3$) δ 6.05 (s, 1H, Ar-*H*), 4.58 (dt, *J* = 2.4, 6.9 Hz, 1H, C*H*(OH)), 2.28 (s, 3H, ArC*H*$_3$), 1.82 (ddq, *J* = 7.3, 14.3, 7.3 Hz, 1H, CH(OH)C$H_aH_b$), 1.66 (ddq, *J* = 7.3, 14.3, 7.3 Hz, 1H, CH(OH)C$H_aH_b$), 0.92 (s, 9H, SiC(C$H_3$)$_3$), 0.91 (t, *J* = 7.3 Hz, 3H, $CH_2CH_3$), 0.27 (s, 3H, Si$Me_a$Me$_b$), and 0.25 (s, 3H, SiMe$_a$$Me_b$).

**$^{13}$C NMR** (125 MHz, $CDCl_3$) δ 156.9, 152.7, 140.9, 104.2, 68.6, 31.2, 26.7, 17.4, 14.1, 10.83, –4.84 and –5.14.

**IR** (neat): 3366, 2956, 2930, 2858, 1606, 1523, 1471, 1463, 1249, 836, and 826 cm$^{-1}$.

**HRMS** (ESI-TOF): Calcd for $(C_{14}H_{26}NaO_2Si)^+$ 277.1594. Found: 277.1596.

**mp** 52.1–56.5 °C.

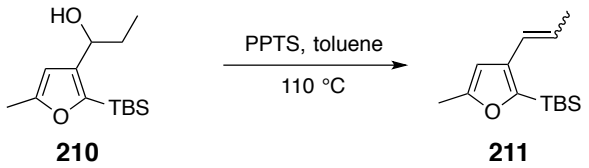


**210** **211**

**Preparation of *E*- and *Z*-*tert*-butyldimethyl(5-methyl-3-(prop-1-en-1-yl)furan-2-yl)silanes (211)**

To a solution of 1-(2-(*tert*-butyldimethylsilyl)-5-methylfuran-3-yl)propan-1-ol (**210**, 1.0 g, 4 mmol) in dry toluene (80 mL) was added *p*-toluenesulfonic acid (15 mg, 0.08 mmol) and 4 Å molecular sieves (ca. 1 g) at room temperature. A reflux condenser was attached and the reaction flask was placed in a 110 °C oil bath and stirred for 2 h. The reaction mixture was then cooled to room temperature and filtered through Celite. The filtrate was concentrated and the residue purified with flash column chromatography on silica gel (pure hexanes) to give a coeluting, 5:1 *E*/*Z* mixture of *tert*-butyldimethyl(5-methyl-3-(prop-1-en-1-yl)furan-2-yl)silane (**211**, 0.73 g, 78% yield) as a colorless liquid. If the reaction mixture was quenched and worked-up by partitioning between aqueous and

organic layers, the resulting crude material showed a decided tendency to decompose (to a red-colored non-elutable material) when subjected to silica gel. The following data were extracted from the spectra of the mixture.

**(*E*)-*tert*-Butyldimethyl(5-methyl-3-(prop-1-en-1-yl)furan-2-yl)silane (*E*-211):**

**$^{1}$H NMR** (500 MHz, $CDCl_3$) δ 6.33 (ddq, *J* = 0.6, 15.5, 1.7 Hz, 1H, C*H*=CHCH$_3$), 6.11 (dq, *J* = 0.5, 1.0 Hz, 1H, Ar-*H*), 5.87 (dq, *J* = 15.5, 6.6 Hz, 1H, CH=C*H*CH$_3$), 2.26 (d, *J* = 0.9 Hz, 3H, Ar-C*H*$_3$), 1.81 (dd, *J* = 1.7, 6.7 Hz, 3H, CH=CHC*H*$_3$), 0.90 (s, 9H, SiC(C*H*$_3$)$_3$), and 0.27 (s, 6H, Si(C*H*$_3$)$_2$).

**$^{13}$C NMR** (125 MHz, $CDCl_3$) δ 156.5, 152.9, 136.5, 124.9, 122.9, 103.9, 26.7, 18.8, 17.8, 13.9, and –5.29.

**GC-LRMS** (ES, 70 eV): $t_R$ = 6.35 min. *m/z*: 236 ($M^+$), and 179 ($M^+$-C(CH$_3$)$_3$).

**(*Z*)-*tert*-Butyldimethyl(5-methyl-3-(prop-1-en-1-yl)furan-2-yl)silane (*Z*-211):**

**$^{1}$H NMR** (500 MHz, $CDCl_3$) δ 6.33 (ddq, *J* = 0.5, 11.4, 1.8 Hz, 1H, C*H*=CHCH$_3$), 6.18 (dq, *J* = 0.5, 0.9 Hz, 1H, Ar-*H*), 5.57 (dq, *J* = 7.1, 11.5 Hz, 1H, CH=C*H*CH$_3$), 2.30 (d, *J* = 0.9 Hz, 3H, Ar-C*H*$_3$), 1.84 (dd, *J* = 1.8, 7.1 Hz, 3H, CH=CHC*H*$_3$), 0.90 (s, 9H, SiC(C*H*$_3$)$_3$), and 0.25 (s, 6H, Si(C*H*$_3$)$_2$).

**$^{13}$C NMR** (125 MHz, $CDCl_3$) δ 156.5, 152.9, 136.5, 125.2, 122.1, 107.3, 26.7, 18.8, 17.8, 14.9, and –5.29.

**GC-LRMS** (ES, 70 eV): $t_R$ = 6.22 min. *m/z*: 236 ($M^+$), and 179 ($M^+$-C(CH$_3$)$_3$).

**IR** (neat, of the *E/Z* mixture of alkenes): 2954, 2928, 2857, 1604, 1502, 1463, 1249, 1111, and 957 cm$^{-1}$.

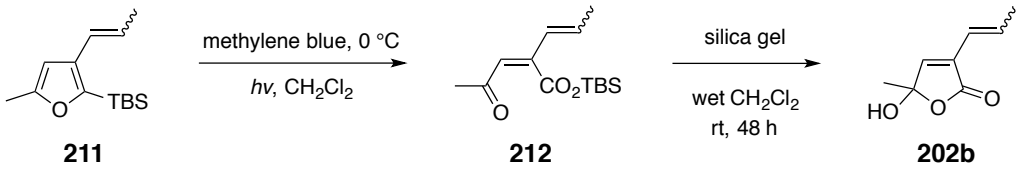


**211** **212** **202b**

**Preparation of 5-hydroxy-5-methyl-3-(prop-1-en-1-yl)furan-2(5H)-one (202b) via (2*Z*)-*tert*-butyldimethylsilyl 4-oxo-2-(prop-1-en-1-yl)pent-2-enoate (212).**

Methylene blue (5 mg) was added to a solution of *tert*-butyldimethyl(5-methyl-3-(prop-1-en-1-yl)furan-2-yl) silane (**211**, 1.83 g, 7.7 mmol) in $CH_2Cl_2$ (250 mL) in a round bottomed flask. The mixture was cooled to 0 °C in an ice-water bath. $O_2$ was introduced into the solution by slow bubbling through a fritted glass tube fitted into a stopper or septum that contained a vent needle. A common 75 W incandescent light bulb was placed directly above the reaction flask (distance < 5 cm). (See photo below of a typical set-up for the experiment.) Ice was periodically added to maintain sub-ambient temperature. After 7 h full consumption of furan **211** was confirmed by TLC analysis. The mixture was concentrated through a short plug of silica gel with $CH_2Cl_2$ elution to give a 6:1 *E*/*Z* crude mixture of (2*Z*)-*tert*-butyldimethylsilyl 4-oxo-2-(prop-1-en-1-yl)pent-2-enoate (**212**) as a pale yellow liquid (2.55 g, 123% mass recovery). Because of the propensity of this silyl ester to undergo desilylation during attempts at more careful chromatographic treatments, this crude mixture was directly used for dimerization studies without further purification.

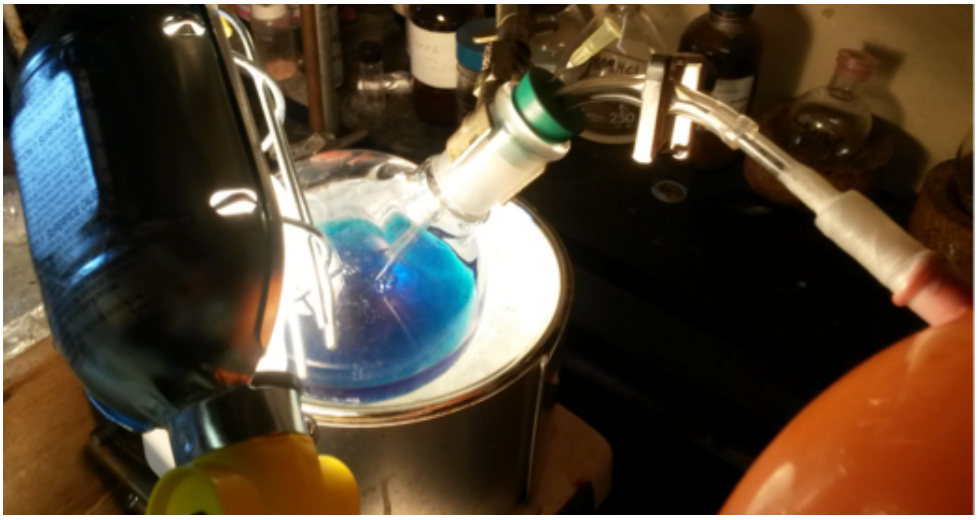

**(2*E*)-*tert*-butyldimethylsilyl 4-oxo-2-((1*E*)-prop-1-en-1-yl)pent-2-enoate (*Z*-212):**

**$^1$H NMR** (500 MHz, $CDCl_3$) δ 6.12 (ddq, *J* = 0.6, 15.7, 6.2 Hz, 1H, C*H*$CH_3$), 6.08 (br d, *J* = 15.7 Hz, 1H, C*H*=$CHCH_3$), 5.97 (br s, 1H, C*H*C(=O)$CH_3$), 2.23 (s, 3H, C(=O)C*H*$_3$), 1.88 (br d, *J* = 5.2 Hz, 3H, CHC*H*$_3$), 0.94, (s, 9H, $SiMe_2C(CH_3)_3$), and 0.42 (s, 6H, $Si(CH_3)_2C(CH_3)_3$).

**$^{13}$C NMR** (125 MHz, $CDCl_3$) δ 196.3, 168.2, 147.0, 138.2, 128.6, 122.6, 30.5, 25.7, 19.3, 17.9, and -4.7.

**GC-LRMS** (ES, 70 eV): $t_R$ = 7.54 min. *m/z*: 268 ($M^+$), 253 ($M^+ - CH_3$) and 211 ($M^+ - C(CH_3)_3$).

**(2*Z*)-*tert*-butyldimethylsilyl 4-oxo-2-((1*Z*)-prop-1-en-1-yl)pent-2-enoate (*Z*-212):**

**$^1$H NMR** (500 MHz, $CDCl_3$) δ obscured under resonances of major isomer between 6.06–6.16 (1H, C*H*C(=O)$CH_3$), 5.96 (ddq, *J* = 0.6, 11.7, 6.9 Hz, 1H, C*H*$CH_3$), 5.92 (br d, *J* = 11.8 Hz, 1H, C*H*=$CHCH_3$), 2.25 (s, 3H, C(=O)C*H*$_3$), 1.85 (br d, *J* = 5.9 Hz, 3H, CHC*H*$_3$), 0.93, (s, 9H, $SiMe_2C(CH_3)_3$), and 0.41 (s, 6H, $Si(CH_3)_2C(CH_3)_3$).

**$^{13}$C NMR** (125 MHz, $CDCl_3$) δ 196.8, 169.0, 143.6, 135.4, 127.7, 125.9, 30.6, 25.6, 17.9, 14.8, and -5.0.

**GC-LRMS** (ES, 70 eV): $t_R$ = 7.39 min. *m/z*: 268 ($M^+$), 253 ($M^+ - CH_3$), and 211 ($M^+ - C(CH_3)_3$).

**IR** (neat, of the *E/Z* mixture of alkenes): 2956, 2932, 2859, 1716, 1689, 1582, 1384, 1375, 1253, 1191, and 961 $cm^{-1}$.

**Hydrolysis of TBS-esters 212 to butenolides 202b.**

A sample of the crude mixture of 3*E*- and 3*Z*-(2*Z*)-*tert*-butyldimethylsilyl 4-oxo-2-(prop-1-en-1-yl)pent-2-enoates (**212**, 156 mg, 0.58 mmol) and wet $CH_2Cl_2$ (12 mL, 1 drop of water was added) were combined in 20 mL glass vial. Silica gel (500 mg) and a stir bar were added, and the slurry was stirred at room temperature for 48 h. This mixture was

filtered. The residue was washed with $CH_2Cl_2$ three times, and combined with the filtrate. This combined solution was then concentrated and purified using column chromatography on silica gel (hexanes:ethyl acetate = 5:1 to 3:1 to 1:1) to give a 7:1 *E*:*Z* mixture of 5-hydroxy-5-methyl-3-(prop-1-en-1-yl)furan-2(5H)-one (**202b**, 52 mg, 58% yield) as a pale yellow oil. The following NMR data were extracted from this mixture.

**(*E*)-5-Hydroxy-5-methyl-3-(prop-1-en-1-yl)furan-2(5H)-one (*E*-202b):**

**$^1$H NMR** (500 MHz, $CDCl_3$) δ 6.83 (d, *J* = 0.6 Hz, 1H, *H4*), 6.81 (dq, *J* = 15.5, 6.9 Hz, 1H, *H2'* ), 6.08 (ddq, *J* = 0.6, 15.9, 1.8 Hz, 1H, *H1'* ), 1.86 (ddd, *J* = 0.6, 1.7, 6.8 Hz, 3H, *H3'* ), and 1.69 (s, 3H, C5-C*H*$_3$).

**$^{13}$C NMR** (125 MHz, $CDCl_3$) δ 170.2, 144.1, 136.0, 130.9, 119.4, 104.2, 25.0, and 19.3.

**(*Z*)-5-Hydroxy-5-methyl-3-(prop-1-en-1-yl)furan-2(5H)-one (*Z*-202b):**

**$^1$H NMR** (500 MHz, $CDCl_3$) δ 7.01 (br s, 1H, *H4*), 6.14 (ddq, *J* = 0.5, 11.5, 7.0 Hz, 1H, *H2'* ), 6.07 (ddq, *J* = 0.9, 12.0, 1.7 Hz, 1H, *H1'* ), 1.86 (ddd, *J* = 0.6, 1.5, 6.9 Hz, 3H, *H3'*), and 1.74 (s, 3H, C5-C*H*$_3$).

**$^{13}$C NMR** (125 MHz, $CDCl_3$) δ 171.5, 146.4, 135.9, 129.8, 117.3, 104.9, 25.1, and 16.0.

**HRMS** (ESI-TOF): Calcd for $(C_8H_{10}NaO_3)^+$ 177.0522. Found: 177.0524.

**IR** (neat, of the *E/Z* mixture of alkenes): 3370, 2994, 2939, 1742, 1665, 1445, 1414, 1167, 1114, 1055, 967, and 925 cm$^{-1}$.

---

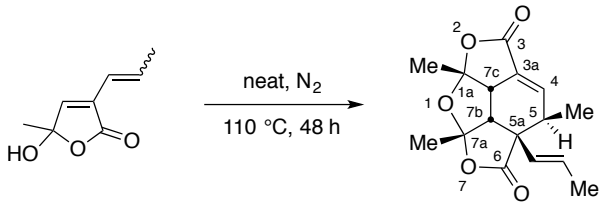


**202b** **(±)-201b**

**Preparation of truncated paracaseolide A**

**(1a*R*,5*R*,5a*S*,7a*S*,7b*R*,7c*S*)-rel-(±)-1a,5,5a,7a,7b,7c-hexahydro-1a,5,7a-trimethyl-5a-(1*E*)-1-propen-1-yldifuro[2,3,4-cd:4',3',2'-hi]isobenzofuran-3,6-dione [(±)-201b]**

5-Hydroxy-5-methyl-3-(prop-1-en-1-yl)furan-2(5H)-one (**202b**, 35 mg, 0.23 mmol) was placed in a 2 mL vial with a Teflon cap. The headspace was flushed with $N_2$. The reaction vial was capped and heated to 110 °C for 48 h. The crude mixture was directly subjected to MPLC (hexanes:ethyl acetate = 1:1) to give unreacted 5-hydroxy-5-methyl-3-(prop-1-en-1-yl)furan-2(5H)-ones (**202b**, 8 mg, *E*:*Z* = 3:4) followed by the truncated paracaseolide A analog **(±)-201b** (13.9 mg, 42%) as a white powder.

**$^1$H NMR** ($CDCl_3$, 500 MHz): δ 7.26 (dd, *J* = 7.6, 3.3 Hz, 1H, *H4*), 5.87 (dq, *J* = 15.7, 6.5 Hz, 1H, =C*H*$CH_3$), 5.53 (dq, *J* = 15.7, 1.6 Hz, 1H, *H*C=C$HCH_3$), 3.38 (dd, *J* = 9.5, 3.3 Hz, 1H, *H7c*), 3.30 (d, *J* = 9.5 Hz, 1H, *H7b*), 3.11 (dq, *J* = 7.4, 7.4 Hz, 1H, *H5*), 1.80 (dd, *J* = 6.5, 1.7 Hz, 3H, =CHC*H*$_3$), 1.76 (s, 3H, (C1a)C*H*$_3$), 1.63, (s, 3H, (C7a)C*H*$_3$), and 1.05 (d, *J* = 7.3 Hz, 3H, H(C5)C*H*$_3$).

**$^{13}$C NMR** ($CDCl_3$) δ 175.3, 166.4, 144.7, 130.0, 129.5, 127.5, 115.6, 114.1, 58.7, 50.4, 46.5, 39.3, 26.9, 25.9, 18.4, and 12.1.

**IR** (neat): 2923, 2854, 1771, 1390, 1312, 1050, and 911 $cm^{-1}$.

**HRMS** (ESI-TOF): Calcd for $(C_{16}H_{18}NaO_5)^+$ 313.1046. Found: 313.1062.

**mp** 200-201 °C.

**X-ray structure determination of (±)-201b**

A single crystal used for X-ray analysis was prepared by dissolving a portion of this purified product in $CH_2Cl_2$. This solution was transferred to a small vial, which was then placed inside a larger capped vial containing pentane. Upon standing at room temperature for several days white crystals of suitable quality were formed.

The crystallographic data (excluding structure factors) for this structure have been deposited into the Cambridge Crystallographic Data Centre (CCDC). The deposition

number is CCDC 1042994. Copies of the data can be obtained (, free of charge) by contacting the CCDC, 12 Union Road, Cambridge CB2 1EZ, UK, or by linking to http://www.ccdc.cam.ac.uk/pages/Home.aspx.

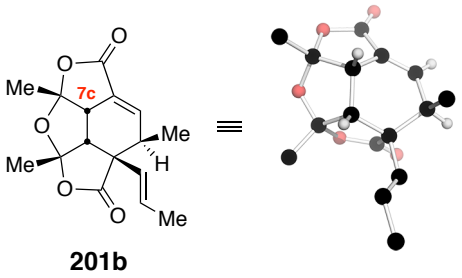


**201b**

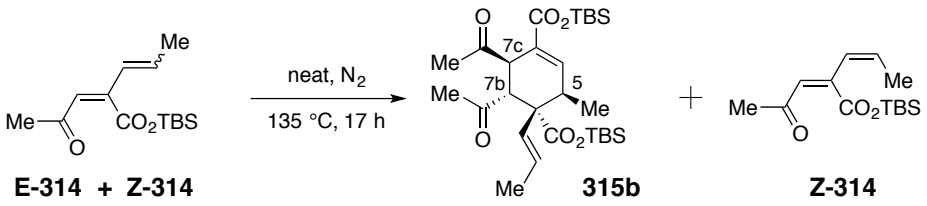


**E-314 + Z-314** **315b** **Z-314**

**Preparation of bis(tert-butyldimethylsilyl) (3R,4S,5R,6R)-5,6-diacetyl-3-methyl-4-((E)-prop-1-en-1-yl)cyclohex-1-ene-1,4-dicarboxylate (315b).**

To a small glass vial was added the crude mixture of *E/Z* isomers of (2*Z*)-*tert*-butyldimethylsilyl 4-oxo-2-(prop-1-en-1-yl)pent-2-enoates (**314**, 158 mg, 0.59 mmol). The headspace was flushed with $N_2$ and the vial was sealed with a Teflon-lined cap. The reaction mixture was placed in a 135 °C oil bath for 17 h to produce a mixture of 151 mg of bis(tert-butyldimethylsilyl) (3R,4S,5R,6R)-5,6-diacetyl-3-methyl-4-((*E*)-prop-1-en-1-yl)cyclohex-1-ene-1,4-dicarboxylate (**315b**) and *tert*-butyldimethylsilyl (*Z*)-4-oxo-2-((*Z*)-prop-1-en-1-yl)pent-2-enoate (***Z*-314**). The small mass loss was due to the fact that some of the ***Z*-314** vaporized and re-condensed on the cap and was not collected). This crude mixture was used directly without purification.

**$^1$H NMR** (500 MHz, $CDCl_3$) δ 6.92 [dd, *J* = 3.1, 1.1 Hz, 1H, =C*H*CH($CH_3$)], 5.56 (dq, *J* = 15.9, 6.5 Hz, 1H, CH=C*H*$CH_3$), 5.23 (dq, *J* = 15.8, 1.7 Hz, 1H, C*H*=CH$CH_3$), 3.75 (ddd, *J* = 2.0, 2.0, 1.3 Hz, 1H, *H*7c), 3.70 (d, *J* = 2.2 Hz, 1H, *H*7b), 3.38 [ddq, *J* = 3.0, 1.9,

7.4 Hz, 1H, *H*5], 2.27 (s, 3H, $C_a$(=O)C$H_3$), 2.26 (s, 3H, $C_b$(=O)C$H_3$), 1.60 (dd, $J$ = 6.5, 1.6 Hz, 3H, CH=CHC$H_3$), 1.28 [d, $J$ = 7.4, 3H, C5(C$H_3$)], 0.95 [s, 9H, -Si$_a$Me$_2$C(C$H_3$)$_3$], 0.94 [s, 9H, -Si$_b$Me$_2$C(C$H_3$)$_3$], 0.29, 0.274, 0.272, and 0.26 (four singlets, 4 × 3H, Si(C$H_3$)$_2$C(CH$_3$)$_3$).

**$^{13}$C NMR** (125 MHz, $CDCl_3$) δ 207.2, 206.3, 174.2, 166.5, 147.9, 129.2, 127.8, 125.8, 58.3, 52.3, 48.7, 34.7, 29.1, 28.1, 25.9, 25.8, 18.2, 18.0, 17.9, 16.7, -4.6, -4.7, -4.79, and -4.80.

**IR** (neat) 2922, 2354, 2320, 1767, 1712, 1454, 1387, 1250, 1196, 1164, 1056, 1021, 973, 919, and 836 cm$^{-1}$.

**HRMS** (ESI-TOF): Calcd for $(C_{28}H_{48}NaO_6Si_2)^+$ 559.2882. Found: 559.2895.

---

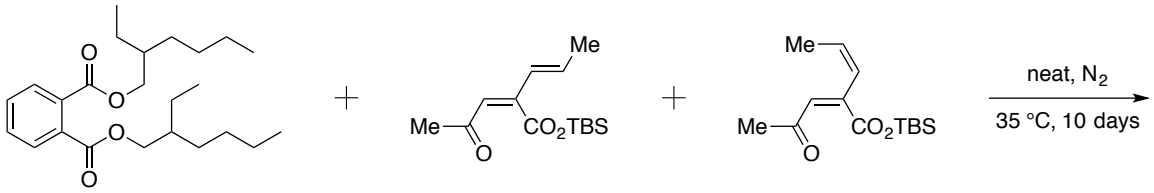


bis(2-ethylhexyl) phthalate **316** *internal standard* : **E-314** : **Z-314**

*1* : *3.6* : *0.66*

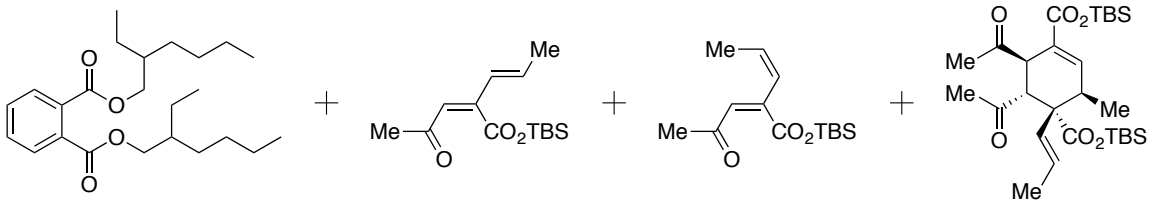


bis(2-ethylhexyl) phthalate **316** *internal standard* : **E-314** : **Z-314** : **315b**

*1* : *0.35* : *0.43* : *1.6*

**Dimerization experiment of (2*Z*)-*tert*-butyldimethylsilyl 4-oxo-2-(prop-1-en-1-yl)pent-2-enoate (314) at ambient temperature (35 °C)**

---

To a small glass vial was added a DCM solution of the crude mixture of *E/Z* isomers (ca. 5.5:1) of (2*Z*)-*tert*-butyldimethylsilyl 4-oxo-2-(prop-1-en-1-yl)pent-2-enoates (**314b**) and bis(2-ethylhexyl) phthalate (DEHP) as an internal standard. The DCM was evaporated. The relative initial quantity of the three components in the resulting neat mixture was measured by $^1$H NMR spectroscopic analysis of an aliquot. The headspace of the vial was flushed with $N_2$ and the vial was sealed with a Teflon-lined cap. The reaction mixture was placed in a 35 °C oil bath for 10 days. The crude reaction mixture was directly subjected to $^1$H NMR analysis. The relative amount of the four components was calculated relative to the DEHP proton resonances.

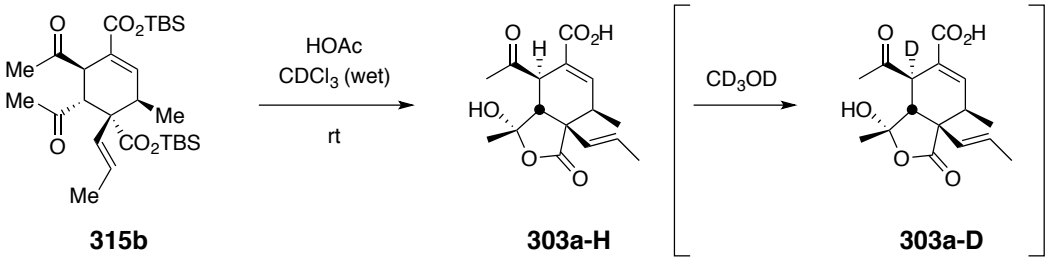


**315b** **303a-H** **303a-D**

**Preparation of (3S,4R,7R,7aS)-4-acetyl-3-hydroxy-3,7-dimethyl-1-oxo-7a-((E)-prop-1-en-1-yl)-1,3,3a,4,7,7a-hexahydroisobenzofuran-5-carboxylic acid (303b-H).**

To a 20 mL glass vial was added the bis(tert-butyldimethylsilyl) ester **315b** (75 mg, 0.14 mmol), $CDCl_3$ (5 mL), and HOAc (1 mL). The reaction mixture was stirred at room temperature for 24 h. The solution was concentrated and the residue purified by flash column chromatography (hexanes:ethyl acetate:acetic acid = 50:50:1) to give (3S,4R,7R,7aS)-4-acetyl-3-hydroxy-3,7-dimethyl-1-oxo-7a-((E)-prop-1-en-1-yl)-1,3,3a,4,7,7a-hexahydroisobenzofuran-5-carboxylic acid (**303b-H**, 31 mg, 72% yield) as an off-white solid. This material showed marginal solubility in $CDCl_3$, but the NMR spectra in that solvent were relatively sharp. They also indicated the presence of at least three distinct species, the major of which comprised >90% of the spectral intensity. Presumably this reflects the presence of epimeric acylals and/or open and closed species among the various ketoacids. The sample was much more soluble in $CD_3OD$, but the

spectra were quite broad, suggestive of dynamic processes.

**$^1$H NMR** (500 MHz, $CDCl_3$) δ 7.07 [dd, *J* = 2.1, 2.1 Hz, 1H, C=C*H*CH($CH_3$)], 5.76 (dq, *J* = 16.0, 6.3 Hz, 1H, CH=C*H*$CH_3$), 5.30 (dq, *J* = 15.7, 1.8 Hz, 1H, C*H*=CH$CH_3$), 3.70 (br s, 1H, *H*7c), 2.99-2.90 (m, 2H, *H*7b and O*H*], 2.57 (br s, 1H, *H*5), 2.29 (s, 3H, C(=O)C*H*$_3$), 1.81 (s, 3H, C(OH)C*H*$_3$), 1.67 (dd, *J* = 6.4, 1.6 Hz, 3H, CH=CHC*H*$_3$), and 1.21 [d, *J* = 7.5, 3H, C5(C*H*$_3$)].

**$^1$H NMR** (500 MHz, $CD_3OD$) δ 6.89 [br s, 1H, C=C*H*CH($CH_3$)], 5.68 (dq, *J* = 15.7, 6.3 Hz, 1H, CH=C*H*$CH_3$), 5.31 (br dq, *J* = 15.9, 1.7 Hz, 1H, C*H*=CH$CH_3$), 3.68 (br s, 1H, *H*7c), 2.94 (br s, 1H, *H*7b), 2.56 (br s, 1H, *H*5), 2.28 (br s, 3H, C(=O)C*H*$_3$), 1.75 (br s, 3H, C(OH)C*H*$_3$), 1.63 (dd, *J* = 6.5, 1.2 Hz, 3H, CH=CHC*H*$_3$), and 1.17 [br d, *J* = 7.3, 3H, C5(C*H*$_3$)].

**$^{13}$C NMR** (125 MHz, $CDCl_3$, chemical shifts taken from the HSQC data) δ 147 (*C*4), 128 (=*C*H$CH_3$), 127 (H*C*=CH$CH_3$), 51 (*C*5), 44 (*C*7c), 34 (*C*7b), 28 (C(=O)*C*H$_3$), 27 C(OH)*C*H$_3$), 18 (=CH*C*H$_3$), and 15 (and C5*C*H).

**$^{13}$C NMR** (125 MHz, $CD_3OD$) δ 209.9 (br s), 178.9, 169.6, 145.2 (br s), 129.8 (br s), 129.1 (br s), 128.9, 106.5, 53.3 (br s), 50.9 (br s), 46.2, 35.7, 28.9 (br s), 26.7 (br s), 18.5, and 15.6 (br s).

**IR** (neat): 2956, 2923, 2854, 2358, 1751, 1699, 1654, 1457, 1355, 1246, 1191, 1163, 1057, 1017, 971, and 914 $cm^{-1}$.

**HRMS** (ESI-TOF): Calcd for $(C_{16}H_{20}NaO_6)^+$ 331.1152 Found: 331.1153.

**mp** 170–174 °C (accompanied by sweating; NMR spectrum of material upon cooling was that of dimer **301b**.

**Deuterium exchange of H7c in $CD_3OD$**

The solution of **303b-H** in $CD_3OD$ was observed to lose signal intensity in the $^1$H NMR spectrum for proton H7c at ambient temperature. The half-life for this exchange was ca. 3.2 days at ambient temperature (ca. 21 °C).

**X-ray structure determination of 303b**

A single crystal used for X-ray analysis was prepared by dissolving a portion of this purified product in $CH_2Cl_2$ (containing ~5% residual EtOAc). This solution was transferred to a small vial, which was then placed inside a larger capped vial containing pentane. Upon standing at room temperature for 3 days white crystals of suitable quality were formed.

The crystallographic data (excluding structure factors) for this structure have been deposited into the Cambridge Crystallographic Data Centre (CCDC). The deposition number is CCDC 1042989. Copies of the data can be obtained (, free of charge) by contacting the CCDC, 12 Union Road, Cambridge CB2 1EZ, UK, or by linking to http://www.ccdc.cam.ac.uk/pages/Home.aspx.

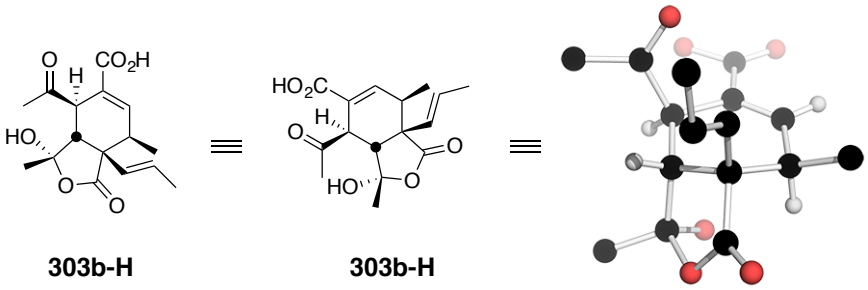


**303b-H** **303b-H**

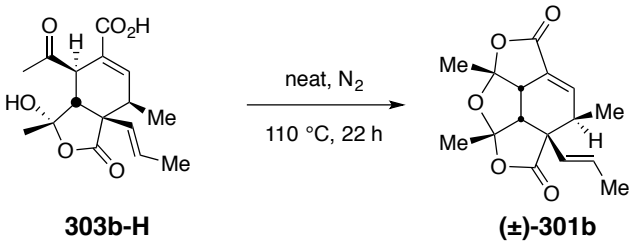


**303b-H** **(±)-301b**

**Preparation of truncated paracaseolide A**

**(1a*R*,5*R*,5a*S*,7a*S*,7b*R*,7c*S*)-rel-(±)-1a,5,5a,7a,7b,7c-hexahydro-1a,5,7a-trimethyl-5a-(1*E*)-1-propen-1-yldifuro[2,3,4-cd:4',3',2'-hi]isobenzofuran-3,6-dione [(±)-301b]**

The acid (**303b-H**, 1.0 mg, 3.2 μmol) was added to a glass vial. The headspace was flushed with $N_2$. The vial was sealed with a Teflon-lined cap and placed in a 110 °C oil bath. After 22 h the $^1$H NMR spectrum of the sample showed that clean conversion had occurred to give the truncated (±)-paracaseolide A (**301b**, 0.7 mg, after re-evaporation of the NMR solvent). The overall cleanliness of this reaction can be seen from inspection of the $^1$H NMR spectrum, a copy of which is included later in this Supplementary Information.

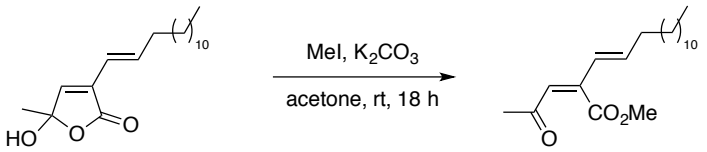


**302a** **318**

**Preparation of methyl (2*Z*,3*E*)-2-(2-oxopropylidene)hexadec-3-enoate (318)**

(±)-(*E*)-5-Hydroxy-5-methyl-3-(tetradec-1-enyl)furan-2(5H)-one (**302a**, 18.3 mg, 0.059 mmol) was placed in a 14x45 mm (1dram) vial. Acetone (2 mL), MeI (25 μL, 0.08 mmol), and $K_2CO_3$ (15 mg, 0.10 mmol) were added. The vial was sealed with a Teflon cap and stirred at room temperature for 18 h. The reaction mixture was partitioned between ethyl acetate and brine. The organic layer was washed again with brine, filtered through a plug of $Na_2SO_4$, concentrated, and purified using MPLC on silica gel (hexanes:ethyl acetate = 4:1) to give methyl (2*Z*,3*E*)-2-(2-oxopropylidene)hexadec-3-enoate (**318**) as a colorless oil (10.4 mg, 55%).

**$^1$H NMR** ($CDCl_3$, 500 MHz): δ 6.12-6.04 (m, 3H, =C*H*s), 3.90 (s, 3H, $CO_2CH_3$), 2.24 (s, 3H, $COCH_3$), 2.21-2.16 (nfom, 2H, $=CHCH_2CH_2$), 1.42 (br pentet, $J$ = 7.3 Hz, 2H, $=CHCH_2CH_2$), 1.32-1.22 (m, 18H, $-(CH_2)_9$), and 0.88, (t, $J$ = 6.9 Hz, 3H, $CH_2CH_3$).

**$^{13}$C NMR** (125 MHz, $CDCl_3$) δ 196.5, 168.9, 145.7, 144.5, 126.7, 124.0, 52.8, 33.6, 32.1, 30.7, 29.87, 29.84 (br), 29.7, 29.60, 29.56, 29.4, 28.6, 22.9, and 14.3.

**IR** (neat): 2924, 2853, 1740, 1690, 1585, 1378, 1250, 1198, 1175, and 963 $cm^{-1}$.

**HRMS** (ESI-TOF): Calcd for $(C_{20}H_{34}NaO_3)^+$ 345.2400 Found: 345.2397.

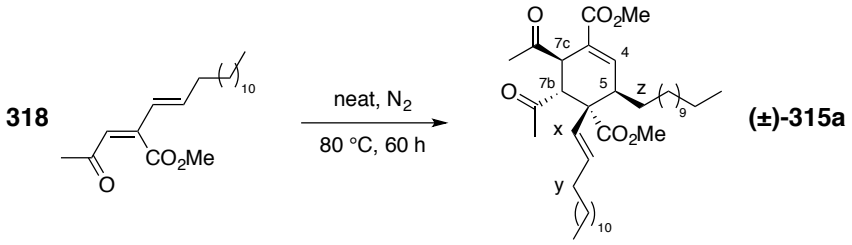


**Preparation of (±)-dimethyl (3*R*,4*S*,5*R*,6*R*)-5,6-diacetyl-3-dodecyl-4-((*E*)-tetradec-1-en-1-yl)cyclohex-1-ene-1,4-dicarboxylate [(±)-315a]**

(±)-Methyl (2*Z*,3*E*)-2-(2-oxopropylidene)hexadec-3-enoate (**318**, 5 mg, 16 $\mu$mol) was placed in a 2 mL vial with a Teflon cap. The headspace was flushed with $N_2$. The reaction vial was heated to 80 °C for 60 h. The crude material was directly purified by flash column chromatography (hexanes: ethyl acetate = 5:1 ~ 3:1) to give of (±)-dimethyl (3*R*,4*S*,5*R*,6*R*)-5,6-diacetyl-3-dodecyl-4-((*E*)-tetradec-1-en-1-yl)cyclohex-1-ene-1,4-dicarboxylate (**(±)-315a**, 5 mg, 100 %) as a colorless oil.

**$^1$H NMR** (500 MHz, $CDCl_3$) δ 7.13 [dd, *J* = 3.1, 1.1 Hz, 1H, =C*H*CH($CH_2CH_2$)], 5.43 (dt, *J* = 15.9, 6.8 Hz, 1H, CH=C*H*$CH_2$), 5.18 (dt, *J* = 15.9, 1.2 Hz, 1H, C*H*=CH$CH_3$), 3.77 (br dt, *J* = 1.2, 2.0 Hz, 1H, *H*7c), 3.75 (s, 3H, $C_aO_2CH_3$), 3.73 (d, *J* = 2.2 Hz, 1H, *H*7b), 3.70 (s, 3H, $C_bO_2CH_3$), 3.08 (br ddt, *J* = 11.1, 2.7, 2.1 Hz, 1H, *H*5), 2.28 [s, 3H, $C_a$(=O)$CH_3$], 2.27 [s, 3H, $C_b$(=O)$CH_3$], 1.96-1.83 (m, 3H), 1.62-1.52 (m, 1H), 1.49-1.40 (m, 1H), 1.40-1.09 (m, 39H), 0.883 (t, *J* = 7.0 Hz, 3H,$CH_2CH_3$), and 0.880 (t, *J* = 7.0 Hz, 3H,$CH_2CH_3$).

**$^{13}$C NMR** (125 MHz, $CDCl_3$) δ 207.3, 206.3, 174.3, 167.0, 145.1, 133.2, 127.9, 124.2, 57.6, 52.3, 51.9, 48.4, 40.0, 32.8, 32.2, 31.0, 29.95, 29.94, 29.90 (br), 29.87, 29.65, 29.61, 29.4, 29.1, 28.8, 28.40, 28.36, 22.9, and 14.4.

**IR** (neat): 2923, 2853, 1770, 1748, 1715, 1436, 1356, 1268, 1241, 1170, and 1048 $cm^{-1}$.

**HRMS** (ESI-TOF): Calcd for $(C_{40}H_{68}NaO_6)^+$ 667.4908 Found: 667.4941

**NMR-based assignment of the relative configuration (i.e., as an *exo* adduct) of (±)-315a**

**Difference NOE experiments** (carried out in $C_6D_6$ for better chemical shift dispersion) gave several key enhancements that were consistent with the assignment of the relative configuration shown above for **(±)-315a**. Namely: irradiation of Hx enhanced H7b, Hy, one of the diastereotopic protons Hz, and one of the two methyl ketone resonance, although we did not make a definitive assignment of which resonance was associated with which methyl group (and it did not enhance H7c or H5) and irradiation of either H7c or H7b enhanced both sets of methyl ketone protons.

**Chemical shift arguments** are also consistent with the assignment. There are close similarities of the shifts and multiplicity of key protons in **(±)-315a** vis-a-vis the bis-TBS ester of the truncated analog **315b**. The relative configuration of that latter compound is secure because it was desilylated to produce **301b**, for which a single crystal X-ray structure had been obtained. Namely, resonances for the following protons had nearly identical chemical shifts and multiplicities in the $^1$H NMR spectra ($CDCl_3$) of **(±)-315a** and **315b**: H7c, H7b, and both methyl ketone Me's.

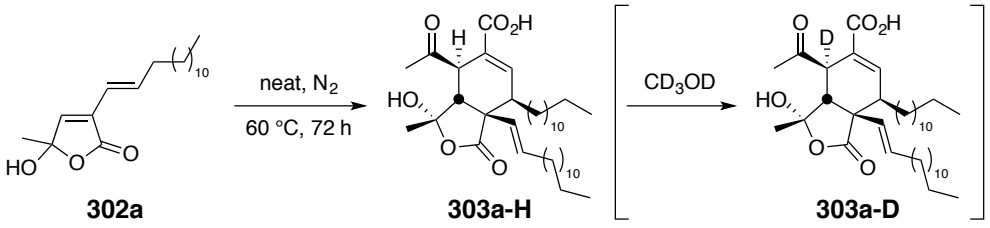


**302a** **303a-H** **303a-D**

**Preparation of (±)-(3*S*,3a*R*,4*R*,7*R*,7a*S*)-4-acetyl-7-dodecyl-3-hydroxy-3-methyl-1-oxo-7a-((*E*)-tetradec-1-en-1-yl)-1,3,3a,4,7,7a-hexahydroisobenzofuran-5-carboxylic acid [(±)-303a]**

(±)-(*E*)-5-Hydroxy-5-methyl-3-(tetradec-1-enyl)furan-2(5H)-one (**302a**, 64 mg, 0.21

mmol) was placed in a 2 mL vial with a Teflon cap. The headspace was flushed with $N_2$. The reaction vial was heated to 60 °C for 72 h. The crude material was directly purified by flash column chromatography (hexanes:ethyl acetate:acetic acid = 50:50:1) to give recovered starting material (**302a**, 23 mg) and (±)-(3*S*,3a*R*,4*R*,7*R*,7a*S*)-4-acetyl-7-dodecyl-3-hydroxy-3-methyl-1-oxo-7a-((*E*)-tetradec-1-en-1-yl)-1,3,3a,4,7,7a-hexahydroisobenzofuran-5-carboxylic acid [**(±)-303a**, 29 mg, 45 %] as a colorless sticky oil.

**$^1$H NMR** (500 MHz, $CDCl_3$) δ 7.28 [br s, 1H, C=C*H*CH($CH_2$)], 5.69 (br dt, *J* = 15.7, 6.4 Hz, 1H, CH=C*H*$CH_2$), 5.26 (br d, *J* = 15.9 Hz, 1H, C*H*=CH$CH_2$), 3.72 (br s, 1H, *H*7c), 2.71 (br s, 1H, *H*7b), 2.61 (br s, 1H, *H*5), 2.25 (very br s, 3H, C(=O)C*H*$_3$), 1.97 (br dt, *J* = 7, 7 Hz, 1H, =CHC*H*$_2$), 1.79 (very br s, 3H, C(OH)C*H*$_3$), 1.51 (br s, 1H), 1.35-1.16 (m, ~41H), and 0.88 [t, *J* = 7.0 Hz, 6H,$CH_2$C*H*$_3$ (2x)]

**$^{13}$C NMR** (125 MHz, $CDCl_3$) δ 133.8, 126.6, 52 (br), 50 (br), 44.8 (br), 40.6 (br), 32.9, 32.1, 29.91 (br), 29.89, 29.87, 29.84, 29.80 (br), 29.7, 29.6, 29.4, 22.9, and 14.4. [Because this compound appears to exist as an equilibrating mixture of pseudo-acids and/or hemiketals ($^1$H NMR), many resonances in the core of this structure were either broad of not observed in this $^{13}$C NMR spectrum.]

**IR** (neat): 2923, 2853, 1770, 1758, 1696, 1464, 1246, 1056, and 911 cm$^{-1}$.

**HRMS** (ESI-TOF): Calcd for $(C_{38}H_{64}NaO_6)^+$ 639.4595 Found: 639.4595.

---

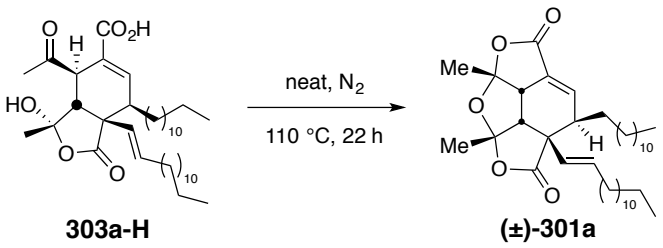


**303a-H** **(±)-301a**

**Preparation of (±)-paracaseolide A (1a*R*,5*R*,5a*S*,7a*S*,7b*R*,7c*S*)-rel-(±)-5-dodecyl-1a,5,5a,7a,7b,7c-hexahydro-1a,7a-dimethyl-5a-(1*E*)-1-tetradecen-1-yldifuro[2,3,4-**

**cd:4',3',2'-hi]isobenzofuran-3,6-dione [(±)-301a]**

In a glass vial was added the acid **303a-H** (4.7 mg, 7.6 μmol). The headspace was flushed with $N_2$. The vial was sealed with a Teflon-lined cap and placed in a 110 °C oil bath. After 22 h the $^1$H NMR spectrum of the sample showed that clean conversion had occurred to give (±)-paracaseolide A (**301a**, 4.3 mg, after re-evaporation of the NMR solvent). The overall cleanliness of this reaction can be seen from inspection of the $^1$H NMR spectrum, a copy of which is included later in this Supplementary Information.

**Computational Methods**

DFT calculations were carried out using Gaussian 09.[100] Geometries were optimized using the M06-2X functional developed by Truhlar et al[101] or the B3LYP[102] functional. The double-ζ 6-31G(d), cc-pVDZ, or triple-ζ 6-311+G(d,p) basis sets were used. The SMD continuum solvation model[46] was used with 2-butanol as the solvent, chosen to mimic the medium for the neat reaction conditions, during the frequency calculation and the geometry optimization (unless otherwise indicated). The "grid=ultrafine" option was applied during the numerical integrations. The harmonic vibrational frequency calculations were carried out using 298 K as the thermal correction for the free energies. Every optimized transition state structure geometry showed only one imaginary frequency.

First, we used DFT calculations to evaluate the relative energies of transition state (TS) structures corresponding to the exo vs. the endo modes of dimerization of **302b** [SMD/M06-2X/6-31G(d) in 2-butanol]. The TS structures for both of these modes of addition are shown on following pages. Both homochiral and heterochiral possibilities (i.e., dimerization of two copies of the same enantiomer or one copy of each enantiomer of **302b**) as well as approaches of the two molecules with inward vs. outward orientations of the hydroxyl groups were examined. The two heterochiral-TS structures for the *exo* mode of addition converged to the same (bis-pericyclic) structure (**$TS_{exo}$-2**) during the

---

[100] M. J. Frisch, G. W. Trucks, H. B. Schlegel, G. E. Scuseria, M. A. Robb, J. R. Cheeseman, G. Scalmani, V. Barone, B. Mennucci, G. A. Petersson, H. Nakatsuji, M. Caricato, X. Li, H. P. Hratchian, A. F. Izmaylov, J. Bloino, G. Zheng, J. L. Sonnenberg, M. Hada, M. Ehara, K. Toyota, R. Fukuda, J. Hasegawa, M. Ishida, T. Nakajima, Y. Honda, O. Kitao, H. Nakai, T. Vreven, J. A. Montgomery, Jr., J. E. Peralta, F. Ogliaro, M. Bearpark, J. J. Heyd, E. Brothers, K. N. Kudin, V. N. Staroverov, R. Kobayashi, J. Normand, K. Raghavachari, A. Rendell, J. C. Burant, S. S. Iyengar, J. Tomasi, M. Cossi, N. Rega, J. M. Millam, M. Klene, J. E. Knox, J. B. Cross, V. Bakken, C. Adamo, J. Jaramillo, R. Gomperts, R. E. Stratmann, O. Yazyev, A. J. Austin, R. Cammi, C. Pomelli, J. W. Ochterski, R. L. Martin, K. Morokuma, V. G. Zakrzewski, G. A. Voth, P. Salvador, J. J. Dannenberg, S. Dapprich, A. D. Daniels, Ö. Farkas, J. B. Foresman, J. V. Ortiz, J. Cioslowski, and D. J. Fox. *Gaussian 09*, revision D.01; Gaussian, Inc.: Wallingform, CT, 2009.

[101] Zhao, Y.; Truhlar, D. G. The M06 suite of density functionals for main group thermochemistry, thermochemical kinetics, noncovalent interactions, excited states, and transition elements: Two new functionals and systematic testing of four M06-class functionals and 12 other functionals. *Theor. Chem. Acc.* **2008**, *120*, 215–241.

[102] Stephens, P. J.; Devlin, F. J.; Chabalowski, C. F.; Frisch, M. J. Ab Initio Calculation of Vibrational Absorption and Circular Dichroism Spectra Using Density Functional Force Fields. *J. Phys. Chem.* **1994**, *98*, 11623-11627.

optimization.

| | $G_{rel}$ (kcal $mol^{-1}$) | |
|---|---|---|
| **$TS_{endo}$-1** | 4.7 | Homochiral: hydroxyls in on diene and out on dienophile |
| **$TS_{endo}$-2** | 2.9 | Heterochiral: hydroxyls in on both diene and dienophile (lowest G, *endo* TS) |
| **$TS_{endo}$-3** | 8.1 | Heterochiral: hydroxyls out on both the diene and dienophile |
| **$TS_{endo}$-4** | 3.7 | Homochiral: hydroxyls out on diene and in on dienophile |
| **$TS_{exo}$-1** | 4.6 | Homochiral: hydroxyls out on both diene and dienophile |
| **$TS_{exo}$-2** | 2.3 | Heterochiral: hydroxyls in on diene and out on dienophile |
| **$TS_{exo}$-3** | 0 | Homochiral: hydroxyls in on both diene and dienophile (lowest G, *exo* TS) |

Second, we optimized the lowest energy *endo* and *exo* TS structures (i.e., **$TS_{endo}$-2** and **$TS_{exo}$-3**) with several other combinations of functional and basis set. A gas-phase calculation (i.e., no SMD) was also performed. Specifically, the following combinations were used: SMD/M06-2X/6-311+G(d,p), SMD/M06-2X/cc-pVDZ, SMD/B3LYP/6-311+G(d,p) in 2-butanol, and M06-2X/6-311+G(d,p) without SMD solvation. All of the resulting TS geometries were very similar; the TS energies are given in Table S1 (below). The optimized structure of **$TS_{endo}$-2** and **$TS_{exo}$-3** at the SMD/M06-2X/6-311+G(d,p) level are those given in the manuscript (as "**$TS_{endo}$**" and "**$TS_{exo}$**").

Third, we examined a conformational analog of **$TS_{endo}$-2** in which the dienophile has an s-trans geometry at the SMD/M06-2X/6-311+G(d,p) level. The resulting **$TS_{endo}$-$2_{s\text{-}trans}$** had a $G_{rel}$ 0.8 kcal•$mol^{-1}$ higher than the energy of the s-cis-containing **$TS_{endo}$-2**.

Last, we optimized monomer **302b** and the product structure **PD** (co-ordinates for both below) from an *exo* DA dimerization at the SMD/M06-2X/6-311+G(d,p) level to determine the computed free energy of reaction (-14.0 kcal•$mol^{-1}$), which is also now

given in the manuscript.

**Table S1.** Energies of $\mathbf{TS_{exo}}$ and $\mathbf{TS_{endo}}$ with different functional/basis set/solvation combinations

| Method | Structure | H (Hartree/Particle) | G (Hartree/Particle) | $H_{rel}$ (kcal•mol$^{-1}$) | $G_{rel}$ (kcal•mol$^{-1}$) |
|---|---|---|---|---|---|
| SMD(2-butanol)/M06-2X/6-31G(d) | $\mathbf{TS_{exo}}$ | -1072.262291 | -1072.333059 | 0.0 | 0.0 |
| | $\mathbf{TS_{endo}}$ | -1072.258385 | -1072.328436 | 2.5 | 2.9 |
| SMD(2-butanol)/M06-2X/6-311+G(d,p)[a] | $\mathbf{TS_{exo}}$ | -1072.595731 | -1072.666831 | 0.0 | 0.0 |
| | $\mathbf{TS_{endo}}$ | -1072.590218 | -1072.660629 | 3.5 | 3.9 |
| M06-2X/6-311+G(d,p) | $\mathbf{TS_{exo}}$ | -1072.558434 | -1072.629637 | 0.0 | 0.0 |
| | $\mathbf{TS_{endo}}$ | -1072.548248 | -1072.619829 | 6.4 | 6.2 |
| SMD(2-butanol)/M06-2X/cc-pVDZ | $\mathbf{TS_{exo}}$ | -1072.384888 | -1072.455101 | 0.0 | 0.0 |
| | $\mathbf{TS_{endo}}$ | -1072.379505 | -1072.450097 | 3.4 | 3.1 |
| SMD(2-butanol)/B3LYP/6-311+G(d,p) | $\mathbf{TS_{exo}}$ | -1073.029730 | -1073.103066 | 0.0 | 0.0 |
| | $\mathbf{TS_{endo}}$ | -1073.023419 | -1073.096053 | 4.0 | 4.4 |

[a] These are the TS structures (and energies) presented in the maintext.

## Coordinates of all structures

**TS structure for $TS_{endo}$-1**

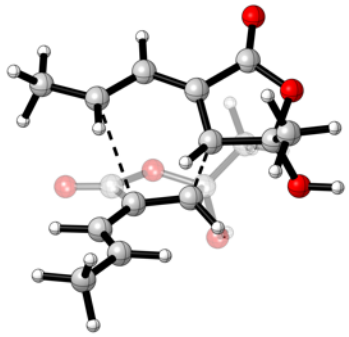

Imaginary frequency: -411.3425 $cm^{-1}$

| Center Number | Atomic Number | Atomic Type | Coordinates (Angstroms) X | Y | Z |
|---|---|---|---|---|---|
| 1 | 6 | 0 | -1.588845 | 0.048150 | -0.541480 |
| 2 | 6 | 0 | -2.529889 | 1.083225 | -0.188519 |
| 3 | 6 | 0 | -2.293487 | 2.401553 | -0.316568 |
| 4 | 6 | 0 | -1.147341 | -0.538479 | 2.148195 |
| 5 | 6 | 0 | 0.143990 | -0.953094 | 1.993001 |
| 6 | 6 | 0 | -0.295266 | 0.178270 | -1.056084 |
| 7 | 1 | 0 | -3.478186 | 0.743661 | 0.228515 |
| 8 | 1 | 0 | -1.392579 | 0.495934 | 1.923016 |
| 9 | 1 | 0 | 0.460493 | -1.920718 | 2.380553 |
| 10 | 1 | 0 | -0.022201 | 1.026521 | -1.678114 |
| 11 | 1 | 0 | -1.355849 | 2.737189 | -0.762081 |
| 12 | 6 | 0 | -1.956040 | -1.372415 | -0.558222 |
| 13 | 8 | 0 | -2.998762 | -1.903819 | -0.238641 |
| 14 | 6 | 0 | 0.047589 | -1.191751 | -1.661607 |
| 15 | 8 | 0 | -0.916731 | -2.089388 | -1.067252 |
| 16 | 6 | 0 | 1.082586 | -0.201397 | 1.260247 |
| 17 | 6 | 0 | 0.829857 | 0.855803 | 0.386021 |
| 18 | 6 | 0 | 2.189289 | 1.339714 | -0.120805 |
| 19 | 1 | 0 | 0.098608 | 1.635463 | 0.609687 |
| 20 | 6 | 0 | 2.504547 | -0.571508 | 1.133589 |
| 21 | 8 | 0 | 3.101844 | -1.480727 | 1.663170 |
| 22 | 8 | 0 | 3.115518 | 0.303596 | 0.302665 |
| 23 | 6 | 0 | -2.212860 | -1.359285 | 2.786517 |
| 24 | 1 | 0 | -1.845620 | -2.350671 | 3.065388 |
| 25 | 1 | 0 | -2.601076 | -0.857085 | 3.680732 |

| | | | | | |
|---|---|---|---|---|---|
| 26 | 1 | 0 | −3.058326 | −1.484637 | 2.097928 |
| 27 | 6 | 0 | −3.261721 | 3.468133 | 0.080660 |
| 28 | 1 | 0 | −2.815391 | 4.147519 | 0.816676 |
| 29 | 1 | 0 | −3.538222 | 4.083188 | −0.784238 |
| 30 | 1 | 0 | −4.172630 | 3.041883 | 0.510050 |
| 31 | 6 | 0 | 1.414722 | −1.815211 | −1.482833 |
| 32 | 1 | 0 | 1.486055 | −2.684648 | −2.145536 |
| 33 | 1 | 0 | 2.193179 | −1.100335 | −1.756731 |
| 34 | 1 | 0 | 1.566519 | −2.169791 | −0.463336 |
| 35 | 8 | 0 | −0.259502 | −1.034519 | −3.018515 |
| 36 | 1 | 0 | −0.041166 | −1.864789 | −3.476463 |
| 37 | 8 | 0 | 2.209254 | 1.417124 | −1.504260 |
| 38 | 1 | 0 | 3.017284 | 1.886905 | −1.775126 |
| 39 | 6 | 0 | 2.621987 | 2.639097 | 0.532466 |
| 40 | 1 | 0 | 3.641292 | 2.883813 | 0.215941 |
| 41 | 1 | 0 | 1.947730 | 3.443645 | 0.227383 |
| 42 | 1 | 0 | 2.602408 | 2.543989 | 1.620953 |

**TS structure for $TS_{endo}$-2**

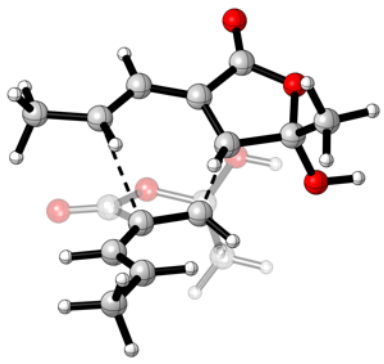

Imaginary frequency: -429.9500 $cm^{-1}$

| Center Number | Atomic Number | Atomic Type | Coordinates (Angstroms) X | Y | Z |
|---|---|---|---|---|---|
| 1 | 6 | 0 | 1.570973 | 0.038078 | 0.559134 |
| 2 | 6 | 0 | 2.690384 | 0.870674 | 0.170578 |
| 3 | 6 | 0 | 2.638739 | 2.208067 | 0.061772 |
| 4 | 6 | 0 | 1.251333 | −0.764880 | −2.005612 |
| 5 | 6 | 0 | −0.042965 | −1.173654 | −1.857347 |
| 6 | 6 | 0 | 0.296531 | 0.420849 | 0.983080 |
| 7 | 1 | 0 | 3.616027 | 0.343864 | −0.061957 |
| 8 | 1 | 0 | 1.473603 | 0.296807 | −1.938029 |

| | | | | | |
|---|---|---|---|---|---|
| 9 | 1 | 0 | −0.328829 | −2.197970 | −2.091930 |
| 10 | 1 | 0 | 0.125469 | 1.406655 | 1.406859 |
| 11 | 1 | 0 | 1.710910 | 2.726119 | 0.309033 |
| 12 | 6 | 0 | 1.711434 | −1.403216 | 0.793344 |
| 13 | 8 | 0 | 2.666644 | −2.130230 | 0.620369 |
| 14 | 6 | 0 | −0.275391 | −0.781374 | 1.749186 |
| 15 | 8 | 0 | 0.552964 | −1.875593 | 1.336995 |
| 16 | 6 | 0 | −1.016269 | −0.335306 | −1.285986 |
| 17 | 6 | 0 | −0.817856 | 0.857030 | −0.595866 |
| 18 | 6 | 0 | −2.199480 | 1.352867 | −0.163676 |
| 19 | 1 | 0 | −0.095626 | 1.611585 | −0.907642 |
| 20 | 6 | 0 | −2.427796 | −0.734525 | −1.120064 |
| 21 | 8 | 0 | −2.986387 | −1.734188 | −1.502470 |
| 22 | 8 | 0 | −3.094228 | 0.263633 | −0.488301 |
| 23 | 6 | 0 | −0.120783 | −0.581829 | 3.250722 |
| 24 | 1 | 0 | −0.756179 | 0.247209 | 3.577863 |
| 25 | 1 | 0 | −0.430987 | −1.495895 | 3.764022 |
| 26 | 1 | 0 | 0.917510 | −0.352816 | 3.506129 |
| 27 | 8 | 0 | −1.574954 | −1.176534 | 1.435448 |
| 28 | 1 | 0 | −2.163831 | −0.444323 | 1.699246 |
| 29 | 6 | 0 | 2.358542 | −1.654812 | −2.453629 |
| 30 | 1 | 0 | 2.045849 | −2.701861 | −2.485497 |
| 31 | 1 | 0 | 2.706811 | −1.356841 | −3.450565 |
| 32 | 1 | 0 | 3.215805 | −1.568906 | −1.776253 |
| 33 | 6 | 0 | 3.789747 | 3.063997 | −0.359690 |
| 34 | 1 | 0 | 3.539884 | 3.645284 | −1.255503 |
| 35 | 1 | 0 | 4.043307 | 3.789395 | 0.422756 |
| 36 | 1 | 0 | 4.677090 | 2.461896 | −0.575014 |
| 37 | 6 | 0 | −2.654888 | 2.579991 | −0.927557 |
| 38 | 1 | 0 | −3.684977 | 2.824874 | −0.649002 |
| 39 | 1 | 0 | −2.005489 | 3.425439 | −0.686304 |
| 40 | 1 | 0 | −2.615418 | 2.390741 | −2.003078 |
| 41 | 8 | 0 | −2.242485 | 1.550008 | 1.218475 |
| 42 | 1 | 0 | −3.076912 | 2.000224 | 1.440408 |

**TS structure for $TS_{endo}$-3**

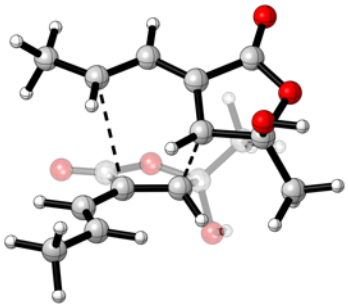

Imaginary frequency: -407.7633 $cm^{-1}$

| Center Number | Atomic Number | Atomic Type | Coordinates (Angstroms) X | Y | Z |
|---|---|---|---|---|---|
| 1 | 6 | 0 | -1.598563 | 0.085071 | -0.535560 |
| 2 | 6 | 0 | -2.503460 | 1.143660 | -0.157200 |
| 3 | 6 | 0 | -2.228920 | 2.456701 | -0.258707 |
| 4 | 6 | 0 | -1.133849 | -0.598582 | 2.131792 |
| 5 | 6 | 0 | 0.157553 | -1.007112 | 1.961511 |
| 6 | 6 | 0 | -0.301551 | 0.178052 | -1.045874 |
| 7 | 1 | 0 | -3.459621 | 0.823864 | 0.257306 |
| 8 | 1 | 0 | -1.380255 | 0.441856 | 1.937232 |
| 9 | 1 | 0 | 0.474683 | -1.985838 | 2.319945 |
| 10 | 1 | 0 | -0.024709 | 1.024150 | -1.669215 |
| 11 | 1 | 0 | -1.284802 | 2.775488 | -0.703051 |
| 12 | 6 | 0 | -2.028864 | -1.315018 | -0.600136 |
| 13 | 8 | 0 | -3.094408 | -1.807307 | -0.293543 |
| 14 | 6 | 0 | 0.009292 | -1.198660 | -1.660654 |
| 15 | 8 | 0 | -1.030176 | -2.060112 | -1.143633 |
| 16 | 6 | 0 | 1.094636 | -0.233335 | 1.249135 |
| 17 | 6 | 0 | 0.843212 | 0.846436 | 0.406186 |
| 18 | 6 | 0 | 2.208576 | 1.359815 | -0.058301 |
| 19 | 1 | 0 | 0.114787 | 1.623705 | 0.641735 |
| 20 | 6 | 0 | 2.515779 | -0.604557 | 1.100212 |
| 21 | 8 | 0 | 3.114065 | -1.530541 | 1.595659 |
| 22 | 8 | 0 | 3.118493 | 0.281171 | 0.269556 |
| 23 | 6 | 0 | -2.196602 | -1.440870 | 2.746289 |
| 24 | 1 | 0 | -1.819506 | -2.430723 | 3.017453 |
| 25 | 1 | 0 | -2.604510 | -0.955266 | 3.640679 |
| 26 | 1 | 0 | -3.031062 | -1.569403 | 2.044303 |
| 27 | 6 | 0 | -3.162398 | 3.542017 | 0.169780 |
| 28 | 1 | 0 | -2.692331 | 4.184581 | 0.923849 |

| | | | | | |
|---|---|---|---|---|---|
| 29 | 1 | 0 | −3.420160 | 4.190016 | −0.676505 |
| 30 | 1 | 0 | −4.085504 | 3.132741 | 0.589484 |
| 31 | 8 | 0 | 2.491149 | 2.450592 | 0.764439 |
| 32 | 1 | 0 | 3.329756 | 2.846440 | 0.469126 |
| 33 | 6 | 0 | 2.399133 | 1.700236 | −1.520625 |
| 34 | 1 | 0 | 1.741392 | 2.532339 | −1.787823 |
| 35 | 1 | 0 | 3.437478 | 2.008393 | −1.679774 |
| 36 | 1 | 0 | 2.185559 | 0.849412 | −2.171044 |
| 37 | 6 | 0 | 1.319580 | −1.915020 | −1.407529 |
| 38 | 1 | 0 | 1.352755 | −2.796725 | −2.057095 |
| 39 | 1 | 0 | 2.171008 | −1.275407 | −1.649271 |
| 40 | 1 | 0 | 1.394828 | −2.266618 | −0.378884 |
| 41 | 8 | 0 | −0.197582 | −0.999156 | −3.029325 |
| 42 | 1 | 0 | 0.026559 | −1.823195 | −3.495587 |

**TS structure for $TS_{endo}$-4**

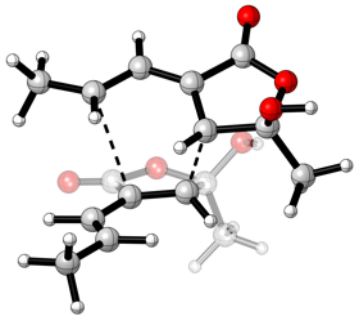

Imaginary frequency: -426.9161 $cm^{-1}$

| Center Number | Atomic Number | Atomic Type | Coordinates (Angstroms) X | Y | Z |
|---|---|---|---|---|---|
| 1 | 6 | 0 | 1.580038 | 0.033963 | 0.565672 |
| 2 | 6 | 0 | 2.614079 | 0.980567 | 0.211805 |
| 3 | 6 | 0 | 2.463838 | 2.315956 | 0.230073 |
| 4 | 6 | 0 | 1.214578 | −0.637520 | −2.061478 |
| 5 | 6 | 0 | −0.075428 | −1.059673 | −1.907216 |
| 6 | 6 | 0 | 0.286723 | 0.285716 | 1.036596 |
| 7 | 1 | 0 | 3.560940 | 0.549192 | −0.113416 |
| 8 | 1 | 0 | 1.437153 | 0.417465 | −1.924463 |
| 9 | 1 | 0 | −0.367005 | −2.064191 | −2.210806 |
| 10 | 1 | 0 | 0.076614 | 1.200099 | 1.587160 |
| 11 | 1 | 0 | 1.520140 | 2.743367 | 0.572618 |

| | | | | | |
|---|---|---|---|---|---|
| 12 | 6 | 0 | 1.832694 | −1.407023 | 0.658687 |
| 13 | 8 | 0 | 2.842865 | −2.033322 | 0.410192 |
| 14 | 6 | 0 | −0.196916 | −1.021193 | 1.670556 |
| 15 | 8 | 0 | 0.724910 | −2.016673 | 1.161784 |
| 16 | 6 | 0 | −1.035609 | −0.260738 | −1.263797 |
| 17 | 6 | 0 | −0.818279 | 0.873675 | −0.486382 |
| 18 | 6 | 0 | −2.200898 | 1.394861 | −0.086012 |
| 19 | 1 | 0 | −0.088038 | 1.640889 | −0.744780 |
| 20 | 6 | 0 | −2.454044 | −0.648010 | −1.115844 |
| 21 | 8 | 0 | −3.022365 | −1.622099 | −1.549558 |
| 22 | 8 | 0 | −3.100072 | 0.309202 | −0.411130 |
| 23 | 6 | 0 | −0.054571 | −0.991024 | 3.184137 |
| 24 | 1 | 0 | −0.732274 | −0.243529 | 3.605929 |
| 25 | 1 | 0 | −0.306719 | −1.975217 | 3.592118 |
| 26 | 1 | 0 | 0.972328 | −0.744664 | 3.466239 |
| 27 | 8 | 0 | −1.482461 | −1.355957 | 1.285105 |
| 28 | 1 | 0 | −1.804916 | −2.074350 | 1.856348 |
| 29 | 6 | 0 | 2.307697 | −1.488982 | −2.607133 |
| 30 | 1 | 0 | 1.996452 | −2.532739 | −2.702283 |
| 31 | 1 | 0 | 2.620291 | −1.120097 | −3.592277 |
| 32 | 1 | 0 | 3.188275 | −1.446481 | −1.955845 |
| 33 | 6 | 0 | 3.528553 | 3.286436 | −0.168739 |
| 34 | 1 | 0 | 3.187891 | 3.926044 | −0.991792 |
| 35 | 1 | 0 | 3.779436 | 3.955240 | 0.663420 |
| 36 | 1 | 0 | 4.439505 | 2.771162 | −0.486334 |
| 37 | 8 | 0 | −2.457444 | 2.465123 | −0.945951 |
| 38 | 1 | 0 | −3.306855 | 2.864415 | −0.688952 |
| 39 | 6 | 0 | −2.440329 | 1.768959 | 1.360503 |
| 40 | 1 | 0 | −1.775201 | 2.589350 | 1.644321 |
| 41 | 1 | 0 | −3.476762 | 2.104175 | 1.472185 |
| 42 | 1 | 0 | −2.277484 | 0.913860 | 2.018498 |

**TS structure for $TS_{exo}$-1**

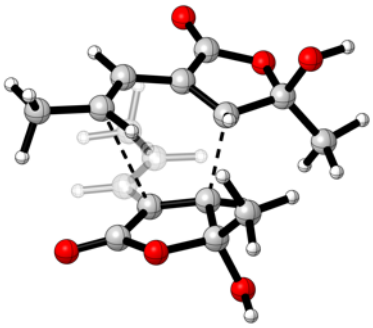

Imaginary frequency: -382.0468 $cm^{-1}$

| Center Number | Atomic Number | Atomic Type | Coordinates (Angstroms) X | Y | Z |
|---|---|---|---|---|---|
| 1 | 6 | 0 | 1.196264 | -0.515698 | -0.888305 |
| 2 | 6 | 0 | 0.475684 | -1.610503 | -1.434422 |
| 3 | 6 | 0 | -0.808807 | -1.491957 | -1.848309 |
| 4 | 6 | 0 | 0.808808 | -1.491951 | 1.848310 |
| 5 | 6 | 0 | -0.475683 | -1.610501 | 1.434424 |
| 6 | 6 | 0 | 0.737420 | 0.784610 | -0.689977 |
| 7 | 1 | 0 | 0.957528 | -2.587143 | -1.416437 |
| 8 | 1 | 0 | 1.255087 | -0.499359 | 1.917244 |
| 9 | 1 | 0 | -0.957525 | -2.587142 | 1.416438 |
| 10 | 1 | 0 | 0.092961 | 1.256933 | -1.421455 |
| 11 | 1 | 0 | -1.255089 | -0.499366 | -1.917241 |
| 12 | 6 | 0 | 2.582652 | -0.604096 | -0.407316 |
| 13 | 8 | 0 | 3.332221 | -1.555350 | -0.392820 |
| 14 | 6 | 0 | 1.960908 | 1.611363 | -0.273670 |
| 15 | 8 | 0 | 2.971919 | 0.620735 | 0.034667 |
| 16 | 6 | 0 | -1.196265 | -0.515698 | 0.888307 |
| 17 | 6 | 0 | -0.737421 | 0.784611 | 0.689977 |
| 18 | 6 | 0 | -1.960910 | 1.611363 | 0.273668 |
| 19 | 1 | 0 | -0.092963 | 1.256935 | 1.421454 |
| 20 | 6 | 0 | -2.582652 | -0.604096 | 0.407316 |
| 21 | 8 | 0 | -3.332221 | -1.555352 | 0.392822 |
| 22 | 8 | 0 | -2.971919 | 0.620733 | -0.034669 |
| 23 | 6 | 0 | 1.657973 | -2.634913 | 2.287153 |
| 24 | 1 | 0 | 2.544901 | -2.711137 | 1.642944 |
| 25 | 1 | 0 | 2.025753 | -2.482259 | 3.308770 |
| 26 | 1 | 0 | 1.112125 | -3.581332 | 2.244505 |
| 27 | 6 | 0 | -1.657969 | -2.634921 | -2.287150 |
| 28 | 1 | 0 | -2.544890 | -2.711156 | -1.642933 |

| | | | | | |
|---|---|---|---|---|---|
| 29 | 1 | 0 | −2.025760 | −2.482264 | −3.308763 |
| 30 | 1 | 0 | −1.112114 | −3.581336 | −2.244514 |
| 31 | 6 | 0 | −1.872667 | 2.541628 | −0.918495 |
| 32 | 1 | 0 | −2.807960 | 3.106019 | −0.993985 |
| 33 | 1 | 0 | −1.045803 | 3.245396 | −0.787501 |
| 34 | 1 | 0 | −1.739997 | 1.990694 | −1.851911 |
| 35 | 8 | 0 | −2.334396 | 2.298275 | 1.430482 |
| 36 | 1 | 0 | −3.092013 | 2.870326 | 1.216213 |
| 37 | 8 | 0 | 2.334393 | 2.298276 | −1.430484 |
| 38 | 1 | 0 | 3.092008 | 2.870329 | −1.216216 |
| 39 | 6 | 0 | 1.872666 | 2.541629 | 0.918493 |
| 40 | 1 | 0 | 2.807959 | 3.106019 | 0.993983 |
| 41 | 1 | 0 | 1.045801 | 3.245396 | 0.787499 |
| 42 | 1 | 0 | 1.739997 | 1.990695 | 1.851909 |

**TS structure for $TS_{exo}$-2**

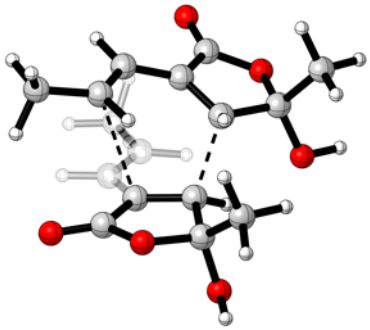

Imaginary frequency: -385.5927 $cm^{-1}$

| Center Number | Atomic Number | Atomic Type | Coordinates (Angstroms) X | Y | Z |
|---|---|---|---|---|---|
| 1 | 6 | 0 | 1.199783 | −0.533092 | −0.858853 |
| 2 | 6 | 0 | 0.495490 | −1.642720 | −1.393504 |
| 3 | 6 | 0 | −0.782015 | −1.534880 | −1.833272 |
| 4 | 6 | 0 | 0.766763 | −1.498703 | 1.878439 |
| 5 | 6 | 0 | −0.515118 | −1.603144 | 1.451787 |
| 6 | 6 | 0 | 0.722263 | 0.767316 | −0.693374 |
| 7 | 1 | 0 | 0.978921 | −2.617623 | −1.345788 |
| 8 | 1 | 0 | 1.229153 | −0.512987 | 1.938803 |
| 9 | 1 | 0 | −1.010095 | −2.573242 | 1.438254 |
| 10 | 1 | 0 | 0.063610 | 1.223998 | −1.424564 |
| 11 | 1 | 0 | −1.227725 | −0.544582 | −1.931280 |

| | | | | | |
|---|---|---|---|---|---|
| 12 | 6 | 0 | 2.574883 | −0.598563 | −0.342469 |
| 13 | 8 | 0 | 3.334384 | −1.540583 | −0.288199 |
| 14 | 6 | 0 | 1.941226 | 1.612432 | −0.303840 |
| 15 | 8 | 0 | 2.938145 | 0.639356 | 0.090199 |
| 16 | 6 | 0 | −1.210369 | −0.505185 | 0.880806 |
| 17 | 6 | 0 | −0.720211 | 0.787265 | 0.681052 |
| 18 | 6 | 0 | −1.912955 | 1.627589 | 0.211926 |
| 19 | 1 | 0 | −0.076870 | 1.238918 | 1.427954 |
| 20 | 6 | 0 | −2.576686 | −0.579209 | 0.347959 |
| 21 | 8 | 0 | −3.343274 | −1.518176 | 0.320393 |
| 22 | 8 | 0 | −2.931912 | 0.646859 | −0.115884 |
| 23 | 6 | 0 | 1.595611 | −2.649873 | 2.334515 |
| 24 | 1 | 0 | 2.480944 | −2.748938 | 1.691012 |
| 25 | 1 | 0 | 1.966478 | −2.490754 | 3.353978 |
| 26 | 1 | 0 | 1.034238 | −3.587662 | 2.303463 |
| 27 | 6 | 0 | −1.622429 | −2.688827 | −2.259141 |
| 28 | 1 | 0 | −2.515844 | −2.754442 | −1.622418 |
| 29 | 1 | 0 | −1.980568 | −2.557042 | −3.287064 |
| 30 | 1 | 0 | −1.074823 | −3.632879 | −2.192299 |
| 31 | 8 | 0 | 2.348591 | 2.212951 | −1.498316 |
| 32 | 1 | 0 | 3.114549 | 2.782353 | −1.308028 |
| 33 | 6 | 0 | 1.823269 | 2.629476 | 0.811492 |
| 34 | 1 | 0 | 2.749887 | 3.210649 | 0.861883 |
| 35 | 1 | 0 | 0.992391 | 3.308426 | 0.598883 |
| 36 | 1 | 0 | 1.673953 | 2.155829 | 1.783879 |
| 37 | 6 | 0 | −2.460681 | 2.507261 | 1.322692 |
| 38 | 1 | 0 | −1.714863 | 3.257555 | 1.598561 |
| 39 | 1 | 0 | −3.367170 | 3.012825 | 0.974491 |
| 40 | 1 | 0 | −2.707137 | 1.905019 | 2.200723 |
| 41 | 8 | 0 | −1.616649 | 2.356970 | −0.929073 |
| 42 | 1 | 0 | −2.356248 | 2.962703 | −1.110682 |

**TS structure for $TS_{exo}$-3**

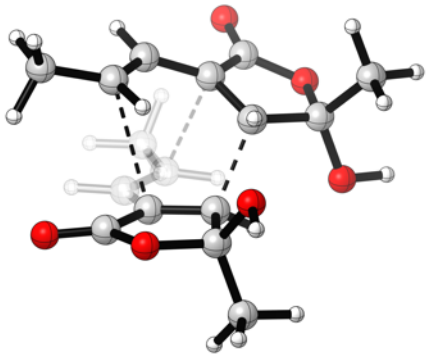

Imaginary frequency: -394.7486 $cm^{-1}$

| Center Number | Atomic Number | Atomic Type | Coordinates (Angstroms) X | Y | Z |
|---|---|---|---|---|---|
| 1 | 6 | 0 | 1.184355 | -0.512468 | -0.894271 |
| 2 | 6 | 0 | 0.461789 | -1.600844 | -1.446535 |
| 3 | 6 | 0 | -0.826603 | -1.476693 | -1.850053 |
| 4 | 6 | 0 | 0.826584 | -1.476690 | 1.850061 |
| 5 | 6 | 0 | -0.461803 | -1.600841 | 1.446530 |
| 6 | 6 | 0 | 0.714612 | 0.786740 | -0.676606 |
| 7 | 1 | 0 | 0.942169 | -2.578355 | -1.440275 |
| 8 | 1 | 0 | 1.270485 | -0.482856 | 1.911701 |
| 9 | 1 | 0 | -0.942186 | -2.578350 | 1.440276 |
| 10 | 1 | 0 | 0.064338 | 1.266644 | -1.401473 |
| 11 | 1 | 0 | -1.270499 | -0.482858 | -1.911706 |
| 12 | 6 | 0 | 2.565777 | -0.607517 | -0.407642 |
| 13 | 8 | 0 | 3.319925 | -1.557458 | -0.410942 |
| 14 | 6 | 0 | 1.927740 | 1.603581 | -0.212657 |
| 15 | 8 | 0 | 2.954716 | 0.610904 | 0.047044 |
| 16 | 6 | 0 | -1.184360 | -0.512464 | 0.894251 |
| 17 | 6 | 0 | -0.714605 | 0.786740 | 0.676593 |
| 18 | 6 | 0 | -1.927724 | 1.603598 | 0.212651 |
| 19 | 1 | 0 | -0.064325 | 1.266630 | 1.401465 |
| 20 | 6 | 0 | -2.565779 | -0.607498 | 0.407614 |
| 21 | 8 | 0 | -3.319940 | -1.557429 | 0.410916 |
| 22 | 8 | 0 | -2.954699 | 0.610924 | -0.047083 |
| 23 | 6 | 0 | -2.438651 | 2.525969 | 1.304431 |
| 24 | 1 | 0 | -1.681372 | 3.284309 | 1.521047 |
| 25 | 1 | 0 | -3.357533 | 3.018225 | 0.969628 |
| 26 | 1 | 0 | -2.651834 | 1.959749 | 2.214553 |
| 27 | 6 | 0 | 2.438657 | 2.525990 | -1.304409 |
| 28 | 1 | 0 | 1.681366 | 3.284324 | -1.521003 |

| | | | | | |
|---|---|---|---|---|---|
| 29 | 1 | 0 | 3.357528 | 3.018253 | -0.969588 |
| 30 | 1 | 0 | 2.651851 | 1.959801 | -2.214548 |
| 31 | 8 | 0 | 1.675205 | 2.288661 | 0.967359 |
| 32 | 1 | 0 | 2.425182 | 2.882657 | 1.144644 |
| 33 | 8 | 0 | -1.675185 | 2.288715 | -0.967342 |
| 34 | 1 | 0 | -2.425042 | 2.882909 | -1.144463 |
| 35 | 6 | 0 | 1.681575 | -2.614928 | 2.289660 |
| 36 | 1 | 0 | 2.561211 | -2.694958 | 1.635646 |
| 37 | 1 | 0 | 2.061335 | -2.453393 | 3.305527 |
| 38 | 1 | 0 | 1.137008 | -3.562661 | 2.261027 |
| 39 | 6 | 0 | -1.681601 | -2.614936 | -2.289622 |
| 40 | 1 | 0 | -2.561223 | -2.694961 | -1.635588 |
| 41 | 1 | 0 | -2.061384 | -2.453415 | -3.305482 |
| 42 | 1 | 0 | -1.137032 | -3.562669 | -2.260990 |

**Structure for $TS_{endo}$-$2_{s\text{-}trans}$**

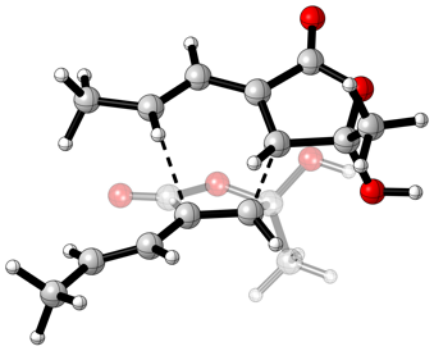

Imaginary frequency: -457.5097 $cm^{-1}$

| Center Number | Atomic Number | Atomic Type | Coordinates (Angstroms) X | Y | Z |
|---|---|---|---|---|---|
| 1 | 6 | 0 | -1.439597 | 0.515449 | 0.265325 |
| 2 | 6 | 0 | -2.456018 | 0.218633 | 1.259751 |
| 3 | 6 | 0 | -3.771392 | 0.083558 | 1.036697 |
| 4 | 6 | 0 | -1.154699 | -2.018970 | -0.378062 |
| 5 | 6 | 0 | 0.080143 | -1.897034 | -0.950805 |
| 6 | 6 | 0 | -0.143181 | 0.964106 | 0.541788 |
| 7 | 1 | 0 | -2.080863 | 0.110891 | 2.276988 |
| 8 | 1 | 0 | -1.233673 | -1.937676 | 0.701333 |
| 9 | 1 | 0 | 0.235180 | -2.157873 | -1.994595 |
| 10 | 1 | 0 | 0.080093 | 1.408695 | 1.505594 |
| 11 | 1 | 0 | -4.156332 | 0.207179 | 0.028840 |
| 12 | 6 | 0 | -1.692044 | 0.732960 | -1.165669 |

| | | | | | |
|---|---|---|---|---|---|
| 13 | 8 | 0 | −2.684152 | 0.539795 | −1.827999 |
| 14 | 6 | 0 | 0.324033 | 1.725145 | −0.706936 |
| 15 | 8 | 0 | −0.582890 | 1.286723 | −1.727617 |
| 16 | 6 | 0 | 1.136452 | −1.299946 | −0.248878 |
| 17 | 6 | 0 | 1.054632 | −0.583286 | 0.940619 |
| 18 | 6 | 0 | 2.469993 | −0.129229 | 1.289577 |
| 19 | 1 | 0 | 0.421390 | −0.879015 | 1.769976 |
| 20 | 6 | 0 | 2.495822 | −1.123292 | −0.795574 |
| 21 | 8 | 0 | 2.953006 | −1.518676 | −1.837289 |
| 22 | 8 | 0 | 3.250224 | −0.462129 | 0.110640 |
| 23 | 6 | 0 | 0.166743 | 3.223899 | −0.504285 |
| 24 | 1 | 0 | 0.861957 | 3.560951 | 0.268362 |
| 25 | 1 | 0 | 0.391742 | 3.735857 | −1.441488 |
| 26 | 1 | 0 | −0.851809 | 3.462891 | −0.192349 |
| 27 | 8 | 0 | 1.586331 | 1.418650 | −1.213987 |
| 28 | 1 | 0 | 2.245554 | 1.773399 | −0.599876 |
| 29 | 6 | 0 | −2.369934 | −2.484737 | −1.092235 |
| 30 | 1 | 0 | −2.236407 | −2.474209 | −2.174807 |
| 31 | 1 | 0 | −2.624849 | −3.501759 | −0.773436 |
| 32 | 1 | 0 | −3.225751 | −1.853112 | −0.829045 |
| 33 | 6 | 0 | −4.766665 | −0.217891 | 2.109956 |
| 34 | 1 | 0 | −5.516447 | 0.576823 | 2.176386 |
| 35 | 1 | 0 | −5.310892 | −1.140277 | 1.882685 |
| 36 | 1 | 0 | −4.287197 | −0.328137 | 3.084589 |
| 37 | 6 | 0 | 3.057485 | −0.878737 | 2.467095 |
| 38 | 1 | 0 | 4.099893 | −0.580352 | 2.604782 |
| 39 | 1 | 0 | 2.490984 | −0.642627 | 3.369389 |
| 40 | 1 | 0 | 3.017180 | −1.953853 | 2.286629 |
| 41 | 8 | 0 | 2.522969 | 1.253311 | 1.466376 |
| 42 | 1 | 0 | 3.365715 | 1.487037 | 1.878846 |

**Structure for 3b**

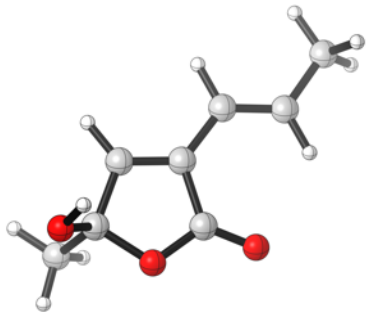

| Center Number | Atomic Number | Atomic Type | Coordinates (Angstroms) X | Y | Z |
|---|---|---|---|---|---|
| 1 | 6 | 0 | 0.391688 | -0.369921 | -0.012026 |
| 2 | 6 | 0 | -0.708362 | -1.131312 | -0.031929 |
| 3 | 6 | 0 | -1.952141 | -0.282238 | -0.037791 |
| 4 | 1 | 0 | -0.762440 | -2.214706 | -0.043272 |
| 5 | 6 | 0 | 1.784803 | -0.799366 | 0.004154 |
| 6 | 1 | 0 | 1.931830 | -1.879032 | 0.006914 |
| 7 | 6 | 0 | 2.849695 | 0.012000 | 0.017400 |
| 8 | 1 | 0 | 2.700884 | 1.088868 | 0.014197 |
| 9 | 6 | 0 | 4.262214 | -0.476648 | 0.036685 |
| 10 | 1 | 0 | 4.812047 | -0.104053 | -0.835711 |
| 11 | 1 | 0 | 4.788854 | -0.101442 | 0.922182 |
| 12 | 1 | 0 | 4.311312 | -1.569348 | 0.039112 |
| 13 | 8 | 0 | -1.426581 | 1.069329 | -0.033945 |
| 14 | 6 | 0 | -0.075367 | 1.051043 | -0.007615 |
| 15 | 8 | 0 | 0.569246 | 2.071514 | 0.017564 |
| 16 | 8 | 0 | -2.742024 | -0.461255 | -1.167824 |
| 17 | 1 | 0 | -2.167805 | -0.429284 | -1.952890 |
| 18 | 6 | 0 | -2.831789 | -0.457979 | 1.181283 |
| 19 | 1 | 0 | -3.669326 | 0.242534 | 1.123671 |
| 20 | 1 | 0 | -3.218460 | -1.479636 | 1.209287 |
| 21 | 1 | 0 | -2.256478 | -0.264075 | 2.089182 |

**Structure for $TS_{exo}$**

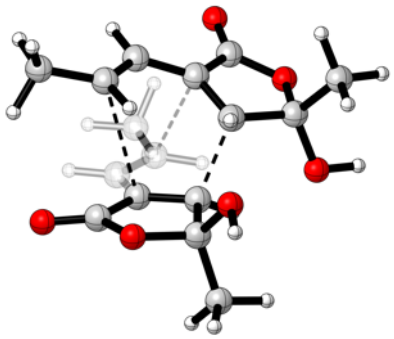

Imaginary frequency: -394.9802 $cm^{-1}$

| Center Number | Atomic Number | Atomic Type | Coordinates (Angstroms) X | Y | Z |
|---|---|---|---|---|---|
| 1 | 6 | 0 | 1.201026 | 0.523337 | 0.863555 |
| 2 | 6 | 0 | 0.504192 | 1.623952 | 1.423021 |
| 3 | 6 | 0 | -0.770231 | 1.515426 | 1.867905 |
| 4 | 6 | 0 | 0.770867 | 1.514391 | -1.868040 |
| 5 | 6 | 0 | -0.503608 | 1.623553 | -1.423417 |
| 6 | 6 | 0 | 0.708891 | -0.771095 | 0.674824 |
| 7 | 1 | 0 | 0.989944 | 2.596349 | 1.393200 |
| 8 | 1 | 0 | 1.220415 | 0.526828 | -1.953415 |
| 9 | 1 | 0 | -0.988941 | 2.596166 | -1.393816 |
| 10 | 1 | 0 | 0.059254 | -1.221752 | 1.415662 |
| 11 | 1 | 0 | -1.220175 | 0.528073 | 1.953598 |
| 12 | 6 | 0 | 2.572609 | 0.586932 | 0.347926 |
| 13 | 8 | 0 | 3.342720 | 1.518537 | 0.319088 |
| 14 | 6 | 0 | 1.903649 | -1.620452 | 0.228570 |
| 15 | 8 | 0 | 2.931532 | -0.642978 | -0.093889 |
| 16 | 6 | 0 | -1.200931 | 0.523339 | -0.863815 |
| 17 | 6 | 0 | -0.709227 | -0.771202 | -0.674723 |
| 18 | 6 | 0 | -1.904247 | -1.620055 | -0.228261 |
| 19 | 1 | 0 | -0.059772 | -1.222316 | -1.415436 |
| 20 | 6 | 0 | -2.572457 | 0.587549 | -0.348095 |
| 21 | 8 | 0 | -3.342249 | 1.519422 | -0.319404 |
| 22 | 8 | 0 | -2.931760 | -0.642134 | 0.094067 |
| 23 | 6 | 0 | -2.427210 | -2.493059 | -1.353048 |
| 24 | 1 | 0 | -1.665722 | -3.226777 | -1.623402 |
| 25 | 1 | 0 | -3.330190 | -3.012320 | -1.022017 |
| 26 | 1 | 0 | -2.667224 | -1.883794 | -2.225816 |
| 27 | 6 | 0 | 2.426224 | -2.493458 | 1.353528 |
| 28 | 1 | 0 | 1.664317 | -3.226611 | 1.624230 |
| 29 | 1 | 0 | 3.328816 | -3.013415 | 1.022520 |

| | | | | | |
|---|---|---|---|---|---|
| 30 | 1 | 0 | 2.666791 | −1.884090 | 2.226072 |
| 31 | 8 | 0 | 1.630571 | −2.356368 | −0.915764 |
| 32 | 1 | 0 | 2.350205 | −2.983615 | −1.067527 |
| 33 | 8 | 0 | −1.631400 | −2.355920 | 0.916175 |
| 34 | 1 | 0 | −2.351336 | −2.982757 | 1.068190 |
| 35 | 6 | 0 | 1.596244 | 2.664405 | −2.328472 |
| 36 | 1 | 0 | 2.504063 | 2.741258 | −1.717671 |
| 37 | 1 | 0 | 1.929415 | 2.515176 | −3.360417 |
| 38 | 1 | 0 | 1.047589 | 3.605337 | −2.263004 |
| 39 | 6 | 0 | −1.595063 | 2.665938 | 2.328080 |
| 40 | 1 | 0 | −2.502647 | 2.743287 | 1.716988 |
| 41 | 1 | 0 | −1.928639 | 2.516950 | 3.359927 |
| 42 | 1 | 0 | −1.045837 | 3.606543 | 2.262711 |

**Structure for $TS_{endo}$**

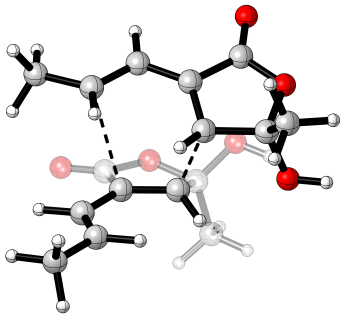

Imaginary frequency: -437.6419 $cm^{-1}$

| Center Number | Atomic Number | Atomic Type | Coordinates (Angstroms) X | Y | Z |
|---|---|---|---|---|---|
| 1 | 6 | 0 | 1.570975 | 0.020680 | 0.537543 |
| 2 | 6 | 0 | 2.681436 | 0.871720 | 0.162343 |
| 3 | 6 | 0 | 2.623684 | 2.210175 | 0.108915 |
| 4 | 6 | 0 | 1.231568 | −0.716476 | −2.028356 |
| 5 | 6 | 0 | −0.057436 | −1.137579 | −1.878688 |
| 6 | 6 | 0 | 0.300251 | 0.387335 | 0.984627 |
| 7 | 1 | 0 | 3.603220 | 0.360321 | −0.108012 |
| 8 | 1 | 0 | 1.442673 | 0.344667 | −1.949445 |
| 9 | 1 | 0 | −0.336300 | −2.158529 | −2.127563 |
| 10 | 1 | 0 | 0.131608 | 1.359956 | 1.433660 |
| 11 | 1 | 0 | 1.699226 | 2.713103 | 0.389775 |
| 12 | 6 | 0 | 1.726434 | −1.419752 | 0.753715 |
| 13 | 8 | 0 | 2.684720 | −2.133984 | 0.569564 |
| 14 | 6 | 0 | −0.254683 | −0.829344 | 1.738739 |

| | | | | | |
|---|---|---|---|---|---|
| 15 | 8 | 0 | 0.579851 | −1.910738 | 1.300240 |
| 16 | 6 | 0 | −1.027559 | −0.315128 | −1.283568 |
| 17 | 6 | 0 | −0.823081 | 0.863609 | −0.574251 |
| 18 | 6 | 0 | −2.198348 | 1.361485 | −0.129593 |
| 19 | 1 | 0 | −0.101415 | 1.619618 | −0.875616 |
| 20 | 6 | 0 | −2.439390 | −0.711711 | −1.118009 |
| 21 | 8 | 0 | −3.001786 | −1.701274 | −1.511614 |
| 22 | 8 | 0 | −3.097440 | 0.272611 | −0.467008 |
| 23 | 6 | 0 | −0.088901 | −0.648479 | 3.239147 |
| 24 | 1 | 0 | −0.724227 | 0.172838 | 3.579281 |
| 25 | 1 | 0 | −0.388061 | −1.569212 | 3.743007 |
| 26 | 1 | 0 | 0.949566 | −0.417403 | 3.483955 |
| 27 | 8 | 0 | −1.551805 | −1.234157 | 1.423819 |
| 28 | 1 | 0 | −2.160750 | −0.563051 | 1.766752 |
| 29 | 6 | 0 | 2.339398 | −1.585093 | −2.509554 |
| 30 | 1 | 0 | 2.058752 | −2.639332 | −2.501816 |
| 31 | 1 | 0 | 2.619754 | −1.300676 | −3.530116 |
| 32 | 1 | 0 | 3.229323 | −1.451176 | −1.888157 |
| 33 | 6 | 0 | 3.763793 | 3.085730 | −0.297751 |
| 34 | 1 | 0 | 3.494069 | 3.698960 | −1.163524 |
| 35 | 1 | 0 | 4.023661 | 3.779811 | 0.507755 |
| 36 | 1 | 0 | 4.647898 | 2.497486 | −0.550315 |
| 37 | 6 | 0 | −2.651964 | 2.595212 | −0.880632 |
| 38 | 1 | 0 | −3.675944 | 2.843635 | −0.590270 |
| 39 | 1 | 0 | −1.994176 | 3.431768 | −0.639178 |
| 40 | 1 | 0 | −2.622655 | 2.412079 | −1.955725 |
| 41 | 8 | 0 | −2.242104 | 1.538189 | 1.252970 |
| 42 | 1 | 0 | −3.044763 | 2.025657 | 1.484012 |

**Structure for PD**

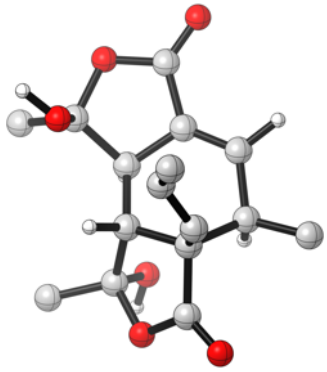

| Center Number | Atomic Number | Atomic Type | Coordinates (Angstroms) X | Y | Z |
|---|---|---|---|---|---|
| 1 | 6 | 0 | 1.350032 | -0.375947 | 0.020502 |
| 2 | 6 | 0 | 1.426013 | -1.550859 | -0.928124 |
| 3 | 6 | 0 | 0.483500 | -1.946668 | -1.778414 |
| 4 | 6 | 0 | 1.156111 | -0.892710 | 1.496801 |
| 5 | 6 | 0 | -0.274401 | -1.343027 | 1.636899 |
| 6 | 6 | 0 | 0.335165 | 0.743781 | -0.342415 |
| 7 | 1 | 0 | 2.352941 | -2.116951 | -0.862227 |
| 8 | 1 | 0 | 1.303777 | -0.030265 | 2.157091 |
| 9 | 1 | 0 | -0.495734 | -2.269007 | 2.161905 |
| 10 | 1 | 0 | 0.209932 | 0.739925 | -1.426889 |
| 11 | 1 | 0 | -0.448035 | -1.392350 | -1.850929 |
| 12 | 6 | 0 | 2.678528 | 0.369291 | -0.081822 |
| 13 | 8 | 0 | 3.784067 | -0.102339 | -0.098726 |
| 14 | 6 | 0 | 1.098073 | 2.038654 | 0.013071 |
| 15 | 8 | 0 | 2.486619 | 1.692427 | -0.199439 |
| 16 | 6 | 0 | -1.244555 | -0.621569 | 1.089226 |
| 17 | 6 | 0 | -1.039610 | 0.655384 | 0.340303 |
| 18 | 6 | 0 | -2.315341 | 0.728305 | -0.531108 |
| 19 | 1 | 0 | -1.124248 | 1.473389 | 1.061976 |
| 20 | 6 | 0 | -2.684793 | -0.934242 | 1.057215 |
| 21 | 8 | 0 | -3.303749 | -1.784453 | 1.644163 |
| 22 | 8 | 0 | -3.289104 | -0.056269 | 0.227519 |
| 23 | 6 | 0 | -2.908475 | 2.102025 | -0.726360 |
| 24 | 1 | 0 | -2.230374 | 2.703970 | -1.333125 |
| 25 | 1 | 0 | -3.864391 | 2.017015 | -1.249604 |
| 26 | 1 | 0 | -3.069522 | 2.592059 | 0.234386 |
| 27 | 6 | 0 | 0.786220 | 3.238065 | -0.847823 |
| 28 | 1 | 0 | -0.250731 | 3.535649 | -0.683985 |
| 29 | 1 | 0 | 1.437457 | 4.070736 | -0.569367 |

| | | | | | |
|---|---|---|---|---|---|
| 30 | 1 | 0 | 0.936026 | 3.003803 | -1.902176 |
| 31 | 8 | 0 | 0.935314 | 2.311967 | 1.373731 |
| 32 | 1 | 0 | 1.352431 | 3.159685 | 1.577754 |
| 33 | 8 | 0 | -2.091643 | 0.075826 | -1.738802 |
| 34 | 1 | 0 | -2.867847 | 0.179343 | -2.305920 |
| 35 | 6 | 0 | 2.124874 | -1.997025 | 1.912332 |
| 36 | 1 | 0 | 3.164258 | -1.694428 | 1.778992 |
| 37 | 1 | 0 | 1.971271 | -2.225318 | 2.969612 |
| 38 | 1 | 0 | 1.951877 | -2.912724 | 1.342741 |
| 39 | 6 | 0 | 0.621910 | -3.142492 | -2.670760 |
| 40 | 1 | 0 | -0.176642 | -3.864261 | -2.474479 |
| 41 | 1 | 0 | 0.533032 | -2.852544 | -3.722193 |
| 42 | 1 | 0 | 1.582998 | -3.640797 | -2.528257 |

# Supplementary information for Section 5.2

## General Experimental Protocols

NMR ($^{1}$H and $^{13}$C) spectra were recorded on Bruker Avance 500 (500 MHz) spectrometers. $^{1}$H NMR chemical shifts ($C_6D_5CD_3$ or $CDCl_3$) are referenced to $C_6D_5CHD_2$ (2.09 ppm) or TMS (0.00 ppm), respectively. The "nfom" designation is used to indicate non-first order multiplets. $^{13}$C NMR chemical shifts are referenced to the *C*$DCl_3$ resonance at 77.23 ppm. The following format is used to report each proton resonance: chemical shift in ppm {multiplicity, *J* values [coupling constant(s)] in Hz, integral value, and assignment}. Coupling constant analysis was performed using protocols we have reported elsewhere.[103] Infrared (IR) spectra were taken of thin film samples on a ZnSe ATR plate with a Prospect MIDAC FT-IR spectrometer. Absorption bands are reported in $cm^{-1}$. Mass spectrometric measurements were performed: i) at low mass accuracy with an Agilent 5975 GC-MS instrument (electron impact ionization (EI) at 70 eV) and ii) at high mass accuracy on a Bruker BioTOF II instrument (<5 ppm mass accuracy) using electrospray ionization (ESI) and PEG as the internal calibrant.

Medium pressure liquid chromatography (MPLC, 50-200 psi) was performed on hand-packed silica gel columns (25-35 μm, 60 Å pores). A Waters HPLC pump fitted with a Waters R401 differential refractive index detector was used to detect the eluants. Flash column chromatography (FCC) was performed on columns packed with silica gel (40-63 μm).

Experiments requiring anhydrous conditions were performed under an atmosphere of nitrogen or argon in oven- or flame-dried glassware. Anhydrous THF, toluene, diethyl ether, and methylene chloride were collected immediately prior to use by being passed through an activated alumina column.

---

[103] Hoye, T. R.; Zhao, H. A method for easily determining coupling constant values: an addendum to "a practical guide to first-order multiplet analysis in $^{1}$H NMR spectroscopy". *J. Org. Chem.* **2002**, *67*, 4014–4016.

## Preparation procedures and characterization data for all key compounds

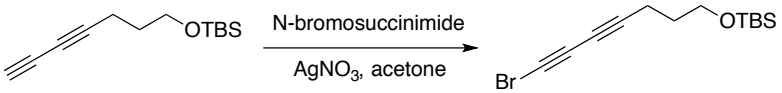


**S501** **523**

**Preparation of ((7-bromohepta-4,6-diyn-1-yl)oxy)(*tert*-butyl)dimethylsilane (523).**

In a round bottom flask (100 mL) wrapped with aluminum foil was added *tert*-butyl(hepta-4,6-diyn-1-yloxy)dimethylsilane[104] (**S501**, 2.2 g, 10 mmol), acetone (50 mL), *N*-bromosuccinimide (2.2 g, 12 mmol), and silver nitrate (170 mg, 1 mmol) at room temperature. The heterogeneous mixture was stirred overnight, filtered, and concentrated to give a light yellow oil. The crude product was then subjected to column chromatography with silica gel (hexanes:ethyl acetate = 12:1) to give ((7-bromohepta-4,6-diyn-1-yl)oxy)(*tert*-butyl)dimethylsilane (**523**, 2.5 g, 8.3 mmol, 83%) as a light yellow oil.

**$^1$H NMR** (500 MHz, $CDCl_3$) δ 3.67 (t, *J* = 5.9 Hz, 2H, -C*H*$_2$OTBS), 2.35 (t, *J* = 7.0 Hz, 2H, -C≡CC*H*$_2$CH$_2$-), 1.72 (tt, *J* = 7.1, 6.1 Hz, 2H, -CH$_2$C*H*$_2$CH$_2$OTBS), 0.89 [s, 9H, Si(CH$_3$)$_2$C(C*H*$_3$)$_3$], and 0.05 [s, 6H, -Si(C*H*$_3$)$_2$C(CH$_3$)$_3$].

**$^{13}$C NMR** (125 MHz, $CDCl_3$) δ 74.7, 66.0, 65.7, 61.5, 37.1, 31.3, 26.1, 18.5, 15.8, and -5.2 ppm.

**IR** (neat) 2954, 2930, 2857, 2369, 2144, 1471, 1462, 1388, 1361, 1252, 1105, 970, 838, and 776 cm$^{-1}$.

**GC-LRMS** (ES, 70 eV): $t_R$ = 7.96 min. *m/z*: 245, 243 ($M^+$-$^t$Bu), 185, 187 ($M^+$-TBS).

[104] Turlington, M.; Du, Y.; Ostrum, S. G.; Santosh, V.; Wren, K.; Lin, T.; Sabat, M.; Pu, L. *J. Am. Chem. Soc.* **2011**, 133, 11780–11794.

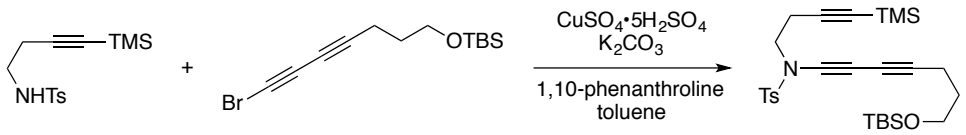


**522** **523** **524**

**Preparation of *N*-(7-((*tert*-Butyldimethylsilyl)oxy)hepta-1,3-diyn-1-yl)-4-methyl-*N*-(4-(trimethylsilyl)but-3-yn-1-yl)benzenesulfonamide (524).**

4-Methyl-*N*-(4-(trimethylsilyl)but-3-yn-1-yl)benzenesulfonamide[105] (**522**, 720 mg, 2.4 mmol), $K_2CO_3$ (1 g, 7.2 mmol), $CuSO_4•5H_2O$ (61 mg, 0.24 mmol), 1,10-phenanthroline (88 mg, 0.49 mmol), and toluene (3.5 mL) were combined in a glass vial. Neat ((7-bromohepta-4,6-diyn-1-yl)oxy)(tert-butyl)dimethylsilane (**523**, 1.1 g, 3.65 mmol) was added with stirring at room temperature. The vial was sealed with a Teflon-lined cap and placed in a 65 °C oil bath with stirring for 15 h. The crude reaction mixture was directly subjected to column chromatography with silica gel (hexanes:ethyl acetate = 12:1) to give *N*-(7-((*tert*-butyldimethylsilyl)oxy)hepta-1,3-diyn-1-yl)-4-methyl-*N*-(4-(trimethylsilyl)but-3-yn-1-yl)benzenesulfonamide (**524**) as an orange-red oil (1.0 g, 80%).

**$^1$H NMR** (500 MHz, $CDCl_3$) δ 7.80 (d, $J$ = 7.5 Hz, 2H, -$SO_2$Ar$H_{ortho}$), 7.36 (d, $J$ = 7.9 Hz, 2H, -$SO_2$Ar$H_{meta}$), 3.68 (t, $J$ = 5.9 Hz, 2H, -C$H_2$OTBS), 3.49 [t, $J$ = 7.7 Hz, 2H, -N(Ts)C$H_2$C$H_2$], 2.55 [t, $J$ = 7.7 Hz, 2H, -N(Ts)C$H_2$C$H_2$], 2.46 (s, 3H, -$SO_2$ArC$H_3$), 2.40 (t, $J$ = 7.0 Hz, 2H, -C$H_2$C$H_2$C$H_2$OTBS), 1.73 (tt, $J$ = 5.9, 7.1 Hz, 2H, -C$H_2$C$H_2$C$H_2$OTBS), 0.90 [s, 9H, -Si(C$H_3$)$_2$C(C$H_3$)$_3$], 0.13 [s, 9H, -Si(C$H_3$)$_3$], and 0.06 [s, 6H, -Si(C$H_3$)$_2$C(C$H_3$)$_3$].

**$^{13}$C NMR** (125 MHz, $CDCl_3$) δ 145.2, 134.8, 130.2, 127.7, 101.7, 87.6, 84.2, 66.8, 64.6, 61.6, 59.1, 50.5, 31.5, 26.1, 21.9, 20.1, 18.5, 16.3, 0.1, and -5.1 ppm.

**IR** (neat) 2954, 2930, 2858, 2252, 2178, 1598, 1375, 1251, 1171, 1093, 970, and 841cm$^{-1}$.

**HRMS** (ESI-TOF): Calcd for $(C_{27}H_{41}NNaO_3SSi_2)^+$ 538.2238; found: 538.2243.

[105] Trost, B. M.; Machacek, M.; Schnaderbeck, M. J. *Org. Lett.* **2000**, *2*, 1761–1764.

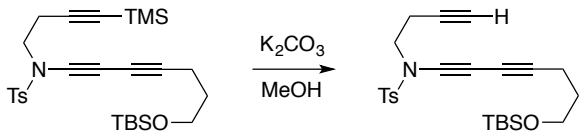


**524** **519a**

**Preparation *N*-(but-3-yn-1-yl)-*N*-(7-((*tert*-butyldimethylsilyl)oxy)hepta-1,3-diyn-1-yl)-4-methylbenzenesulfonamide (519a).**

*N*-(7-((*tert*-Butyldimethylsilyl)oxy)hepta-1,3-diyn-1-yl)-4-methyl-*N*-(4-(trimethylsilyl)but-3-yn-1-yl)benzenesulfonamide (**524**, 700 mg, 1.36 mmol), $K_2CO_3$ (200 mg, 1.45 mmol), and methanol (3 mL) were combined in a glass vial. The vial was capped and the contents were stirred at room temperature for 4 h. The crude mixture was partitioned between ethyl acetate and brine. The organic layer was dried over $Na_2SO_4$, concentrated, and purified with column chromatography on silica gel (hexanes:ethyl acetate = 12:1) to give *N*-(but-3-yn-1-yl)-*N*-(7-((*tert*-butyldimethylsilyl)oxy)hepta-1,3-diyn-1-yl)-4-methylbenzenesulfonamide (**519a**) as a pale yellow oil (501 mg, 83%).

**$^1$H NMR** (500 MHz, $CDCl_3$) δ 7.80 (d, *J* = 7.9 Hz, 2H, -$SO_2$Ar$H_{ortho}$), 7.36 (d, *J* = 8.0 Hz, 2H, -$SO_2$Ar$H_{meta}$), 3.68 (t, *J* = 5.9 Hz, 2H, -C$H_2$OTBS), 3.50 [t, *J* = 7.7 Hz, 2H, -N(Ts)C$H_2$$CH_2$], 2.52 [dt, *J* = 3.1, 7.9 Hz, 2H, -N(Ts)$CH_2$C$H_2$], 2.46 (s, 3H, -$SO_2$ArC$H_3$), 2.40 (t, *J* = 7.0 Hz, 2H, -C$H_2$$CH_2$$CH_2$OTBS), 1.97 (t, *J* = 2.7 Hz, 1H, -C≡C*H*), 1.73 (tt, *J* = 5.9, 7.1 Hz, 2H, -$CH_2$C$H_2$$CH_2$OTBS), 0.90 [s, 9H, -Si$(CH_3)_2$C(C$H_3$)$_3$], and 0.06 [s, 6H, -Si(C$H_3$)$_2$C$(CH_3)_3$].

**$^{13}$C NMR** (125 MHz, $CDCl_3$) δ 145.3, 134.7, 130.2, 127.8, 84.3, 79.6, 70.9, 66.6, 64.5, 61.6, 59.3, 50.2, 31.5, 26.1, 21.9, 18.6, 18.5, 16.3, and -5.1 ppm.

**IR** (neat) 3290, 2952, 2933, 2860, 2252, 2165, 1598, 1373, 1250, 1171, 1093, 1057, 1033, 970, and 838 $cm^{-1}$.

**HRMS** (ESI-TOF): Calcd for $(C_{24}H_{33}NNaO_3SSi)^+$ 466.1843. Found: 466.1857.

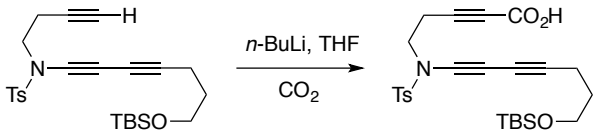


**519a** **S502**

**Preparation of 5-((*N*-(7-((*tert*-butyldimethylsilyl)oxy)hepta-1,3-diyn-1-yl)-4-methylphenyl)sulfonamido)pent-2-ynoic acid (S502).**

In a glass vial was added *N*-(but-3-yn-1-yl)-*N*-(7-((*tert*-butyldimethylsilyl)oxy)hepta-1,3-diyn-1-yl)-4-methylbenzenesulfonamide (**519a**, 100 mg, 0.22 mmol) and THF (3 mL). The vial was sealed with a septum, fitted with an Ar balloon, and cooled to -78 °C in a dry-ice acetone bath. A solution of *n*-BuLi (0.15 mL, 2.5 M in hexanes) was added and the mixture was stirred at -78 °C for 1 h. A balloon filled with anhydrous $CO_2$ (from a lecture cylinder) was attached and the solution was allowed to warm to room temperature and stirred overnight. The color of the acetylide solution dissipated in the first few minutes. The crude mixture was partitioned between ethyl acetate and 1:1 HCl (3M, aq)/$NH_4Cl$ (aq) solution. The organic layer was dried over anhydrous $Na_2SO_4$, concentrated, and purified with column chromatography (hexanes:ethyl acetate:methanol = 5:5:1) to give 5-((*N*-(7-((*tert*-butyldimethylsilyl)oxy)hepta-1,3-diyn-1-yl)-4-methylphenyl)sulfonamido)pent-2-ynoic acid (**S502**, 77.9 mg, 71%) as a yellow oil. A portion of the starting terminal alkyne was also recovered (15.0 mg, 15%).

**$^1$H NMR** (500 MHz, $CDCl_3$) δ 9.08 (br s, 1H, $CO_2H$), 7.79 (d, $J$ = 8.0 Hz, 2H, -$SO_2ArH_{ortho}$), 7.37 (d, $J$ = 8.1 Hz, 2H, -$SO_2ArH_{meta}$), 3.69 (t, $J$ = 5.9 Hz, 2H, -$CH_2$OTBS), 3.55 [br t, $J$ = 7.4 Hz, 2H, -N(Ts)$CH_2CH_2$], 2.65 [br t, $J$ = 7.2 Hz, 2H, -N(Ts)$CH_2CH_2$], 2.45 (s, 3H, -$SO_2ArCH_3$), 2.40 (t, $J$ = 7.1 Hz, 2H, -$CH_2CH_2CH_2$OTBS), 1.73 (tt, $J$ = 6.3, 6.3 Hz, 2H, -$CH_2CH_2CH_2$OTBS), 0.90 [s, 9H, -$Si(CH_3)_2C(CH_3)_3$], and 0.07 [s, 6H, -$Si(CH_3)_2C(CH_3)_3$].

**$^{13}$C NMR** (125 MHz, $CDCl_3$) δ 157.3 (br), 145.6, 134.3, 130.3, 127.8, 84.7 (br), 84.5, 75.6 (br), 66.2, 64.4, 61.7, 59.7, 49.3 (br), 31.4, 26.1, 21.9, 18.9, 18.5, 16.2, and -5.2 ppm.

**IR** (neat) 2953, 2930, 2857, 2245, 2165, 1713 (w), 1696 (w), 1596, 1372, 1252, 1170,

1093, 966, and 837 $cm^{-1}$.

**HRMS** (ESI-TOF): Calcd for $(C_{25}H_{33}NNaO_5SSi)^+$ 510.1741. Found: 510.1731.

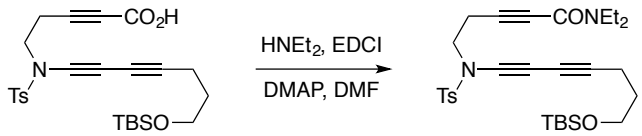


**S502** **519b**

**Preparation of 5-((*N*-(7-((*tert*-butyldimethylsilyl)oxy)hepta-1,3-diyn-1-yl)-4-methylphenyl)sulfonamido)-*N*,*N*-diethylpent-2-ynamide (519b).**

In a glass vial (2 mL) was added 5-((*N*-(7-((*tert*-butyldimethylsilyl)oxy)hepta-1,3-diyn-1-yl)-4-methylphenyl)sulfonamido)pent-2-ynoic acid (**S502**, 50 mg, 0.1 mmol), dimethylformamide (0.2 mL), diethylamine (20 μL, 0.2 mmol), 4-dimethylaminopyridine (4 mg, 0.03 mmol), and 1-(3-dimethylaminopropyl)-3-ethylcarbodiimide hydrochloride (EDCI, 40 mg, 0.2 mmol) at room temperature. This mixture was stirred overnight and then partitioned between ethyl acetate and brine. The organic layer was dried over anhydrous $Na_2SO_4$, concentrated, and purified by column chromatography (silica gel, hexanes:ethyl acetate = 1:1) to give 5-((*N*-(7-((*tert*-butyldimethylsilyl)oxy)hepta-1,3-diyn-1-yl)-4-methylphenyl)sulfonamido)-*N*,*N*-diethylpent-2-ynamide (**519b**, 30.4 mg, 0.06 mmol, 57%) as a pale yellow oil.

**$^1$H NMR** (500 MHz, $CDCl_3$) δ 7.79 (d, $J$ = 8.2 Hz, 2H, -$SO_2$Ar$H_{ortho}$), 7.37 (d, $J$ = 8.1 Hz, 2H, -$SO_2$Ar$H_{meta}$), 3.68 (t, $J$ = 5.9 Hz, 2H, -C$H_2$OTBS), 3.57 [q, $J$ = 7.1 Hz, 2H, -N(C$H_2$$CH_3$)$_a$($CH_2CH_3$)$_b$], 3.53 [t, $J$ = 7.3 Hz, 2H, -N(Ts)C$H_2$$CH_2$], 3.40 [q, $J$ = 7.2 Hz, 2H, -N($CH_2CH_3$)$_a$(C$H_2$$CH_3$)$_b$], 2.72 [t, $J$ = 7.3 Hz, 2H, -N(Ts)$CH_2$C$H_2$], 2.46 (s, 3H, -$SO_2$ArC$H_3$), 2.40 (t, $J$ = 7.0 Hz, 2H, -C$H_2$$CH_2CH_2$OTBS), 1.73 (tt, $J$ = 7.0, 6.1 Hz, 2H, -$CH_2$C$H_2$$CH_2$OTBS), 1.21 [t, $J$ = 7.1 Hz, 3H, -N($CH_2$C$H_3$)$_a$($CH_2CH_3$)$_b$], 1.13 [t, $J$ = 7.1 Hz, 3H, -N($CH_2CH_3$)$_a$($CH_2$C$H_3$)$_b$], 0.90 [s, 9H, -Si($CH_3$)$_2$C(C$H_3$)$_3$], and 0.06 [s, 6H, -Si(C$H_3$)$_2$C($CH_3$)$_3$].

**$^{13}$C NMR** (125 MHz, $CDCl_3$) δ 153.6, 145.5, 134.4, 130.3, 127.8, 86.3, 84.5, 76.5, 66.4, 64.4, 61.6, 59.5, 49.6, 43.7, 39.3, 31.5, 26.1, 21.9, 19.1, 18.5, 16.2, 14.5, 13.0, and -5.2 ppm.

**IR** (neat) 2953, 2932, 2857, 2252, 2165, 1627, 1428, 1373, 1281, 1171, 1092, 969, and 838 $cm^{-1}$.

**HRMS** (ESI-TOF): Calcd for $(C_{29}H_{42}N_2NaO_4SSi)^+$ 565.2527. Found: 565.2533.

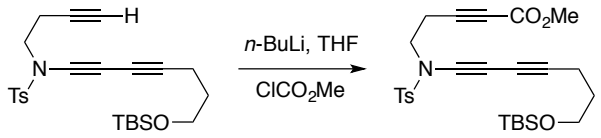


**519a** **519c**

**Preparation of methyl 5-((*N*-(7-((tert-butyldimethylsilyl)oxy)hepta-1,3-diyn-1-yl)-4-methylphenyl)sulfonamido)pent-2-ynoate (519c).**

In a glass vial was added *N*-(but-3-yn-1-yl)-*N*-(7-((*tert*-butyldimethylsilyl)oxy)hepta-1,3-diyn-1-yl)-4-methylbenzenesulfonamide (**519a**, 50 mg, 0.11 mmol) and THF (1.5 mL). The vial was sealed with a septum, connected to an Ar balloon, and cooled to -78 °C in a dry-ice acetone bath. A solution of *n*-BuLi (0.07 mL, 2.5 M in hexanes) was added and the solution was stirred at -78 °C for 1 h. Methyl chloroformate ($ClCO_2Me$, 0.03 mL) was added. The reaction vial was allowed to warm to room temperature and stirred overnight. The crude mixture was partitioned between ethyl acetate and $NH_4Cl$ (aq) solution. The organic layer was dried over anhydrous $Na_2SO_4$, concentrated, and purified by column chromatography (silica gel, hexanes:ethyl acetate = 5:1) to give methyl 5-((*N*-(7-((tert-butyldimethylsilyl)oxy)hepta-1,3-diyn-1-yl)-4-methylphenyl)sulfonamido) pent-2-ynoate (**519c**, 36.2 mg, 64%) as a yellow oil. Some starting material (10.4 mg, 20%) was also recovered.

**$^{1}$H NMR** (500 MHz, $CDCl_3$) δ 7.80 (d, $J$ = 8.1 Hz, 2H, -$SO_2Ar$$H_{ortho}$), 7.37 (d, $J$ = 8.1 Hz,

2H, -$SO_2$Ar$H_{meta}$), 3.76 (s, 3H, $CO_2CH_3$), 3.68 (t, $J$ = 5.9 Hz, 2H, -$CH_2$OTBS), 3.55 [t, $J$ = 7.5 Hz, 2H, -N(Ts)$CH_2CH_2$], 2.68 [t, $J$ = 7.7 Hz, 2H, -N(Ts)$CH_2CH_2$], 2.46 (s, 3H, -$SO_2ArCH_3$), 2.41 (t, $J$ = 7.0 Hz, 2H, -$CH_2CH_2CH_2$OTBS), 1.73 (tt, $J$ = 6.5, 6.4 Hz, 2H, -$CH_2CH_2CH_2$OTBS), 0.90 [s, 9H, -Si$(CH_3)_2C(CH_3)_3$], and 0.06 [s, 6H, -Si$(CH_3)_2C(CH_3)_3$].

**$^{13}$C NMR** (125 MHz, $CDCl_3$) δ 153.8, 145.5, 134.4, 130.2, 127.8, 84.6, 84.1, 74.7, 66.2, 64.3, 61.5, 59.7, 52.9, 49.2, 31.4, 26.1, 21.9, 18.8, 18.5, 16.2, and -5.2 ppm.

**IR** (neat) 2952, 2931, 2858, 2246, 2165, 1717, 1597, 1435, 1373, 1257, 1171, 1091, 966, and 838 $cm^{-1}$.

**HRMS** (ESI-TOF): Calcd for $(C_{26}H_{35}NNaO_5SSi)^+$ 524.1897. Found: 524.1951.

---

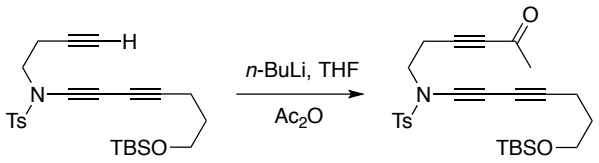


**519a** **519d**

**Preparation of *N*-(7-((tert-butyldimethylsilyl)oxy)hepta-1,3-diyn-1-yl)-4-methyl-*N*-(5-oxohex-3-yn-1-yl)benzenesulfonamide (519d).**

In a glass vial was added *N*-(but-3-yn-1-yl)-*N*-(7-((*tert*-butyldimethylsilyl)oxy)hepta-1,3-diyn-1-yl)-4-methylbenzenesulfonamide (**519a**, 100 mg, 0.22 mmol) and THF (3 mL). The vial was then sealed with a septum, connected to an Ar balloon, and cooled to -78 °C in a dry-ice acetone bath. A solution of *n*-BuLi (0.15 mL, 2.5 M in hexanes) was added. This solution was stirred at -78 °C for 1 h. The reaction mixture was then taken up in a syringe and added dropwise to an ambient temperature solution of acetic anhydride (0.1 mL) in THF (1 mL). This mixture was stirred overnight and then partitioned between ethyl acetate and $NH_4Cl$ (aq) solution. The organic layer was dried over anhydrous $Na_2SO_4$, concentrated, and purified with column chromatography (silica gel, hexanes:ethyl acetate = 5:1) to give **519d** (55.4 mg, 51%) as a yellow oil. Some starting material was also recovered (30 mg, 30%).

**$^1$H NMR** (500 MHz, $CDCl_3$) δ 7.80 (d, *J* = 7.4 Hz, 2H, -$SO_2Ar\mathit{H}_{ortho}$), 7.37 (d, *J* = 7.9 Hz, 2H, -$SO_2Ar\mathit{H}_{meta}$), 3.68 (t, *J* = 5.9 Hz, 2H, -$C\mathit{H}_2$OTBS), 3.55 [t, *J* = 6.9 Hz, 2H, -N(Ts)$C\mathit{H}_2CH_2$], 2.72 [t, *J* = 6.9 Hz, 2H, -N(Ts)$CH_2C\mathit{H}_2$], 2.46 (s, 3H, -$SO_2ArC\mathit{H}_3$), 2.40 (t, *J* = 6.7 Hz, 2H, -$C\mathit{H}_2CH_2CH_2$OTBS), 2.31 (s, 3H, -$COC\mathit{H}_3$), 1.73 (tt, *J* = 7.1, 5.9 Hz, 2H, -$CH_2C\mathit{H}_2CH_2$OTBS), 0.90 [s, 9H, -$Si(CH_3)_2C(C\mathit{H}_3)_3$], and 0.06 [s, 6H, -$Si(C\mathit{H}_3)_2C(CH_3)_3$].

**$^{13}$C NMR** (125 MHz, $CDCl_3$) δ 184.5, 145.5, 134.5, 130.3, 127.8, 88.1, 84.7, 82.9, 66.5, 64.4, 61.6, 59.6, 49.5, 32.8, 31.5, 26.1, 21.9, 19.3, 18.5, 16.2, and -5.2 ppm.

**IR** (neat) 2953, 2930, 2857, 2216, 2164, 1679, 1373, 1250, 1232, 1170, 1092, 969, and 837 $cm^{-1}$.

**HRMS** (ESI-TOF): Calcd for $(C_{26}H_{35}NNaO_4SSi)^+$ 508.1948. Found: 508.1962.

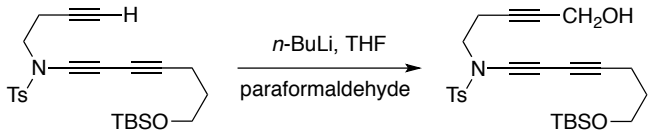


**519a** **S503**

**Preparation of *N*-(7-((*tert*-butyldimethylsilyl)oxy)hepta-1,3-diyn-1-yl)-*N*-(5-hydroxypent-3-yn-1-yl)-4-methylbenzenesulfonamide (S503).**

In a glass vial was added *N*-(but-3-yn-1-yl)-*N*-(7-((*tert*-butyldimethylsilyl)oxy)hepta-1,3-diyn-1-yl)-4-methylbenzenesulfonamide (**519a**, 100 mg, 0.22 mmol) and THF (3 mL). The vial was then sealed with a septum, connected with an Ar balloon, and cooled to -78 °C in a dry-ice acetone bath. A solution of *n*-BuLi (0.15 mL, 2.5 M in hexanes) was added and the solution was stirred at -78 °C for 1 h. Solid paraformaldehyde (30 mg, 1.0 mmol) was added in one portion. The reaction vial was allowed to warm to room temperature overnight. The crude mixture was partitioned between ethyl acetate and $NH_4Cl$ (aq) solution. The organic layer was dried over anhydrous $Na_2SO_4$ and

concentrated. The residue was purified with column chromatography (silica gel, hexanes:ethyl acetate = 5:1) to give *N*-(7-((*tert*-butyldimethylsilyl)oxy)hepta-1,3-diyn-1-yl)-*N*-(5-hydroxypent-3-yn-1-yl)-4-methylbenzenesulfonamide (**S503**, 41.0 mg, 38%) as a yellow oil. Some starting material was also recovered (25.3 mg, 25%).

**$^1$H NMR** (500 MHz, $CDCl_3$) δ 7.80 (d, *J* = 8.1 Hz, 2H, -$SO_2$Ar$H_{ortho}$), 7.37 (d, *J* = 8.1 Hz, 2H, -$SO_2$Ar$H_{meta}$), 4.19 (s, 2H, C$H_2$OH), 3.68 (t, *J* = 5.9 Hz, 2H, -C$H_2$OTBS), 3.49 [t, *J* = 7.4 Hz, 2H, -N(Ts)C$H_2$$CH_2$], 2.55 [tt, *J* = 7.5, 2.1 Hz, 2H, -N(Ts)$CH_2$C$H_2$], 2.46 (s, 3H, -$SO_2$ArC$H_3$), 2.40 (t, *J* = 7.0 Hz, 2H, -C$H_2$$CH_2$$CH_2$OTBS), 1.73 (tt, *J* = 6.6, 6.3 Hz, 2H, -$CH_2$C$H_2$$CH_2$OTBS), 0.90 [s, 9H, -Si($CH_3$)$_2$C(C$H_3$)$_3$], and 0.06 [s, 6H, -Si(C$H_3$)$_2$C($CH_3$)$_3$].

**$^{13}$C NMR** (125 MHz, $CDCl_3$) δ 145.3, 134.7, 130.1, 127.7, 84.4, 81.6, 81.1, 66.8, 64.5, 61.6, 59.2, 51.3, 50.4, 31.5, 26.1, 21.9, 19.0, 18.5, 16.2, and -5.2 ppm.

**IR** (neat) 3450 (br), 2952, 2929, 2857, 2251, 2165, 1597, 1372, 1252, 1171, 1093, 1017, 967, and 838 $cm^{-1}$.

**HRMS** (ESI-TOF): Calcd for $(C_{25}H_{35}NNaO_4SSi)^+$ 496.1948. Found: 496.1959.

---

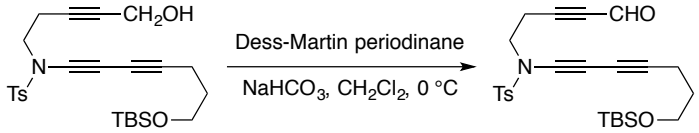


**S503** **519e**

**Preparation of *N*-(7-((*tert*-butyldimethylsilyl)oxy)hepta-1,3-diyn-1-yl)-4-methyl-*N*-(5-oxopent-3-yn-1-yl)benzenesulfonamide (519e).**

In a glass vial was added alcohol **S503** (45 mg, 0.09 mmol), $CH_2Cl_2$ (2 mL), and $NaHCO_3$ (84 mg, 1 mmol). The vial was cooled to 0 °C and Dess-Martin periodinane (85 mg, 0.2 mmol) was added in a single portion. The mixture was stirred at 0 °C for 3 h and a 1:1 mixture of $NaHCO_3$ (aq) and $Na_2S_2O_3$ (aq) was added. The aqueous phase was extracted 2 times with EtOAc. The organic layer was dried over anhydrous $Na_2SO_4$ and concentrated. The residue was purified with column chromatography (silica gel,

hexanes:ethyl acetate = 5:1) to give *N*-(7-((*tert*-butyldimethylsilyl)oxy)hepta-1,3-diyn-1-yl)-4-methyl-*N*-(5-oxopent-3-yn-1-yl)benzenesulfonamide (**519e**, 40.8 mg, 0.09 mmol, 91%) as a pale yellow oil.

**$^1$H NMR** (500 MHz, $CDCl_3$) δ 9.12 (t, *J* = 0.9 Hz, 1H, -C*H*O), 7.80 (d, *J* = 8.4 Hz, 2H, -$SO_2$Ar$H_{ortho}$), 7.37 (d, *J* = 8.0 Hz, 2H, -$SO_2$Ar$H_{meta}$), 3.68 (t, *J* = 5.9 Hz, 2H, -C$H_2$OTBS), 3.58 [t, *J* = 7.4 Hz, 2H, -N(Ts)C$H_2$$CH_2$], 2.77 [dt, *J* = 0.9, 7.5 Hz, 2H, -N(Ts)$CH_2$C$H_2$], 2.46 (s, 3H, -$SO_2$ArC$H_3$), 2.41 (t, *J* = 7.1 Hz, 2H, -C$H_2$$CH_2$$CH_2$OTBS), 1.73 (tt, *J* = 7.1, 5.9 Hz, 2H, -$CH_2$C$H_2$$CH_2$OTBS), 0.90 [s, 9H, -Si($CH_3$)$_2$C(C$H_3$)$_3$], and 0.06 [s, 6H, -Si(C$H_3$)$_2$C($CH_3$)$_3$].

**$^{13}$C NMR** (125 MHz, $CDCl_3$) δ 176.7, 145.6, 134.4, 130.3, 127.8, 93.1, 84.8, 82.9, 66.2, 64.3, 61.6, 59.8, 49.2, 31.4, 26.1, 21.9, 19.3, 18.5, 16.2, and -5.2 ppm.

**IR** (neat) 2952, 2930, 2858, 2207, 2165, 1669, 1372, 1252, 1170, 1092, 967, and 838cm$^{-1}$.

**HRMS** (ESI-TOF): Calcd for $(C_{26}H_{37}NNaO_5SSi)^+$ (M+$CH_3OH$+$Na^+$) 526.2054. Found: 526.2077.

---

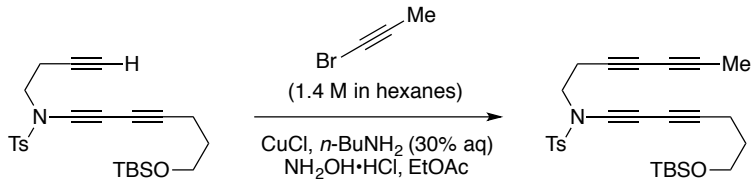


***519a*** ***519f***

**Preparation of *N*-(7-((*tert*-butyldimethylsilyl)oxy)hepta-1,3-diyn-1-yl)-*N*-(hepta-3,5-diyn-1-yl)-4-methylbenzenesulfonamide (519f)**

In a glass vial (2 mL) was added CuCl (1 mg, 0.01 mmol), $NH_2OH$•HCl (10 mg), and *n*-$BuNH_2$ (0.6 mL, 30% aq solution). The reaction was cooled to 0 °C before addition of alkyne **519a** (50 mg, 0.11 mmol) as an ethyl acetate (0.6 mL) solution. A solution of 1-

bromopropyne[106] (160 μL, 1.4 M in hexanes) was added. The vial was sealed with a Teflon-lined cap. After 5 min of stirring at 0 °C, the cooling bath was removed. The reaction was allowed to stir at room temperature for 1 h and saturated $NH_4Cl$ (aq) solution was added. The aqueous phase was extracted with ethyl acetate. The organic layer was washed with brine, dried over anhydrous $Na_2SO_4$, and concentrated. The residue was purified by column chromatography (silica gel, hexanes:ethyl acetate = 12:1) to give *N*-(7-((*tert*-butyldimethylsilyl)oxy)hepta-1,3-diyn-1-yl)-*N*-(hepta-3,5-diyn-1-yl)-4-methylbenzenesulfonamide (**519f**, 49.3 mg, 0.1 mmol, 91%) as a pale yellow oil.

**$^1$H NMR** (500 MHz, $CDCl_3$) δ 7.79 (d, $J$ = 8.4 Hz, 2H, -$SO_2$Ar$H_{ortho}$), 7.36 (d, $J$ = 8.0 Hz, 2H, -$SO_2$Ar$H_{meta}$), 3.68 (t, $J$ = 5.9 Hz, 2H, -C$H_2$OTBS), 3.49 [t, $J$ = 7.4 Hz, 2H, -N(Ts)C$H_2$C$H_2$], 2.57 [tq, $J$ = 6.9, 1.2 Hz, 2H, -N(Ts)C$H_2$C$H_2$], 2.46 (s, 3H, -$SO_2$ArC$H_3$), 2.40 (t, $J$ = 7.1 Hz, 2H, -C$H_2$C$H_2$C$H_2$OTBS), 1.90 (t, $J$ = 1.2 Hz, 3H, -C≡CC$H_3$), 1.73 (tt,

---

[106] a) Procedure for preparation of bromopropyne[4b]:
"A 2 L three-neck round-bottom flask containing a magnetic stir bar was charged with a solution of KOH (85% tech. grade, 260 g, 3.94 mol) in 250 mL of water, and the flask was placed in an ice-salt bath. The flask was fitted with a thermocouple, a pressure equalizing dropping funnel, and a rubber septum. When the KOH solution had cooled to –3 °C (internal temperature), bromine (40 mL, 0.78 mol, ca. 1.5 equiv) was added dropwise to the stirred solution at such a rate so that the internal temperature did not rise above 0 °C. A precipitate formed over the course of the addition. After the addition was complete, the yellow slurry was stirred for an additional 30 min at 0 °C.
A 250 mL Erlenmeyer flask containing a ground-glass joint was charged with 150 mL of hexanes and the flask was cooled in a dry ice-acetone bath. Gaseous propyne (bp -23 °C, 95%, ca. 30 mL, 0.50 mol) was then slowly introduced via an 18 gauge syringe needle into the headspace of the flask. Condensation is more efficient if the needle tip is close to the surface of the cold hexane. Condensation was allowed to continue until the total volume of the solution had grown to ca. 180 mL. It is advisable to attach a bubbler to the headspace to ensure that the gas is not being introduced too rapidly.
The addition funnel on 2 L the three-neck flask was replaced by a Dewar condenser filled with a dry ice-acetone mixture. The hexanes solution of propyne, still at -78 °C, was added slowly to the aqueous KOBr solution, still maintained at ≤0 °C, via cannula over approximately 1 h. Depending on the rate of addition, the internal temperature of the reaction mixture may or may not increase. The reaction mixture was allowed to warm to room temperature, using internal temperature monitoring to guide the intermittent use of the cooling bath. As the mixture warmed, propyne reflux was observed, and the rate or reflux qualitatively indicated the progress of reaction. After the cessation of propyne reflux (ca. 2 h), the reaction mixture was transferred to a 2 L separatory funnel. The aqueous layer was drained and combined with brine (100 mL) to minimize emulsion formation. The combined aqueous layers were extracted with hexanes (2x50 mL), and the combined organic layers were washed with brine (100 mL), dried over $Na_2SO_4$, and filtered to give a dried stock solution of 1-bromopropyne (ca. 300 mL total volume). *Caution*: neat 1-bromopropyne (reported bp 64 °C) has been reported to ignite upon exposure to oxygen;[4c] hence, we have opted to titer the hexanes solution by $^1$H NMR analysis of an aliquot and use that solution directly for subsequent coupling reactions. The concentration of the stock solution described here was judged to be 27 wt%. Such solutions have been stored multiple times in a freezer (ca. -20 °C) for months with no obvious loss in titer (NMR) or discoloration."[4b]
b) Chen, J.; Palani, V.; Hoye, T. R. *J. Am. Chem. Soc.* **2016**, *138*, 4318–4321.
c) Brandsma, L.; Verkruijsse, H. D. *Synthesis* **1990**, 984–985.

*J* = 7.1, 5.9 Hz, 2H, -$CH_2CH_2CH_2$OTBS), 0.90 [s, 9H, -$Si(CH_3)_2C(CH_3)_3$], and 0.06 [s, 6H, -$Si(CH_3)_2C(CH_3)_3$].

**$^{13}$C NMR** (125 MHz, $CDCl_3$) δ 145.3, 134.5, 130.2, 127.8, 84.4, 74.5, 71.3, 67.8, 66.4, 64.5, 64.3, 61.6, 59.4, 49.9, 31.5, 26.1, 21.9, 19.3, 18.5, 16.2, 4.4, and -5.2 ppm.

**IR** (neat) 2953, 2929, 2857, 2252, 2165, 1372, 1171, 1092, 967, and 838 $cm^{-1}$.

**HRMS** (ESI-TOF): Calcd for $(C_{27}H_{35}NNaO_3SSi)^+$ 504.1999. Found: 504.2018.

---

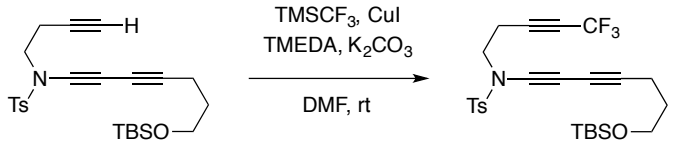


**519a** **519g**

**Preparation of *N*-(7-((*tert*-butyldimethylsilyl)oxy)hepta-1,3-diyn-1-yl)-4-methyl-*N*-(5,5,5-trifluoropent-3-yn-1-yl)benzenesulfonamide (519g).**

CuI (64 mg, 0.34 mmol, 1.7 eq.), $K_2CO_3$ (93 mg, 0.68 mmol, 3.4 eq.), and dry DMF (1.0 mL, ca. 5 mL•$mmol^{-1}$ of alkyne substrate) were combined in a 20 mL scintillation vial equipped with a stir bar and capped with a rubber septum. A balloon filled with dry air was attached. The mixture was stirred vigorously at room temperature while anhydrous TMEDA was introduced via syringe. The white suspension immediately turned blue. This suspension was allowed to stir at ambient temperature for 15 min before addition of $TMSCF_3$ (70 μL, 2.4 eq.) The resulting deep green solution was allowed to stir at room temperature for an additional 5 min before being cooled to 0 °C in an ice-water bath. A solution of triyne **519a** (90 mg, 0.20 mmol) and $TMSCF_3$ (70 μL, 2.4 equiv) in dry DMF (1.0 mL, ca. 5 mL•$mmol^{-1}$ of alkyne substrate) was slowly added over 10 min at 0 °C. The deep green reaction mixture was allowed to warm to room temperature overnight with stirring. After 15 h TLC analysis confirmed full consumption of starting material. The resulting mixture was partitioned between ethyl acetate and brine. The organic layer was washed with brine twice, dried over anhydrous $Na_2SO_4$, and concentrated. The

residue was purified with column chromatography on silica gel (hexanes:ethyl acetate = 5:1) to give the trifluoromethylated triyne **519g** (89 mg, 0.17 mmol, 86%) as a pale yellow oil.

**$^1$H NMR** (500 MHz, $CDCl_3$) δ 7.80 (d, $J$ = 8.4 Hz, 2H, -$SO_2$Ar$H_{ortho}$), 7.37 (d, $J$ = 8.6 Hz, 2H, -$SO_2$Ar$H_{meta}$), 3.68 (t, $J$ = 5.9 Hz, 2H, -C$H_2$OTBS), 3.56 [br d, $J$ = 7.4 Hz, 2H, -N(Ts)C$H_2$C$H_2$], 2.68 [br tq, $J$ = 7.4, 3.6 Hz, 2H, -N(Ts)C$H_2$C$H_2$], 2.46 (s, 3H, -$SO_2$ArC$H_3$), 2.41 (t, $J$ = 7.1 Hz, 2H, -C$H_2$C$H_2$C$H_2$OTBS), 1.73 (tt, $J$ = 5.9, 7.1 Hz, 2H, -C$H_2$C$H_2$C$H_2$OTBS), 0.90 [s, 9H, -Si(C$H_3$)$_2$C(C$H_3$)$_3$], and 0.06 [s, 6H, -Si(C$H_3$)$_2$C(C$H_3$)$_3$].

**$^{13}$C NMR** (125 MHz, $CDCl_3$) δ 145.6, 134.5, 130.3, 127.8, 114.0 (q, $J$ = 257.0 Hz), 84.8, 84.2 (q, $J$ = 6.4 Hz), 70.6 (q, $J$ = 52.4 Hz), 66.2, 64.3, 61.6, 59.9, 49.0, 31.5, 26.1, 21.9, 18.54, 18.52, 16.3, and -5.1 ppm.

**IR** (neat) 2954, 2930, 2858, 2274, 2256, 2165, 1597, 1375, 1286, 1171, 1141, 1092, 970, and 838 $cm^{-1}$.

**HRMS** (ESI-TOF): Calcd for $(C_{25}H_{32}F_3NNaO_3SSi)^+$ 534.1716. Found: 534.1724.

---

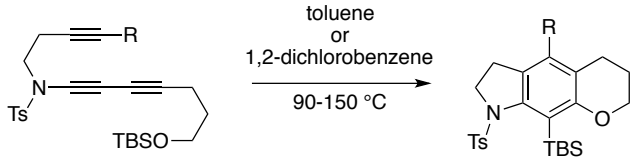


**519a-g** **521a-g**

**General procedure for the hexadehydro-Diels-Alder reaction**

Triyne precursor **519a-g**, a stir bar, and degassed ($N_2$ sparge) toluene or, for experiments performed at >140 °C, 1,2-dichlorobenzene (100 mL/1 mmol triyne precursor) were combined in a glass vial. The headspace was flushed with $N_2$, and the vial was closed with a Teflon-lined cap and placed in a hot oil bath, pre-equilibrated to the indicated temperature, for 16–24 h. The crude reaction mixture was concentrated and directly subjected to flash column chromatography (FCC) on silica gel to obtain the purified

product. It should be noted that the NMR data for these products suggest that the sulfonamide nitrogen atom is puckered and that inversion of that atom is slow on the NMR time scale. Namely, this stereogenic center renders each of the methylene group geminal protons (and the TBS-methyl resonances) diastereotopic and, therefore, inequivalent in chemical shift in the $^{1}$H (and $^{13}$C) NMR spectrum for each compound.

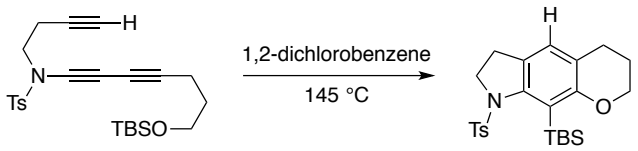


**519a** **521a**

**Preparation of 9-(*tert*-butyldimethylsilyl)-8-tosyl-2,3,4,6,7,8-hexahydropyrano[3,2-*f*]indole (521a).**

The general HDDA reaction procedure was followed using: 12 mg (27 μmol) of triyne **519a**, 1,2-dichlorobenzene, 145 °C oil bath, 15 h reaction time, and FCC elution with hexanes:ethyl acetate = 5:1. Product: 9-(*tert*-butyldimethylsilyl)-8-tosyl-2,3,4,6,7,8-hexahydropyrano[3,2-*f*]indole (**521a**, 6 mg, 14 μmol, 50%) as a pale yellow oil.

**$^{1}$H NMR** (500 MHz, $CDCl_3$) δ 7.26 (d, $J$ = 8.1 Hz, 2H, -$SO_2$Ar$H_{ortho}$), 7.12 (d, $J$ = 8.0 Hz, 2H, -$SO_2$Ar$H_{meta}$), 6.66 (t, $J$ = 1.0 Hz, 1H, Ar-H), 4.23 (dddd, $J$ = 10.6, 6.7, 3.2, 0.9 Hz, 1H, -OC$H_a$H$_b$-), 4.10 (ddd, $J$ = 10.7, 7.9, 3.0 Hz, 1H, -OCH$_a$$H_b$-), 4.00 [ddd, $J$ = 13.1, 7.9, 0.9 Hz, 1H, -N(Ts)C$H_a$H$_b$-], 3.70 [ddd, $J$ = 13.1, 11.9, 8.3 Hz, 1H, -N(Ts)CH$_a$$H_b$-], 2.77 (ddd, $J$ = 16.2, 6.0, 6.0 Hz, 1H, -OCH$_2$CH$_2$C$H_a$H$_b$Ar-), 2.72 (ddd, $J$ = 16.4, 7.1, 6.2 Hz, 1H, -OCH$_2$CH$_2$CH$_a$$H_b$Ar-), 2.38 (s, 3H, -$SO_2$ArC$H_3$), 2.09 (dd, $J$ = 15.1, 8.2 Hz, 1H, -N(Ts)CH$_2$C$H_a$H$_b$-), 2.06 (ddddd, $J$ = 13.8, 9.4, 7.8, 6.1, 3.4 Hz, 1H, -OCH$_2$C$H_a$H$_b$-), 1.94 (ddddd, $J$ = 13.4, 6.5, 6.5, 6.5, 3.1 Hz, 1H, -OCH$_2$CH$_a$$H_b$-), 1.59 (dddd, $J$ = 15.2, 11.9, 7.9, 1.2 Hz, 1H, -N(Ts)CH$_2$CH$_a$$H_b$-), 1.03 [s, 9H, -Si(CH$_3$)$_2$C(C$H_3$)$_3$], 0.53 [s, 3H, -Si(C$H_3$)$_a$(CH$_3$)$_b$C(CH$_3$)$_3$], and 0.25 [s, 3H, -Si(CH$_3$)$_a$(C$H_3$)$_b$C(CH$_3$)$_3$].

**$^{13}$C NMR** (125 MHz, $CDCl_3$) δ 159.2, 146.9, 143.7, 134.8, 129.4, 128.8, 128.2, 126.2,

122.3, 119.7, 65.8, 52.0, 29.3, 27.7, 25.5, 22.4, 21.8, 17.8, 0.098, and 0.084 ppm.

**IR** (neat) 2951, 2929, 2856, 1571, 1461, 1401, 1351, 1242, 1164, 1087, 1021, and 865 $cm^{-1}$.

**HRMS** (ESI-TOF): Calcd for $(C_{24}H_{33}NNaO_3SSi)^+$ 466.1843. Found: 466.1852.

---

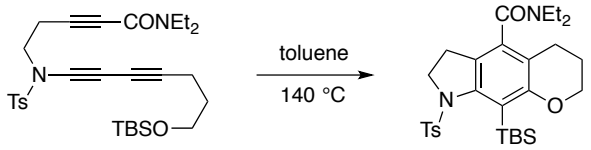


**519b** **521b**

**Preparation of 9-(*tert*-butyldimethylsilyl)-*N*,*N*-diethyl-8-tosyl-2,3,4,6,7,8-hexahydropyrano[3,2-*f*]indole-5-carboxamide (521b).**

The general HDDA reaction procedure was followed using: 12 mg (24 μmol) of triyne **519b**, 140 °C bath temperature, 24 h reaction time, and FCC elution with hexanes:ethyl acetate:methanol = 10:10:1. Product: 9-(*tert*-butyldimethylsilyl)-*N*,*N*-diethyl-8-tosyl-2,3,4,6,7,8-hexahydropyrano[3,2-*f*]indole-5-carboxamide (**521b**, 5 mg, 10 μmol, 42%) as a pale yellow oil. The compound was an ca. 4:1 mixture of diastereomeric atropisomers, presumably involving slow inversion about a puckered NTs nitrogen atom along with slow rotation about the Ar–CO bond, that interconverted slowly on the NMR time scale but rapidly on the chromatography time scale; hence it eluted from the silica column as a single spot.

**$^1$H NMR** (500 MHz, $CDCl_3$) δ 7.41 (d, $J$ = 8.2 Hz, 2H, -$SO_2$Ar$H_{ortho}$), 7.14 (d, $J$ = 8.0 Hz, 2H, -$SO_2$Ar$H_{meta}$), 4.23 (dddd, $J$ = 10.6, 6.5, 3.4, 0.8 Hz, 1H, -OC$H_a$$H_b$-), 4.14 [ddd, $J$ = 13.0, 7.9, 0.8 Hz, 1H, -N(Ts)C$H_a$$H_b$-], 4.11 (dddd, $J$ = 10.9, 8.1, 2.9, 0.6 Hz, 1H, -OC$H_a$$H_b$-), 3.78 [ddd, $J$ = 13.1, 11.9, 8.3 Hz, 1H, -N(Ts)C$H_a$$H_b$-], 3.51 [dq, $J$ = 13.7, 7.1 Hz, -N(C$H_a$$H_b$$CH_3$)$_x$($CH_2CH_3$)$_y$], 3.34 [dq, $J$ = 13.6, 7.1 Hz, -N(C$H_a$$H_b$$CH_3$)$_x$($CH_2CH_3$)$_y$], 2.79 (ddd, $J$ = 16.5, 8.1, 6.0 Hz, 1H, -$OCH_2CH_2$C$H_a$$H_b$Ar-), 2.73 [dq, $J$ = 14.2, 7.2 Hz, -N($CH_2CH_3$)$_x$(C$H_a$$H_b$$CH_3$)$_y$], 2.63 [dq, $J$ = 14.2, 7.1 Hz, -N($CH_2CH_3$)$_x$(C$H_a$$H_b$$CH_3$)$_y$], 2.46

(ddd, $J$ = 16.6, 5.7, 5.7 Hz, 1H, -$OCH_2CH_2CH_aH_bAr$-), 2.36 (s, 3H, -$SO_2ArCH_3$), 2.19 (ddd, $J$ = 15.1, 8.0, 0.8 Hz, 1H, -$N(Ts)CH_2CH_aH_b$-), 2.04 (ddddd, $J$ = 16.1, 9.0, 8.1, 5.8, 3.4 Hz, 1H, -$OCH_2CH_aH_b$-), 1.94 (ddddd, $J$ = 17.0, 6.4, 6.4, 6.4, 3.2 Hz, 1H, -$OCH_2CH_aH_b$-), 1.66 (ddd, $J$ = 15.2, 11.9, 8.1 Hz, 1H, -$N(Ts)CH_2CH_aH_b$-), 1.11 [t, $J$ = 7.2 Hz, -$N(CH_2CH_3)_x(CH_2CH_3)_y$], 1.10 [s, 9H, -$Si(CH_3)_2C(CH_3)_3$], 0.90 [t, $J$ = 7.1 Hz, -$N(CH_2CH_3)_x(CH_2CH_3)_y$], 0.52 [s, 3H, -$Si(CH_3)_a(CH_3)_bC(CH_3)_3$], and 0.15 [s, 3H, -$Si(CH_3)_a(CH_3)_bC(CH_3)_3$].

**$^{13}$C NMR** (125 MHz, $CDCl_3$) δ 168.5, 159.9, 146.8, 143.5, 135.8, 134.5, 129.6, 128.3, 128.0, 124.9, 115.7, 65.7, 52.1, 42.1, 38.4, 29.5, 26.3, 22.7, 21.9, 21.8, 17.7, 14.6, 13.0, 0.6, and 0.2 ppm.

**IR** (neat) 2932, 2854, 1633, 1354, 1164, 1098, and 841 $cm^{-1}$.

**HRMS** (ESI-TOF): Calcd for $(C_{29}H_{42}N_2NaO_4SSi)^+$ 565.2527. Found: 565.2544.

The following NMR data are have been extracted from the minor set of resonances (ca. 4:1 major:minor species) present in the proton spectrum of the purified material:

**$^1$H NMR** (500 MHz, $CDCl_3$) δ 7.25 (d, $J$ = 8.2 Hz, 2H, -$SO_2ArH_{ortho}$), 7.18 (d, $J$ = 8.2 Hz, 2H, -$SO_2ArH_{meta}$), 4.26 (dddd, $J$ = 10.8, 6.5, 3.3, 1.0 Hz, 1H, -$OCH_aH_b$-), 4.09 (ddd, $J$ = 10.6, 8.4, 2.9 Hz, 1H, -$OCH_aH_b$-), 3.97 [ddd, $J$ = 13.1, 8.2, 0.8 Hz, 1H, -$N(Ts)CH_aH_b$-], 3.70 [ddd, $J$ = 13.0, 12.1, 8.1 Hz, 1H, -$N(Ts)CH_aH_b$-], resonances for the following protons in the range of 3.6–2.4 ppm were too severely overlapped with those of the major isomer to explicitly discern: -$N(CH_aH_bCH_3)_x(CH_2CH_3)_y$, -$OCH_2CH_2CH_aH_bAr$, -$N(CH_2CH_3)_x(CH_aH_bCH_3)_y$; 2.37 (s, 3H, -$SO_2ArCH_3$), resonances for the following protons in the range of 2.2–1.6 ppm were too severely overlapped with those of the major isomer to explicitly discern: -$N(Ts)CH_2CH_aH_b$- and -$OCH_2CH_aH_b$-; 1.14 [t, $J$ = 7.1 Hz, -$N(CH_2CH_3)_x(CH_2CH_3)_y$], 0.99 [s, 9H, -$Si(CH_3)_2C(CH_3)_3$], 0.95 [t, $J$ = 7.1 Hz, -$N(CH_2CH_3)_x(CH_2CH_3)_y$], 0.54 [s, 3H, -$Si(CH_3)_a(CH_3)_bC(CH_3)_3$], and 0.31 [s, 3H, -$Si(CH_3)_a(CH_3)_bC(CH_3)_3$].

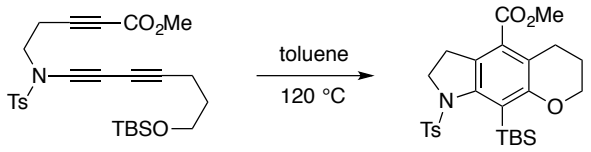


**519c** **521c**

**Preparation of methyl 9-(*tert*-butyldimethylsilyl)-8-tosyl-2,3,4,6,7,8-hexahydropyrano[3,2-*f*]indole-5-carboxylate (521c).**

The general HDDA reaction procedure was followed using: 11 mg (22 μmol) of triyne **519c**, 120 °C oil bath, 24 h reaction time, and FCC elution with hexanes:ethyl acetate = 3:1. Product: methyl 9-(*tert*-butyldimethylsilyl)-8-tosyl-2,3,4,6,7,8-hexahydropyrano[3,2-*f*]indole-5-carboxylate (**521c**, 7 mg, 14 μmol, 64%) as a pale yellow oil.

**$^1$H NMR** (500 MHz, $CDCl_3$) δ 7.23 (d, $J$ = 8.2 Hz, 2H, -$SO_2$Ar$H_{ortho}$), 7.14 (d, $J$ = 7.9 Hz, 2H, -$SO_2$Ar$H_{meta}$), 4.27 (dddd, $J$ = 10.6, 6.0, 3.4, 1.2 Hz, 1H, -OC$H_a$$H_b$-), 4.08 (ddd, $J$ = 10.6, 8.6, 2.8 Hz, 1H, -OC$H_a$$H_b$-), 3.97 [ddd, $J$ = 13.1, 8.3, 1.2 Hz, 1H, -N(Ts)C$H_a$$H_b$-], 3.73 (s, 3H, $CO_2CH_3$), 3.69 [ddd, $J$ = 13.1, 11.9, 8.4 Hz, 1H, -N(Ts)C$H_a$$H_b$-], 2.94 (ddd, $J$ = 17.3, 8.6, 6.1 Hz, 1H, -$OCH_2CH_2CH_a$$H_b$Ar-), 2.87 (dddd, $J$ = 17.3, 5.9, 5.9, 1.1 Hz, 1H, -$OCH_2CH_2CH_a$$H_b$Ar-), 2.39 (s, 3H, -$SO_2$Ar$CH_3$), 2.30 (ddd, $J$ = 16.2, 8.4, 0.9 Hz, 1H, -N(Ts)$CH_2CH_a$$H_b$-), 2.04 (ddddd, $J$ = 13.7, 9.3, 8.5, 5.8, 3.4 Hz, 1H, -$OCH_2CH_a$$H_b$-), 1.96 (ddddd, $J$ = 13.7, 6.0, 6.0, 6.0, 2.9 Hz, 1H, -$OCH_2CH_a$$H_b$-), 1.64 (ddd, $J$ = 16.2, 12.0, 8.1 Hz, 1H, -N(Ts)$CH_2CH_a$$H_b$-), 1.01 [s, 9H, -$Si(CH_3)_2C(CH_3)_3$], 0.53 [s, 3H, -$Si(CH_3)_a(CH_3)_bC(CH_3)_3$], and 0.28 [s, 3H, -$Si(CH_3)_a(CH_3)_bC(CH_3)_3$].

**$^{13}$C NMR** (125 MHz, $CDCl_3$) δ 167.9, 159.6, 147.2, 144.1, 134.3, 129.5, 128.7, 128.1, 126.5, 119.0, 65.6, 51.8, 51.4, 29.1, 28.3, 24.1, 22.1, 21.8, 18.0, 0.1 and -0.1 ppm.

**IR** (neat) 2950, 2861, 1719, 1442, 1357, 1251, 1164, 1102, 1054, 1033, 1010, and 834 $cm^{-1}$.

**HRMS** (ESI-TOF): Calcd for $(C_{26}H_{36}NO_5SSi)^+$ 502.2078. Found: 502.2060.

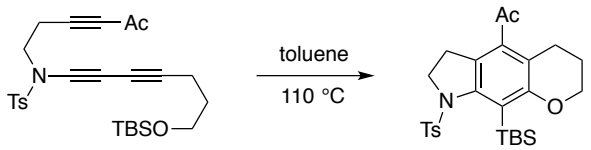


**519d** **521d**

**Preparation of 1-(9-(*tert*-butyldimethylsilyl)-8-tosyl-2,3,4,6,7,8-hexahydropyrano[3,2-*f*]indol-5-yl)ethan-1-one (521d).**

The general HDDA reaction procedure was followed using: 14 mg (28 μmol) of triyne **519d**, 110 °C heating bath, 24 h reaction time, and FCC elution with hexanes:ethyl acetate = 3:1. Product: methyl 1-(9-(*tert*-butyldimethylsilyl)-8-tosyl-2,3,4,6,7,8-hexahydropyrano[3,2-*f*]indol-5-yl)ethan-1-one (**521d**, 11 mg, 23 μmol, 80%) as a pale yellow oil.

**$^1$H NMR** (500 MHz, $CDCl_3$) δ 7.26 (d, *J* = 8.1 Hz, 2H, -$SO_2$Ar$H_{ortho}$), 7.16 (d, *J* = 7.9 Hz, 2H, -$SO_2$Ar$H_{meta}$), 4.28 (dddd, *J* = 10.7, 6.2, 3.4, 1.2 Hz, 1H, -OC$H_a$$H_b$-), 4.09 (dddd, *J* = 10.7, 8.5, 3.0, 0.7 Hz, 1H, -OC$H_a$$H_b$-), 4.02 [ddd, *J* = 13.2, 8.0, 1.0 Hz, 1H, -N(Ts)C$H_a$$H_b$-], 3.68 [ddd, *J* = 13.2, 11.7, 8.3 Hz, 1H, -N(Ts)C$H_a$$H_b$-], 2.78 (dddd, *J* = 16.7, 8.6, 6.1, 0.6 Hz, 1H, -$OCH_2CH_2CH_a$$H_b$Ar-), 2.64 (dddd, *J* = 16.6, 5.8, 5.8, 1.2 Hz, 1H, -$OCH_2CH_2CH_a$$H_b$Ar-), 2.39 (s, 3H, -$SO_2$ArC$H_3$), 2.15 (s, 3H, ArCOC$H_3$), 2.08 (ddd, *J* = 15.3, 8.3, 0.9 Hz, 1H, -N(Ts)$CH_2$C$H_a$$H_b$-), 2.04 (ddddd, *J* = 13.5, 8.9, 8.4, 5.6, 3.4 Hz, 1H, -$OCH_2$C$H_a$$H_b$-), 1.95 (ddddd, *J* = 13.7, 6.0, 6.0, 6.0, 2.9 Hz, 1H, -$OCH_2CH_a$$H_b$-), 1.51 (ddd, *J* = 15.4, 11.7, 8.0 Hz, 1H, -N(Ts)$CH_2CH_a$$H_b$-), 1.02 [s, 9H, -$Si(CH_3)_2C(CH_3)_3$], 0.53 [s, 3H, -$Si(CH_3)_a(CH_3)_bC(CH_3)_3$], and 0.26 [s, 3H, -$Si(CH_3)_a(CH_3)_bC(CH_3)_3$].

**$^{13}$C NMR** (125 MHz, $CDCl_3$) δ 204.4, 159.6, 147.3, 144.2, 139.0, 134.3, 129.4, 128.2, 125.0, 124.8, 115.4, 65.6, 51.6, 31.1, 29.2, 27.0, 23.3, 21.9, 21.8, 17.9, 0.02 and -0.03 ppm.

**IR** (neat) 2950, 2931, 2894, 2855, 1698, 1355, 1245, 1164, 1096, and 830 $cm^{-1}$.

**HRMS** (ESI-TOF): Calcd for $(C_{26}H_{35}NNaO_4SSi)^+$ 508.1948. Found: 508.1954.

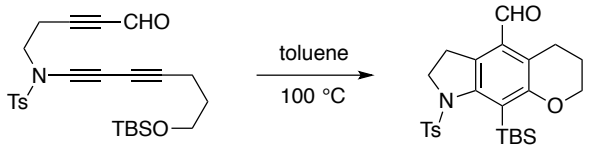


**519e** **521e**

**Preparation of 9-(*tert*-butyldimethylsilyl)-8-tosyl-2,3,4,6,7,8-hexahydropyrano[3,2-*f*]indole-5-carbaldehyde (521e).**

The general HDDA reaction procedure was followed using: 14 mg (29 μmol) of triyne **519e**, 100 °C heating bath, 24 h reaction time, and FCC elution with hexanes:ethyl acetate = 3:1. Product: methyl 9-(*tert*-butyldimethylsilyl)-8-tosyl-2,3,4,6,7,8-hexahydropyrano[3,2-*f*]indole-5-carbaldehyde (**521e**, 9.1 mg, 19 μmol, 66%) as a pale yellow oil.

**$^1$H NMR** (500 MHz, $CDCl_3$) δ 10.17 (s, 1H, ArC*H*O), 7.22 (d, *J* = 8.2 Hz, 2H, -$SO_2$Ar$H_{ortho}$), 7.11 (d, *J* = 8.1 Hz, 2H, -$SO_2$Ar$H_{meta}$), 4.30 (ddd, *J* = 10.6, 6.1, 3.3 Hz, 1H, -OC$H_a$H$_b$-), 4.12 (ddd, *J* = 10.5, 8.5, 2.9 Hz, 1H, -OCH$_a$$H_b$-), 4.07 [ddd, *J* = 13.1, 8.1, 1.0 Hz, 1H, -N(Ts)C$H_a$H$_b$-], 3.71 [ddd, *J* = 13.2, 11.7, 8.4 Hz, 1H, -N(Ts)CH$_a$$H_b$-], 3.19 (t, *J* = 6.4 Hz, 2H, -OCH$_2$CH$_2$C$H_2$Ar-), 2.63 (ddd, *J* = 16.8, 8.5, 1.0 Hz, 1H, -N(Ts)CH$_2$C$H_a$H$_b$-), 2.37 (s, 3H, -$SO_2$ArC$H_3$), 2.12 (ddddd, *J* = 13.8, 8.5, 7.2, 7.2, 3.4 Hz, 1H, -OCH$_2$C$H_a$H$_b$-), 2.03 (ddddd, *J* = 13.9, 6.1, 6.1, 6.1, 2.9 Hz, 1H, -OCH$_2$CH$_a$$H_b$-), 1.81 (ddd, *J* = 16.8, 11.7, 8.1 Hz, 1H, -N(Ts)CH$_2$CH$_a$$H_b$-), 1.03 [s, 9H, -Si(CH$_3$)$_2$C(C$H_3$)$_3$], 0.55 [s, 3H, -Si(C$H_3$)$_a$(CH$_3$)$_b$C(CH$_3$)$_3$], and 0.29 [s, 3H, -Si(CH$_3$)$_a$(C$H_3$)$_b$C(CH$_3$)$_3$].

**$^{13}$C NMR** (125 MHz, $CDCl_3$) δ 191.3, 159.9, 147.9, 144.4, 134.2, 132.7, 130.9, 129.7, 129.6, 128.1, 120.9, 65.5, 51.7, 29.1, 27.4, 22.8, 21.9, 21.8, 18.0, 0.1 and -0.1 ppm.

**IR** (neat) 2949, 2928, 2893, 2855, 1687, 1356, 1244, 1164, 1110, 1089, and 842 cm$^{-1}$.

**HRMS** (ESI-TOF): Calcd for $(C_{25}H_{33}NNaO_4SSi)^+$ 494.1792. Found: 494.1813.

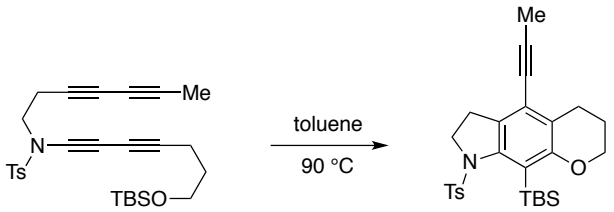


**519f** **521f**

**Preparation of 9-(*tert*-butyldimethylsilyl)-5-(prop-1-yn-1-yl)-8-tosyl-2,3,4,6,7,8-hexahydropyrano[3,2-*f*]indole (521f).**

The general HDDA reaction procedure was followed using: 17 mg (35 μmol) of triyne **519f**, 90 °C heating bath, 16 h reaction time, and FCC elution with hexanes:ethyl acetate = 12:1. Product: 9-(*tert*-butyldimethylsilyl)-5-(prop-1-yn-1-yl)-8-tosyl-2,3,4,6,7,8-hexahydropyrano[3,2-*f*]indole (**521f**, 14 mg, 29 μmol, 82%) as a pale yellow oil.

**$^1$H NMR** (500 MHz, $CDCl_3$) δ 7.25 (d, $J$ = 8.2 Hz, 2H, -$SO_2$Ar$H_{ortho}$), 7.14 (d, $J$ = 7.9 Hz, 2H, -$SO_2$Ar$H_{meta}$), 4.22 (dddd, $J$ = 10.6, 6.4, 3.3, 0.7 Hz, 1H, -OC$H_a$$H_b$-), 4.05 (dddd, $J$ = 10.8, 8.4, 3.0, 0.4 Hz, 1H, -OC$H_a$$H_b$-), 3.98 [ddd, $J$ = 13.1, 8.0, 1.0 Hz, 1H, -N(Ts)C$H_a$$H_b$-], 3.69 [ddd, $J$ = 13.1, 11.9, 8.4 Hz, 1H, -N(Ts)C$H_a$$H_b$-], 2.82 (ddd, $J$ = 17.1, 6.4, 6.4 Hz, 1H, -$OCH_2CH_2$C$H_a$$H_b$Ar-), 2.80 (dddd, $J$ = 17.2, 7.5, 6.2 Hz, 1H, -$OCH_2CH_2$C$H_a$$H_b$Ar-), 2.39 (s, 3H, -$SO_2$ArC$H_3$), 2.23 (ddd, $J$ = 15.8, 8.4, 0.9 Hz, 1H, -N(Ts)$CH_2$C$H_a$$H_b$-), 2.11–2.02 (nfom, 1H, -$OCH_2$C$H_a$$H_b$-), 2.01 (t, $J$ = 1.2 Hz, 3H, -C≡CC$H_3$), 2.00-1.92 (nfom, 1H, -$OCH_2$C$H_a$$H_b$-), 1.58 (ddd, $J$ = 15.8, 11.8, 8.0 Hz, 1H, -N(Ts)$CH_2$C$H_a$$H_b$-), 1.01 [s, 9H, -Si$(CH_3)_2$C$(CH_3)_3$], 0.52 [s, 3H, -Si$(CH_3)_a$$(CH_3)_b$C$(CH_3)_3$], and 0.25 [s, 3H, -Si$(CH_3)_a$$(CH_3)_b$C$(CH_3)_3$].

**$^{13}$C NMR** (125 MHz, $CDCl_3$) δ 159.3, 146.2, 143.9, 134.6, 131.7, 129.4, 128.1, 122.5, 121.1, 121.0, 94.1, 75.8, 65.6, 51.6, 29.2, 27.9, 24.3, 22.2, 21.8, 17.9, 4.8, 0.1, and 0.0 ppm.

**IR** (neat) 2949, 2930, 2854, 1582, 1463, 1393, 1354, 1243, 1164, 1136, 1083, and 909 $cm^{-1}$.

**HRMS** (ESI-TOF): Calcd for $(C_{27}H_{35}NNaO_3SSi)^+$ 504.1999. Found: 504.1965.

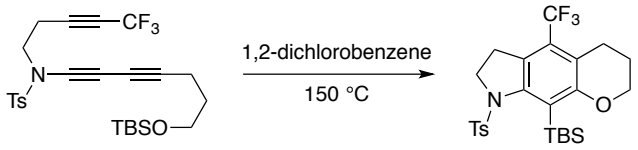


**519g** **521g**

**Preparation of 9-(*tert*-butyldimethylsilyl)-8-tosyl-5-(trifluoromethyl)-2,3,4,6,7,8-hexahydropyrano[3,2-*f*]indole (521g)**

The general HDDA reaction procedure was followed using: 12 mg (23 μmol) of triyne **519g**, 1,2-dichlorobenzene as solvent, 150 °C oil bath, 14 h reaction time, and FCC elution with hexanes:ethyl acetate = 5:1. Product: methyl 9-(*tert*-butyldimethylsilyl)-8-tosyl-5-(trifluoromethyl)-2,3,4,6,7,8-hexahydropyrano[3,2-*f*]indole (**521g**, 5 mg, 10 μmol, 42%) as a pale yellow oil.

**$^1$H NMR** (500 MHz, $CDCl_3$) δ 7.18 (d, $J$ = 8.1 Hz, 2H, -$SO_2$Ar$H_{ortho}$), 7.13 (d, $J$ = 8.4 Hz, 2H, -$SO_2$Ar$H_{meta}$), 4.27 (ddd, $J$ = 10.5, 6.8, 3.3 Hz, 1H, -OC$H_a$$H_b$-), 4.13 (ddd, $J$ = 10.5, 7.8, 3.0 Hz, 1H, -OC$H_a$$H_b$-), 3.98 [dd, $J$ = 13.2, 8.0 Hz, 1H, -N(Ts)C$H_a$$H_b$-], 3.64 [ddd, $J$ = 13.3, 11.6, 8.4 Hz, 1H, -N(Ts)C$H_a$$H_b$-], 2.92 (ddd, $J$ = 17.8, 6.7, 6.7 Hz, 1H, -$OCH_2CH_2$C$H_a$$H_b$Ar-), 2.89 (dddd, $J$ = 17.6, 6.2, 6.2 Hz, 1H, -$OCH_2CH_2$C$H_a$$H_b$Ar-), 2.39 (s, 3H, -$SO_2$ArC$H_3$), 2.30 (ddq, $J$ = 16.7, 8.3, 3.1 Hz, 1H, -N(Ts)$CH_2$C$H_a$$H_b$-), 2.08 (ddddd, $J$ = 13.8, 7.7, 7.7, 6.0, 3.4 Hz, 1H, -$OCH_2$C$H_a$$H_b$-), 1.97 (ddddd, $J$ = 13.7, 6.5, 6.5, 6.5, 3.1 Hz, 1H, -$OCH_2$C$H_a$$H_b$-), 1.62 (dddq, $J$ = 16.8, 11.2, 8.2, 2.6 Hz, 1H, -N(Ts)$CH_2$C$H_a$$H_b$-), 1.01 [s, 9H, -$Si(CH_3)_2C(CH_3)_3$], 0.54 [s, 3H, -$Si(CH_3)_a(CH_3)_bC(CH_3)_3$], and 0.30 [s, 3H, -$Si(CH_3)_a(CH_3)_bC(CH_3)_3$].

**$^{13}$C NMR** (125 MHz, $CDCl_3$) δ 159.9, 147.7, 144.4, 133.9, 129.4, 128.1, 127.8 (q, $J$ = 2.7

Hz), 127.4, 125.6 (q, $J$ = 30.0 Hz), 124.8 (q, $J$ = 275 Hz), 118.0 (q, $J$ = 1.7 Hz), 65.5, 50.9, 29.1, 28.2 (q, $J$ = 3.6 Hz), 22.7 (q, $J$ = 3.5 Hz), 21.8, 21.7, 18.0, 0.0, and -0.2 ppm.

**IR** (neat) 2951, 2930, 2895, 2857, 1727 (w), 1597, 1567, 1442, 1396, 1360, 1299, 1262, 1166, 1154, 1116, 1103, 1033, and 942 $cm^{-1}$.

**HRMS** (ESI-TOF): Calcd for $(C_{25}H_{32}F_3NNaO_3SSi)^+$ 534.1716. Found: 534.1744.

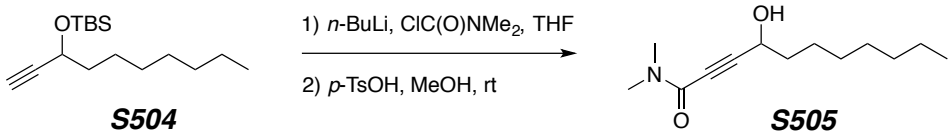


***S504*** ***S505***

**Preparation of 4-hydroxy-*N*,*N*-dimethylundec-2-ynamide (S505).**

In a glass vial was added *tert*-butyl(dec-1-yn-3-yloxy)dimethylsilane[107] (**S504**, 806 mg, 3.0 mmol) and anhydrous THF (6 mL). The vial was then sealed with a septum, placed under a balloon of Ar, and cooled to -78 °C in a dry-ice acetone bath. A solution of *n*-BuLi (1.8 mL, 2.5 M in hexanes) was added, and the mixture was stirred at -78 °C for 1 h. This solution was transferred to a THF solution of dimethylcarbamoyl chloride (540 mg in 5 mL of dry THF, 5 mmol) at -78 °C with stirring. The reaction vial was allowed to warm to room temperature and stirred overnight. The crude mixture was partitioned between ethyl acetate and $NH_4Cl$ (aq) solution. The organic layer was dried over anhydrous $Na_2SO_4$ and concentrated. The residue was redissolved in MeOH (10 mL). Solid *p*-toluenesulfonic acid monohydrate (1.14 g, 6 mmol) was added at room temperature with stirring. This mixture was stirred at room temperature for 4 h. The reaction solution was concentrated, the residue was partitioned between EtOAc and a saturated solution of $NaHCO_3$(aq). The organic layer was washed with brine, dried over anhydrous $Na_2SO_4$, concentrated, and purified with FCC on silica gel (hexanes:ethyl acetate:methanol=10:10:1) to give 4-hydroxy-*N*,*N*-dimethylundec-2-ynamide (**S505**, 601 mg, 89 % yield, 2 steps) as a colorless oil.

[107] Jung, M. E.; Min, S.-J. *J. Am. Chem. Soc.* **2005**, *127*, 10834–10835.

**$^1$H NMR** (500 MHz, $CDCl_3$) δ 4.52 (t, *J* = 6.7 Hz, 1H, -C*H*OH-), 3.20 [s, 3H, -C(O)N(C*H*$_3$)$_a$(CH$_3$)$_b$], 2.97 [s, 3H, -C(O)N(CH$_3$)$_a$(C*H*$_3$)$_b$], 1.82–1.71 [nfom, 2H, -CH(OH)C*H*$_2$], 1.52–1.42 [m, 2H, -CH(OH)CH$_2$C*H*$_2$], 1.36–1.22 [m, 8H, -CH(OH)CH$_2$CH$_2$(C*H*$_2$)$_4$-], and 0.88 (t, *J* = 7.2 Hz, 3H, -C*H*$_3$).

**$^{13}$C NMR** (125 MHz, $CDCl_3$) δ 154.5, 92.9, 77.3, 62.4, 38.6, 37.3, 34.3, 31.9, 29.4, 29.3, 25.3, 22.8, and 14.3 ppm.

**IR** (neat) 3377 (br), 2927, 2856, 2233, 1622, 1496, 1459, 1400, 1267, 1183, and 1073 cm$^{-1}$.

**HRMS** (ESI-TOF): Calcd for $(C_{13}H_{23}NNaO_2)^+$ 248.1621. Found: 248.1629.

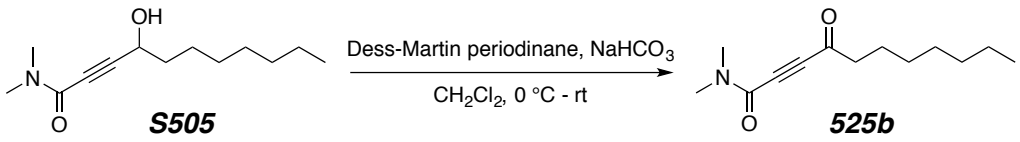


**Preparation of *N*,*N*-dimethyl-4-oxoundec-2-ynamide (525b).**

In a glass vial was added alcohol **S505** (226 mg, 1 mmol), $CH_2Cl_2$ (5 mL), and $NaHCO_3$ (840 mg, 10 mmol). The vial was cooled to 0 °C and Dess-Martin periodinane (640 mg, 1.5 mmol) was added in a single portion. This reaction mixture was stirred overnight, and a 1:1 mixture of $NaHCO_3$ (aq) and $Na_2S_2O_3$ (aq) was added. The aqueous phase was extracted 2 times with EtOAc. The organic layer was dried over anhydrous $Na_2SO_4$, filtered, and concentrated. The residue was purified by FCC (silica gel, hexanes:ethyl acetate = 1:1) to give *N*,*N*-dimethyl-4-oxoundec-2-ynamide (**525b**, 216 mg, 0.97 mmol, 97%) as a pale yellow oil.

**$^1$H NMR** (500 MHz, $CDCl_3$) δ 3.21 [s, 3H, -C(O)N(C*H*$_3$)$_a$(CH$_3$)$_b$], 3.01 [s, 3H, -C(O)N(CH$_3$)$_a$(C*H*$_3$)$_b$], 2.64 [t, *J* = 7.4 Hz, 2H, C(O)C*H*$_2$], 1.69 [br pentet, *J* = 7.3 Hz, 2H, -C(O)CH$_2$C*H*$_2$], 1.36–1.23 [m, 8H, - (C*H*$_2$)$_4$CH$_3$-], and 0.88 (t, *J* = 7.2 Hz, 3H, -C*H*$_3$).

**$^{13}$C NMR** (125 MHz, $CDCl_3$) δ 186.9, 152.7, 86.0, 79.7, 45.6, 38.3, 34.4, 31.8, 29.1, 29.0, 23.8, 22.8, and 14.2 ppm.

**IR** (neat) 2954, 2928, 2858, 1683, 1647, 1397, 1265, 1172, and 1060 $cm^{-1}$.

**HRMS** (ESI-TOF): Calcd for $(C_{13}H_{21}NNaO_2)^+$ 246.1465. Found: 246.1465.

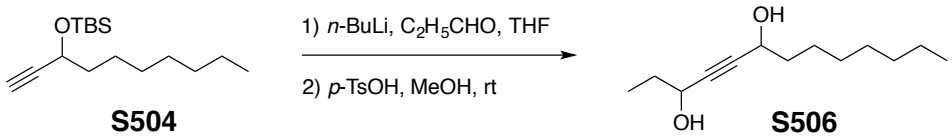


**S504** **S506**

**Preparation of tridec-4-yne-3,6-diol (S506).**

In a glass vial was added *tert*-butyl(dec-1-yn-3-yloxy)dimethylsilane (**S504**, 806 mg, 3.0 mmol) and anhydrous THF (6 mL). The vial was then sealed with a septum, placed under a balloon of Ar, and cooled to -78 °C in a dry-ice acetone bath. A solution of *n*-BuLi (1.8 mL, 2.5 M in hexanes) was added and the mixture was stirred at -78 °C for 1 h. This solution was transferred to a THF solution of propanal (870 mg in 5 mL of dry THF, 15 mmol) under -78 °C with stirring. The reaction vial was allowed to warm to room temperature and stirred overnight. The crude mixture was partitioned between ethyl acetate and $NH_4Cl$ (aq) solution. The organic layer was dried over anhydrous $Na_2SO_4$ and concentrated. The residue was redissolved in MeOH (10 mL). Solid *p*-toluenesulfonic acid monohydrate (1.14 g, 6 mmol) was added at room temperature with stirring. This mixture was stirred at room temperature for 4 h. The reaction solution was concentrated, the residue was partitioned between EtOAc, and saturated solution of $NaHCO_3$(aq). The organic layer was washed with brine, dried over anhydrous $Na_2SO_4$, concentrated, and purified by FCC on silica gel (hexanes:ethyl acetate = 3:1) to give tridec-4-yne-3,6-diol (**S506**, 561 mg, 88 % yield, 2 steps) as a colorless oil.

**$^1$H NMR** (500 MHz, $CDCl_3$) δ 4.40 (t, $J$ = 6.4 Hz, 1H, -C*H*OHCH$_2$CH$_3$), 4.36 (t, $J$ = 6.2 Hz, 1H, -C*H*OHCH$_2$CH$_2$-), 1.99 (br s, 2H, two -O*H*), 1.78–1.63 [m, 4H, -

CH(OH)C*H*$_2$CH$_3$ and -CH(OH)C*H*$_2$CH$_2$-], 1.48–1.39 [m, 2H, -CH(OH)CH$_2$C*H*$_2$], 1.36–1.23 [m, 8H, - CH(OH)CH$_2$CH$_2$(C*H*$_2$)$_4$-], 1.01 (dt, *J* = 7.4, 1.4 Hz, 3H, -CHOHCH$_2$C*H*$_3$), and 0.88 (t, *J* = 7.1 Hz, 3H, -C*H*$_3$).

**$^{13}$C NMR** (125 MHz, $CDCl_3$) δ 86.3 (br), 85.9 (br), 63.9 (br), 62.7 (br), 38.0 (br), 32.0, 31.0 (br), 29.42, 29.39, 25.4, 22.8, 14.3, and 9.6 ppm.

**IR** (neat) 3321 (br), 2954, 2927, 2856, 1730 (w), 1624, 1458, 1336, 1242, 1149, 1099, 1038, and 964 cm$^{-1}$.

**HRMS** (ESI-TOF): Calcd for $(C_{13}H_{24}NaO_2)^+$ 235.1669. Found: 235.1671.

---

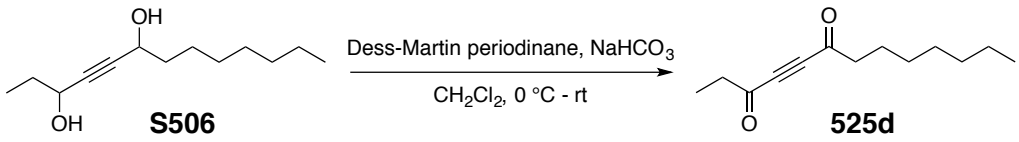


**Preparation of tridec-4-yne-3,6-dione (525d).**

In a glass vial was added alcohol **S506** (215 mg, 1 mmol), $CH_2Cl_2$ (5 mL), and $NaHCO_3$ (1.7 g, 20 mmol). The vial was cooled to 0 °C and Dess-Martin periodinane (1.28 g, 3 mmol) was added in a single portion. The reaction was stirred overnight and a 1:1 mixture of $NaHCO_3$ (aq) and $Na_2S_2O_3$ (aq) was added. The aqueous phase was extracted 2 times with EtOAc. The organic layer was dried over anhydrous $Na_2SO_4$ and concentrated. The residue was purified using FCC (silica gel, hexanes:ethyl acetate = 5:1) to give tridec-4-yne-3,6-dione (**525d**, 198 mg, 0.95 mmol, 95%) as a pale yellow oil.

**$^1$H NMR** (500 MHz, $CDCl_3$) δ 2.67 [q, *J* = 7.3 Hz, 2H, C(O)C*H*$_2$CH$_3$], 2.63 [t, *J* = 7.4 Hz, 2H, C(O)C*H*$_2$CH$_2$], 1.68 [br pentet, *J* = 7.2 Hz, 2H, -C(O)CH$_2$C*H*$_2$], 1.36–1.23 [m, 8H, -(C*H*$_2$)$_4$CH$_3$-], 1.18 [t, *J* = 7.3, 3H, C(O)CH$_2$C*H*$_3$], and 0.88 [t, *J* = 7.0 Hz, 3H, -(CH$_2$)$_6$C*H*$_3$].

**$^{13}$C NMR** (125 MHz, $CDCl_3$) δ 187.1, 186.8, 84.6, 84.3, 45.5, 38.9, 31.8, 29.1, 29.0, 23.8, 22.8, 14.2, and 7.7 ppm.

---

**IR** (neat) 2954, 2929, 2858, 1685, 1459, 1405, 1151, 1088, and 1033 $cm^{-1}$.

**HRMS** (ESI-TOF): Calcd for $(C_{13}H_{20}NaO_2 \bullet MeOH)^+$ ($M^+$+MeOH) 263.1618. Found: 263.1609.

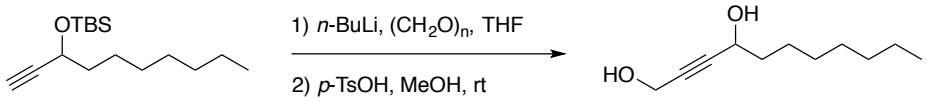


**S504** **S507**

**Preparation of undec-2-yne-1,4-diol (S507).**

In a glass vial was added *tert*-butyl(dec-1-yn-3-yloxy)dimethylsilane (**S504**, 806 mg, 3.0 mmol) and anhydrous THF (6 mL). The vial was then sealed with a septum, placed under a balloon of Ar, and cooled to -78 °C in a dry-ice acetone bath. A solution of *n*-BuLi (1.8 mL, 2.5 M in hexanes) was added and the mixture was stirred at -78 °C for 1 h. Solid paraformaldehyde (1.8 g, 60 mmol) was added to the solution under -78 °C. The reaction vial was allowed to warm to room temperature and stirred overnight. The crude mixture was partitioned between ethyl acetate and $NH_4Cl$ (aq) solution. The organic layer was dried over anhydrous $Na_2SO_4$ and concentrated. The residue was redissolved in MeOH (10 mL). Solid *p*-toluenesulfonic acid monohydrate (1.14 g, 6 mmol) was added at room temperature with stirring. This mixture was stirred at room temperature for 4 h. The reaction solution was concentrated, and the residue was partitioned between EtOAc and a saturated solution of $NaHCO_3$(aq). The organic layer was washed with brine, dried over anhydrous $Na_2SO_4$, filtered, concentrated, and purified by FCC on silica gel (hexanes:ethyl acetate = 3:1) to give undec-2-yne-1,4-diol (**S507**, 450 mg, 82 % yield, 2 steps) as a colorless oil.

**$^1$H NMR** (500 MHz, $CDCl_3$) δ 4.41 (br t with nfom character, $J$ = 6.6 Hz, 1H, -C*H*OH-), 4.31–4.30 (m, *2*H, C$H_2$OH), 2.54 (br s, 1H, -O$H_a$), 2.24 (br s, 1H, -O$H_b$), 1.76–1.64 [m, 2H, -CH(OH)C$H_2$], 1.49–1.39 [m, 2H, -CH(OH)CH$_2$C$H_2$], 1.36–1.23 [m, 8H, -CH(OH)CH$_2$CH$_2$(C$H_2$)$_4$-], 1.01 (dt, $J$ = 7.4, 1.4 Hz, 3H, -CHOHCH$_2$C$H_3$), and 0.88 (t, $J$

= 7.1 Hz, 3H, -C*H*$_3$).

**$^{13}$C NMR** (125 MHz, $CDCl_3$) δ 87.2, 83.2, 62.7, 51.2, 37.9, 32.0, 29.44, 29.40, 25.4, 22.8, and 14.3 ppm.

**IR** (neat) 3305 (br), 2926, 2856, 1464, 1241, 1142, 1108, and 1019 cm$^{-1}$.

**HRMS** (ESI-TOF): Calcd for $(C_{11}H_{20}NaO_2)^+$ 207.1356. Found: 207.1360.

---

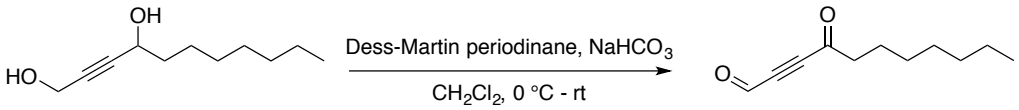


**S507** **525e**

**Preparation of 4-oxoundec-2-ynal (525e).**

In a glass vial was added alcohol **S507** (184 mg, 1 mmol), $CH_2Cl_2$ (5 mL), and $NaHCO_3$ (1.7 g, 20 mmol). The vial was cooled to 0 °C and Dess-Martin periodinane (1.28 g, 3 mmol) was added in a single portion. The reaction was stirred overnight and a 1:1 mixture of $NaHCO_3$ (aq) and $Na_2S_2O_3$ (aq) was added. The aqueous phase was extracted 2 times with EtOAc. The organic layer was dried over anhydrous $Na_2SO_4$ and concentrated. The crude material of 4-oxoundec-2-ynal (**525e**, 140 mg, 0.78 mmol, 78%) was obtained as a red oil and was directly used without purification.

**$^1$H NMR** (500 MHz, $CDCl_3$) δ 9.37 (s, *J* = 7.4 Hz, 1H, -C*H*O), 2.65 [t, *J* = 7.4 Hz, 2H, C(O)C*H*$_2$], 1.69 [br pentet, *J* = 7.2 Hz, 2H, -C(O)CH$_2$C*H*$_2$], 1.38–1.17 [m, 8H, -(C*H*$_2$)$_4$CH$_3$-], and 0.89 [t, *J* = 7.2 Hz, 3H, -(CH$_2$)$_6$C*H*$_3$].

**$^{13}$C NMR** (125 MHz, $CDCl_3$) δ 186.3, 175.4, 87.7, 83.5, 45.5, 31.8, 29.1, 29.0, 23.7, 22.8, and 14.2 ppm.

**IR** (neat) 2954, 2927, 2858, 1773 (w), 1674, 1458, 1401, 1244, 1140, 1055, 1033, and 1013 cm$^{-1}$.

---

**HRMS** (ESI-TOF): Calcd for $(C_{11}H_{16}NaO_2 \bullet MeOH)^+$ ($M^+$+MeOH) 235.1305. Found: 235.1300.

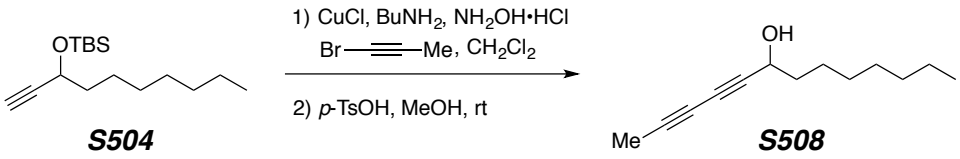


***S504*** ***S508***

**Preparation of trideca-2,4-diyn-6-ol (S508).**

In a round bottom flash (50 mL) was added CuCl (20 mg, 0.2 mmol), $NH_2OH \bullet HCl$ (200 mg), and *n*-$BuNH_2$ (10 mL, 30% aq solution). The reaction mixture was cooled to 0 °C before addition of alkyne **S504** (538 mg, 2 mmol) as an ethyl acetate (10 mL) solution. A solution of 1-bromopropyne (2 mL, 1.4 M in hexanes) was added. The flask was sealed with rubber stopper and placed under a balloon filled with Ar. After 5 min of stirring at 0 °C, the cooling bath was removed. The reaction mixture was allowed to stir at room temperature for 1 h and saturated $NH_4Cl$ (aq) solution was added. The aqueous phase was extracted with ethyl acetate. The organic layer was washed with brine, dried over anhydrous $Na_2SO_4$, and concentrated. The residue was redissolved in MeOH (10 mL). Solid *p*-toluenesulfonic acid monohydrate (760 mg, 4 mmol) was added at room temperature with stirring. This mixture was stirred at room temperature for 4 h. The reaction solution was concentrated, and the residue was partitioned between EtOAc and saturated solution of $NaHCO_3$(aq). The organic layer was washed with brine, dried over anhydrous $Na_2SO_4$, filtered, concentrated, and purified by FCC on silica gel (hexanes:ethyl acetate = 5:1) to give trideca-2,4-diyn-6-ol (**S508**, 360 mg, 94 % yield, 2 steps) as a colorless oil.

**$^1$H NMR** (500 MHz, $CDCl_3$) δ 4.39 (tq, *J* = 6.6, 1.0 Hz, 1H, -C*H*OH-), 1.94 (d, *J* = 1.0 Hz, 3H, C-C*H*$_3$), 1.76–1.64 [nfom, 2H, -CH(OH)C*H*$_2$], 1.51–1.39 [m, 2H, -CH(OH)CH$_2$C*H*$_2$], 1.37–1.22 [m, 8H, - CH(OH)CH$_2$CH$_2$(C*H*$_2$)$_4$-], 0.92 (s, 1H, -O*H*), and 0.88 (t, *J* = 7.1 Hz, 3H, -C*H*$_3$).

**$^{13}$C NMR** (125 MHz, $CDCl_3$) δ 77.4, 76.2, 70.1, 63.9, 63.1, 37.9, 32.0, 29.41, 29.37, 25.3, 22.8, 14.3, and 4.5 ppm.

**IR** (neat) 3334 (br), 2926, 2855, 2258, 1732 (w), 1464, 1376, 1336, 1038, 1025, and 834 $cm^{-1}$.

**GC-LRMS** (ES, 70 eV): $t_R$ = 7.77 min. *m/z*: 174 $(M–H_2O)^{\bullet+}$, 93 $(M–99)^+$.

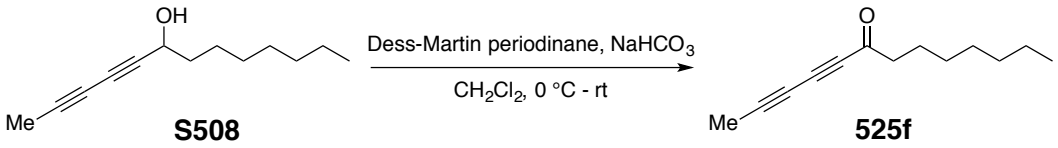


**Preparation of trideca-2,4-diyn-6-one (525f).**

To a glass vial was added alcohol **S508** (195 mg, 1 mmol), $CH_2Cl_2$ (5 mL), and $NaHCO_3$ (840 mg, 10 mmol). The vial was cooled to 0 °C and Dess-Martin periodinane (640 mg, 1.5 mmol) was added in a single portion. The reaction mixture was stirred overnight, and a 1:1 mixture of $NaHCO_3$ (aq) and $Na_2S_2O_3$ (aq) was added. The aqueous phase was extracted 2 times with EtOAc. The organic layer was dried over anhydrous $Na_2SO_4$, filtered, and concentrated. The residue was purified by FCC (silica gel, hexanes:ethyl acetate = 12:1) to give trideca-2,4-diyn-6-one (**525f**, 186 mg, 0.98 mmol, 98%) as a pale yellow oil.

**$^1$H NMR** (500 MHz, $CDCl_3$) δ 2.55 [t, *J* = 7.5 Hz, 2H, C(O)C$H_2$], 2.04 (s, 3H, C-C$H_3$), 1.66 [br pentet, *J* = 7.3 Hz, 2H, -C(O)$CH_2$C$H_2$], 1.34–1.22 [m, 8H, - (C$H_2$)$_4$$CH_3$-], and 0.88 (t, *J* = 7.1 Hz, 3H, -C$H_3$).

**$^{13}$C NMR** (125 MHz, $CDCl_3$) δ 187.6, 86.3, 76.3, 71.9, 63.3, 45.8, 31.8, 29.2, 29.1, 24.2, 22.8, 14.3, and 5.0 ppm.

**IR** (neat) 2955, 2928, 2857, 2238, 2150, 1671, 1458, 1272, and 1068 $cm^{-1}$.

**HRMS** (ESI-TOF): Calcd for $(C_{13}H_{18}NaO)^+$ 213.1250. Found: 213.1255.

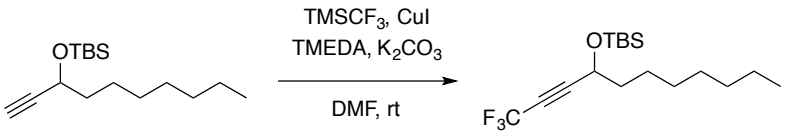


**S504** **S509**

**Preparation of *tert*-butyldimethyl((1,1,1-trifluorodec-2-yn-4-yl)oxy)silane (S509).**

CuI (1.07 g, 5.62 mmol, 1.5 equiv), $K_2CO_3$ (1.54 g, 11.2 mmol, 3 equiv), and dry DMF (17 mL, ca. 5 mL•mmol$^{-1}$ of alkyne substrate) were combined in a 200 mL round-bottomed flask equipped with a stir bar and capped with a rubber septum. A balloon filled with dry air was attached. The mixture was stirred vigorously at room temperature while anhydrous TMEDA was introduced via syringe. The white suspension immediately turned blue. This suspension was allowed to stir at ambient temperature for 15 min before addition of $TMSCF_3$ (1.1 mL, 2 equiv). The resulting deep green solution was allowed to stir at room temperature for an additional 5 min before being cooled to 0 °C in an ice-water bath. A solution of alkyne **S504** (1 g, 3.72 mmol) and $TMSCF_3$ (1.1 mL, 2 equiv) in dry DMF (17 mL, ca. 5 mL•mmol$^{-1}$ of alkyne substrate) was slowly added over 10 min at 0 °C. The deep green reaction mixture was allowed to warm to room temperature and stirred overnight. After 15 h TLC analysis confirmed full consumption of starting material. The resulting mixture was partitioned between ethyl acetate and brine. The organic layer was washed with brine twice, dried over anhydrous $Na_2SO_4$, filtered, and concentrated. The residue was purified by FCC on silica gel (hexanes:ethyl acetate = 12:1) to give the trifluoromethylated alkyne **S509** (632 mg, 2 mmol, 54%) as a colorless oil.

**$^1$H NMR** (500 MHz, $CDCl_3$) δ 4.41 [tq, $J$ = 6.1, 3.0 Hz, 1H, -C*H*(OTBS)-], 1.72 [dddd, 13.3, 9.1, 6.4, 6.4 Hz, 1H, CH(OTBS)C$H_a$H$_b$], 1.70 [dddd, 13.4, 8.8, 6.3, 6.3 Hz, 1H, CH(OTBS)CH$_a$$H_b$], 1.48–1.35 (m, 2H-CH(OTBS)CH$_2$C$H_2$-), 1.35–1.22 [m, 8H, -(C$H_2$)$_4$CH$_3$], 0.90 [s, 9H, -Si(CH$_3$)$_2$C(C$H_3$)$_3$], 0.89 (t, $J$ = 7.1 Hz, 3H, -CH$_2$C$H_3$), 0.13 [s, 3H, -Si(C$H_3$)$_a$(CH$_3$)$_b$C(CH$_3$)$_3$], and 0.11 [s, 3H, -Si(CH$_3$)$_a$(C$H_3$)$_b$C(CH$_3$)$_3$].

**$^{13}$C NMR** (125 MHz, $CDCl_3$) δ 114.4 (q, $J$ = 257.0 Hz), 89.4 (q, $J$ = 6.4 Hz), 71.5 (q, $J$ = 51.9 Hz), 62.5, 37.7, 32.0, 29.31, 29.25, 25.8, 25.0, 22.8, 18.3, 14.3, -4.5, and -4.9 ppm.

**IR** (neat) 2956, 2929, 2862, 1277, 1147, 1097, and 839 $cm^{-1}$.

**GC-LRMS** (ES, 70 eV): $t_R$ = 6.39 min. *m/z*: 336 ($M^+$), and 279 ($M^+$–Bu•).

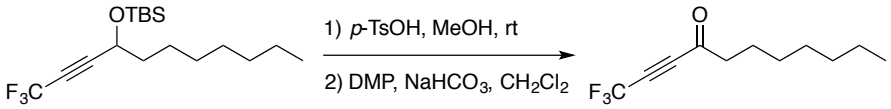


**S509** **525g**

**Preparation of 1,1,1-trifluorodec-2-yn-4-one (525g).**

*tert*-Butyldimethyl((1,1,1-trifluorodec-2-yn-4-yl)oxy)silane (**S509**, 325 mg, 1 mmol), MeOH (10 mL), and *para*-toluenesulfonic acid (200 mg, 1 mmol) were combined in a 20 mL glass vial equipped with a stir bar, and the mixture was stirred at room temperature. After 2 h TLC analysis indicated completion of reaction. The crude mixture was partitioned between $Et_2O$ and $NaHCO_3$ (aq). The aqueous layer was extracted with $Et_2O$. The combined organic layers were washed with brine, dried over anhydrous $Na_2SO_4$, and concentrated. The crude material was then re-dissolved in $CH_2Cl_2$ (5 mL), and cooled to 0 °C before addition of $NaHCO_3$ (0.84 g, 10 mmol) and Dess-Martin periodinane (DMP, 0.84 g, 2 mmol). The ice bath was removed after 5 min. The reaction mixture was allowed to stir overnight at room temperature. The crude mixture was then partitioned between EtOAc and $Na_2S_2O_3$. The organic layer was washed with brine, dried over anhydrous $Na_2SO_4$, and concentrated. The residue was purified by column chromatography on silica gel (hexanes:ethyl acetate = 20:1) to give 1,1,1-trifluorodec-2-yn-4-one (**525g**, 165 mg, 80%) as a colorless oil.

**$^1$H NMR** (500 MHz, $CDCl_3$) δ 2.66 [t, $J$ = 7.4 Hz, 2H, C(O)C$H_2$], 1.69 (br pentet, $J$ = 7.1 Hz, 2H, -C(O)$CH_2$C$H_2$-), 1.36–1.23 [m, 8H, -(C$H_2$)$_4$$CH_3$], and 0.89 (t, $J$ = 7.1 Hz, 3H, -C$H_3$).

**$^{13}$C NMR** (125 MHz, $CDCl_3$) δ 185.2 (q, *J* = 2.0 Hz), 114.0 (q, *J* = 259.7 Hz), 80.9 (q, *J* = 6.6 Hz), 73.1 (q, *J* = 54.4 Hz), 45.5, 31.7, 29.1, 28.9, 23.5, 22.8, and 14.2 ppm.

**IR** (neat) 2960, 2931, 2862, 1701, 1257, 1221, 1155, and 1088 $cm^{-1}$.

**HRMS** (ESI-TOF): Calcd for $(C_{11}H_{15}F_3NaO•MeOH)^+$ (M+$Na^+$+MeOH) 275.1229. Found: 275.1240.

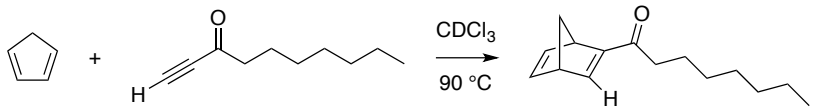


**525a** **526a**

**Preparation of methyl 1-(bicyclo[2.2.1]hepta-2,5-dien-2-yl)octan-1-one (526a).**

Freshly cracked cyclopentadiene (1 M solution in $CDCl_3$, 0.15 mL, 1.5 equiv) was directly added to dec-1-yn-3-one[108] (**525a**, 0.2 M solution in $CDCl_3$, 15 mg in 0.5 mL of $CDCl_3$) in an NMR tube at room temperature. $^1$H NMR analysis was performed to monitor the reaction progress. The NMR tube was placed in a 90 °C oil bath. After 15 h the reaction was judged to be complete (>5 half-lives), and the reaction mixture was concentrated. The residue was purified by column chromatography on silica gel (hexanes:ethyl acetate = 12:1) to give 1-(bicyclo[2.2.1]hepta-2,5-dien-2-yl)octan-1-one (**526a**, 20 mg, 0.09 mmol, 92%) as a pale yellow oil.

**$^1$H NMR** (500 MHz, $CDCl_3$) δ 7.59 [d, *J* = 3.2 Hz, 1H, -C*H*=C(octanoyl)-], 6.87 (dd, *J* = 5.0, 3.2 Hz, 1H, -C$H_a$=C$H_b$-), 6.72 (ddd, *J* = 4.8, 3.2, 0.3 Hz, 1H, -C$H_a$=C$H_b$-), 4.00–3.97 (br s, 1H, bridgehead $H_a$), 3.74–3.71 (br s, 1H, bridgehead $H_b$), 2.58 (ddd, *J* = 15.4, 8.0, 7.2 Hz, 1H, -C(O)C$H_a$H$_b$), 2.53 (ddd, *J* = 15.5, 7.7, 7.1 Hz, 1H, -C(O)CH$_a$$H_b$-), 2.09 (ddd, *J* = 6.6, 1.6, 1.6 Hz, C$H_a$H$_b$CHC=C), 2.07 (ddd, *J* = 6.5, 1.6, 1.6 Hz, CH$_a$$H_b$CHC=C),

[108] Yan, W.; Li, Z.; Kishi, Y. Selective activation/coupling of polyhalogenated nucleophiles in Ni/Cr-mediated reactions: synthesis of C1–C19 building block of halichondrin Bs. *J. Am. Chem. Soc.* **2015**, *137*, 6219–6225.

1.58 (br pentet, $J$ = 7.1 Hz, 2H, -C(O)CH$_2$C$H_2$-), 1.34–1.20 [m, 8H, -(C$H_2$)$_4$CH$_3$], and 0.87 (t, $J$ = 7.1 Hz, 3H, -C$H_3$).

**$^{13}$C NMR** (125 MHz, $CDCl_3$) δ 197.5, 158.2, 155.6, 144.0, 141.9, 73.6, 51.9, 48.9, 39.1, 31.9, 29.6, 29.3, 25.1, 22.8, and 14.3 ppm.

**IR** (neat) 2956, 2929, 2857, 1656, 1584, 1553, 1460, 1370, 1219, 1141, and 876 cm$^{-1}$.

**HRMS** (ESI-TOF): Calcd for $(C_{15}H_{22}NaO)^+$ 241.1563. Found: 241.1572.

---

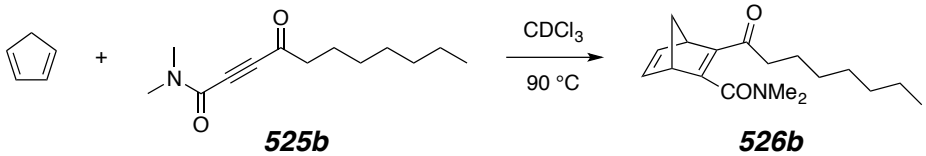


***525b*** ***526b***

**Preparation of *N*,*N*-dimethyl-3-octanoylbicyclo[2.2.1]hepta-2,5-diene-2-carboxamide (526b).**

Freshly cracked cyclopentadiene (1 M solution in $CDCl_3$, 0.15 mL, 1.5 equiv) was directly added to *N*,*N*-dimethyl-4-oxoundec-2-ynamide (**525b**, 0.2 M solution in $CDCl_3$, 22 mg in 0.5 mL of $CDCl_3$) in an NMR tube at room temperature. $^1$H NMR analysis was performed to monitor the reaction progress. The NMR tube was sealed with a plastic cap, wrapped with black electrical tape, and placed in a 90 °C oil bath. After 3 h the reaction was judged to be complete (>5 half-lives), and the crude mixture was concentrated. The residue was purified by column chromatography on silica gel (hexanes:ethyl acetate = 1:1) to give *N*,*N*-dimethyl-3-octanoylbicyclo[2.2.1]hepta-2,5-diene-2-carboxamide (**526b**, 28 mg, 0.10 mmol, 97%) as a pale yellow oil.

**$^1$H NMR** (500 MHz, $CDCl_3$) δ 6.92-6.90 (m, 2H, -C$H$=C$H$-), 4.07 (dddd, $J$ = 4.0, 2.4, 1.6, 1.6 Hz, 1H, bridgehead $H_a$), 3.74 (dddd, $J$ = 3.9, 2.3, 1.6, 1.6 Hz, 1H, bridgehead $H_b$), 3.05 (s, 3H, -CON(C$H_3$)$_a$(CH$_3$)$_b$], 2.84 (s, 3H, -CON(CH$_3$)$_a$(C$H_3$)$_b$], 2.51 [dt, $J$ = 16.9, 7.5 Hz, 1H, -C(O)C$H_a$H$_b$], 2.44 [dt, $J$ = 16.8, 7.4 Hz, 1H, -C(O)CH$_a$$H_b$], 2.26 (ddd, $J$ = 6.8, 1.6, 1.6 Hz, 1H, C$H_a$H$_b$CHC=C), 2.08 (ddd, $J$ = 6.8, 1.5, 1.5 Hz, 1H, CH$_a$$H_b$CHC=C),

1.55 [br pentet, $J$ = 7.2 Hz, 2H, -C(O)CH$_2$C$H_2$-], 1.32–1.20 [m, 8H, -(C$H_2$)$_4$CH$_3$], and 0.87 [t, $J$ = 7.1 Hz, 3H, -(CH$_2$)$_6$C$H_3$].

**$^{13}$C NMR** (125 MHz, $CDCl_3$) δ 197.0, 169.1, 159.7, 149.5, 142.8, 141.6, 72.0, 56.0, 50.7, 40.6, 37.5, 34.4, 31.8, 29.4, 29.2, 23.9, 22.8, and 14.2 ppm.

**IR** (neat) 2928, 2856, 1658, 1634, 1613, 1557, 1455, 1395, 1290, 1217, 1139, and 1042 cm$^{-1}$.

**HRMS** (ESI-TOF): Calcd for $(C_{18}H_{27}NNaO_2)^+$ 312.1934. Found: 312.1922.

---

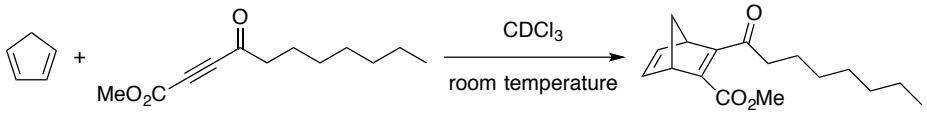


**525c** **526c**

**Preparation of methyl 3-octanoylbicyclo[2.2.1]hepta-2,5-diene-2-carboxylate (526c).**

Freshly cracked cyclopentadiene (1 M solution in $CDCl_3$, 0.15 mL, 1.5 equiv) was directly added to methyl 4-oxoundec-2-ynoate[109] (**525c**, 0.2 M solution in $CDCl_3$, 21 mg in 0.5 mL of solvent) in an NMR tube at room temperature. $^1$H NMR analysis was performed to monitor the reaction progress. After 4 h the reaction was judged to be complete (>5 half-lives), and the crude mixture was concentrated. The residue was purified by column chromatography on silica gel (hexanes:ethyl acetate = 5:1) to give methyl 3-octanoylbicyclo[2.2.1]hepta-2,5-diene-2-carboxylate (**526c**, 25 mg, 0.09 mmol, 90%) as a pale yellow oil.

**$^1$H NMR** (500 MHz, $CDCl_3$) δ 6.93 (dd, $J$ = 5.0, 3.2 Hz, 1H, -C$H_a$=CH$_b$-), 6.88 (dd, $J$ = 5.0, 3.1 Hz, 1H, -CH$_a$=C$H_b$-), 4.00–3.97 (br s, 1H, bridgehead $H_a$), 3.86–3.83 (br s, 1H, bridgehead $H_b$), 3.76 (s, 3H, -CO$_2$C$H_3$), 2.65 (t, $J$ = 7.3 Hz, 1H, -C(O)C$H_2$), 2.22 (dddd, $J$ = 6.8, 1.7, 1.7, 0.4 Hz, C$H_a$H$_b$CHC=C), 2.05 (ddd, $J$ = 6.8, 1.5, 1.5 Hz, CH$_a$$H_b$CHC=C), 1.58 (br pentet, $J$ = 7.1 Hz, 2H, -C(O)CH$_2$C$H_2$-), 1.33–1.23 [m, 8H, -(C$H_2$)$_4$CH$_3$], and

[109] Yue, Y.; Yu, X.-Q.; Pu, L. *Chem. Eur. J.* **2009**, *15*, 5104–5107.

0.88 (t, *J* = 7.1 Hz, 3H, -C*H*$_3$).

**$^{13}$C NMR** (125 MHz, $CDCl_3$) δ 203.4, 165.2, 163.7, 147.2, 143.2, 142.1, 72.4, 54.7, 53.0, 52.1, 42.4, 31.9, 29.4, 29.3, 23.9, 22.8, and 14.3 ppm.

**IR** (neat) 2951, 2929, 2855, 1717, 1612, 1435, 1290, 1238, 1100, and 1072 cm$^{-1}$.

**HRMS** (ESI-TOF): Calcd for $(C_{17}H_{24}NaO_3)^+$ 299.1618. Found: 299.1625.

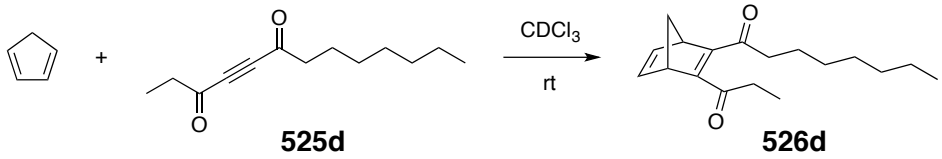


**525d** **526d**

**Preparation of 3-propionylbicyclo[2.2.1]hepta-2,5-dien-2-yl)octan-1-one (526d).**

Freshly cracked cyclopentadiene (1 M solution in $CDCl_3$, 0.15 mL, 1.5 equiv) was directly added to tridec-4-yne-3,6-dione (**525d**, 0.2 M solution in $CDCl_3$, 21 mg in 0.5 mL of solvent) in an NMR tube at room temperature. $^1$H NMR analysis was performed to monitor the reaction progress. After 1.5 h the reaction was judged to be complete (>5 half-lives), and the reaction mixture was concentrated. The residue was purified by column chromatography on silica gel (hexanes:ethyl acetate = 12:1) to give 3-propionylbicyclo[2.2.1]hepta-2,5-dien-2-yl)octan-1-one (**526d**, 25 mg, 0.09 mmol, 93%) as a pale yellow oil.

**$^1$H NMR** (500 MHz, $CDCl_3$) δ 6.93–6.91 (m, 2H, -C*H*=C*H*-), 3.93–3.88 (m, 2H, bridgehead *Hs*), 2.57 [q, *J* = 7.3 Hz, 2H, C(O)C*H*$_2$CH$_3$], 2.56–2.52 (overlapping nfoms, 2H, -C(O)C*H*$_2$), 2.20 (ddd, *J* = 6.8, 1.6, 1.6, Hz, C*H*$_a$H$_b$CHC=C), 2.07 (ddd, *J* = 6.9, 1.5, 1.5 Hz, CH$_a$*H*$_b$CHC=C), 1.58 [br pentet, *J* = 7.3 Hz, 2H, -C(O)CH$_2$C*H*$_2$-], 1.33–1.23 [m, 8H, -(C*H*$_2$)$_4$CH$_3$], 1.09 [t, *J* = 7.3 Hz, C(O)CH$_2$C*H*$_3$], and 0.87 (t, *J* = 7.1 Hz, 3H, -C*H*$_3$).

**$^{13}$C NMR** (125 MHz, $CDCl_3$) δ 201.90, 201.88, 158.7, 158.2, 142.7, 142.6, 71.9, 53.7, 53.6, 41.8, 35.0, 31.9, 29.4, 29.3, 23.9, 22.8, 14.3, and 7.9 ppm.

**IR** (neat) 2930, 2858, 1692, 1665, 1598, 1556, 1456, 1357, 1293, 1214, 1164, 1135, 1089, and 809 $cm^{-1}$.

**HRMS** (ESI-TOF): Calcd for $(C_{18}H_{26}NaO_2)^+$ 297.1825. Found: 297.1819.

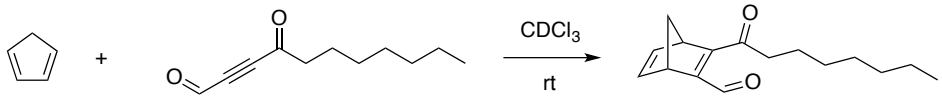


**525e** **526e**

**Preparation of 3-octanoylbicyclo[2.2.1]hepta-2,5-diene-2-carbaldehyde (526e).**

Freshly cracked cyclopentadiene (1 M solution in $CDCl_3$, 0.15 mL, 1.5 equiv) was directly added to 4-oxoundec-2-ynal (**525e**, 0.2 M solution in $CDCl_3$, 18 mg in 0.5 mL of solvent) in an NMR tube at room temperature. $^1$H NMR analysis was performed to monitor the reaction progress. After 25 min the reaction was judged to be complete (>5 half-lives), and the reaction mixture was concentrated. The residue was purified by column chromatography on silica gel (hexanes:ethyl acetate = 12:1) to give 3-octanoylbicyclo[2.2.1]hepta-2,5-diene-2-carbaldehyde (**526e**, 18 mg, 0.07 mmol, 73%) as a pale yellow oil.

**$^1$H NMR** (500 MHz, $CDCl_3$) δ 10.20 (s, 1H, C*H*O), 6.89 (ddd, *J* = 5.1, 2.9, 1.1 Hz, 1H, -C*H*$_a$=CH$_b$-), 6.88 (ddd, *J* = 5.1, 2.9, 1.0 Hz, 1H, -CH$_a$=C*H*$_b$-), 4.17–4.14 (dddd, *J* = 3.9, 2.8, 1.4, 1.4, 0.4 Hz, 1H, bridgehead *H*$_a$), 3.98 (dddd, *J* = 4.0, 2.6, 1.3, 1.3 Hz, 1H, bridgehead *H*$_b$), 2.71 [ddd, *J* = 16.9, 8.1, 6.7 Hz, 1H, -C(O)C*H*$_a$H$_b$], 2.63 [dt, *J* = 16.9, 8.0, 6.6 Hz, 1H, -C(O)CH$_a$*H*$_b$], 2.20–2.15 (m, C*H*$_2$CHC=C), 1.68–1.60 (m, 2H, -C(O)CH$_2$C*H*$_2$-), 1.37–1.22 [m, 8H, -(C*H*$_2$)$_4$CH$_3$], and 0.89 (t, *J* = 7.2 Hz, 3H, -C*H*$_3$).

**$^{13}$C NMR** (125 MHz, $CDCl_3$) δ 199.3, 188.1, 166.7, 159.5, 143.3, 141.8, 72.1, 53.6, 49.2, 42.4, 31.8, 29.31, 29.28, 23.7, 22.8, and 14.3 ppm.

**IR** (neat) 2926, 2857, 1663, 1589, 1557, 1285, 1210, 1054, 1033, and 1015 $cm^{-1}$.

**HRMS** (ESI-TOF): Calcd for $(C_{17}H_{26}NaO_3)^+$ 301.1774. Found: 301.1769.

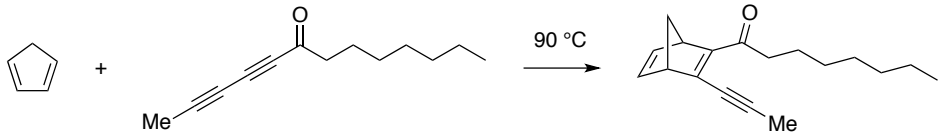


***525f*** ***526f***

**Preparation of 3-(prop-1-yn-1-yl)bicyclo[2.2.1]hepta-2,5-dien-2-yl)octan-1-one (526f).**

Freshly cracked cyclopentadiene (0.15 mL) was directly added to trideca-2,4-diyn-6-one (**525f**, 38 mg, 0.2 mmol) in a small vial. The headspace was flushed with $N_2$. The vial was sealed with Teflon-lined cap and placed in a 90 °C oil bath. After 24 h the reaction mixture was concentrated, and the residue was purified by column chromatography on silica gel (hexanes:ethyl acetate = 30:1) to give 3-(prop-1-yn-1-yl)bicyclo[2.2.1]hepta-2,5-dien-2-yl)octan-1-one (**526f**, 35 mg, 1.4 mmol, 68%) as a pale yellow oil. This sample was contaminated with a small portion of coeluting **526a**, arising from a small portion of **525a** present in the starting sample of **525f.**

**$^1$H NMR** (500 MHz, $CDCl_3$) δ 6.82 (ddd, *J* = 5.2, 3.1, 0.8 Hz, 1H, -C*H*$_a$=CH$_b$-), 6.77 (ddd, *J* = 5.1, 3.1, 0.9 Hz, 1H, -CH$_a$=C*H*$_b$-), 4.08–4.06 (br s, 1H, bridgehead *H*$_a$), 3.67–3.65 (br s, 1H, bridgehead *H*$_b$), 2.87–2.76 [nfom, 2H, -C(O)C*H*$_2$], 2.17 (s, 3H, C-C*H*$_3$), 2.07 (ddd, *J* = 7.0, 1.7, 1.7 Hz, C*H*$_a$H$_b$CHC=C), 2.01 (ddd, *J* = 6.8, 1.5, 1.5 Hz, CH$_a$*H*$_b$CHC=C), 1.59 (br pentet, *J* = 6.9 Hz, 2H, -C(O)CH$_2$C*H*$_2$-), 1.35–1.21 [m, 8H, -(C*H*$_2$)$_4$CH$_3$], and 0.88 (t, *J* = 7.1 Hz, 3H, -C*H*$_3$).

**$^{13}$C NMR** (125 MHz, $CDCl_3$) δ 197.3, 155.9, 148.0, 143.2, 141.3, 106.2, 77.5, 70.7, 59.2, 50.2, 41.0, 32.0, 29.7, 29.4, 24.9, 22.9, 14.3, and 5.6 ppm.

**IR** (neat) 2954, 2927, 2855, 2237, 1650, 1575, 1556, 1456, 1378, and 1294 cm$^{-1}$.

**HRMS** (ESI-TOF): Calcd for $(C_{18}H_{24}NaO)^+$ 279.1719. Found: 279.1721.

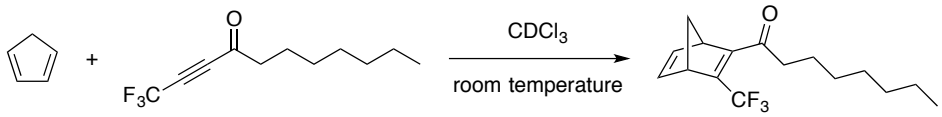


**525g** **526g**

**Preparation of 1-((1*R*,4*S*)-3-(trifluoromethyl)bicyclo[2.2.1]hepta-2,5-dien-2-yl)decan-1-one (526g).**

Freshly cracked cyclopentadiene (1 M solution in $CDCl_3$, 0.15 mL, 1.5 equiv) was directly added to 1,1,1-trifluorodec-2-yn-4-one (**525g**, 0.2 M solution in $CDCl_3$, 22 mg in 0.5 mL solvent) in an NMR tube at room temperature. $^1$H NMR analysis was performed to monitor the reaction progress. After 40 min the reaction was judged to be complete (>5 half-lives), and the reaction mixture was concentrated. The residue was purified by column chromatography on silica gel (hexanes:ethyl acetate = 12:1) to give 1-(3-(trifluoromethyl)bicyclo[2.2.1]hepta-2,5-dien-2-yl)decan-1-one (**526g**, 24 mg, 0.084 mmol, 84%) as a colorless oil.

**$^1$H NMR** (500 MHz, $CDCl_3$) δ 6.94 (dd, $J$ = 5.1, 1.8 Hz, 1H, -C$H_a$=CH$_b$-), 6.93 (dd, $J$ = 5.1, 1.8 Hz, 1H, -CH$_a$=C$H_b$-), 3.87–3.85 (m, 2H, bridgehead *H*'s), 2.58 (dt, $J$ = 16.9, 7.4 Hz, 1H, -C(O)C$H_a$H$_b$), 2.56 (dt, $J$ = 17.0, 7.2 Hz, 1H, -C(O)CH$_a$$H_b$-), 2.22 (ddd, $J$ = 6.9, 1.7, 1.7 Hz, C$H_a$H$_b$CHC=C), 2.04 (br d, $J$ = 6.9 Hz, CH$_a$$H_b$CHC=C), 1.58 (br pentet, $J$ = 7.1 Hz, 2H, -C(O)CH$_2$C$H_2$-), 1.33–1.21 [m, 8H, -(C$H_2$)$_4$CH$_3$], and 0.88 (t, $J$ = 7.1 Hz, 3H, -C$H_3$).

**$^{13}$C NMR** (125 MHz, $CDCl_3$) δ 201.3, 158.7, 144.6 (q, $J$ = 35.1 Hz), 142.5, 142.4 (br), 123.1 (q, $J$ = 268.9 Hz), 72.2, 54.6, 52.0 (q, $J$ = 1.8 Hz), 42.4 (q, $J$ = 1.8 Hz), 31.8, 29.2 (2C), 23.8, 22.8, and 14.3 ppm.

**IR** (neat) 2930, 2858, 1695, 1335, 1293, 1257, 1157, and 1120 cm$^{-1}$.

**HRMS** (ESI-TOF): Calcd for $(C_{16}H_{21}F_3NaO)^+$ 309.1437. Found: 309.1447.

**Table S2.** Relative rates of hexadehydro-Diels–Alder reactions of **519a-g**

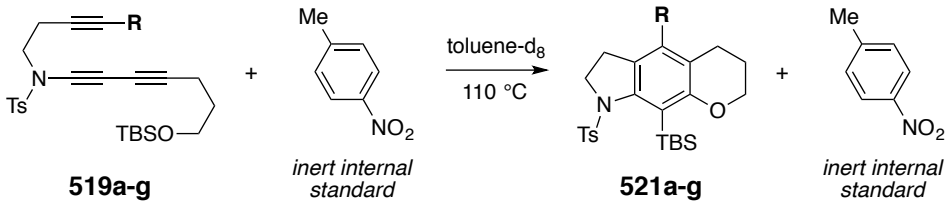


| substrate | 519g | 519a | 519b | 519c | 519d | 519e | 519f |
|---|---|---|---|---|---|---|---|
| ***R*** |  | H | 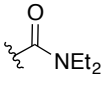 | 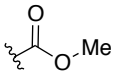 |  |  | 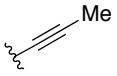 |
| $t_{1/2}$ **(h)** | > 600 | > 400 | 84 | 9.2 | 5.1 | 0.82 | 0.26 |

## General procedure for measuring the relative rates of HDDA reaction of substrates 519a-g

Each of the triyne precursors **519a-g** (ca. 3 mg, 6 μmol), along with the internal standard *p*-nitrotoluene (1 mg, 7 μmol), was dissolved in 0.6 mL of toluene-$d_8$ and transferred to an NMR tube. A $^1$H NMR spectrum was recorded for each sample to determine the ratio of the starting material and the inert internal standard *p*-nitrotoluene present in each. Each tube was then capped and sealed with electrical tape. All tubes were placed in a pre-equilibrated 110 °C oil bath. The reaction progress of each was monitored by periodic removal of the tube and analyzing the $^1$H NMR spectrum. The reaction half-lives were determined based on integration of the product peaks against the internal standard peak. First order kinetics was assumed for the rate-determining, HDDA cycloisomerization of **519** to its derived benzyne **520**.

**Table S3.** Relative rates of bimolecular Diels–Alder reactions of **525a-g** with **CPD**

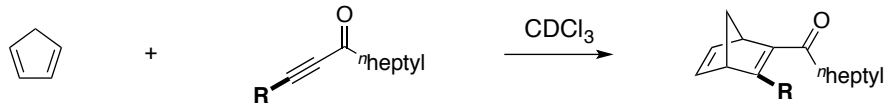


**CPD** **525a-g** **526a-g**

| dienophile | 525f | 525a | 525b | 525c | 525d | 525g | 525e |
|---|---|---|---|---|---|---|---|
| ***R*** | 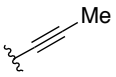 | H |  | 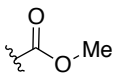 | 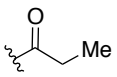 |  |  |
| $k_{rel}$ | 1 | 10 | 50 | 840 | 2,100 | 16,800 | 47,000 |



**General procedure for measuring the relative rates of bimolecular Diels–Alder reactions of 525a-g with CPD**

For each adjacent pair of ynones in Table S3 above (i.e. **525f** vs. **525a**, **525a** vs. **525b**, **525b** vs. **525c**, and so on), the following competition experiment was conducted: 0.1 mmol of each ynone (ca. 20 mg) was dissolved in 0.5 mL of $CDCl_3$ and the solution was transferred into an NMR tube. $^1$H NMR analysis was then performed to determine the initial ratio of the two ynones. A solution of freshly cracked cyclopentadiene (0.1 mL, 0.1 M, 0.01 mmol) was then added to this NMR tube. The reaction progress was constantly monitored by $^1$H NMR analysis. Heating of the NMR tube was required for several of the slower Diels–Alder reaction partners (namely, experiments involving **525f**, **525a**, or **525b** as the dienophile). The $k_{rel}$ values shown in Table S3 are the average of two separate measurements.

# Supplementary information for Section 5.4

## Supporting information for subsection 5.4.1

DFT calculations were performed with the Gaussian 09[100] software package. All geometries were optimized using the M06-2X functional.[101] The following basis sets were used: double-ζ split-valence 6-31G(d), triple-ζ split-valence 6-311G(d,p), and Dunning's correlation consistent, triple-ζ cc-pVTZ. Acetonitrile solvation was approximated by the continuum solvation model SMD[46] for both the geometry optimizations and the frequency calculations ["scrf=(SMD,solvent=acetonitrile)" keyword]. All calculations used the grid=ultrafine option to specify the integration grid used during the numerical integrations ["integral(grid=ultrafine)" keyword]. Harmonic vibrational frequency calculations were performed at 298 K to provide thermal corrections to the enthalpies. The optimized geometry for each reactant, intermediate, and product was found to have no imaginary frequencies; the optimized geometry for each transition structure (TS) was found to have one (and only one) imaginary frequency. Analysis of the imaginary frequency (by following the normal modes associated with each) for each TS identified it with each associated starting material and product.

**Computed energy and geometry of 536**

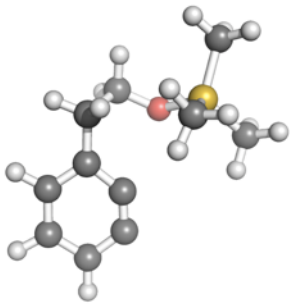

**M06-2X/6-311G(d,p)**

Sum of electronic and thermal Enthalpies = −793.117704 A.U.[a]

| Center Number | Atomic Number | Atomic Type | Coordinates (Angstroms) X | Y | Z |
|---|---|---|---|---|---|
| 1 | 6 | 0 | 3.111267 | −0.998053 | 0.121095 |
| 2 | 6 | 0 | 4.126298 | −0.034227 | −0.012413 |
| 3 | 6 | 0 | 3.859705 | 1.339338 | −0.123289 |
| 4 | 6 | 0 | 2.488893 | 1.582846 | −0.093020 |
| 5 | 6 | 0 | 1.632208 | 0.694844 | 0.031945 |
| 6 | 6 | 0 | 1.736895 | −0.678469 | 0.154165 |
| 7 | 1 | 0 | 3.389243 | −2.044572 | 0.205405 |
| 8 | 1 | 0 | 5.158689 | −0.367942 | −0.032971 |
| 9 | 1 | 0 | 4.645359 | 2.076792 | −0.223836 |
| 10 | 6 | 0 | 0.631015 | −1.676567 | 0.300000 |
| 11 | 1 | 0 | 1.042176 | −2.687371 | 0.249871 |
| 12 | 1 | 0 | 0.163054 | −1.556582 | 1.281827 |
| 13 | 6 | 0 | −0.433712 | −1.517375 | −0.786017 |
| 14 | 1 | 0 | 0.010349 | −1.716095 | −1.765070 |
| 15 | 1 | 0 | −1.226258 | −2.257741 | −0.622125 |
| 16 | 8 | 0 | −0.955633 | −0.201267 | −0.813938 |
| 17 | 14 | 0 | −2.310463 | 0.298363 | 0.036710 |
| 18 | 6 | 0 | −2.129952 | −0.085990 | 1.859243 |
| 19 | 1 | 0 | −2.988497 | 0.317713 | 2.406011 |
| 20 | 1 | 0 | −2.097592 | −1.163274 | 2.047424 |
| 21 | 1 | 0 | −1.225447 | 0.364218 | 2.278718 |
| 22 | 6 | 0 | −2.396702 | 2.137106 | −0.250228 |
| 23 | 1 | 0 | −3.258590 | 2.571586 | 0.264608 |
| 24 | 1 | 0 | −1.496268 | 2.631766 | 0.125358 |
| 25 | 1 | 0 | −2.489473 | 2.366249 | −1.315343 |

| | | | | | |
|---|---|---|---|---|---|
| 26 | 6 | 0 | −3.824473 | −0.571806 | −0.633678 |
| 27 | 1 | 0 | −4.722186 | −0.225717 | −0.111652 |
| 28 | 1 | 0 | −3.958588 | −0.370323 | −1.700254 |
| 29 | 1 | 0 | −3.763069 | −1.655535 | −0.497228 |

[a] Atomic Units = Hartrees

**M06-2X/6-31G(d)**

Sum of electronic and thermal Enthalpies = −792.947189 A.U.[a]

| Center Number | Atomic Number | Atomic Type | Coordinates (Angstroms) X | Y | Z |
|---|---|---|---|---|---|
| 1 | 6 | 0 | 3.036817 | −0.983305 | 0.139713 |
| 2 | 6 | 0 | 4.013023 | 0.022502 | 0.011526 |
| 3 | 6 | 0 | 3.689965 | 1.384087 | −0.123542 |
| 4 | 6 | 0 | 2.309827 | 1.571105 | −0.123308 |
| 5 | 6 | 0 | 1.485428 | 0.644877 | 0.000084 |
| 6 | 6 | 0 | 1.648405 | −0.722387 | 0.142482 |
| 7 | 1 | 0 | 3.359970 | −2.016950 | 0.244070 |
| 8 | 1 | 0 | 5.060351 | −0.268841 | 0.014471 |
| 9 | 1 | 0 | 4.448091 | 2.153818 | −0.220209 |
| 10 | 6 | 0 | 0.577963 | −1.760683 | 0.288680 |
| 11 | 1 | 0 | 1.023407 | −2.760087 | 0.254718 |
| 12 | 1 | 0 | 0.100781 | −1.651026 | 1.269621 |
| 13 | 6 | 0 | −0.486528 | −1.654123 | −0.808091 |
| 14 | 1 | 0 | −0.041614 | −1.918841 | −1.773288 |
| 15 | 1 | 0 | −1.290045 | −2.375277 | −0.603511 |
| 16 | 8 | 0 | −0.996860 | −0.341928 | −0.931672 |
| 17 | 14 | 0 | −2.193812 | 0.316945 | 0.040668 |
| 18 | 6 | 0 | −1.715503 | 0.307692 | 1.855925 |
| 19 | 1 | 0 | −2.419795 | 0.930286 | 2.421812 |
| 20 | 1 | 0 | −1.748879 | −0.698456 | 2.288115 |
| 21 | 1 | 0 | −0.710709 | 0.716481 | 2.014244 |
| 22 | 6 | 0 | −2.362289 | 2.072689 | −0.575775 |
| 23 | 1 | 0 | −3.144949 | 2.611393 | −0.029848 |
| 24 | 1 | 0 | −1.422765 | 2.621778 | −0.445201 |
| 25 | 1 | 0 | −2.618599 | 2.095284 | −1.640577 |
| 26 | 6 | 0 | −3.785443 | −0.648767 | −0.181297 |
| 27 | 1 | 0 | −4.592800 | −0.191027 | 0.402636 |
| 28 | 1 | 0 | −4.100131 | −0.666828 | −1.230523 |
| 29 | 1 | 0 | −3.684057 | −1.685628 | 0.159120 |

[a] Atomic Units = Hartrees

**M06-2X/ccpVTZ**

Sum of electronic and thermal Enthalpies = −793.181349 A.U.[a]

| Center Number | Atomic Number | Atomic Type | Coordinates (Angstroms) X | Y | Z |
|---|---|---|---|---|---|
| 1 | 6 | 0 | 3.162187 | −1.012205 | 0.113273 |
| 2 | 6 | 0 | 4.213509 | −0.093670 | −0.020563 |
| 3 | 6 | 0 | 4.005349 | 1.287924 | −0.122962 |
| 4 | 6 | 0 | 2.649091 | 1.584984 | −0.080343 |
| 5 | 6 | 0 | 1.758477 | 0.734978 | 0.042693 |
| 6 | 6 | 0 | 1.804182 | −0.638777 | 0.157109 |
| 7 | 1 | 0 | 3.396300 | −2.068153 | 0.188839 |
| 8 | 1 | 0 | 5.228868 | −0.470253 | −0.047702 |
| 9 | 1 | 0 | 4.818619 | 1.991530 | −0.224112 |
| 10 | 6 | 0 | 0.665081 | −1.595062 | 0.298158 |
| 11 | 1 | 0 | 1.037782 | −2.616906 | 0.224718 |
| 12 | 1 | 0 | 0.211343 | −1.476566 | 1.285352 |
| 13 | 6 | 0 | −0.409485 | −1.374696 | −0.761190 |
| 14 | 1 | 0 | 0.019626 | −1.511681 | −1.756117 |
| 15 | 1 | 0 | −1.193062 | −2.129184 | −0.634211 |
| 16 | 8 | 0 | −0.937397 | −0.064972 | −0.687943 |
| 17 | 14 | 0 | −2.399872 | 0.280632 | 0.038276 |
| 18 | 6 | 0 | −2.424660 | −0.392632 | 1.782901 |
| 19 | 1 | 0 | −3.391383 | −0.192728 | 2.251158 |
| 20 | 1 | 0 | −2.271936 | −1.474268 | 1.794192 |
| 21 | 1 | 0 | −1.650928 | 0.070034 | 2.398714 |
| 22 | 6 | 0 | −2.518094 | 2.138692 | 0.024710 |
| 23 | 1 | 0 | −3.443856 | 2.470604 | 0.499121 |
| 24 | 1 | 0 | −1.682481 | 2.584772 | 0.567619 |
| 25 | 1 | 0 | −2.505169 | 2.524564 | −0.996312 |
| 26 | 6 | 0 | −3.781473 | −0.496306 | −0.952412 |
| 27 | 1 | 0 | −4.752110 | −0.246406 | −0.518265 |
| 28 | 1 | 0 | −3.771117 | −0.138713 | −1.983936 |
| 29 | 1 | 0 | −3.698104 | −1.585095 | −0.969619 |

[a] Atomic Units = Hartrees

**Computed energy and geometry of 537‡**

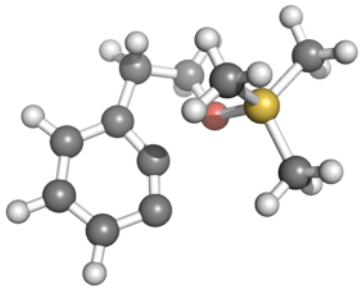

**M06-2X/6-311G(d,p)**

Sum of electronic and thermal Enthalpies = −793.112966 A.U.[a]
Imaginary frequency: −163.4714 $cm^{-1}$

| Center Number | Atomic Number | Atomic Type | Coordinates (Angstroms) X | Y | Z |
|---|---|---|---|---|---|
| 1 | 6 | 0 | 3.013861 | −0.821534 | 0.366797 |
| 2 | 6 | 0 | 3.695884 | 0.400567 | 0.249491 |
| 3 | 6 | 0 | 3.052741 | 1.566140 | −0.176619 |
| 4 | 6 | 0 | 1.670642 | 1.528038 | −0.513676 |
| 5 | 6 | 0 | 1.220420 | 0.341792 | −0.344513 |
| 6 | 6 | 0 | 1.651876 | −0.897110 | 0.049004 |
| 7 | 1 | 0 | 3.532960 | −1.713558 | 0.700953 |
| 8 | 1 | 0 | 4.752069 | 0.434741 | 0.496128 |
| 9 | 1 | 0 | 3.626418 | 2.486254 | −0.250175 |
| 10 | 6 | 0 | 0.703993 | −2.053174 | 0.096381 |
| 11 | 1 | 0 | 1.179743 | −2.987190 | −0.204735 |
| 12 | 1 | 0 | 0.323253 | −2.177198 | 1.114754 |
| 13 | 6 | 0 | −0.433388 | −1.687163 | −0.861787 |
| 14 | 1 | 0 | −0.142414 | −1.885799 | −1.894464 |
| 15 | 1 | 0 | −1.343369 | −2.248513 | −0.636644 |
| 16 | 8 | 0 | −0.670642 | −0.275777 | −0.758478 |
| 17 | 14 | 0 | −1.994338 | 0.343781 | 0.136873 |
| 18 | 6 | 0 | −1.889794 | −0.335964 | 1.870452 |
| 19 | 1 | 0 | −2.705811 | 0.069302 | 2.477047 |
| 20 | 1 | 0 | −1.974273 | −1.426334 | 1.887255 |
| 21 | 1 | 0 | −0.947130 | −0.052125 | 2.347641 |
| 22 | 6 | 0 | −1.811005 | 2.192495 | 0.092555 |
| 23 | 1 | 0 | −2.721378 | 2.656979 | 0.484344 |
| 24 | 1 | 0 | −0.968968 | 2.534235 | 0.698099 |
| 25 | 1 | 0 | −1.665546 | 2.551158 | −0.929914 |

| | | | | | |
|---|---|---|---|---|---|
| 26 | 6 | 0 | −3.546438 | −0.214084 | −0.730383 |
| 27 | 1 | 0 | −4.425933 | 0.181983 | −0.213335 |
| 28 | 1 | 0 | −3.569178 | 0.152778 | −1.760234 |
| 29 | 1 | 0 | −3.637329 | −1.303453 | −0.751322 |

[a] Atomic Units = Hartrees

**M06-2X/6-31G(d)**

Sum of electronic and thermal Enthalpies = −792.942197 A.U.[a]
Imaginary frequency: −169.7033 $cm^{-1}$

| Center Number | Atomic Number | Atomic Type | Coordinates (Angstroms) X | Y | Z |
|---|---|---|---|---|---|
| 1 | 6 | 0 | −2.968182 | 0.812981 | 0.382676 |
| 2 | 6 | 0 | −3.630697 | −0.421564 | 0.268993 |
| 3 | 6 | 0 | −2.972238 | −1.573616 | −0.177832 |
| 4 | 6 | 0 | −1.599599 | −1.513885 | −0.547312 |
| 5 | 6 | 0 | −1.170673 | −0.312950 | −0.385374 |
| 6 | 6 | 0 | −1.613387 | 0.914873 | 0.036276 |
| 7 | 1 | 0 | −3.496313 | 1.692860 | 0.740506 |
| 8 | 1 | 0 | −4.682179 | −0.477038 | 0.539260 |
| 9 | 1 | 0 | −3.533498 | −2.505798 | −0.238626 |
| 10 | 6 | 0 | −0.675967 | 2.079853 | 0.089707 |
| 11 | 1 | 0 | −1.160279 | 3.017273 | −0.195960 |
| 12 | 1 | 0 | −0.288158 | 2.199822 | 1.108310 |
| 13 | 6 | 0 | 0.457503 | 1.736666 | −0.883809 |
| 14 | 1 | 0 | 0.159572 | 1.963354 | −1.910858 |
| 15 | 1 | 0 | 1.371810 | 2.290766 | −0.651888 |
| 16 | 8 | 0 | 0.698817 | 0.324436 | −0.831937 |
| 17 | 14 | 0 | 1.936104 | −0.355437 | 0.147748 |
| 18 | 6 | 0 | 1.465882 | −0.150005 | 1.945027 |
| 19 | 1 | 0 | 2.214945 | −0.631167 | 2.585238 |
| 20 | 1 | 0 | 1.420397 | 0.907449 | 2.228712 |
| 21 | 1 | 0 | 0.494985 | −0.607851 | 2.163174 |
| 22 | 6 | 0 | 2.024729 | −2.141104 | −0.375249 |
| 23 | 1 | 0 | 2.814896 | −2.660349 | 0.179145 |
| 24 | 1 | 0 | 1.080100 | −2.662604 | −0.194013 |
| 25 | 1 | 0 | 2.255469 | −2.221147 | −1.443174 |
| 26 | 6 | 0 | 3.524472 | 0.550338 | −0.244843 |
| 27 | 1 | 0 | 4.368198 | 0.027548 | 0.221205 |
| 28 | 1 | 0 | 3.705562 | 0.579424 | −1.325012 |
| 29 | 1 | 0 | 3.527439 | 1.578573 | 0.131440 |

[a] Atomic Units = Hartrees

**M06-2X/ccpVTZ**

Sum of electronic and thermal Enthalpies = −793.175463 A.U.[a]
Imaginary frequency: −164.1869 $cm^{-1}$

| Center Number | Atomic Number | Atomic Type | Coordinates (Angstroms) X | Y | Z |
|---|---|---|---|---|---|
| 1 | 6 | 0 | 3.014060 | −0.823674 | 0.362346 |
| 2 | 6 | 0 | 3.698570 | 0.392997 | 0.246301 |
| 3 | 6 | 0 | 3.060459 | 1.559514 | −0.173998 |
| 4 | 6 | 0 | 1.679248 | 1.528250 | −0.504816 |
| 5 | 6 | 0 | 1.227631 | 0.344674 | −0.337549 |
| 6 | 6 | 0 | 1.653509 | −0.893816 | 0.049958 |
| 7 | 1 | 0 | 3.530284 | −1.716922 | 0.691323 |
| 8 | 1 | 0 | 4.753838 | 0.422350 | 0.489017 |
| 9 | 1 | 0 | 3.635976 | 2.475852 | −0.248032 |
| 10 | 6 | 0 | 0.705292 | −2.044998 | 0.094628 |
| 11 | 1 | 0 | 1.175468 | −2.977801 | −0.210860 |
| 12 | 1 | 0 | 0.328226 | −2.173250 | 1.111735 |
| 13 | 6 | 0 | −0.433187 | −1.671788 | −0.854379 |
| 14 | 1 | 0 | −0.149075 | −1.871887 | −1.887020 |
| 15 | 1 | 0 | −1.341728 | −2.230667 | −0.626704 |
| 16 | 8 | 0 | −0.666619 | −0.263371 | −0.747473 |
| 17 | 14 | 0 | −1.995341 | 0.341982 | 0.133410 |
| 18 | 6 | 0 | −1.918957 | −0.357027 | 1.859272 |
| 19 | 1 | 0 | −2.747365 | 0.034290 | 2.454332 |
| 20 | 1 | 0 | −1.997094 | −1.445964 | 1.857797 |
| 21 | 1 | 0 | −0.988384 | −0.075031 | 2.356090 |
| 22 | 6 | 0 | −1.814204 | 2.190232 | 0.115379 |
| 23 | 1 | 0 | −2.725615 | 2.646601 | 0.508643 |
| 24 | 1 | 0 | −0.977440 | 2.521601 | 0.730554 |
| 25 | 1 | 0 | −1.663273 | 2.562044 | −0.899460 |
| 26 | 6 | 0 | −3.535673 | −0.208202 | −0.756973 |
| 27 | 1 | 0 | −4.419743 | 0.187141 | −0.251768 |
| 28 | 1 | 0 | −3.541942 | 0.159520 | −1.784590 |
| 29 | 1 | 0 | −3.624892 | −1.295620 | −0.780022 |

[a] Atomic Units = Hartrees

**Computed energy and geometry of 538**

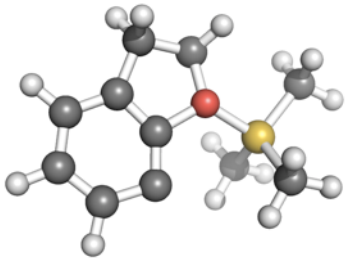

**M06-2X/6-311G(d,p)**

Sum of electronic and thermal Enthalpies = −793.124734 A.U.[a]

| Center Number | Atomic Number | Atomic Type | Coordinates (Angstroms) X | Y | Z |
|---|---|---|---|---|---|
| 1 | 6 | 0 | 3.198375 | 0.482288 | 0.036669 |
| 2 | 6 | 0 | 3.458829 | −0.891791 | 0.078975 |
| 3 | 6 | 0 | 2.418036 | −1.823990 | 0.011205 |
| 4 | 6 | 0 | 1.040094 | −1.489997 | −0.094204 |
| 5 | 6 | 0 | 0.927787 | −0.130134 | −0.120055 |
| 6 | 6 | 0 | 1.873671 | 0.880866 | −0.067105 |
| 7 | 1 | 0 | 3.998951 | 1.212040 | 0.084402 |
| 8 | 1 | 0 | 4.485701 | −1.233732 | 0.166397 |
| 9 | 1 | 0 | 2.705447 | −2.874525 | 0.048108 |
| 10 | 6 | 0 | 1.245626 | 2.243601 | −0.174148 |
| 11 | 1 | 0 | 1.656946 | 2.967400 | 0.529358 |
| 12 | 1 | 0 | 1.353949 | 2.641442 | −1.186084 |
| 13 | 6 | 0 | −0.219447 | 1.957346 | 0.144779 |
| 14 | 1 | 0 | −0.430251 | 2.033321 | 1.212354 |
| 15 | 1 | 0 | −0.929225 | 2.535983 | −0.438258 |
| 16 | 8 | 0 | −0.398446 | 0.536323 | −0.226654 |
| 17 | 14 | 0 | −1.946415 | −0.346380 | 0.017966 |
| 18 | 6 | 0 | −2.159798 | −1.498537 | −1.416851 |
| 19 | 1 | 0 | −3.226611 | −1.707607 | −1.546585 |
| 20 | 1 | 0 | −1.800460 | −1.026523 | −2.335728 |
| 21 | 1 | 0 | −1.627103 | −2.438536 | −1.279574 |
| 22 | 6 | 0 | −1.889452 | −1.080516 | 1.719580 |
| 23 | 1 | 0 | −2.907591 | −1.329023 | 2.035744 |
| 24 | 1 | 0 | −1.277700 | −1.981187 | 1.763366 |
| 25 | 1 | 0 | −1.490273 | −0.352628 | 2.432981 |
| 26 | 6 | 0 | −3.177582 | 1.044302 | −0.065391 |
| 27 | 1 | 0 | −4.178257 | 0.610437 | 0.032294 |

| | | | | | |
|---|---|---|---|---|---|
| 28 | 1 | 0 | −3.053540 | 1.768296 | 0.743675 |
| 29 | 1 | 0 | −3.139439 | 1.572951 | −1.021469 |

[a] Atomic Units = Hartrees

**M06-2X/6-31G(d)**

Sum of electronic and thermal Enthalpies = −792.953718 A.U.[a]

| Center Number | Atomic Number | Atomic Type | Coordinates (Angstroms) X | Y | Z |
|---|---|---|---|---|---|
| 1 | 6 | 0 | 3.187445 | −0.468167 | −0.066262 |
| 2 | 6 | 0 | 3.429029 | 0.911302 | −0.101432 |
| 3 | 6 | 0 | 2.378535 | 1.831911 | 0.008518 |
| 4 | 6 | 0 | 1.006703 | 1.484811 | 0.155068 |
| 5 | 6 | 0 | 0.919460 | 0.121855 | 0.168494 |
| 6 | 6 | 0 | 1.869226 | −0.883939 | 0.074109 |
| 7 | 1 | 0 | 3.996665 | −1.188275 | −0.148971 |
| 8 | 1 | 0 | 4.450807 | 1.266260 | −0.218525 |
| 9 | 1 | 0 | 2.658431 | 2.887820 | −0.029012 |
| 10 | 6 | 0 | 1.250151 | −2.252344 | 0.177621 |
| 11 | 1 | 0 | 1.641236 | −2.966249 | −0.550922 |
| 12 | 1 | 0 | 1.388909 | −2.673096 | 1.179022 |
| 13 | 6 | 0 | −0.227241 | −1.965246 | −0.093410 |
| 14 | 1 | 0 | −0.467768 | −2.026660 | −1.157828 |
| 15 | 1 | 0 | −0.921692 | −2.557132 | 0.498793 |
| 16 | 8 | 0 | −0.401053 | −0.555104 | 0.310655 |
| 17 | 14 | 0 | −1.922306 | 0.347107 | −0.035427 |
| 18 | 6 | 0 | −2.200564 | 1.559491 | 1.343950 |
| 19 | 1 | 0 | −3.272851 | 1.777498 | 1.416407 |
| 20 | 1 | 0 | −1.884271 | 1.126532 | 2.299435 |
| 21 | 1 | 0 | −1.654277 | 2.491322 | 1.191705 |
| 22 | 6 | 0 | −1.785298 | 1.010120 | −1.766853 |
| 23 | 1 | 0 | −2.786636 | 1.253243 | −2.141537 |
| 24 | 1 | 0 | −1.161411 | 1.904380 | −1.817614 |
| 25 | 1 | 0 | −1.358497 | 0.251893 | −2.434006 |
| 26 | 6 | 0 | −3.179763 | −1.027847 | 0.052340 |
| 27 | 1 | 0 | −4.175850 | −0.585714 | −0.072640 |
| 28 | 1 | 0 | −3.051566 | −1.774401 | −0.738053 |
| 29 | 1 | 0 | −3.166619 | −1.537764 | 1.021625 |

[a] Atomic Units = Hartrees

**M06-2X/ccpVTZ**

Sum of electronic and thermal Enthalpies = −793.186682 A.U.[a]

| Center Number | Atomic Number | Atomic Type | Coordinates (Angstroms) X | Y | Z |
|---|---|---|---|---|---|
| 1 | 6 | 0 | 3.182143 | 0.487908 | 0.056617 |
| 2 | 6 | 0 | 3.447542 | −0.881739 | 0.092841 |
| 3 | 6 | 0 | 2.415466 | −1.816371 | −0.002014 |
| 4 | 6 | 0 | 1.042231 | −1.486293 | −0.130587 |
| 5 | 6 | 0 | 0.920589 | −0.129480 | −0.145183 |
| 6 | 6 | 0 | 1.861015 | 0.881161 | −0.068058 |
| 7 | 1 | 0 | 3.977402 | 1.218966 | 0.124255 |
| 8 | 1 | 0 | 4.472312 | −1.219387 | 0.196257 |
| 9 | 1 | 0 | 2.706338 | −2.863649 | 0.030652 |
| 10 | 6 | 0 | 1.232995 | 2.240299 | −0.176238 |
| 11 | 1 | 0 | 1.623781 | 2.957233 | 0.542473 |
| 12 | 1 | 0 | 1.365413 | 2.649843 | −1.178371 |
| 13 | 6 | 0 | −0.235642 | 1.946743 | 0.103192 |
| 14 | 1 | 0 | −0.472751 | 2.021784 | 1.163308 |
| 15 | 1 | 0 | −0.931981 | 2.524517 | −0.492898 |
| 16 | 8 | 0 | −0.404388 | 0.528491 | −0.275831 |
| 17 | 14 | 0 | −1.934246 | −0.345885 | 0.029905 |
| 18 | 6 | 0 | −2.171786 | −1.559219 | −1.349149 |
| 19 | 1 | 0 | −3.241887 | −1.679469 | −1.534158 |
| 20 | 1 | 0 | −1.713942 | −1.185261 | −2.266673 |
| 21 | 1 | 0 | −1.740170 | −2.531081 | −1.121050 |
| 22 | 6 | 0 | −1.834674 | −1.011395 | 1.755950 |
| 23 | 1 | 0 | −2.845147 | −1.216831 | 2.117072 |
| 24 | 1 | 0 | −1.248811 | −1.926258 | 1.813832 |
| 25 | 1 | 0 | −1.390396 | −0.268685 | 2.422757 |
| 26 | 6 | 0 | −3.174109 | 1.032904 | −0.086883 |
| 27 | 1 | 0 | −4.169290 | 0.594231 | 0.021237 |
| 28 | 1 | 0 | −3.053706 | 1.776739 | 0.701521 |
| 29 | 1 | 0 | −3.137231 | 1.534663 | −1.055166 |

[a] Atomic Units = Hartrees

**Computed energy and geometry of 539‡**

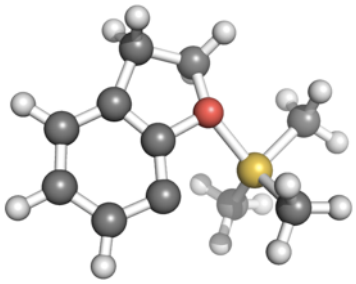

**M06-2X/6-311G(d,p)**

Sum of electronic and thermal Enthalpies = −793.115579 A.U.[a]
Imaginary frequency: −163.8221 $cm^{-1}$

| Center Number | Atomic Number | Atomic Type | Coordinates (Angstroms) X | Y | Z |
|---|---|---|---|---|---|
| 1 | 6 | 0 | 3.137571 | −0.030714 | 0.056369 |
| 2 | 6 | 0 | 2.969904 | −1.424588 | 0.082634 |
| 3 | 6 | 0 | 1.707561 | −2.036191 | −0.010065 |
| 4 | 6 | 0 | 0.518390 | −1.284945 | −0.156597 |
| 5 | 6 | 0 | 0.832104 | 0.036159 | −0.220523 |
| 6 | 6 | 0 | 1.996704 | 0.751813 | −0.092794 |
| 7 | 1 | 0 | 4.121752 | 0.410160 | 0.167022 |
| 8 | 1 | 0 | 3.849401 | −2.048493 | 0.206652 |
| 9 | 1 | 0 | 1.675656 | −3.121525 | 0.059851 |
| 10 | 6 | 0 | 1.653813 | 2.226756 | −0.128655 |
| 11 | 1 | 0 | 2.166951 | 2.813813 | 0.632871 |
| 12 | 1 | 0 | 1.877290 | 2.657445 | −1.107623 |
| 13 | 6 | 0 | 0.129742 | 2.218314 | 0.131032 |
| 14 | 1 | 0 | −0.101467 | 2.278168 | 1.195450 |
| 15 | 1 | 0 | −0.431634 | 2.956195 | −0.434253 |
| 16 | 8 | 0 | −0.292308 | 0.884074 | −0.331632 |
| 17 | 14 | 0 | −1.729449 | −0.339012 | 0.021119 |
| 18 | 6 | 0 | −2.304660 | −1.351527 | −1.440158 |
| 19 | 1 | 0 | −3.380864 | −1.232114 | −1.599156 |
| 20 | 1 | 0 | −1.792635 | −1.005702 | −2.343487 |
| 21 | 1 | 0 | −2.065612 | −2.408068 | −1.308336 |
| 22 | 6 | 0 | −1.786381 | −0.995737 | 1.771109 |
| 23 | 1 | 0 | −2.770036 | −0.815719 | 2.216307 |
| 24 | 1 | 0 | −1.554638 | −2.061191 | 1.811334 |
| 25 | 1 | 0 | −1.043558 | −0.470870 | 2.381148 |

| | | | | | |
|---|---|---|---|---|---|
| 26 | 6 | 0 | −2.925787 | 1.130698 | 0.054885 |
| 27 | 1 | 0 | −3.942274 | 0.760568 | 0.226980 |
| 28 | 1 | 0 | −2.696968 | 1.837509 | 0.859480 |
| 29 | 1 | 0 | −2.934376 | 1.683181 | −0.890271 |

[a] Atomic Units = Hartrees

**M06-2X/6-31G(d)**

Sum of electronic and thermal Enthalpies = −792.948388 A.U.[a]

Imaginary frequency: −135.0053 $cm^{-1}$

| Center Number | Atomic Number | Atomic Type | Coordinates (Angstroms) X | Y | Z |
|---|---|---|---|---|---|
| 1 | 6 | 0 | 3.143331 | 0.045112 | 0.063824 |
| 2 | 6 | 0 | 3.027622 | −1.354911 | 0.091781 |
| 3 | 6 | 0 | 1.787726 | −2.011082 | −0.013052 |
| 4 | 6 | 0 | 0.566721 | −1.312316 | −0.175073 |
| 5 | 6 | 0 | 0.836505 | 0.020670 | −0.238374 |
| 6 | 6 | 0 | 1.973524 | 0.782856 | −0.099386 |
| 7 | 1 | 0 | 4.109818 | 0.525880 | 0.184401 |
| 8 | 1 | 0 | 3.930078 | −1.946543 | 0.227226 |
| 9 | 1 | 0 | 1.798847 | −3.099499 | 0.060036 |
| 10 | 6 | 0 | 1.582436 | 2.245453 | −0.134343 |
| 11 | 1 | 0 | 2.073039 | 2.851017 | 0.631013 |
| 12 | 1 | 0 | 1.792924 | 2.691637 | −1.111867 |
| 13 | 6 | 0 | 0.059666 | 2.184237 | 0.121966 |
| 14 | 1 | 0 | −0.176216 | 2.220931 | 1.188310 |
| 15 | 1 | 0 | −0.528521 | 2.911253 | −0.433946 |
| 16 | 8 | 0 | −0.316939 | 0.845044 | −0.363894 |
| 17 | 14 | 0 | −1.732839 | −0.347162 | 0.025033 |
| 18 | 6 | 0 | −2.304403 | −1.384588 | −1.424507 |
| 19 | 1 | 0 | −3.383988 | −1.272854 | −1.579332 |
| 20 | 1 | 0 | −1.799920 | −1.050500 | −2.338430 |
| 21 | 1 | 0 | −2.062249 | −2.440521 | −1.279965 |
| 22 | 6 | 0 | −1.732232 | −1.001237 | 1.780517 |
| 23 | 1 | 0 | −2.704009 | −0.819268 | 2.254712 |
| 24 | 1 | 0 | −1.502097 | −2.068900 | 1.818268 |
| 25 | 1 | 0 | −0.970765 | −0.477264 | 2.371049 |
| 26 | 6 | 0 | −2.956126 | 1.101069 | 0.075921 |
| 27 | 1 | 0 | −3.965877 | 0.711498 | 0.258000 |
| 28 | 1 | 0 | −2.735650 | 1.811136 | 0.882622 |
| 29 | 1 | 0 | −2.988772 | 1.660330 | −0.867048 |

[a] Atomic Units = Hartrees

**M06-2X/ccpVTZ**

Sum of electronic and thermal Enthalpies = −793.176756 A.U.[a]
Imaginary frequency: −165.4977 $cm^{-1}$

| Center Number | Atomic Number | Atomic Type | Coordinates (Angstroms) X | Y | Z |
|---|---|---|---|---|---|
| 1 | 6 | 0 | 3.123004 | −0.035403 | 0.060352 |
| 2 | 6 | 0 | 2.951600 | −1.425893 | 0.085402 |
| 3 | 6 | 0 | 1.691335 | −2.033021 | −0.013703 |
| 4 | 6 | 0 | 0.508672 | −1.278758 | −0.169100 |
| 5 | 6 | 0 | 0.824677 | 0.038515 | −0.231366 |
| 6 | 6 | 0 | 1.988395 | 0.749096 | −0.095388 |
| 7 | 1 | 0 | 4.106425 | 0.400710 | 0.177757 |
| 8 | 1 | 0 | 3.827114 | −2.050955 | 0.214683 |
| 9 | 1 | 0 | 1.656181 | −3.116144 | 0.057713 |
| 10 | 6 | 0 | 1.650005 | 2.222201 | −0.126126 |
| 11 | 1 | 0 | 2.159209 | 2.804008 | 0.638967 |
| 12 | 1 | 0 | 1.879379 | 2.657945 | −1.099243 |
| 13 | 6 | 0 | 0.127437 | 2.214828 | 0.124798 |
| 14 | 1 | 0 | −0.108052 | 2.269419 | 1.186426 |
| 15 | 1 | 0 | −0.428646 | 2.957850 | −0.435323 |
| 16 | 8 | 0 | −0.297070 | 0.887052 | −0.348419 |
| 17 | 14 | 0 | −1.708011 | −0.337574 | 0.021596 |
| 18 | 6 | 0 | −2.309403 | −1.350851 | −1.428318 |
| 19 | 1 | 0 | −3.382636 | −1.218153 | −1.581444 |
| 20 | 1 | 0 | −1.797929 | −1.020742 | −2.335417 |
| 21 | 1 | 0 | −2.085142 | −2.407691 | −1.288576 |
| 22 | 6 | 0 | −1.758078 | −0.987675 | 1.773680 |
| 23 | 1 | 0 | −2.734257 | −0.797826 | 2.225747 |
| 24 | 1 | 0 | −1.537038 | −2.053402 | 1.814991 |
| 25 | 1 | 0 | −1.006050 | −0.468868 | 2.374014 |
| 26 | 6 | 0 | −2.916165 | 1.124083 | 0.067964 |
| 27 | 1 | 0 | −3.924827 | 0.744558 | 0.252092 |
| 28 | 1 | 0 | −2.683547 | 1.830862 | 0.868821 |
| 29 | 1 | 0 | −2.940326 | 1.675320 | −0.875378 |

[a] Atomic Units = Hartrees

**Computed energy and geometry of 540**

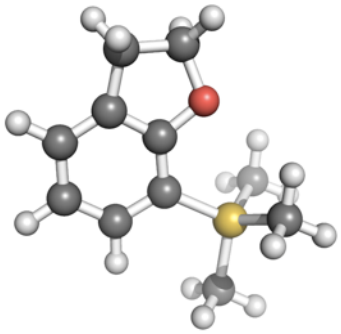

**M06-2X/6-311G(d,p)**

Sum of electronic and thermal Enthalpies = −793.206783 A.U.[a]

| Center Number | Atomic Number | Atomic Type | Coordinates (Angstroms) X | Y | Z |
|---|---|---|---|---|---|
| 1 | 6 | 0 | 2.418791 | 1.688131 | −0.005979 |
| 2 | 6 | 0 | 1.302196 | 2.529640 | −0.047917 |
| 3 | 6 | 0 | 0.015965 | 1.994439 | −0.042624 |
| 4 | 6 | 0 | −0.221993 | 0.608657 | −0.005282 |
| 5 | 6 | 0 | 0.920772 | −0.185719 | 0.026644 |
| 6 | 6 | 0 | 2.220168 | 0.318692 | 0.027953 |
| 7 | 1 | 0 | 3.421544 | 2.101649 | 0.000053 |
| 8 | 1 | 0 | 1.438501 | 3.604190 | −0.081871 |
| 9 | 1 | 0 | −0.830858 | 2.673645 | −0.073104 |
| 10 | 6 | 0 | 3.170885 | −0.847850 | 0.139803 |
| 11 | 1 | 0 | 4.012415 | −0.793207 | −0.550573 |
| 12 | 1 | 0 | 3.562581 | −0.924774 | 1.157924 |
| 13 | 6 | 0 | 2.232758 | −2.018036 | −0.194508 |
| 14 | 1 | 0 | 2.289270 | −2.275635 | −1.255373 |
| 15 | 1 | 0 | 2.398527 | −2.908258 | 0.408108 |
| 16 | 8 | 0 | 0.888145 | −1.548446 | 0.072325 |
| 17 | 14 | 0 | −1.945459 | −0.159212 | 0.006667 |
| 18 | 6 | 0 | −3.207499 | 1.226735 | −0.038864 |
| 19 | 1 | 0 | −4.219795 | 0.813192 | 0.003516 |
| 20 | 1 | 0 | −3.091736 | 1.908294 | 0.808742 |
| 21 | 1 | 0 | −3.126967 | 1.812077 | −0.959476 |
| 22 | 6 | 0 | −2.140626 | −1.265475 | −1.496406 |
| 23 | 1 | 0 | −3.124346 | −1.744451 | −1.503984 |
| 24 | 1 | 0 | −2.035671 | −0.694563 | −2.423441 |
| 25 | 1 | 0 | −1.379447 | −2.050127 | −1.492492 |

| | | | | | |
|---|---|---|---|---|---|
| 26 | 6 | 0 | −2.147718 | −1.173865 | 1.571303 |
| 27 | 1 | 0 | −3.135194 | −1.643809 | 1.608220 |
| 28 | 1 | 0 | −1.392866 | −1.963548 | 1.614096 |
| 29 | 1 | 0 | −2.036885 | −0.550253 | 2.462974 |

[a] Atomic Units = Hartrees

**M06-2X/6-31G(d)**

Sum of electronic and thermal Enthalpies = −793.041642 A.U.[a]

| Center Number | Atomic Number | Atomic Type | Coordinates (Angstroms) X | Y | Z |
|---|---|---|---|---|---|
| 1 | 6 | 0 | 2.421984 | −1.691189 | 0.005097 |
| 2 | 6 | 0 | 1.303557 | −2.532635 | 0.045658 |
| 3 | 6 | 0 | 0.016530 | −1.994894 | 0.041413 |
| 4 | 6 | 0 | −0.221910 | −0.607917 | 0.006617 |
| 5 | 6 | 0 | 0.924114 | 0.185127 | −0.023706 |
| 6 | 6 | 0 | 2.224930 | −0.319557 | −0.027009 |
| 7 | 1 | 0 | 3.426193 | −2.106535 | −0.001293 |
| 8 | 1 | 0 | 1.439377 | −3.609296 | 0.077790 |
| 9 | 1 | 0 | −0.832508 | −2.674801 | 0.070511 |
| 10 | 6 | 0 | 3.177053 | 0.847283 | −0.130916 |
| 11 | 1 | 0 | 4.009138 | 0.797791 | 0.575192 |
| 12 | 1 | 0 | 3.592843 | 0.920280 | −1.142059 |
| 13 | 6 | 0 | 2.234537 | 2.023283 | 0.180720 |
| 14 | 1 | 0 | 2.298227 | 2.313175 | 1.234969 |
| 15 | 1 | 0 | 2.396503 | 2.900708 | −0.445927 |
| 16 | 8 | 0 | 0.890051 | 1.549356 | −0.065697 |
| 17 | 14 | 0 | −1.944722 | 0.158541 | −0.006221 |
| 18 | 6 | 0 | −3.211250 | −1.229547 | 0.040727 |
| 19 | 1 | 0 | −4.225704 | −0.816357 | −0.004920 |
| 20 | 1 | 0 | −3.096346 | −1.916136 | −0.805504 |
| 21 | 1 | 0 | −3.135059 | −1.815008 | 0.963981 |
| 22 | 6 | 0 | −2.148179 | 1.269087 | 1.498097 |
| 23 | 1 | 0 | −3.129521 | 1.757441 | 1.495488 |
| 24 | 1 | 0 | −2.059355 | 0.698652 | 2.429436 |
| 25 | 1 | 0 | −1.380467 | 2.049997 | 1.504998 |
| 26 | 6 | 0 | −2.155081 | 1.172458 | −1.575643 |
| 27 | 1 | 0 | −3.142664 | 1.647231 | −1.607094 |
| 28 | 1 | 0 | −1.397863 | 1.961903 | −1.629188 |
| 29 | 1 | 0 | −2.054792 | 0.547534 | −2.470037 |

[a] Atomic Units = Hartrees

**M06-2X/ccpVTZ**

Sum of electronic and thermal Enthalpies = −793.266761 A.U.[a]

| Center Number | Atomic Number | Atomic Type | Coordinates (Angstroms) X | Y | Z |
|---|---|---|---|---|---|
| 1 | 6 | 0 | 2.410186 | 1.689837 | −0.006165 |
| 2 | 6 | 0 | 1.291849 | 2.524025 | −0.046229 |
| 3 | 6 | 0 | 0.011740 | 1.982915 | −0.041398 |
| 4 | 6 | 0 | −0.220133 | 0.599152 | −0.005710 |
| 5 | 6 | 0 | 0.924634 | −0.186845 | 0.024455 |
| 6 | 6 | 0 | 2.219145 | 0.322644 | 0.028367 |
| 7 | 1 | 0 | 3.408888 | 2.108306 | −0.000120 |
| 8 | 1 | 0 | 1.422169 | 3.597432 | −0.079257 |
| 9 | 1 | 0 | −0.836705 | 2.656946 | −0.070388 |
| 10 | 6 | 0 | 3.176680 | −0.835228 | 0.133398 |
| 11 | 1 | 0 | 4.010013 | −0.775970 | −0.563230 |
| 12 | 1 | 0 | 3.580744 | −0.906545 | 1.144872 |
| 13 | 6 | 0 | 2.247138 | −2.012796 | −0.186386 |
| 14 | 1 | 0 | 2.308168 | −2.286826 | −1.240947 |
| 15 | 1 | 0 | 2.418970 | −2.892050 | 0.427479 |
| 16 | 8 | 0 | 0.900705 | −1.549459 | 0.070593 |
| 17 | 14 | 0 | −1.945110 | −0.162531 | 0.006263 |
| 18 | 6 | 0 | −3.197718 | 1.229799 | −0.037703 |
| 19 | 1 | 0 | −4.210230 | 0.821955 | 0.000728 |
| 20 | 1 | 0 | −3.078606 | 1.905574 | 0.811318 |
| 21 | 1 | 0 | −3.109990 | 1.815975 | −0.954586 |
| 22 | 6 | 0 | −2.153069 | −1.263798 | −1.496887 |
| 23 | 1 | 0 | −3.141074 | −1.729226 | −1.500517 |
| 24 | 1 | 0 | −2.046264 | −0.691638 | −2.420488 |
| 25 | 1 | 0 | −1.403077 | −2.056205 | −1.498734 |
| 26 | 6 | 0 | −2.158441 | −1.173886 | 1.569806 |
| 27 | 1 | 0 | −3.150880 | −1.628649 | 1.603920 |
| 28 | 1 | 0 | −1.416194 | −1.972317 | 1.615810 |
| 29 | 1 | 0 | −2.042099 | −0.550580 | 2.458435 |

[a] Atomic Units = Hartrees

**Computed energy and geometry of 541**

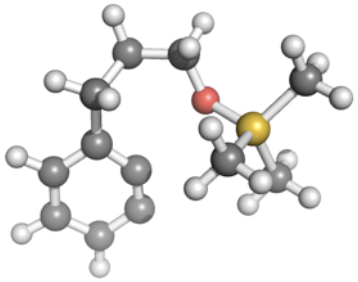

**M06-2X/6-311G(d,p)**

Sum of electronic and thermal Enthalpies = −832.391922 A.U.[a]

| Center Number | Atomic Number | Atomic Type | Coordinates (Angstroms) X | Y | Z |
|---|---|---|---|---|---|
| 1 | 6 | 0 | −3.118714 | 0.509202 | 0.617470 |
| 2 | 6 | 0 | −3.841835 | −0.663371 | 0.341866 |
| 3 | 6 | 0 | −3.304097 | −1.724101 | −0.403053 |
| 4 | 6 | 0 | −1.994770 | −1.461835 | −0.810152 |
| 5 | 6 | 0 | −1.422667 | −0.396427 | −0.524005 |
| 6 | 6 | 0 | −1.791535 | 0.727315 | 0.182781 |
| 7 | 1 | 0 | −3.596211 | 1.300184 | 1.188890 |
| 8 | 1 | 0 | −4.857238 | −0.746767 | 0.715806 |
| 9 | 1 | 0 | −3.869886 | −2.622720 | −0.614748 |
| 10 | 6 | 0 | −1.012148 | 1.977118 | 0.475859 |
| 11 | 1 | 0 | −1.728264 | 2.752826 | 0.754565 |
| 12 | 1 | 0 | −0.383948 | 1.801370 | 1.358044 |
| 13 | 6 | 0 | −0.126172 | 2.462755 | −0.681037 |
| 14 | 1 | 0 | −0.614874 | 2.262021 | −1.639257 |
| 15 | 1 | 0 | 0.001355 | 3.546073 | −0.603341 |
| 16 | 6 | 0 | 1.259085 | 1.841226 | −0.674521 |
| 17 | 1 | 0 | 1.858429 | 2.249187 | −1.495128 |
| 18 | 1 | 0 | 1.760598 | 2.107994 | 0.266040 |
| 19 | 8 | 0 | 1.177593 | 0.428361 | −0.821180 |
| 20 | 14 | 0 | 2.072620 | −0.609592 | 0.145373 |
| 21 | 6 | 0 | 1.440474 | −0.522824 | 1.904529 |
| 22 | 1 | 0 | 1.993397 | −1.220786 | 2.541489 |
| 23 | 1 | 0 | 1.562192 | 0.477978 | 2.329812 |
| 24 | 1 | 0 | 0.380539 | −0.789945 | 1.955782 |
| 25 | 6 | 0 | 1.850381 | −2.316008 | −0.569671 |
| 26 | 1 | 0 | 2.466231 | −3.036267 | −0.022212 |

| | | | | | |
|---|---|---|---|---|---|
| 27 | 1 | 0 | 0.811288 | −2.648664 | −0.510018 |
| 28 | 1 | 0 | 2.157444 | −2.342564 | −1.618947 |
| 29 | 6 | 0 | 3.872319 | −0.098662 | 0.088594 |
| 30 | 1 | 0 | 4.481695 | −0.768782 | 0.703058 |
| 31 | 1 | 0 | 4.259757 | −0.137779 | −0.933824 |
| 32 | 1 | 0 | 4.018149 | 0.917705 | 0.466246 |

[a] Atomic Units = Hartrees

**M06-2X/6-31G(d)**

Sum of electronic and thermal Enthalpies = −832.210755 A.U.[a]

| Center Number | Atomic Number | Atomic Type | Coordinates (Angstroms) X | Y | Z |
|---|---|---|---|---|---|
| 1 | 6 | 0 | −3.256917 | 0.521997 | 0.408351 |
| 2 | 6 | 0 | −3.921372 | −0.692971 | 0.160962 |
| 3 | 6 | 0 | −3.257023 | −1.831890 | −0.324015 |
| 4 | 6 | 0 | −1.893584 | −1.600950 | −0.523566 |
| 5 | 6 | 0 | −1.382743 | −0.489087 | −0.274158 |
| 6 | 6 | 0 | −1.870560 | 0.710547 | 0.198656 |
| 7 | 1 | 0 | −3.830423 | 1.369420 | 0.778868 |
| 8 | 1 | 0 | −4.990765 | −0.746445 | 0.349089 |
| 9 | 1 | 0 | −3.779643 | −2.764159 | −0.513308 |
| 10 | 6 | 0 | −1.153325 | 2.002570 | 0.473467 |
| 11 | 1 | 0 | −1.913511 | 2.767250 | 0.660017 |
| 12 | 1 | 0 | −0.578171 | 1.902155 | 1.404917 |
| 13 | 6 | 0 | −0.207714 | 2.468401 | −0.645183 |
| 14 | 1 | 0 | −0.648196 | 2.256602 | −1.626330 |
| 15 | 1 | 0 | −0.084804 | 3.554959 | −0.573642 |
| 16 | 6 | 0 | 1.177350 | 1.850030 | −0.563828 |
| 17 | 1 | 0 | 1.829354 | 2.280107 | −1.335433 |
| 18 | 1 | 0 | 1.617195 | 2.099800 | 0.414105 |
| 19 | 8 | 0 | 1.107593 | 0.442132 | −0.745138 |
| 20 | 14 | 0 | 2.137001 | −0.571415 | 0.112807 |
| 21 | 6 | 0 | 1.636752 | −0.579534 | 1.920295 |
| 22 | 1 | 0 | 2.284400 | −1.249527 | 2.498495 |
| 23 | 1 | 0 | 1.716721 | 0.418069 | 2.367754 |
| 24 | 1 | 0 | 0.603729 | −0.924906 | 2.042654 |
| 25 | 6 | 0 | 1.961601 | −2.266786 | −0.652389 |
| 26 | 1 | 0 | 2.643317 | −2.976981 | −0.170079 |
| 27 | 1 | 0 | 0.943076 | −2.654876 | −0.550557 |
| 28 | 1 | 0 | 2.207432 | −2.240800 | −1.719803 |

| | | | | | |
|---|---|---|---|---|---|
| 29 | 6 | 0 | 3.898092 | 0.049078 | −0.066936 |
| 30 | 1 | 0 | 4.596599 | −0.611570 | 0.459975 |
| 31 | 1 | 0 | 4.198293 | 0.078644 | −1.120720 |
| 32 | 1 | 0 | 4.023289 | 1.056601 | 0.345858 |

[a] Atomic Units = Hartrees

**M06-2X/ccpVTZ**

Sum of electronic and thermal Enthalpies = −832.458474 A.U.[a]

| Center Number | Atomic Number | Atomic Type | Coordinates (Angstroms) X | Y | Z |
|---|---|---|---|---|---|
| 1 | 6 | 0 | −3.236930 | 0.548248 | 0.492097 |
| 2 | 6 | 0 | −3.964928 | −0.620679 | 0.229321 |
| 3 | 6 | 0 | −3.385833 | −1.755314 | −0.351986 |
| 4 | 6 | 0 | −2.032982 | −1.560505 | −0.619575 |
| 5 | 6 | 0 | −1.457835 | −0.495331 | −0.353984 |
| 6 | 6 | 0 | −1.863476 | 0.694044 | 0.204665 |
| 7 | 1 | 0 | −3.746961 | 1.395297 | 0.937527 |
| 8 | 1 | 0 | −5.018123 | −0.642219 | 0.482476 |
| 9 | 1 | 0 | −3.954460 | −2.651497 | −0.555346 |
| 10 | 6 | 0 | −1.081333 | 1.939849 | 0.487996 |
| 11 | 1 | 0 | −1.793951 | 2.718458 | 0.757581 |
| 12 | 1 | 0 | −0.454554 | 1.769922 | 1.369704 |
| 13 | 6 | 0 | −0.191561 | 2.415613 | −0.668518 |
| 14 | 1 | 0 | −0.666274 | 2.191149 | −1.625979 |
| 15 | 1 | 0 | −0.081674 | 3.499828 | −0.609471 |
| 16 | 6 | 0 | 1.201099 | 1.819464 | −0.636903 |
| 17 | 1 | 0 | 1.804022 | 2.229933 | −1.451624 |
| 18 | 1 | 0 | 1.683981 | 2.107005 | 0.305219 |
| 19 | 8 | 0 | 1.149331 | 0.406504 | −0.762928 |
| 20 | 14 | 0 | 2.166729 | −0.576808 | 0.123340 |
| 21 | 6 | 0 | 1.670986 | −0.515440 | 1.925420 |
| 22 | 1 | 0 | 2.322671 | −1.154583 | 2.526053 |
| 23 | 1 | 0 | 1.744906 | 0.497976 | 2.326118 |
| 24 | 1 | 0 | 0.644466 | −0.863459 | 2.060951 |
| 25 | 6 | 0 | 1.967901 | −2.291757 | −0.575495 |
| 26 | 1 | 0 | 2.650437 | −2.985728 | −0.080140 |
| 27 | 1 | 0 | 0.951241 | −2.663217 | −0.438259 |
| 28 | 1 | 0 | 2.193133 | −2.303525 | −1.643684 |
| 29 | 6 | 0 | 3.925572 | 0.026836 | −0.073803 |
| 30 | 1 | 0 | 4.617320 | −0.623607 | 0.466090 |

| | | | | | |
|---|---|---|---|---|---|
| 31 | 1 | 0 | 4.221778 | 0.033106 | −1.124912 |
| 32 | 1 | 0 | 4.049114 | 1.038270 | 0.318946 |

[a] Atomic Units = Hartrees

**Computed energy and geometry of 542[‡]**

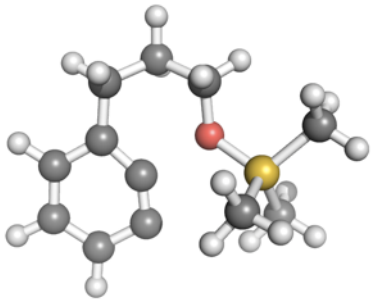

**M06-2X/6-311G(d,p)**

Sum of electronic and thermal Enthalpies = −832.388976 A.U.[a]
Imaginary frequency: −154.6740 $cm^{-1}$

| Center Number | Atomic Number | Atomic Type | Coordinates (Angstroms) X | Y | Z |
|---|---|---|---|---|---|
| 1 | 6 | 0 | −3.287091 | 0.116342 | 0.224369 |
| 2 | 6 | 0 | −3.514331 | −1.257049 | 0.073288 |
| 3 | 6 | 0 | −2.466463 | −2.140184 | −0.203536 |
| 4 | 6 | 0 | −1.160276 | −1.614142 | −0.331691 |
| 5 | 6 | 0 | −1.124694 | −0.348295 | −0.160513 |
| 6 | 6 | 0 | −1.999404 | 0.672530 | 0.112034 |
| 7 | 1 | 0 | −4.115008 | 0.787722 | 0.431496 |
| 8 | 1 | 0 | −4.526842 | −1.635525 | 0.169618 |
| 9 | 1 | 0 | −2.676586 | −3.200064 | −0.317065 |
| 10 | 6 | 0 | −1.706848 | 2.137756 | 0.280585 |
| 11 | 1 | 0 | −2.599754 | 2.701699 | 0.002673 |
| 12 | 1 | 0 | −1.519404 | 2.342131 | 1.340959 |
| 13 | 6 | 0 | −0.503748 | 2.600060 | −0.535560 |
| 14 | 1 | 0 | −0.662509 | 2.392429 | −1.597972 |
| 15 | 1 | 0 | −0.383720 | 3.680367 | −0.422928 |
| 16 | 6 | 0 | 0.786786 | 1.946406 | −0.086199 |
| 17 | 1 | 0 | 1.633920 | 2.367059 | −0.633564 |
| 18 | 1 | 0 | 0.943589 | 2.119078 | 0.985321 |
| 19 | 8 | 0 | 0.729713 | 0.531930 | −0.340965 |
| 20 | 14 | 0 | 2.055428 | −0.477675 | 0.066208 |

| | | | | | |
|---|---|---|---|---|---|
| 21 | 6 | 0 | 1.744723 | −1.207424 | 1.754462 |
| 22 | 1 | 0 | 2.646295 | −1.710529 | 2.117714 |
| 23 | 1 | 0 | 1.490290 | −0.421102 | 2.471998 |
| 24 | 1 | 0 | 0.930753 | −1.935004 | 1.740571 |
| 25 | 6 | 0 | 2.251909 | −1.757986 | −1.271937 |
| 26 | 1 | 0 | 3.206838 | −2.277407 | −1.140595 |
| 27 | 1 | 0 | 1.453247 | −2.500658 | −1.258906 |
| 28 | 1 | 0 | 2.265253 | −1.282482 | −2.256857 |
| 29 | 6 | 0 | 3.575764 | 0.609428 | 0.111582 |
| 30 | 1 | 0 | 4.443509 | −0.015415 | 0.347029 |
| 31 | 1 | 0 | 3.764843 | 1.085385 | −0.854721 |
| 32 | 1 | 0 | 3.513628 | 1.389672 | 0.874749 |

[a] Atomic Units = Hartrees

**M06-2X/6-31G(d)**

Sum of electronic and thermal Enthalpies = −832.207909 A.U.[a]
Imaginary frequency: −160.9336 $cm^{-1}$

| Center Number | Atomic Number | Atomic Type | Coordinates (Angstroms) X | Y | Z |
|---|---|---|---|---|---|
| 1 | 6 | 0 | −3.280752 | 0.103723 | 0.213072 |
| 2 | 6 | 0 | −3.494158 | −1.274635 | 0.079042 |
| 3 | 6 | 0 | −2.434106 | −2.150556 | −0.186231 |
| 4 | 6 | 0 | −1.132643 | −1.617253 | −0.323711 |
| 5 | 6 | 0 | −1.110785 | −0.343204 | −0.166964 |
| 6 | 6 | 0 | −1.997516 | 0.673006 | 0.093757 |
| 7 | 1 | 0 | −4.117299 | 0.769697 | 0.413528 |
| 8 | 1 | 0 | −4.504645 | −1.662737 | 0.179918 |
| 9 | 1 | 0 | −2.636664 | −3.216323 | −0.284779 |
| 10 | 6 | 0 | −1.725143 | 2.144713 | 0.252555 |
| 11 | 1 | 0 | −2.613633 | 2.699429 | −0.065388 |
| 12 | 1 | 0 | −1.580987 | 2.367969 | 1.318196 |
| 13 | 6 | 0 | −0.496949 | 2.613692 | −0.521756 |
| 14 | 1 | 0 | −0.626409 | 2.428906 | −1.594388 |
| 15 | 1 | 0 | −0.373548 | 3.692863 | −0.384604 |
| 16 | 6 | 0 | 0.777540 | 1.937618 | −0.054073 |
| 17 | 1 | 0 | 1.646796 | 2.383636 | −0.548159 |
| 18 | 1 | 0 | 0.895279 | 2.059231 | 1.031685 |
| 19 | 8 | 0 | 0.729760 | 0.540234 | −0.382957 |
| 20 | 14 | 0 | 2.044437 | −0.474512 | 0.062200 |
| 21 | 6 | 0 | 1.702424 | −1.194474 | 1.753779 |

| | | | | | |
|---|---|---|---|---|---|
| 22 | 1 | 0 | 2.601767 | −1.683552 | 2.146161 |
| 23 | 1 | 0 | 1.420593 | −0.403722 | 2.459223 |
| 24 | 1 | 0 | 0.894687 | −1.931148 | 1.728936 |
| 25 | 6 | 0 | 2.260232 | −1.759022 | −1.274520 |
| 26 | 1 | 0 | 3.154534 | −2.360002 | −1.070263 |
| 27 | 1 | 0 | 1.400446 | −2.430316 | −1.340211 |
| 28 | 1 | 0 | 2.396973 | −1.279122 | −2.250162 |
| 29 | 6 | 0 | 3.574297 | 0.606123 | 0.134997 |
| 30 | 1 | 0 | 4.440337 | −0.027242 | 0.363127 |
| 31 | 1 | 0 | 3.772204 | 1.100539 | −0.822520 |
| 32 | 1 | 0 | 3.514736 | 1.374798 | 0.912879 |

[a] Atomic Units = Hartrees

**M06-2X/ccpVTZ**

Sum of electronic and thermal Enthalpies = −832.453974 A.U.[a]
Imaginary frequency: −167.2388 $cm^{-1}$

| Center Number | Atomic Number | Atomic Type | Coordinates (Angstroms) X | Y | Z |
|---|---|---|---|---|---|
| 1 | 6 | 0 | −3.272975 | 0.113668 | 0.231595 |
| 2 | 6 | 0 | −3.499737 | −1.255594 | 0.078605 |
| 3 | 6 | 0 | −2.455309 | −2.134272 | −0.208515 |
| 4 | 6 | 0 | −1.151849 | −1.610463 | −0.344274 |
| 5 | 6 | 0 | −1.116161 | −0.345752 | −0.168991 |
| 6 | 6 | 0 | −1.989467 | 0.669955 | 0.111563 |
| 7 | 1 | 0 | −4.098113 | 0.783338 | 0.445034 |
| 8 | 1 | 0 | −4.509484 | −1.634615 | 0.180594 |
| 9 | 1 | 0 | −2.665584 | −3.191740 | −0.324938 |
| 10 | 6 | 0 | −1.702696 | 2.133195 | 0.276618 |
| 11 | 1 | 0 | −2.595743 | 2.692781 | −0.001078 |
| 12 | 1 | 0 | −1.516293 | 2.340994 | 1.334425 |
| 13 | 6 | 0 | −0.502816 | 2.594311 | −0.537602 |
| 14 | 1 | 0 | −0.665194 | 2.396818 | −1.599327 |
| 15 | 1 | 0 | −0.374636 | 3.670556 | −0.417513 |
| 16 | 6 | 0 | 0.781189 | 1.929388 | −0.096832 |
| 17 | 1 | 0 | 1.628980 | 2.350204 | −0.638321 |
| 18 | 1 | 0 | 0.939726 | 2.091832 | 0.974095 |
| 19 | 8 | 0 | 0.722015 | 0.518666 | −0.363226 |
| 20 | 14 | 0 | 2.044755 | −0.473645 | 0.069216 |
| 21 | 6 | 0 | 1.737265 | −1.153954 | 1.776839 |
| 22 | 1 | 0 | 2.638252 | −1.643104 | 2.153918 |
| 23 | 1 | 0 | 1.480230 | −0.348669 | 2.468911 |

| | | | | | |
|---|---|---|---|---|---|
| 24 | 1 | 0 | 0.926608 | −1.882425 | 1.781584 |
| 25 | 6 | 0 | 2.246499 | −1.793502 | −1.227893 |
| 26 | 1 | 0 | 3.225073 | −2.265920 | −1.111283 |
| 27 | 1 | 0 | 1.482588 | −2.565881 | −1.158058 |
| 28 | 1 | 0 | 2.203640 | −1.357694 | −2.228061 |
| 29 | 6 | 0 | 3.562955 | 0.614901 | 0.079907 |
| 30 | 1 | 0 | 4.431271 | −0.005672 | 0.314690 |
| 31 | 1 | 0 | 3.737995 | 1.074878 | −0.894454 |
| 32 | 1 | 0 | 3.506611 | 1.404729 | 0.830442 |

[a] Atomic Units = Hartrees

**Computed energy and geometry of 543**

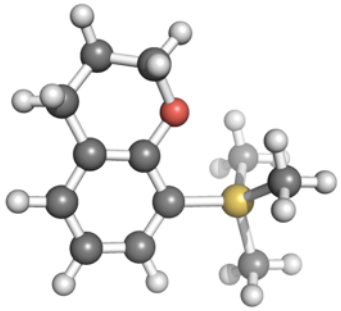

**M06-2X/6-311G(d,p)**

Sum of electronic and thermal Enthalpies = −832.488052 A.U.[a]

| Center Number | Atomic Number | Atomic Type | Coordinates (Angstroms) X | Y | Z |
|---|---|---|---|---|---|
| 1 | 6 | 0 | 1.923479 | 2.128566 | 0.039610 |
| 2 | 6 | 0 | 0.718544 | 2.817778 | 0.024949 |
| 3 | 6 | 0 | −0.477693 | 2.101184 | 0.000102 |
| 4 | 6 | 0 | −0.489160 | 0.704618 | 0.001631 |
| 5 | 6 | 0 | 0.749460 | 0.041054 | 0.029747 |
| 6 | 6 | 0 | 1.966877 | 0.732995 | 0.040302 |
| 7 | 1 | 0 | 2.862506 | 2.674303 | 0.042600 |
| 8 | 1 | 0 | 0.708997 | 3.901553 | 0.024561 |
| 9 | 1 | 0 | −1.418040 | 2.643618 | −0.019386 |
| 10 | 6 | 0 | 3.284671 | −0.009791 | 0.027677 |
| 11 | 1 | 0 | 3.984664 | 0.505225 | −0.634174 |
| 12 | 1 | 0 | 3.722997 | 0.007594 | 1.031255 |
| 13 | 6 | 0 | 3.077008 | −1.457162 | −0.409174 |
| 14 | 1 | 0 | 2.869836 | −1.508072 | −1.482186 |

| | | | | | |
|---|---|---|---|---|---|
| 15 | 1 | 0 | 3.963712 | −2.060501 | −0.206421 |
| 16 | 6 | 0 | 1.892211 | −2.027091 | 0.345894 |
| 17 | 1 | 0 | 1.697315 | −3.066351 | 0.085298 |
| 18 | 1 | 0 | 2.059085 | −1.958742 | 1.427498 |
| 19 | 8 | 0 | 0.688693 | −1.323834 | 0.021946 |
| 20 | 14 | 0 | −2.098090 | −0.287974 | −0.020195 |
| 21 | 6 | 0 | −2.237768 | −1.323604 | 1.538912 |
| 22 | 1 | 0 | −3.190546 | −1.861854 | 1.559553 |
| 23 | 1 | 0 | −1.430380 | −2.058212 | 1.587801 |
| 24 | 1 | 0 | −2.185314 | −0.698782 | 2.435214 |
| 25 | 6 | 0 | −3.528827 | 0.926907 | −0.085368 |
| 26 | 1 | 0 | −4.473505 | 0.374021 | −0.105378 |
| 27 | 1 | 0 | −3.549963 | 1.584214 | 0.788665 |
| 28 | 1 | 0 | −3.493762 | 1.552345 | −0.982026 |
| 29 | 6 | 0 | −2.165015 | −1.392792 | −1.536617 |
| 30 | 1 | 0 | −3.115850 | −1.933437 | −1.575833 |
| 31 | 1 | 0 | −2.075964 | −0.805351 | −2.455213 |
| 32 | 1 | 0 | −1.354801 | −2.125226 | −1.520662 |

[a] Atomic Units = Hartrees

**M06-2X/6-31G(d)**

Sum of electronic and thermal Enthalpies = −832.312045 A.U.[a]

| Center Number | Atomic Number | Atomic Type | Coordinates (Angstroms) X | Y | Z |
|---|---|---|---|---|---|
| 1 | 6 | 0 | −1.927298 | −2.129796 | 0.039409 |
| 2 | 6 | 0 | −0.720668 | −2.819736 | 0.024371 |
| 3 | 6 | 0 | 0.475940 | −2.101057 | −0.000436 |
| 4 | 6 | 0 | 0.488262 | −0.702764 | 0.002422 |
| 5 | 6 | 0 | −0.752558 | −0.040350 | 0.031824 |
| 6 | 6 | 0 | −1.971473 | −0.732804 | 0.041314 |
| 7 | 1 | 0 | −2.867943 | −2.676812 | 0.041680 |
| 8 | 1 | 0 | −0.710754 | −3.905491 | 0.023065 |
| 9 | 1 | 0 | 1.418576 | −2.643710 | −0.021009 |
| 10 | 6 | 0 | −3.289131 | 0.011085 | 0.028037 |
| 11 | 1 | 0 | −3.993456 | −0.503567 | −0.633732 |
| 12 | 1 | 0 | −3.731882 | −0.003581 | 1.032285 |
| 13 | 6 | 0 | −3.080059 | 1.458386 | −0.410732 |
| 14 | 1 | 0 | −2.872039 | 1.508664 | −1.485660 |
| 15 | 1 | 0 | −3.968748 | 2.063670 | −0.210290 |
| 16 | 6 | 0 | −1.894166 | 2.028421 | 0.345108 |

| | | | | | |
|---|---|---|---|---|---|
| 17 | 1 | 0 | −1.697586 | 3.069613 | 0.082960 |
| 18 | 1 | 0 | −2.064710 | 1.965213 | 1.428677 |
| 19 | 8 | 0 | −0.691518 | 1.326104 | 0.025402 |
| 20 | 14 | 0 | 2.097539 | 0.286993 | −0.020504 |
| 21 | 6 | 0 | 2.254058 | 1.313382 | 1.548357 |
| 22 | 1 | 0 | 3.198346 | 1.870709 | 1.552881 |
| 23 | 1 | 0 | 1.434071 | 2.034054 | 1.628216 |
| 24 | 1 | 0 | 2.236888 | 0.679419 | 2.442084 |
| 25 | 6 | 0 | 3.531482 | −0.930588 | −0.098582 |
| 26 | 1 | 0 | 4.479106 | −0.378902 | −0.119586 |
| 27 | 1 | 0 | 3.557950 | −1.594687 | 0.772703 |
| 28 | 1 | 0 | 3.494725 | −1.553843 | −0.999118 |
| 29 | 6 | 0 | 2.167892 | 1.402517 | −1.534660 |
| 30 | 1 | 0 | 3.118081 | 1.948760 | −1.566743 |
| 31 | 1 | 0 | 2.088218 | 0.819681 | −2.459412 |
| 32 | 1 | 0 | 1.354079 | 2.133894 | −1.523739 |

[a] Atomic Units = Hartrees

**M06-2X/ccpVTZ**

Sum of electronic and thermal Enthalpies = −832.550958 A.U.[a]

| Center Number | Atomic Number | Atomic Type | Coordinates (Angstroms) X | Y | Z |
|---|---|---|---|---|---|
| 1 | 6 | 0 | 1.916361 | 2.125432 | 0.039306 |
| 2 | 6 | 0 | 0.711822 | 2.808868 | 0.021628 |
| 3 | 6 | 0 | −0.478484 | 2.088731 | −0.003861 |
| 4 | 6 | 0 | −0.486074 | 0.695371 | −0.001117 |
| 5 | 6 | 0 | 0.752648 | 0.038317 | 0.028825 |
| 6 | 6 | 0 | 1.964953 | 0.733351 | 0.041640 |
| 7 | 1 | 0 | 2.851791 | 2.673597 | 0.043209 |
| 8 | 1 | 0 | 0.698043 | 3.890700 | 0.020012 |
| 9 | 1 | 0 | −1.418936 | 2.626853 | −0.025248 |
| 10 | 6 | 0 | 3.283066 | −0.002000 | 0.033140 |
| 11 | 1 | 0 | 3.984076 | 0.519072 | −0.619332 |
| 12 | 1 | 0 | 3.715212 | 0.012831 | 1.037240 |
| 13 | 6 | 0 | 3.086043 | −1.445531 | −0.409265 |
| 14 | 1 | 0 | 2.883552 | −1.493588 | −1.481291 |
| 15 | 1 | 0 | 3.973673 | −2.043849 | −0.207041 |
| 16 | 6 | 0 | 1.905389 | −2.023779 | 0.339045 |
| 17 | 1 | 0 | 1.717302 | −3.061396 | 0.073406 |
| 18 | 1 | 0 | 2.072462 | −1.963013 | 1.419293 |

| | | | | | |
|---|---|---|---|---|---|
| 19 | 8 | 0 | 0.700322 | −1.325550 | 0.021363 |
| 20 | 14 | 0 | −2.098624 | −0.289372 | −0.019659 |
| 21 | 6 | 0 | −2.253119 | −1.306468 | 1.548500 |
| 22 | 1 | 0 | −3.201835 | −1.848071 | 1.558980 |
| 23 | 1 | 0 | −1.444852 | −2.034900 | 1.622333 |
| 24 | 1 | 0 | −2.220506 | −0.669380 | 2.434551 |
| 25 | 6 | 0 | −3.520345 | 0.932511 | −0.098983 |
| 26 | 1 | 0 | −4.465854 | 0.385122 | −0.116066 |
| 27 | 1 | 0 | −3.537708 | 1.596315 | 0.767474 |
| 28 | 1 | 0 | −3.477627 | 1.547467 | −0.999955 |
| 29 | 6 | 0 | −2.175553 | −1.406738 | −1.524745 |
| 30 | 1 | 0 | −3.133063 | −1.931617 | −1.558118 |
| 31 | 1 | 0 | −2.079137 | −0.828546 | −2.446003 |
| 32 | 1 | 0 | −1.378669 | −2.150373 | −1.503802 |

[a] Atomic Units = Hartrees

## Supporting information for subsection 5.4.2

DFT calculations were carried out with the Gaussian 09 software package.[100] All geometries were optimized using the M06-2X functional[101] and the triple-ζ split-valence 6-311+G(d,p) basis set. The SMD continuum solvation model was used during both the geometry optimization and frequency calculation with methanol as the solvent. The "grid=ultrafine" option was used to specify the integration grid applied during the numerical integrations. Harmonic vibrational frequency calculations for thermal corrections of the enthalpies were performed at 298 K. Starting geometries for the DFT calculations of all alcohol donors were found through Monte Carlo conformational searches performed with the OPLS_2005 force field in MacroModel version 9.9.[110] Each conformer was then subjected to geometry optimization using DFT. The optimized reactant and product geometries were checked and found to have no imaginary frequencies, and each of the optimized transition state structure geometries was found to have only one imaginary frequency. The value for the "Sum of electronic and thermal Free Energies=" was used to determine the free energy (G) of each of the two reactants ($G_{Benzyne}$ and $G_{Alcohol}$) and of the transition state structure ($G_{TS}$) for each reaction. The $\Delta G^{\ddagger}$ value was determined using the following equation:

$$\Delta G^{\ddagger} = G_{TS} - (G_{Benzyne} + G_{Alcohol})$$

where G is the free energy of the lowest energy geometry of the alcohol, benzyne, and transition state structure.

[110] MacroModel, version 9.9, Schrödinger, LLC, New York, NY, 2011.

**548**

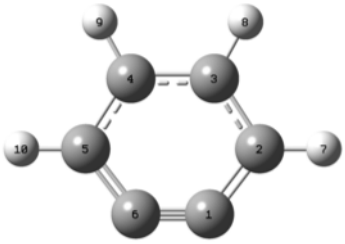

Sum of electronic and thermal Free Energies[a] = -230.825373 A.U.[b]

| Atom Type | Cartesian Coordinates (x,y,z) | | |
|---|---|---|---|
| C | 0.619852 | -1.229395 | -0.000097 |
| C | 1.46399 | -0.1319 | 0.000151 |
| C | 0.702906 | 1.050096 | -0.000035 |
| C | -0.702924 | 1.050086 | -0.000036 |
| C | -1.463992 | -0.131923 | 0.000156 |
| C | -0.619827 | -1.229392 | -0.000096 |
| H | 2.54578 | -0.133741 | 0.000058 |
| H | 1.225887 | 2.00106 | -0.000175 |
| H | -1.225922 | 2.001041 | -0.000187 |
| H | -2.545781 | -0.133784 | 0.00005 |

[a] Used for the $\Delta G^{\ddagger}_{M06\text{-}2X}$ calculation.
[b] Atomic Units = Hartrees

**549**

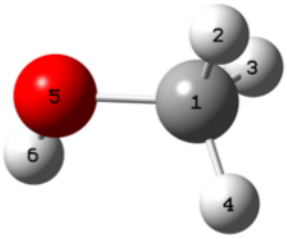

Sum of electronic and thermal Free Energies[a] = -115.684827 A.U.[b]

| Atom Type | Cartesian Coordinates (x,y,z) | | |
|---|---|---|---|
| C | 0.668899 | -0.01991 | 0.000007 |
| H | 1.093991 | 0.9835 | -0.001203 |
| H | 1.013727 | -0.551469 | -0.891174 |
| H | 1.013919 | -0.549492 | 0.892295 |

| | | | |
|---|---|---|---|
| O | -0.748958 | 0.123931 | 0.00001 |
| H | -1.143363 | -0.754526 | -0.000037 |

[a] Used for the $\Delta G^{\ddagger}_{M06\text{-}2X}$ calculation.
[b] Atomic Units = Hartrees

**550**

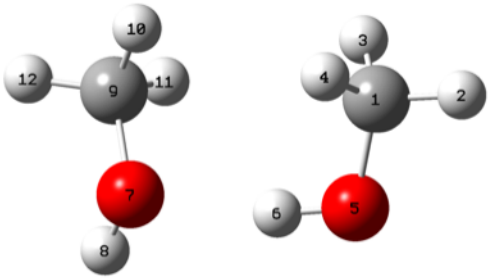


Sum of electronic and thermal Free Energies[a] = -231.361766 A.U.[b]

| Atom Type | Cartesian Coordinates (x,y,z) | | |
|---|---|---|---|
| C | 1.798512 | 0.590066 | 0.133295 |
| H | 2.883777 | 0.664265 | 0.053223 |
| H | 1.35038 | 1.336365 | -0.530643 |
| H | 1.511811 | 0.812352 | 1.165999 |
| O | 1.426132 | -0.730513 | -0.238258 |
| H | 0.472062 | -0.823927 | -0.073228 |
| O | -1.319354 | -0.645029 | 0.294518 |
| H | -1.810679 | -1.318622 | -0.189578 |
| C | -1.749204 | 0.641566 | -0.151986 |
| H | -1.240118 | 1.383557 | 0.462173 |
| H | -1.489408 | 0.802485 | -1.20173 |
| H | -2.827898 | 0.758068 | -0.024143 |

[a] Used for the $\Delta G^{\ddagger}_{M06\text{-}2X}$ calculation.
[b] Atomic Units = Hartrees

**554**

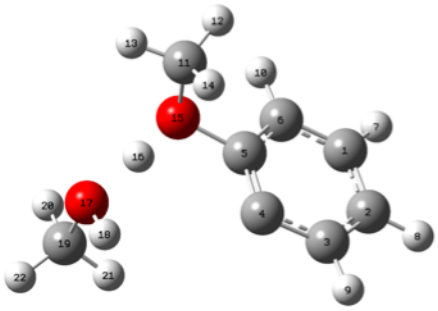

Sum of electronic and thermal Free Energies[a] = -462.190021 A.U.[b]

| Atom Type | Cartesian Coordinates (x,y,z) | | |
|---|---|---|---|
| C | 2.626184 | 0.187325 | -0.84804 |
| C | 2.84433 | -0.828607 | 0.083908 |
| C | 1.815142 | -1.234227 | 0.937519 |
| C | 0.519111 | -0.664627 | 0.939847 |
| C | 0.411076 | 0.321907 | -0.016936 |
| C | 1.370773 | 0.782718 | -0.910008 |
| H | 3.415858 | 0.506984 | -1.518561 |
| H | 3.819355 | -1.303792 | 0.140428 |
| H | 2.046439 | -2.035433 | 1.638927 |
| H | 1.146933 | 1.570642 | -1.622103 |
| C | -1.007459 | 2.199818 | 0.664366 |
| H | -0.279852 | 2.92281 | 0.301783 |
| H | -2.021575 | 2.566077 | 0.518464 |
| H | -0.825049 | 1.94707 | 1.709226 |
| O | -0.877136 | 1.003471 | -0.14491 |
| H | -1.69234 | 0.309815 | 0.065324 |
| O | -2.732088 | -0.517489 | 0.244782 |
| H | -2.604953 | -0.979545 | 1.0862 |
| C | -2.835183 | -1.478893 | -0.824068 |
| H | -2.919829 | -0.910194 | -1.74801 |
| H | -1.946156 | -2.110715 | -0.852307 |
| H | -3.72888 | -2.08406 | -0.677867 |

[a] Used for the $\Delta G^{\ddagger}_{M06\text{-}2X}$ calculation.
[b] Atomic Units = Hartrees

**555**

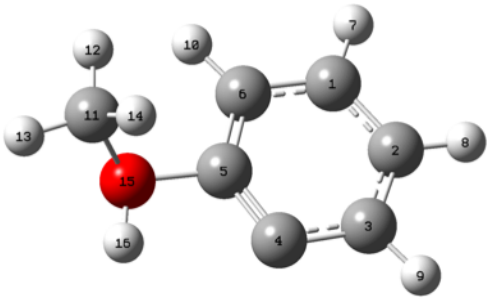


Sum of electronic and thermal Free Energies[a] = -346.503683 A.U.[b]

| Atom Type | Cartesian Coordinates (x,y,z) | | |
|---|---|---|---|
| C | 1.514088 | 1.260609 | -0.005828 |
| C | 2.289716 | 0.115475 | 0.187594 |
| C | 1.703304 | -1.151945 | 0.150058 |
| C | 0.321212 | -1.364141 | -0.066067 |
| C | -0.330165 | -0.17478 | -0.23573 |
| C | 0.148156 | 1.125407 | -0.23429 |
| H | 1.964375 | 2.246328 | 0.011629 |
| H | 3.356144 | 0.217417 | 0.364405 |
| H | 2.360096 | -2.007199 | 0.300858 |
| H | -0.490096 | 1.985143 | -0.406695 |
| C | -2.687865 | 0.220756 | 0.544209 |
| H | -2.541487 | 1.295914 | 0.565385 |
| H | -3.696665 | -0.032518 | 0.23062 |
| H | -2.422078 | -0.247273 | 1.490341 |
| O | -1.792977 | -0.29826 | -0.496175 |
| H | -1.93714 | -1.260015 | -0.62682 |

[a] Used for the $\Delta G^{\ddagger}_{M06\text{-}2X}$ calculation.
[b] Atomic Units = Hartrees

**556**

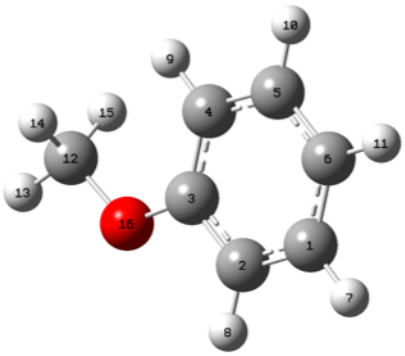


Sum of electronic and thermal Free Energies[a] = -346.619102 A.U.[b]

| Atom Type | Cartesian Coordinates (x,y,z) | | |
|---|---|---|---|
| C | 1.85251 | -0.991177 | 0.00981 |
| C | 0.501621 | -1.302718 | -0.002009 |
| C | -0.450326 | -0.278315 | -0.013414 |
| C | -0.044116 | 1.055389 | -0.014579 |
| C | 1.320211 | 1.351163 | -0.003227 |
| C | 2.272488 | 0.340355 | 0.009413 |
| H | 2.583083 | -1.792489 | 0.020853 |
| H | 0.160697 | -2.332036 | -0.000069 |
| H | -0.766175 | 1.861336 | -0.024733 |
| H | 1.630966 | 2.390094 | -0.004426 |
| H | 3.328791 | 0.58152 | 0.019433 |
| C | -2.757819 | 0.327928 | 0.024768 |
| H | -3.708371 | -0.201452 | 0.042597 |
| H | -2.6592 | 0.933781 | 0.929319 |
| H | -2.714035 | 0.968546 | -0.860079 |
| O | -1.752897 | -0.678131 | -0.023433 |

[a] Used for the $\Delta G^{\ddagger}_{M06\text{-}2X}$ calculation.
[b] Atomic Units = Hartrees

**556•MeOH**

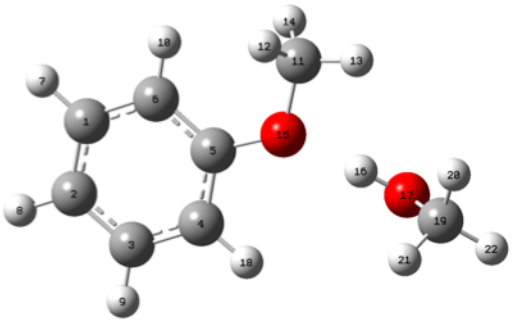

Sum of electronic and thermal Free Energies[a] = -462.294760 A.U.[b]

| Atom Type | Cartesian Coordinates (x,y,z) | | |
|---|---|---|---|
| C | -2.857576 | 0.5686 | -0.221009 |
| C | -3.064102 | -0.798272 | -0.086411 |
| C | -1.972637 | -1.633041 | 0.159766 |
| C | -0.694816 | -1.105459 | 0.269081 |
| C | -0.499103 | 0.271192 | 0.131988 |
| C | -1.578361 | 1.116791 | -0.11435 |
| H | -3.69618 | 1.228568 | -0.413038 |
| H | -4.061655 | -1.212451 | -0.171502 |
| H | -2.118479 | -2.701988 | 0.267394 |
| H | -1.441138 | 2.184521 | -0.223228 |
| C | 1.051626 | 2.096697 | 0.122265 |
| H | 0.531209 | 2.660434 | 0.900089 |
| H | 2.126795 | 2.212337 | 0.246913 |
| H | 0.755617 | 2.456836 | -0.866002 |
| O | 0.792197 | 0.701451 | 0.253412 |
| H | 2.091734 | -0.31178 | -0.688824 |
| O | 2.906982 | -0.802065 | -0.87056 |
| H | 0.163918 | -1.739804 | 0.461123 |
| C | 3.677316 | -0.78398 | 0.325347 |
| H | 3.956895 | 0.23606 | 0.606783 |
| H | 3.13655 | -1.247075 | 1.156584 |
| H | 4.587227 | -1.355927 | 0.140839 |

[a] Used for the $\Delta G^{\ddagger}_{M06\text{-}2X}$ calculation.
[b] Atomic Units = Hartrees

**553**‡

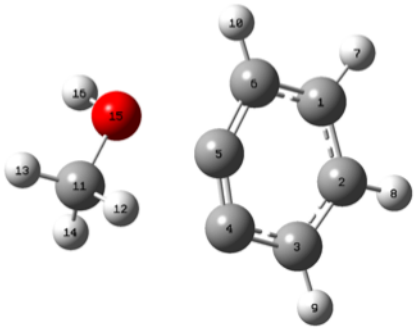


Sum of electronic and thermal Free Energies[a] = -346.492191 A.U.[b]

| Atom Type | Cartesian Coordinates (x,y,z) | | |
|---|---|---|---|
| C | 1.935835 | 1.044163 | 0.037483 |
| C | 2.431584 | -0.26912 | 0.003583 |
| C | 1.579032 | -1.378153 | -0.032931 |
| C | 0.18845 | -1.125668 | -0.037609 |
| C | -0.100868 | 0.104999 | -0.005172 |
| C | 0.555136 | 1.302339 | 0.036794 |
| H | 2.623797 | 1.882217 | 0.066701 |
| H | 3.50565 | -0.423471 | 0.007252 |
| H | 1.994474 | -2.380947 | -0.055773 |
| H | 0.125711 | 2.294538 | 0.066 |
| C | -3.003745 | -0.535339 | 0.086756 |
| H | -2.886269 | -0.912244 | 1.101954 |
| H | -4.056989 | -0.314576 | -0.098643 |
| H | -2.655556 | -1.291635 | -0.621254 |
| O | -2.226404 | 0.656201 | -0.013446 |
| H | -2.352129 | 1.037187 | -0.892103 |

[a] Used for the $\Delta G^{\ddagger}_{M06\text{-}2X}$ calculation.
[b] Atomic Units = Hartrees

**557**‡

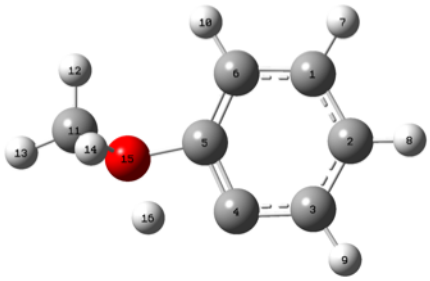

Sum of electronic and thermal Free Energies[a] = -346.497103 A.U.[b]

| Atom Type | Cartesian Coordinates (x,y,z) | | |
|---|---|---|---|
| C | 1.594634 | 1.213883 | 0.026802 |
| C | 2.274092 | 0.004062 | 0.17988 |
| C | 1.599225 | -1.223508 | 0.122383 |
| C | 0.213613 | -1.264926 | -0.08539 |
| C | -0.359251 | -0.023493 | -0.235315 |
| C | 0.213878 | 1.227693 | -0.195968 |
| H | 2.136804 | 2.151263 | 0.075881 |
| H | 3.345895 | 0.020825 | 0.350272 |
| H | 2.17567 | -2.135948 | 0.2517 |
| H | -0.343508 | 2.147868 | -0.326619 |
| C | -2.714217 | 0.194132 | 0.483907 |
| H | -2.70925 | 1.279385 | 0.414016 |
| H | -3.682041 | -0.207981 | 0.196912 |
| H | -2.420571 | -0.13995 | 1.479678 |
| O | -1.756073 | -0.312607 | -0.484735 |
| H | -1.38625 | -1.381667 | -0.341753 |

[a] Used for the $\Delta G^{\ddagger}_{M06\text{-}2X}$ calculation.
[b] Atomic Units = Hartrees

**552**‡

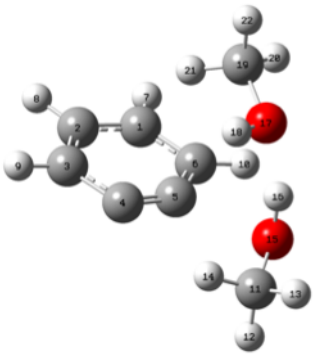

Sum of electronic and thermal Free Energies[a] = -462.172519 A.U.[b]

| Atom Type | Cartesian Coordinates (x,y,z) | | |
|---|---|---|---|
| C | -2.258428 | -0.14238 | 1.032719 |
| C | -2.772757 | -0.015517 | -0.26803 |
| C | -2.005724 | 0.498523 | -1.320954 |
| C | -0.679965 | 0.870399 | -1.01128 |
| C | -0.35953 | 0.702953 | 0.196254 |
| C | -0.939958 | 0.235673 | 1.340702 |
| H | -2.884543 | -0.540024 | 1.824363 |
| H | -3.794858 | -0.32617 | -0.458798 |
| H | -2.431656 | 0.586558 | -2.315348 |
| H | -0.501268 | 0.153661 | 2.325873 |
| C | 2.453219 | 1.740611 | -0.235874 |
| H | 2.319746 | 2.785058 | 0.04665 |
| H | 3.521948 | 1.518141 | -0.296058 |
| H | 1.995485 | 1.578527 | -1.217943 |
| O | 1.828162 | 0.939247 | 0.75741 |
| H | 1.953446 | 0.005249 | 0.496406 |
| O | 1.956346 | -1.566865 | -0.367572 |
| H | 2.024028 | -1.4404 | -1.321068 |
| C | 0.859483 | -2.440592 | -0.095889 |
| H | 0.759227 | -2.504057 | 0.987275 |
| H | -0.07087 | -2.054356 | -0.521509 |
| H | 1.055214 | -3.439271 | -0.494428 |

[a] Used for the $\Delta G^{\ddagger}_{M06\text{-}2X}$ calculation.
[b] Atomic Units = Hartrees

**558**‡

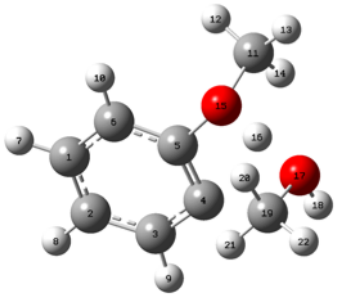

Sum of electronic and thermal Free Energies[a] = -462.189450 A.U.[b]

| Atom Type | Cartesian Coordinates (x,y,z) | | |
|---|---|---|---|
| C | -2.618989 | 0.186784 | 0.843874 |
| C | -2.830818 | -0.831461 | -0.086973 |
| C | -1.797917 | -1.234366 | -0.93739 |
| C | -0.503977 | -0.660041 | -0.937229 |
| C | -0.401984 | 0.327944 | 0.018847 |
| C | -1.365864 | 0.786726 | 0.908389 |
| H | -3.411749 | 0.504886 | 1.511485 |
| H | -3.803874 | -1.310441 | -0.145349 |
| H | -2.024451 | -2.037314 | -1.638353 |
| H | -1.146916 | 1.576926 | 1.619481 |
| C | 1.012013 | 2.208019 | -0.664393 |
| H | 0.281841 | 2.930564 | -0.306087 |
| H | 2.024906 | 2.577756 | -0.518874 |
| H | 0.831864 | 1.950435 | -1.708478 |
| O | 0.883843 | 1.014771 | 0.149679 |
| H | 1.696521 | 0.317087 | -0.061717 |
| O | 2.703328 | -0.543254 | -0.258022 |
| H | 2.502554 | -1.024135 | -1.074728 |
| C | 2.811392 | -1.478787 | 0.833275 |
| H | 2.966427 | -0.890477 | 1.735406 |
| H | 1.89549 | -2.065223 | 0.920485 |
| H | 3.666881 | -2.131105 | 0.66307 |

[a] Used for the $\Delta G^{\ddagger}_{M06\text{-}2X}$ calculation.
[b] Atomic Units = Hartrees

**551**‡

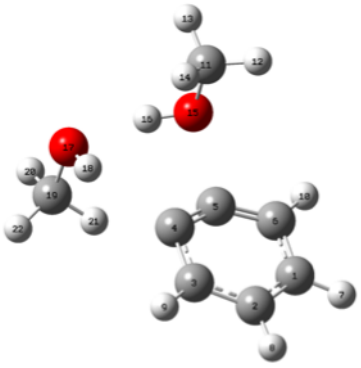

"Sum of electronic and thermal Free Energies[a] = -462.168576 A.U.[b]

| Atom Type | Cartesian Coordinates (x,y,z) | | |
|---|---|---|---|
| C | -2.737438 | 0.427598 | 0.627094 |
| C | -2.90836 | -0.705091 | -0.185034 |
| C | -1.834925 | -1.311043 | -0.848128 |
| C | -0.5631 | -0.723254 | -0.662561 |
| C | -0.575601 | 0.283585 | 0.096799 |
| C | -1.473156 | 1.013813 | 0.817947 |
| H | -3.593566 | 0.871229 | 1.123964 |
| H | -3.904615 | -1.118989 | -0.300808 |
| H | -1.996556 | -2.185981 | -1.469005 |
| H | -1.291902 | 1.884872 | 1.431819 |
| C | 1.521471 | 2.230494 | -0.782019 |
| H | 0.790479 | 3.036188 | -0.707452 |
| H | 2.521817 | 2.662468 | -0.872727 |
| H | 1.306329 | 1.634906 | -1.674917 |
| O | 1.416339 | 1.43989 | 0.398535 |
| H | 1.987765 | 0.659393 | 0.277306 |
| O | 2.540675 | -0.992431 | -0.338976 |
| H | 1.708446 | -1.090857 | -0.827321 |
| C | 2.472369 | -1.842498 | 0.80591 |
| H | 3.410561 | -1.730166 | 1.348725 |
| H | 1.644526 | -1.55624 | 1.462173 |
| H | 2.353047 | -2.888128 | 0.511721 |

[a] Used for the $\Delta G^{\ddagger}_{M06\text{-}2X}$ calculation.
[b] Atomic Units = Hartrees

## Supporting information for subsection 5.4.3

DFT calculations were performed with the Gaussian 09 software package.[100] Geometries were optimized using the M06-2X functional;[101] the basis set was the double-ζ split-valence 6-31G(d). The SMD continuum solvation model[46] with chloroform as the solvent was used during both geometry optimization and the frequency calculation. The "grid=ultrafine" option was applied during the numerical integrations. Harmonic vibrational frequency calculations were performed at 298 K for thermal corrections of the enthalpies. The optimized transition state structure geometries were found to have only one imaginary frequency.

### TS structure for Diels-Alder trapping leading to 561a-maj

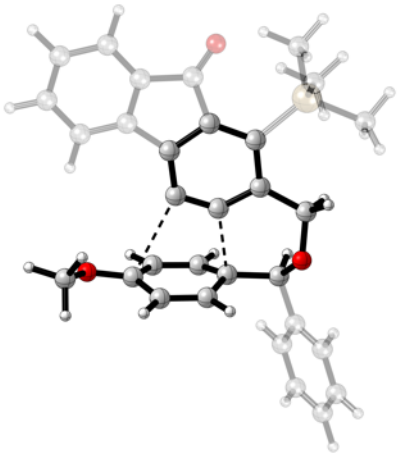

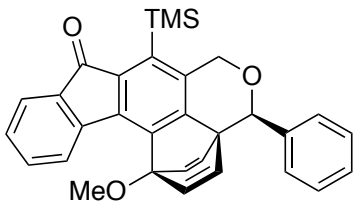


***561a-maj***

Imaginary frequency: -132.0574 $cm^{-1}$.
Sum of electronic and thermal Free Energies: -1712.173050 Hartree/Particle

| Center Number | Atomic Number | Atomic Type | Coordinates (Angstroms) X | Y | Z |
|---|---|---|---|---|---|
| 1 | 6 | 0 | 0.173740 | 0.118232 | 0.080520 |
| 2 | 6 | 0 | 0.009524 | -1.246970 | -0.019560 |
| 3 | 6 | 0 | -1.364379 | -1.654034 | -0.014564 |
| 4 | 6 | 0 | -2.323982 | -0.628065 | 0.022751 |
| 5 | 6 | 0 | -1.994684 | 0.753392 | 0.080220 |
| 6 | 6 | 0 | -0.659623 | 1.108275 | 0.112433 |
| 7 | 6 | 0 | -4.330416 | 0.693794 | -0.012665 |
| 8 | 6 | 0 | -5.632856 | 1.159996 | -0.038515 |
| 9 | 6 | 0 | -5.833192 | 2.543037 | 0.032804 |

| | | | | | |
|---|---|---|---|---|---|
| 10 | 6 | 0 | -4.744747 | 3.411512 | 0.128370 |
| 11 | 6 | 0 | -3.429365 | 2.931199 | 0.152215 |
| 12 | 6 | 0 | -3.235743 | 1.561419 | 0.077011 |
| 13 | 1 | 0 | -6.467771 | 0.468668 | -0.109960 |
| 14 | 1 | 0 | -6.841064 | 2.945573 | 0.016831 |
| 15 | 1 | 0 | -4.923076 | 4.481292 | 0.187042 |
| 16 | 1 | 0 | -2.583449 | 3.608855 | 0.236458 |
| 17 | 6 | 0 | -3.824177 | -0.714720 | -0.066045 |
| 18 | 8 | 0 | -4.515344 | -1.707428 | -0.185954 |
| 19 | 6 | 0 | -3.020651 | -3.745704 | 1.553335 |
| 20 | 6 | 0 | -2.786955 | -3.919375 | -1.607834 |
| 21 | 6 | 0 | -0.570480 | -4.749886 | 0.240670 |
| 22 | 1 | 0 | -3.540389 | -4.708630 | 1.473980 |
| 23 | 1 | 0 | -2.379983 | -3.794229 | 2.441900 |
| 24 | 1 | 0 | -3.774468 | -2.972941 | 1.709760 |
| 25 | 1 | 0 | -2.056422 | -3.879065 | -2.424337 |
| 26 | 1 | 0 | -3.175943 | -4.944007 | -1.564637 |
| 27 | 1 | 0 | -3.615434 | -3.250292 | -1.848449 |
| 28 | 1 | 0 | -1.070785 | -5.715238 | 0.396579 |
| 29 | 1 | 0 | 0.082967 | -4.870070 | -0.628115 |
| 30 | 1 | 0 | 0.051311 | -4.572429 | 1.123839 |
| 31 | 14 | 0 | -1.956281 | -3.482571 | 0.021635 |
| 32 | 6 | 0 | 1.173966 | -2.204229 | -0.170083 |
| 33 | 1 | 0 | 1.345855 | -2.763232 | 0.761385 |
| 34 | 1 | 0 | 0.961741 | -2.925030 | -0.962048 |
| 35 | 6 | 0 | 2.907125 | -0.691250 | 0.404140 |
| 36 | 1 | 0 | 2.724262 | -1.094901 | 1.412837 |
| 37 | 8 | 0 | 2.370285 | -1.566739 | -0.563251 |
| 38 | 6 | 0 | 2.240016 | 0.675296 | 0.310192 |
| 39 | 6 | 0 | 2.050187 | 1.454020 | 1.484917 |
| 40 | 6 | 0 | 2.231501 | 1.345188 | -0.941883 |
| 41 | 6 | 0 | 1.492278 | 2.698111 | 1.389514 |
| 42 | 1 | 0 | 2.232676 | 1.005164 | 2.457927 |
| 43 | 6 | 0 | 1.685104 | 2.599569 | -1.053868 |
| 44 | 1 | 0 | 2.569414 | 0.808957 | -1.824757 |
| 45 | 6 | 0 | 1.168006 | 3.212090 | 0.109204 |
| 46 | 1 | 0 | 1.226774 | 3.285069 | 2.262564 |
| 47 | 1 | 0 | 1.587373 | 3.075319 | -2.022195 |
| 48 | 6 | 0 | 4.408568 | -0.587371 | 0.185083 |
| 49 | 6 | 0 | 5.195713 | 0.084012 | 1.125240 |
| 50 | 6 | 0 | 5.014282 | -1.133335 | -0.945867 |
| 51 | 6 | 0 | 6.568228 | 0.207036 | 0.937888 |
| 52 | 1 | 0 | 4.731405 | 0.512814 | 2.010557 |
| 53 | 6 | 0 | 6.390595 | -1.006183 | -1.134688 |
| 54 | 1 | 0 | 4.407968 | -1.664261 | -1.671338 |
| 55 | 6 | 0 | 7.170725 | -0.337708 | -0.196216 |

| | | | | | |
|---|---|---|---|---|---|
| 56 | 1 | 0 | 7.168952 | 0.726694 | 1.678488 |
| 57 | 1 | 0 | 6.852171 | -1.436034 | -2.018971 |
| 58 | 1 | 0 | 8.242291 | -0.242516 | -0.343837 |
| 59 | 8 | 0 | 0.509028 | 4.379090 | 0.103613 |
| 60 | 6 | 0 | 0.037813 | 4.866157 | -1.146489 |
| 61 | 1 | 0 | -0.536788 | 4.092575 | -1.667664 |
| 62 | 1 | 0 | -0.606789 | 5.713874 | -0.914403 |
| 63 | 1 | 0 | 0.866649 | 5.203609 | -1.776959 |

**TS structure for Diels-Alder trapping leading to 561a-min**

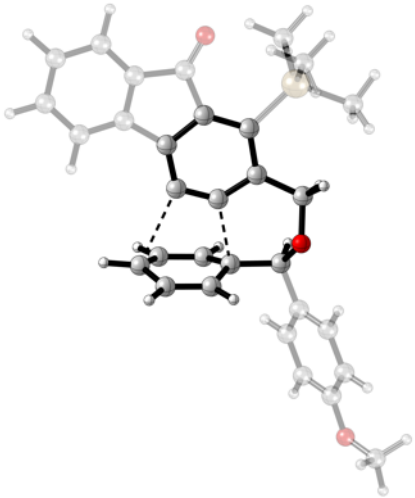

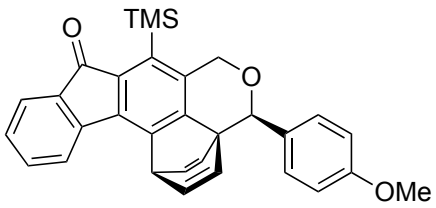


***561a-min***

Imaginary frequency: -249.6773 $cm^{-1}$.
Sum of electronic and thermal Free Energies: -1712.167076 Hartree/Particle

| Center Number | Atomic Number | Atomic Type | Coordinates (Angstroms) X | Y | Z |
|---|---|---|---|---|---|
| 1 | 6 | 0 | 0.369524 | -0.442818 | 0.075710 |
| 2 | 6 | 0 | 0.521853 | 0.926515 | 0.035974 |
| 3 | 6 | 0 | 1.890361 | 1.351115 | 0.018971 |
| 4 | 6 | 0 | 2.863522 | 0.340033 | -0.042600 |
| 5 | 6 | 0 | 2.561252 | -1.051652 | -0.057575 |
| 6 | 6 | 0 | 1.231250 | -1.403288 | 0.023805 |
| 7 | 6 | 0 | 4.887633 | -0.938288 | -0.247810 |
| 8 | 6 | 0 | 6.195878 | -1.370984 | -0.370756 |
| 9 | 6 | 0 | 6.426238 | -2.750128 | -0.418082 |
| 10 | 6 | 0 | 5.359644 | -3.646891 | -0.344537 |
| 11 | 6 | 0 | 4.038044 | -3.199660 | -0.222587 |
| 12 | 6 | 0 | 3.813817 | -1.833385 | -0.174360 |

| | | | | | |
|---|---|---|---|---|---|
| 13 | 1 | 0 | 7.011987 | −0.656382 | −0.428687 |
| 14 | 1 | 0 | 7.439638 | −3.127017 | −0.513167 |
| 15 | 1 | 0 | 5.559046 | −4.713783 | −0.384236 |
| 16 | 1 | 0 | 3.212434 | −3.903402 | −0.169088 |
| 17 | 6 | 0 | 4.357173 | 0.459579 | −0.183004 |
| 18 | 8 | 0 | 5.026930 | 1.470579 | −0.262832 |
| 19 | 6 | 0 | 3.555123 | 3.365942 | 1.669621 |
| 20 | 6 | 0 | 3.216995 | 3.746653 | −1.466531 |
| 21 | 6 | 0 | 1.043361 | 4.399491 | 0.500546 |
| 22 | 1 | 0 | 2.957472 | 3.226363 | 2.578271 |
| 23 | 1 | 0 | 4.391440 | 2.666191 | 1.692900 |
| 24 | 1 | 0 | 3.964573 | 4.383124 | 1.703302 |
| 25 | 1 | 0 | 2.459218 | 3.741155 | −2.258848 |
| 26 | 1 | 0 | 3.585258 | 4.775335 | −1.371163 |
| 27 | 1 | 0 | 4.050471 | 3.114018 | −1.777980 |
| 28 | 1 | 0 | 1.524652 | 5.369352 | 0.685445 |
| 29 | 1 | 0 | 0.347953 | 4.546237 | −0.330534 |
| 30 | 1 | 0 | 0.467118 | 4.159057 | 1.399728 |
| 31 | 14 | 0 | 2.450615 | 3.185590 | 0.155061 |
| 32 | 6 | 0 | −0.665594 | 1.864519 | −0.049908 |
| 33 | 1 | 0 | −0.829691 | 2.387626 | 0.903404 |
| 34 | 1 | 0 | −0.489454 | 2.617427 | −0.821079 |
| 35 | 6 | 0 | −2.358279 | 0.302758 | 0.518842 |
| 36 | 1 | 0 | −2.162832 | 0.691561 | 1.531146 |
| 37 | 8 | 0 | −1.854384 | 1.209289 | −0.438508 |
| 38 | 6 | 0 | −1.664414 | −1.048717 | 0.389301 |
| 39 | 6 | 0 | −1.380329 | −1.804459 | 1.559828 |
| 40 | 6 | 0 | −1.716314 | −1.727029 | −0.863331 |
| 41 | 6 | 0 | −0.727840 | −3.003192 | 1.429212 |
| 42 | 1 | 0 | −1.552835 | −1.359015 | 2.536329 |
| 43 | 6 | 0 | −1.074692 | −2.930962 | −0.991171 |
| 44 | 1 | 0 | −2.161250 | −1.221729 | −1.716393 |
| 45 | 6 | 0 | −0.410160 | −3.464688 | 0.133618 |
| 46 | 1 | 0 | −0.379179 | −3.549592 | 2.299714 |
| 47 | 1 | 0 | −0.991958 | −3.423254 | −1.954619 |
| 48 | 6 | 0 | −3.858998 | 0.170864 | 0.321587 |
| 49 | 6 | 0 | −4.615224 | −0.584073 | 1.227787 |
| 50 | 6 | 0 | −4.510100 | 0.771423 | −0.749437 |
| 51 | 6 | 0 | −5.982501 | −0.726005 | 1.068384 |
| 52 | 1 | 0 | −4.125916 | −1.066262 | 2.071267 |
| 53 | 6 | 0 | −5.889440 | 0.633594 | −0.926996 |
| 54 | 1 | 0 | −3.938961 | 1.363456 | −1.456076 |
| 55 | 6 | 0 | −6.630388 | −0.115702 | −0.014433 |
| 56 | 1 | 0 | −6.575285 | −1.304064 | 1.770258 |

| | | | | | |
|---|---|---|---|---|---|
| 57 | 1 | 0 | -6.366438 | 1.115399 | -1.772703 |
| 58 | 1 | 0 | 0.176345 | -4.372090 | 0.023422 |
| 59 | 8 | 0 | -7.972677 | -0.308760 | -0.085932 |
| 60 | 6 | 0 | -8.663725 | 0.308154 | -1.155971 |
| 61 | 1 | 0 | -8.317690 | -0.069684 | -2.125181 |
| 62 | 1 | 0 | -9.715574 | 0.052311 | -1.024527 |
| 63 | 1 | 0 | -8.550120 | 1.398219 | -1.128173 |

**TS structure for Diels-Alder trapping leading to 561b-maj**

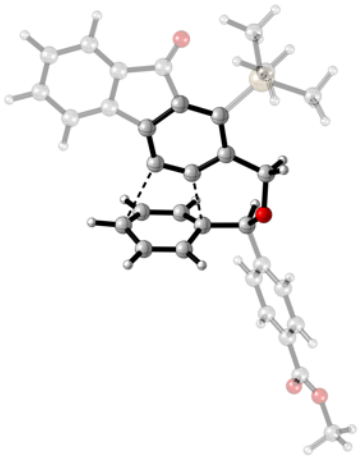

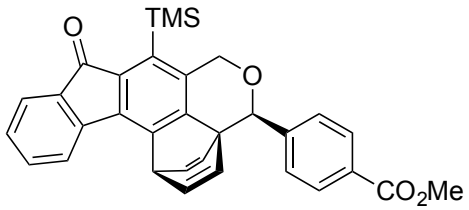


***561b-maj***

Imaginary frequency: -250.8086 $cm^{-1}$.
Sum of electronic and thermal Free Energies: -1825.477912 Hartree/Particle

| Center Number | Atomic Number | Atomic Type | Coordinates (Angstroms) X | Y | Z |
|---|---|---|---|---|---|
| 1 | 6 | 0 | 0.871714 | -0.419533 | 0.102520 |
| 2 | 6 | 0 | 1.048290 | 0.946792 | 0.063871 |
| 3 | 6 | 0 | 2.424029 | 1.345631 | 0.020613 |
| 4 | 6 | 0 | 3.376802 | 0.316588 | -0.061242 |
| 5 | 6 | 0 | 3.048899 | -1.069409 | -0.072442 |
| 6 | 6 | 0 | 1.714072 | -1.395128 | 0.032362 |
| 7 | 6 | 0 | 5.372772 | -0.999093 | -0.304456 |
| 8 | 6 | 0 | 6.670418 | -1.455970 | -0.450327 |
| 9 | 6 | 0 | 6.873874 | -2.839104 | -0.503462 |
| 10 | 6 | 0 | 5.792132 | -3.715972 | -0.413525 |
| 11 | 6 | 0 | 4.481475 | -3.244315 | -0.268204 |
| 12 | 6 | 0 | 4.283966 | -1.874166 | -0.213954 |
| 13 | 1 | 0 | 7.498772 | -0.756791 | -0.520930 |

| | | | | | |
|---|---|---|---|---|---|
| 14 | 1 | 0 | 7.878240 | −3.234828 | −0.616003 |
| 15 | 1 | 0 | 5.970816 | −4.786279 | −0.458181 |
| 16 | 1 | 0 | 3.643793 | −3.932442 | −0.201443 |
| 17 | 6 | 0 | 4.869877 | 0.408271 | −0.228903 |
| 18 | 8 | 0 | 5.556633 | 1.406644 | −0.320439 |
| 19 | 6 | 0 | 4.160184 | 3.326811 | 1.638549 |
| 20 | 6 | 0 | 3.763945 | 3.719142 | −1.488368 |
| 21 | 6 | 0 | 1.642575 | 4.408152 | 0.523544 |
| 22 | 1 | 0 | 3.578567 | 3.207488 | 2.560404 |
| 23 | 1 | 0 | 4.977502 | 2.604706 | 1.646968 |
| 24 | 1 | 0 | 4.597562 | 4.332630 | 1.658584 |
| 25 | 1 | 0 | 2.993854 | 3.715883 | −2.268733 |
| 26 | 1 | 0 | 4.140338 | 4.745724 | −1.402444 |
| 27 | 1 | 0 | 4.588051 | 3.079828 | −1.810869 |
| 28 | 1 | 0 | 2.146144 | 5.366329 | 0.709764 |
| 29 | 1 | 0 | 0.939142 | 4.576008 | −0.296807 |
| 30 | 1 | 0 | 1.073822 | 4.172172 | 1.428717 |
| 31 | 14 | 0 | 3.020713 | 3.169773 | 0.147654 |
| 32 | 6 | 0 | −0.123450 | 1.906156 | 0.007508 |
| 33 | 1 | 0 | −0.264029 | 2.421126 | 0.968839 |
| 34 | 1 | 0 | 0.051106 | 2.664488 | −0.758331 |
| 35 | 6 | 0 | −1.834808 | 0.368383 | 0.586360 |
| 36 | 1 | 0 | −1.628712 | 0.743180 | 1.601346 |
| 37 | 8 | 0 | −1.330524 | 1.274734 | −0.368525 |
| 38 | 6 | 0 | −1.170510 | −0.996308 | 0.436400 |
| 39 | 6 | 0 | −0.888516 | −1.768344 | 1.596551 |
| 40 | 6 | 0 | −1.247385 | −1.659959 | −0.822660 |
| 41 | 6 | 0 | −0.255813 | −2.975158 | 1.446541 |
| 42 | 1 | 0 | −1.044494 | −1.330947 | 2.579391 |
| 43 | 6 | 0 | −0.626727 | −2.872841 | −0.969154 |
| 44 | 1 | 0 | −1.690345 | −1.138703 | −1.667133 |
| 45 | 6 | 0 | 0.041751 | −3.427741 | 0.142826 |
| 46 | 1 | 0 | 0.092810 | −3.536120 | 2.307706 |
| 47 | 1 | 0 | −0.562388 | −3.356383 | −1.938339 |
| 48 | 1 | 0 | 0.613492 | −4.342497 | 0.017219 |
| 49 | 6 | 0 | −3.339350 | 0.257659 | 0.406640 |
| 50 | 6 | 0 | −4.094839 | −0.430088 | 1.362305 |
| 51 | 6 | 0 | −3.975824 | 0.809187 | −0.705246 |
| 52 | 6 | 0 | −5.466760 | −0.561557 | 1.209766 |
| 53 | 1 | 0 | −3.603662 | −0.863711 | 2.230023 |
| 54 | 6 | 0 | −5.352338 | 0.674191 | −0.864136 |
| 55 | 1 | 0 | −3.391772 | 1.350397 | −1.440783 |
| 56 | 6 | 0 | −6.101446 | −0.010401 | 0.093005 |
| 57 | 1 | 0 | −6.062010 | −1.088472 | 1.948527 |

| | | | | | |
|---|---|---|---|---|---|
| 58 | 1 | 0 | −5.844625 | 1.103061 | −1.730339 |
| 59 | 6 | 0 | −7.576339 | −0.180259 | −0.025398 |
| 60 | 8 | 0 | −8.263784 | −0.750466 | 0.793228 |
| 61 | 8 | 0 | −8.071579 | 0.365863 | −1.142814 |
| 62 | 6 | 0 | −9.484475 | 0.229380 | −1.312486 |
| 63 | 1 | 0 | −9.716601 | 0.708337 | −2.262690 |
| 64 | 1 | 0 | −9.764657 | −0.825912 | −1.338937 |
| 65 | 1 | 0 | −10.015820 | 0.724715 | −0.496665 |

**TS structure for Diels-Alder trapping leading to 561b-min**

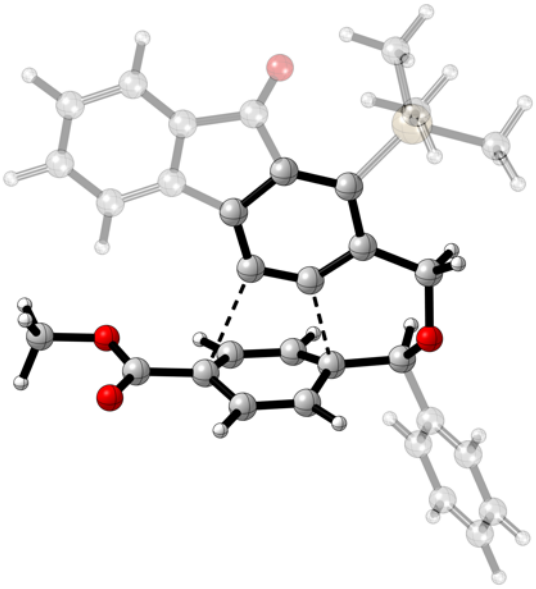

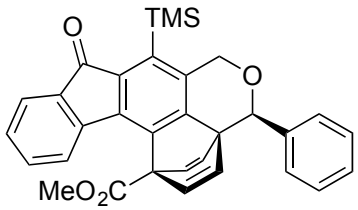


***561b-min***

Imaginary frequency: -251.9179 $cm^{-1}$.
Sum of electronic and thermal Free Energies: -1825.475535 Hartree/Particle

| Center Number | Atomic Number | Atomic Type | Coordinates (Angstroms) X | Y | Z |
|---|---|---|---|---|---|
| 1 | 6 | 0 | 0.278103 | −0.161547 | 0.066332 |
| 2 | 6 | 0 | 0.206690 | −1.538598 | 0.032894 |
| 3 | 6 | 0 | −1.134210 | −2.043735 | 0.028374 |
| 4 | 6 | 0 | −2.169068 | −1.094210 | 0.001647 |
| 5 | 6 | 0 | −1.956534 | 0.314101 | 0.003679 |
| 6 | 6 | 0 | −0.647029 | 0.736266 | 0.034066 |
| 7 | 6 | 0 | −4.273973 | 0.061474 | −0.124285 |
| 8 | 6 | 0 | −5.608525 | 0.419480 | −0.195121 |
| 9 | 6 | 0 | −5.920910 | 1.783423 | −0.185671 |

| | | | | | |
|---|---|---|---|---|---|
| 10 | 6 | 0 | −4.908475 | 2.740420 | −0.102013 |
| 11 | 6 | 0 | −3.560536 | 2.368611 | −0.033590 |
| 12 | 6 | 0 | −3.255588 | 1.018234 | −0.049589 |
| 13 | 1 | 0 | −6.383690 | −0.339204 | −0.254810 |
| 14 | 1 | 0 | −6.957329 | 2.101240 | −0.239779 |
| 15 | 1 | 0 | −5.171432 | 3.794326 | −0.090750 |
| 16 | 1 | 0 | −2.772995 | 3.112649 | 0.041184 |
| 17 | 6 | 0 | −3.657880 | −1.302238 | −0.103580 |
| 18 | 8 | 0 | −4.264905 | −2.351832 | −0.177866 |
| 19 | 6 | 0 | −2.632545 | −4.186020 | 1.672019 |
| 20 | 6 | 0 | −2.371676 | −4.467248 | −1.487250 |
| 21 | 6 | 0 | −0.115028 | −5.064166 | 0.388150 |
| 22 | 1 | 0 | −3.034079 | −5.206828 | 1.664454 |
| 23 | 1 | 0 | −1.999118 | −4.092691 | 2.562273 |
| 24 | 1 | 0 | −3.472357 | −3.496839 | 1.769657 |
| 25 | 1 | 0 | −2.708511 | −5.507351 | −1.398851 |
| 26 | 1 | 0 | −3.228421 | −3.856922 | −1.778758 |
| 27 | 1 | 0 | −1.627156 | −4.431336 | −2.291279 |
| 28 | 1 | 0 | −0.545887 | −6.055481 | 0.583792 |
| 29 | 1 | 0 | 0.535793 | −5.172141 | −0.484447 |
| 30 | 1 | 0 | 0.502538 | −4.813187 | 1.256168 |
| 31 | 14 | 0 | −1.589729 | −3.910921 | 0.128818 |
| 32 | 6 | 0 | 1.449157 | −2.402343 | −0.038330 |
| 33 | 1 | 0 | 1.663813 | −2.864654 | 0.936565 |
| 34 | 1 | 0 | 1.309871 | −3.201215 | −0.767955 |
| 35 | 6 | 0 | 3.056310 | −0.715184 | 0.418549 |
| 36 | 1 | 0 | 2.909884 | −1.061988 | 1.453376 |
| 37 | 8 | 0 | 2.587120 | −1.692831 | −0.483055 |
| 38 | 6 | 0 | 2.281150 | 0.585017 | 0.237095 |
| 39 | 6 | 0 | 2.027197 | 1.414842 | 1.365010 |
| 40 | 6 | 0 | 2.218044 | 1.168618 | −1.063013 |
| 41 | 6 | 0 | 1.280958 | 2.548749 | 1.194205 |
| 42 | 1 | 0 | 2.298975 | 1.066222 | 2.357665 |
| 43 | 6 | 0 | 1.487954 | 2.312419 | −1.236760 |
| 44 | 1 | 0 | 2.645976 | 0.630740 | −1.904233 |
| 45 | 6 | 0 | 0.840889 | 2.871508 | −0.112029 |
| 46 | 1 | 0 | 0.947223 | 3.142209 | 2.037958 |
| 47 | 1 | 0 | 1.302939 | 2.736869 | −2.217467 |
| 48 | 6 | 0 | 4.541292 | −0.497324 | 0.176500 |
| 49 | 6 | 0 | 5.282637 | 0.263608 | 1.084352 |
| 50 | 6 | 0 | 5.172295 | −1.025973 | −0.948873 |
| 51 | 6 | 0 | 6.638047 | 0.491455 | 0.870977 |
| 52 | 1 | 0 | 4.797267 | 0.678164 | 1.965103 |
| 53 | 6 | 0 | 6.530911 | −0.794801 | −1.162765 |

| | | | | | |
|---|---|---|---|---|---|
| 54 | 1 | 0 | 4.600270 | −1.625351 | −1.648473 |
| 55 | 6 | 0 | 7.266597 | −0.037256 | −0.256284 |
| 56 | 1 | 0 | 7.205022 | 1.079743 | 1.586269 |
| 57 | 1 | 0 | 7.013681 | −1.212455 | −2.041428 |
| 58 | 1 | 0 | 8.324664 | 0.139826 | −0.423911 |
| 59 | 6 | 0 | −0.085849 | 4.020242 | −0.354970 |
| 60 | 8 | 0 | −0.292642 | 4.505921 | −1.443234 |
| 61 | 8 | 0 | −0.666555 | 4.455243 | 0.769645 |
| 62 | 6 | 0 | −1.525345 | 5.589920 | 0.617294 |
| 63 | 1 | 0 | −2.296241 | 5.393078 | −0.131027 |
| 64 | 1 | 0 | −1.974896 | 5.753056 | 1.595747 |
| 65 | 1 | 0 | −0.944100 | 6.463938 | 0.313460 |

**TS structure for Diels-Alder trapping leading to 561c-maj**

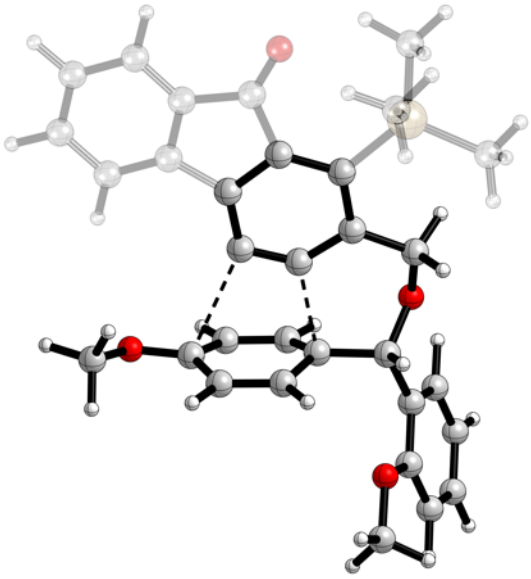

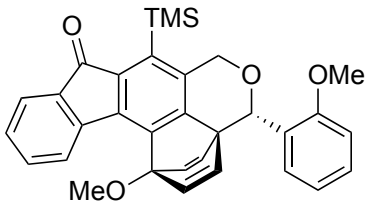


***561c-maj***

Imaginary frequency: -146.1104 $cm^{-1}$.
Sum of electronic and thermal Free Energies: -1826.621386 Hartree/Particle

| Center Number | Atomic Number | Atomic Type | Coordinates (Angstroms) X | Y | Z |
|---|---|---|---|---|---|
| 1 | 6 | 0 | −0.130157 | 0.078660 | −0.174146 |
| 2 | 6 | 0 | −0.329476 | −1.285241 | −0.136619 |
| 3 | 6 | 0 | −1.705129 | −1.657265 | 0.009200 |
| 4 | 6 | 0 | −2.642827 | −0.611014 | −0.003058 |
| 5 | 6 | 0 | −2.286691 | 0.759127 | −0.135339 |

| | | | | | |
|---|---|---|---|---|---|
| 6 | 6 | 0 | −0.945196 | 1.085937 | −0.188315 |
| 7 | 6 | 0 | −4.624717 | 0.744251 | −0.073808 |
| 8 | 6 | 0 | −5.919192 | 1.232200 | −0.091297 |
| 9 | 6 | 0 | −6.095054 | 2.613622 | −0.228559 |
| 10 | 6 | 0 | −4.990645 | 3.458034 | −0.350917 |
| 11 | 6 | 0 | −3.683629 | 2.955027 | −0.333817 |
| 12 | 6 | 0 | −3.513539 | 1.587839 | −0.187096 |
| 13 | 1 | 0 | −6.766775 | 0.558291 | −0.004008 |
| 14 | 1 | 0 | −7.096008 | 3.033021 | −0.245678 |
| 15 | 1 | 0 | −5.149331 | 4.526351 | −0.465921 |
| 16 | 1 | 0 | −2.825409 | 3.612466 | −0.446723 |
| 17 | 6 | 0 | −4.145569 | −0.670474 | 0.034299 |
| 18 | 8 | 0 | −4.860415 | −1.651144 | 0.107289 |
| 19 | 6 | 0 | −3.230172 | −3.529984 | 1.933542 |
| 20 | 6 | 0 | −3.299990 | −4.053706 | −1.194398 |
| 21 | 6 | 0 | −0.923914 | −4.720516 | 0.522317 |
| 22 | 1 | 0 | −3.668998 | −4.527106 | 2.063638 |
| 23 | 1 | 0 | −2.523456 | −3.375330 | 2.757640 |
| 24 | 1 | 0 | −4.032580 | −2.796542 | 2.022432 |
| 25 | 1 | 0 | −3.706241 | −5.052714 | −0.994230 |
| 26 | 1 | 0 | −4.132846 | −3.390592 | −1.436510 |
| 27 | 1 | 0 | −2.650266 | −4.133585 | −2.073753 |
| 28 | 1 | 0 | −1.418082 | −5.658178 | 0.810445 |
| 29 | 1 | 0 | −0.339756 | −4.934363 | −0.377013 |
| 30 | 1 | 0 | −0.235547 | −4.466905 | 1.334756 |
| 31 | 14 | 0 | −2.312465 | −3.458380 | 0.290581 |
| 32 | 6 | 0 | 0.803012 | −2.276283 | −0.311162 |
| 33 | 1 | 0 | 1.055752 | −2.763915 | 0.641805 |
| 34 | 1 | 0 | 0.508431 | −3.053004 | −1.020128 |
| 35 | 6 | 0 | 2.607623 | −0.779549 | 0.005367 |
| 36 | 1 | 0 | 2.524562 | −1.132019 | 1.044456 |
| 37 | 8 | 0 | 1.962370 | −1.690270 | −0.861045 |
| 38 | 6 | 0 | 1.951786 | 0.596616 | −0.082936 |
| 39 | 6 | 0 | 1.798958 | 1.381177 | 1.088114 |
| 40 | 6 | 0 | 1.924445 | 1.266897 | −1.342619 |
| 41 | 6 | 0 | 1.249250 | 2.635897 | 1.011345 |
| 42 | 6 | 0 | 1.391881 | 2.521116 | −1.435590 |
| 43 | 6 | 0 | 0.902921 | 3.145750 | −0.261667 |
| 44 | 1 | 0 | 1.029150 | 3.196718 | 1.911567 |
| 45 | 1 | 0 | 1.259351 | 3.029279 | −2.384794 |
| 46 | 6 | 0 | 4.073274 | −0.723265 | −0.381398 |
| 47 | 6 | 0 | 5.005497 | −0.193772 | 0.528177 |
| 48 | 6 | 0 | 4.518993 | −1.166803 | −1.621256 |
| 49 | 6 | 0 | 6.355639 | −0.111978 | 0.189645 |

| | | | | | |
|---|---|---|---|---|---|
| 50 | 6 | 0 | 5.868217 | −1.085093 | −1.970369 |
| 51 | 1 | 0 | 3.797969 | −1.591614 | −2.311890 |
| 52 | 6 | 0 | 6.778302 | −0.557342 | −1.063846 |
| 53 | 1 | 0 | 7.078303 | 0.292084 | 0.889036 |
| 54 | 1 | 0 | 6.199915 | −1.435823 | −2.942363 |
| 55 | 1 | 0 | 7.831169 | −0.489287 | −1.321184 |
| 56 | 1 | 0 | 2.015409 | 0.933884 | 2.053427 |
| 57 | 1 | 0 | 2.238399 | 0.728036 | −2.232603 |
| 58 | 8 | 0 | 4.493921 | 0.205501 | 1.723501 |
| 59 | 6 | 0 | 5.388473 | 0.740949 | 2.681791 |
| 60 | 1 | 0 | 5.879810 | 1.644643 | 2.304375 |
| 61 | 1 | 0 | 4.781502 | 0.995614 | 3.551380 |
| 62 | 1 | 0 | 6.146793 | 0.004674 | 2.970952 |
| 63 | 8 | 0 | 0.274163 | 4.315154 | −0.445649 |
| 64 | 6 | 0 | −0.314229 | 4.936800 | 0.688917 |
| 65 | 1 | 0 | 0.451490 | 5.316783 | 1.373221 |
| 66 | 1 | 0 | −0.898284 | 5.772550 | 0.303721 |
| 67 | 1 | 0 | −0.969114 | 4.234296 | 1.216018 |

---

**TS structure for Diels-Alder trapping leading to 561c-min-anti via the intermediate enol ether S561c-anti.**

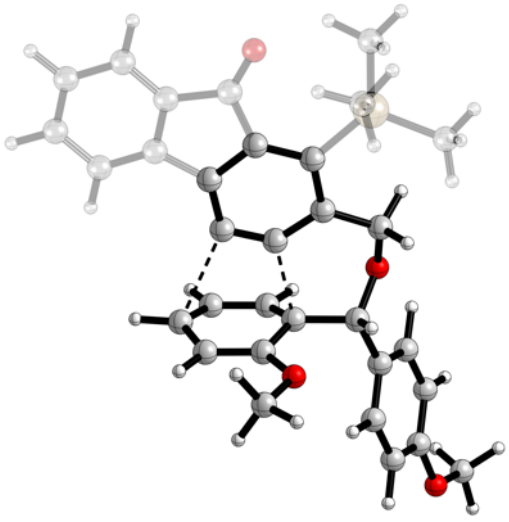

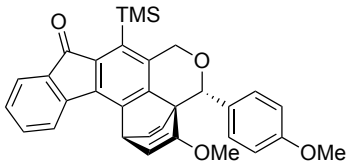


***S561c-min-anti***

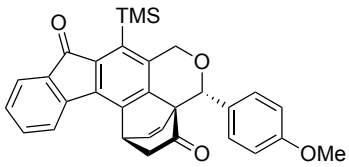


***561c-min-anti***

Imaginary frequency: -236.3594 $cm^{-1}$.
Sum of electronic and thermal Free Energies: -1826.617815 Hartree/Particle

---

| Center Number | Atomic Number | Atomic Type | Coordinates (Angstroms) X | Y | Z |
|---|---|---|---|---|---|
| 1 | 6 | 0 | 0.453833 | -0.349317 | -0.149499 |
| 2 | 6 | 0 | 0.629147 | 1.018382 | -0.070704 |
| 3 | 6 | 0 | 2.001703 | 1.422808 | -0.012858 |
| 4 | 6 | 0 | 2.963098 | 0.406452 | -0.134601 |
| 5 | 6 | 0 | 2.637144 | -0.968406 | -0.296450 |
| 6 | 6 | 0 | 1.302690 | -1.319719 | -0.288805 |
| 7 | 6 | 0 | 4.971625 | -0.881141 | -0.415569 |
| 8 | 6 | 0 | 6.275215 | -1.325979 | -0.546308 |
| 9 | 6 | 0 | 6.482253 | -2.697386 | -0.730679 |
| 10 | 6 | 0 | 5.398002 | -3.574604 | -0.781243 |
| 11 | 6 | 0 | 4.081704 | -3.114890 | -0.649452 |
| 12 | 6 | 0 | 3.880269 | -1.756402 | -0.466776 |
| 13 | 1 | 0 | 7.105857 | -0.626975 | -0.506020 |
| 14 | 1 | 0 | 7.491189 | -3.083408 | -0.836151 |
| 15 | 1 | 0 | 5.579561 | -4.635620 | -0.926007 |
| 16 | 1 | 0 | 3.241023 | -3.801714 | -0.690252 |
| 17 | 6 | 0 | 4.462196 | 0.512526 | -0.219597 |
| 18 | 8 | 0 | 5.150688 | 1.513102 | -0.169494 |
| 19 | 6 | 0 | 3.630468 | 3.263016 | 1.851226 |
| 20 | 6 | 0 | 3.432606 | 3.896919 | -1.256577 |
| 21 | 6 | 0 | 1.198038 | 4.452827 | 0.667756 |
| 22 | 1 | 0 | 4.088432 | 4.253197 | 1.966860 |
| 23 | 1 | 0 | 2.985416 | 3.098923 | 2.722646 |
| 24 | 1 | 0 | 4.429372 | 2.520605 | 1.864916 |
| 25 | 1 | 0 | 3.858927 | 4.885669 | -1.047360 |
| 26 | 1 | 0 | 4.236212 | 3.249668 | -1.612771 |
| 27 | 1 | 0 | 2.700430 | 4.020124 | -2.063340 |
| 28 | 1 | 0 | 1.698138 | 5.390859 | 0.944526 |
| 29 | 1 | 0 | 0.537751 | 4.680980 | -0.173521 |
| 30 | 1 | 0 | 0.582985 | 4.162024 | 1.525316 |
| 31 | 14 | 0 | 2.587007 | 3.229174 | 0.283840 |
| 32 | 6 | 0 | -0.529640 | 1.993165 | -0.132870 |
| 33 | 1 | 0 | -0.713097 | 2.459431 | 0.845789 |
| 34 | 1 | 0 | -0.304305 | 2.787361 | -0.848311 |
| 35 | 6 | 0 | -2.252155 | 0.437512 | 0.288127 |
| 36 | 1 | 0 | -2.053973 | 0.746014 | 1.322989 |
| 37 | 8 | 0 | -1.720926 | 1.397826 | -0.600215 |
| 38 | 6 | 0 | -1.578691 | -0.911703 | 0.045350 |
| 39 | 6 | 0 | -1.369728 | -1.800261 | 1.148996 |
| 40 | 6 | 0 | -1.621150 | -1.469078 | -1.264008 |
| 41 | 6 | 0 | -0.782402 | -3.024959 | 0.919184 |

| | | | | | |
|---|---|---|---|---|---|
| 42 | 6 | 0 | −1.031487 | −2.682783 | −1.498598 |
| 43 | 1 | 0 | −2.000677 | −0.849265 | −2.071888 |
| 44 | 6 | 0 | −0.462596 | −3.367810 | −0.406079 |
| 45 | 1 | 0 | −0.471456 | −3.670733 | 1.731402 |
| 46 | 1 | 0 | −0.926570 | −3.075183 | −2.504122 |
| 47 | 6 | 0 | −3.752040 | 0.344700 | 0.076975 |
| 48 | 6 | 0 | −4.537774 | −0.380821 | 0.982433 |
| 49 | 6 | 0 | −4.372118 | 0.943982 | −1.013164 |
| 50 | 6 | 0 | −5.904919 | −0.497720 | 0.799414 |
| 51 | 1 | 0 | −4.068894 | −0.851082 | 1.843449 |
| 52 | 6 | 0 | −5.750847 | 0.832840 | −1.211820 |
| 53 | 1 | 0 | −3.777097 | 1.517073 | −1.716167 |
| 54 | 6 | 0 | −6.521728 | 0.109567 | −0.302715 |
| 55 | 1 | 0 | −6.522231 | −1.051745 | 1.499677 |
| 56 | 1 | 0 | −6.204422 | 1.314914 | −2.070190 |
| 57 | 1 | 0 | 0.078364 | −4.293003 | −0.583082 |
| 58 | 8 | 0 | −1.663280 | −1.297897 | 2.368424 |
| 59 | 6 | 0 | −1.323844 | −2.087240 | 3.499549 |
| 60 | 1 | 0 | −0.244290 | −2.266245 | 3.539599 |
| 61 | 1 | 0 | −1.633004 | −1.511009 | 4.371317 |
| 62 | 1 | 0 | −1.857982 | −3.043085 | 3.483346 |
| 63 | 8 | 0 | −7.866735 | −0.058124 | −0.395423 |
| 64 | 6 | 0 | −8.526232 | 0.557849 | −1.485512 |
| 65 | 1 | 0 | −8.394945 | 1.646184 | −1.467582 |
| 66 | 1 | 0 | −8.167935 | 0.163388 | −2.443604 |
| 67 | 1 | 0 | −9.584671 | 0.321014 | −1.372339 |

**TS structure for Diels-Alder trapping leading to (the unobserved) 561c-min-syn via the intermediate enol ether S561c-syn**

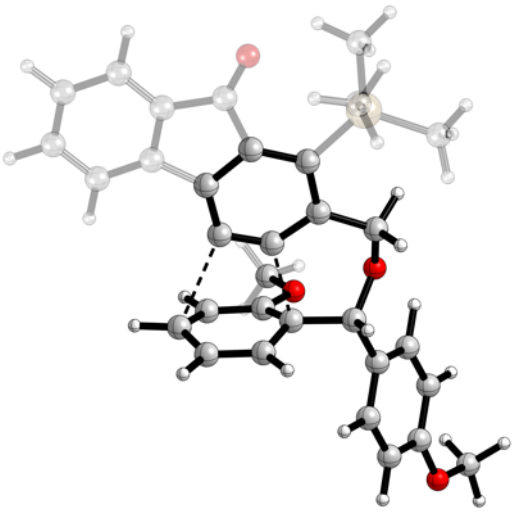

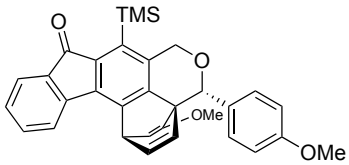


***S561c-min-syn***

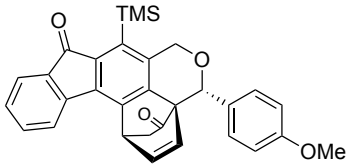


***561c-min-anti***

Imaginary frequency: -217.7592 $cm^{-1}$.
Sum of electronic and thermal Free Energies: -1826.615067 Hartree/Particle

| Center Number | Atomic Number | Atomic Type | Coordinates (Angstroms) X | Y | Z |
|---|---|---|---|---|---|
| 1 | 6 | 0 | -0.509876 | -0.376946 | -0.215745 |
| 2 | 6 | 0 | -0.676129 | 0.991209 | -0.117764 |
| 3 | 6 | 0 | -2.045038 | 1.405948 | -0.044345 |
| 4 | 6 | 0 | -3.011353 | 0.386836 | -0.019703 |
| 5 | 6 | 0 | -2.695684 | -0.997679 | -0.089651 |
| 6 | 6 | 0 | -1.367279 | -1.349752 | -0.214432 |
| 7 | 6 | 0 | -5.024762 | -0.917404 | 0.104981 |
| 8 | 6 | 0 | -6.329341 | -1.369077 | 0.195162 |
| 9 | 6 | 0 | -6.546661 | -2.750682 | 0.157044 |
| 10 | 6 | 0 | -5.471184 | -3.631295 | 0.033134 |
| 11 | 6 | 0 | -4.153621 | -3.164776 | -0.056590 |
| 12 | 6 | 0 | -3.942253 | -1.796101 | -0.019619 |
| 13 | 1 | 0 | -7.152658 | -0.667027 | 0.292065 |
| 14 | 1 | 0 | -7.556705 | -3.142312 | 0.224221 |
| 15 | 1 | 0 | -5.660701 | -4.700424 | 0.006429 |
| 16 | 1 | 0 | -3.320209 | -3.855000 | -0.151773 |
| 17 | 6 | 0 | -4.506448 | 0.486347 | 0.122009 |
| 18 | 8 | 0 | -5.186584 | 1.485863 | 0.248369 |
| 19 | 6 | 0 | -3.747000 | 3.515692 | -1.535841 |

| | | | | | |
|---|---|---|---|---|---|
| 20 | 6 | 0 | −3.408331 | 3.653482 | 1.622396 |
| 21 | 6 | 0 | −1.265508 | 4.517917 | −0.279271 |
| 22 | 1 | 0 | −4.287014 | 4.463394 | −1.418197 |
| 23 | 1 | 0 | −3.129837 | 3.602941 | −2.438041 |
| 24 | 1 | 0 | −4.485660 | 2.728863 | −1.694994 |
| 25 | 1 | 0 | −3.799436 | 4.678134 | 1.601630 |
| 26 | 1 | 0 | −4.226742 | 2.982791 | 1.890297 |
| 27 | 1 | 0 | −2.646849 | 3.609494 | 2.409928 |
| 28 | 1 | 0 | −1.779728 | 5.477213 | −0.427538 |
| 29 | 1 | 0 | −0.606896 | 4.644247 | 0.585021 |
| 30 | 1 | 0 | −0.647751 | 4.350889 | −1.166847 |
| 31 | 14 | 0 | −2.635134 | 3.236402 | −0.040701 |
| 32 | 6 | 0 | 0.490965 | 1.955647 | −0.070382 |
| 33 | 1 | 0 | 0.600887 | 2.475554 | −1.034757 |
| 34 | 1 | 0 | 0.320939 | 2.709619 | 0.699834 |
| 35 | 6 | 0 | 2.196012 | 0.432115 | −0.680542 |
| 36 | 1 | 0 | 1.975406 | 0.821058 | −1.688636 |
| 37 | 8 | 0 | 1.709053 | 1.341155 | 0.279034 |
| 38 | 6 | 0 | 1.505256 | −0.924410 | −0.573158 |
| 39 | 6 | 0 | 1.221988 | −1.637916 | −1.771539 |
| 40 | 6 | 0 | 1.612059 | −1.679053 | 0.645298 |
| 41 | 6 | 0 | 0.616436 | −2.863687 | −1.703081 |
| 42 | 6 | 0 | 1.027653 | −2.929764 | 0.713369 |
| 43 | 6 | 0 | 0.383936 | −3.423829 | −0.428905 |
| 44 | 1 | 0 | 0.258124 | −3.368120 | −2.593887 |
| 45 | 1 | 0 | 0.963154 | −3.475252 | 1.646858 |
| 46 | 6 | 0 | 3.705516 | 0.316977 | −0.536942 |
| 47 | 6 | 0 | 4.440044 | −0.399226 | −1.489230 |
| 48 | 6 | 0 | 4.387207 | 0.914957 | 0.516343 |
| 49 | 6 | 0 | 5.817527 | −0.508462 | −1.392103 |
| 50 | 1 | 0 | 3.927835 | −0.877407 | −2.321367 |
| 51 | 6 | 0 | 5.775362 | 0.815211 | 0.628762 |
| 52 | 1 | 0 | 3.827465 | 1.468087 | 1.262236 |
| 53 | 6 | 0 | 6.495602 | 0.101514 | −0.329467 |
| 54 | 1 | 0 | 6.393284 | −1.057730 | −2.130400 |
| 55 | 1 | 0 | 6.277080 | 1.294647 | 1.461524 |
| 56 | 1 | 0 | −0.159406 | −4.361362 | −0.353286 |
| 57 | 1 | 0 | 1.346546 | −1.123856 | −2.721157 |
| 58 | 8 | 0 | 2.201449 | −1.049936 | 1.671860 |
| 59 | 6 | 0 | 2.252908 | −1.725457 | 2.918997 |
| 60 | 1 | 0 | 2.798813 | −1.064969 | 3.592399 |
| 61 | 1 | 0 | 1.245309 | −1.899874 | 3.311407 |
| 62 | 1 | 0 | 2.786262 | −2.677630 | 2.827525 |
| 63 | 8 | 0 | 7.845443 | −0.055106 | −0.319330 |

| | | | | | |
|---|---|---|---|---|---|
| 64 | 6 | 0 | 8.565841 | 0.569336 | 0.726203 |
| 65 | 1 | 0 | 8.424044 | 1.656465 | 0.714664 |
| 66 | 1 | 0 | 8.271131 | 0.174647 | 1.705655 |
| 67 | 1 | 0 | 9.617237 | 0.341471 | 0.547203 |

# Supplementary information for Section 6.1

## General Experimental Protocols

NMR spectra were recorded on either a Bruker Avance 400 or 500 (400 and 500 MHz, respectively) spectrometer in $CDCl_3$. The following format is used to report the $^1H$ NMR data: chemical shift in ppm [multiplicity, coupling constant(s) in Hz, integral (to the nearest whole number of protons), and assignment]. Coupling constant analysis was guided by methods we have previously reported.[103] Chemical shifts for proton spectra are referenced to TMS (δ 0.00 ppm). Non-first order multiplets are listed as "nfom". Chemical shifts for carbon spectra are referenced to $CHCl_3$ (δ 77.23 ppm). TMS is detectable in some of the $^{13}C$ NMR samples (δ ca. 0.0 ppm). Several compounds contain $CF_3$ groups. The resonances for several carbon atoms in the $^{13}C$ NMR spectra for these are observed as quartets; for each, the midpoint of the multiplet (i.e., the actual chemical shift) is given in the line listing. Infrared spectral data were recorded on an Midac Corporation Prospect 4000 FT-IR spectrometer. Spectra were taken of thin film samples in attenuated total reflectance (ATR) mode on a germanium window. Electrospray ionization (ESI) mass spectrometry data were collected on a Bruker BioTOF II (ESI-TOF) instrument. Samples for high-resolution mass spectral (HRMS) analysis were doped with PEG as the internal calibrant. Samples were introduced as methanolic solutions.

Flash chromatography was performed on E. Merck silica gel (230-400 mesh). Thin layer chromatography (TLC) was performed on glass or plastic backed plates of silica gel. Spots were visualized by dipping in a solution of ceric ammonium molybdate followed by heat treatment and/or UV irradiation.

Reactions requiring anhydrous conditions were performed in flame- or oven-dried glassware under an atmosphere of nitrogen or argon. Anhydrous toluene, diethyl ether, THF, and methylene chloride were passed through a column of activated alumina and taken immediately prior to use. $CHCl_3$ used for HDDA reactions was ethanol-free. Reported reaction temperatures are the temperature of the external heating oil-bath. HDDA-initiated reactions, including those that were carried out at temperatures above the

boiling point of the solvent, were typically performed in a threaded vial fitted with an inert, Teflon®-lined screw-cap.

Procedures for preparation and spectral data are provided for i) all new compounds specifically shown in the manuscript and ii) all new (previously unreported) intermediates used in the synthetic route by which the former were made. The latter are specified by **S#**, since they only appear here in the Supporting Information (SI). A citation is provided for each known but non-commercially available compound that is used; these have not been given a structure number.

## Preparation and characterization data for all key compounds

## General Procedures A–B

*A. Alkyne coupling with the Cadiot–Chodkiewicz reaction*

To a solution of CuCl (0.10 equiv or 10% with respect to (wrt) the terminal alkyne substrate) in 40:60 (v:v) *n*-$BuNH_2$:$H_2O$ (5 mL/mmol) was added an excess of $NH_2OH$•HCl (typically a few crystals on a reaction scale ≤1 mmol) with stirring. The reaction vessel was immediately capped with a Teflon®-lined cap and placed in an ice-water bath. The color of this mixture turned from deep purple-blue to colorless within seconds, indicating full reduction of Cu(II) to Cu(I). A mixed solution of the terminal alkyne (1.0 equiv) and the 1-bromoalkyne (1.2–1.5 equiv) in $CH_2Cl_2$ (5 mL/mmol wrt the terminal alkyne) was added dropwise. The mixture was stirred for 1 h at 0 °C, during which time a few crystals of $NH_2OH$•HCl were periodically added whenever the solution turned bluish. After complete consumption of the terminal alkyne substrate (as monitored by TLC analysis), the mixture was diluted with saturated aqueous $NH_4Cl$ and extracted with EtOAc. The organic extracts were washed with brine, dried ($Na_2SO_4$), filtered, and concentrated. The residue was typically purified by flash chromatography on silica gel.

*B. Carbazole synthesis with the HDDA reaction*

The indicated triyne (or tetrayne) precursor was added to a glass vial. 1,2-Dichloroethane (DCE) or chloroform was added to bring the concentration of the multi-yne to 0.02 M. The indicated trapping agent (2–10 equiv) was then added. The vial was sealed with a Teflon-lined cap and placed in an oil bath held at 90, 100, or 120 °C. After 15 h, the reaction vessel was allowed to cool to room temperature, concentrated, and directly subjected to flash column chromatography on silica gel for purification.

**Preparation of the multi-yne precursors for HDDA cycloisomerization**

***HDDA precursors prepared***

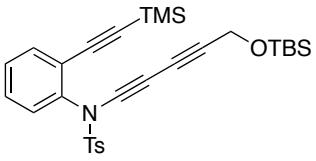


**604–TMS/CH2OTBS**

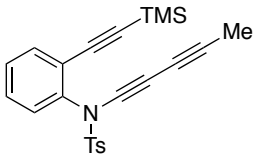


**601**

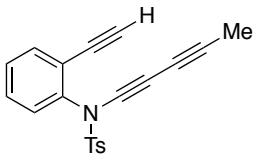


**604–H/Me**

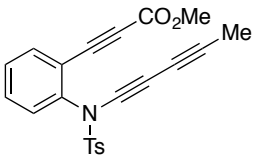


**604–E/Me**

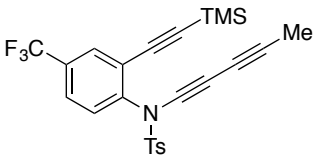


**604–(CF3)TMS/Me**

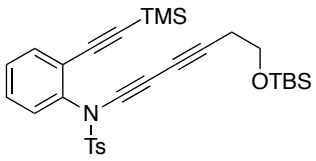


**604–TMS/tOTBS**

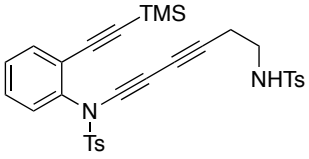


**604–TMS/tNHTs**

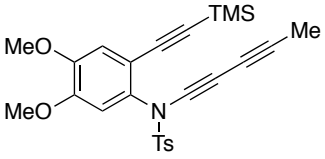


**617**

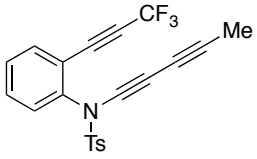


**620**

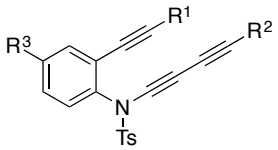


**604–($R^3$)$R^1$/$R^2$**

or

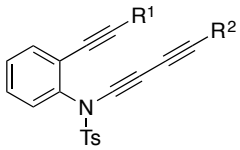


**604–$R^1$/$R^2$**

Naming logic for substrates **604**: **604–($R^3$)$R^1$/$R^2$** or **604–$R^1$/$R^2$** is used for HDDA precursors with the following structure unless otherwise defined. For any substrate with an intramolecularly tethered trapping group R, "tR" is used in lieu of $R^2$ (e.g., "tOTBS" signifies that an OTBS group is tethered as the intramolecular trapping agent).

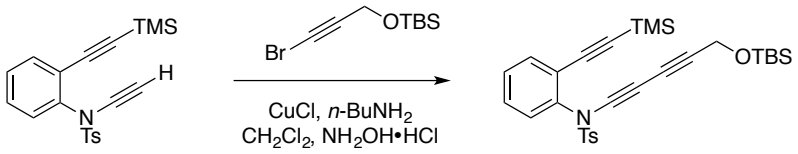


**S601** **604–TMS/CH2OTBS**

**Preparation of *N*-(5-((*tert*-butyldimethylsilyl)oxy)penta-1,3-diyn-1-yl)-4-methyl-*N*-(2-((trimethylsilyl)ethynyl)phenyl)benzenesulfonamide (604–TMS/CH2OTBS)**

Triyne **604–TMS/CH2OTBS** was prepared following General Procedure A using diyne precursor *N*-ethynyl-4-methyl-*N*-(2-((trimethylsilyl)ethynyl)phenyl)benzenesulfonamide[111] (43 mg, 0.12 mmol), ((3-bromoprop-2-yn-1-yl)oxy)(*tert*-butyl)dimethylsilane (50 μL), CuCl (1 mg, 0.01 mmol), *n*-$BuNH_2$ (0.5 mL), and $CH_2Cl_2$ (0.5 mL). Purification by flash column chromatography (hexanes: ethyl acetate = 5:1) gave the triyne **604–TMS/CH2OTBS** (46.1 mg, 0.086 mmol, 74%) as a pale yellow oil.

**$^1$H NMR** (500 MHz, $CDCl_3$): δ 7.68 (d, $J$ = 8.3 Hz, 2H, $SO_2Ar\mathit{H}_{ortho}$), 7.48-7.45 (nfom, 1H, Ar*H*), 7.35-7.28 (nfom, 5H, ArH), 4.40 (s, 2H, C$\mathit{H}_2$OTBS), 2.46 (s, 3H, $SO_2$Ar-C$\mathit{H}_3$), 0.89 (s, 9H, Si($CH_3$)C(C$\mathit{H}_3$)$_3$), 0.16 (s, 9H, Si(C$\mathit{H}_3$)$_3$), and 0.10 (s, 6H, Si(C$\mathit{H}_3$)C($CH_3$)$_3$).

**$^{13}$C NMR** (125 MHz, $CDCl_3$): δ 145.3, 138.4, 134.1, 130.0, 129.32, 129.30, 129.2, 128.7, 127.4, 122.7, 102.2, 99.4, 81.9, 70.1, 69.6, 58.6, 52.5, 26.0, 22.0, 18.5, -0.1, and -5.0.

**IR**: 2955, 2929, 2857, 2246, 2166, 1483, 1445, 1380, 1250, 1175, 1089, 1023, and 842 $cm^{-1}$.

**HRMS** (ESI-TOF): Calcd for $C_{29}H_{37}NNaO_3SSi_2^+$ $[M+Na]^+$ requires 558.1925; found 558.1931.

[111] Laroche, C.; Li, J.; Freyer, M. W.; Kerwin, S. M. Coupling reactions of bromoalkynes with imidazoles mediated by copper salts: synthesis of novel N-alkynylimidazoles. *J. Org. Chem.* **2008**, *73*, 6462–6465.

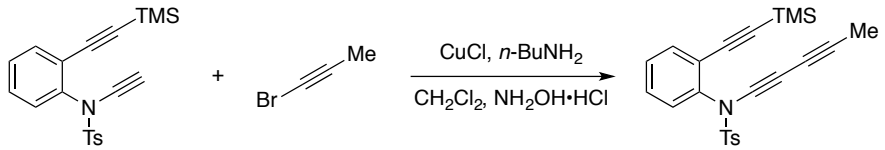


**S601** **S602** **601**

**Preparation of 4-methyl-*N*-(penta-1,3-diyn-1-yl)-*N*-(2-((trimethylsilyl)ethynyl)phenyl)benzenesulfonamide (601)**

Triyne **601** was prepared following General Procedure A using the diyne precursor *N*-ethynyl-4-methyl-*N*-(2-((trimethylsilyl)ethynyl)phenyl)benzenesulfonamide[87b] (**S601**, 201 mg, 0.55 mmol), 1-bromopropyne[106] (**S602**, 0.8 mL, 1.4 M in hexanes), CuCl (6 mg, 0.06 mmol), *n*-$BuNH_2$ (2 mL), and $CH_2Cl_2$ (2 mL). Purification by flash column chromatography (hexanes: ethyl acetate 12:1 to 5:1) gave the triyne **601** (193 mg, 0.48 mmol, 87%) as a pale yellow oil.

**$^1$H NMR** (500 MHz, $CDCl_3$): δ 7.67 (d, $J$ = 8.3 Hz, 2H, $SO_2Ar\mathit{H}_{ortho}$), 7.48-7.44 (nfom, 1H, Ar*H*), 7.34-7.27 (nfom, 5H, ArH), 2.45 (s, 3H, $SO_2$Ar-C$\mathit{H}_3$), 1.94 (s, 3H, C≡C-C$\mathit{H}_3$), and 0.17 (s, 9H, -Si(C$\mathit{H}_3$)$_3$).

**$^{13}$C NMR** (125 MHz, $CDCl_3$): δ 145.1, 138.7, 134.7, 134.2, 130.0 (br, 2C), 129.3, 129.1, 128.7, 122.7, 102.2, 99.6, 80.4, 66.4, 64.2, 59.1, 22.0, 4.8, and 0.2.

**IR**: 2958, 2257, 2172, 1596, 1483, 1445, 1379, 1174, 857, and 845 $cm^{-1}$.

**HRMS** (ESI-TOF): Calcd for $C_{23}H_{23}NNaO_2SSi^+$ $[M+Na]^+$ requires 428.1111; found 428.1107.

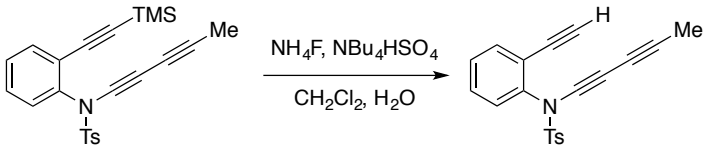


**601** **604–H/Me**

**Preparation of *N*-(2-ethynylphenyl)-4-methyl-*N*-(penta-1,3-diyn-1-yl)benzenesulfonamide (604–H/Me)**

Triyne **601** (30 mg, 0.074 mmol), $CH_2Cl_2$ (1 mL), and $NBu_4HSO_4$ (2 mg, 5.9 μmol) were combined in a small glass vial. A stir bar was added. $NH_4F$ (aq, 10 M) was added to the suspension at room temperature. The reaction mixture was stirred vigorously at room temperature for 2 h. The mixture was partitioned between $NH_4Cl$ (aq) and ethyl acetate. The organic layer was washed with brine, dried with anhydrous $Na_2SO_4$, concentrated, and purified by column chromatography (hexanes: ethyl acetate = 5: 1) to give **604–H/Me** (15 mg, 0.045 mmol, 61%) as a pale yellow oil.

**$^1$H NMR** (500 MHz, $CDCl_3$): δ 7.71 (d, $J$ = 8.3 Hz, 2H, $SO_2Ar\mathit{H}_{ortho}$), 7.52-7.48 (nfom, 1H, Ar*H*), 7.37-7.33 (nfom, 2H, Ar*H*), 7.33 (d, $J$ = 8.1 Hz, 2H, $ArSO_2Ar\mathit{H}_{meta}$), 7.22-7.18 (m, 1H, Ar*H*), 3.03 (s, 1H, C≡C*H*), 2.46 (s, 3H, $SO_2Ar$-C$\mathit{H}_3$), and 1.95 (s, 3H, C≡C-C$\mathit{H}_3$).

**$^{13}$C NMR** (125 MHz, $CDCl_3$): δ 145.4, 139.3, 134.32, 134.27, 129.9, 129.8, 129.4, 129.2, 128.7, 122.3, 83.5, 80.5, 78.6, 66.7, 63.9, 58.5, 21.9, and 4.9.

**IR**: 3283, 2923, 2256, 2173, 1482, 1445, 1375, 1172, 1089, and 918 $cm^{-1}$.

**HRMS** (ESI-TOF): Calcd for $C_{20}H_{15}NNaO_2S^+$ $[M+Na]^+$ requires 356.0716; found 356.0719.

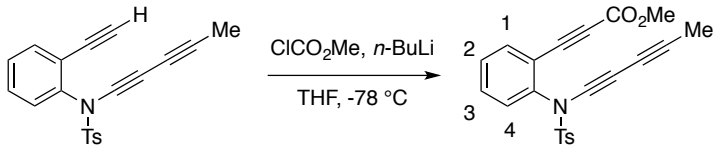


**604–H/Me** **604–E/Me**

**Preparation of methyl 3-(2-((4-methyl-*N*-(penta-1,3-diyn-1-yl)phenyl)sulfonamido)phenyl)propiolate (604–E/Me)**

A solution of *N*-(2-ethynylphenyl)-4-methyl-*N*-(penta-1,3-diyn-1-yl)benzenesulfonamide (**604–H/Me**, 40 mg, 0.12 mmol) in THF (2 mL) was cooled to -78 °C inside of a septum-sealed vial under a slight positive pressure of $N_2$. A solution of *n*-BuLi (0.07 mL, 0.18 mmol, 2.5 M in hexanes) was added dropwise via a syringe. This mixture was stirred at -78 °C for 2 h, and methyl chloroformate (30 μL, 0.39 mmol) was added. The vial was allowed to warm to room temperature over ca. 30 min. The reaction mixture was partitioned between ethyl acetate and saturated aqueous solution of $NH_4Cl$. The organic layer was washed with brine, dried with anhydrous $Na_2SO_4$, filtered, and concentrated. The residue was purified by column chromatography on silica gel (hexanes:ethyl acetate = 5:1) to give methyl 3-(2-((4-methyl-*N*-(penta-1,3-diyn-1-yl)phenyl)sulfonamido)phenyl)propiolate (**604–E/Me**, 38 mg, 0.1 mmol, 81% yield) as a yellow oil.

**$^1$H NMR** (500 MHz, $CDCl_3$): δ 7.69 (d, *J* = 8.3 Hz, 2H, $SO_2Ar\mathit{H}_{ortho}$), 7.55 (br dd, *J* = 7.6, 1.5 Hz, 1H, $Ar\mathit{H}_1$), 7.47 (br ddd, *J* = 1.6, 7.7, 7.8 Hz, 1H, $Ar\mathit{H}_3$), 7.39 (br ddd, *J* = 1.1, 7.6, 7.6 Hz, 1H, $Ar\mathit{H}_2$), 7.36 (br dd, *J* = 8.0, 0.8 Hz, 1H, $Ar\mathit{H}_4$), 7.30 (d, *J* = 8.0 Hz, 2H, $ArSO_2Ar\mathit{H}_{meta}$), 3.81 (s, 3H, $CO_2C\mathit{H}_3$), 2.44 (s, 3H, $SO_2Ar\text{-}C\mathit{H}_3$), and 1.95 (s, 3H, C≡C-$C\mathit{H}_3$).

**$^{13}$C NMR** (125 MHz, $CDCl_3$): δ 153.9, 145.7, 139.8, 135.0, 133.6, 131.6, 130.0, 129.9, 129.5, 128.7, 119.7, 85.4, 81.1, 80.6, 66.2, 63.8, 59.2, 52.9, 21.9, and 4.8.

**IR**: 2950 (w), 2900 (w), 2229, 2173, 1714, 1596, 1486, 1446, 1378, 1301, 1210, 1174, 1089, and 1029 $cm^{-1}$.

**HRMS** (ESI-TOF): Calcd for $C_{22}H_{17}NNaO_4S^+$ $[M+Na]^+$ requires 414.0770; found 414.0783.

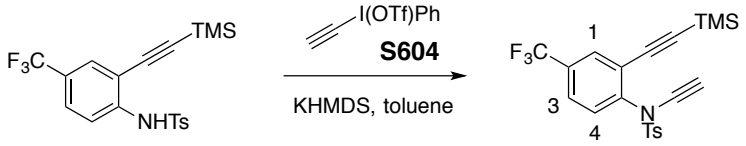


**S603** **S605**

**Preparation of *N*-ethynyl-4-methyl-*N*-(4-(trifluoromethyl)-2-((trimethylsilyl)ethynyl)phenyl)benzene-sulfonamide (S605)**

A solution of amide **S603**[112] (105 mg, 0.26 mmol) in anhydrous toluene (13 mL) was added to a 100 mL round bottom flask. The reaction flask was cooled to 0 °C in an ice-water bath under $N_2$ protection. A solution of KHMDS (0.8 mL, 0.5 M in toluene, 0.4 mmol) was added dropwise. After 45 min, alkynyliodonium salt **S604**[113] (200 mg, 0.53 mmol) was added as a slurry in $CH_2Cl_2$ (25 mL). After overnight stirring at room temperature, the reaction mixture was concentrated and partitioned between ethyl acetate and brine. The organic layer was dried with anhydrous $Na_2SO_4$, filtered, and concentrated. The residue was purified with column chromatography (hexanes: ethyl acetate = 12:1 to 5:1) to give **S605** (82 mg, 0.19, 74%) as a pale yellow oil.

**$^1$H NMR** (500 MHz, $CDCl_3$): δ 7.75 (ddq, $J$ = 2.2, 0.5, 0.7 Hz, 1H, Ar$H_1$), 7.70 (d, $J$ = 8.3 Hz, 2H, $ArSO_2ArH_{ortho}$), 7.57 (ddq, $J$ = 8.4, 2.2, 0.7 Hz, 1H, Ar$H_3$), 7.44 (ddq, $J$ = 8.4, 0.5, 0.8 Hz, 1H, Ar$H_4$), 7.33 (d, $J$ = 8.1 Hz, 2H, $ArSO_2ArH_{meta}$), 2.85 (s, 1H, C≡C-$H$), 2.46 (s, 3H, $SO_2$Ar-C$H_3$), and 0.17 (s, 9H, -Si(C$H_3$)$_3$).

**$^{13}$C NMR** (125 MHz, $CDCl_3$): δ 145.5, 141.6 (br), 134.5, 131.4 (q, $J$ = 33.3 Hz), 131.3 (q,

[112] Ohta, Y.; Chiba, H.; Oishi, S.; Fujii, N.; Ohno, H. Construction of nitrogen heterocycles bearing an aminomethyl group by copper-catalyzed domino three-component coupling−cyclization. *J. Org. Chem.* **2009**, *74*, 7052–7058.

[113] Kitamura, T.; Morshed, M. H.; Tsukada, S.; Miyazaki, Y.; Iguchi, N.; Inoue, D. Alkynylation of benzotriazole with silylethynyliodonium triflates. regioselective synthesis of 2-ethynyl-2H-benzotriazole derivatives. *J. Org. Chem.* **2011**, *76*, 8117–8120.

$J$ = 3.7 Hz), 130.03, 129.97, 128.7, 125.9 (3.6 Hz), 123.8, 123.4 (q, $J$ = 272.5 Hz), 104.2, 98.4, 74.9, 60.1, 22.0, and -0.2.

**IR**: 3299, 2961, 2135, 1597, 1493, 1413, 1379, 1332, 1251, 1173, 1132, 884, and 845 $cm^{-1}$.

**HRMS** (ESI-TOF): Calcd for $C_{21}H_{20}F_3NNaO_2SSi^+$ $[M+Na]^+$ requires 458.0828; found 458.0831.

---

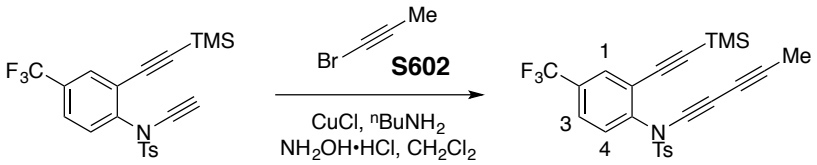


**S605** **604–(CF3)TMS/Me**

**Preparation of 4-methyl-*N*-(penta-1,3-diyn-1-yl)-*N*-(4-(trifluoromethyl)-2-((trimethylsilyl)ethynyl)phenyl)benzenesulfonamide (604–(CF3)TMS/Me)**

Triyne **604–(CF3)TMS/Me** was prepared following General Procedure A using the diyne precursor *N*-ethynyl-4-methyl-*N*-(2-((trimethylsilyl)ethynyl)phenyl)benzenesulfonamide (**S605**, 40 mg, 0.092 mmol), 1-bromopropyne (**S602**, 0.13 mL, 1.4 M in hexanes), CuCl (1 mg, 0.01 mmol), *n*-$BuNH_2$ (0.5 mL), and $CH_2Cl_2$ (0.5 mL). Purification by flash column chromatography (hexanes: ethyl acetate 12:1 to 5:1) gave the triyne **604–(CF3)TMS/Me** (41.4 mg, 0.087 mmol, 95%) as a pale yellow oil.

**$^1$H NMR** (500 MHz, $CDCl_3$): δ 7.72 (ddq, $J$ = 2.2, 0.5, 0.8 Hz, 1H, Ar$H_1$), 7.67 (d, $J$ = 8.3 Hz, 2H, $ArSO_2ArH_{ortho}$), 7.56 (ddq, $J$ = 8.4, 2.2, 0.7 Hz, 1H, Ar$H_3$), 7.45 (ddq, $J$ = 8.4, 0.8, 0.4 Hz, 1H, Ar$H_4$), 7.33 (d, $J$ = 8.1 Hz, 2H, $ArSO_2ArH_{meta}$), 2.46 (s, 3H, $SO_2Ar$-C$H_3$), 1.95 (s, 3H, C≡C-C$H_3$), and 0.17 (s, 9H, Si(C$H_3$)$_3$).

**$^{13}$C NMR** (125 MHz, $CDCl_3$): δ 145.6, 141.5 (br), 134.4, 131.3 (q, $J$ = 33.5 Hz), 131.3 (q, $J$ = 3.7 Hz), 130.1, 129.9, 128.6, 125.8 (q, $J$ = 3.5 Hz), 123.3, 123.3 (q, $J$ = 273.2 Hz), 104.6, 98.0, 80.9, 65.5, 63.9, 60.1, 22.0, 4.7, and -0.3.

---

**IR**: 2960, 2920, 2258, 2173, 1492, 1414, 1382, 1330, 1251, 1174, 1133, 1122, 878, and 845 $cm^{-1}$.

**HRMS** (ESI-TOF): Calcd for $C_{24}H_{22}F_3NNaO_2SSi^+$ $[M+Na]^+$ requires 496.0985; found 496.0987.

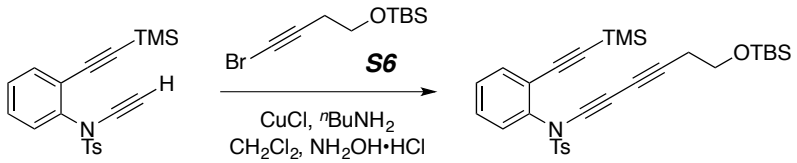


***S1*** ***4–TMS/tOTBS***

**_N_-(6-((_tert_-butyldimethylsilyl)oxy)hexa-1,3-diyn-1-yl)-4-methyl-_N_-(2-((trimethylsilyl)ethynyl)phenyl) benzenesulfonamide (604–TMS/tOTBS)**

Triyne **604–TMS/tOTBS** was prepared following General Procedure A using the diyne precursor *N*-ethynyl-4-methyl-*N*-(2-((trimethylsilyl)ethynyl)phenyl)benzenesulfonamide (**S601**, 20 mg, 0.054 mmol), ((4-bromobut-3-yn-1-yl)oxy)(*tert*-butyl)dimethylsilane[114] (**S606**, 21.5 mg, 0.082 mmol), CuCl (1 mg, 0.01 mmol), *n*-$BuNH_2$ (0.3 mL), and $CH_2Cl_2$ (0.5 mL). Purification by flash column chromatography (hexanes: ethyl acteate 12:1 to 5:1) gave the triyne **604–TMS/tOTBS** (17.2 mg, 0.031 mmol, 57%) as a pale yellow oil.

**$^1$H NMR** (500 MHz, $CDCl_3$): δ 7.67 (d, $J$ = 8.3 Hz, 2H, $SO_2Ar\mathit{H}_{ortho}$), 7.47-7.44 (nfom, 1H, Ar*H*), 7.33-7.27 (nfom, 5H, ArH), 3.71 (t, $J$ = 7.3 Hz, 2H, $C\mathit{H}_2OTBS$), 2.51 (t, $J$ = 7.3 Hz, 2H, $C\mathit{H}_2CH_2OTBS$), 2.45 (s, 3H, $SO_2Ar\text{-}C\mathit{H}_3$), 0.89 (s, 9H, $Si(CH_3)_2C(C\mathit{H}_3)_3$), 0.16 (s, 9H, $-Si(C\mathit{H}_3)_3$), and 0.06 (s, 6H, $Si(C\mathit{H}_3)_2C(CH_3)_3$).

**$^{13}$C NMR** (125 MHz, $CDCl_3$): δ 145.1, 138.6, 134.7, 134.1, 129.9, 129.3 (2C), 129.1, 128.6, 122.7, 102.1, 99.5, 81.4, 67.2, 66.2, 61.8, 59.0, 26.1, 24.2, 22.0, 18.5, -0.1, and -5.1.

[114] Li, L.-S.; Wu, Y.-L. An efficient method for synthesis of α-keto acid esters from terminal alkynes. *Tetrahedron Lett.* **2002**, *43*, 2427–2430.

**IR**: 2955, 2928, 2857, 2253, 2169, 1380, 1250, 1175, 1104, and 843 $cm^{-1}$.

**HRMS** (ESI-TOF): Calcd for $C_{30}H_{39}NNaO_3SSi_2^+$ $[M+Na]^+$ requires 572.2081; found 572.2092.

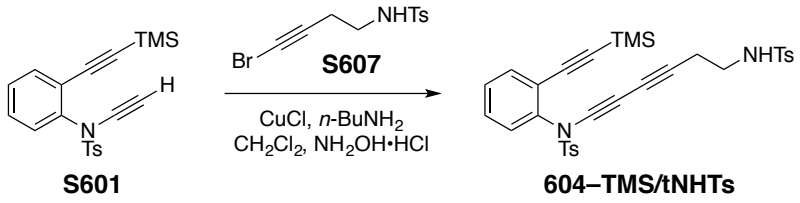


**Preparation of 4-methyl-*N*-(6-((4-methylphenyl)sulfonamido)hexa-1,3-diyn-1-yl)-*N*-(2-((trimethylsilyl)ethynyl)phenyl)benzenesulfonamide (604–TMS/tNHTs)**

Triyne **604–TMS/tNHTs** was prepared following General Procedure A using the diyne precursor *N*-ethynyl-4-methyl-*N*-(2-((trimethylsilyl)ethynyl)phenyl)benzenesulfonamide (**S601**, 50 mg, 0.14 mmol), *N*-(4-bromobut-3-yn-1-yl)-4-methylbenzenesulfonamide[115] (**S607**, 62 mg, 0.21 mmol), CuCl (1 mg, 0.01 mmol), *n*-$BuNH_2$ (1 mL), and $CH_2Cl_2$ (1 mL). Purification by flash column chromatography (hexanes: ethyl acteate = 3:1) gave the triyne **604–TMS/tNHTs** (73 mg, 0.12 mmol, 91%) as a pale yellow oil. This yield is of chromatographed material that still contains a small amount of a co-eluting impurity containing *i*-Pr resonances.

**$^1$H NMR** (500 MHz, $CDCl_3$): δ 7.74 (d, $J$ = 8.2 Hz, 2H, $SO_2Ar_aH_{ortho}$), 7.66 (d, $J$ = 8.2 Hz, 2H, $SO_2Ar_bH_{ortho}$), 7.48-7.45 (nfom, 1H, Ar*H*), 7.36-7.28 (nfom, 7H, ArH), 4.77-4.72 (br m, 1H, N*H*Ts), 3.09 (dt, $J$ = 6.5, 6.5 Hz, 2H, $CH_2CH_2$NHTs), 2.46 (t, $J$ = 6.5 Hz, 2H, $CH_2CH_2$NHTs), 2.46 (s, 3H, $SO_2Ar_a$-$CH_3$), 2.42 (s, 3H, $SO_2Ar_b$-$CH_3$), and 0.16 (s, 9H, $Si(CH_3)_3$).

**$^{13}$C NMR** (125 MHz, $CDCl_3$): δ 145.4, 143.9, 138.3, 137.0, 134.5, 134.2, 130.03, 130.02,

[115] Yoo, W.-J.; Allen, A.; Villeneuve, K.; Tam, W. Rhodium-catalyzed intramolecular [4 + 2] cycloadditions of alkynyl halides. *Org. Lett.* **2005**, *7*, 5853–5856.

129.4, 129.30, 129.29, 128.6, 127.3, 122.7, 102.2, 99.5, 80.1, 68.0, 67.4, 58.5, 41.8, 22.0, 21.7, 21.3, and -0.1.

**IR**: 3292, 2962, 2252, 2169, 1597, 1482, 1445, 1378, 1331, 1161, 1090, and 845 $cm^{-1}$.

**HRMS** (ESI-TOF): Calcd for $C_{31}H_{32}N_2NaO_4S_2Si^+$ $[M+Na]^+$ requires 611.1465; found 611.1494.

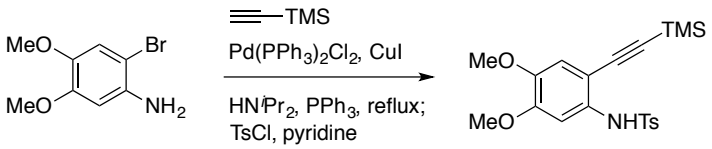


***613*** ***614***

**Preparation of *N*-(4,5-dimethoxy-2-((trimethylsilyl)ethynyl)phenyl)-4-methylbenzenesulfonamide (614)**

A mixture of 2-bromo-4,5-dimethoxyaniline[116] (**613**, 7 g, 30 mmol), ethynyltrimethylsilane (7 mL, 49 mmol), triphenylphosphine (510 mg, 2 mmol), and diisopropylamine (130 mL) were combined in a 200 mL round bottom flask. A reflux condenser was attached with a rubber septum on the top. Oxygen dissolved in this solution was removed via bubbling of nitrogen gas through an 18-gauge needle with stirring at room temperature for 10 min. A powdered mixture of $Pd(PPh_3)_2Cl_2$ (680 mg, 0.97 mmol) and CuI (185 mg, 0.97 mmol) was added. The reaction mixture was kept under a slight positive pressure of $N_2$ and was brought to reflux through heating in an oil bath. After 2 days, the reaction was cooled to room temperature. Additional ethynyltrimethylsilane (1 mL, 7 mmol), triphenylphosphine (340 mg, 1.3 mmol), $Pd(PPh_3)_2Cl_2$ (450 mg, 0.64 mmol) and CuI (120 mg, 0.63 mmol) were added. The solution was sparged again with $N_2$ gas for 10 min. The mixture was heated to reflux temperature for one additional day under a slight positive pressure of $N_2$. This reaction mixture was cooled to room temperature, filtered through a short pad of Celite, and

[116] De Leon, P.; Egbertson, M.; Hills, I. D.; Johnson, A. W.; Machacek, M. Quinolinone PDE2 inhibitors. U.S. Patent 2456440 B1, August 19, 2015.

concentrated to give a dark brown oil. This oil was redissolved in pyridine (60 mL). Toluenesulfonyl chloride (5.72 g, 30 mmol) was added and the mixture was allowed to stir at room temperature overnight. This mixture was concentrated, and the residue was partitioned between ethyl acetate and 2M HCl (aq). The organic layer was washed with brine, dried with $Na_2SO_4$, filtered, and concentrated. The residue was purified by flash column chromatrography (hexanes:ethyl acetate = 12:1 to 3:1) to give *N*-(4,5-dimethoxy-2-((trimethylsilyl)ethynyl)phenyl)-4-methylbenzenesulfonamide (**614**, 6.8 g, 16.8 mmol, 56%) as an off-white solid.

**$^1$H NMR** (500 MHz, $CDCl_3$): δ 7.58 (d, $J$ = 8.4 Hz, 2H, $SO_2Ar\mathit{H}_{ortho}$), 7.22 (s, 1H, Ar*H*), 7.18 (d, $J$ = 8.5 Hz, 2H, $ArSO_2Ar\mathit{H}_{meta}$), 6.93 (br s, 1H, N*H*Ts), 6.72 (s, 1H, Ar*H*), 3.92 [s, 3H, $Ar(OC\mathit{H}_3)_a$], 3.79 [s, 3H, $Ar(OC\mathit{H}_3)_b$], 2.37 (s, 3H, $SO_2Ar\text{-}C\mathit{H}_3$), and 0.24 (s, 9H, $C{\equiv}C\text{-}Si(C\mathit{H}_3)_3$).

**$^{13}$C NMR** (125 MHz, $CDCl_3$): δ 150.6, 146.3, 144.1, 136.1, 132.7, 129.7, 127.5, 113.6, 107.0, 105.6, 100.4, 100.0, 56.4, 56.2, 21.8, and 0.2.

**IR**: 3300, 2959, 2147, 1609, 1510, 1391, 1350, 1215, 1164, 1005, and 846 $cm^{-1}$.

**HRMS** (ESI-TOF): Calcd for $C_{20}H_{25}NNaO_4SSi^+$ $[M+Na]^+$ requires 426.1166; found 426.1164.

**mp:** 119–120 °C.

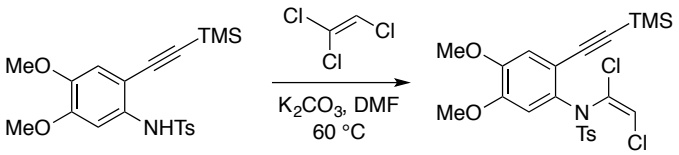


**614** **615**

**Preparation of (*E*)-*N*-(1,2-dichlorovinyl)-*N*-(4,5-dimethoxy-2-((trimethylsilyl)ethynyl)phenyl)-4-methylbenzenesulfonamide (615)**

A mixture of *N*-(4,5-dimethoxy-2-((trimethylsilyl)ethynyl)phenyl)-4-methylbenzenesulfonamide (**614**, 2 g, 5 mmol), $K_2CO_3$ (2.1 g, 15 mmol), trichloroethylene (1.35 mL, 15 mmol), and DMF (4 mL) were combined in a 20 mL vial. This vial was closed with a Teflon-lined cap and placed in a 60 °C oil bath with stirring overnight. The crude reaction mixture was partitioned between ethyl acetate and brine. The organic layer was dried with anhydrous $Na_2SO_4$, filtered, and concentrated. The residue was purified by column chromatography on silica gel (hexanes:ethyl acetate=3:1) to give (*E*)-*N*-(1,2-dichlorovinyl)-*N*-(4,5-dimethoxy-2-((trimethylsilyl)ethynyl)phenyl)-4-methylbenzenesulfonamide (**615**, 1.8 g, 3.6 mmol) as a white foam-like solid.

**$^1$H NMR** (500 MHz, $CDCl_3$): δ 7.70 (d, $J$ = 8.4 Hz, 2H, $SO_2ArH_{ortho}$), 7.24 (d, $J$ = 8.5 Hz, 2H, $ArSO_2ArH_{meta}$), 7.06 (s, 1H, Ar*H*), 6.91 (s, 1H, Ar*H*), 6.36 (s, 1H, NCCl=C*H*Cl), 3.88 [s, 3H, Ar(OC$H_3$)$_a$], 3.80 [s, 3H, Ar(OC$H_3$)$_b$], 2.42 (s, 3H, $SO_2$Ar-C$H_3$), and 0.15 (s, 9H, C≡C-Si(C$H_3$)$_3$).

**$^{13}$C NMR** (125 MHz, $CDCl_3$): δ 149.4, 149.1, 144.7, 136.2, 131.5, 130.8, 129.6, 129.2, 118.5, 117.4, 116.1, 115.5, 101.6, 98.9, 56.31, 56.26, 21.9, and 0.0.

**IR**: 2962, 2159, 1599, 1512, 1353, 1220, 1169, 1073, 1006, and 845 cm$^{-1}$.

**HRMS** (ESI-TOF): Calcd for $C_{22}H_{25}Cl_2NNaO_4SSi^+$ $[M+Na]^+$ requires 520.0543; found 520.0571.

**mp:** 45–47 °C.

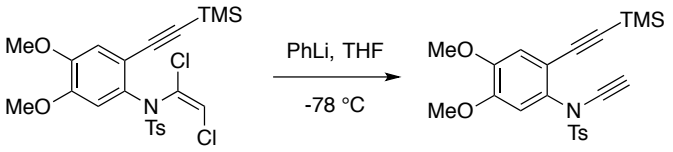


***615*** ***616***

**Preparation of *N*-(4,5-dimethoxy-2-((trimethylsilyl)ethynyl)phenyl)-*N*-ethynyl-4-methylbenzenesulfonamide (616)**

A solution of (*E*)-*N*-(1,2-dichlorovinyl)-*N*-(4,5-dimethoxy-2-((trimethylsilyl)ethynyl)phenyl)-4-methylbenzenesulfonamide (**615**, 1.5 g, 3 mmol) in THF (30 mL, 10 mL/mmol) was cooled to -78 °C in a septum-sealed round bottom flask equipped with a $N_2$ line. A solution of PhLi (5.1 mL, 1.3 M in diethyl ether) was added slowly over 10 min to form an orange-red solution. This mixture was stirred at -78 °C for 4 h before addition of $H_2O/Et_2O$ (2 mL, 1:1) at this temperature. The reaction flask was then allowed to warm to room temperature. The reaction mixture was partitioned between ethyl acetate and a saturated aqueous solution of $NH_4Cl$. The organic layer was washed with brine, dried with anhydrous $Na_2SO_4$, filtered, and concentrated. The residue was purified with column chromatography on silica gel (hexanes:ethyl acetate=5:1) to give *N*-(4,5-dimethoxy-2-((trimethylsilyl)ethynyl)phenyl)-*N*-ethynyl-4-methylbenzenesulfonamide (**616**, 1.2 g, 2.8 mmol, 93%) as a pale yellow oil.

**$^1$H NMR** (500 MHz, $CDCl_3$): δ 7.71 (d, $J$ = 7.9 Hz, 2H, $SO_2ArH_{ortho}$), 7.30 (d, $J$ = 8.0 Hz, 2H, $ArSO_2ArH_{meta}$), 6.90 (s, 1H, Ar*H*), 6.75 (s, 1H, Ar*H*), 3.87 [s, 3H, $Ar(OCH_3)_a$], 3.82 [s, 3H, $Ar(OCH_3)_b$], 2.84 (s, 1H, C C*H*), 2.44 (s, 3H, $SO_2Ar$-$CH_3$), and 0.15 (s, 9H, C≡C-Si($CH_3$)$_3$).

**$^{13}$C NMR** (125 MHz, $CDCl_3$): δ 149.7, 149.3, 145.0, 134.7, 132.1, 129.8, 128.7, 115.2, 115.1, 112.3, 100.0, 99.8, 75.8, 58.9, 56.3 (2C), 21.9, and 0.1.

**IR**: 3294, 2966, 2160, 2133, 1600, 1511, 1374, 1223, 1173, 1003, and 848 $cm^{-1}$.

**HRMS** (ESI-TOF): Calcd for $C_{22}H_{25}NNaO_4SSi^+$ $[M+Na]^+$ requires 450.1166; found 450.1172.

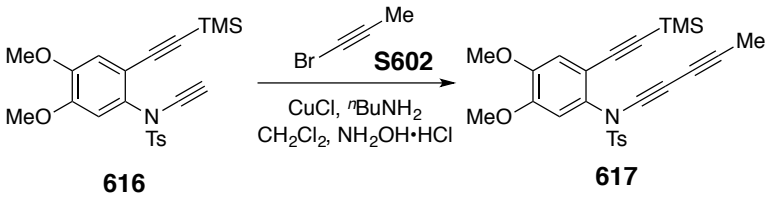


**616** **617**

**Preparation of *N*-(4,5-dimethoxy-2-((trimethylsilyl)ethynyl)phenyl)-4-methyl-*N*-(penta-1,3-diyn-1-yl)benzenesulfonamide (617)**

Triyne **617** was prepared following General Procedure A using the diyne precursor *N*-(4,5-dimethoxy-2-((trimethylsilyl)ethynyl)phenyl)-*N*-ethynyl-4-methylbenzenesulfonamide (**616**, 630 mg, 1.47 mmol), 1-bromopropyne (**S602**, 1.7 mL, 1.3 M in hexanes), CuCl (15 mg, 0.15 mmol), *n*-$BuNH_2$ (8 mL), and $CH_2Cl_2$ (8 mL). Purification by flash column chromatography (hexanes:ethyl acetate=5:1) gave the triyne **617** (670 mg, 1.44 mmol, 98%) as a pale yellow oil.

**$^1$H NMR** (500 MHz, $CDCl_3$): δ 7.68 (d, $J$ = 8.3 Hz, 2H, $SO_2Ar\mathit{H}_{ortho}$), 7.30 (d, $J$ = 8.0 Hz, 2H, $ArSO_2Ar\mathit{H}_{meta}$), 6.87 (s, 1H, Ar*H*), 6.76 (s, 1H, Ar*H*), 3.87 [s, 3H, $Ar(OC\mathit{H}_3)_a$], 3.83 [s, 3H, $Ar(OC\mathit{H}_3)_b$], 2.45 (s, 3H, $SO_2Ar\text{-}C\mathit{H}_3$), 1.95 (s, 3H, $C{\equiv}C\text{-}C\mathit{H}_3$), and 0.15 (s, 9H, $C{\equiv}C\text{-}Si(C\mathit{H}_3)_3$).

**$^{13}$C NMR** (125 MHz, $CDCl_3$): δ 149.6, 149.2, 145.1, 134.6, 132.1, 129.9, 128.7, 115.1, 114.9, 112.3, 100.2, 99.7, 80.3, 66.5, 64.2, 58.9, 56.4, 56.3, 22.0, 4.8, and -0.1.

**IR**: 2965, 2258, 2161, 1601, 1510, 1375, 1220, 1173, 1033, and 845 $cm^{-1}$.

**HRMS** (ESI-TOF): Calcd for $C_{25}H_{27}NNaO_4SSi^+$ $[M+Na]^+$ requires 488.1322; found 488.1338.

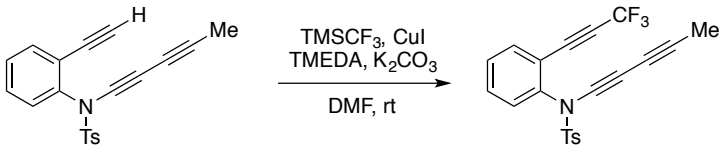


**604–H/Me** **620**

**Preparation of 4-methyl-*N*-(penta-1,3-diyn-1-yl)-*N*-(2-(3,3,3-trifluoroprop-1-yn-1-yl)phenyl)benzenesulfonamide (620)**[117]

CuI (57 mg, 0.3 mmol, 1.5 equiv), $K_2CO_3$ (83 mg, 0.6 mmol, 3 equiv), and dry DMF (1.0 mL, ca. 5 mL•mmol$^{-1}$ of alkyne substrate) were combined in a 20 mL scintillation vial equipped with a stir bar and capped with a rubber septum. A large reaction container with a flat bottom is preferred, in order to facilitate $O_2$ dissolution. A balloon filled with dry air was attached. The mixture was stirred vigorously at room temperature while anhydrous TMEDA was introduced via syringe. The white suspension immediately turned blue. This suspension was allowed to stir at ambient temperature for 15 min before addition of $TMSCF_3$ (70 μL, 2.4 eq.) The resulting deep green solution was allowed to stir at room temperature for an additional 5 min before being cooled to 0 °C in an ice-water bath. A solution of triyne **604-H/Me** (66 mg, 0.20 mmol) and $TMSCF_3$ (70 μL, 2.4 equiv) in dry DMF (1.0 mL, ca. 5 mL•mmol$^{-1}$ of alkyne substrate) was slowly added over 10 min at 0 °C. The deep green reaction mixture was allowed to warm to room temperature overnight with stirring. After 16 h TLC analysis confirmed full consumption of the starting alkyne. The resulting mixture was partitioned between ethyl acetate and brine. The organic layer was washed with brine twice, dried over anhydrous $Na_2SO_4$, and concentrated. The residue was purified by column chromatography on silica gel (hexanes:ethyl acetate = 5:1) to give the trifluoromethylated triyne **620** (73 mg, 0.18 mmol, 92%) as a pale yellow oil.

**$^1$H NMR** (500 MHz, $CDCl_3$): δ 7.64 (d, $J$ = 8.3 Hz, 2H, $SO_2Ar\mathit{H}_{ortho}$), 7.55-7.49 (m, 2H, Ar*H*), 7.45 (br d, $J$ = 7.4 Hz, 1H, Ar*H*), 7.39 (br dd, $J$ = 8, 8 Hz, 1H, Ar*H*), 7.32 (d, $J$ = 8.0 Hz, 2H, $ArSO_2Ar\mathit{H}_{meta}$), 2.45 (s, 3H, $SO_2Ar$-C$\mathit{H}_3$), and 1.96 (s, 3H, C≡C-C$\mathit{H}_3$).

[117] Tresse, C.; Guissart, C.; Schweizer, S.; Bouhoute, Y.; Chany, A.-C.; Goddard, M.-L.; Blanchard, N.; Evano, G. *Adv. Synth. Catal.* **2014**, *356*, 2051–2060.

**$^{13}$C NMR** (125 MHz, $CDCl_3$): δ 146.0, 139.7, 134.7, 133.6, 132.0, 130.3, 130.2, 129.5, 128.4, 118.2, 114.5 (q, J = 257.7), 81.5 (q, *J* = 6.5 Hz), 81.0 (q, *J* = 53.2 Hz), 80.9, 65.8, 63.5, 59.6, 21.9, and 4.8.

**IR**: 2258, 2174, 1487, 1448, 1381, 1316, 1175, 1143, 1090, and 813 $cm^{-1}$.

**HRMS** (ESI-TOF): Calcd for $C_{21}H_{14}F_3NNaO_2S^+$ $[M+Na]^+$ requires 424.0590; found 424.0607.

**Preparation of carbazole derivatives from HDDA cycloisomerization reaction**

***Carbazoles prepared***

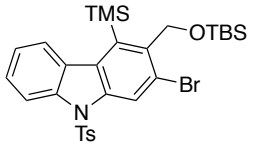


***6a***

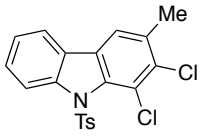


***6b***

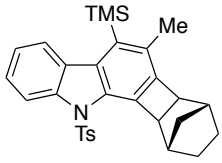


***6c***

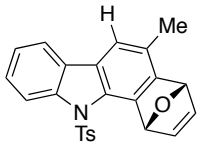


***6d***

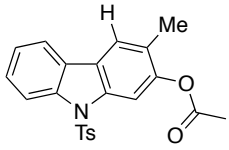


***6e***

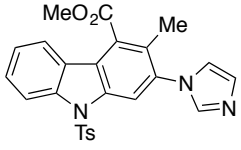


***6f***

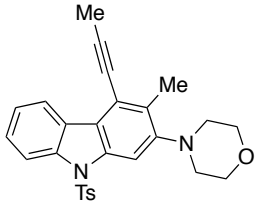


***6g***

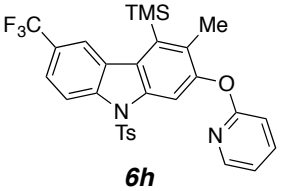


***6h***

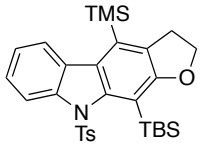


***6i***

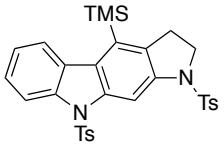


***6j***

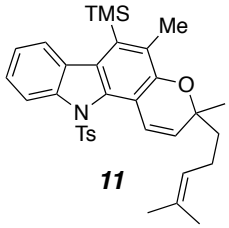


***11***

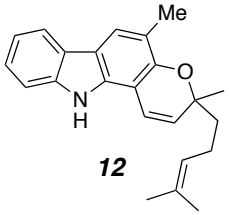


***12***

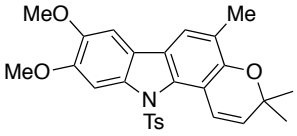


***19***

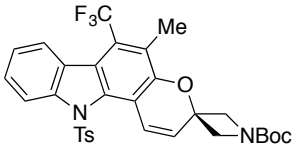


***22***

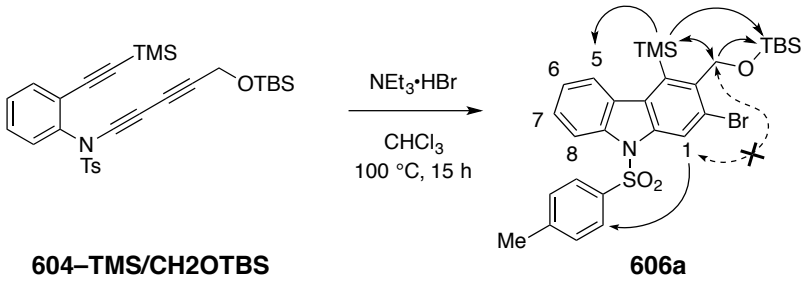


**604–TMS/CH2OTBS** **606a**

**Preparation of 2-bromo-3-methyl-9-tosyl-4-(trimethylsilyl)-9*H*-carbazole (606a)**

Compound **606a** was prepared following General Procedure B using **601** (25 mg, 47 μmol), $NEt_3$•HBr (18 mg, 99 μmol), and $CHCl_3$ (2.3 mL). Purification by column chromatography (hexanes: ethyl acetate = 5:1) gave product **606a** (25 mg, 41 μmol, 87%) as a pale yellow oil.

**$^1$H NMR** (500 MHz, $CDCl_3$): δ 8.66 (s, 1H, Ar$H_1$), 8.35 (ddd, $J$ = 8.4, 1.1, 0.6 Hz, 1H, Ar$H_8$), 8.06 (ddd, $J$ = 8.1, 1.2, 0.6 Hz, 1H, Ar$H_5$), 7.67 (d, $J$ = 8.4 Hz, 2H, $ArSO_2Ar H_{ortho}$), 7.46 (ddd, $J$ = 8.4, 7.2, 1.2 Hz, 1H, Ar$H_7$), 7.31 (ddd, $J$ = 8.1, 7.3, 1.1 Hz, 1H, Ar$H_6$), 7.12 (d, $J$ = 8.7 Hz, 2H, $ArSO_2Ar H_{meta}$), 5.04 (s, 2H, -C$H_2$OTBS), 2.28 (tt, $J$ = 0.6, 0.3 Hz, 3H, $SO_2ArCH_3$), 0.86 [s, 9H, $Si(CH_3)_2C(CH_3)_3$], 0.53 (s, 9H, $Si(CH_3)_3$), and 0.09 [s, 6H, $Si(CH_3)_2C(CH_3)_3$]. Key difference nOe results are indicated by the arrows in structure **606a** above. These allow definitive assignment of protons H5 vs. H8 as well as assessment of the sense of regioselectivity in the trapping of the benzyne by the bromide nucleophile.

**$^{13}$C NMR** (125 MHz, $CDCl_3$): δ 145.3, 141.4, 139.1, 138.6, 138.4, 135.0, 131.5, 130.0, 127.3, 126.8(2C), 125.7, 124.2, 123.1, 120.0, 115.1, 65.3, 26.3, 21.7, 18.6, 3.1, and -4.5.

**IR**: 2954, 2928, 2856, 1598, 1567, 1459, 1368, 1251, 1187, 1174, 1082, and 839 $cm^{-1}$.

**HRMS** (ESI-TOF): Calcd for $C_{29}H_{38}BrNNaO_3SSi_2^+$ $[M+Na]^+$ requires 638.1187; found 638.1188.

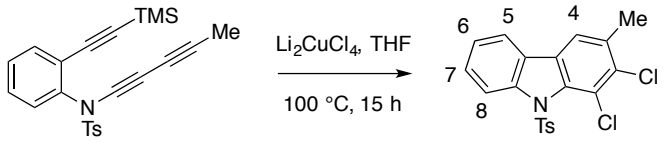


**601** **606b**

**Preparation of 1,2-dichloro-3-methyl-9-tosyl-9*H*-carbazole (606b)**

Compound **606b** was prepared following General Procedure B using **601** (15 mg, 37 μmol), $Li_2CuCl_4$ (180 μL, 1M in THF, 180 μmol), and THF (2 mL). Purification by column chromatography (hexanes: ethyl acetate = 5:1) gave product **606b** (14 mg, 35 μmol, 94%) as an off-white solid.

**$^1$H NMR** (500 MHz, $CDCl_3$): δ 8.15 (ddd, *J* = 8.3, 0.8, 0.8 Hz, 1H, Ar$H_8$), 7.68 (ddd, *J* = 7.7, 1.3, 0.7 Hz, 1H, Ar$H_5$), 7.57 (q, *J* = 0.8 Hz, 1H, Ar$H_4$), 7.45 (ddd, *J* = 8.5, 7.3, 1.3 Hz, 1H, Ar$H_7$), 7.40 (d, *J* = 8.4 Hz, 2H, $ArSO_2Ar$$H_{ortho}$), 7.33 (ddd, *J* = 7.7, 7.3, 1.0 Hz, 1H, Ar$H_6$), 7.05 (d, *J* = 8.1 Hz, 2H, $ArSO_2Ar$$H_{meta}$), 2.53 (s, 3H, $Ar_{carbazole}C$$H_3$), and 2.30 (s, 3H, $SO_2ArC$$H_3$).

**$^{13}$C NMR** (125 MHz, $CDCl_3$): δ 144.6, 142.3, 137.5, 135.5, 134.8, 133.4, 130.1, 129.3, 127.9, 127.8, 127.1, 125.6, 123.8, 119.9, 119.4, 119.3, 22.0, and 21.8.

**IR**: 3205, 2923, 1738 (w), 1452, 1422, 1349, 1167, 1095, 1033, and 940 $cm^{-1}$.

**HRMS** (ESI-TOF): Calcd for $C_{20}H_{15}Cl_2NNaO_2S^+$ $[M+Na]^+$ requires 426.0093; found 426.0097.

**mp:** 212–216 °C.

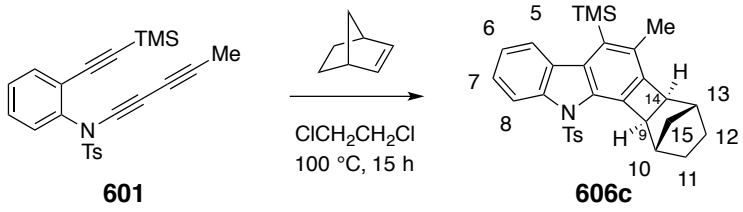


**Preparation of 6-methyl-11-tosyl-5-(trimethylsilyl)-6b,8,9,10,10a,11-hexahydro-7*H*-7,10-methanobenzo[3,4]cyclobuta[1,2-*a*]carbazole (606c)**

Compound **606c** was prepared following General Procedure B using **1** (20 mg, 49 μmol), norbornene (50 mg, 0.53 mmol), dichloroethane (3 mL). Purification by column chromatography (hexanes: ethyl acetate = 12:1) gave product **606c** (9 mg, 18 μmol, 37%) as an off-white oil.

**$^1$H NMR** (500 MHz, $CDCl_3$): δ 8.24 (d, *J* = 8.3 Hz, 1H, Ar$H_8$), 8.00 (d, *J* = 8.1 Hz, 1H, Ar$H_5$), 7.60 (d, *J* = 8.3 Hz, 2H, $ArSO_2ArH_{ortho}$), 7.36 (dd, *J* = 8.2, 7.4 Hz, 1H, Ar$H_7$), 7.24 (dd, *J* = 8.0, 7.3 Hz, 1H, Ar$H_6$), 7.08 (d, *J* = 8.4 Hz, 2H, $ArSO_2ArH_{meta}$), 3.65 (d, *J* = 3.9 Hz, 1H, $H_9$), 3.20 (d, *J* = 3.7 Hz, 1H, $H_{14}$), 2.76 (br d, *J* = 2.7 Hz, 1H, $H_{10}$), 2.39 (s, 3H, $Ar_{carbazole}CH_3$), 2.36 (br d, *J* = 2.6 Hz, 1H, $H_{13}$), 2.27 (s, 3H, $SO_2ArCH_3$), 1.72–1.61 (m, 2H), 1.37–1.31 (nfom, 1H), 1.30–1.24 (nfom, 1H), 0.98 (d, *J* = 10.0 Hz, 1H, C15$H_a$$H_b$), 0.86 (br d, *J* =10.5 Hz, 1H, C15$H_a$$H_b$), and 0.49 (s, 9H, $Si(CH_3)_3$).

**$^{13}$C NMR** (125 MHz, $CDCl_3$): δ 146.2, 144.5, 138.1, 135.6, 134.3, 132.3, 131.9, 131.6, 131.5, 129.8, 128.4, 126.8, 126.0, 125.0, 122.5, 114.9, 52.0, 49.6, 36.7, 36.2, 32.1, 28.33, 28.28, 21.7, 19.1, and 3.7.

**IR**: 2950, 2869, 1598, 1471, 1421, 1371, 1230, 1175, 1090, and 969 $cm^{-1}$.

**GC-LRMS** (ES, 70 eV): $t_R$ = 16.10 min. *m/z*: 499 $(M)^{\bullet+}$, 484 $(M–Me)^+$, 344 $(M–Ts)^+$.

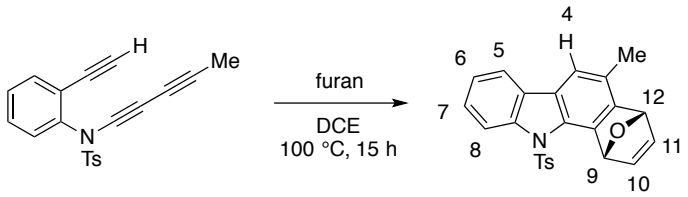


**604–H/Me** **606d**

**Preparation of 5-methyl-11-tosyl-4,11-dihydro-1*H*-1,4-epoxybenzo[*a*]carbazole (606d)**

Compound **606d** was prepared following General Procedure B using **604–H/Me** (15 mg, 45 μmol), furan (15 mg, 0.22 mmol), and dichloroethane (2.5 mL). Purification by column chromatography (hexanes: ethyl acetate = 12:1) gave product **606d** (13 mg, 32 μmol, 72%) as a pale yellow oil.

**$^1$H NMR** (500 MHz, $CDCl_3$): δ 8.15 (dd, *J* = 8.3, 0.8 Hz, 1H, Ar$H_8$), 7.69 (ddd, *J* = 7.7, 1.3, 0.7 Hz, 1H, Ar$H_5$), 7.39 (dd, *J* = 5.6, 1.9 Hz, 1H, $H_{10}$), 7.37 (ddd, *J* = 8.4, 7.3, 1.2 Hz, 1H, Ar$H_7$), 7.28 (s, 1H, $H_4$), 7.25 (ddd, *J* = 7.5, 7.5, 1.0 Hz, 1H, Ar$H_6$), 7.24 (d, *J* = 8.4 Hz, 2H, $ArSO_2Ar H_{ortho}$), 7.18 (dd, *J* = 5.5, 1.9 Hz, 1H, $H_{11}$), 6.97 (d, *J* = 8.4 Hz, 2H, $ArSO_2Ar H_{meta}$), 6.57 (dd, *J* = 2.0, 1.0 Hz, 1H, $H_9$), 5.92 (dd, *J* = 2.0, 1.0 Hz, 1H, $H_{12}$), 2.46 (s, 3H, $Ar_{carbazole}CH_3$), and 2.21 (s, 3H, $SO_2ArCH_3$).

**$^{13}$C NMR** (125 MHz, $CDCl_3$): δ 149.5, 144.7, 143.8, 143.3, 139.9, 137.8, 134.1, 131.8, 129.5, 128.8, 128.1, 127.4, 126.95, 126.91, 124.8, 120.1, 118.0, 117.0, 84.1, 81.3, 21.7, and 18.4.

**IR**: 2922, 1598, 1469, 1419, 1367, 1173, 1090, 1033, 964, 873, and 844 $cm^{-1}$.

**HRMS** (ESI-TOF): Calcd for $C_{24}H_{19}NNaO_3S^+$ $[M+Na]^+$ requires 424.0978; found 424.0990.

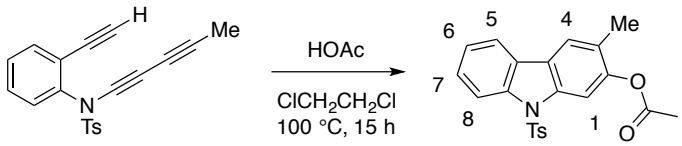


**604–H/Me** **606e**

**Preparation of 3-methyl-9-tosyl-9*H*-carbazol-2-yl acetate (606e)**

Compound **606e** was prepared following General Procedure B using **604–H/Me** (12 mg, 36 μmol), acetic acid (5 μL, 79 μmol), and dichloroethane (1.8 mL). Purification by column chromatography (hexanes: ethyl acetate = 5:1) gave product **606e** (10 mg, 25 μmol, 71%) as a pale yellow oil.

**$^1$H NMR** (500 MHz, $CDCl_3$): δ 8.28 (ddd, *J* = 8.4, 1.0, 0.8 Hz, 1H, Ar*H*$_8$), 8.03 (dq, *J* = 0.4, 0.4 Hz, 1H, Ar*H*$_1$), 7.82 (ddd, *J* = 7.7, 1.3, 0.7 Hz, 1H, Ar*H*$_5$), 7.71 (dd, *J* = 0.8, 0.5 Hz, 1H, Ar*H*$_4$), 7.68 (d, *J* = 8.7 Hz, 2H, $ArSO_2Ar$*H*$_{ortho}$), 7.45 (ddd, *J* = 8.4, 7.3, 1.3 Hz, 1H, Ar*H*$_7$), 7.33 (ddd, *J* = 7.7, 7.3, 1.0 Hz, 1H, Ar*H*$_6$), 7.10 (d, *J* = 8.7 Hz, 2H, $ArSO_2Ar$*H*$_{meta}$), 2.41 (s, 3H, OC(O)C*H*$_3$), 2.29 (dd, *J* = 0.9, 0.4, 3H, $Ar_{carbazole}C$*H*$_3$), and 2.25 (tt, *J* = 0.7, 0.3 Hz, 3H, $SO_2ArC$*H*$_3$).

**$^{13}$C NMR** (125 MHz, $CDCl_3$): δ 169.6, 148.9, 145.2, 139.0, 137.2, 134.8, 129.9, 127.3, 126.8, 126.7, 126.2, 124.7, 124.2, 121.7, 120.0, 115.4, 109.7, 21.7, 21.1, and 16.6.

**IR**: 2970, 1739, 1448, 1366, 1227, 1216, 1205, 1169, 1033, and 908 $cm^{-1}$.

**HRMS** (ESI-TOF): Calcd for $C_{22}H_{19}NNaO_4S^+$ $[M+Na]^+$ requires 416.0927; found 416.0933.

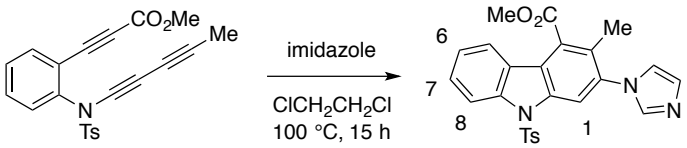


**604–E/Me** **606f**

**Preparation of methyl 2-(1*H*-imidazol-1-yl)-3-methyl-9-tosyl-9*H*-carbazole-4-carboxylate (606f)**

Compound **606f** was prepared following General Procedure B using **604–E/Me** (13 mg, 33 μmol), imidazole (11 mg, 162 μmol), and dichloroethane (1.7 mL). Purification by column chromatography (hexanes: ethyl acetate:methanol = 10:10:1) gave product **606f** [12 mg, 26 μmol, 79%, if pure; this material was contaminated with two coeluting impurities to the extent of 7 mol% and 2 mol% (from $^1$H NMR integration)] as a brown oil. The sample was rechromatographed and the resulting material showed no appreciable change in the impurity profile (nor its color).

**$^1$H NMR** (400 MHz, $CDCl_3$): δ 8.38 (ddd, *J* = 8.5, 1.0, 0.7 Hz, 1H, Ar*H*$_8$), 8.33 (q, *J* = 0.4 Hz, 1H, $ArH_1$), 7.70 (ddd, *J* = 8.0, 1.3, 0.7 Hz, 1H, Ar*H*$_5$), 7.67 (d, *J* = 8.4 Hz, 2H, $ArSO_2Ar$*H*$_{ortho}$), 7.66 (dd, *J* = 1.2, 0.9 Hz, 1H, $Ar_{imid}$*H*$_2$), 7.57 (ddd, *J* = 8.5, 7.3, 1.3 Hz, 1H, Ar*H*$_7$), 7.38 (ddd, *J* = 8.0, 7.3, 1.0 Hz, 1H, Ar*H*$_6$), 7.29 (dd, *J* = 1.3, 0.9 Hz, 1H, $Ar_{imid}$*H*$_5$), 7.16 (d, *J* = 8.6 Hz, 2H, $ArSO_2Ar$*H*$_{meta}$), 7.13 (dd, *J* = 1.3, 1.3 Hz, 1H, $Ar_{imid}$*H*$_4$), 4.10 (s, 3H, $CO_2C$*H*$_3$), 2.31 (tt, *J* = 0.6, 0.3 Hz, 3H, $SO_2ArC$*H*$_3$), and 2.17 (d, *J* = 0.4 Hz, 3H, $Ar_{carbazole}C$*H*$_3$).

**$^{13}$C NMR** (125 MHz, $CDCl_3$): δ 168.9, 145.9, 139.5, 138.0, 136.8, 135.8, 134.7, 130.2, 130.0, 128.9, 128.3, 127.2, 126.7, 124.6, 123.6, 123.3, 121.6, 121.2, 115.3, 114.9, 53.1, 21.8, and 14.8.

**IR**: 3111, 2954, 2927, 1731, 1597, 1494, 1465, 1372, 1215, 1174, 1091, 1072, 1048, and 1028 $cm^{-1}$.

**HRMS** (ESI-TOF): Calcd for $C_{25}H_{22}N_3O_4S^+$ $[M+H]^+$ requires 460.1326; found 460.1332.

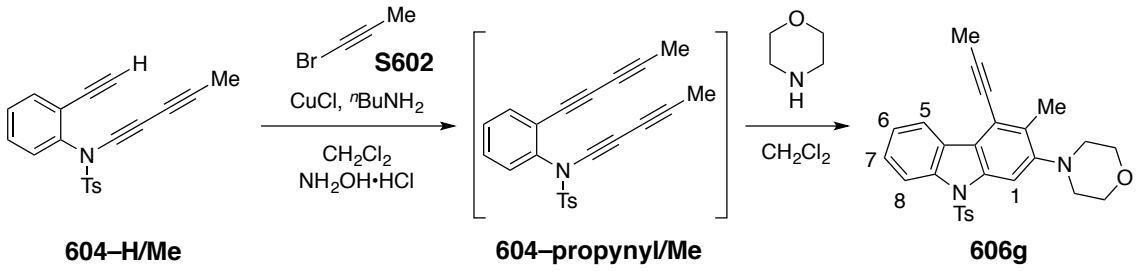


**604–H/Me** **604–propynyl/Me** **606g**

**Preparation of 4-(3-methyl-4-(prop-1-yn-1-yl)-9-tosyl-9*H*-carbazol-2-yl)morpholine (606g)**

Tetrayne **604–propynyl/Me** was prepared following General Procedure A using triyne precursor *N*-(2-ethynylphenyl)-4-methyl-*N*-(penta-1,3-diyn-1-yl)benzenesulfonamide (**604–H/Me**, 20 mg, 60 μmol), 1-bromopropyne (0.1 mL, 1.3 M in hexanes), CuCl (1 mg, 0.01 mmol), *n*-$BuNH_2$ (0.5 mL), and $CH_2Cl_2$ (0.5 mL). The total reaction time was ca. 40 min. After aqueous work-up, the crude material was not purified. [A $^1$H NMR spectrum of this sample, still containing ethyl acetate, suggested that the tetrayne **604-propynyl/Me** had been formed relatively cleanly and showed the following resonances: δ 7.71 (d, $J$ = 8.4 Hz, 2H, $ArSO_2Ar\mathit{H}_{ortho}$), 7.45 – 7.43 (nfom, 1H), 7.33 (d, $J$ = 8.9 Hz, 2H, $ArSO_2Ar\mathit{H}_{meta}$), 7.35–7.26 (m, 3H), 2.46 (s, 3H, $SO_2ArC\mathit{H}_3$), 2.02 (s, 3H, -C≡CC$\mathit{H}_3$), and 1.96 (s, 3H, -C≡CC$\mathit{H}_3$).] The yellow oily residue obtained after concentration was re-dissolved in $CH_2Cl_2$. Morpholine (30 μL, 0.3 mmol) was added. The solution was held at room temperature. After completion of reaction as monitored by TLC (ca. 2 days), the reaction mixture was concentrated. The residue was purified by column chromatography on silica gel (hexanes:ethyl acetate=3:1) to give 4-(3-methyl-4-(prop-1-yn-1-yl)-9-tosyl-9*H*-carbazol-2-yl)morpholine [**606g**, 22 mg, this sample contained 2% (by mass) of EtOAc (from integration of $^1$H NMR resonances); the corrected yield is 47 μmol, 78%] as a white solid.

**$^1$H NMR** (500 MHz, $CDCl_3$): δ 8.52 (ddd, $J$ = 7.9, 1.4, 0.6 Hz, 1H, Ar$\mathit{H}_5$), 8.31 (ddd, $J$ = 8.3, 1.1, 0.7 Hz, 1H, Ar$\mathit{H}_8$), 8.00 (q, $J$ = 0.4 Hz, 1H, Ar$\mathit{H}_1$), 7.61 (d, $J$ = 8.6 Hz, 2H, $ArSO_2Ar\mathit{H}_{ortho}$), 7.44 (ddd, $J$ = 8.3, 7.4, 1.4 Hz, 1H, Ar$\mathit{H}_7$), 7.34 (ddd, $J$ = 7.7, 7.3, 1.2 Hz, 1H, Ar$\mathit{H}_6$), 7.06 (d, $J$ = 8.1 Hz, 2H, $ArSO_2Ar\mathit{H}_{meta}$), 3.94–3.90 (nfom, 4H, -C$\mathit{H}_2$OC$\mathit{H}_2$-),

3.03–2.98 (nfom, 4H, -C$H_2$NC$H_2$-), 2.49 (d, $J$ = 0.3 Hz, 3H, Ar$_{carbazole}$C$H_3$), 2.28 (tt, $J$ = 0.7, 0.3 Hz, 3H, $SO_2$ArC$H_3$), and 2.24 (s, 3H, -C≡CC$H_3$).

**$^{13}$C NMR** (125 MHz, $CDCl_3$): δ 151.1, 145.0, 138.8, 137.5, 134.9, 132.2, 129.7, 126.81, 126.80, 126.6, 124.0, 122.2, 121.5, 118.1, 114.9, 106.1, 96.0, 77.5, 67.5, 52.9, 21.7, 15.9, and 5.0.

**IR**: 2957, 2919, 2855, 2822, 1587, 1438, 1369, 1211, 1172, 1153, 1117, 1067, 1034, and 961 cm$^{-1}$.

**HRMS** (ESI-TOF): Calcd for $C_{27}H_{27}N_2O_3S^+$ $[M+H]^+$ requires 459.1737; found 459.1748.

**mp:** 217–218°C.

---

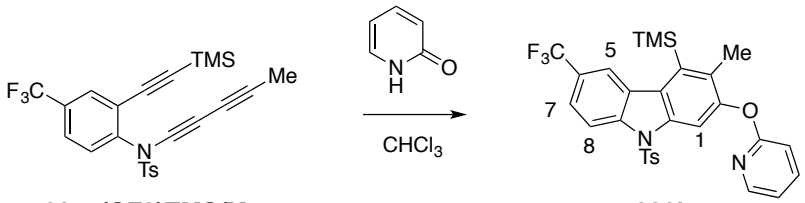


**604–(CF3)TMS/Me** **606h**

**Preparation of 3-methyl-2-(pyridin-2-yloxy)-9-tosyl-4-(trimethylsilyl)-9*H*-carbazole (606h)**

Compound **606h** was prepared following General Procedure B using **604–(CF3)TMS/Me** (19 mg, 0.04 mmol), 2-pyridone (38 mg, 0.40 mmol), and $CHCl_3$ (4 mL). Purification by column chromatography (hexanes: ethyl acetate = 5:1) gave product **606h** (22.2 mg, 0.039 mmol, 97%) as an off-white solid.

**$^1$H NMR** (500 MHz, $CDCl_3$): δ 8.47 (ddq, $J$ = 8.8, 0.7, 0.7 Hz, 1H, Ar$H_8$), 8.33 (ddq, $J$ = 1.9, 0.7, 0.7 Hz, 1H, Ar$H_5$), 8.20 (ddd, $J$ = 5.0, 2.0, 0.8 Hz, 1H, Ar$_{pyridine}H_6$), 8.17 (q, $J$ = 0.5 Hz, 1H, Ar$H_1$), 7.75 (ddd, $J$ = 8.3, 7.2, 2.0 Hz, 1H, Ar$_{pyridine}H_4$), 7.69 (d, $J$ = 8.5 Hz, 2H, $ArSO_2ArH_{ortho}$), 7.67 (ddq, $J$ = 8.8, 1.8, 0.5 Hz, 1H, Ar$H_7$), 7.14 (d, $J$ = 8.1 Hz, 2H, $ArSO_2ArH_{meta}$), 7.04 (ddd, $J$ = 7.2, 5.0, 0.9 Hz, 1H, Ar$_{pyridine}H_5$), 6.99 (dt, $J$ = 8.3, 0.9 Hz,

1H, $Ar_{pyridine}H_3$), 2.41 (d, $J$ = 0.5 Hz, 3H, $Ar_{carbazole}CH_3$), 2.30 (s, 3H, $SO_2ArCH_3$), and 0.53 (s, 9H, $Si(CH_3)_3$).

**$^{13}$C NMR** (125 MHz, $CDCl_3$): δ 163.9, 152.1, 147.9, 145.6, 140.8, 139.9, 138.1, 136.4, 134.8, 134.1, 130.1, 127.6, 126.9, 125.1, 125.0 (q, $J$ = 32.3 Hz), 124.8 (q, $J$ = 272.2 Hz), 123.0 (q, $J$ = 3.5 Hz), 122.3 (q, $J$ = 4.4 Hz), 118.7, 114.9, 111.5, 109.8, 21.8, 18.3, and 3.3. These carbon NMR chemical shifts compare much more favorably with literature reports of 2-aryloxypyridine derivatives than those of *N*-aryl-2-pyridone derivatives.[118]

**IR**: 2927, 1595, 1572, 1468, 1430, 1372, 1326, 1269, 1169, 1120, 1050, and 846 $cm^{-1}$.

**HRMS** (ESI-TOF): Calcd for $C_{29}H_{27}F_3N_2NaO_3SSi^+$ $[M+Na]^+$ requires 591.1356; found 591.1368.

**mp:** 149–151 °C.

---

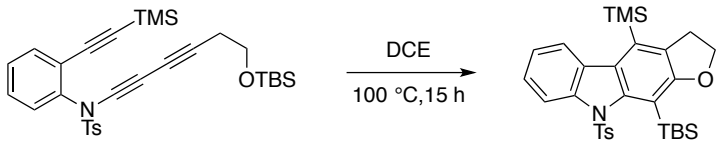


**604–TMS/tOTBS** **606i**

**Preparation of 10-(*tert*-butyldimethylsilyl)-9-tosyl-4-(trimethylsilyl)-3,9-dihydro-2*H*-furo[2,3-*b*]carbazole (606i)**

In a glass vial was added triyne precursor **604–TMS/tOTBS** (12 mg, 0.022 mmol) and DCE (1 mL). The vial was sealed with a Teflon-lined cap and placed in a 100 °C oil bath for 15 h. The crude reaction mixture was concentrated and directly subjected to column chromatographic purification on silica gel (hexanes:ethyl acetate = 5:1) to give **606i** (10 mg, 0.018 mmol, 83%) as a pale yellow oil.

---

[118] For example, a) Zhang, C.; Sun, P. Palladium-catalyzed direct C(sp2)–H alkoxylation of 2-aryloxypyridines using 2-pyridyloxyl as the directing group. *J. Org. Chem.* **2014**, *79*, 8457−8461 vs. b) Panda, N.; Jena, A. K.; Mohapatra, S.; Rout, S. R. Copper ferrite nanoparticle-mediated N-arylation of heterocycles: a ligand-free reaction. *Tetrahedron Lett.* **2011**, *52*, 1924–1927.

**$^1$H NMR** (500 MHz, $CDCl_3$): δ 8.06 (ddd, *J* = 8.0, 1.2, 0.6 Hz, 1H, Ar$H_8$), 7.47 (ddd, *J* = 7.9, 1.2, 0.6 Hz, 1H, Ar$H_5$), 7.23 (ddd, *J* = 8.1, 7.3, 1.2 Hz, 1H, Ar$H_7$), 7.14 (ddd, *J* = 7.9, 7.3, 1.2 Hz, 1H, Ar$H_6$), 6.70 (d, *J* = 8.2 Hz, 2H, $ArSO_2Ar$$H_{ortho}$), 6.67 (d, *J* = 8.5 Hz, 2H, $ArSO_2Ar$$H_{meta}$), 4.69 (ddd, *J* = 10.0, 8.5, 5.0 Hz, 1H, C$H_a$$H_b$O), 4.46 (ddd, *J* = 9.6, 9.6, 8.5 Hz, 1H, $CH_a$$H_b$O), 3.44 (ddd, *J* = 15.1, 10.1, 9.5 Hz, 1H, C$H_a$$H_b$$CH_2$O), 3.25 (ddd, *J* = 15.1, 9.6, 5.1 Hz, 1H, $CH_a$$H_b$$CH_2$O), 2.14 (s, 3H, $SO_2$Ar-C$H_3$), 1.06 (s, 9H, $Si(CH_3)_2C(CH_3)_3$), 0.68 (s, 3H, $Si(CH_3)_a(CH_3)_bC(CH_3)_3$), 0.33 (s, 3H, $Si(CH_3)_a(CH_3)_b$ $C(CH_3)_3$), and 0.28 (s, 9H, -$Si(CH_3)_3$).

**$^{13}$C NMR** (125 MHz, $CDCl_3$): δ 164.6, 147.6, 143.8, 142.1, 132.3, 130.7, 130.6, 130.3, 129.5, 128.0, 127.6, 125.0, 124.7, 122.8, 120.4, 115.1, 70.7, 32.3, 29.3, 21.5, 18.1, 1.8, -0.1, and -0.6.

**IR**: 2950, 2929, 2894, 2855, 1461, 1364, 1315, 1254, 1171, 1090, 1039, and 839 $cm^{-1}$.

**HRMS** (ESI-TOF): Calcd for $C_{30}H_{39}NNaO_3SSi_2^+$ $[M+Na]^+$ requires 572.2081; found 572.2067.

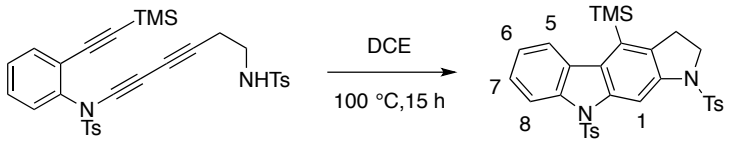


**604–TMS/tNHTs** **606j**

**Preparation of 1,9-ditosyl-4-(trimethylsilyl)-1,2,3,9-tetrahydropyrrolo[2,3-*b*]carbazole (606j)**

In a glass vial was added triyne precursor **604–TMS/tNHTs** (25 mg, 0.042 mmol) and DCE (2 mL). The vial was sealed with a Teflon-lined cap and placed in a 100 °C oil bath for 15 h. The crude reaction mixture was concentrated and directly subjected to column chromatography (hexanes:ethyl acetate = 3:1) to give **606j** (18 mg, 0.018 mmol, 72%) as a pale yellow oil.

**$^1$H NMR** (500 MHz, $CDCl_3$): δ 8.63 (s, 1H, Ar$H_1$), 8.44 (d, $J$ = 8.4 Hz, 1H, Ar$H_8$), 7.93 (d, $J$ = 8.0 Hz, 1H, Ar$H_5$), 7.802 (d, $J$ = 8.4 Hz, 2H, $SO_2Ar_aH_{ortho}$), 7.796 (d, $J$ = 8.4 Hz, 2H, $SO_2Ar_bH_{ortho}$), 7.41 (ddd, $J$ = 8.5, 7.2, 1.2 Hz, 1H, Ar$H_7$), 7.28 (ddd, $J$ = 8.1, 7.3, 1.1 Hz, 1H, Ar$H_6$), 7.24 (d, $J$ = 8.1 Hz, 2H, $SO_2Ar_aH_{meta}$), 7.15 (d, $J$ = 8.1 Hz, 2H, $SO_2Ar_bH_{meta}$), 3.97 (t, $J$ = 8.3 Hz, 2H, $CH_2CH_2$NTs), 3.11 (t, $J$ = 8.3 Hz, 2H, $CH_2CH_2$NTs), 2.36 (s, 3H, $SO_2Ar_a$-$CH_3$), 2.30 (s, 3H, $SO_2Ar_b$-$CH_3$), and 0.43 (s, 9H, $Si(CH_3)_3$).

**$^{13}$C NMR** (125 MHz, $CDCl_3$): δ 145.0, 144.3, 140.7, 139.2, 138.3, 135.4, 134.0, 133.9, 130.5, 130.0, 129.9, 127.9, 127.1, 126.4, 126.2, 126.0, 123.9, 122.8, 114.8, 102.0, 50.4, 30.3, 21.8, 21.7, and 2.4.

**IR**: 2949, 1599, 1578, 1465, 1401, 1356, 1265, 1166, 1091, 1052, 1033, and 844 $cm^{-1}$.

**HRMS** (ESI-TOF): Calcd for $C_{31}H_{32}N_2NaO_4S_2Si^+$ $[M+Na]^+$ requires 611.1465; found 611.1470.

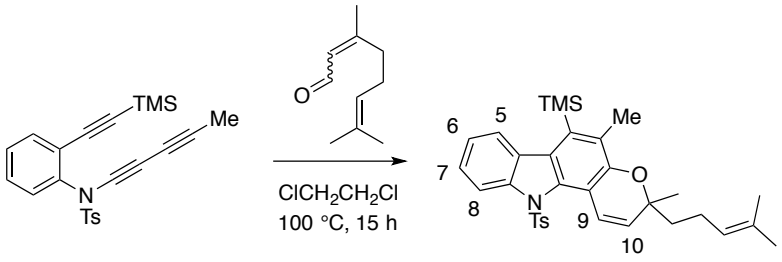


**601** **611**

**Preparation of 3,5-dimethyl-3-(4-methylpent-3-en-1-yl)-11-tosyl-6-(trimethylsilyl)-3,11-dihydropyrano[3,2-*a*]carbazole (611)**

Compound **611** was prepared following General Procedure B using **601** (40 mg, 99 μmol), citral (30 mg, 0.20 mmol), and DCE (5 mL). Purification by column chromatography (hexanes:ethyl acetate = 5:1) gave product **611** (49 mg, 88 μmol, 89%) as a pale yellow oil.

**$^1$H NMR** (500 MHz, $CDCl_3$): δ 8.11 (ddd, *J* = 8.0, 1.2, 0.6 Hz, 1H, Ar$H_8$), 7.50 (ddd, *J* = 7.9, 1.2, 0.6 Hz, 1H, Ar$H_5$), 7.25 (ddd, *J* = 8.1, 7.4, 1.2 Hz, 1H, Ar$H_7$), 7.23 (d, *J* = 9.8 Hz, 1H, Ar$H_9$), 7.18 (ddd, *J* = 7.9, 7.3, 1.2 Hz, Ar$H_6$), 6.87 (d, *J* = 8.3 Hz, 2H, $SO_2$Ar$H_{ortho}$), 6.77 (d, *J* = 8.1 Hz, 2H, $SO_2$Ar$H_{meta}$), 5.71 (d, *J* = 9.9 Hz, 1H, $H_{10}$), 5.16 [tqq, *J* = 7.2, 1.4, 1.4 Hz, 1H, $CH_2CH$=$C(CH_3)_2$], 2.35 (s, 3H, $Ar_{carbazole}CH_3$), 2.19 (dt, *J* = 8.3, 7.5 Hz, 2H, $CH_2CH$=$C(CH_3)_2$), 2.16 (s, 3H, $SO_2ArCH_3$), 1.86–1.79 (m, 2H, $CH_2CH_2CH$=), 1.68 (d, *J* = 1.1 Hz, 3H, CH=$C(CH_3)_a(CH_3)_b$, 1.59 (d, *J* = 0.8 Hz, 3H, CH=$C(CH_3)_a(CH_3)_b$), 1.52 (s, 3H, $C(CH_3)CH_2CH_2$), and 0.26 (s, 9H, $Si(CH_3)_3$).

**$^{13}$C NMR** (125 MHz, $CDCl_3$): δ 150.5, 144.2, 141.9, 136.6, 133.9, 132.5, 131.8, 131.0, 130.8, 129.7, 128.3, 127.5, 127.5, 125.1, 125.0, 124.4, 123.6, 122.3, 120.3, 115.1, 78.4, 41.1, 26.2, 25.9, 23.0, 21.5, 17.9, 17.8, and 2.9.

**IR**: 2969, 2924, 1598, 1538, 1453, 1367, 1306, 1253, 1174, 1075, and 841cm$^{-1}$.

**HRMS** (ESI-TOF): Calcd for $C_{33}H_{39}NNaO_3SSi^+$ $[M+Na]^+$ requires 580.2312; found 580.2330.

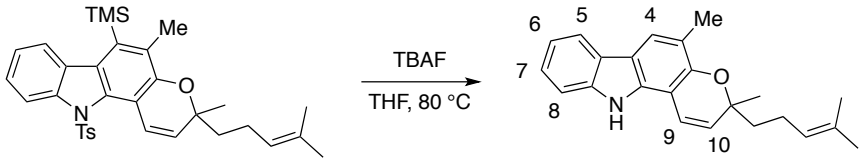


**611** **612**

**Preparation of mahanimbine (612)**

In a glass vial was added **611** (15 mg, 0.027 mmol), THF (0.3 mL), and TBAF (0.2 mL, 1 M in THF) at room temperature. The vial was sealed with a Teflon-lined cap and placed in an 80 °C oil bath for 6 h. The reaction mixture was partitioned between $NH_4Cl$ (aq) and ethyl acetate. The organic layer was washed with brine, dried over anhydrous $Na_2SO_4$, filtered, and concentrated. The residue was purified by column chromatography (hexanes: ethyl acetate = 5:1) to give mahanimbine (**612**, 8.1 mg, 0.024 mmol, 91%) as a

pale yellow oil. The NMR data were essentially identical with those previously reported.[119]

**$^1$H NMR** (500 MHz, $CDCl_3$): δ 7.91 (ddd, *J* = 7.8, 1.2, 0.6 Hz, 1H, Ar*H*$_5$), 7.86 (br s, 1H, N*H*), 7.66 (s, 1H, Ar*H*$_4$), 7.37 (ddd, *J* = 8.0, 1.1, 0.6 Hz, 1H, Ar*H*$_8$), 7.30 (ddd, *J* = 8.0, 7.2, 1.2 Hz, 1H, Ar*H*$_7$), 7.17 (ddd, *J* = 7.7, 7.2, 1.1 Hz, 1H, Ar*H*$_6$), 6.64 (d, *J* = 9.8 Hz, 1H, *H*$_9$), 5.66 (d, *J* = 9.8 Hz, 1H, *H*$_{10}$), 5.11 (tqq, *J* = 7.2, 1.4, 1.4 Hz, 1H, $CH_2CH$=$C(CH_3)_2$), 2.33 (s, 3H, $Ar_{carbazole}CH_3$), 2.24–2.10 (m, 2H, $CH_2CH$=$C(CH_3)_2$), 1.79–1.74 (nfom, *2*H, $CH_2CH_2CH$=), 1.66 (br s, 3H, CH=$C(CH_3)_a(CH_3)_b$, 1.58 (br s, 3H, CH=$C(CH_3)_a(CH_3)_b$), and 1.44 (s, 3H, $C(CH_3)CH_2CH_2$).

**$^{13}$C NMR** (125 MHz, $CDCl_3$): δ 150.1, 139.7, 135.1, 131.9, 128.7, 124.42, 124.40, 124.1, 121.4, 119.7, 119.5, 118.6, 117.7, 116.8, 110.6, 104.4, 78.4, 40.1, 26.1, 25.9, 23.0, 17.8, and 16.3.

**IR**: 2922, 2865, 2844, 1456, 1055, 1033, 1014, 909, and 840 $cm^{-1}$.

**HRMS** (ESI-TOF): Calcd for $C_{23}H_{25}NNaO^+$ $[M+Na]^+$ requires 354.1828; found 354.1809.

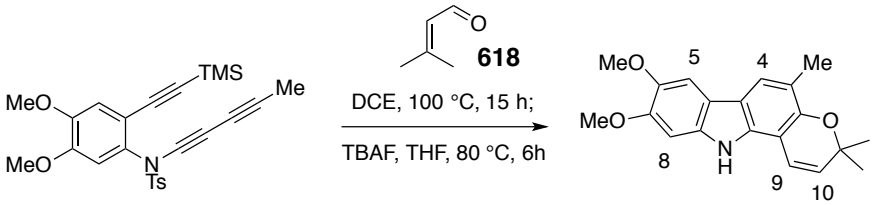


**617** **619**

**Preparation of koenidine (619)**

Following General Procedure B, **617** (47 mg, 0.1 mmol), 3-methylbut-2-enal (**618**, 42 mg, 0.5 mmol), and DCE (5 mL) were used. The crude reaction mixture was concentrated and re-dissolved in THF (1 mL). TBAF (0.2 mL, 1 M in THF) was added slowly at room temperature. The vial was sealed with a Teflon-lined cap and placed in an 80 °C oil bath for 6 h. The cooled reaction mixture was partitioned between $NH_4Cl$ (aq) and ethyl

[119] Tachibana, Y.; Kikuzaki, H.; Lajis, N. H.; Nakatani, N. Antioxidative activity of carbazoles from murraya koenigii leaves. *J. Agric. Food Chem.* **2001**, *49*, 5589–5594.

acetate. The organic layer was washed with brine, dried over anhydrous $Na_2SO_4$, filtered, and concentrated. The residue was purified by column chromatography (hexanes: ethyl acetate = 5:1) to give koenidine (**619**, 22 mg, 0.084 mmol, 84%) as a pale-yellow oil.

**$^1$H NMR** (500 MHz, $CDCl_3$): δ 7.70 (br s, 1H, carbazole N*H*), 7.55 (s, 1H, Ar*H4*), 7.38 (s, 1H, Ar*H5*), 6.91 (s, 1H, Ar*H8*), 6.60 (d, *J* = 9.7 Hz, 1H, *H9*), 5.69 (d, *J* = 9.7 Hz, 1H, *H10*), 3.98 [s, 3H, Ar(OC$H_3$)$_a$], 3.94 [s, 3H, Ar(OC$H_3$)$_b$], 2.32 (d, *J* = 0.8 Hz, 3H, carbazole C$H_3$), and 1.48 (s, 6H, C(C$H_3$)$_2$).

**$^{13}$C NMR** (125 MHz, $CDCl_3$): δ 149.0, 148.5, 144.7, 135.0, 134.3, 129.8, 120.4, 118.6, 117.5 (2xC[120]), 116.4, 104.9, 102.5, 95.0, 76.0, 56.8, 56.5, 27.8, and 16.3.

**IR**: 3424, 3363, 2973, 2939, 1644, 1628, 1494, 1474, 1444, 1426, 1276, 1209, 1161, 1129, 1118, and 768 $cm^{-1}$.

**HRMS** (ESI-TOF): Calcd for $C_{20}H_{21}NNaO_3^+$ $[M+Na]^+$ requires 346.1414; found 346.1415.

**mp:** 223–224 °C (lit.,[121] 224–225 °C)

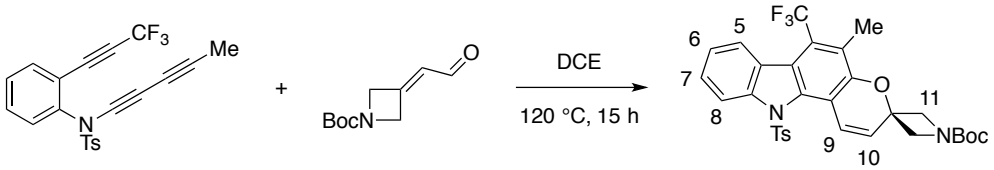


**620** **621** **622**

**Preparation of *tert*-butyl 5'-methyl-11'-tosyl-6'-(trifluoromethyl)-11'*H*-spiro[azetidine-3,3'-pyrano[3,2-*a*]carbazole]-1-carboxylate (622)**

[120] Patel, O. P. S.; Mishra, A.; Maurya, R.; Saini, D.; Pandey, J.; Taneja, I.; Raju, K. S. R.; Kanojiya, S.; Shukla, S. K.; Srivastava, M. N.; Wahajuddin, M.; Tamrakar, A. K.; Srivastava, A. K.; Yadav, P. P. naturally occurring carbazole alkaloids from Murraya koenigii as potential antidiabetic agents. *J. Nat. Prod*. **2016**, *79*, 1276–1284.

[121] Kureel, S. P.; Kapil, R. S.; Popli, S. P. New alkaloids from Murraya koenigii Spreng. *Experientia* **1969**, *25*, 790–791.

Compound **622** was prepared following General Procedure B using **620** (14 mg, 35 μmol), *tert*-butyl 3-(2-oxoethylidene)azetidine-1-carboxylate[122] (35 mg, 0.18 mmol), and DCE (2 mL). Purification by column chromatography (hexanes: ethyl acetate = 5:1) gave product **622** (15 mg, 25 μmol, 72%) as a pale yellow oil.

**$^1$H NMR** (500 MHz, $CDCl_3$): δ 8.15 (ddd, *J* = 8.2, 1.2, 0.6 Hz, 1H, Ar$H_8$), 7.80 (dddq, *J* = 8.2, 1.7, 1.4, 0.6 Hz, 1H, Ar$H_5$), 7.38 (ddd, *J* = 8.2, 7.3, 1.2 Hz, 1H, Ar$H_7$ or Ar$H_6$), 7.37 (d, *J* = 9.8 Hz, 1H, $H_9$), 7.27 (ddd, *J* = 8.2, 7.3, 1.2 Hz, 1H, Ar$H_7$ or Ar$H_6$), 6.85 (s, 4H, $ArSO_2ArH_{o,m}$), 6.12 (d, *J* = 9.8 Hz, 1H, $H_{10}$), 4.33 (dd, *J* = 9.5, 1.0 Hz, 2H, $H_{11a}$), 4.17 (d, *J* = 9.5, 1.0 Hz, 2H, $H_{11b}$), 2.50 (q, *J* = 3.6 Hz, 3H, $Ar_{carbazole}CH_3$), 2.20 (s, 3H, tosyl $CH_3$), and 1.50 [s, 9H, $NCO_2C(CH_3)_3$].

**$^{13}$C NMR** (125 MHz, $CDCl_3$): δ 156.5, 150.1, 145.1, 141.9, 137.0, 131.1, 130.0, 128.8, 128.2, 127.15, 127.11, 126.2, 124.9 (q, *J* = 275.1 Hz), 124.2, 123.6, 123.4 (q, *J* = 7.5 Hz), 123.4 (q, *J* = 2.7 Hz), 122.0 (q, *J* = 29.9 Hz), 119.6, 116.8, 80.4, 74.1, 63.7 (br), 28.6, 21.6, and 12.8 (q, *J* = 4.6 Hz).

**IR**: 2978, 2885, 1704, 1391, 1375, 1324, 1248, 1176, 1118, 1083, 1021, and 759 $cm^{-1}$.

**HRMS** (ESI-TOF): Calcd for $C_{31}H_{29}F_3N_2NaO_5S^+$ $[M+Na]^+$ requires 621.1641; found 621.1656.

[122] Burkhard, J. A.; Guérot, C.; Knust, H.; Rogers-Evans, M.; Carreira, E. M. Synthesis and structural analysis of a new class of azaspiro[3.3]heptanes as building blocks for medicinal chemistry. *Org. Lett.* **2010**, *12*, 1944–1947.

## Computational methods and coordinates of structures

DFT calculations were carried out using the Gaussian 09 software package.[100] Geometries were optimized using the M06-2X functional developed by Truhlar et al[101] and the double-ζ 6-31G(d) basis set. The SMD continuum solvation model46 was used with 1,2-dichloroethane as the solvent during geometry optimization and frequency calculation. The "grid=ultrafine" option was applied during the numerical integrations. The harmonic vibrational frequency calculations were carried out using 298 K as the thermal correction for the free energies.

The following benzyne geometries were optimized:

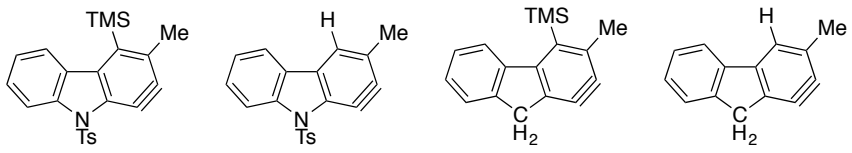


**602** **602$_{-TMS}$** **602$_{CH2}$** **602$_{CH2-TMS}$**

**Coordinates:**

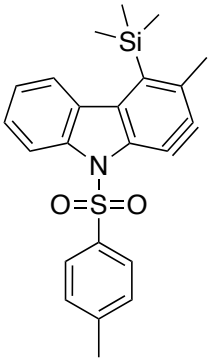


**602**

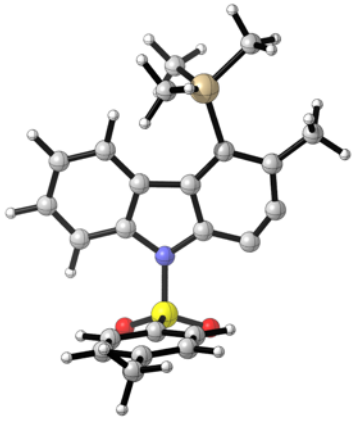

| Center Number | Atomic Number | Atomic Type | Coordinates (Angstroms) X | Y | Z |
|---|---|---|---|---|---|
| 1 | 6 | 0 | -0.351992 | 3.794026 | 0.615937 |
| 2 | 6 | 0 | -0.980089 | 2.899438 | -0.239702 |
| 3 | 6 | 0 | -0.323447 | 1.701516 | -0.522051 |
| 4 | 6 | 0 | 0.946250 | 1.376750 | 0.012950 |
| 5 | 6 | 0 | 1.551668 | 2.313982 | 0.864353 |
| 6 | 6 | 0 | 0.902217 | 3.504039 | 1.162180 |
| 7 | 1 | 0 | -0.842800 | 4.732315 | 0.854133 |
| 8 | 1 | 0 | -1.941100 | 3.128562 | -0.681564 |
| 9 | 1 | 0 | 2.522452 | 2.131673 | 1.304851 |
| 10 | 1 | 0 | 1.380133 | 4.218009 | 1.825139 |
| 11 | 6 | 0 | 1.320417 | 0.044240 | -0.486674 |
| 12 | 6 | 0 | 2.459420 | -0.800928 | -0.300155 |
| 13 | 6 | 0 | 0.218703 | -0.362398 | -1.298469 |
| 14 | 6 | 0 | 2.491399 | -2.094612 | -0.900321 |
| 15 | 6 | 0 | 0.282607 | -1.619596 | -1.868153 |
| 16 | 6 | 0 | 1.320493 | -2.259978 | -1.608019 |
| 17 | 16 | 0 | -2.363640 | 0.325931 | -1.762754 |
| 18 | 8 | 0 | -2.973800 | 1.615780 | -2.031521 |
| 19 | 8 | 0 | -2.314250 | -0.699487 | -2.786386 |
| 20 | 6 | 0 | 3.581543 | -3.126513 | -0.805046 |
| 21 | 1 | 0 | 4.513844 | -2.771360 | -1.251156 |
| 22 | 1 | 0 | 3.784196 | -3.402242 | 0.232710 |
| 23 | 1 | 0 | 3.275307 | -4.027721 | -1.339476 |
| 24 | 14 | 0 | 3.930559 | -0.159825 | 0.746315 |
| 25 | 6 | 0 | 5.455848 | -1.256823 | 0.851146 |
| 26 | 1 | 0 | 5.293510 | -2.208480 | 1.364013 |

| | | | | | |
|---|---|---|---|---|---|
| 27 | 1 | 0 | 5.921561 | −1.452510 | −0.118877 |
| 28 | 1 | 0 | 6.182213 | −0.686756 | 1.446981 |
| 29 | 6 | 0 | 4.555353 | 1.427282 | −0.065979 |
| 30 | 1 | 0 | 5.329011 | 1.154883 | −0.793608 |
| 31 | 1 | 0 | 3.788202 | 1.994487 | −0.599398 |
| 32 | 1 | 0 | 5.021141 | 2.093602 | 0.669932 |
| 33 | 6 | 0 | 3.323352 | 0.023082 | 2.524982 |
| 34 | 1 | 0 | 2.277190 | 0.328159 | 2.613031 |
| 35 | 1 | 0 | 3.425318 | −0.947205 | 3.025625 |
| 36 | 1 | 0 | 3.936800 | 0.742337 | 3.080738 |
| 37 | 7 | 0 | −0.748422 | 0.651350 | −1.361950 |
| 38 | 6 | 0 | −4.056057 | −1.411311 | 2.077625 |
| 39 | 6 | 0 | −4.166387 | −0.040838 | 1.809085 |
| 40 | 6 | 0 | −3.667196 | 0.501392 | 0.632345 |
| 41 | 6 | 0 | −3.052298 | −0.350680 | −0.284609 |
| 42 | 6 | 0 | −2.923637 | −1.717361 | −0.048735 |
| 43 | 6 | 0 | −3.430484 | −2.236498 | 1.137462 |
| 44 | 1 | 0 | −4.653938 | 0.607750 | 2.531793 |
| 45 | 1 | 0 | −3.764410 | 1.561376 | 0.420247 |
| 46 | 1 | 0 | −2.445681 | −2.360477 | −0.781221 |
| 47 | 1 | 0 | −3.342582 | −3.300854 | 1.334957 |
| 48 | 6 | 0 | −4.623303 | −1.980414 | 3.349377 |
| 49 | 1 | 0 | −4.315304 | −1.387257 | 4.215695 |
| 50 | 1 | 0 | −5.718515 | −1.969586 | 3.319708 |
| 51 | 1 | 0 | −4.299055 | −3.012638 | 3.501134 |

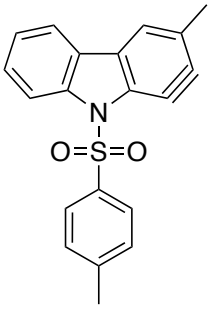


**602$_{-TMS}$**

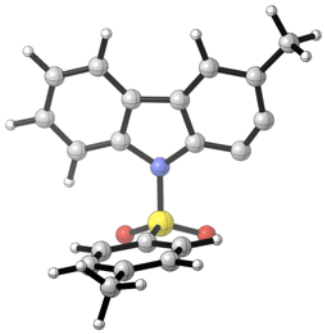

| Center Number | Atomic Number | Atomic Type | Coordinates (Angstroms) X | Y | Z |
|---|---|---|---|---|---|
| 1 | 6 | 0 | -0.528750 | 3.796261 | -0.891991 |
| 2 | 6 | 0 | -0.096557 | 2.909228 | 0.088350 |
| 3 | 6 | 0 | -0.747840 | 1.678874 | 0.170343 |
| 4 | 6 | 0 | -1.807585 | 1.339334 | -0.697286 |
| 5 | 6 | 0 | -2.231879 | 2.253946 | -1.663854 |
| 6 | 6 | 0 | -1.584304 | 3.478446 | -1.757571 |
| 7 | 1 | 0 | -0.037900 | 4.760493 | -0.979256 |
| 8 | 1 | 0 | 0.705747 | 3.171087 | 0.766798 |
| 9 | 1 | 0 | -3.052342 | 2.004337 | -2.329899 |
| 10 | 1 | 0 | -1.899838 | 4.198987 | -2.505332 |
| 11 | 6 | 0 | -2.247907 | -0.002760 | -0.353609 |
| 12 | 6 | 0 | -3.250410 | -0.839959 | -0.879467 |
| 13 | 6 | 0 | -1.424945 | -0.426268 | 0.719264 |
| 14 | 6 | 0 | -3.483148 | -2.140610 | -0.391532 |
| 15 | 6 | 0 | -1.667677 | -1.707538 | 1.184544 |
| 16 | 6 | 0 | -2.573902 | -2.361705 | 0.633685 |
| 17 | 16 | 0 | 0.920956 | 0.293751 | 1.870422 |
| 18 | 8 | 0 | 1.408315 | 1.584394 | 2.323289 |
| 19 | 8 | 0 | 0.623400 | -0.767585 | 2.812955 |
| 20 | 6 | 0 | -4.536768 | -3.063797 | -0.921869 |
| 21 | 1 | 0 | -5.253950 | -3.328017 | -0.138836 |
| 22 | 1 | 0 | -5.079189 | -2.589011 | -1.742465 |
| 23 | 1 | 0 | -4.092651 | -3.993413 | -1.290407 |
| 24 | 7 | 0 | -0.538953 | 0.606549 | 1.072695 |
| 25 | 6 | 0 | 1.988611 | -0.324455 | 0.607338 |
| 26 | 6 | 0 | 1.947287 | -1.681947 | 0.297917 |
| 27 | 6 | 0 | 2.810183 | 0.565190 | -0.084068 |
| 28 | 6 | 0 | 2.757053 | -2.152745 | -0.729822 |
| 29 | 1 | 0 | 1.302426 | -2.355543 | 0.854060 |

| | | | | | |
|---|---|---|---|---|---|
| 30 | 6 | 0 | 3.610942 | 0.070791 | −1.105030 |
| 31 | 1 | 0 | 2.829093 | 1.617086 | 0.182685 |
| 32 | 6 | 0 | 3.595477 | −1.288930 | −1.441825 |
| 33 | 1 | 0 | 2.740804 | −3.209413 | −0.980303 |
| 34 | 1 | 0 | 4.262484 | 0.749020 | −1.649325 |
| 35 | 1 | 0 | −3.873485 | −0.483303 | −1.696829 |
| 36 | 6 | 0 | 4.483997 | −1.805040 | −2.540798 |
| 37 | 1 | 0 | 4.372256 | −1.204131 | −3.448498 |
| 38 | 1 | 0 | 5.536516 | −1.751340 | −2.241880 |
| 39 | 1 | 0 | 4.252409 | −2.845068 | −2.782392 |

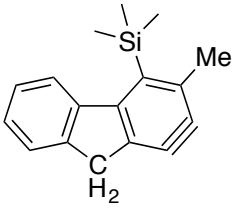


**602$_{CH2}$**

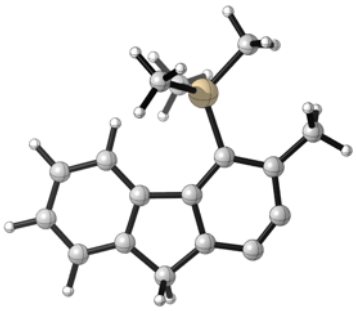

| Center Number | Atomic Number | Atomic Type | Coordinates (Angstroms) X | Y | Z |
|---|---|---|---|---|---|
| 1 | 6 | 0 | −4.047768 | −1.239515 | −0.000683 |
| 2 | 6 | 0 | −3.920886 | 0.147896 | 0.000109 |
| 3 | 6 | 0 | −2.653495 | 0.713413 | 0.000396 |
| 4 | 6 | 0 | −1.483022 | −0.076101 | −0.000063 |
| 5 | 6 | 0 | −1.630243 | −1.469267 | −0.000963 |
| 6 | 6 | 0 | −2.904077 | −2.036275 | −0.001192 |
| 7 | 1 | 0 | −5.031905 | −1.698093 | −0.000918 |
| 8 | 1 | 0 | −4.800881 | 0.785799 | 0.000477 |
| 9 | 1 | 0 | −0.781417 | −2.138630 | −0.001313 |
| 10 | 1 | 0 | −2.998690 | −3.117954 | −0.001824 |
| 11 | 6 | 0 | −0.288972 | 0.829518 | 0.000246 |
| 12 | 6 | 0 | 1.116023 | 0.565706 | −0.000315 |
| 13 | 6 | 0 | −0.825251 | 2.156220 | 0.000603 |
| 14 | 6 | 0 | 2.049518 | 1.653473 | −0.000685 |
| 15 | 6 | 0 | 0.143022 | 3.139321 | 0.000315 |
| 16 | 6 | 0 | 1.353431 | 2.843014 | −0.000123 |
| 17 | 6 | 0 | 3.551801 | 1.564976 | −0.001938 |
| 18 | 1 | 0 | 3.927437 | 1.044242 | 0.882334 |

| | | | | | |
|---|---|---|---|---|---|
| 19 | 1 | 0 | 3.925653 | 1.043045 | -0.886270 |
| 20 | 1 | 0 | 3.972291 | 2.572416 | -0.003054 |
| 21 | 14 | 0 | 1.745908 | -1.243096 | 0.000387 |
| 22 | 6 | 0 | 1.161830 | -2.063714 | -1.599232 |
| 23 | 1 | 0 | 1.084200 | -3.151255 | -1.480050 |
| 24 | 1 | 0 | 0.203983 | -1.694351 | -1.974546 |
| 25 | 1 | 0 | 1.913875 | -1.875407 | -2.374888 |
| 26 | 6 | 0 | 3.608346 | -1.528950 | 0.001950 |
| 27 | 1 | 0 | 4.118701 | -1.149482 | 0.891309 |
| 28 | 1 | 0 | 3.728898 | -2.621315 | 0.002403 |
| 29 | 1 | 0 | 4.120257 | -1.150042 | -0.886728 |
| 30 | 6 | 0 | 1.160050 | -2.063111 | 1.599684 |
| 31 | 1 | 0 | 1.911322 | -1.874451 | 2.376003 |
| 32 | 1 | 0 | 0.201779 | -1.693921 | 1.974043 |
| 33 | 1 | 0 | 1.082791 | -3.150707 | 1.480710 |
| 34 | 6 | 0 | -2.320527 | 2.177861 | 0.000950 |
| 35 | 1 | 0 | -2.719624 | 2.692948 | 0.883046 |
| 36 | 1 | 0 | -2.720062 | 2.693702 | -0.880506 |

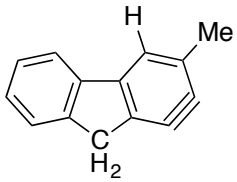


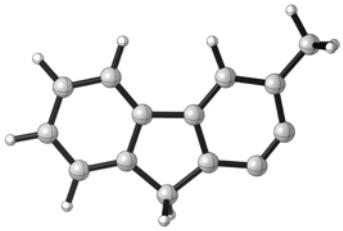

**602$_{CH2-TMS}$**

| Center Number | Atomic Number | Atomic Type | Coordinates (Angstroms) X | Y | Z |
|---|---|---|---|---|---|
| 1 | 6 | 0 | 3.710103 | -0.463080 | -0.000028 |
| 2 | 6 | 0 | 3.063211 | 0.774484 | -0.000027 |
| 3 | 6 | 0 | 1.675278 | 0.807463 | -0.000002 |
| 4 | 6 | 0 | 0.934794 | -0.389420 | 0.000012 |
| 5 | 6 | 0 | 1.580799 | -1.624290 | 0.000009 |
| 6 | 6 | 0 | 2.974581 | -1.650687 | 0.000002 |
| 7 | 1 | 0 | 4.795299 | -0.502640 | -0.000048 |
| 8 | 1 | 0 | 3.638545 | 1.696376 | -0.000058 |
| 9 | 1 | 0 | 1.011438 | -2.549640 | 0.000053 |
| 10 | 1 | 0 | 3.493687 | -2.604486 | 0.000020 |
| 11 | 6 | 0 | -0.500717 | -0.058017 | 0.000095 |

| | | | | | |
|---|---|---|---|---|---|
| 12 | 6 | 0 | −1.622450 | −0.904998 | 0.000053 |
| 13 | 6 | 0 | −0.602918 | 1.357841 | 0.000042 |
| 14 | 6 | 0 | −2.946267 | −0.414515 | 0.000023 |
| 15 | 6 | 0 | −1.928371 | 1.748542 | 0.000012 |
| 16 | 6 | 0 | −2.906334 | 0.976261 | 0.000022 |
| 17 | 6 | 0 | −4.158700 | −1.295994 | −0.000092 |
| 18 | 1 | 0 | −4.778484 | −1.105352 | −0.881859 |
| 19 | 1 | 0 | −3.870238 | −2.349686 | −0.000996 |
| 20 | 1 | 0 | −4.777658 | −1.106728 | 0.882585 |
| 21 | 6 | 0 | 0.753470 | 2.006952 | −0.000031 |
| 22 | 1 | 0 | 0.903443 | 2.641168 | −0.881683 |
| 23 | 1 | 0 | 0.903550 | 2.641370 | 0.881449 |
| 24 | 1 | 0 | −1.478450 | −1.983636 | −0.000005 |

# Bibliography


1. Chen, X.-L.; Liu, H.-L.; Li, J.; Xin, G.-R.; Guo, Y.-W. Paracaseolide A, first α-alkylbutenolide dimer with an unusual tetraquinane oxa-cage bislactone skeleton from Chinese mangrove *Sonneratia paracaseolaris*. *Org. Lett.* **2011**, *13*, 5032–5035.
2. Lammer, C.; Wagerer, S.; Saffrich, R.; Mertens, D.; Ansorge, W.; Hoffmann, I. The cdc25B phosphatase is essential for the G2/M phase transition in human cells. *J. Cell Sci.* **1998**, *111*, 2445–2453.
3. Yin, J.-P.; Tang, C.-L.; Gao, L.-X.; Ma, W.-P.; Li, J.-Y.; Li, Y.; Li, J.; Nan, F.-J. Design and synthesis of paracaseolide A analogues as selective inhibitors of protein tyrosine phosphatase 1B inhibitors. *Org. Biomol. Chem.* **2014**, *12*, 3441–3445.
4. For example: (a) Shults, E. E.; Velder, J.; Schmalz, H.-G.; Chernov, S. V.; Rubalava, T. V.; Gatilov, Y. V.; Henze, G.; Tolstikov, G. A.; Prokop, A. Gram-scale synthesis of pinusolide and evaluation of its antileukemic potential. *Bioorg. Med. Chem. Lett.* **2006**, *16*, 4228–4232 and references cited therein. (b) Koo, K. A.; Lee, M. K.; Kim, S. H.; Jeong, E. J.; Oh, T. H.; Kim, Y. C. Pinusolide and 15-methoxypinusolidic acid attenuate the neurotoxic effect of staurosporine in primary cultures of rat cortical cells. *Br. J. Pharmacol.* **2007**, *150*, 65–71. (c) Kikuchi, H.; Tsukitani, Y.; Nakanishi, H.; Shimizu, I.; Saitoh, S.; Iguchi, K.; Yamada, Y. Studies on marine natural products. VIII. New Butenolides from the Gorgonian Euplexaura flava (Nutting). *Chem. Pharm. Bull.* **1983**, *31*, 1172–1176. (d) Boukouvalas, J.; Loach, R. P. General, regiodefined access to α-substituted butenolides through metal−halogen exchange of 3-bromo-2-silyloxyfurans. Efficient synthesis of an anti-inflammatory gorgonian lipid. *J. Org. Chem.* **2008**, *73*, 8109–8112.
5. Gravel, E.; Poupon, E. Biogenesis and biomimetic chemistry: Can complex natural products be assembled spontaneously? *Eur. J. Org. Chem*. **2008**, 27–42
6. (a) Zhao, Q.; Qing, C.; Hao, X. J.; Han, J.; Zuo, G. Y.; Zou, C.; Xu, G. L. Cytotoxicity of labdane-type diterpenoids from Hedychium forrestii. *Chem. Pharm. Bull.* **2008**, *56*, 210–212. (b) Nakamura, S.; Okazaki, Y.; Ninomiya, K.; Morikawa, T.; Matsuda, H.; Yoshikawa, M. Medicinal flowers. XXIV. Chemical structures and hepatoprotective effects of constituents from flowers of Hedychium coronarium. *Chem. Pharm. Bull.* **2008**, *56*, 1704–1709. (c) Suresh, G.; Reddy, P. P.; Babu, K. S.; Shaik, T. B.; Kalivendi, S. V. Two new cytotoxic labdane diterpenes from the

rhizomes of Hedychium coronarium. *Bioorg. Med. Chem. Lett.* **2010**, *20*, 7544–7548. (d) Shirota, O.; Nagamatsu, K.; Sekita, S.; Neo-clerodane diterpenes from the hallucinogenic sage Salvia divinorum. *J. Nat. Prod.* **2006**, *69*, 1782–1786. (e) Gamard, P.; Sauriol, F.; Benhamou, N.; Belanger, R. R.; Paulitz, T. C. Novel butyrolactones with antifungal activity produced by Pseudomonas aureofaciens strain 63-28. *J. Antibiot.* **1997**, *50*, 742–749. (f) Kikuchi, H.; Tsukitani, Y.; Nakanishi, H.; Shimizu, I. New butenolides from the gorgonian euplexaura flava(nutting). *Chem. Lett.* **1982**, *11*, 233–236.

7. Jung, M. E.; Zimmerman, C. N. New synthesis of methyl 1,3-butadiene-2-carboxylate by the cheletropic extrusion of carbon monoxide from 3-carbomethoxy-3,4-pentadienal and a study of its dimerization to give dimethyl mikanecate (dimethyl 4-ethenyl-1-cyclohexene-1,4-dicarboxylate). *J. Am. Chem. Soc.* **1991**, *113*, 7813–7814.

8. Hoye, T. R.; Donaldson, S. M.; Vos, T. J. An enyne metathesis/(4 + 2)-dimerization route to (±)-differolide. *Org. Lett.* **1999**, *1*, 277–279.

9. Keller-Schierlein, W.; Bahnmüller, U.; Dobler, M.; Bielecki, J.; Stümpfel, J.; Zähner, H. Isolation and structure elucidation of differolide. *Helv. Chim. Acta* **1986**, *69*, 1833–1836.

10. (a) Stocking, E. M.; Williams, R. M. Chemistry and biology of biosynthetic Diels–Alder reactions. *Angew. Chem. Int. Ed.* **2003**, *42*, 3078–3115. (b) Hideaki Oikawa, H.; Tokiwano, T. Enzymatic catalysis of the Diels–Alder reaction in the biosynthesis of natural products. *Nat. Prod. Rep.* **2004**, *21*, 321–352.

11. (a) Kim, A. H. J.; Ruszczycky, M. W.; Choi, S.-H.; Liu, Y.-N.; Liu, H.-W. Enzyme-catalyzed [4+2] cycloaddition is a key step in the biosynthesis of spinosyn. *Nature* **2011**, *473*, 109–112. (b) Hashimoto, T.; Hashimoto, J.; Teruya, K.; Hirano, T.; Shin-Ya, K.; Ikeda, H.; Liu, H-w.; Nishiyama, M.; Kuzuyama, T. Biosynthesis of versipelostatin: Identification of an enzyme-catalyzed [4+2]-cycloaddition required for macrocyclization of spirotetronate-containing polyketides. *J. Am. Chem. Soc.* **2015**, *137*, 572–575.

12. (a) Brophy, G. C.; Mohandas, J.; Slaytor, M.; Sternhell, S.; Watson, T. R.; Wilson, L. A. Novel lignans from a *Cinnamomum* sp. from Bougainville. *Tetrahedron Lett.* **1969**, *10*, 5159–5162. (b) Chapman, O. L.; Engel, M. R.; Springer, J. P.; Clardy, J. C. The total synthesis of carpanone. *J. Am. Chem. Soc.* **1971**, *93*, 6696–6698.

13. (a) Bandaranayake, W. M.; Banfield, J. E.; Black, D. St. C. Postulated electrocyclic reactions leading to endiandric acid and related natural products. *J. Chem. Soc. Chem. Comm.* **1980**, 902–903. (b) Nicolaou, K. C.; Petasis, N. A.; Zipkin, R. E.; Uenishi, J. The endiandric acid cascade. Electrocyclizations in organic synthesis. 1. Stepwise, stereocontrolled total synthesis of endiandric acids A and B. *J. Am. Chem. Soc.* **1982**, *104,* 5555–5557.

14. (a) Noutsias, D.; Vassilikogiannakis, G. First total synthesis of paracaseolide A. *Org. Lett*. **2012**, *14*, 3565–3567. (b) Vasamsetty, L.; Khan, F. A.; Mehta G. Total synthesis of a novel oxa-bowl natural product paracaseolide A via a 'putative' biomimetic pathway. *Tetrahedron Lett*. **2013**, *54*, 3522–3525. (c) Giera, D. S.; Stark, C. B. W. Total synthesis of (±)-paracaseolide A and initial attempts at a Lewis acid mediated dimerization of its putative biosynthetic precursor. *RSC Adv.* **2013**, *3*, 21280–21284. (d) Boukouvalas, J.; Jean, M.–A. Streamlined biomimetic synthesis of paracaseolide A via aerobic oxidation of a 2-silyloxyfuran. *Tetrahedron Lett*. **2014**, *55*, 4248–4250.

15. Vasamsetty, L.; Sahu, D.; Ganguly, B.; Khan, F. A.; Mehta, G. Total synthesis of novel bioactive natural product paracaseolide A and analogues: Computational evaluation of a 'proposed' biomimetic Diels–Alder reaction. *Tetrahedron* **2014**, *70*, 8488–8497.

16. Adam, W.; Rodriguez, A. Intramolecular silyl migration in the singlet oxygenation of 2-methyl-5-trimethylsilylfuran. *Tetrahedron Lett.* **1981**, *22*, 3505–3508.

17. Guney, T.; Kraus, G. A. Total synthesis of paracaseolide A. *Org. Lett.* **2013**, *15*, 613–615.

18. This chapter is largely adapted from: Wang, T.; Hoye, T. R. Diels–Alderase-free, bis-pericyclic, [4+2] dimerization in the biosynthesis of (±)-paracaseolide A. *Nature Chem.* **2015**, *7*, 641–645.

19. Caramella, P.; Quadrelli, P.; Toma, L. Unexpected bispericyclic transition structure leading to 4+2 and 2+4 cycloadducts in the endo dimerization of cyclopentadiene. *J. Am. Chem. Soc.* **2002**, *124*, 1130–1131.

20. Ess, D. H.; Wheeler, S. E.; Iafe, R. G.; Xu, L.; Çelebi-Ölçüm, N.; Houk, K. N. Bifurcations on potential energy surfaces of organic reactions. *Angew. Chem. Int. Ed.* **2008**, *47*, 7592–7601.

21. Toma, L.; Romano, S.; Quadrelli, P.; Caramella, P. Merging of 4+2 and 2+4 cycloaddition paths in the regiospecific dimerization of methacrolein. A case of concerted crypto-diradical cycloaddition. *Tetrahedron Lett.* **2001**, *42*, 5077–5080.

22. Alston, P. V.; Ottenbrite, R. M.; Shillady, D. D. Secondary orbital interactions determining regioselectivity in the Diels-Alder reaction. *J. Org. Chem.* **1973**, *38*, 4075–4077.

23. Limanto, J.; Khuong, K. S.; Houk, K. N.; Snapper, M. L. Intramolecular cycloadditions of cyclobutadiene with dienes: Experimental and computational studies of the competing (2 + 2) and (4 + 2) modes of reaction. *J. Am. Chem. Soc.* **2003**, *125*, 16310–16321.

24. Gagnepain, J.; Castet, F.; Quideau, S. Total synthesis of (+)-aquaticol by biomimetic phenol dearomatization: Double diastereofacial differentiation in the Diels–Alder dimerization of orthoquinols with a $C_2$-symmetric transition state. *Angew. Chem.* **2007**, *119*, 1555–1557.

25. Miles, W. H.; Duca, D. G.; Selfridge, B. R.; Palha De Sousa, C. A.; Hamman, K. B.; Goodzeit, E. O.; Freedman, J. T. Amine-catalyzed epimerization of -hydroxybutenolides. *Tetrahedron Lett.* **2007**, *48*, 7809–7812.

26. Diels, O. & Alder, K. Syntheses in the hydroaromatic series [in German]. *Justus Liebigs Ann. Chem.* **1928**, *460*, 98–122.

27. (a) Onishchenko, A. S. Diene Synthesis (Israel Program for Scientific Translations,1964). (b) Nicolaou, K. C., Snyder, S. A., Montagnon, T.; Vassilikogiannakis, G. The Diels–Alder reaction in total synthesis. *Angew. Chem. Int. Ed.* **2002**, *41*, 1668–1698.

28. Michael, A.; Bucher, J. E. Über die einwirkung von eissigsäureanhydrid auf phenylpropiolsäure. *Chem. Zentrblt.* **1898**, 731–733.

29. Hoye, T. R.; Baire, B.; Niu, D.; Willoughby, P. H.; Woods, B. P. The hexadehydro-Diels–Alder reaction. *Nature*, **2012**, *490*, 208–212.

30. Wenk, H. H.; Winkler, M.; Sander, W. One century of aryne chemistry. *Angew. Chem. Int. Ed.* **2003**, 42, 502–528.

31. Hoffmann, R. W. Dehydrobenzene and cycloalkynes (Organic chemistry, a series of monographs, vol. 11, academic, 1967).

32. (a) Pellissier, H.; Santelli, M. The use of arynes in organic synthesis. *Tetrahedron* **2003**, *59*, 701–730. (b) Dyke, A. M.; Hester, A. J.; Lloyd-Jones, G. C. Organometallic generation and capture of ortho-arynes. *Synthesis* **2006**, 4093–4112. (c) Sanz, R. Recent applications of aryne chemistry to organic synthesis. A review. *Org. Prep. Proced. Int.* **2008**, *40*, 215–291. (d) Gilchrist, T. L. in Science of Synthesis Vol.43 (ed. Hopf, H.) 151–215 (Georg Thieme, 2008). (e) Chen, Y.; Larock, R. C. in Modern arylation methods (ed. Ackermann, L.) 401–473 (Wiley-VCH, 2009). (f) Kitamura, T. Synthetic methods for the generation and preparative application of benzyne. *Aust. J. Chem.* **2010**, *63*, 987–1001. (g) Tadross, P. M.; Stoltz, B. M. A comprehensive history of arynes in natural product total synthesis. *Chem. Rev.* **2012**, 112, 3550–3577. (h) Gampe, C. M.; Carreira, E. M. Arynes and cyclohexyne in natural product synthesis. *Angew. Chem. Int. Ed.* **2012**, *51*, 3766–3778.

33. Niu, D.; Willoughby, P. H.; Woods, B. P.; Baire, B.; Hoye, T. R. Alkane desaturation by concerted double hydrogen atom transfer to benzyne. *Nature* **501**, 531–534.

34. Himeshima, Y.; Sonoda, T.; Kobayashi, H. Fluoride-induced 1,2-elimination of *o*-trimethylsilylphenyl triflate to benzyne under mild conditions. *Chem. Lett.* **1983**, *12*, 1211–1214.

35. Zhang, J.; Niu, D.; Brinker, V. A.; Hoye, T. R. The phenol–ene reaction: biaryl synthesis via trapping reactions between HDDA-generated benzynes and phenolics. *Org. Lett.* **2016**, *18*, 5596–5599.

36. Niu, D.; Hoye, T. R. The aromatic ene reaction. *Nat. Chem.* **2014**, *6*, 34–40.

37. (a) Brinkley, Y. J.; Friedman, L. Novel ene and insertion reactions of benzyne and alkylbenzenes. *Tetrahedron Lett.* **1972**, *13*, 4141–4142. (b) Tabushi, I.; Yamada, H.; Yoshida, Z.; Oda, R. Reactions of benzyne with substituted benzenes. *Bull. Chem. Soc. Jpn.* **1977**, *50*, 285–290.

38. Chen, J.; Palani, V.; Hoye, T. R. Reactions of HDDA-derived benzynes with sulfides: mechanism, modes, and three-component reactions. *J. Am. Chem. Soc.* **2016**, *138*, 4318–4321.

39. Xu, F.; Hershey, K. W.; Holmes, R. J.; Hoye, T. R. Blue-Emitting Arylalkynyl Naphthalene Derivatives via a Hexadehydro-Diels–Alder Cascade Reaction. *J. Am. Chem. Soc.* **2016**, *138*, 12739–12742.

40. Miyawaki, K.; Suzuki, R., Kawano, T.; Ueda, I. Cycloaromatization of a nonconjugated polyenyne system: synthesis of 5H-benzo[d]fluoreno[3,2-b]pyrans via diradicals generated from 1-[2-{4-(2-alkoxymethylphenyl)butan-1,3-diynyl}]phenylpentan-2,4-diyn-l-ols and trapping evidence for the 1,2-didehydrobenzene diradical. *Tetrahedron Lett.* **1997**, *38*, 3943–3946.

41. (a) Ajaz, A.; Bradley, A. Z.; Burrell, R. C.; Li, W. H. H.; Daoust, K. J.; Bovee, L. B.; DiRico, K. J.; Johnson, R. P. Concerted vs stepwise mechanisms in dehydro-Diels–Alder reactions. *J. Org. Chem.* **2011**, *76*, 9320–9328. (b) Liang, Y.; Hong, X.; Yu, P.; Houk, K. N. Why alkynyl substituents dramatically accelerate hexadehydro-Diels–Alder (HDDA) reactions: stepwise mechanisms of HDDA cycloadditions. *Org. Lett.* **2014**, *16*, 5702–5705. (c) Kerisit, N.; Toupet, L.; Larini, P.; Perrin, L.; Guillemin, J.-C.; Trolez, Y. Straightforward synthesis of 5-bromopenta-2,4-diynenitrile and its reactivity towards terminal alkynes: a direct access to diene and benzofulvene scaffolds. *Chem.-Eur. J.* **2015**, *21*, 6042−6047. (d) Skraba-Joiner, S. L.; Johnson, R. P.; Agarwal, J. Dehydropericyclic reactions: symmetry-controlled routes to strained reactive intermediates. *J. Org. Chem.* **2015**, *80*, 11779–11787. (e) Marell, D. J.; Furan, L. R.; Woods, B. P.; Lei, X.; Bendelsmith, A. J.; Cramer, C. J.; Hoye, T. R.; Kuwata, K. T. Mechanism of the intramolecular hexadehydro-Diels–Alder reaction. *J. Org. Chem.* **2015**, *80*, 11744–11754. (f) [SMD(*o*-dichlorobenzene)/B3LYP-D3BJ/6-311+G(d,p)//M06-2X/6-311+G(d,p)]

42. Paton, R. S.; Kim, S.; Ross, A. G.; Danishefsky, S. J.; Houk, K. N. Experimental Diels–Alder reactivities of cycloalkenones and cyclic dienes explained through transition-state distortion energies. *Angew. Chem. Int. Ed.* **2011**, *50*, 10366–10368.

43. (a) Becke, A. D. Density-functional exchange-energy approximation with correct asymptotic behavior. *Phys. Rev. A: At., Mol., Opt. Phys.* **1988**, *38*, 3098−3100. (b) Lee, C.; Yang, W.; Parr, R. G. Development of the Colle-Salvetti correlation-energy formula into a functional of the electron density. *Phys. Rev. B: Condens. Matter Mater. Phys.* **1988**, *37*, 785−789. (c) Becke, A. D. Density-functional thermochemistry. III. The role of exact exchange. *J. Chem. Phys.* **1993**, *98*, 5648−5652. (d) Stephens, P. J.; Devlin, F. J.; Chabalowski, C. F.; Frisch, M. J. Ab initio calculation of vibrational absorption and circular dichroism spectra using density functional force fields. *J. Phys. Chem.* **1994**, *98*, 11623−11627.

44. Grimme, S.; Antony, J.; Ehrlich, S.; Krieg, H. A consistent and accurate ab initio parametrization of density functional dispersion correction (DFT-D) for the 94 elements H-Pu. *J. Chem. Phys.* 2010, 132, 154104.

45. Johnson, E. R.; Becke, A. D. A post-Hartree-Fock model of intermolecular interactions: Inclusion of higher-order corrections. *J. Chem. Phys.* **2006**, *124*, 174104.

46. Marenich, A. V.; Cramer, C. J.; Truhlar, D. G. Universal solvation model based on solute electron density and on a continuum model of the solvent defined by the bulk dielectric constant and atomic surface tensions. *J. Phys. Chem.* B **2009**, *113*, 6378−6396.

47. For a review describing cycloaromatization reactions via diradicals, see: Mohamed, R. K.; Peterson, P. W.; Alabugin, I. V. *Chem. Rev.* **2013**, *113*, 7089–7129.

48. Woods, B. P.; Baire, B.; Hoye, T. R. Rates of hexadehydro-Diels−Alder (HDDA) cyclizations: impact of the linker structure. *Org. Lett.* **2014**, *16*, 4578−4581.

49. This part is largely adapted from: Wang, T.; Niu, D.; Hoye, T. R. The hexadehydro-Diels−Alder cycloisomerization reaction proceeds by a stepwise mechanism. *J. Am. Chem. Soc.* **2016**, *138*, 7832−7835.

50. Baire, B.; Niu, D.; Willoughby, P. H.; Woods, B. P.; Hoye, T. R. Synthesis of complex benzenoids via the intermediate generation of o-benzynes through the hexadehydro-Diels–Alder reaction. *Nat. Protoc.* **2013**, *8*, 501−508.

51. Yun, S. Y.; Wang, K.-P.; Lee, N.-K.; Mamidipalli, P.; Lee, D. Alkane C–H insertion by aryne intermediates with a silver catalyst. *J. Am. Chem. Soc.*, **2013**, *135*, 4668–4671.

52. In the case of the slowest reacting members, formation of 3-butynyl *p*-toluenesulfonamide-containing byproducts were observed, presumably arising from a slow hydrolysis of the ynamide bond in **519a** or **519g** under the HDDA cyclization conditions. Other than **521**, no product arising from an initial HDDA cyclization event was ever observed for any of the examples.

53. Hansch, C.; Leo, A.; Taft, R. W. A survey of Hammett substituent constants and resonance and field parameters. *Chem. Rev.* **1991**, *91*, 165–195.

54. (a) Onishchenko, A. S. *Diene Synthesis* (Israel Program for Scientific Translations, 1964). (b) Diels-Alder reactions with ethylenic and acetylenic dienophiles: Holmes, H. L. *Org. React*. **1948**, 4, 60.

55. (a) Pasto, D. J.; Krasnansky, R.; Zercher, C. Stabilization energies and structures of substituted methyl radicals. *J. Org. Chem.* **1987**, *52*, 3062–3072. (b) Henry, D. J.; Parkinson, C. J.; Mayer, P. M.; Radom, L. Bond dissociation energies and radical stabilization energies associated with substituted methyl radicals. *J. Phys. Chem. A* **2001**, *105*, 6750–6756. (c) Zipse, H. Radical stability—a theoretical perspective. *Top. Curr. Chem.* **2006**, *263*, 163–189.

56. (a) Sauer, J.; Wiest, H.; Mielert, A. *Chem. Ber.* **1964**, *97*, 3183–3207. (b) Konovalov, A. I.; Kamasheva, G. I.; Loskutov, M. P. *J. Org. Chem. USSR* **1973**, *9*, 2064–2071.

57. (a) Hamura, T.; Ibusuki, Y.; Sato, K.; Matsumoto, T.; Osamura, Y.; Suzuki, K. Strain-induced regioselectivities in reactions of benzyne possessing a fused four-membered ring. *Org. Lett.* **2003**, *5*, 3551−3554. (b) Cheong, P. H. Y.; Paton, R. S.; Bronner, S. M.; Im, G.-Y. J.; Garg, N. K.; Houk, K. N. Indolyne experimental and computational studies: synthetic applications and origins of selectivities of nucleophilic additions. *J. Am. Chem. Soc.* **2010**, *132*, 1267−1269. (c) Garr, A. N.; Luo, D.; Brown, N.; Cramer, C. J.; Buszek, K. R.; VanderVelde, D. Experimental and theoretical investigations into the unusual regioselectivity of 4,5-, 5,6-, and 6,7-indole aryne cycloadditions. *Org. Lett.* **2010**, *12*, 96−99.

58. (a) Duanmu, K.; Wang, B.; Marenich, A. V.; Cramer, C. J.; Truhlar, D. G. CM5PAC version 2015, University of Minnesota, Minneapolis, 2015. http://comp.chem.umn.edu/cm5pac/ (b) Marenich, A. V.; Jerome, S. V.; Cramer, C. J.; Truhlar, D. G. Charge Model 5: an extension of Hirshfeld population analysis for the accurate description of molecular interactions in gaseous and condensed phases. *J. Chem. Theor. Comput.* **2012**, *8*, 527–541. (c) Duanmu, K.; Truhlar, D. G. Partial ionic character beyond the pauling paradigm: metal nanoparticles. *J. Phys. Chem. C* **2014**, *118*, 28069–28074.

59. Goetz, A. E.; Garg, N. K. Regioselective reactions of 3,4-pyridynes enabled by the aryne distortion model. *Nat. Chem.* **2013**, *5*, 54–60.

60. This section is largely adapted from: Hoye, T. R.; Baire, B.; Wang, T. Tactics for probing aryne reactivity: mechanistic studies of silicon-oxygen bond cleavage during

the trapping of (HDDA-generated) benzynes by silyl ethers. *Chem. Sci.* **2014**, *5*, 545–550.

61. This section is largely adapted from: Willoughby, P. H.; Niu, D.; Wang, T.; Haj, M. K.; Cramer, C. J.; Hoye, T. R. Mechanism of the reactions of alcohols with o-benzynes. *J. Am. Chem. Soc.* **2014**, *136*, 13657–13665.

62. (a) The possibility of a direct, single-step, O-H insertion mechanism[62b] to produce anisole directly from methanol and *o*-benzyne (not shown) was considered. Numerous attempts to locate a TS structure were unsuccessful. (b) Im, G.-Y. J.; Bronner, S. M.; Goetz, A. E.; Paton, R. S.; Cheong, P. H.-Y.; Houk, K. N.; Garg, N. K. Indolyne experimental and computational studies: synthetic applications and origins of selectivities of nucleophilic additions. *J. Am. Chem. Soc.* **2010**, *132*, 17933–17944.

63. (a) Xia, Y.; Liang, Y.; Chen, Y.; Wang, M.; Jiao, L.; Huang, F.; Liu, S.; Li, Y.; Yu, Z.-X. An unexpected role of a trace amount of water in catalyzing proton transfer in phosphine-catalyzed (3 + 2) cycloaddition of allenoates and alkenes. *J. Am. Chem. Soc.* **2007**, *129*, 3470–3471. (b) Patil, M. P.; Sunoj, R. B. Insights on Co-catalyst-promoted enamine formation between dimethylamine and propanal through ab initio and density functional theory study. *J. Org. Chem.* **2007**, *72*, 8202-8215. (c) Cheong, P. H.-Y.; Legault, C. Y.; Um, J. M.; Çelebi-Ölcüm, N.; Houk, K. N. Quantum mechanical investigations of organocatalysis: mechanisms, reactivities, and selectivities. *Chem. Rev.* **2011**, *111*, 5042–5137.

64. (a) Hull, J. F.; Balcells, D.; Sauer, E. L. O.; Raynaud, C.; Brudvig, G. W.; Crabtree, R. H.; Eisenstein, O. Manganese catalysts for C−H activation: an experimental/theoretical study identifies the stereoelectronic factor that controls the switch between hydroxylation and desaturation pathways. *J. Am. Chem. Soc.* **2010**, *132*, 7605-7616. (b) Lonsdale, R.; Harvey, J. N.; Mulholland, A. J. A practical guide to modelling enzyme-catalyzed reactions. *Chem. Soc. Rev.* **2012**, *41*, 3025-3038.

65. This part is largely adapted from: Pogula, V. D.; Wang, T.; Hoye, T. R. Intramolecular [4 + 2] trapping of a hexadehydro-Diels–Alder (HDDA) benzyne by tethered arenes. *Org. Lett.* **2015**, *17*, 856–859.

66. (a) Yun, S. Y.; Wang, K.; Lee, N.; Mamidipalli, P.; Lee, D. Alkane C–H insertion by aryne intermediates with a silver catalyst. *J. Am. Chem. Soc.* **2013**, *135*, 4668−4671. (b) Karmakar, R.; Mamidipalli, P.; Yun, S. Y.; Lee, D. Alder-ene reactions of arynes. *Org. Lett.* **2013**, *15*, 1938−1941. (c) Wang, K.; Yun, S. Y.; Mamidipalli, P.;

Lee, D. Silver-mediated fluorination, trifluoromethylation, and trifluoromethylthiolation of arynes. *Chem. Sci.* **2013**, 4, 3205−3211. (d) Mamidipalli, P.; Yun, S. Y.; Wang, K.; Zhou, T.; Xia, Y.; Lee, D. Formal hydrogenation of arynes with silyl $C_\beta$–H bonds as an active hydride source. *Chem. Sci.* **2014**, *5*, 2362−2367. (e) Lee, N.; Yun, S. Y.; Mamidipalli, P.; Salzman, R. M.; Lee, D.; Zhou, T.; Xia, Y. Hydroarylation of arynes catalyzed by silver for biaryl synthesis. *J. Am. Chem. Soc.* **2014**, 136, 4363−4368. (f) Karmakar, R.; Yun, S. Y.; Wang, K.; Lee, D. Regioselectivity in the nucleophile trapping of arynes: the electronic and steric effects of nucleophiles and substituents. *Org. Lett.* **2014**, *16*, 6−9. (g) Karmakar, R.; Yun, S. Y.; Chen, J.; Xia, Y.; Lee, D. Benzannulation of triynes to generate functionalized arenes by spontaneous incorporation of nucleophiles. *Angew. Chem. Int. Ed.* **2015**, *54*, 6582−6586. (h) Karmakar, K.; Ghorai, S.; Xia, Y.; Lee, D. Synthesis of phenolic compounds by trapping arynes with a hydroxy surrogate. *Molecules* **2015**, *20*, 15862−15880. (i) Karmakar, R.; Wang, K.-P.; Yun, S. Y.; Mamidipalli, P.; Lee, D. Hydrohalogenative aromatization of multiynes promoted by ruthenium alkylidene complexes. *Org. Biomol. Chem.* **2016**, *14*, 4782–4788.

67. (a) Vandavasi, J. K.; Hu, W.; Hsiao, C.; Senadia, G. C.; Wang, J. J. A new approach for fused isoindolines via hexadehydro-Diels–Alder reaction (HDDA) by Fe(0) catalysis. *RSC Adv.* **2014**, *4*, 57547−57552. (b) Liang, Y.; Hong, X.; Yu, P.; Houk, K. N. Why alkynyl substituents dramatically accelerate hexadehydro-Diels–Alder (HDDA) reactions: stepwise mechanisms of HDDA cycloadditions. *Org. Lett.* **2014**, *16*, 5702−5705. (c) Nobusue, S.; Yamane, H.; Miyoshi, H.; Tobe, Y. [4.2](2,2')(2,2')Biphenylophanetriyne: a twisted biphenylophane with a highly distorted diacetylene bridge. *Org. Lett.* **2014**, *16*, 1940−1943. (d) Kerisit, N.; Toupet, L.; Larini, P.; Perrin, L.; Guillemin, J.; Trolez, Y. Straightforward synthesis of 5-bromopenta-2,4-diynenitrile and its reactivity towards terminal alkynes: a direct access to diene and benzofulvene scaffolds. *Chem. - Eur. J.* **2015**, *21*, 6042−6047. (e) Watanabe, T.; Curran, D. P.; Taniguchi, T. Hydroboration of arynes formed by hexadehydro-Diels–Alder cyclizations with N-heterocyclic carbene boranes. *Org. Lett.* **2015**, *17*, 3450−3453. (f) Chen, Z.; Shan, W.; Yin, J.; Yu, G.; Liu, S. Efficient construction of carbazole derivatives via new benzyne precursors of four acetylene modules. *Acta Chimica Sinica* **2015**, *73*, 1007–1012. (g) Zhang, M.-X.; Shan, W.; Chen, Z.; Yin, J.; Yu, G.-A.; Liu, S. H. Diels–Alder reactions of arynes in situ generated from DA reaction between bis-1,3-diynes and alkynes. *Tetrahedron Lett.* **2015**, *56*, 6833–6838.

68. (a) Niu, D.; Hoye, T. R. The aromatic ene reaction. *Nat. Chem.* **2014**, 6, 34−40. (b) Chen, J.; Baire, B.; Hoye, T. R. Cycloaddition reactions of azide, furan, and pyrrole units with benzynes generated by the hexadehydro-Diels–Alder (HDDA) reaction. *Heterocycles* **2014**, *88*, 1191−1200. (c) Woods, B. P.; Baire, B.; Hoye, T. R. Rates of hexadehydro-Diels–Alder (HDDA) cyclizations: impact of the linker structure. *Org. Lett.* **2014**, *16*, 4578−4581. (d) Woods, B. P.; Hoye, T. R. Differential scanning calorimetry (DSC) as a tool for probing the reactivity of polyynes relevant to hexadehydro-Diels–Alder (HDDA) cascades. *Org. Lett.* **2014**, *16*, 6370−6373. (e) Pogula, V. D.; Wang, T.; Hoye, T. R. Intramolecular [4 + 2] trapping of a hexadehydro-Diels–Alder (HDDA) benzyne by tethered arenes. *Org. Lett.* **2015**, *17*, 856−859. (f) Luu Nguyen, Q.; Baire, B.; Hoye, T. R. Competition between classical and hexadehydro-Diels–Alder (HDDA) reactions of HDDA triynes with furan. *Tetrahedron Lett.* **2015**, *56*, 3265−3267. (g) Chen, J.; Palani, V.; Hoye, T. R. Reactions of HDDA-derived benzynes with sulfides: mechanism, modes, and three-component reactions. *J. Am. Chem. Soc.* **2016**, *138*, 4318–4321.

69. For a summary of these methods see, e.g.: Tadross, P. M.; Stoltz, B. M. A comprehensive history of arynes in natural product total synthesis. *Chem. Rev*. **2012**, *112*, 3550–3577 and references therein.

70. This section is largely adapted from: Wang, T.; Hoye, T. R. Hexadehydro-Diels–Alder (HDDA)-enabled carbazolyne chemistry: single step, de novo construction of the pyranocarbazole core of alkaloids of the murraya koenigii (curry tree) family. *J. Am. Chem. Soc.* **2016**, *138*, 13870–13873.

71. Campbell, N.; Barclay, B. M. Recent advances in the chemistry of carbazole.*Chem. Rev.* **1947**, 359-380.

72. Jiang, H.; Sun, J.; Zhang, J. A review on synthesis of carbazole-based chromophores as organic light-emitting materials. *Curr. Org. Chem.* **2012**, *16*, 2014–2025.

73. (a) Knölker, H.-J.; Reddy, K. R. Isolation and synthesis of biologically active carbazole alkaloids. *Chem. Rev*. **2002**, *102*, 4303–4427. (b) Knölker, H.-J.; Reddy, K. R. In *The Alkaloids: Chemistry and biology of carbazole alkaloids*; Cordell, G. A., Ed.; Academic Press: New York, 2008; Vol. 65, pp 1–430. (c) Occurrence, biogenesis, and synthesis of biologically active carbazole alkaloids.Schmidt, A. W.; Reddy, K. R.; Knölker, H.-J. *Chem. Rev*. **2011**, *112*, 3193–3328.

74. Głuszyńska, A. Biological potential of carbazole derivatives. *Eur. J. Med. Chem*. **2015**, *94*, 405–426.

75. For recent reviews of carbazole synthesis see: (a) Roy, J.; Jana, A. K.; Mal, D. Recent trends in the synthesis of carbazoles: an update. *Tetrahedron*, **2012**, *68*, 6099–6121. (b) Bauer, I.; Knölker, H.-J. Synthesis of pyrrole and carbazole alkaloids. *Top. Curr. Chem.* **2012**, *309*, 203–253.

76. Tohyama, S.; Choshi, T.; Azuma, S.; Fujioka, H.; Hibino, S. A new synthetic route to the 1-oxygenated carbazole alkaloids, mukonine and clausine E (clauzoline I). *Heterocycles*, **2009**, *79*, 955–965.

77. Witulski, B.; Alayrac, C. A highly efficient and flexible synthesis of substituted carbazoles by rhodium-catalyzed inter- and intramolecular alkyne cyclotrimerizations. *Angew. Chem. Int. Ed.* **2002**, *41*, 3281–3284.

78. Martínez-Esperón, M. F.; Rodríguez, D.; Castedo, L.; Saá, C. Synthesis of carbazoles from ynamides by intramolecular dehydro Diels−Alder reactions. *Org. Lett.* **2005**, *7*, 2213–2216.

79. (a) Brown, R. F. C.; Choi, N.; Coulston, K. J.; Eastwood, F. W.; Ercole, F.; Horvath, J. M.; Mattinson, M.; Mulder, R. J.; Ooi, H. C. Pyrolytic generation and rearrangement of n-substituted 1,2-didehydrocarbazoles. *Liebigs Ann./Recueil* **1997**, 1931−1940. (b) Goetz, A. E.; Silberstein, A. L.; Corsello, M. A.; Garg, N. K. Concise enantiospecific total synthesis of tubingensin A. *J. Am. Chem. Soc.* **2014**, *136*, 3036−3039.

80. Isolation: (a) Joshi, B. S.; Kamat, V. N.; Gawd, D. H. On the structures of girinimbine, mahanimbine, isomahanimbine, koenimbidine and murrayacine. *Tetrahedron* **1970**, *26*, 1475−1482. Recent syntheses: (b) Hesse, R.; Gruner, K. K.; Kataeva, O.; Schmidt, A. W.; Knölker, H.-J. Efficient construction of pyrano[3,2-a]carbazoles: application to a biomimetic total synthesis of cyclized monoterpenoid pyrano[3,2-a]carbazole alkaloids. *Chem. Eur. J.* **2013**, *19*, 14098–14111. (c) Li, X.; Song, W.; Tang, W. Rhodium-catalyzed tandem annulation and (5 + 1) cycloaddition: 3-hydroxy-1,4-enyne as the 5-carbon component. *J. Am. Chem. Soc.* **2013**, *135*, 16797–16800.

81. Isolation: (a) Narasimhan, N. S.; Paradkar, M. V.; Chitguppi, V. P.; Kelkar, S. L. *Indian J. Chem*. **1975**, *13*, 993−999. Recent synthesis: (b) Schuster, C.; Rönnefahrt, M.; Julich-Gruner, K. K.; Jäger, A.; Schmidt, A. W.; Knölker, H.–J. Synthesis of the pyrano[3,2-a]carbazole alkaloids koenine, koenimbine, koenigine, koenigicine, and structural reassignment of mukonicine. *Synthesis* **2016**, *48*, 150–160.

82. Our analytical methods should have allowed detection of as little as 1% of such a byproduct.

83. Patel, O. P. S.; Mishra, A.; Maurya, R.; Saini, D.; Pandey, J.; Taneja, I.; Raju, K. S. R.; Kanojiya, S.; Shukla, S. K.; Srivastava, M. N.; Wahajuddin, M.; Tamrakar, A. K.; Srivastava, A. K.; Yadav, P. P. Naturally occurring carbazole alkaloids from murraya koenigii as potential antidiabetic agents. *J. Nat. Prod*. **2016**, *79*, 1276–1284.

84. Zhang, T.; Huang, C.; Wu, L. A facile synthesis of 2H-chromenes and 9-functionalized phenanthrenes through reactions between α,β-unsaturated compounds and arynes. *Eur. J. Org. Chem*. **2012**, 3507–3519.

85. DeKorver, K. A.; Li, H.; Lohse, A. G.; Hayashi, R.; Lu, Z.; Zhang, Y.; Hsung, R. P. Ynamides: a modern functional group for the new millennium. *Chem. Rev*. **2010**, *110*, 5064–5106.

86. Mansfield, S. J.; Campbell, C. D.; Jones, M. W.; Anderson, E. A. A robust and modular synthesis of ynamides. *Chem. Commun*. **2015**, *51*, 3316–3319.

87. (a) Witulski, B.; Stengel, B. Rhodium(I)-catalyzed [2+2+2] cycloadditions with N-functionalized 1-alkynylamides: a conceptually new strategy for the regiospecific synthesis of substituted indolines. *Angew. Chem., Int. Ed.* **1999**, *38*, 2426–2430. (b) Alayrac, C.; Schollmeyer, D.; Witulski, B. First total synthesis of antiostatin $A_1$, a potent carbazole-based naturally occurring antioxidant. *Chem. Commun.* **2009**, 1464–1466.

88. Tresse, C.; Guissart, C.; Schweizer, S.; Bouhoute, Y.; Chany, A.-C.; Goddard, M.-L.; Blanchard, N.; Evano, G. Practical methods for the synthesis of trifluoromethylated alkynes: oxidative trifluoromethylation of copper acetylides and alkynes. *Adv. Synth. Catal.* **2014**, *356*, 2051–2060.

89. Burkhard, J. A.; Guérot, C.; Knust, H.; Rogers-Evans, M.; Carreira, E. M. Synthesis and structural analysis of a new class of azaspiro[3.3]heptanes as building blocks for medicinal chemistry. *Org. Lett*. **2010**, *12*, 1944–1947.

90. (a) This HDDA cycloisomerization proceeds more slowly than the other examples reported here, consistent with the presence of the $CF_3$-group, one of the rare substituents that destabilizes adjacent radical character relative to a hydrogen atom. In turn, this outcome is entirely in line with previous mechanistic studies supporting the stepwise (diradical) nature of the HDDA cyclization reaction.[49]

91. It was once deemed that "bonds within aromatic rings are not considered to have potential strategic character."Corey, E. J.; Howe, W. J.; Orf, H. W.; Pensak, D. A.; Petersson, G. General methods of synthetic analysis. Strategic bond disconnections for bridged polycyclic structures. *J. Am. Chem. Soc.* **1975**, *97*, 6116–6124.

92. This part is largely adapted from: Niu, D.; Wang, T.; Woods, B. P.; Hoye, T. R. Dichlorination of (hexadehydro-Diels–Alder generated) benzynes and a protocol for interrogating the kinetic order of bimolecular aryne trapping reactions. *Org. Lett.* **2014**, 16, 254–257.

93. Noyori, S.; Nishihara, Y. "Recent advances in cross-coupling reactions with aryl chlorides, tosylates, and mesylates." In *Applied Cross-Coupling Reactions*, pp. 177-202. Springer Berlin Heidelberg, 2013.

94. a) Friedman, L.; Logullo, F. M. *Angew. Chem., Int. Ed.* **1965**, *4*, 239–240. b) Birkett, M. A.; Knight, D. W.; Little, P. B.; Mitchell, M. B. *Tetrahedron* **2000**, *56*, 1013. c) Perry, R. J.; Turner, S. R. *J. Org. Chem.* **1991**, *56*, 6573. d) Rodríguez-Lojo, D.; Cobas, A.; Peña, D.; Pérez, D.; Guitián, E. *Org. Lett.* **2012**, *14*, 1363–1365.

95. Buchwald, S. L.; Lucas, E. A.; Davis, W. M. *J. Am. Chem. Soc.* **1989**, *111*, 397.

96. a) Rodebaugh, R.; Debenham, J. S.; Fraser-Reid, B.; Snyder, J. P. *J. Org. Chem.* **1999**, *64*, 1758–1761. b) Uemura, S.; Sasaki, O.; Okano, M. *J. Chem. Soc. D*, **1971**, 1064–1065. c) Uemura, S.; Onoe, A.; Okano, M. *Bull. Chem. Soc. Jap.* **1974**, *47*, 692–697. See also, d) Kovacic, P.; Brace, N. O. *J. Am. Chem. Soc.* **1954**, *76*, 5491–5494. e) Yang, L.; Lu, Z.; Stahl, S. S. *Chem. Commun.* **2009**, 6460–6462.

97. Xie, C.; Liu, L.; Zhang, Y.; Xu, P. Copper-catalyzed alkyne-aryne and alkyne-alkene-aryne coupling reactions. *Org. Lett.* **2008**, *10*, 2393–2396.

98. Garve, L. K. B.; Werz, D. B. Pd-catalyzed three-component coupling of terminal alkynes, arynes, and vinyl cyclopropane dicarboxylate. *Org. Lett.* **2015**, *17*, 596−599.

99. Abson, A.; Broom, N. J. P.; Coates, P. A.; Elder, J. S.; Forrest, A. K.; Hannan, P. C. T.; Hicks, A. J.; O'Hanlon, P. J.; Masson, N. D.; Pearson, N. D.; Pons, J. E.; Wilson, J. M. Chemistry of Pseudomonic Acid. Part 16 Aryl and Heteroaryl Ketone Derivatives of Monic Acid. *J. Antibiot.* **49**, 390–394 (1996).

100. M. J. Frisch, G. W. Trucks, H. B. Schlegel, G. E. Scuseria, M. A. Robb, J. R. Cheeseman, G. Scalmani, V. Barone, B. Mennucci, G. A. Petersson, H. Nakatsuji, M. Caricato, X. Li, H. P. Hratchian, A. F. Izmaylov, J. Bloino, G. Zheng, J. L.

Sonnenberg, M. Hada, M. Ehara, K. Toyota, R. Fukuda, J. Hasegawa, M. Ishida, T. Nakajima, Y. Honda, O. Kitao, H. Nakai, T. Vreven, J. A. Montgomery, Jr., J. E. Peralta, F. Ogliaro, M. Bearpark, J. J. Heyd, E. Brothers, K. N. Kudin, V. N. Staroverov, R. Kobayashi, J. Normand, K. Raghavachari, A. Rendell, J. C. Burant, S. S. Iyengar, J. Tomasi, M. Cossi, N. Rega, J. M. Millam, M. Klene, J. E. Knox, J. B. Cross, V. Bakken, C. Adamo, J. Jaramillo, R. Gomperts, R. E. Stratmann, O. Yazyev, A. J. Austin, R. Cammi, C. Pomelli, J. W. Ochterski, R. L. Martin, K. Morokuma, V. G. Zakrzewski, G. A. Voth, P. Salvador, J. J. Dannenberg, S. Dapprich, A. D. Daniels, Ö. Farkas, J. B. Foresman, J. V. Ortiz, J. Cioslowski, and D. J. Fox. *Gaussian 09*, revision D.01; Gaussian, Inc.: Wallingform, CT, 2009.

101. Zhao, Y.; Truhlar, D. G. The M06 suite of density functionals for main group thermochemistry, thermochemical kinetics, noncovalent interactions, excited states, and transition elements: Two new functionals and systematic testing of four M06-class functionals and 12 other functionals. *Theor. Chem. Acc.* **2008**, *120*, 215–241.

102. Stephens, P. J.; Devlin, F. J.; Chabalowski, C. F.; Frisch, M. J. Ab Initio Calculation of Vibrational Absorption and Circular Dichroism Spectra Using Density Functional Force Fields. *J. Phys. Chem.* **1994**, *98*, 11623-11627.

103. Hoye, T. R.; Zhao, H. A method for easily determining coupling constant values: an addendum to "a practical guide to first-order multiplet analysis in $^{1}$H NMR spectroscopy". *J. Org. Chem.* **2002**, *67*, 4014–4016.

104. Turlington, M.; Du, Y.; Ostrum, S. G.; Santosh, V.; Wren, K.; Lin, T.; Sabat, M.; Pu, L. *J. Am. Chem. Soc.* **2011**, 133, 11780–11794.

105. Trost, B. M.; Machacek, M.; Schnaderbeck, M. J. *Org. Lett.* **2000**, *2*, 1761–1764.

106. a) Procedure for preparation of bromopropyne[4b]:

"A 2 L three-neck round-bottom flask containing a magnetic stir bar was charged with a solution of KOH (85% tech. grade, 260 g, 3.94 mol) in 250 mL of water, and the flask was placed in an ice-salt bath. The flask was fitted with a thermocouple, a pressure equalizing dropping funnel, and a rubber septum. When the KOH solution had cooled to –3 °C (internal temperature), bromine (40 mL, 0.78 mol, ca. 1.5 equiv) was added dropwise to the stirred solution at such a rate so that the internal temperature did not rise above 0 °C. A precipitate formed over the course of the addition. After the addition was complete, the yellow slurry was stirred for an additional 30 min at 0 °C.

A 250 mL Erlenmeyer flask containing a ground-glass joint was charged with 150

mL of hexanes and the flask was cooled in a dry ice-acetone bath. Gaseous propyne (bp -23 °C, 95%, ca. 30 mL, 0.50 mol) was then slowly introduced via an 18 gauge syringe needle into the headspace of the flask. Condensation is more efficient if the needle tip is close to the surface of the cold hexane. Condensation was allowed to continue until the total volume of the solution had grown to ca. 180 mL. It is advisable to attach a bubbler to the headspace to ensure that the gas is not being introduced too rapidly.

The addition funnel on 2 L the three-neck flask was replaced by a Dewar condenser filled with a dry ice-acetone mixture. The hexanes solution of propyne, still at -78 °C, was added slowly to the aqueous KOBr solution, still maintained at ≤0 °C, via cannula over approximately 1 h. Depending on the rate of addition, the internal temperature of the reaction mixture may or may not increase. The reaction mixture was allowed to warm to room temperature, using internal temperature monitoring to guide the intermittent use of the cooling bath. As the mixture warmed, propyne reflux was observed, and the rate or reflux qualitatively indicated the progress of reaction. After the cessation of propyne reflux (ca. 2 h), the reaction mixture was transferred to a 2 L separatory funnel. The aqueous layer was drained and combined with brine (100 mL) to minimize emulsion formation. The combined aqueous layers were extracted with hexanes (2x50 mL), and the combined organic layers were washed with brine (100 mL), dried over $Na_2SO_4$, and filtered to give a dried stock solution of 1-bromopropyne (ca. 300 mL total volume). *Caution*: neat 1-bromopropyne (reported bp 64 °C) has been reported to ignite upon exposure to oxygen;[4c] hence, we have opted to titer the hexanes solution by $^1$H NMR analysis of an aliquot and use that solution directly for subsequent coupling reactions. The concentration of the stock solution described here was judged to be 27 wt%. Such solutions have been stored multiple times in a freezer (ca. -20 °C) for months with no obvious loss in titer (NMR) or discoloration."[4b]

b) Chen, J.; Palani, V.; Hoye, T. R. *J. Am. Chem. Soc.* **2016**, *138*, 4318–4321.

c) Brandsma, L.; Verkruijsse, H. D. *Synthesis* **1990**, 984–985.

107. Jung, M. E.; Min, S.-J. *J. Am. Chem. Soc.* **2005**, *127*, 10834–10835.

108. Yan, W.; Li, Z.; Kishi, Y. Selective activation/coupling of polyhalogenated nucleophiles in Ni/Cr-mediated reactions: synthesis of C1–C19 building block of halichondrin Bs. *J. Am. Chem. Soc.* **2015**, *137*, 6219–6225.

109. Yue, Y.; Yu, X.-Q.; Pu, L. *Chem. Eur. J.* **2009**, *15*, 5104–5107.

110. MacroModel, version 9.9, Schrödinger, LLC, New York, NY, 2011.

111. Laroche, C.; Li, J.; Freyer, M. W.; Kerwin, S. M. Coupling reactions of bromoalkynes with imidazoles mediated by copper salts: synthesis of novel N-alkynylimidazoles. *J. Org. Chem.* **2008**, *73*, 6462–6465.

112. Ohta, Y.; Chiba, H.; Oishi, S.; Fujii, N.; Ohno, H. Construction of nitrogen heterocycles bearing an aminomethyl group by copper-catalyzed domino three-component coupling−cyclization. *J. Org. Chem.* **2009**, *74*, 7052–7058.

113. Kitamura, T.; Morshed, M. H.; Tsukada, S.; Miyazaki, Y.; Iguchi, N.; Inoue, D. Alkynylation of benzotriazole with silylethynyliodonium triflates. regioselective synthesis of 2-ethynyl-2H-benzotriazole derivatives. *J. Org. Chem.* **2011**, *76*, 8117–8120.

114. Li, L.-S.; Wu, Y.-L. An efficient method for synthesis of α-keto acid esters from terminal alkynes. *Tetrahedron Lett.* **2002**, *43*, 2427–2430.

115. Yoo, W.-J.; Allen, A.; Villeneuve, K.; Tam, W. Rhodium-catalyzed intramolecular [4 + 2] cycloadditions of alkynyl halides. *Org. Lett.* **2005**, *7*, 5853–5856.

116. De Leon, P.; Egbertson, M.; Hills, I. D.; Johnson, A. W.; Machacek, M. Quinolinone PDE2 inhibitors. U.S. Patent 2456440 B1, August 19, 2015.

117. Tresse, C.; Guissart, C.; Schweizer, S.; Bouhoute, Y.; Chany, A.-C.; Goddard, M.-L.; Blanchard, N.; Evano, G. *Adv. Synth. Catal.* **2014**, *356*, 2051–2060.

118. For example, a) Zhang, C.; Sun, P. Palladium-catalyzed direct C(sp2)–H alkoxylation of 2-aryloxypyridines using 2-pyridyloxyl as the directing group. *J. Org. Chem.* **2014**, *79*, 8457−8461 vs. b) Panda, N.; Jena, A. K.; Mohapatra, S.; Rout, S. R. Copper ferrite nanoparticle-mediated N-arylation of heterocycles: a ligand-free reaction. *Tetrahedron Lett.* **2011**, *52*, 1924–1927.

119. Tachibana, Y.; Kikuzaki, H.; Lajis, N. H.; Nakatani, N. Antioxidative activity of carbazoles from murraya koenigii leaves. *J. Agric. Food Chem.* **2001**, *49*, 5589–5594.

120. Patel, O. P. S.; Mishra, A.; Maurya, R.; Saini, D.; Pandey, J.; Taneja, I.; Raju, K. S. R.; Kanojiya, S.;
Shukla, S. K.; Srivastava, M. N.; Wahajuddin, M.; Tamrakar, A. K.; Srivastava, A. K.; Yadav, P. P. naturally occurring carbazole alkaloids from Murraya koenigii as potential antidiabetic agents. *J. Nat. Prod*. **2016**, *79*, 1276–1284.

121. Kureel, S. P.; Kapil, R. S.; Popli, S. P. New alkaloids from Murraya koenigii Spreng. *Experientia* **1969**, *25*, 790–791.

122. Burkhard, J. A.; Guérot, C.; Knust, H.; Rogers-Evans, M.; Carreira, E. M. Synthesis and structural analysis of a new class of azaspiro[3.3]heptanes as building blocks for medicinal chemistry. *Org. Lett.* **2010**, *12*, 1944–1947.